

JPL NO. 9950-519

**BOEING  
ENGINEERING &  
CONSTRUCTION**  
*THE BOEING ENERGY  
AND ENVIRONMENT DIVISION*

Report No. DOE/JPL 954833-81/3  
Distribution Category UC-63b

(NASA-CR-164454) WIND LOADS ON FLAT PLATE N81-25431  
PHOTOVOLTAIC ARRAY FIELDS Final Report  
(Boeing Engineering and Construction) 384 p  
HC A17/MF A01 C5CL 20K Unclas  
G3/39 26604

## WIND LOADS ON FLAT PLATE PHOTOVOLTAIC ARRAY FIELDS

JPL CONTRACT NO. 954833

LOW COST SOLAR ARRAY PROJECT  
ENGINEERING AREA

Phase III Final Report

April 1981

Ronald D. Miller  
Donald K. Zimmerman



The JPL Low Cost Solar Array Project is sponsored by the U.S. Department of Energy and forms part of the Solar Photovoltaic Conversion Program to initiate a major effort toward the development of low-cost solar arrays. This work was performed for the Jet Propulsion Laboratory, California Institute of Technology by agreement between NASA and DOE.

Prepared for  
Jet Propulsion Laboratory  
4800 Oak Grove Drive  
Pasadena, California 91103

By the  
Boeing Engineering and Construction Company  
(A Division of The Boeing Company)  
Seattle, Washington 98124

**WIND LOADS ON  
FLAT PLATE PHOTOVOLTAIC ARRAY FIELDS**

**JPL Contract No. 954833**

**Low Cost Solar Array Project  
Engineering Area**

**Phase III Final Report**

**April, 1981**

**Ronald D. Miller  
Donald K. Zimmerman**

**"The JPL Low Cost Solar Array Project is sponsored by the U.S. Department of Energy and forms part of the Solar Photovoltaic Conversion Program to initiate a major effort toward the development of low-cost solar arrays. This work was performed for the Jet Propulsion Laboratory, California Institute of Technology by agreement between NASA and DOE."**

**Prepared for**

**Jet Propulsion Laboratory  
4800 Oak Grove Drive  
Pasadena, California 91103**

**By the**

**Boeing Engineering and Construction Company  
(A Division of The Boeing Company)  
Seattle, Washington**

"This report was prepared as an account of work sponsored by the United States Government. Neither the United States nor the United States Department of Energy, nor any of their employees, nor any of their contractors, subcontractors, or their employees makes any warranty, express or implied, or assumes any legal liability or responsibility for the accuracy, completeness or usefulness of any information, apparatus, product or process disclosed, or represents that its use would not infringe privately owned rights."

### Acknowledgements

Management and engineering on this project was provided by the Solar Systems organization of the Boeing Engineering and Construction Company (a Division of The Boeing Company). Dr. Ronald Ross and Mr. Robert Weaver, Manager and technical monitor, respectively, in the Engineering area of the Low Cost Solar Array Project, Jet Propulsion Laboratory, California Institute of Technology, contributed many helpful suggestions during the program, particularly in the preparation of the wind tunnel test plan. The wind tunnel test was performed by the Fluid Dynamics Laboratory staff of Colorado State University, Fort Collins, Colorado. The responsible Manager for the testing was Dr. Jack E. Cermak, the Project Director was Dr. Jon A. Peterka, and Principal Investigators were N. Hosoya and Dr. Mike Poreh.



## Table of Contents

1.0	SUMMARY	1
2.0	INTRODUCTION	5
2.1	Study Objectives	5
2.2	Discussion and Background	6
2.3	Study Requirements	7
2.4	Report Organization	8
3.0	BASIC AERODYNAMIC EQUATIONS AND DEFINITIONS	13
3.1	Analysis Definitions and Nomenclature	13
3.2	Solar Energy-Aerodynamic Synonyms	16
3.3	Aerodynamic Sign Convention and Basic Equations	17
4.0	WIND TUNNEL TEST PROGRAM AND RESULTS	19
4.1	Uniform Wind Velocity Profile	20
4.2	1/7 Power Law Wind Velocity Profile	22
4.2.1	Array Mid-Span Wind Loads Without a Protective Wind Barrier (Fence)	22
4.2.2	Array Mid-Span Wind Loads With a Protective Wind Barrier (Fence)	23
4.2.3	Array Edge Wind Loads for Straight-On Winds	24
4.2.4	Array Edge Wind Loads for Oblique Winds	25
4.3	Comparison of Wind Tunnel Test Results for Uniform Wind Profile and 1/7 Power Law Wind Profile	28
4.4	Test Results Summary	29
5.0	THEORETICAL - EXPERIMENTAL RESULTS COMPARISON	73
6.0	DISCUSSION AND CONCLUSIONS	83
7.0	STEADY STATE WIND LOADS DESIGN GUIDELINES	87
7.1	Wind Loads on Arrays Behind a Protective Wind Barrier	87
7.2	Wind Loads on Arrays Without a Protective Wind Barrier	91
7.3	Array Edge Wind Loads	92
8.0	NEW TECHNOLOGY	101
9.0	REFERENCES	103
	APPENDIX A	1A
	APPENDIX B	1B
	APPENDIX C	1C

**PRECEDING PAGE BLANK NOT FILMED**



## Figures

No.		Page
1-1	Steady State Wind Normal Force and Normalized Pressure Coefficient Envelope for Arrays Behind a Protective Wind Barrier	3
2-1	Array Variables Used to Study Aerodynamic Loads	10
2-2	Photovoltaic Array Field	11
2-3	Definition of an Array	11
4-1a	Array Chordwise Pressure Coefficient Distribution in Uniform Wind Velocity Profile (Tilt Angle = 20°, Wind from Front).	30
4-1b	Array Chordwise Pressure Coefficient Distribution in Uniform Wind Velocity Profile (Tilt Angle = 20° Wind from Rear)	31
4-1c	Array Chordwise Pressure Coefficient Distribution in Uniform Wind Velocity Profile (Tilt Angle = 35°, Wind from Front)	32
4-1d	Array Chordwise Pressure Coefficient Distribution in Uniform Wind Velocity Profile (Tilt Angle = 35°, Wind from Rear)	33
4-1e	Array Chordwise Pressure Coefficient Distribution in Uniform Wind Velocity Profile (Tilt Angle = 60°, Wind from Front)	34
4-1f	Array Chordwise Pressure Coefficient Distribution in Uniform Wind Velocity Profile (Tilt Angle = 60°, Wind from Rear)	35
4-1g	Array Chordwise Pressure Coefficient Distribution in Uniform Wind Velocity Profile (Tilt Angle = 90°)	36
4-2	1/7 Power Law Wind Velocity Profile	37

**PRECEDING PAGE BLANK NOT FILMED**

	Page
4-3a	38
Array Chordwise Pressure Coefficient Distribution in Boundary Layer Wind (Tilt Angle = 20°, Wind from Front)	
4-3b	39
Array Chordwise Pressure Coefficient Distribution in Boundary Layer Wind (Tilt Angle = 20°, Wind from Rear)	
4-3c	40
Array Chordwise Pressure Coefficient Distribution in Boundary Layer Wind (Tilt Angle = 35°, Wind from Front)	
4-3d	41
Array Chordwise Pressure Coefficient Distribution in Boundary Layer Wind (Tilt Angle = 35°, Wind from Rear)	
4-3e	42
Array Chordwise Pressure Coefficient Distribution in Boundary Layer Wind (Tilt Angle = 60°, Wind from Front)	
4-3f	43
Array Chordwise Pressure Coefficient Distribution in Boundary Layer Wind (Tilt Angle = 60°, Wind from Rear)	
4-3g	44
Array Chordwise Pressure Coefficient Distribution in Boundary Layer Wind (Tilt Angle = 90°)	
4-4	45
Effect of Head-On and Rearward Winds on Array Normal Force Coefficients (No Fence)	
4-5	46
Effect of a Fence on Array Chordwise Pressure Coefficient Distribution for Head-On and Rearward Winds	
4-6	47
Effect of a Fence on Array Normal Force Coefficients for Head-On and Rearward Winds	
4-7	48
Array Chordwise Pressure Coefficient Distribution Located .15 Chord Lengths from Side Edge for Head-On and Rearward Winds (No Fence)	
4-8	49
Effect of Fence on Array Chordwise Pressure Coefficient Distribution Located .15 Chord Lengths from Side Edge for Head-On and Rearward Winds	
4-9	50
Comparison Between Array Edge and Center of Span Normal Force Coefficients for Head-On and Rearward Winds (No Fence)	

	Page	
4-10	Effect of Fence on Array Edge Normal Force Coefficients for Head-On and Rearward Winds	50
4-11a	Effect of Oblique Winds on Array Edge Pressure Distribution (No Fence, Wind from Front)	51
4-11b	Effect of Oblique Winds on Array Edge Pressure Distribution (No Fence, Wind from Rear)	53
4-11c	Effect of Oblique Winds on Array Edge Pressure Distribution (Conventional Fence, Wind from Front)	54
4-11d	Effect of Oblique Winds on Array Edge Pressure Distribution (Conventional Fence, Wind from Rear)	55
4-11e	Effect of Oblique Winds on Array Edge Pressure Distribution (Conventional Fence, Endplated Arrays, Wind from Front)	56
4-11f	Effect of Oblique Winds on Array Edge Pressure Distribution (Conventional Fence, Endplated Arrays, Wind from Rear)	57
4-11g	Effect of Oblique Winds on Array Edge Pressure Distribution (Modified Fence Corner, Wind from Front)	58
4-11h	Effect of Oblique Winds on Array Edge Pressure Distribution (Modified Fence Corner, Wind from Rear)	59
4-12	Effect of Oblique Winds on Array Normal Force Coefficients at Array Edge	60
4-13	Maximum Pressure Coefficient at Array Side Edge Due to Oblique Winds	61
4-14a	Array Pressure Coefficient Comparison Between Uniform and Boundary Layer Wind Profiles (Tilt Angle = 20°, Wind from Front)	62
4-14b	Array Pressure Coefficient Comparison Between Uniform and Boundary Layer Wind Profiles (Tilt Angle = 20°, Wind from Rear)	63
4-14c	Array Pressure Coefficient Comparison Between Uniform and Boundary Layer Wind Profiles (Tilt Angle = 35°, Wind from Front)	64
4-14d	Array Pressure Coefficient Comparison Between Uniform and Boundary Layer Wind Profiles (Tilt Angle = 35°, Wind from Rear)	65
4-14e	Array Pressure Coefficient Comparison Between Uniform and Boundary Layer Wind Profiles (Tilt Angle = 60°, Wind from Front)	66

	<u>Page</u>	
4-14f	Array Pressure Coefficient Comparison Between Uniform and Boundary Layer Wind Profiles (Tilt Angle = 60°, Wind from Rear)	67
4-14g	Array Pressure Coefficient Comparison Between Uniform and Boundary Layer Wind Profiles (Tilt Angle = 90°)	68
4-15	Array Normal Force Coefficient Comparison Between Uniform and Boundary Layer Wind Profiles	69
4-16	Configurations for Edge Load Reduction Study	71
5-1	Array Pressure Coefficient Distribution Comparison Between Wind Tunnel Test and Theoretical Methods in Free Air	76
5-2a	Array Pressure Coefficient Distribution Comparison Between Wind Tunnel Test and Theoretical Methods in Close Ground Proximity (Tilt Angle = 20°)	77
5-2b	Array Pressure Coefficient Distribution Comparison Between Wind Tunnel Test and Theoretical Methods in Close Ground Proximity (Tilt Angle = 35°)	78
5-2c	Array Pressure Coefficient Distribution Comparison Between Wind Tunnel Test and Theoretical Methods in Close Ground Proximity (Tilt Angle = 60°)	79
5-3	Effect of Ground Clearance on Front and Back Array Pressures in Uniform Flow (Tilt Angle = 60°, Wind from Back)	80
5-4	Array Normal Force Coefficient Comparison Between Wind Tunnel Test and Theoretical Methods	81
5-5	Theoretical Key Wind Loads Parameters and Their Sensitivity in Separated Flow analyses (Reference 5)	82
7-1a	Steady State Wind Normal Force Coefficient Envelope for Arrays Within an Array Field or Behind a Protective Wind Barrier	94
7-1b	Steady State Wind Normalized Pressure Coefficient Envelope for Arrays Within an Array Field or Behind a Protective Wind Barrier	95
7-2a	Steady State Wind Normal Force Coefficient Envelope for the Two Outer Boundary Array Rows in an Array Field Unprotected from the Wind	96
7-2b	Steady State Wind Normalized Pressure Coefficient Envelope for the Two Outer Boundary Array Rows in an Array Field Unprotected from the Wind	97

7-3a	Steady State Wind Pressure Coefficient and Normal Force Coefficient Guidelines for Edge Arrays in an Array Field (No Fence)	98
7-3b.	Steady State Wind Pressure Coefficient and Normal Force Coefficient Guidelines for Edge Arrays in an Array Field (Fence)	99
7-3c	Steady State Wind Pressure Coefficient and Normal Force Coefficient Guidelines for Edge Arrays in an Array Field (Fence with Modified Corners)	100

## Tables

No.		Page
4-1	Array Test Conditions	22
5-1	Example of Average Normal Wind Forces on Arrays Behind Protective Fences by Theoretical and Wind Tunnel Test Methods	75

## 1.0 SUMMARY

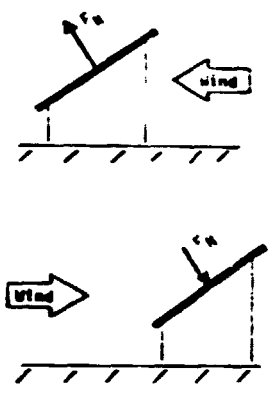
This report presents the results of an experimental analysis (boundary layer wind tunnel test) of the aerodynamic forces resulting from winds acting on flat plate photovoltaic arrays. Local pressure coefficient distributions and normal force coefficients on the arrays are shown and compared to theoretical results. Parameters that were varied when determining the aerodynamic forces included tilt angle, array separation, ground clearance, protective wind barriers, and the effect of the wind velocity profile. Recommended design wind forces and pressures are presented, which envelop the test results for winds perpendicular to the array's longitudinal axis. This wind direction produces the maximum wind loads on the arrays except at the array edge where oblique winds produce larger edge pressure loads.

The arrays located at the outer boundary of an array field have a protective influence on the interior arrays of the field. A significant decrease of the array wind loads were recorded in the wind tunnel test on array panels located behind a fence and/or interior to the array field compared to the arrays on the boundary and unprotected from the wind. The magnitude of this decrease was the same whether caused by a fence or upwind arrays. Figure 1-1 shows typical envelopes of the wind loads on arrays that are presented in this report. This figure is for arrays interior to an array field or on the boundary of a field when a fence exists to protect the front arrays. Since these loads envelop the measured wind tunnel results, they can be used as guideline design steady-state wind loads on photovoltaic arrays with wind protection. Similar guideline wind loads are given in the report for arrays unprotected from the wind.

The wind loads on the arrays within two slant heights from the side edges are considerably different from the remainder of the array field. Vortices are produced by the array corners and at the fence corner if a fence exists. These vortices cause local high pressure loads on or near the array edges. Several methods to reduce the strength of the vortices and resulting pressures were tried with limited success. Endplating the arrays (completely enclosing the ends of the arrays with a 50% porosity plate to simulate shrubs or gates at the array ends) was the most successful in reducing the wind loads on the array side edges, decreasing these loads by approximately 50%. Modifying the fence corner was also successful but to a lesser extent than endplating the arrays.

However, the edge pressures are, at best, several times larger than the pressure several slant heights away from the side edge.

Theoretically calculated steady state wind loads were larger in magnitude than wind tunnel determined wind loads. Wind tunnel determined wind loads using a uniform wind profile and a 1/7 boundary layer wind profile were similar in shape and magnitude. The magnitude of the wind loads for the uniform wind profile, although similar to the boundary layer profile, were not consistently larger or smaller than the boundary layer profile results and thus could not be used reliably for design purposes in preference to the boundary layer results.



•  $C_N$  based on wind reference velocity at 10 meters

exception: not valid within two slant heights from the side edges

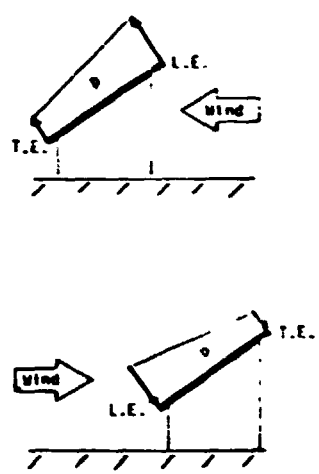
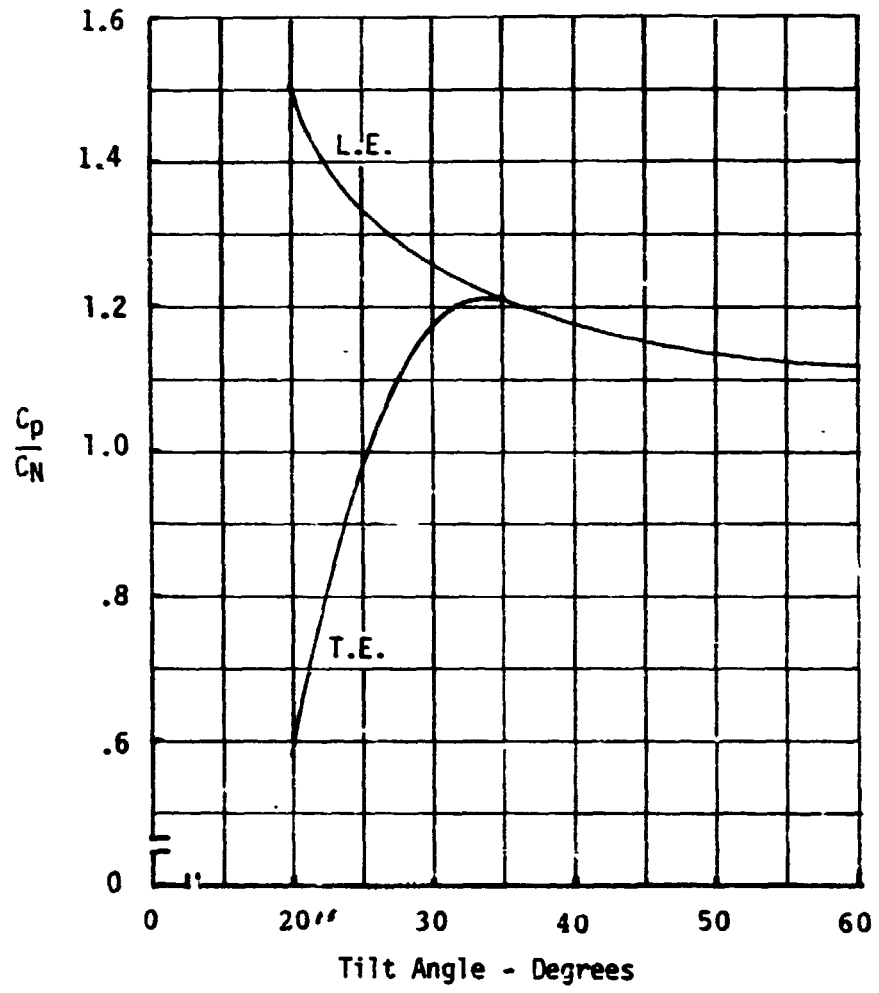


Figure 1-1. Steady State Wind Normal Force and Normalized Pressure Coefficient Envelope for Arrays Behind a Protective Wind Barrier



## 2.0 INTRODUCTION

This report summarizes an experimental analysis (wind tunnel test) of the aerodynamic loading on long, flat plate photovoltaic arrays resulting from exposure to the wind environments, evaluates and compares test results to theoretical results, and presents guidelines for aerodynamic loads to be used in the design of specific photovoltaic arrays. This report is an extension to the theoretical analysis reported in DOE/JPL 954833-79/2. The study was performed under contract number 954833 to the Jet Propulsion Laboratory as part of the Engineering Area Task of the Low-Cost Solar Array (LSA) Project. This project is being managed by JPL for the Department of Energy, Division of Solar Technology.

### 2.1 Study Objectives

The Department of Energy (DOE) photovoltaic program<sup>1</sup> has the overall objective to ensure that photovoltaic conversion systems will contribute significantly (50 Gwe) to the nation's energy supply by the year 2000. The cost associated with the design and construction of solar photovoltaic arrays to produce electric energy from sunlight is an important factor in the acceptance and use of solar energy. DOE has established specific price goals to produce energy at 55-92 mills/KW-h by 1986 (expressed in constant 1980 dollars) which are deemed necessary to achieve the desired industry growth and market penetration. Therefore, it is necessary in the trade-off phase of system design to ensure that the design requirements are realistic. The objective of this study was to establish wind load guidelines for flat plate photovoltaic arrays with various configurations in relation to chord lengths, array spacings, height of arrays from the ground, wind direction, array angles of attack, and with and without protective fences used to reduce the wind loading (see Figure 2-1). The guidelines were to be established by theoretical aerodynamic methods and experimental techniques. Wind tunnel testing was to be used to verify the theoretical results reported in reference 5 and to determine steady state wind loads on arrays for conditions that cannot presently be obtained by theoretical methods. These loads are required to ensure realistic design requirements.

PRECEDING PAGE BLANK NOT FILMED

## 2.2 Discussion and Background

The load due to wind on an array and on its support structure strongly influences the design and ultimately the cost of the photovoltaic panels, panel and array support structure and foundations of the arrays. A previous design study of flat plate array support structure showed that the arrays (structural framework and foundation) costs were of the same order of magnitude as the photovoltaic module costs. Furthermore, the array costs were strongly dependent on the assumed wind loading for loading in the range of 35 to 75 psf. Another study, using transparent inflated enclosures to protect the modules<sup>3</sup>, predicted wind loadings on the enclosures near the low end of the range compared to those used in reference 2, and showed significant cost savings compared to conventional arrays with similar wind loading criteria. It is, therefore, essential to determine the true maximum wind load that the array will experience during its lifetime in order to minimize the structure cost.

Three factors affect the amount of wind loading on a body: the flow field in which the body is placed, the aerodynamic characteristics of the body itself, and the dynamic response of the body due to the wind loading. Although the structural loads resulting from this latter factor are not totally composed of aerodynamic forces (they also include inertia forces), these structural loads do result from the wind loading, or more precisely, the fluctuations in wind loading.

A flow field of the type that would be found around arrays in an array field situated in an open terrain, as depicted in Figure 2-2, has three aspects: 1) the steady state flow before it encounters any obstacles, 2) atmospheric gusts, and 3) turbulence. The steady state flow consists of a shear layer adjacent to the ground whose shearing effects decrease with elevation above the ground until a uniform flow is attained. The shear layer for most open flatlands can be modeled as a 1/7 power law<sup>4</sup>. Gusting is the result of velocity variations and changes in the direction of the prevailing wind due to atmospheric instabilities. Turbulence may be caused by several factors. Gusting can cause turbulence when adjacent volumes of air are moving at different velocities, thus producing a shearing effect. The roughness of the land causes turbulence because of shearing effects. An obstacle in the path of the flow can also create turbulence by upsetting the flow and thus causing eddies and vortices to

form. In addition, the shape of the body will affect the characteristics of the turbulence. Turbulent flow is highly complex, with varying frequencies and intensities occurring in a random manner.

The body in the case of a photovoltaic array consists of modules assembled on a framework that is mounted on a support structure (Fig. 2-3). The aerodynamic characteristics of an array are the same as those of a flat plate when only steady state flow is considered. When gusting and turbulence are introduced, these characteristics are not as well defined; however, the aerodynamics for a flat plate are a good approximation in lieu of a more detailed structural design. The effect on the array forces due to the flow field are a function of the type of impingement and the resulting pressure distribution over the array. When the flow is turbulent, the pressure distribution and, consequently, the forces exerted on the array are nonuniform in frequency and intensity. These forces may cause vibrations in the structure resulting in additional structural dynamic forces on the array. Since turbulence varies in frequency and intensity, the resulting loading will also vary as a function of the frequency and intensity.

### 2.3 Study Requirements

The requirements of this study involve analysis and test within five specific areas. They are:

1. Wind tunnel test plan.
2. Wind tunnel test.
3. Test and theoretical results analysis and comparison.
4. Modification of theoretical results to reflect empirical results.
5. Establishment of design guidelines for estimating wind loads on photovoltaic arrays.

The following is a summary of the statement of work for Phase III.

- o Verify the analytic results obtained in Phase II and expand the effort to establish wind load and pressure distributions that can be used

as module and support structure design guidelines by performing the following four tasks.

1) Task 1 - Pre-Test Planning

Review the data requirements from the Phase II work for meeting Phase III objectives and optimize the wind tunnel test conditions and configurations that will meet the data requirements.

2) Task 2 - Wind Tunnel Testing

Based on the requirements determined in Task 1, perform the required wind tunnel tests. Review the preliminary data during the test program and modify the test plan as required to ensure that the data requirements are met.

3) Task 3 - Data Analysis

- a) Compare the wind tunnel results with the results of Phase II and determine the validity of the analytically identified key load parameters.
- b) Modify the results of Phase II to reflect the empirical results.

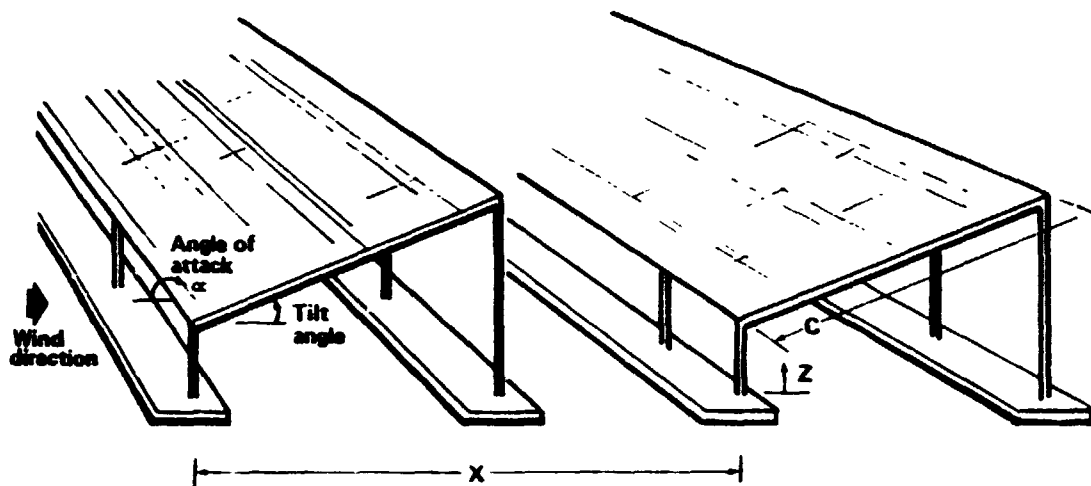
4) Task 4 - Design Guidelines

- a) Establish design guidelines for estimating the wind loads on the support structure as a function of the wind velocity and array field configuration.
- b) Establish design guidelines for estimating the pressure distribution on flat plate modules for varying wind velocities and array field configurations.

## 2.4 Report Organization

The remainder of this report presents the results of the wind tunnel test and its comparison to the theoretical results presented in reference 5 and the proposed design wind loads and conclusions. Section 3.0 presents basic

aerodynamic equations, definitions, and nomenclature for use in understanding the results. Section 4.0 presents the wind tunnel program and results. A comparison of theoretical results to experimental results is presented in Section 5.0. A discussion of the results of Sections 4.0 and 5.0 is included in Section 6.0 together with conclusions obtained from the results. Section 7.0 presents array wind load envelopes that may be used for design guidelines. New technology and References are outlined in Sections 8.0 and 9.0, respectively. The wind tunnel test report which includes test description and data from the tests conducted at Colorado State University in their Meteorological Wind Tunnel Facility is presented in the Appendix.



Ground clearance (Z)  
Array spacing (X)  
Tilt angle  
Wind direction

*Figure 2-1. Array Variables Used to Study Aerodynamic Loads*

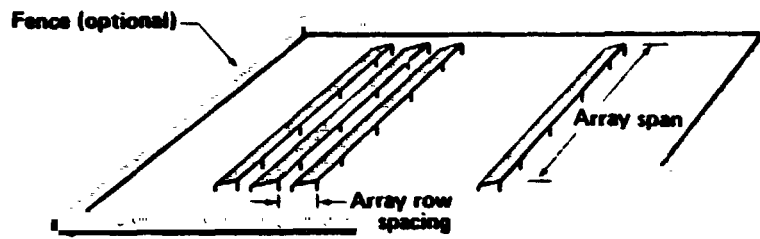


**Figure 2-2. Photovoltaic Array Field**

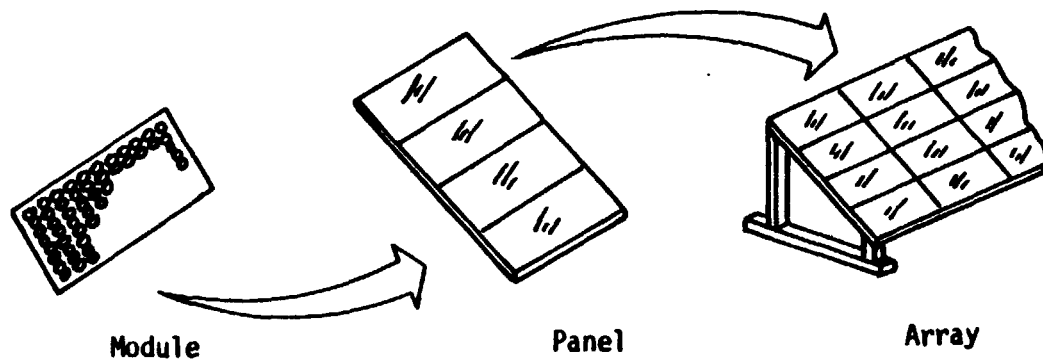


**Figure 2-3. Definition of an Array**



### 3.0 BASIC AERODYNAMIC EQUATIONS AND DEFINITIONS

The analyses used in this report required the use of aerodynamic results that were calculated in aerodynamic terms. Since these terms may be unfamiliar to designers of photovoltaic arrays, this section explains the basic aerodynamic terms and nomenclature and defines basic aerodynamic equations to assist those without an aerodynamic background to understand the results. In addition, synonyms between aerodynamic and solar energy terms are given where applicable.

#### 3.1 Analysis Definitions and Nomenclature

Aerodynamic coefficients:	non-dimensional coefficients.
pressure coefficient ( $C_p$ ):	relates lifting surface pressure to reference freestream dynamic pressure, $C_p = p/q$ .
$C_{p\alpha}$	slope of the pressure coefficient curve; relates pressure coefficient to angle of attack, $C_p = C_{p\alpha}\alpha$ .
$\Delta C_p$	net pressure coefficient on lifting surface = windward face pressure coefficient minus base pressure coefficient.
normal force ( $F_n, F_N$ ):	force normal to the lifting surface (positive out of base pressure face).
normal force coefficient ( $C_n, C_N$ ):	relates lifting surface normal force to reference freestream dynamic pressure and reference area, $C_N = F_N/qA$ .
$C_{N\alpha}$	slope of the normal force coefficient curve, relates normal force coefficient to angle of attack, $C_N = C_{N\alpha}\alpha$ .

lift (L)	force on the lifting surface perpendicular to the freestream velocity (positive up).
lift coefficient ( $C_L$ )	relates lift to reference freestream dynamic pressure and reference area, $C_L = L/qA$ .
drag (D)	force on the lifting surface parallel to the freestream velocity (positive in the wind direction).
drag coefficient ( $C_D$ )	relates drag to reference freestream dynamic pressure and reference area, $C_D = D/qA$ .
center of pressure (X)	location of total force on lifting surface measured from the leading edge.
Angle of attack:	angle measured from the wind vector to the plane of the lifting surface.
Array:	a mechanically integrated assembly of panels together with support structure (including foundations).
Array field:	the aggregate of all arrays.
Array spacing:	horizontal distance measured from one array to the identical location on the next array.
Aspect ratio (AR):	aerodynamic geometric parameter (span/chord for a rectangular array).
Base pressure face:	downwind side of lifting surface.

<b>Bluff body:</b>	a nonstreamline body that causes airflow about itself to become separated and turbulent.
<b>Chord (C):</b>	distance of array between leading and trailing edges and perpendicular to the edges, i.e.: slant height of array.
<b>Dynamic pressure (q):</b>	pressure due to freestream velocity at a reference height ( $q = .5\rho V^2$ ).
<b>Ground clearance (Z):</b>	distance between the ground and the lowest point on the panels forming the array.
<b>Inviscid:</b>	frictionless flow.
<b>Leading edge (L.E.):</b>	windward edge of the array.
<b>Module:</b>	the smallest complete environmentally protected assembly of solar cells.
<b>Normal wash, downwash:</b>	flow of air perpendicular to the lifting surface plane.
<b>Panel:</b>	a collection of one or more modules fastened together forming a field installable unit.
<b>Plate:</b>	thin rectangular shaped structure that acts as a lifting surface.
<b>Pressure (p):</b>	force per unit area.
<b>Span (b):</b>	distance of an array between the two side edges i.e.: length of array.

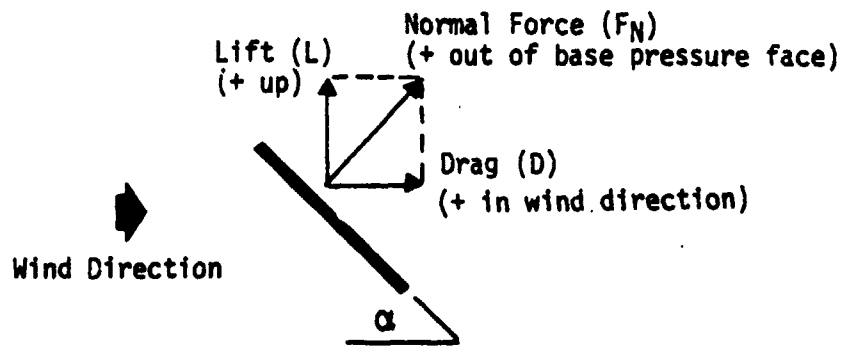
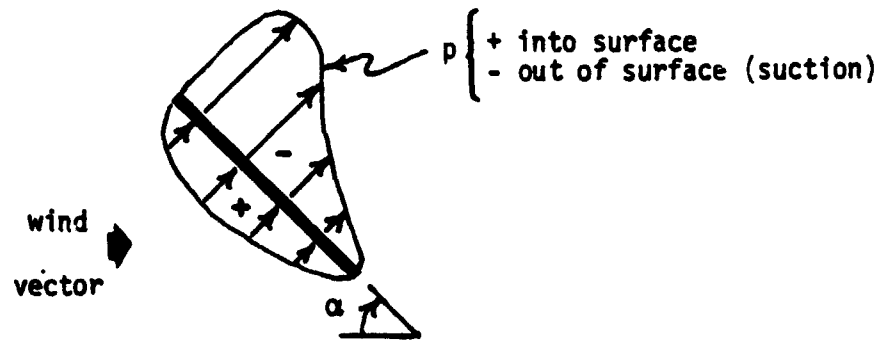
Tilt Angle:	angle measured from the horizontal to the plane of the array panels.
Trailing Edge (TE):	downwind edge of the array
Viscous:	flow that has friction.
Windward face:	windward side of lifting surface.
Yaw angle:	angle measured from wind direction to the normal of the array leading edge.
A:	reference area of array or portion of the array
$l$ :	length
V:	velocity.
$\rho$ :	air density.
$\mu$ :	coefficient of viscosity.
$S$ :	area of lifting surface.
S:	distance measured along the chord from a reference point.

### 3.2 Solar Energy - Aerodynamic Synonyms

<u>Solar Energy</u>	<u>Aerodynamics</u>	<u>Comments</u>
Tilt angle and wind direction	Angle of attack, symbol is $\alpha$	Restricted to horizontal winds
Slant height	Chord	
Wind angle	Yaw angle	

### 3.3 Aerodynamic Sign Convention and Basic Equations

Sign Convention:



### Aerodynamic Equations:

1. Pressures and pressure coefficients are related by:

$$p = q C_p$$

2. Normal forces and normal force coefficients are related by:

$$F_N = q S C_n$$

3. When the pressure coefficients and normal force coefficients are linear with respect to angle of attack, the above expressions can be changed to:

$$p = q C_{p\alpha} \alpha$$

$$F_n = q S C_{n\alpha} \alpha$$

4. Normal force coefficient for chordwise strips can be obtained from the pressure coefficients by integrating the pressure coefficient along the chord and is expressed by:

$$C_n = \frac{1}{c} \int_c C_p$$

or for a surface as:

$$C_n = -\frac{1}{S} \int_s C_p$$

5. Lift and drag coefficients are related to the normal force coefficient by the angle of attack as:

$$C_L = C_n \cos \alpha$$

$$C_D = C_n \sin \alpha$$

6. Lift and drag forces are given by:

$$L = q S C_L$$

$$D = q S C_D$$

#### 4.0 WIND TUNNEL TEST PROGRAM AND RESULTS

A wind tunnel test program was developed to verify the theoretical results in reference 5 and to obtain test data for conditions not presently suitable for theoretical analysis. The test plan included the testing of wind loads on single arrays, arrays within an array field, the effect of fences on arrays in an array field, and the effect of wind velocity profiles (uniform and 1/7 power law). The emphasis of the program was the testing of arrays in an array field with a boundary layer wind having a 1/7 power law velocity profile referenced at 10 meters. This wind profile was used to represent the winds found in nature in open flat terrain. The array parameters varied using this wind profile were: (1) array separation (1.5, 2.0, and 3.0C), (2) tilt angle (20°, 35°, 60°, and 90°), (3) wind direction (front, rear, and oblique winds of 45° and 135° from the front), (4) fence (with and without), (5) fence porosity (0% and 30%), and (6) fence-array separation (1.25, 2.5, and 5.0C). The array parameters not varied were the slant height (C) and the array ground clearance of .25C. Several modifications to the fence corner and array edges were tested with oblique winds in an attempt to reduce the array edge loads. A complete list of the test configurations is listed in Table 18, Appendix A. The fence corner modifications are detailed in Table 17, Appendix A, and the array edge modifications are shown in Figure 24, Appendix A.

A number of test runs were conducted utilizing a uniform velocity profile. These tests did not include any fence effects or effects of oblique winds. The tests included variations of tilt angle and array separation in an array field. Single arrays were also tested varying the tilt angle and the array ground clearance. Corresponding single array tests were performed with a 1/7 power law velocity profile for comparison to the uniform velocity profile results.

The wind tunnel testing was conducted in the Meteorological Wind Tunnel at Colorado State University (see Figure 1, Appendix A). This tunnel is characterized by a long (96 ft.) test section that is 6 ft. 8 in. wide by 6 ft. high. The long test section is required to properly develop and stabilize the boundary layer velocity profile used in the tests. Testing in a boundary layer wind profile is performed at the rear of the test section whereas testing in a uniform wind velocity profile is performed at the front of the test section.

The array model tested was a 1:24 scale of an eight ft. chord full size array. Pressure taps were located at the mid-span and edge locations as shown in Figure 10, Appendix A. Ten pressure taps were located on each of the front and rear faces of the array and at each span location. The spacing of the taps were varied such as to have more taps near the leading and trailing edges of the array. Pressures at each tap were recorded digitally for 16 seconds by means of a pressure switch to a Setra differential transducer which was sampled at 250 times per second. The test data acquisition, data reduction as well as the testing procedures are detailed in Appendix A. The recorded test data in its entirety is presented in Appendix B and the computer plotted test data in Appendix C.

The following sections present significant findings from the test results. Section 4.1 details the results from the uniform wind velocity profile for an array field. Section 4.2 presents the results from the 1/7 power law wind profile and section 4.3 shows the comparison of the wind loads on a single array due to a uniform and a boundary layer wind. Section 4.4 summarizes the significant test results.

#### 4.1 Uniform Wind Velocity Profile

Figures 4-1a through 4-1g, show the net or delta pressure coefficient distribution (the windward face pressure coefficient minus the base pressure coefficient) along the chord for an array field positioned at four tilt angles and with a uniform velocity profile wind from both front and rearward directions. In all of these cases, the arrays are .25 slant heights above the ground and separated by a distance of two slant heights. Other array separation distances (1.5 and 3.0 slant heights) were tested. Since the results from the three array separations are similar, only the results of the 2.0 slant height separation tests are used to discuss significant findings. The pressures on the arrays, each recorded in the test for sixteen seconds, were used to calculate average and rms pressure coefficients. The rms pressures are an indication of the pressures to be expected from the turbulence generated by the arrays. However, the rms pressures do not reveal any characteristics of the flow such as the phase angle of the pressure between locations or the frequency content of the pressures. These parameters are very important to predict dynamic pressures and forces on the structure and will be reported in a future report.

The first windward array in the array field experiences by far the highest mean pressure coefficients and resulting normal forces for all tilt angles. In contrast to the mean pressures, the rms values of the unsteady pressure coefficients caused by the array induced wind turbulence is the smallest on the first windward array. The turbulence in the wind tunnel for the free stream wind prior to the array field is essentially zero.

The first array behind the windward array (2nd array) experiences considerably lower mean pressures than the first array but the rms pressures caused by the array induced wind turbulence are greatly increased. This is caused primarily by the turbulence created in the wind by the first array. In addition, the pressure distribution on the second array is significantly changed by the effects from the first array, especially when the wind is from the front. For this wind condition, the pressures on the windward array face become negative over a portion of the chord for several tilt angles, and  $\Delta\dot{u}_p$  may be negative over part of the chord for several tilt angles as shown for the 35° tilt angle case. In this condition, if only normal forces were recorded on the array, they would indicate essentially zero force. From the pressure coefficient distribution shown in Figure 4-1c to 4-1f, it can be seen that there are varying pressures on the array and a significant pitching moment is felt by the array.

The loads on the fifth array downwind from the edge of the array field experience larger fluctuating pressure coefficients than the first array, but smaller than the second array. Although the fluctuating pressure coefficients are of the same order as the steady state pressures on the fifth array, the total of these pressures is much smaller than only the steady state pressures on the first array. Another noteworthy aspect of the loads on the fifth array is the flatness of the pressure distribution along the chord. The pressure distribution is essentially constant over the chord for each tilt angle considered. An exception is the 20° tilt angle configuration with the wind approaching the array from the back, where the pressure distribution along the chord linearly increases from the trailing edge to the leading edge.

## 4.2 1/7 Power Law Wind Velocity Profile

The major portion of the wind tunnel test program was devoted to the wind loading on the arrays in a boundary layer wind of 1/7 power law velocity profile shown in Figure 4-2. This section presents and discusses the significant findings of the wind tunnel test results performed in the boundary layer wind. The array test configuration, pressure measurement locations and wind direction are given in Table 4.1.

*Table 4-1. Array Test Conditions*

Array Configuration (Tilt Angle)	Fence	Pressure Measurement Location	Wind Direction
20°, 35°, 60°, 90°	No	Center of Span	0° (Head-On), 180°
20°, 35°, 60°, 90°	Yes	Center of Span	0° (Head-On), 180°
35°	No	Edge of Span	0° (Head-On), 180°
35°	Yes	Edge of Span	0° (Head-On), 180°
35°	No	Edge of Span	45°, 225°
35°	Yes	Edge of Span	45°, 225°

### 4.2.1 Array Mid-Span Wind Loads Without a Protective Wind Barrier (Fence)

Figure 4-3 presents the mean and rms delta pressure coefficient distributions on the arrays in an array field with an identical configuration as in Figure 4-1, except for the wind profile. The pressure coefficients are based on the freestream reference velocity located at a height of ten meters. The results for the mean and rms  $\Delta C_p$  chordwise distributions are very similar in shape to those from the uniform wind profile test results presented in Section 4.1. Because the magnitude of the coefficients are a function of the reference velocity that varies with elevation above the ground in a boundary layer wind, a direct magnitude comparison with the uniform flow results cannot be made with the boundary layer results referenced to the freestream velocity at 10 meters. The trends of the results plotted in Figure 4-3 are the same as those for the uniform velocity profile results shown in Figure 4-1. That is, the highest

steady state or mean pressures are on the first array. The downwind arrays have lower steady state pressure than the front array because of the protection afforded by the upwind arrays, but the rms pressures are slightly higher within the array field than for the front array. In addition, with increasing tilt angle, the greater the amount of protection from the wind is received by the downwind arrays from the upwind arrays.

The effect that the upwind arrays have on reducing the resulting forces on downwind arrays is shown by examining the normal force coefficients presented in Figure 4-4. The normal force coefficients were obtained by integrating the delta pressure coefficients along the chord for each array and array configuration for the steady state wind. The maximum normal force coefficient on the array is due to a wind from the rear and on the first windward array for all tilt angles. Regardless of the wind direction, the first windward array acts as a barrier to the wind for the downwind arrays and removes most of the wind energy. Consequently, the steady state wind load on the second array is significantly reduced, and the steady state wind load on succeeding arrays beyond the second array are only slightly reduced from that of the second array.

#### 4.2.2 Array Mid-Span Loads with a Protective Wind Barrier (Fence)

The protective influence on the high aspect ratio photovoltaic arrays by a fence is presented in Figure 4-5 and 4-6. Figure 4-5 shows the  $\Delta C_p$  on the first array behind a six foot fence (.75C). The corresponding normal force coefficients for the first, second and fifth arrays are shown in Figure 4-6, with the results without a fence for comparison. With a fence to protect the arrays from the wind, the wind-caused normal force coefficients are approximately the same on the first and succeeding arrays except for the arrays with tilt angles of 60°. The top of the array at a tilt angle of 60° is approximately .375 chord lengths above the top of the fence, so the upper portion of the first array is exposed to the freestream velocity resulting in increased loads. Of significant conclusion from Figure 4-6 is that the normal force on arrays several rows into the array field are the same with or without a fence. Thus, the fence only protects the first couple of rows of arrays and the remaining arrays are protected by the windward arrays.

### 4.2.3 Array Edge Wind Loads for Straight-On Winds

Figure 4-7 and 4-8 presents the pressure distribution at a location .15 chord lengths from the side edge for arrays having a tilt angle of  $35^\circ$  and for an array field without and with a protective fence respectively. Figures 4-9 and 4-10 show the normal force coefficients for the same conditions and compare the normal force coefficients at the array edge location to the mid-span location. Figure 10 of the Appendix A shows the location of the edge and center of span pressure taps on the model used in the test.) Without a fence to protect the arrays, the first windward array pressure distribution at the edge is essentially the same as at the center of the array (compare Figure 4-7 to Figure 4-3c and d). The arrays downwind from the first array have an edge pressure coefficient distribution whose magnitude is reduced from the first array but not nearly as much as for the mid-span pressure coefficients at similar conditions. The edge pressures are affected by the formation of vortices resulting from the array corners. This can be seen by the significant increase in the rms pressure coefficient levels between mid-span and edge locations and by the increased steady state pressure coefficient at the array corners, especially for winds approaching from the rear. The normal force coefficients shown in Figure 4-9 also show this trend.

The fence reduces the wind by such an amount that no large differences occur in pressure coefficient distributions at the edges compared to the mid-span pressure locations as seen by comparing Figure 4-8 to Figure 4-5 for identical array positions. One aspect of Figure 4-8 that is important is that the pressure coefficients for the fifth array downwind are larger than the first array. It is conceivable that the array edge pressures behind a protective fence will approach those without a protective fence for downward arrays when the wind is straight-on to the arrays. This results because the side fence has no effect on the straight-on wind and the fence perpendicular to the wind has a decreasing effect on the wind with increasing distance downwind from the fence. Extrapolating the normal force coefficients in Figure 4-10 further downwind supports this conclusion and suggests that loads on the arrays with a fence will approach those without a fence further downstream than five arrays.

#### 4.2.4 Array Edge Wind Loads for Oblique Winds

Downwind effects of vortices formed at the array corners can cause large pressure coefficients near the array edges when the winds are at an angle to the arrays, because of increased vortex strength. Several wind tunnel test runs were performed with oblique winds at  $45^\circ$  approaching the arrays from the front and the rear directions. The array configurations were: tilt angle of  $35^\circ$ , array separation =  $2C$  and array ground clearance =  $.25C$ . Large local pressures on the array edges due to oblique winds were measured as shown by the pressure coefficient distributions located  $.15$  chord lengths from the array edge in Figures 4-11, a through d, for an array field without and with a protective fence.

The leading edge pressure coefficients, especially for unobstructed winds approaching from the front, were very large and can result in pressures at the leading edge approaching  $45$  psf for a  $90$  mph wind, based on the pressure coefficients in Figures 4-11a and 4-11b. When no fence exists, the array edges for arrays downwind from the first array do not receive any protection from the upwind arrays; therefore, their edge pressure distribution is essentially the same as the first array, as shown in Figures 4-11a and b. Figure 4-11a also shows the pressure distribution located  $.9$  chord lengths from the edge on the first array. The trend implies that the magnitude of the pressure coefficients are decreasing with distance away from the side edge.

Even when the arrays are protected by a fence, the edge pressure coefficients due to an oblique wind are much larger than for straight-on winds as shown by comparing Figures 4-11c and d to Figure 4-8. The fence does give some protection to the arrays because the overall array edge pressure coefficient distribution is somewhat lower in magnitude than the corresponding conditions without a fence. This can be seen more easily by comparing the normal force coefficients at the edge with and without a fence as shown in Figure 4-12. Figure 4-12 also shows the reduction in normal force coefficients from  $.15$  chord lengths to  $.9$  chord lengths from the edge with and without a fence. The combination of a fence corner and an oblique wind causes a strong vortex to be generated at the fence corner which sweeps downwind and causes localized high pressure loadings. The high pressure loading caused by this vortex can be seen by the twin large humps in the pressure coefficient distribution shown on the first array in Figure 4-11c and by the large pressure coefficients at the

leading edge in Figure 4-11d. Figures 4-12 and 4-13 also show the effect of the vortex. Although the normal force coefficient for an array behind a fence is lower than without a fence (Figure 4-12), the corresponding maximum pressure coefficient is higher (Figure 4-13) on the first windward array when the wind approaches from the rear. This maximum pressure coefficient is at the leading edge which is directly downwind and in the vortex from the fence.

Because of the high edge pressures on the arrays, several modified configurations were tested in the wind tunnel in an attempt to reduce these pressures. The modifications (described in more detail in the Appendix) are as follows:

- 1) A short fence of the same porosity and height as the protective fence placed in front of the corner of the protective fence and at  $45^\circ$  to each side. This short fence would be perpendicular to a oblique wind that is at  $45^\circ$  to the protective fence and array field (See Figure 4-16, Configuration 1)
- 2) Three short fences overlapping each other and placed in front of the corner of the protective fence as in (1) (see Figure 4-16, Configuration 2)
- 3) Additional eight foot length added to the array with the added length having 50% porosity (See Figure 4-16, Configuration 3)
- 4) Endplating of the array ends completely closing the rows of the arrays with a 50% porosity end plate. This is to simulate shrubs etc., at the ends of the arrays (see Figure 4-16, Configuration 4)
- 5) Addition of a 50% porosity extension to the top of the array at the corner of the existing protective fence (see Figure 4-16, Configuration 5 and Figure 4-11g).

The data from the wind tunnel test for all of these configurations is given in Appendix B, and plots of the data are presented in Appendix C. The results from the configurations in (1) through (3) are not presented in the main body of the report for the following reasons. Configuration (3) did not produce any reduction in edge pressures. Configurations (1) and (2) did show reductions in the pressure coefficient distributions for the pressure taps on the model. However, this configuration would require more pressure readings over the total

array area near the edge to adequately define this reduction. It is believed, and somewhat supported by the data, that the vortex caused by the main fence corner is significantly reduced, but that other vortices are being generated at the corners of the smaller fences, thus pushing the location of the high pressure loading points inwards from the array side edge.

Configuration (4), endplating of the arrays, produced the smallest edge pressure coefficients of the configurations tested. The edge pressure coefficient distributions for the endplating effect is shown in Figures 4-11e and f. Unfortunately, this method of reducing the loads may be impractical for several reasons: (1) the endplating would cause varying amounts of shadowing on the arrays depending upon the time of day, (2) if mechanized equipment is required to be moved down each row of the arrays, a gate would be required at the end of each row.

The addition of a 50% porosity extension to the fence corner is shown with the results in Figures 4-11g and h. This extension does significantly reduce the edge pressure coefficient distributions from those of just a regular protective fence. It appears that the increased porosity and height at the corner reduces the tightness and strength of the corner vortex. Additional benefits may be realized by increased porosity and/or height of this corner addition. However, these parameters were not varied to optimize the reduction in the array edge pressure loadings.

In summary, the array and fence corners produce vortices whose strength is increased from a straight on wind to an oblique wind. The wind loads on the areas affected by the corner vortices are considerably larger than the loads at the non-affected areas. In order to reduce the corner vortex induced loads, it is necessary to reduce the strength of the corner vortex. This is best accomplished by lowering the wind velocity prior to reaching the arrays by utilizing a fence and by modifying the fence corner to reduce the vortex generated by it. From the modifications investigated in the test, the most practical modification is that of increasing the height of the fence at the corner and by varying the local fence porosity in this area as shown by the figure insert in Figure 4-11g.

#### 4.3 Comparison of Wind Tunnel Test Results for Uniform Wind Profile and 1/7 Power Law Wind Profile

In order to compare the test results between the uniform wind profile and the 1/7 power law wind profile, it is necessary to select a reference height above the ground for defining the reference velocity in the 1/7 power law wind profile. In Phase II, reference 5, the velocity at the highest edge of the array was recommended as the reference velocity when using data obtained by a uniform velocity profile because the base pressure (the major contribution to total pressure in most cases) is affected predominately by the velocity at the array edge. The mean  $\Delta C_p$  was calculated with this reference velocity for the 1/7 power law wind profile results and compared in Figure 4-14 to the  $\Delta C_p$  obtained by the uniform wind profile test. The comparison of the shape of the  $\Delta C_p$  distribution from the two wind profile tests is very close, the magnitude is also close except for a few configurations, such as the windward array with the wind from the rear for the 20° tilt angle configuration and the wind from the front for the 60° tilt angle configuration, where the magnitudes differ by as much as .25. The second array with a tilt angle of 35° and the wind from the rear also compares poorly; the loads from the 1/7 power law wind profile are approximately half the loads from the uniform wind profile.

Integration of the  $\Delta C_p$  values over the chord to obtain normal force coefficients produced the results presented in Figure 4-15. The comparison of the normal force coefficients between the uniform wind profile and the 1/7 power law wind profile is much closer than the pressure distribution, primarily because the integration of large pressure differences over a small fraction of the total area does not have a pronounced effect on the total normal force coefficient.

From the results shown in Figure 4-14 and 4-15, the uniform velocity profile normal force coefficients results would be satisfactory for use in performing preliminary design studies and in most cases for use in the final design of array structural supports. The pressure coefficient distribution results are not as definitive; the uniform velocity profile results would be satisfactory for use in preliminary design studies but are probably not accurate enough for final design of the photovoltaic panels. However, from the results, it is certainly apparent that a uniform velocity wind tunnel can be used to evaluate parameter studies for photovoltaic arrays such as load alleviation devices.

Since environmental wind tunnels (required to model the boundary layer wind) are few in number, and sometimes difficult to obtain time in their use, the close comparison in the results between the two wind profiles is important in allowing more flexibility in the testing of array models and configuration changes.

#### 4.4 Test Results Summary

The use of a fence to protect the arrays from the wind significantly reduces the mid-span loads on the first windward array compared to the loads on an unprotected first array. The arrays located downwind from the first array are protected by the upwind arrays and the mid-span loads are approximately the same as the first array when protected by a fence. Localized array edge loads, caused by corner vortices, are considerably larger than the array mid-span loads. These edge loads can be reduced by using a fence to protect the arrays and by appropriate modifications to the fence corners shown previously in this section. To optimize the fence corner modifications or other modifications to the arrays for minimum wind loads would require an extensive test program. Since the large wind loads are a localized effect caused by the corner vortices, the arrays could be designed for higher strength in the edge areas to withstand the high vortex induced loads.

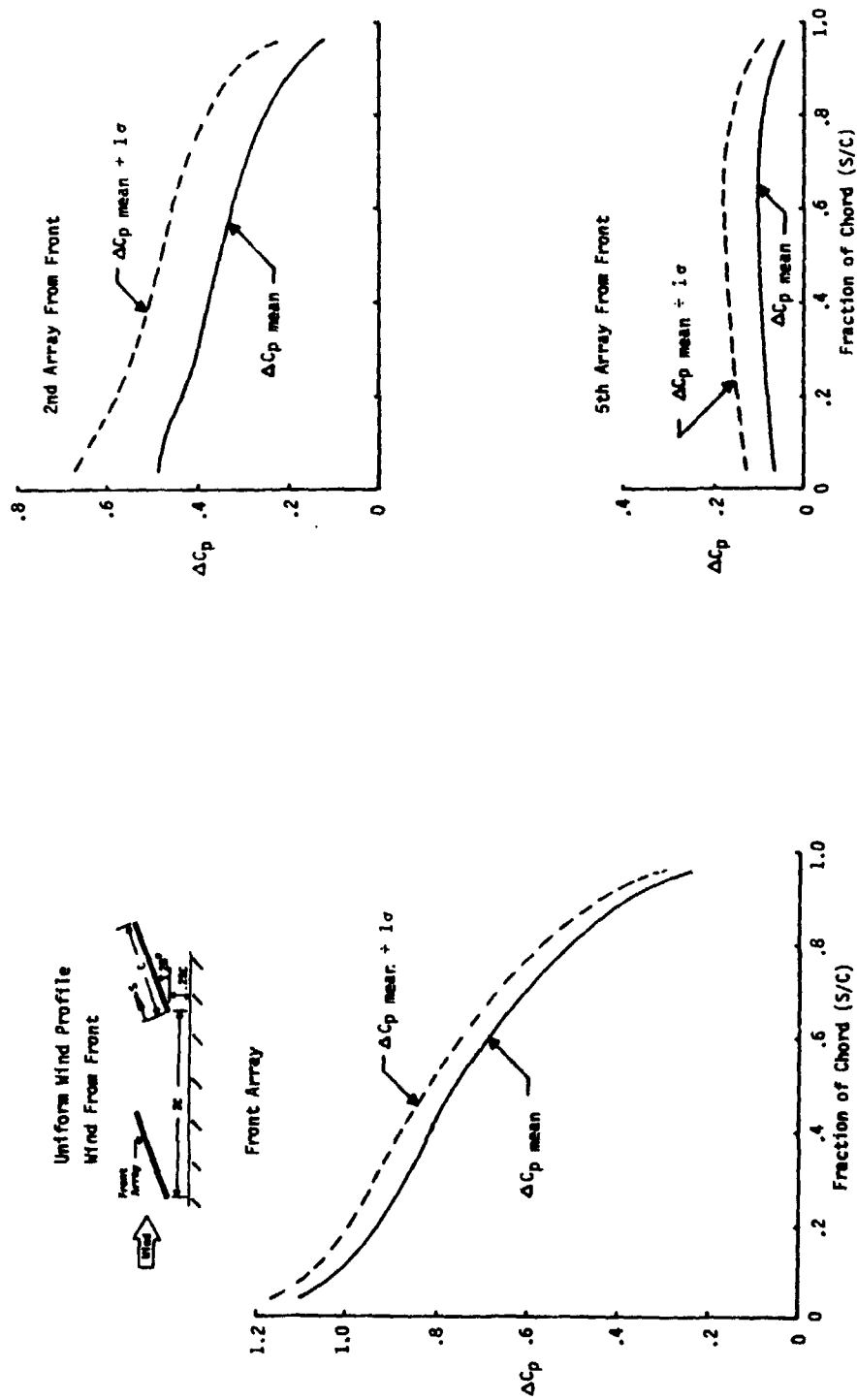


Figure 4-1a. Array Chordwise Pressure Coefficient Distribution in Uniform Wind Velocity Profile (Tilt Angle =  $20^\circ$ , Wind from Front).

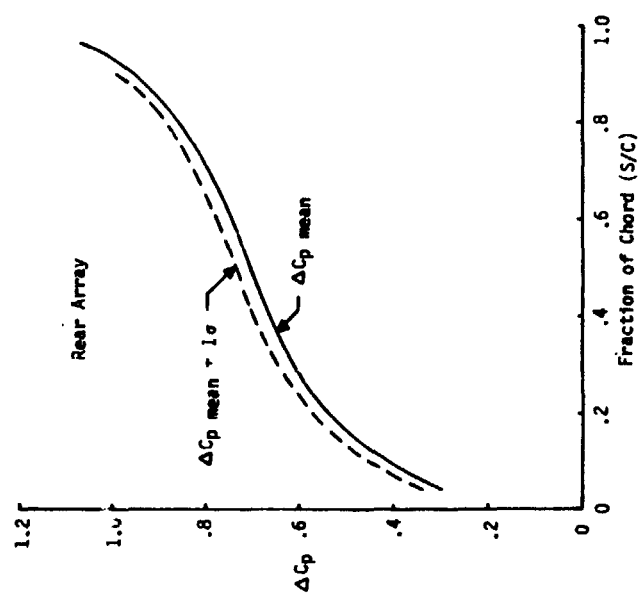
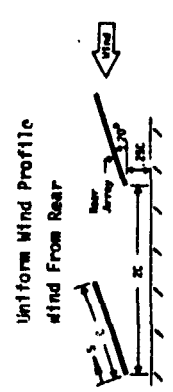
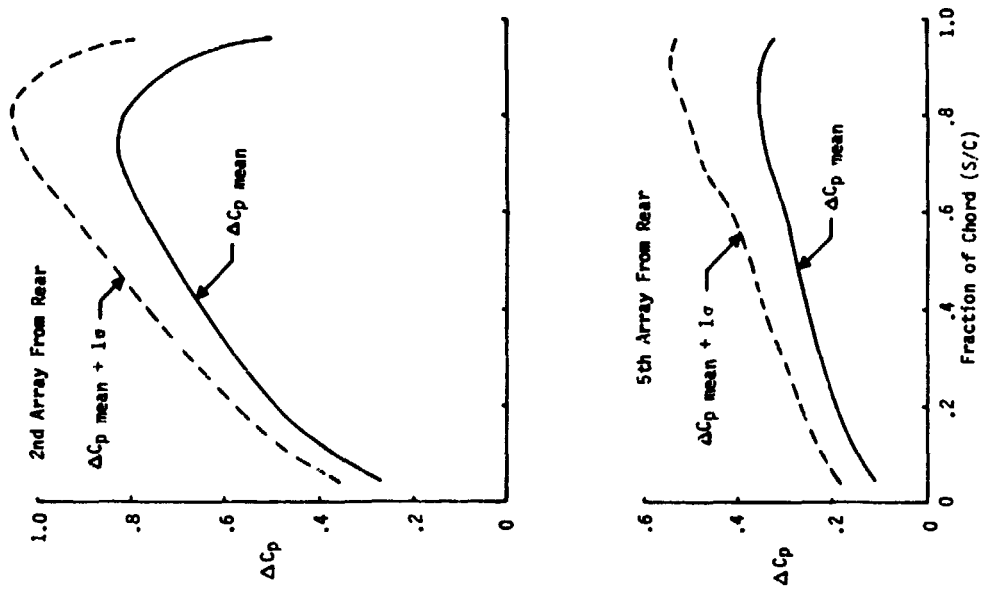


Figure 4-1b. Array Chordwise Pressure Coefficient Distribution in Uniform Wind Velocity Profile (Tilt Angle = 20°, Wind from Rear).

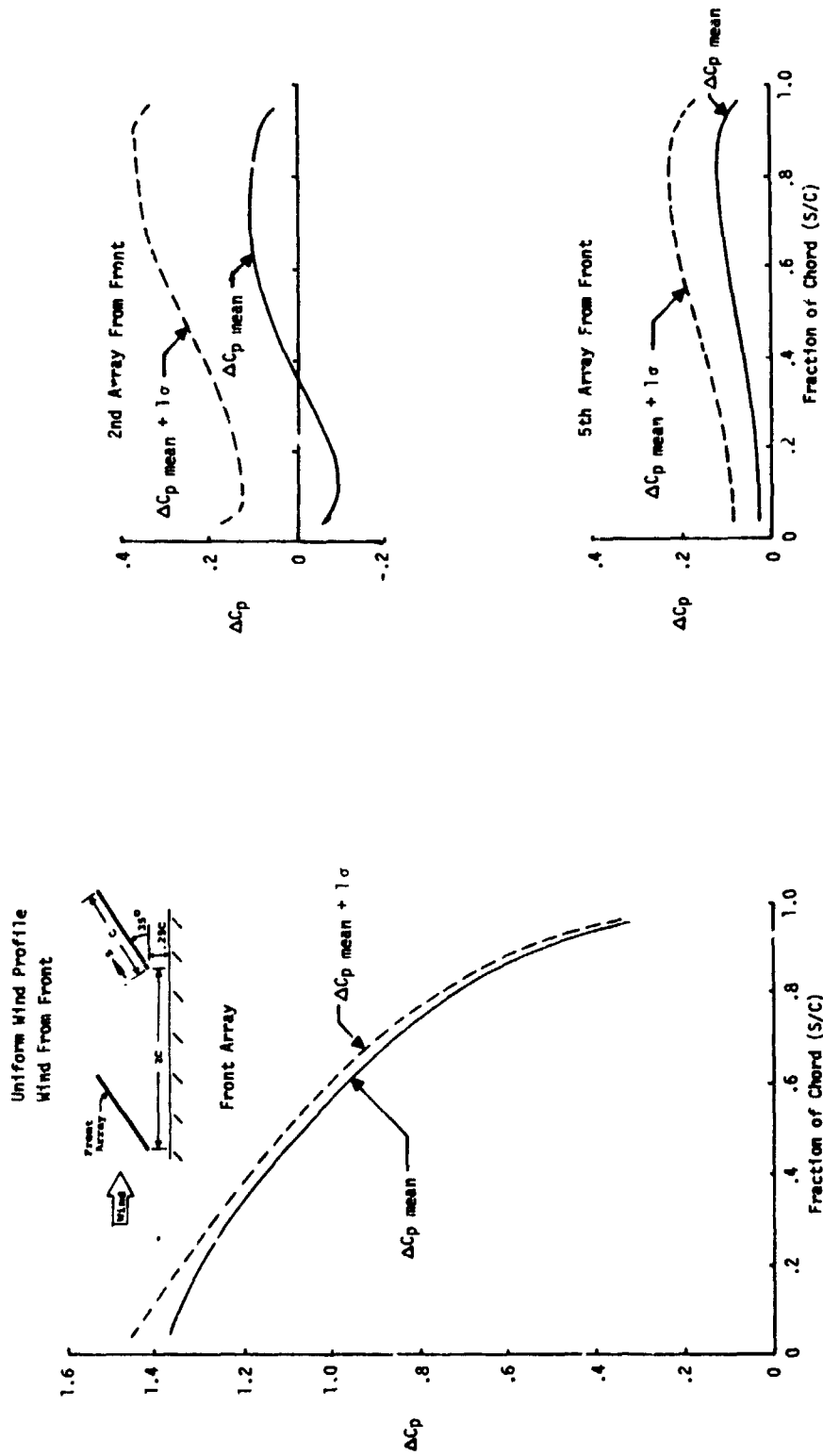


Figure 4-1c. Array Chordwise Pressure Coefficient Distribution in Uniform Wind Velocity Profile (Tilt Angle = 35°, Wind from Front!)

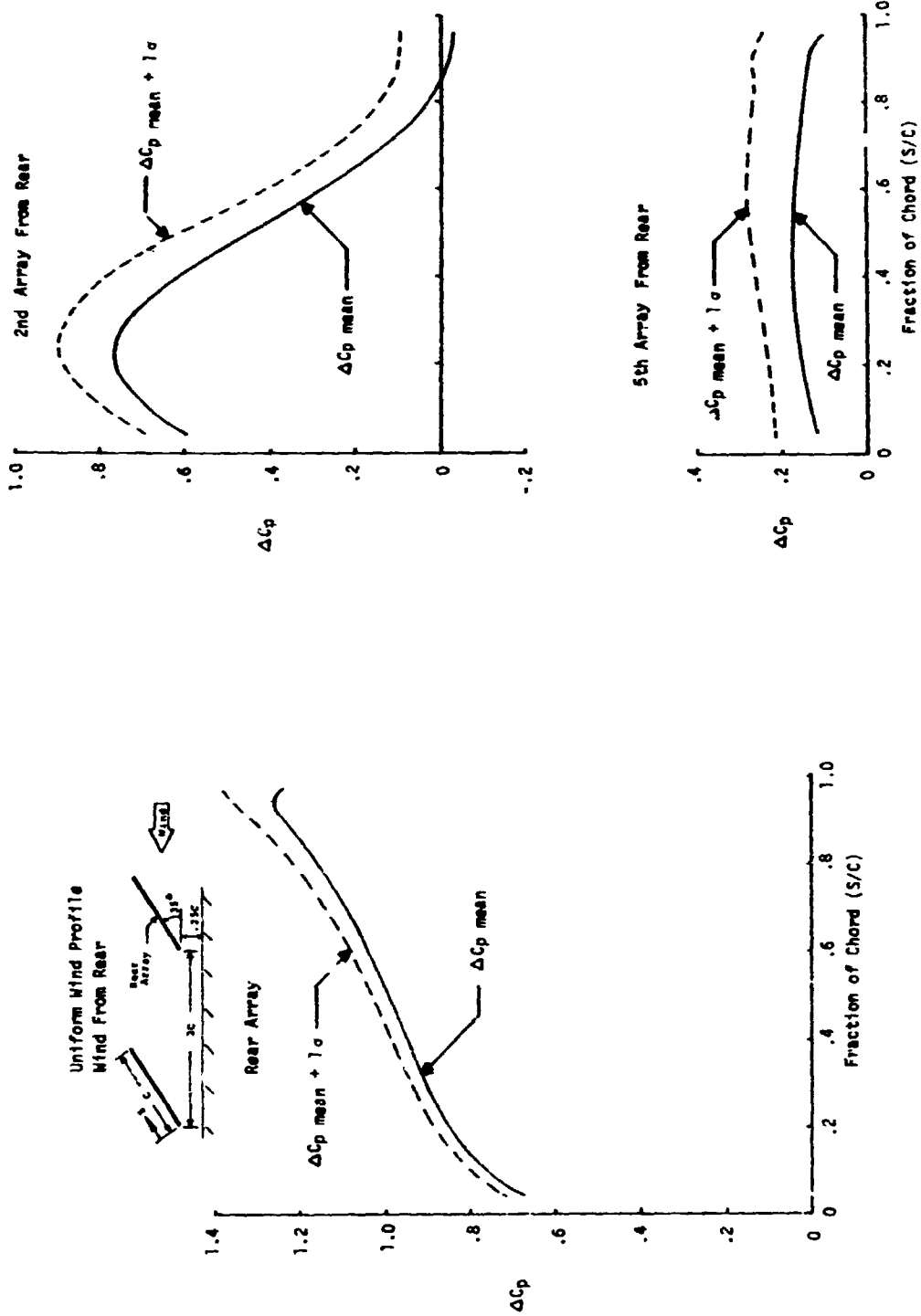


Figure 4-1d. Array Chordwise Pressure Coefficient Distribution in Uniform Wind Velocity Profile (Tilt Angle = 36°, Wind from Rear)

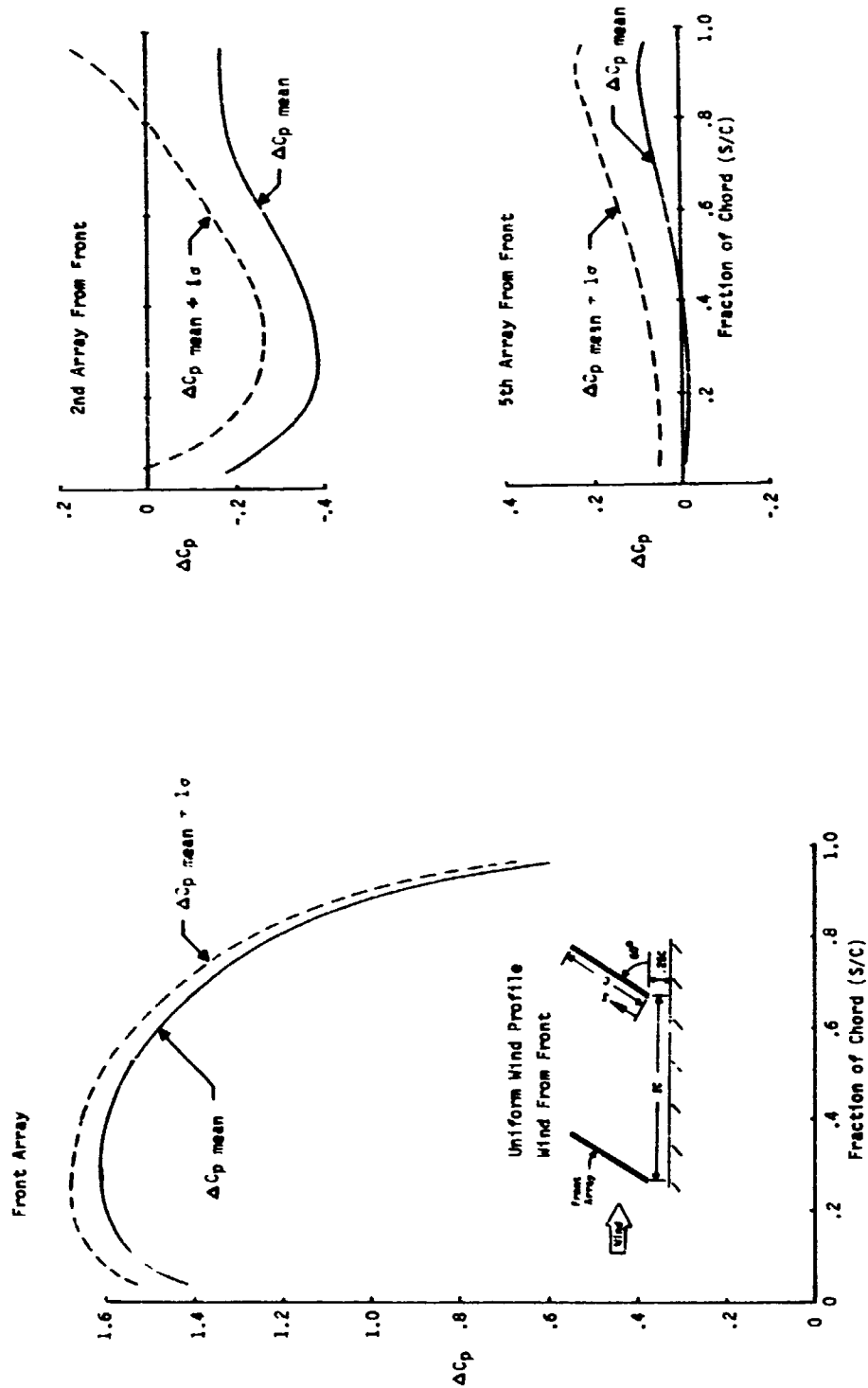


Figure 4-1e. Array Chordwise Pressure Coefficient Distribution in Uniform Wind Velocity Profile (Tilt Angle =  $60^\circ$ , Wind from Front)

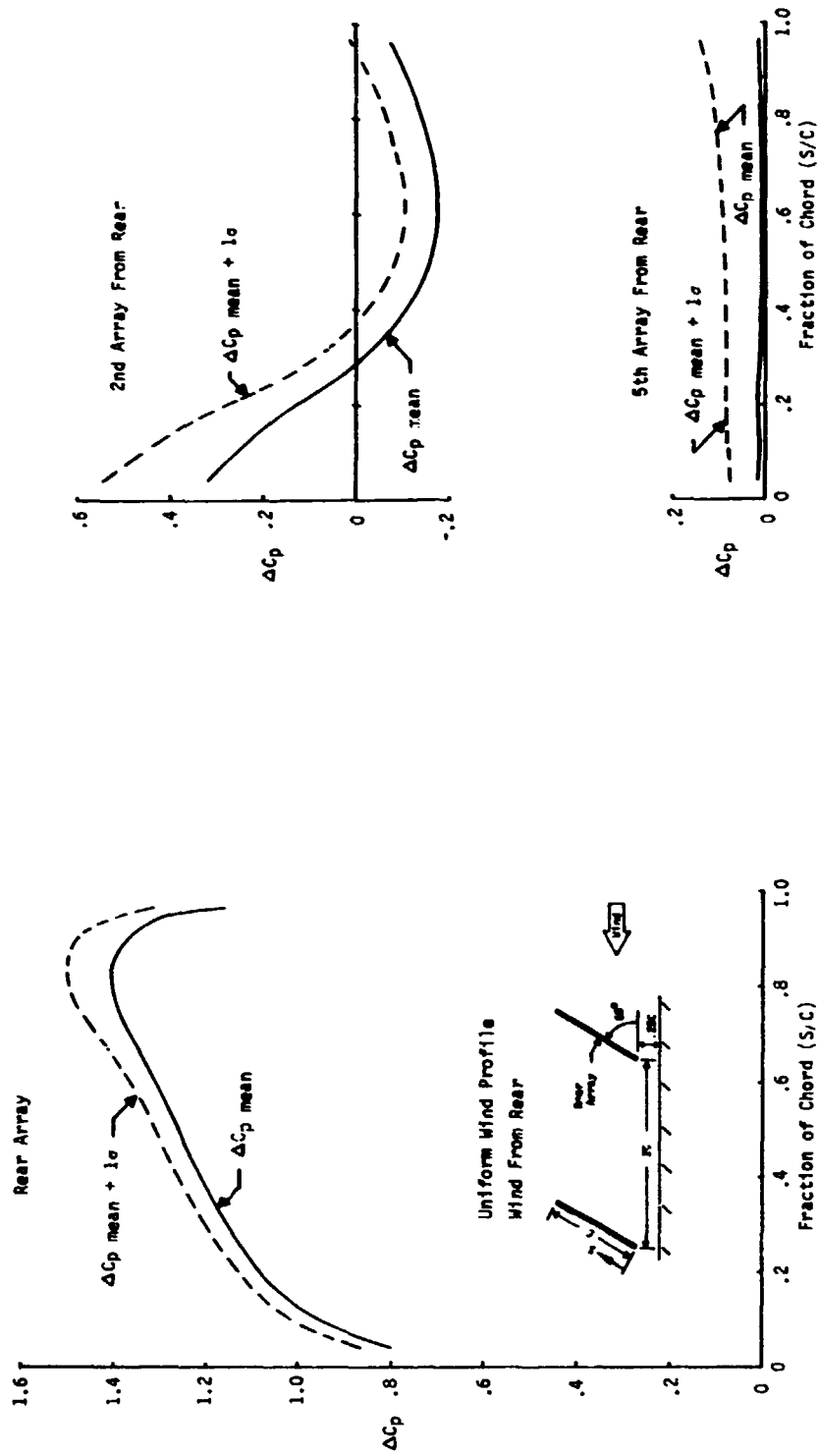


Figure 4-11. Array Chordwise Pressure Coefficient Distribution in Uniform Wind Velocity Profile (Tilt Angle = 60°, Wind from Rear)

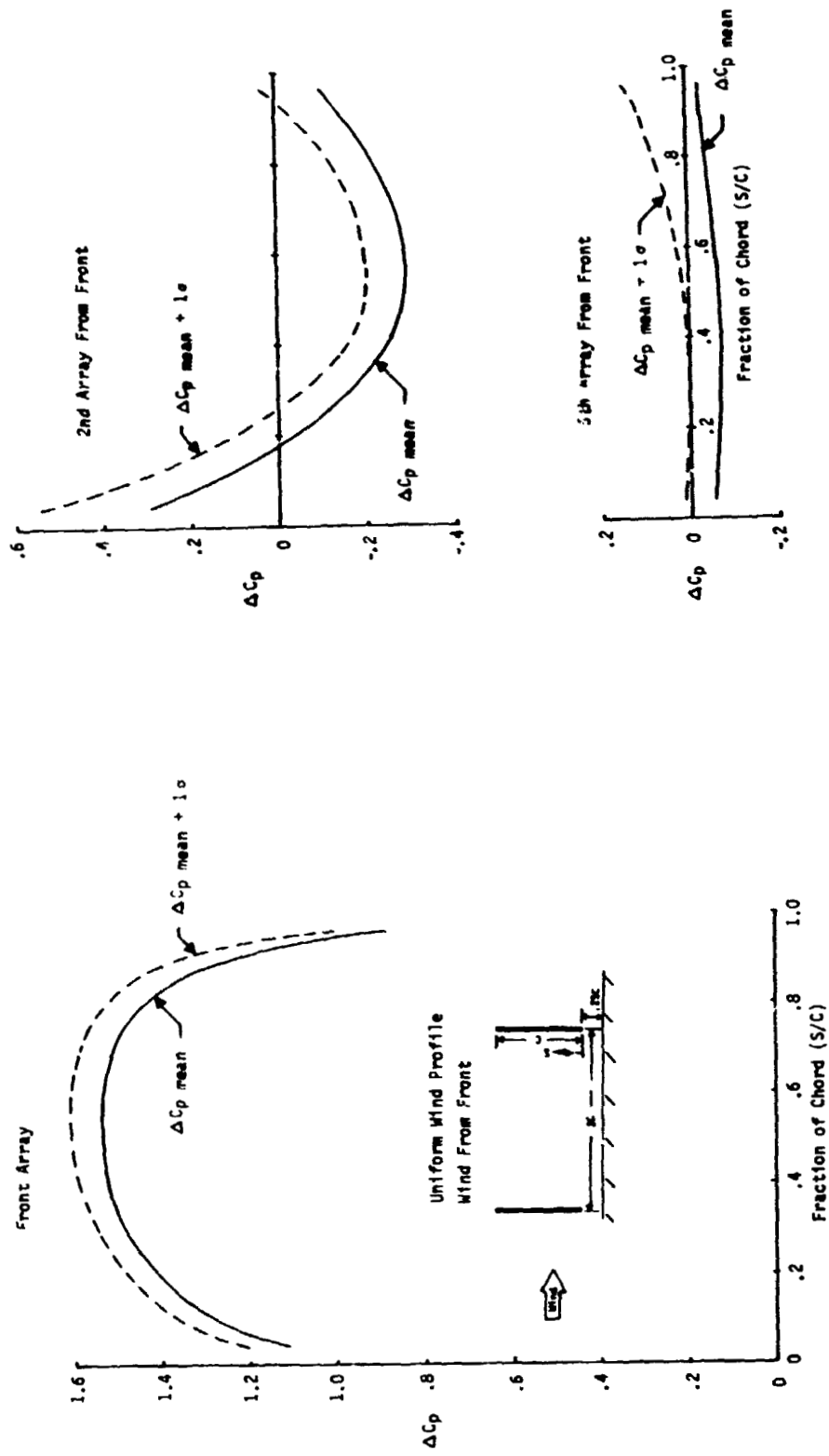
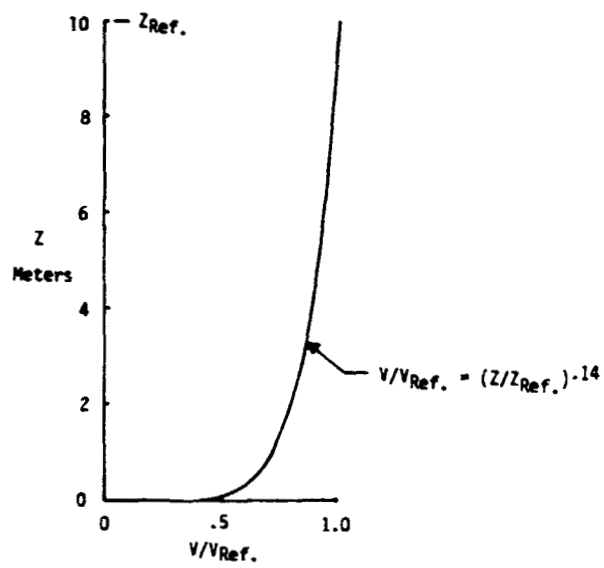


Figure 4-1g. Array Chordwise Pressure Coefficient Distribution in Uniform Wind Velocity Profile (Tilt Angle = 90°)



**Figure 4-2. 1/7 Power Law Wind Velocity Profile**

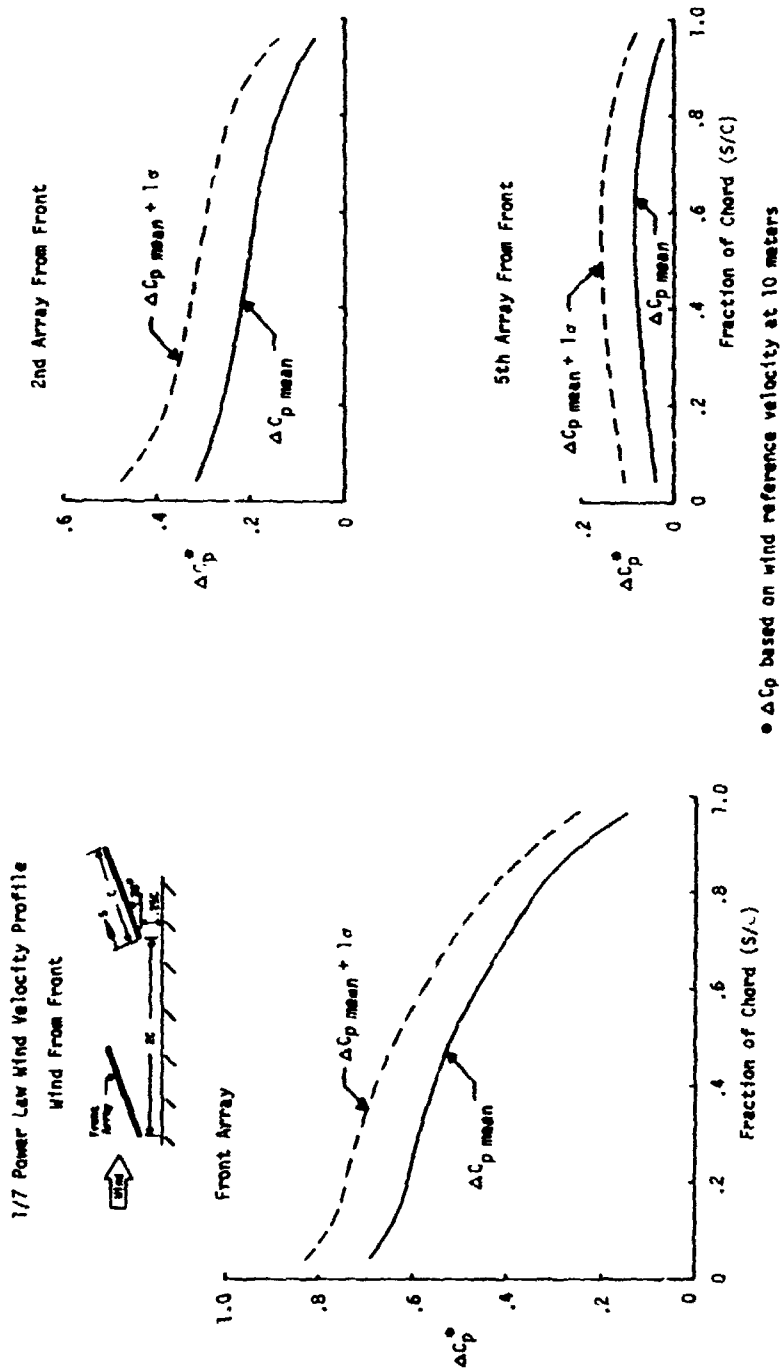
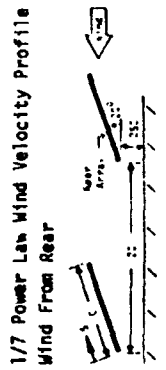
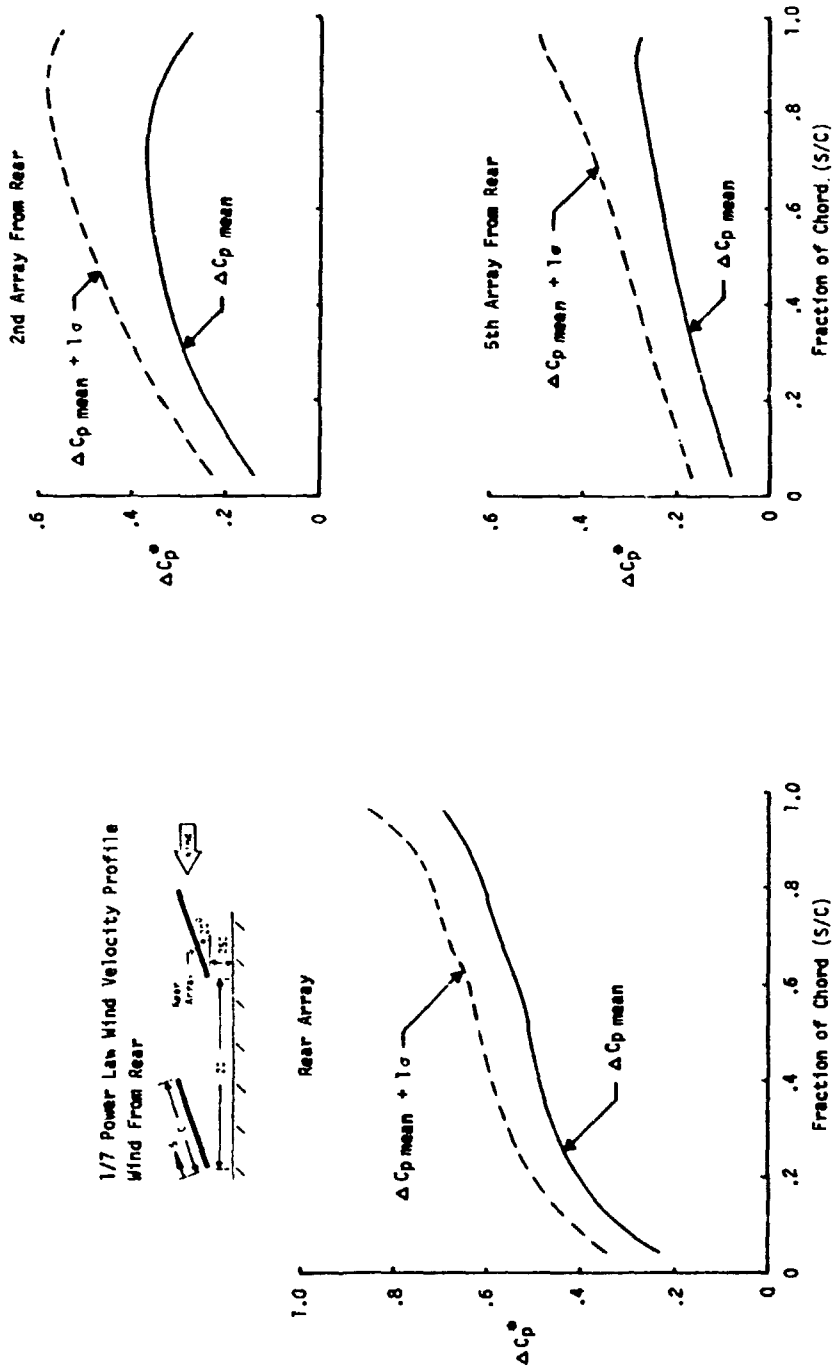


Figure 4-3a. Array Chordwise Pressure Coefficient Distribution in Boundary Layer  
Wind (Tilt Angle = 20°, Wind from Front)



\*  $\Delta C_p$  based on wind reference velocity at 10 meters

Figure 4-3b. Array Chordwise Pressure Coefficient Distribution In Boundary Layer  
Wind (Tilt Angle =  $20^\circ$ , Wind from Rear)

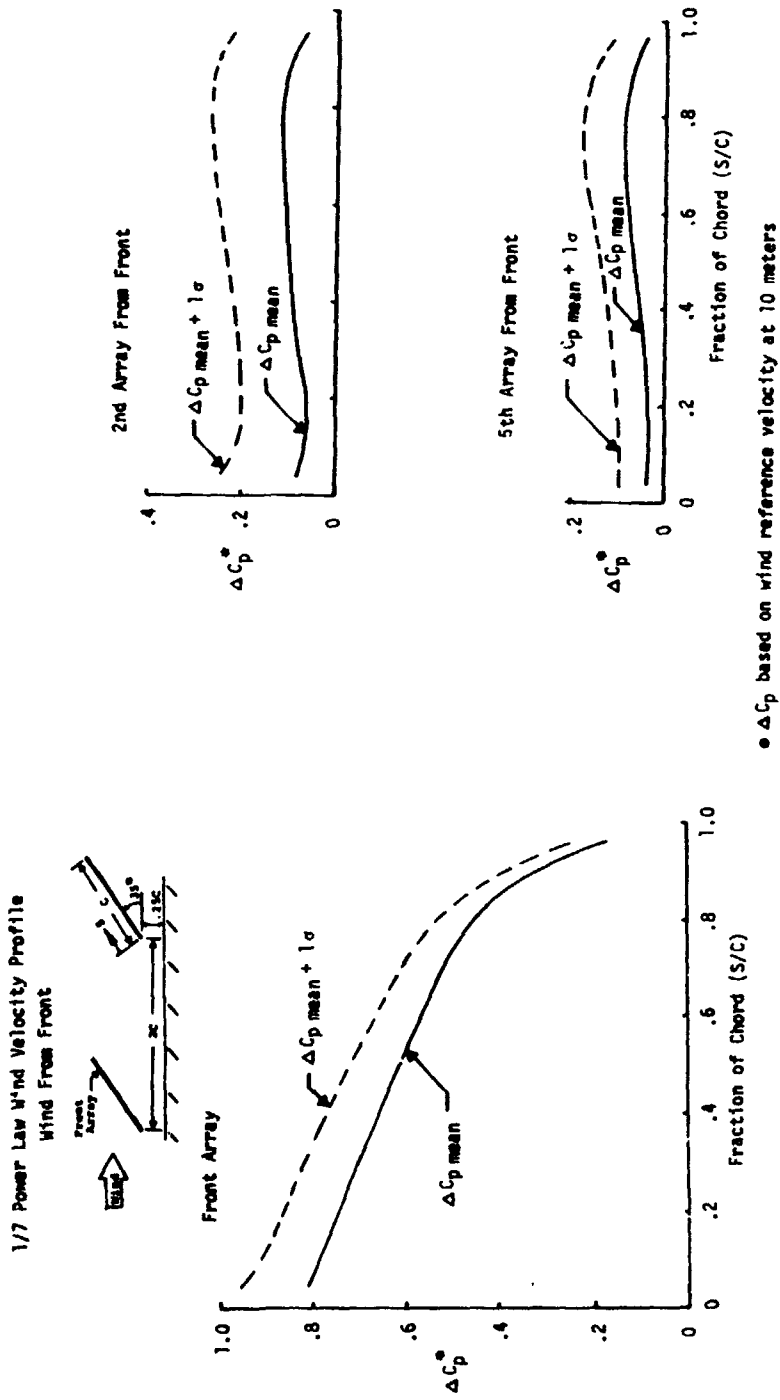
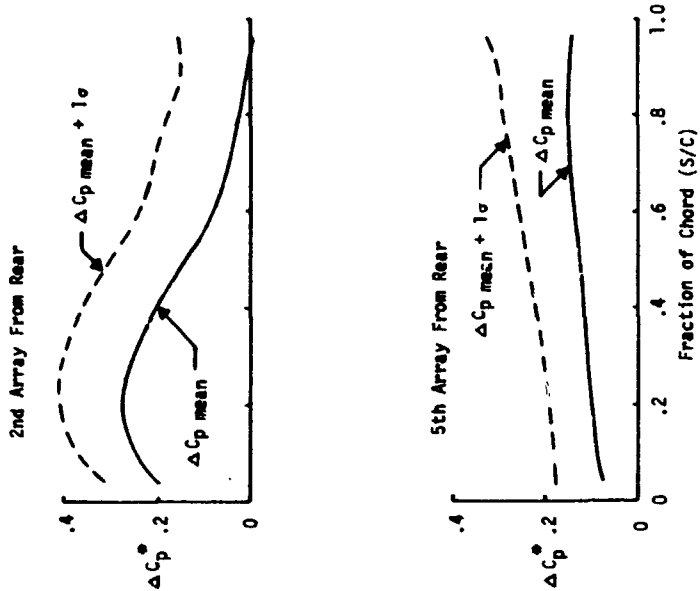
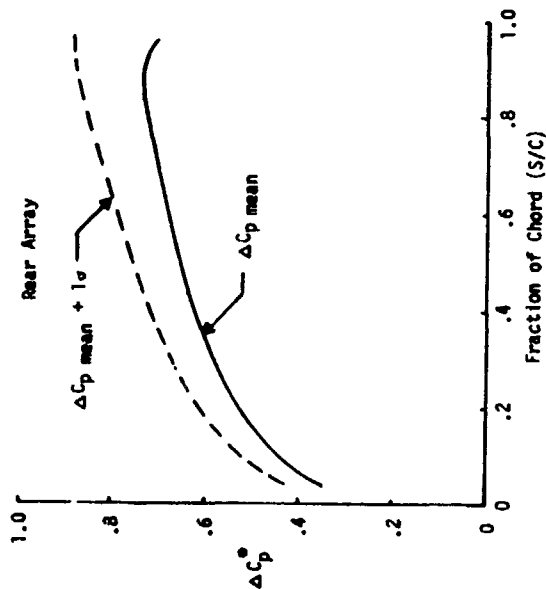


Figure 4-3c. Array Chordwise Pressure Coefficient Distribution in Boundary Layer  
Wind (Tilt Angle = 35°, Wind from Front)

1/7 Power Law Wind Velocity Profile  
Wind From Rear



•  $\Delta C_p$  based on wind reference velocity at 10 meters

Figure 4-3d. Array Chordwise Pressure Coefficient Distribution in Boundary Layer  
Wind (Tilt Angle = 35°, Wind from Rear)

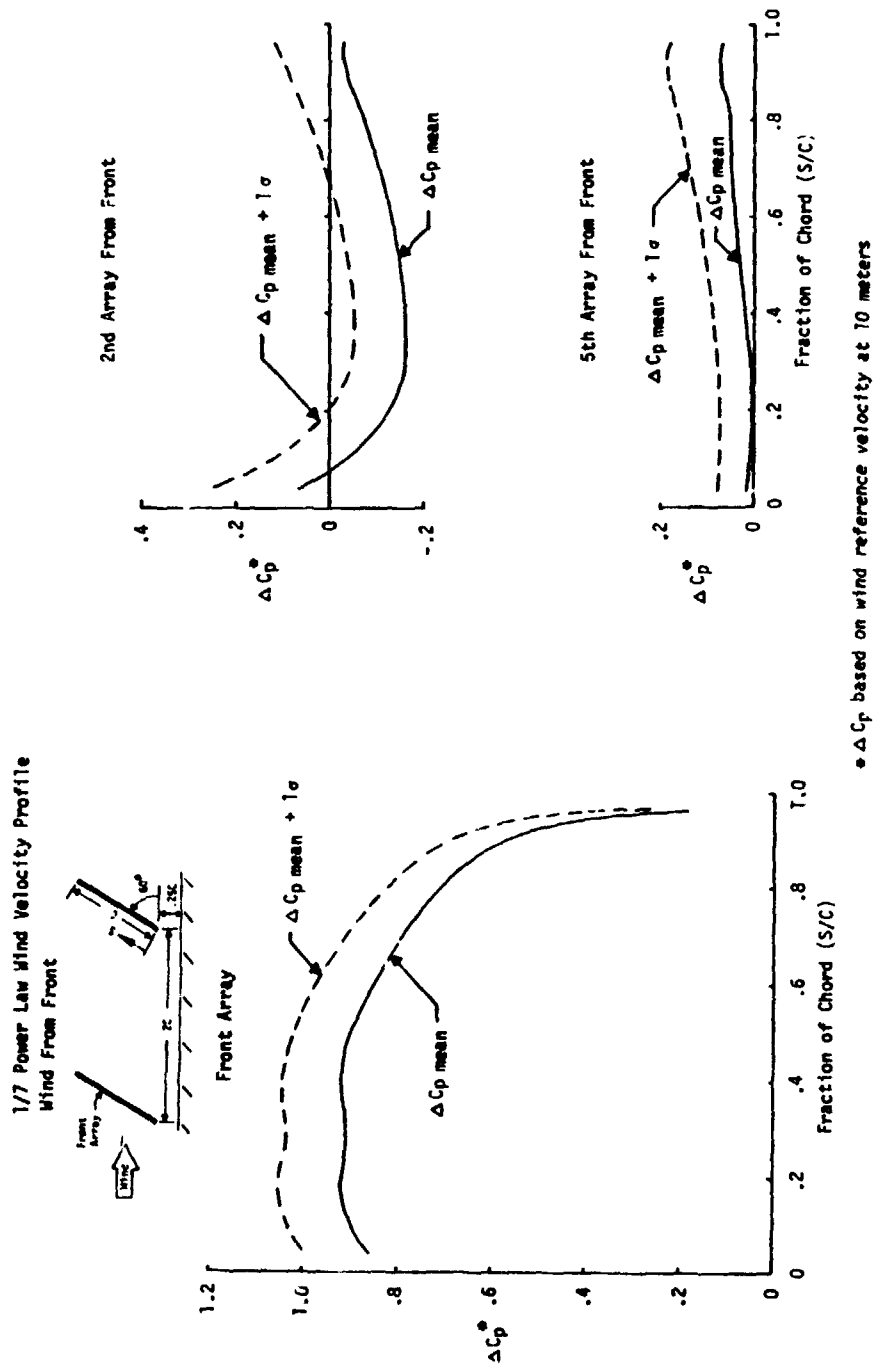


Figure 4-3e. Array Chordwise Pressure Coefficient Distribution in Boundary Layer  
Wind (Tilt Angle = 60°, Wind from Front)

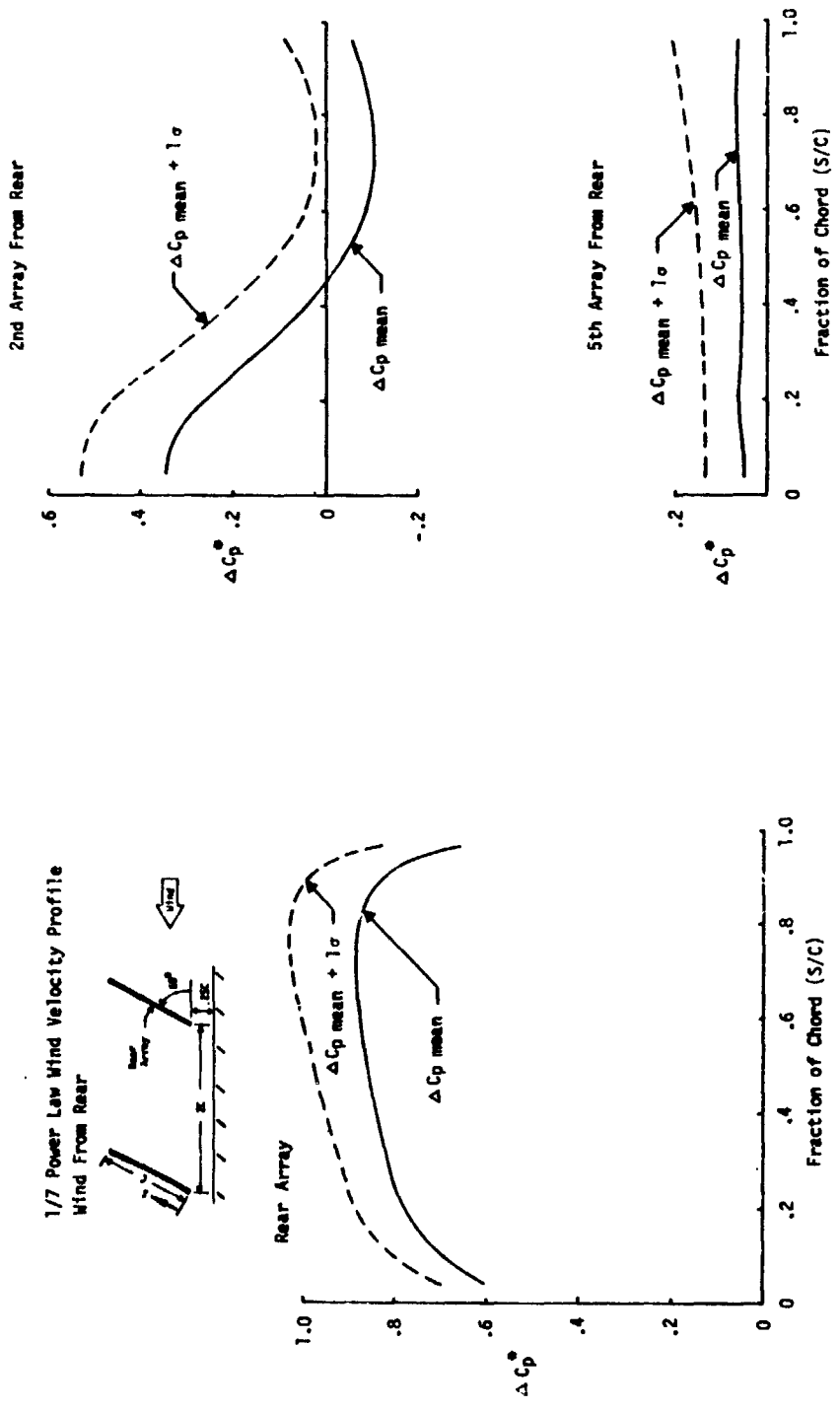


Figure 4-31. Array Chordwise Pressure Coefficient Distribution in Boundary Layer  
Wind (Tilt Angle = 60°, Wind from Rear)

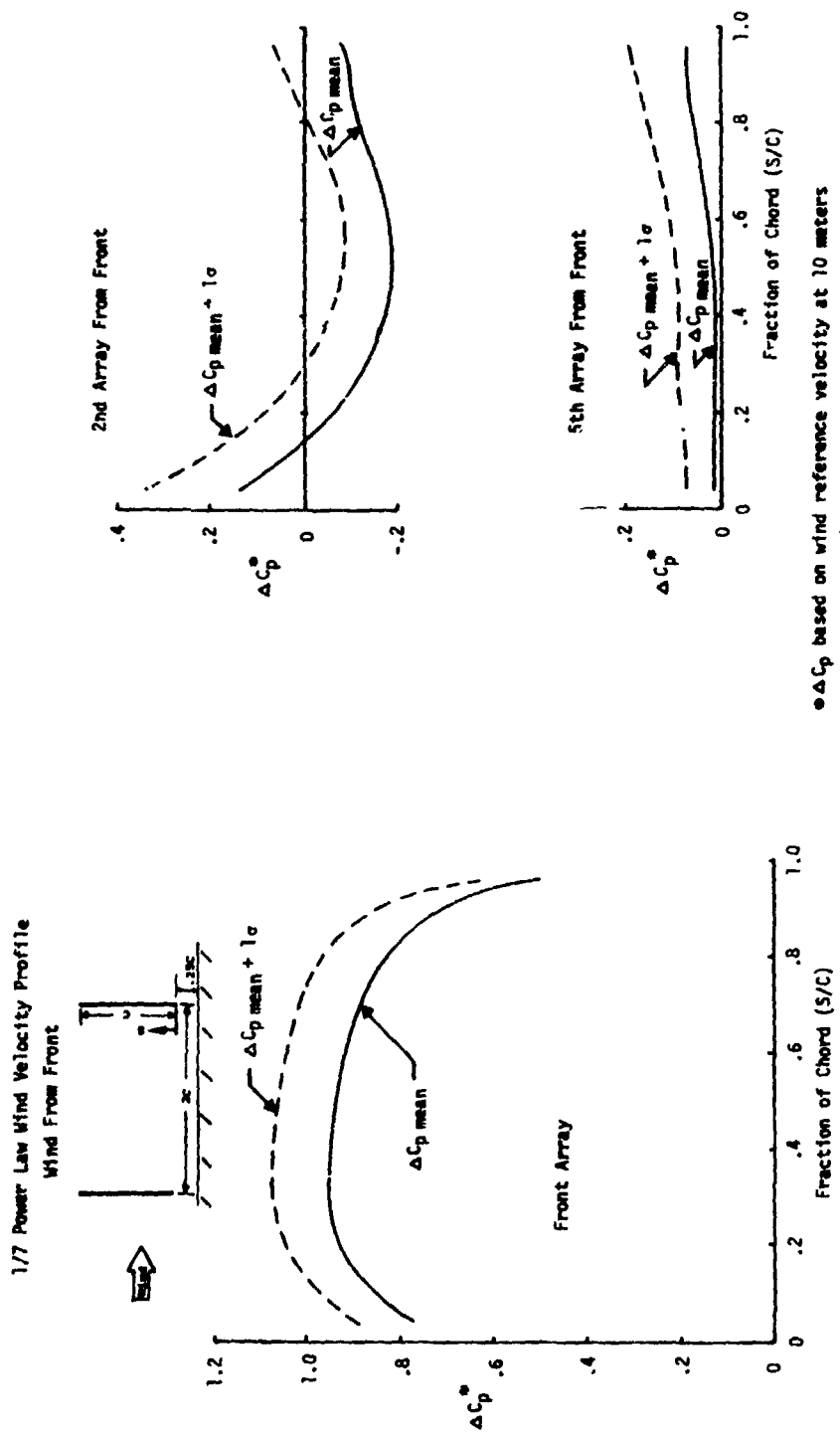


Figure 4-3g. Array Chordwise Pressure Coefficient Distribution in Boundary Layer  
Wind (Tilt Angle = 90°)

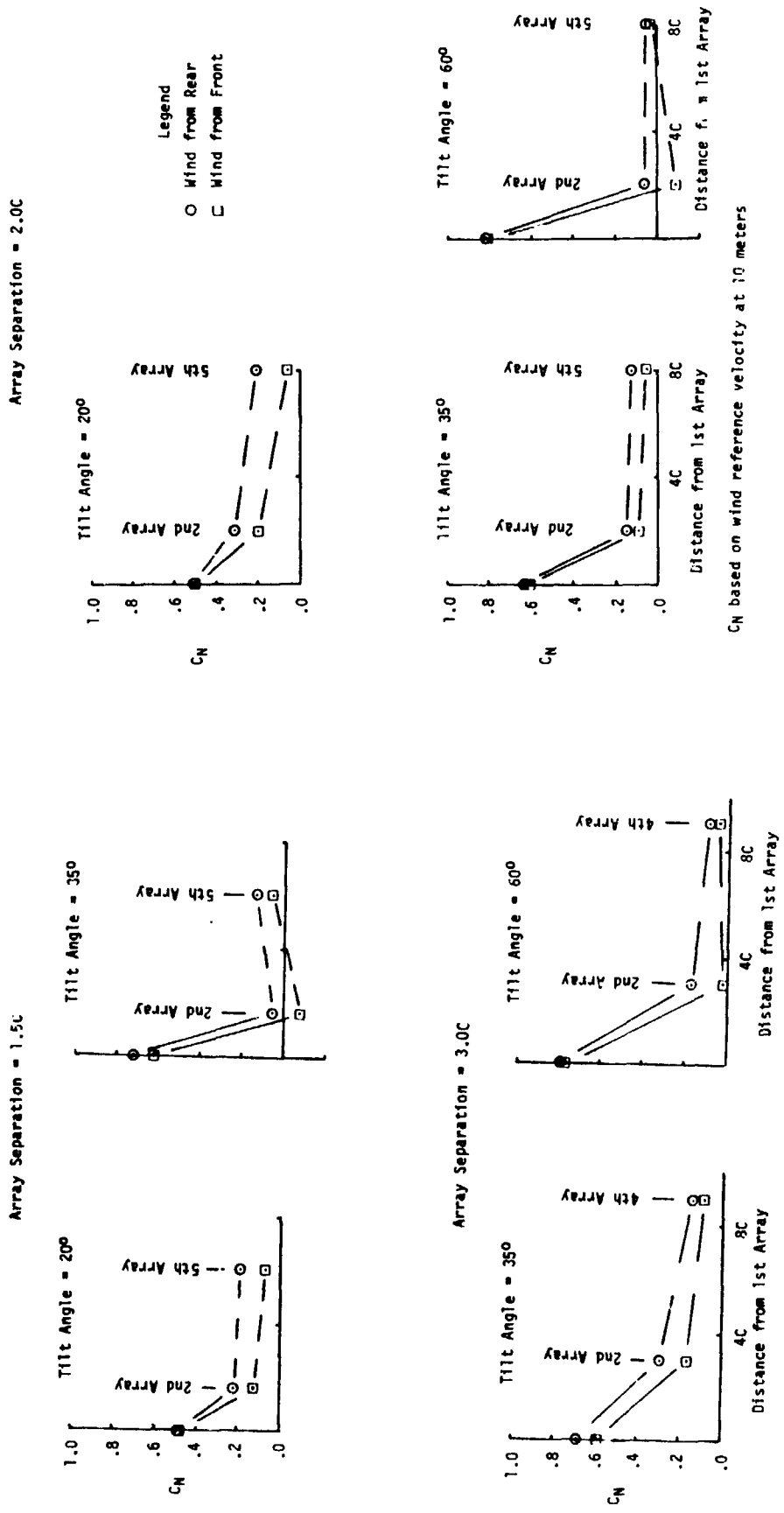
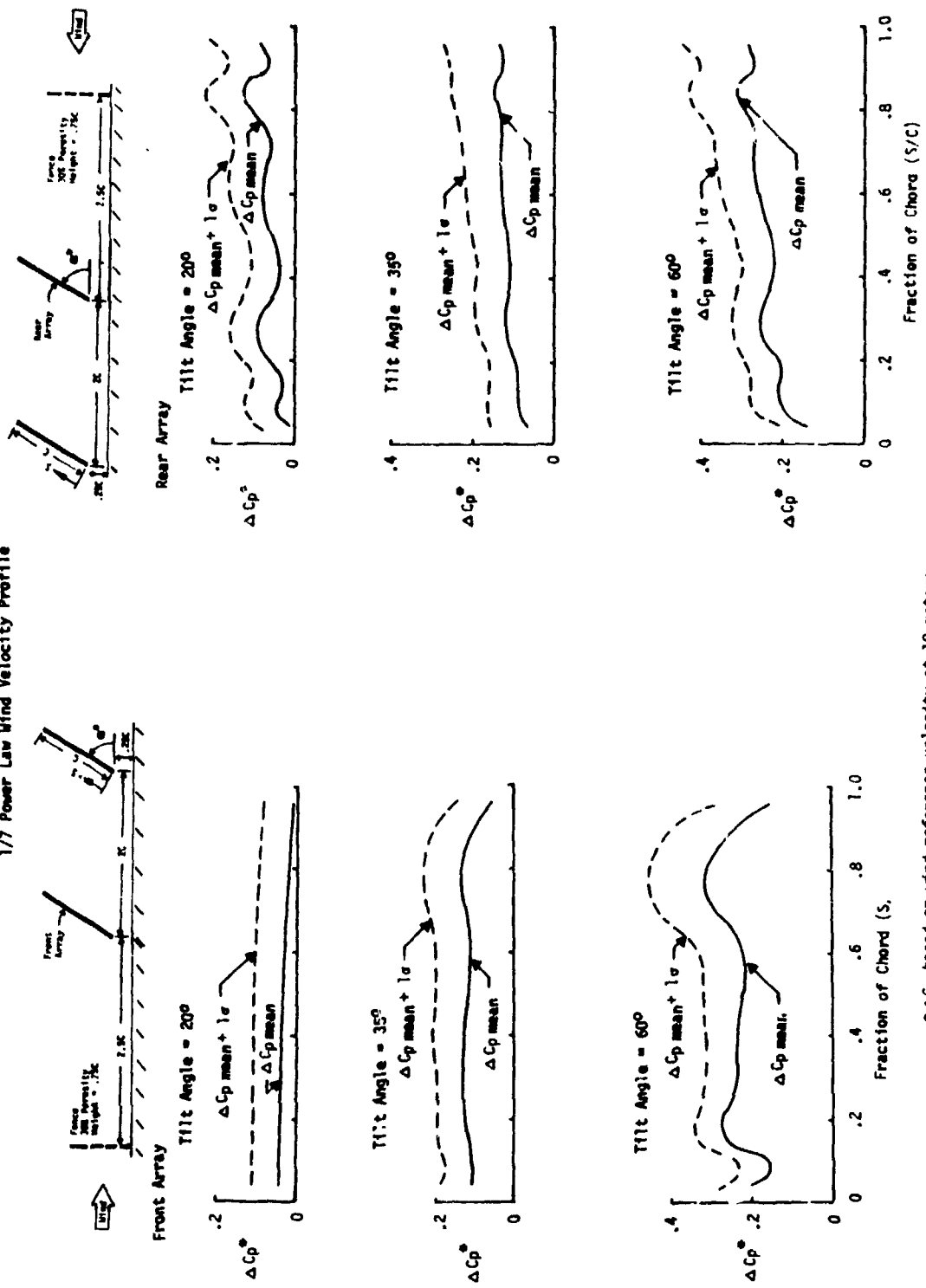


Figure 4-4. Effect of Head-On and Rearward Winds on Array Normal Force Coefficients ( $N_s$  Fence)

1/7 Power Law Wind Velocity Profile



$\Delta C_p$  based on wind reference velocity at 10 meters

Figure 4-5. Effect of a Fence on Array Chordwise Pressure Coefficient Distribution for Head-On and Rearward Winds.

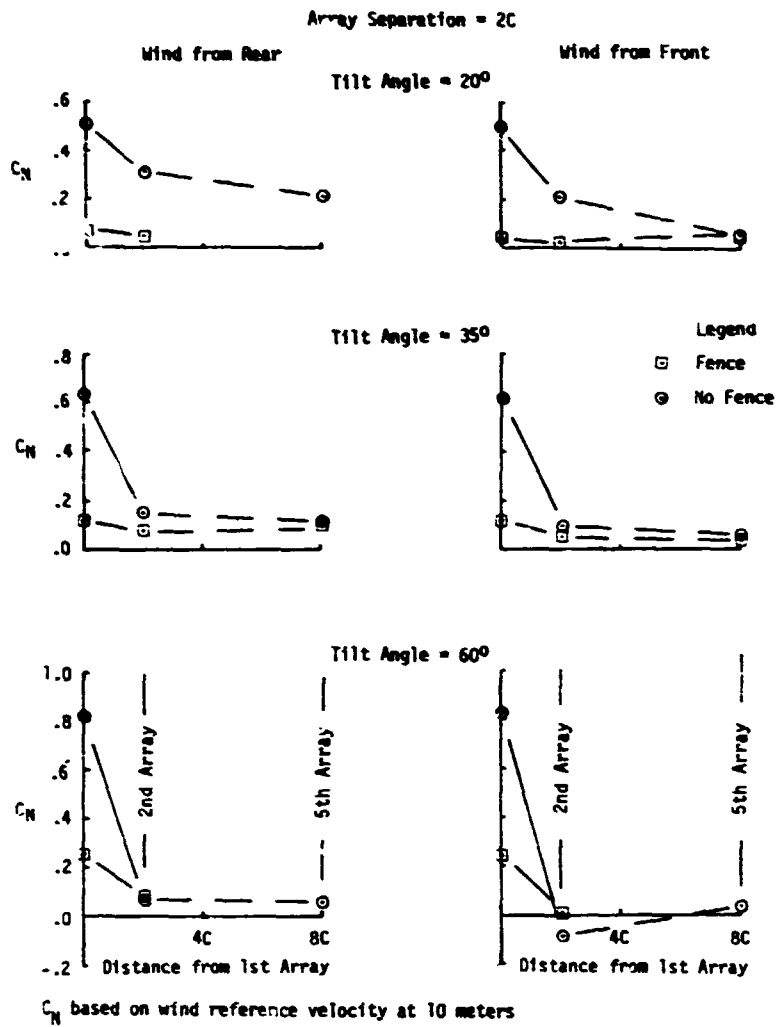


**Figure 4-6. Effect of a Fence on Array Normal Force Coefficients for Head-On and Rearward Winds.**

1/7 Power Law Wind Velocity Profile

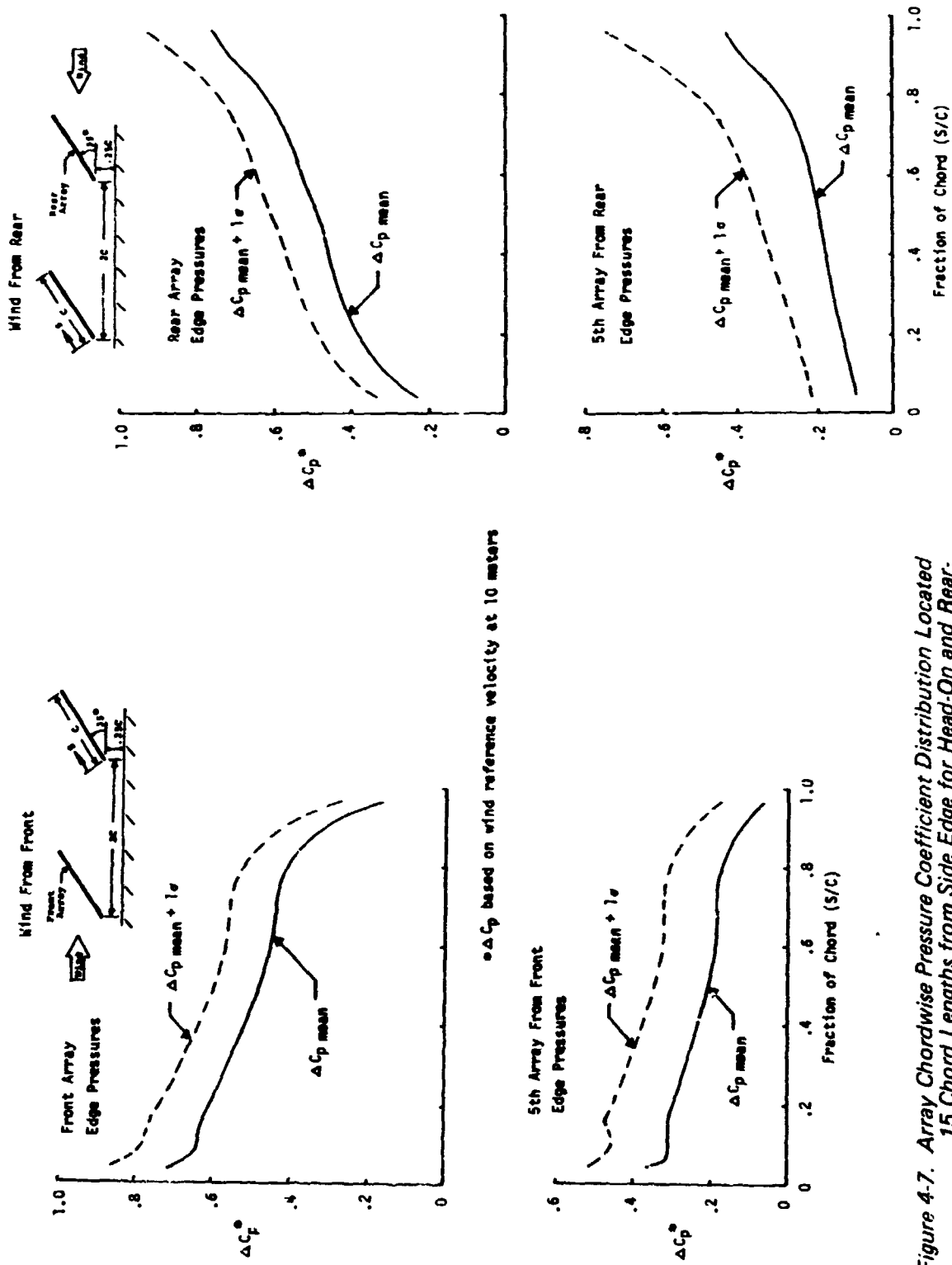
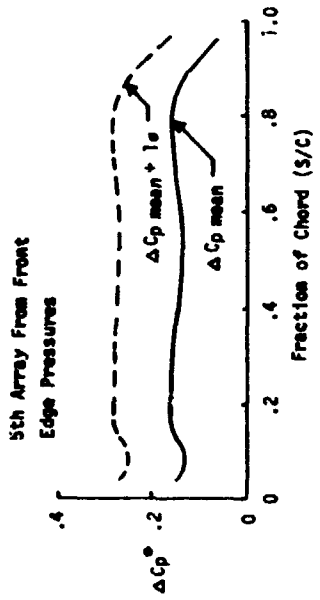
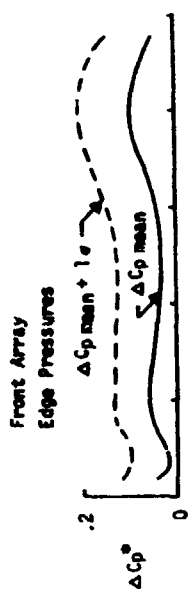
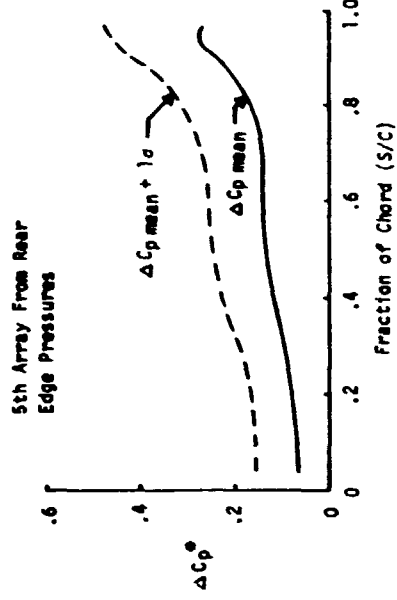
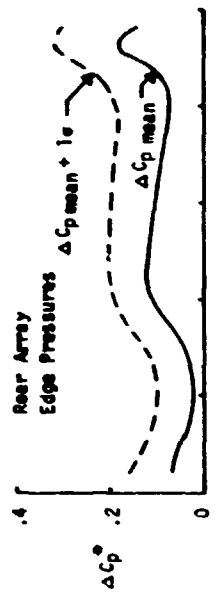


Figure 4-7. Array Chordwise Pressure Coefficient Distribution Located .15 Chord Lengths from Side Edge for Head-On and Rearward Winds (No Ferrel)

1/7 Power Law Wind Velocity Profile



•  $\Delta C_p$  based on wind reference velocity at 10 meters

Figure 4-8. Effect of Fence on Array Chordwise Pressure Coefficient Distribution Located .15 Chord Lengths from Side Edge for Head-On and Rearward Winds

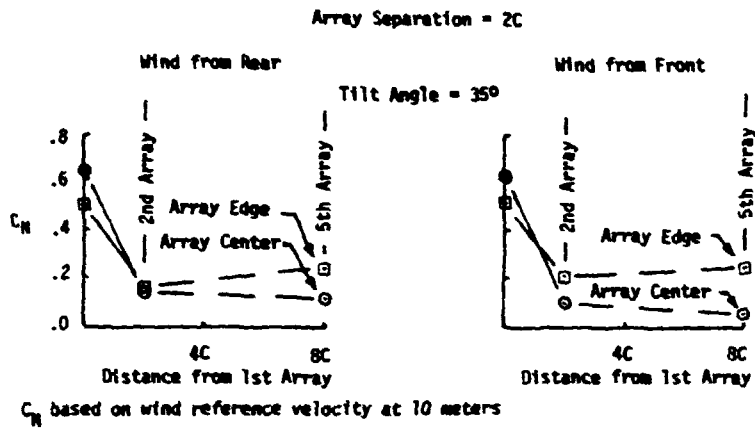


**Figure 4-9. Comparison Between Array Edge and Center of Span Normal Force Coefficients for Head-On and Rearward Winds (No Fence)**

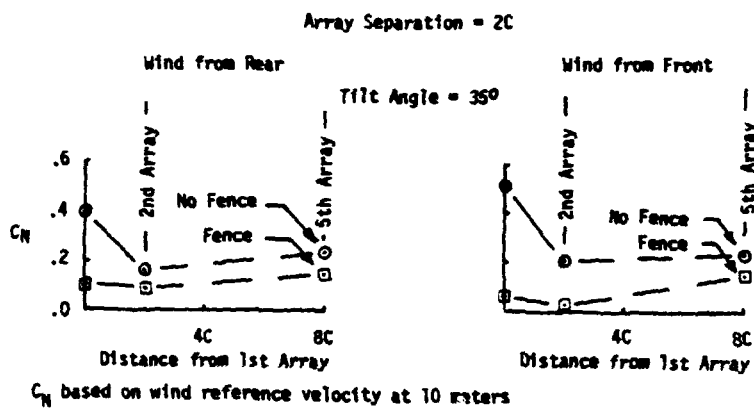
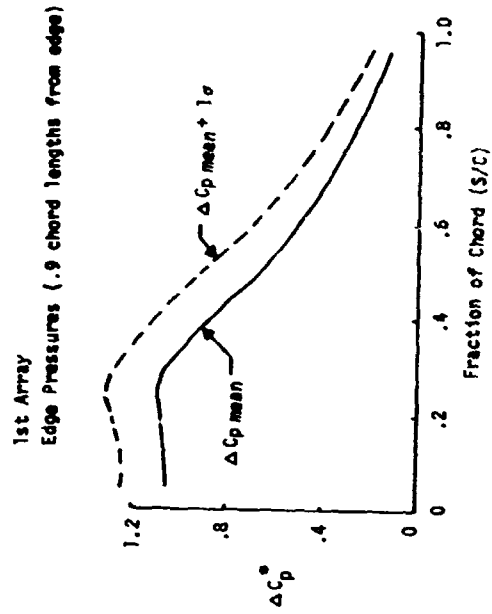
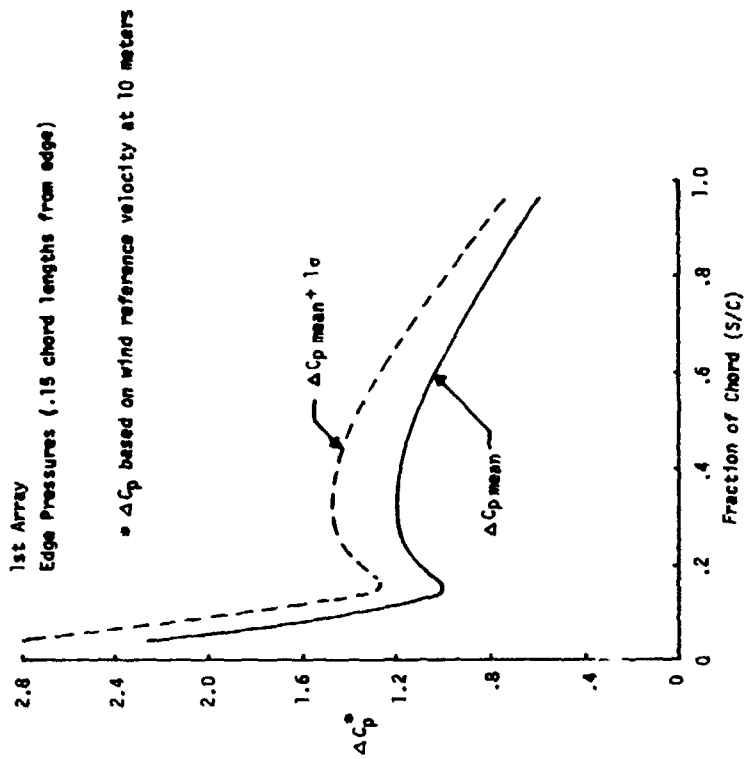
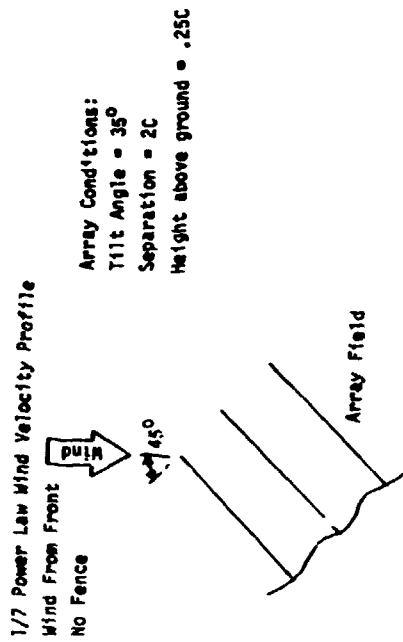


**Figure 4-10. Effect of Fence on Array Edge Normal Force Coefficients for Head-On and Rearward Winds**



$\Delta C_p$  based on wind reference velocity at 10 meters

Figure 4-11a Effect of Oblique Winds on Array Edge Pressure Distribution  
 (No Fence, Wind from Front)

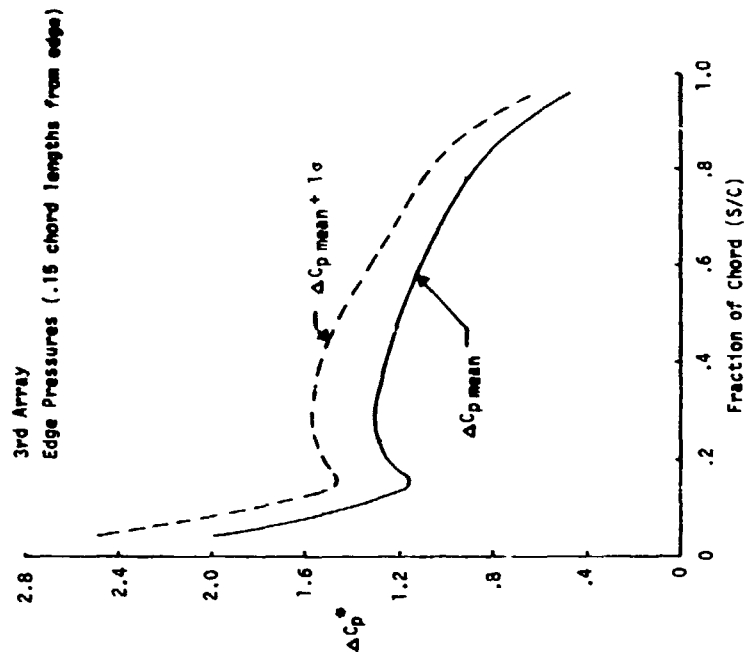
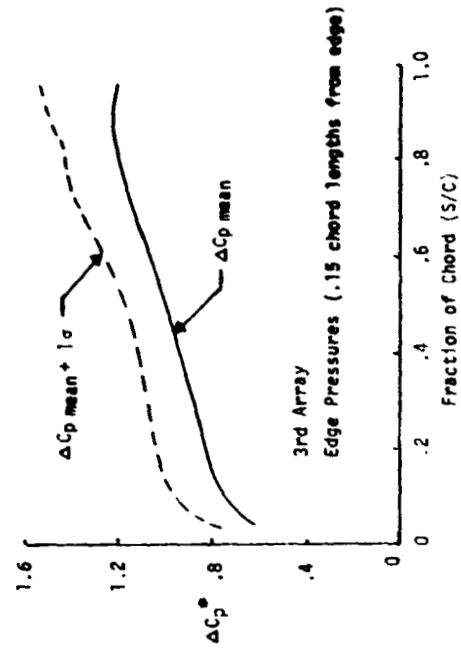
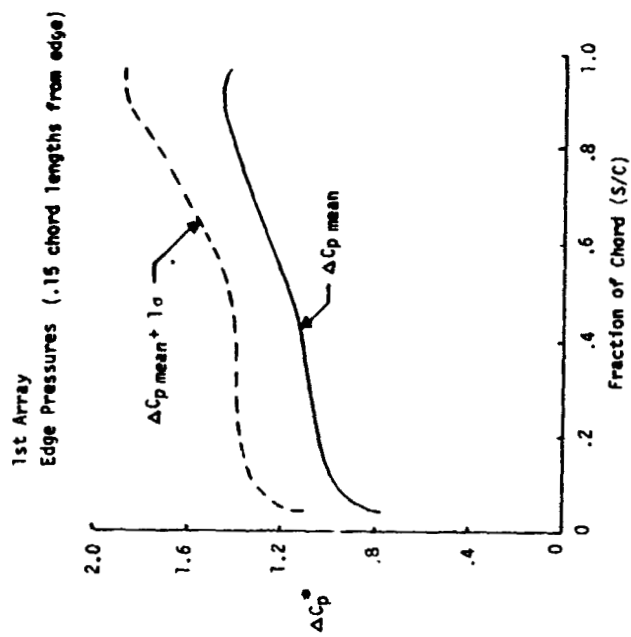
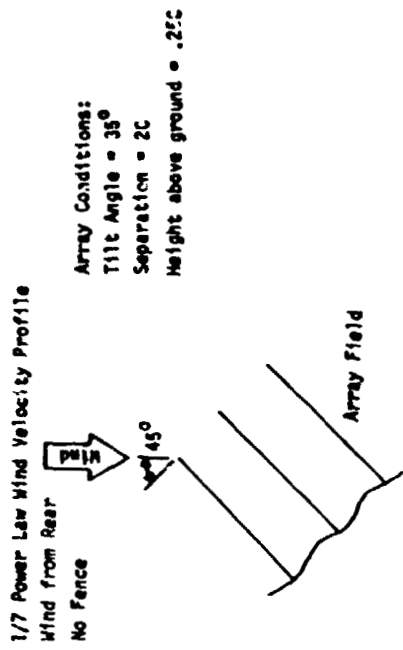


Figure 4-11a. Concluded



\*  $\Delta C_p$  based on wind reference velocity at 10 meters

Figure 4-11b. Effect of Oblique Winds on Array Edge Pressure Distribution  
 (No Fence, Wind from Rear)

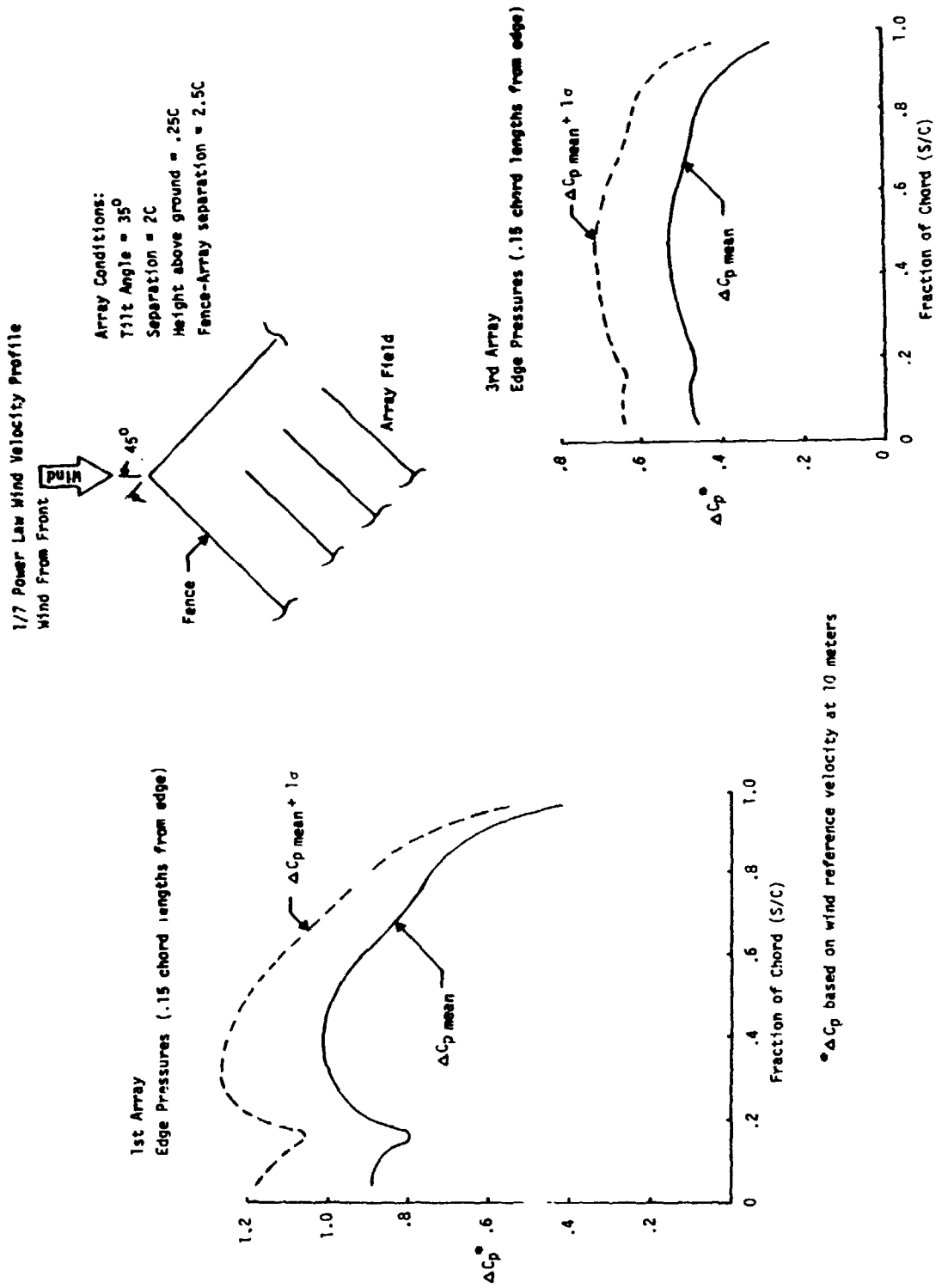


Figure 4-11c. Effect of Oblique Winds on Array Edge Pressure Distribution  
(Conventional Fence, Wind from Front)

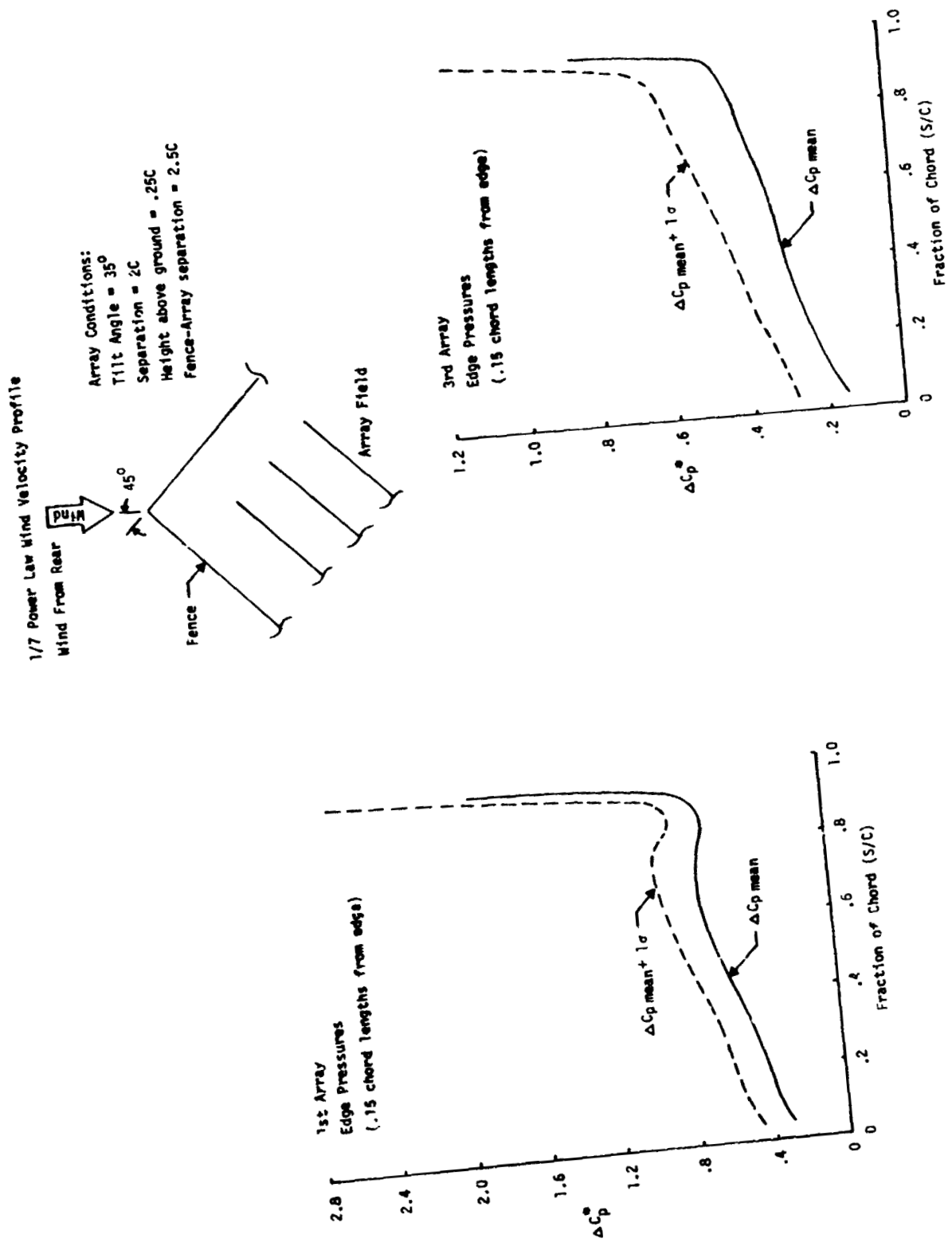
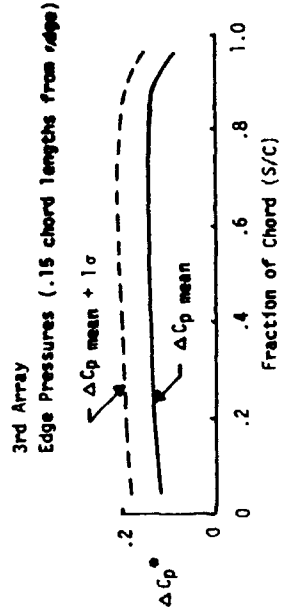
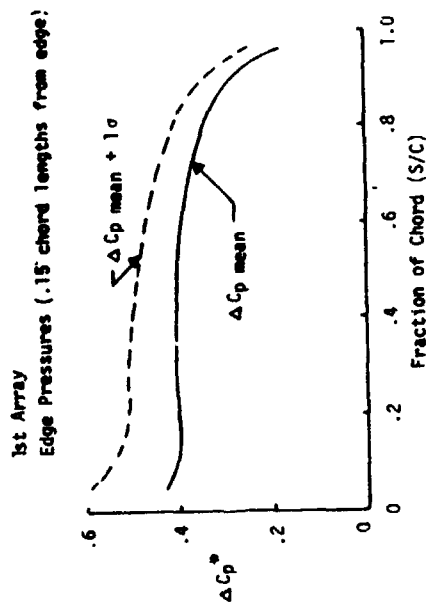
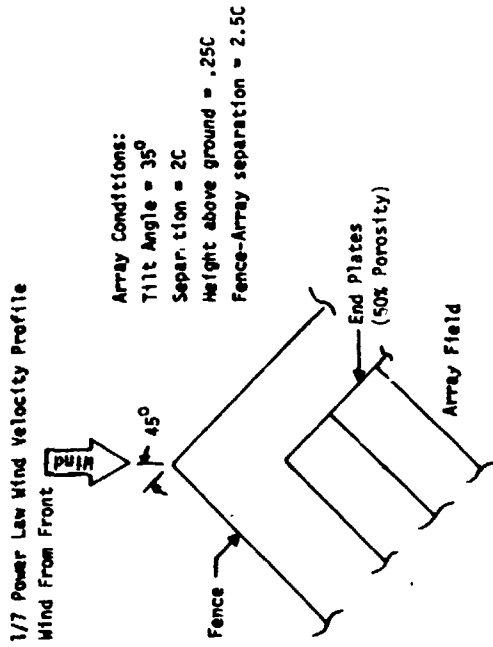
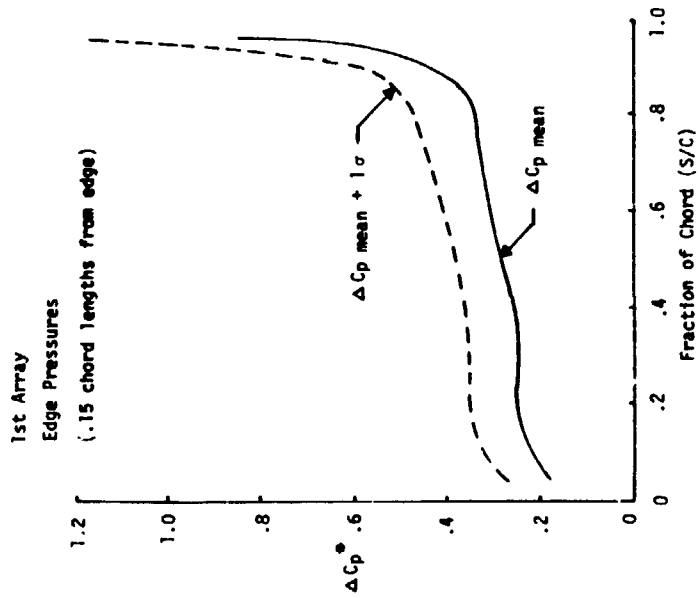
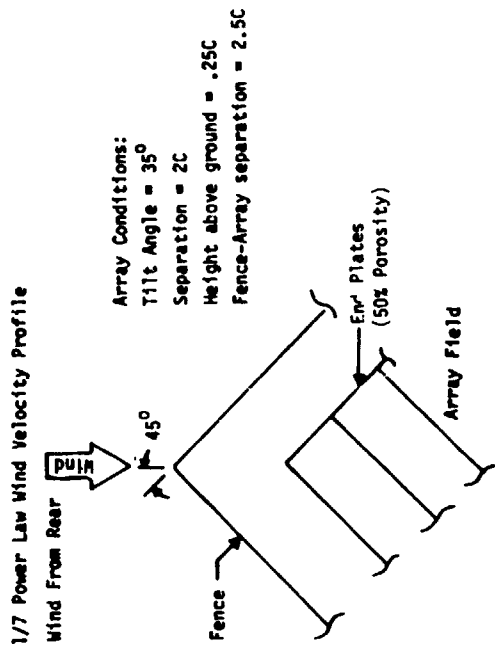


Figure 4-11d. Effect of Oblique Winds on Array Edge Pressure Distribution (Conventional Fence, Wind from Rear)



\*  $\Delta C_p$  based on wind reference velocity at 10 meters

Figure 4-11e. Effect of Oblique Winds on Array Edge Pressure Distribution (Conventional Fence, Endplated Arrays, Wind from Front)



\*  $\Delta C_p$  based on wind reference velocity at 10 meters

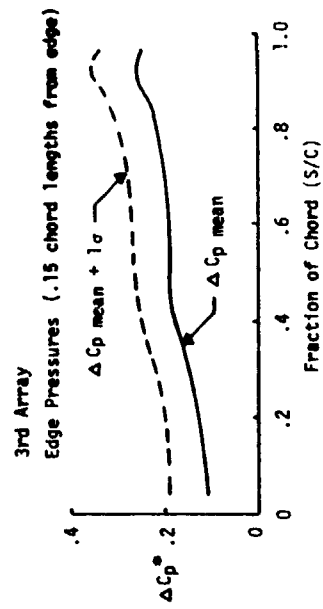
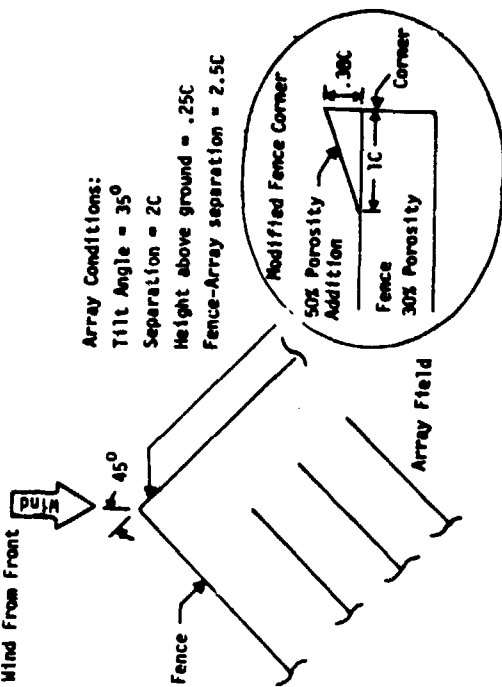
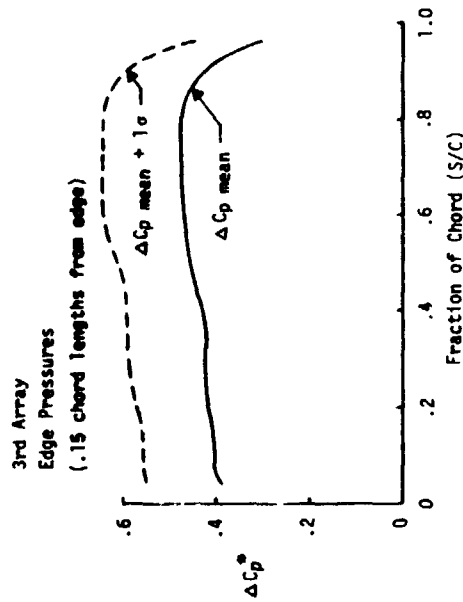
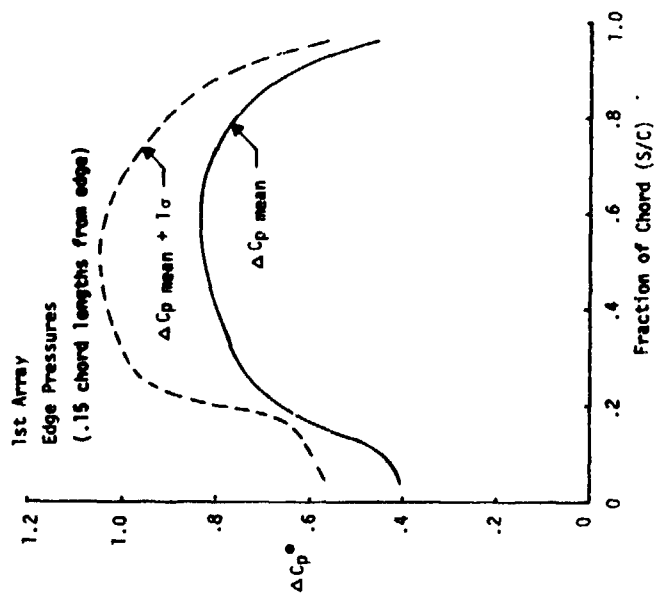


Figure 4-11f. Effect of Oblique Winds on Array Edge Pressure Distribution (Conventional Fence, Endplated Arrays, Wind from Rear)

1/7 Power Law Wind Velocity Profile  
Wind From Front



Array Conditions:  
Tilt Angle =  $35^\circ$   
Separation =  $2C$   
Height above ground =  $.25C$   
Fence-Array separation =  $2.5C$



\*  $\Delta C_p$  based on wind reference velocity at 10 meters

Figure 4-11g. Effect of Oblique Winds on Array Edge Pressure Distribution (Modified Fence Corner, Wind from Front)

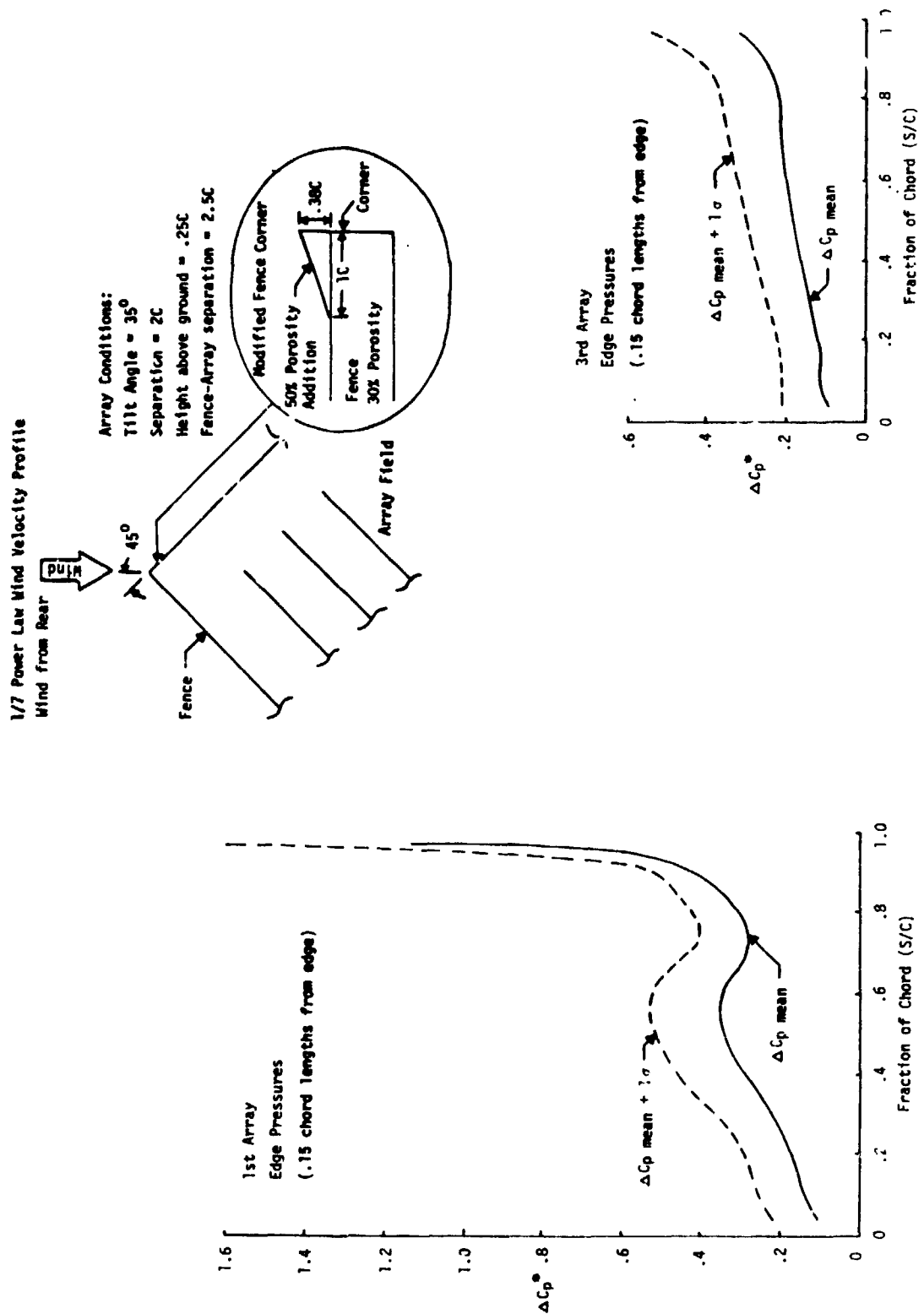


Figure 4-11h. Effect of Oblique Winds on Array Edge Pressure Distribution (Modified Fence Corner, Wind from Rear)

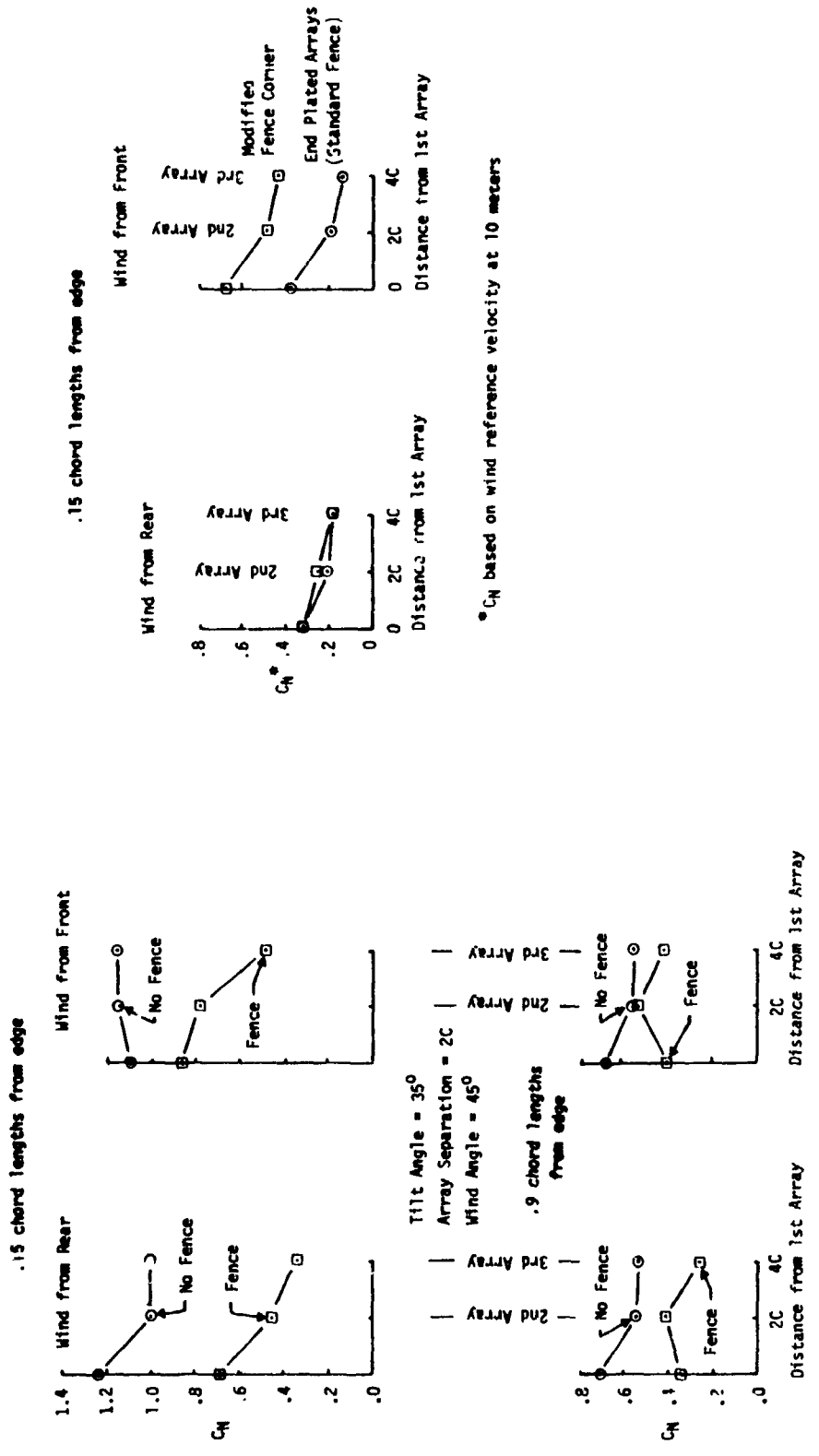
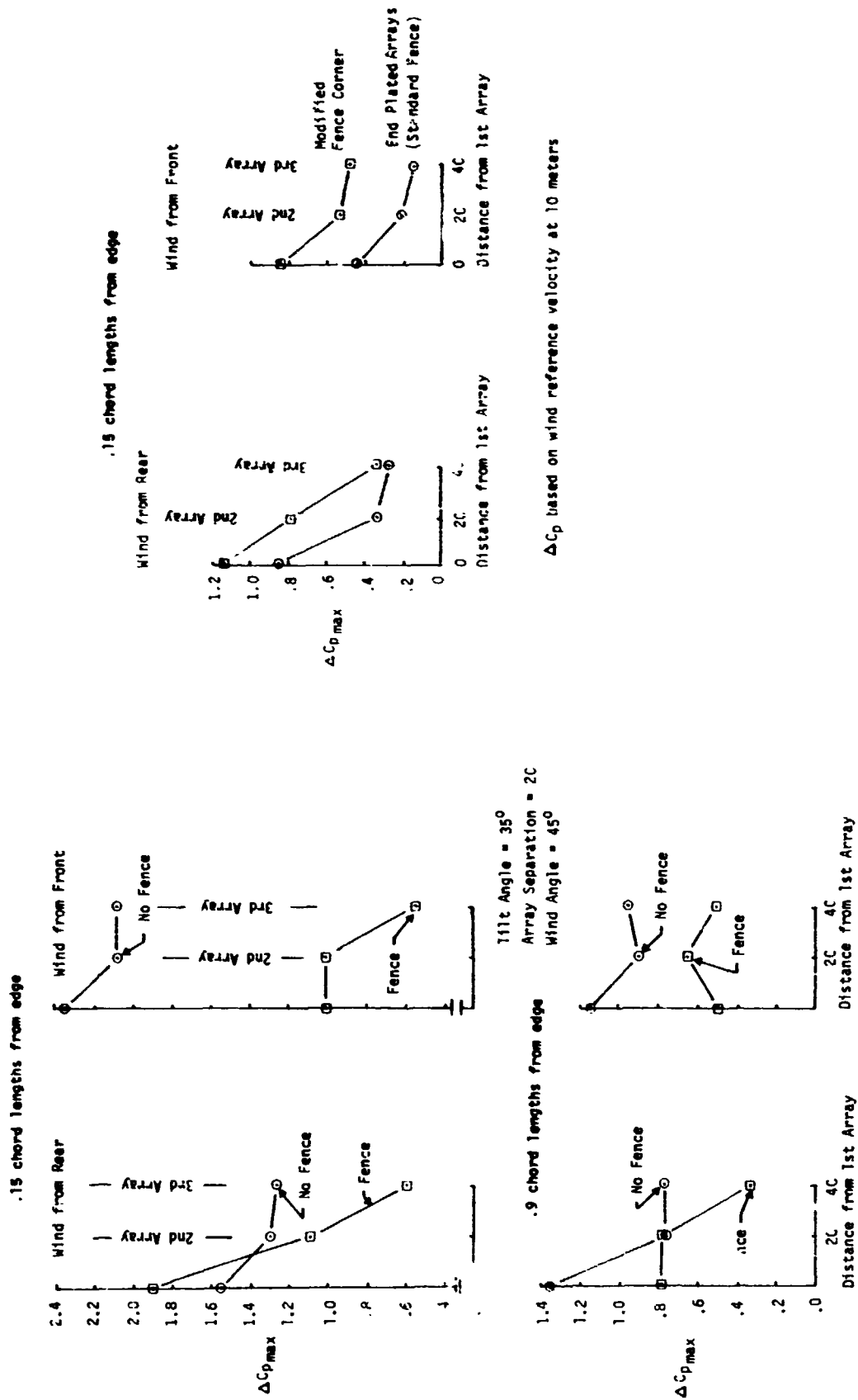


Figure 4-12. Effect of Oblique Winds on Array Normal Force Coefficients at Array Edge



$\Delta C_p$  based on wind reference velocity at 10 meters

Figure 4-13. Maximum Pressure Coefficient at Array Side Edge Due to Oblique Winds

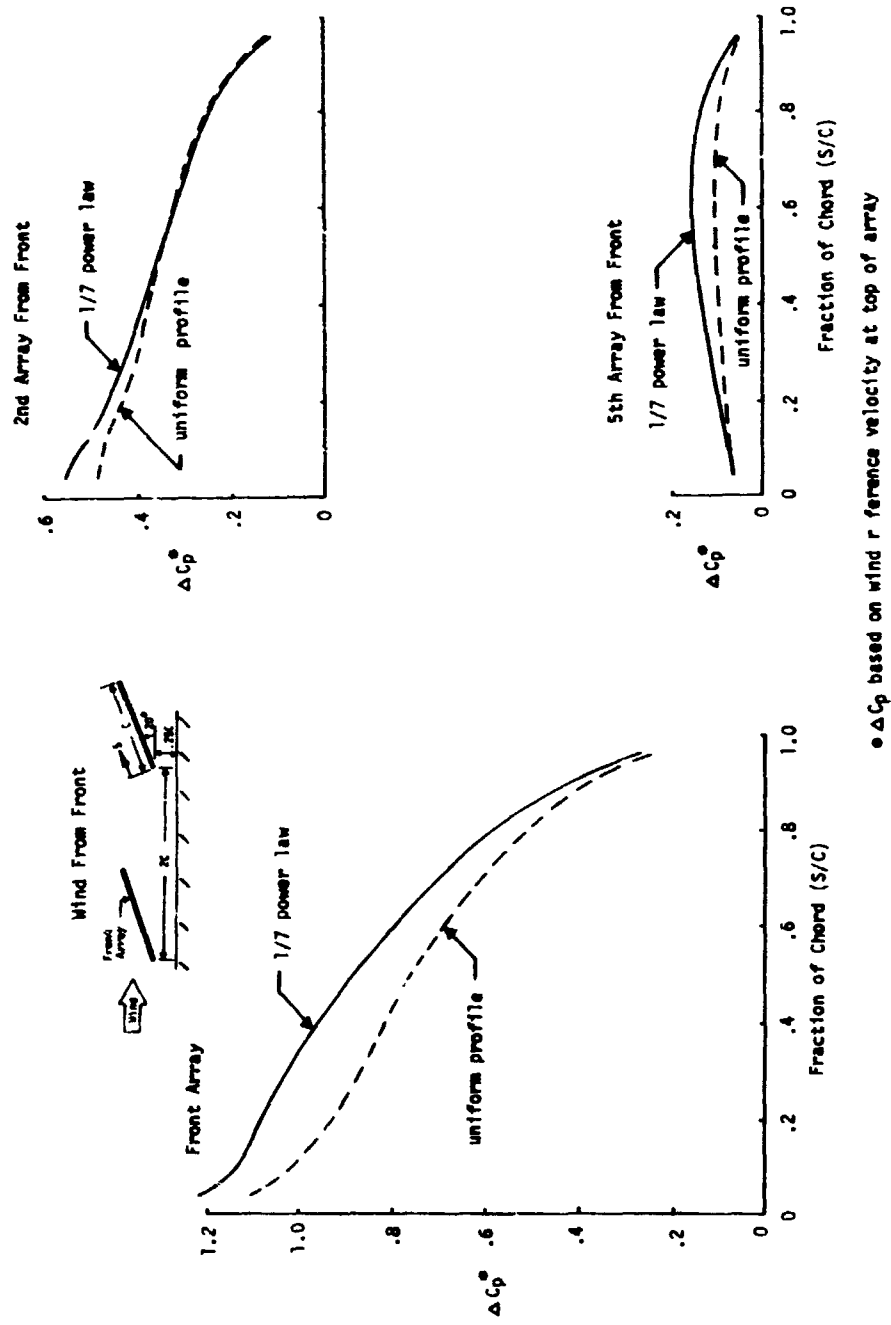


Figure 4-14a. Array Pressure Coefficient Comparison Between Uniform and Boundary Layer Wind Profiles (Tilt Angle =  $20^\circ$ , Wind from Front)

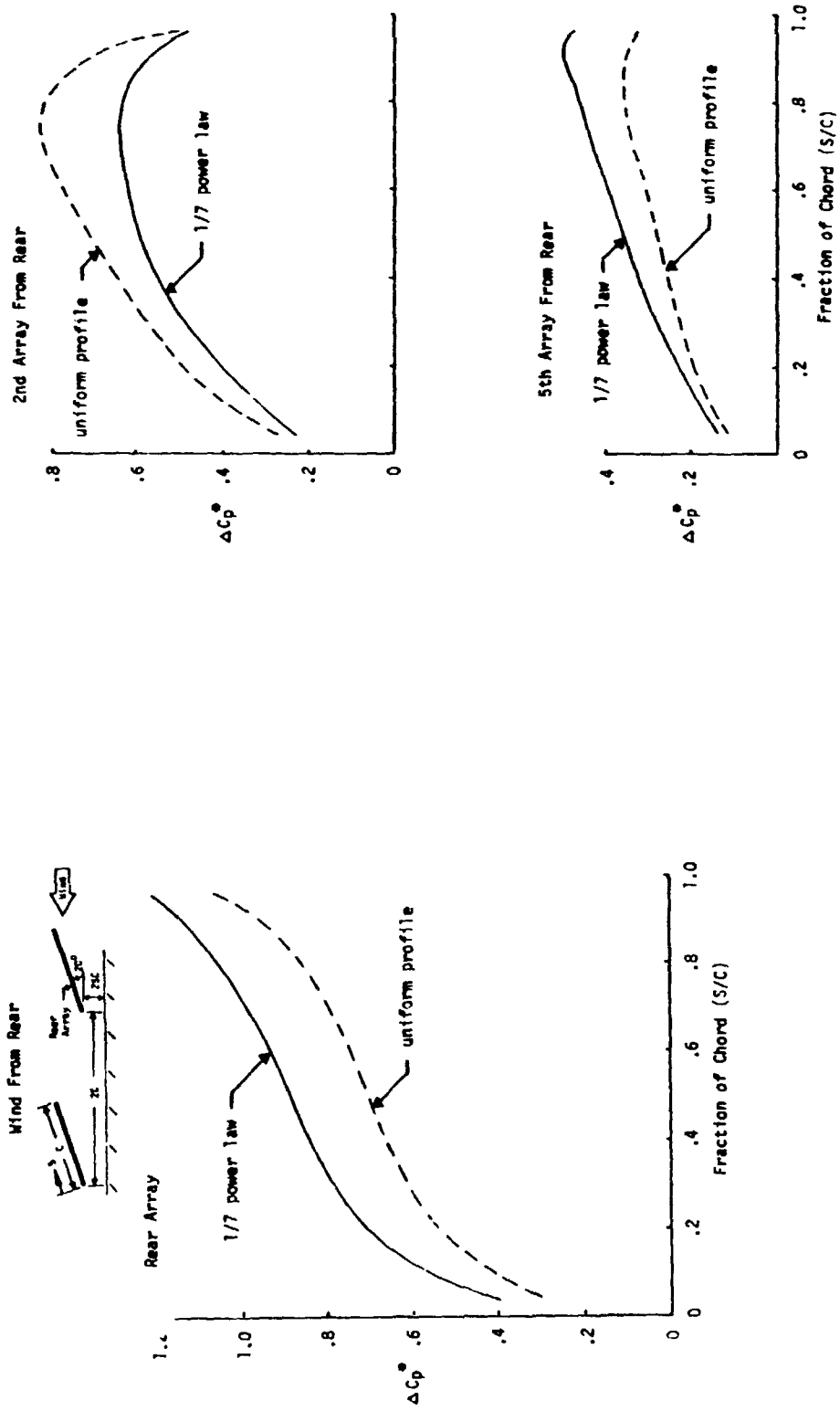


Figure 4-14b. Array Pressure Coefficient Comparison Between Uniform and Boundary Layer Wind Profiles (Tilt Angle = 20°, Wind from Rear)

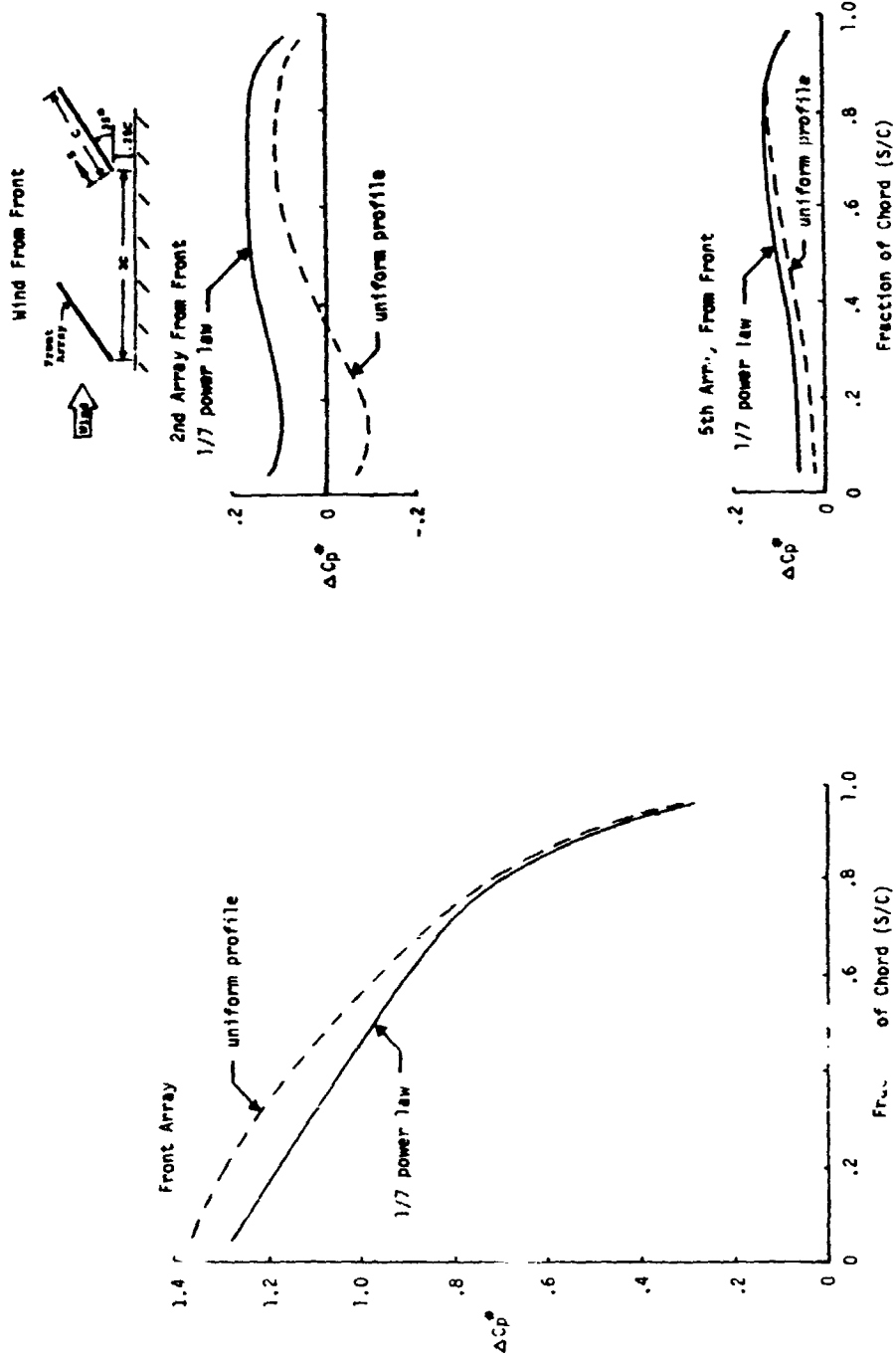


Figure 4-14c. Array Pressure Coefficient Comparison Between Uniform and Boundary Layer Wind Profiles (Tilt Angle = 35°, Wind from Front)

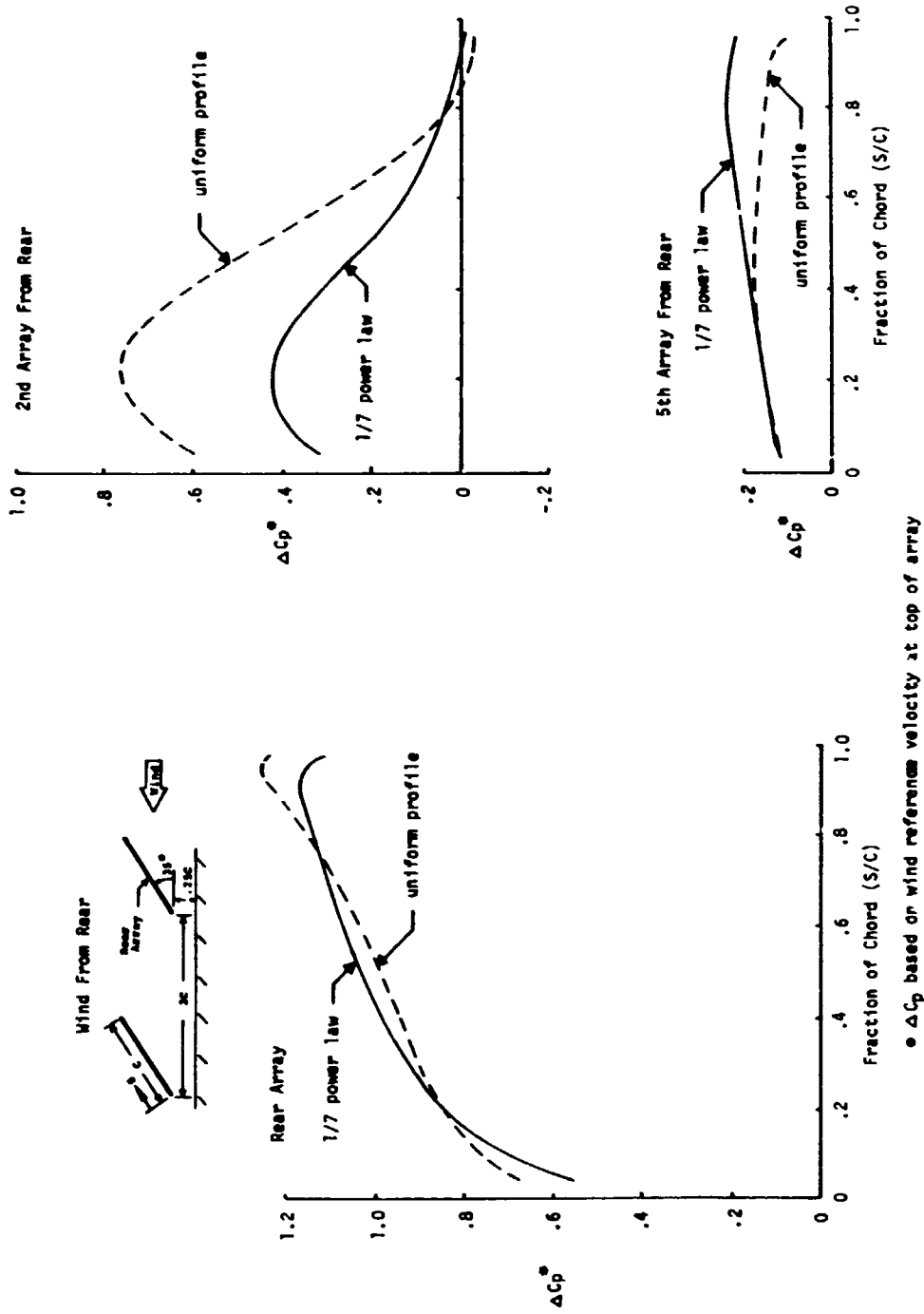


Figure 4-14d. Array Pressure Coefficient Comparison Between Uniform and Boundary Layer Wind Profiles (Tilt Angle=35°, Wind from Rear)

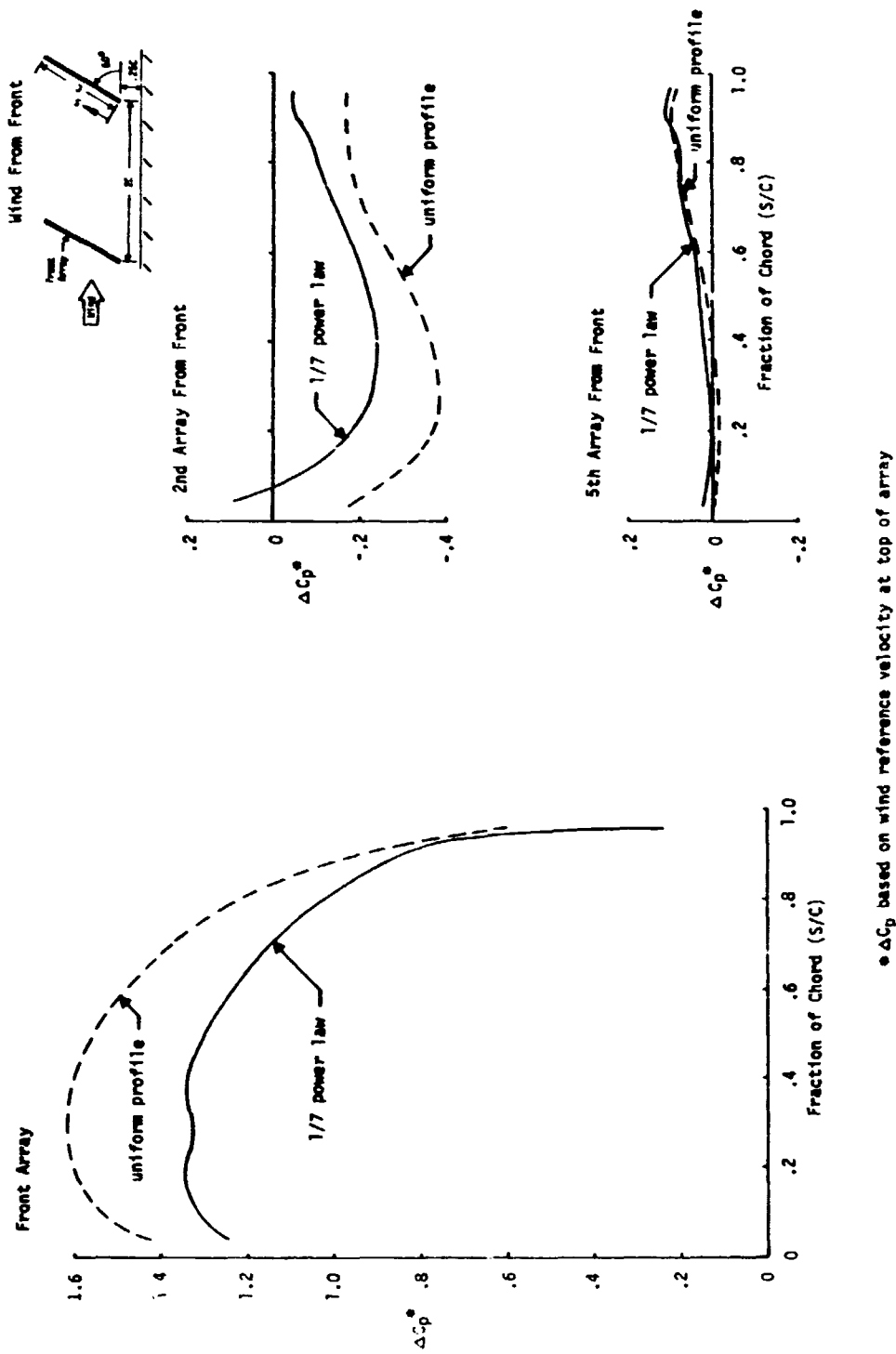


Figure 4-14e. Array Pressure Coefficient Comparison Between Uniform and Boundary Layer Wind Profiles (Tilt Angle = 60°, Wind from Front)

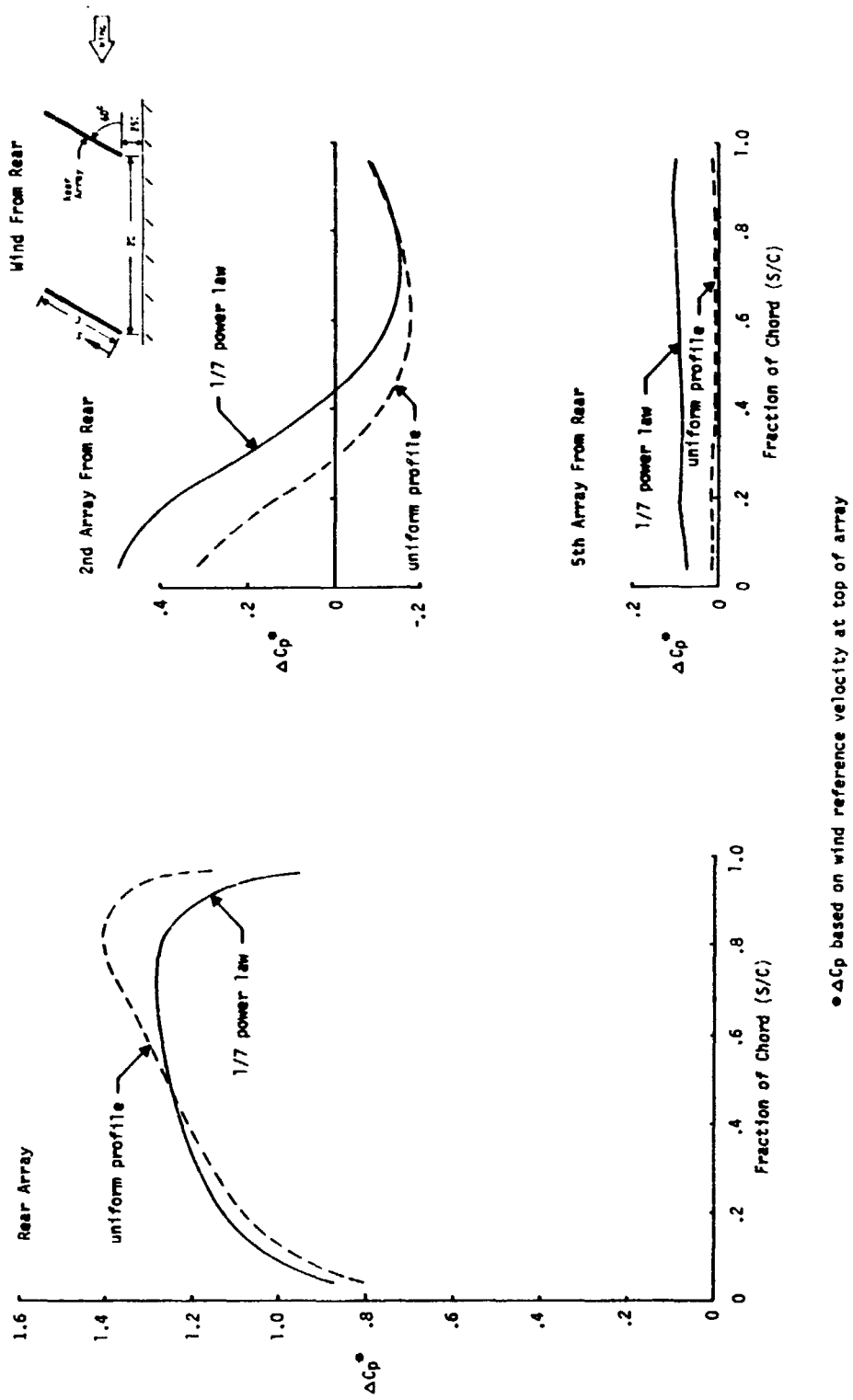
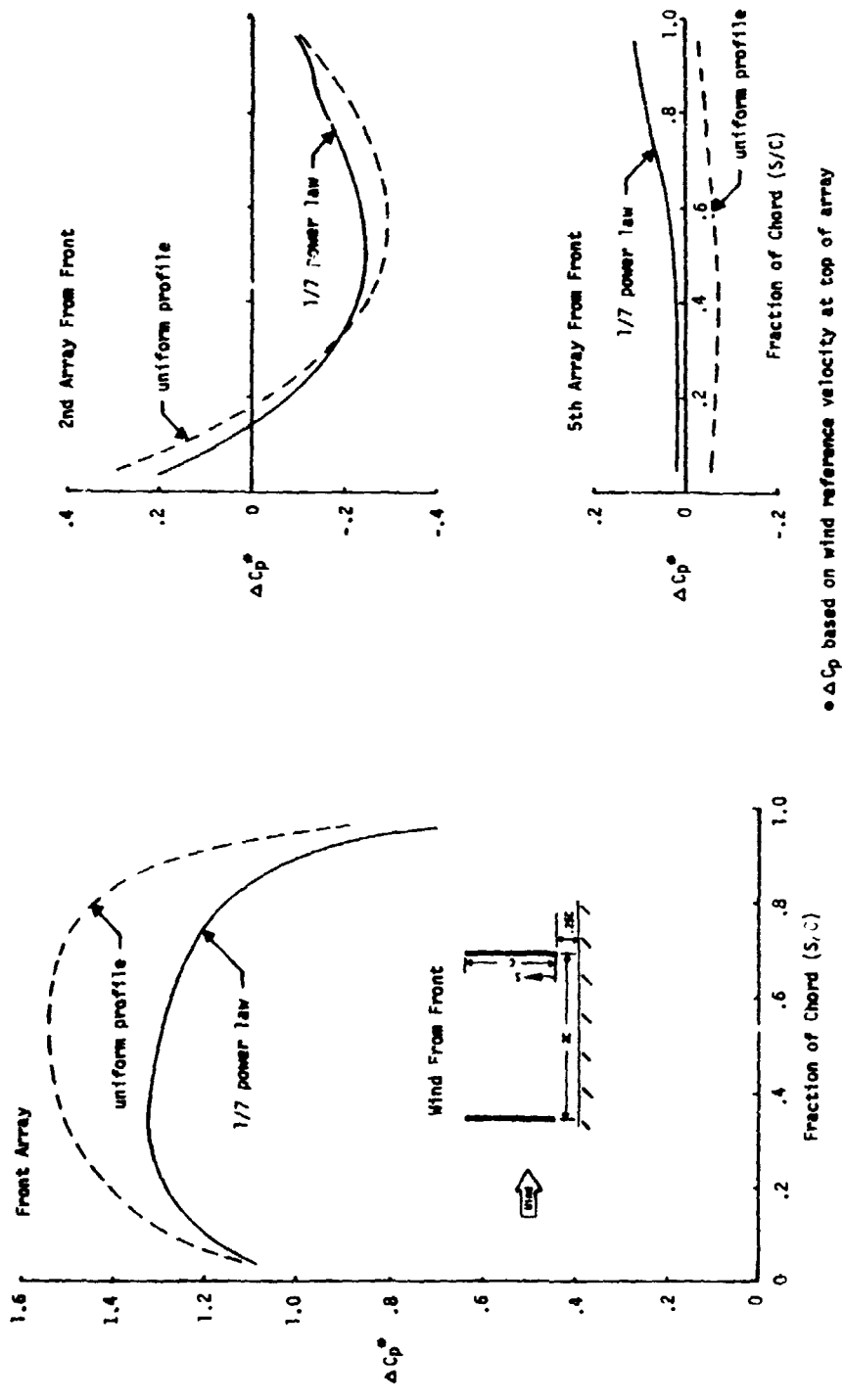


Figure 4-14f. Array Pressure Coefficient Comparison Between Uniform and Boundary Layer Wind Profiles (Tilt Angle = 60°, Wind from Rear)



•  $\Delta C_p$  based on wind reference velocity at top of array

Figure 4-14g. Array Pressure Coefficient Comparison Between Uniform and Boundary Layer Wind Profiles (Tilt Angle = 90°)

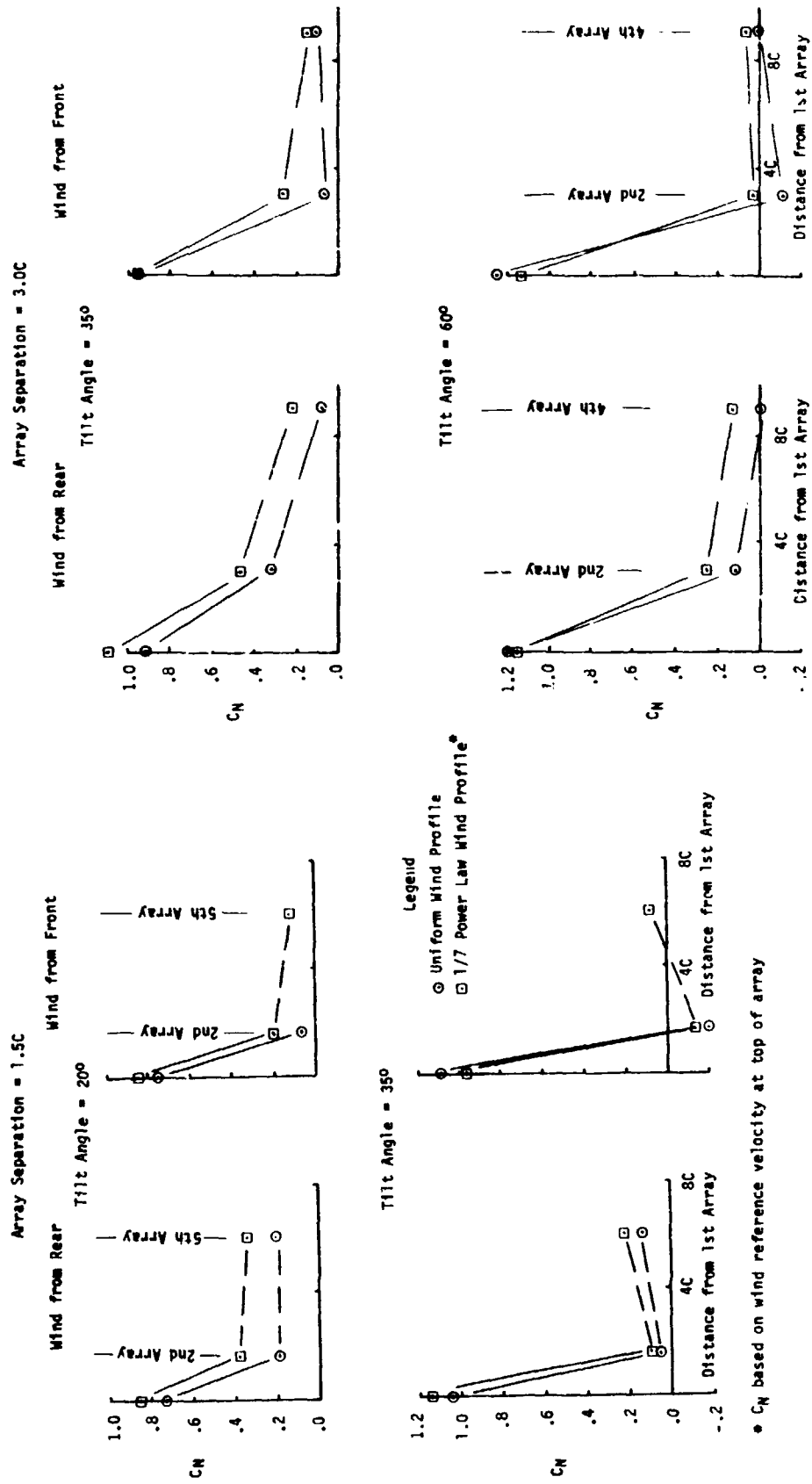
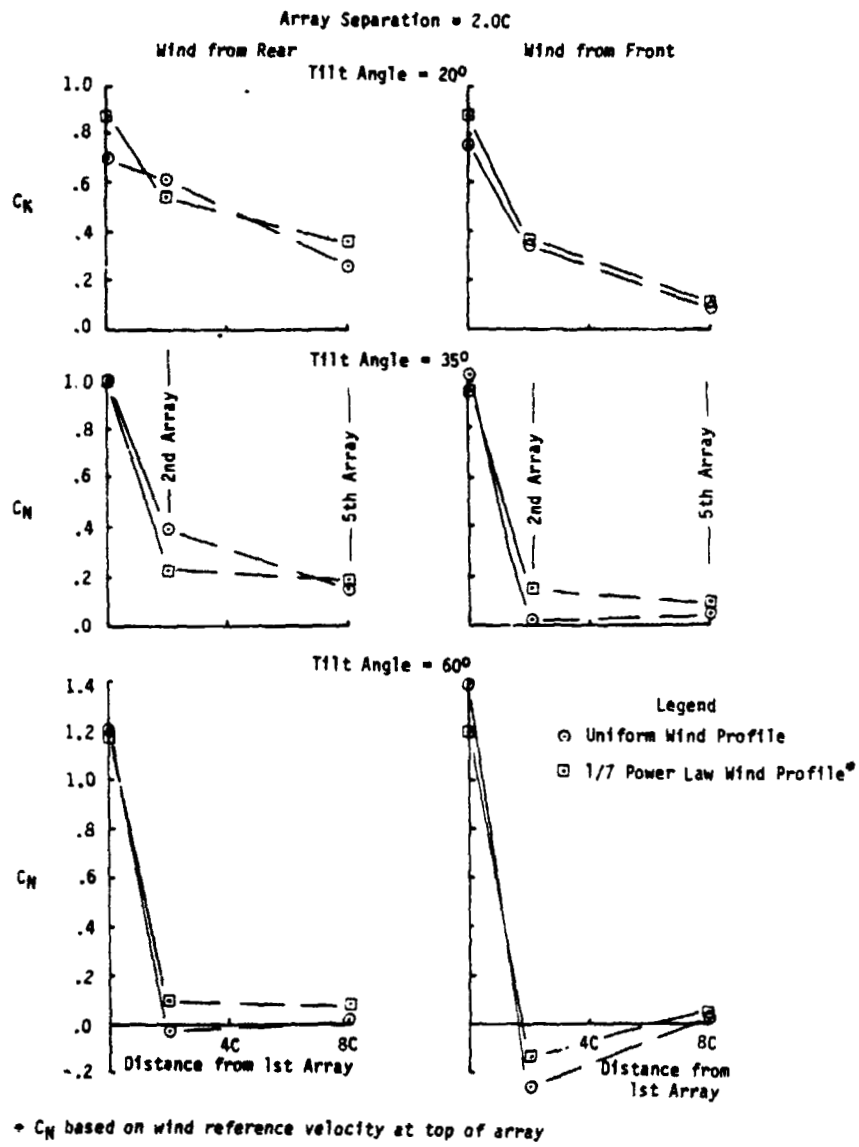


Figure 4-15. Array Normal Force Coefficient Comparison Between Uniform and Boundary Layer Wind Profiles.



**Figure 4-15. Concluded**

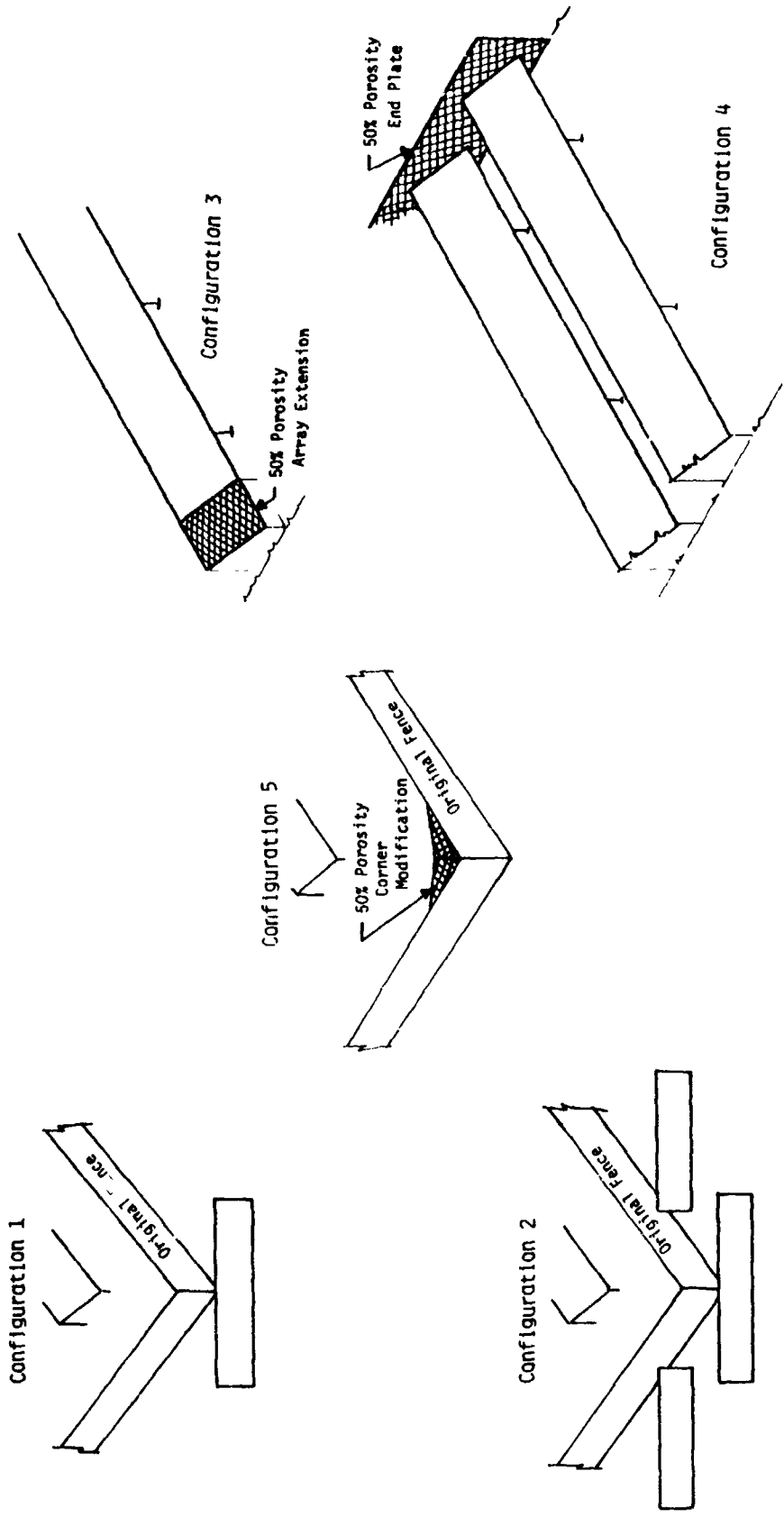


Figure 4-16. Configurations for Edge Load Reduction Study



## 5.0 THEORETICAL - EXPERIMENTAL RESULTS COMPARISON

The theoretical results developed in Phase II and presented in reference 5 were calculated based on a uniform velocity profile and were then adjusted to reflect the boundary layer velocity profile. Figure 5-1 shows the comparison of the theoretical results to the wind tunnel test results for the net pressure coefficient distribution along the chord of a single array located out of the influence of the ground and in a uniform velocity profile for three angles of attack (20°, 35°, and 60°). (Since the theoretical results were based on an infinite aspect ratio array, all theoretical-experimental comparisons utilize the mid-span test results.) The results differ by approximately 5% to 10% except for very low pressure coefficients; this comparison is considered very good and demonstrates that theoretical methods can be used to accurately predict the aerodynamic loads on an array located sufficiently far from the ground so that ground effects are not a consideration.

When the array is located in close ground proximity, the theoretical method tends to overpredict the pressure coefficients as compared to the wind tunnel test; this is shown in Figure 5-2. When the tilt angle of the array is small (20°), the theoretical results match the wind tunnel test results within approximately 20% or less. However, as the tilt angle increases (35° and 60°), the theoretical-experimental results become increasingly farther apart. The difference is due (at least in part, to the blockage effect that occurs to the air flow because of the restricted area between the ground and the lower edge of the array and the effects of air viscosity (not considered in the theoretical model) in this restricted flow regime. From the test results, of which Figure 5-3 is a typical example, flow blockage is seen to occur because of the ground-to-array gap. Figure 5-3 indicates that the flow is blocked and decreases in velocity as the gap is reduced in value from  $H/C = \infty$  to .25 as evidenced by the increase in pressure on the lower edge ( $S/C = 0$ ) on the windward face of the array and by the smaller negative pressure on the base pressure face. Because of the flow restriction at the gap, the flow in front of the windward face of the array is also affected, and the windward face pressure distribution is modified across the total face depending on the amount of restriction of the flow. In contrast to the test results, the theoretical separated inviscid flow method predicts that the air flow increases in velocity to allow a given mass of air to flow through the gap to compensate for the restricted gap area. This increase in velocity is further intensified as the

array presents a more bluff configuration to the wind at increasing tilt angles. Consequently, because of the inviscid flow assumptions in the theoretical method, there is an increasing spread with tilt angle between theoretical and test results as the tilt angle is increased from 20°.

In the Phase II study, reference 5, it was recommended that the theoretical normal force and pressure coefficients for all downwind arrays be calculated as 60% of the windward array. The amount of protection afforded to the downwind arrays in an array field is more complex than can be covered by a blanket percent reduction as shown in Figure 5-4; it is a function of the tilt angle and to a lesser extent, the wind direction. In general, the larger the tilt angle, the greater is the protection afforded to the downwind arrays by the windward array and the greater the load reduction. From the theoretical - experimental data comparison, the theoretical results presented in reference 5 are conservative for steady state wind loads on arrays without protective fences and can be used for design studies of photovoltaic flat plate arrays in lieu of specific test data relating to the design. However, the design would be penalized in terms of structural costs by the conservative loads.

When a fence is used as a protective wind barrier for the arrays, reference 5 recommended using the velocity isotachs behind a fence to calculate the dynamic pressure. Using this dynamic pressure with the theoretical normal force coefficients, the average normal forces per unit area were calculated and presented in reference 5 as Table 6-2 for various tilt angles and for an 8.2 foot fence. The appropriate results were extracted and are presented in Table 5-1 of this document, together with the results from the wind tunnel test for arrays positioned behind a 6 foot fence and in a boundary layer wind. The comparison is reasonably satisfactory at the 20° tilt angle, less so at 35°, and poor at 60°. Thus, the technique suggested in reference 5 should only be used for the smaller tilt angles and only when more reliable results are not available.

**Table 5-1. Example of Average Normal Wind Forces on Arrays behind Protective Fences by Theoretical and Wind Tunnel Test Methods (Behind)**

Wind from Front			
	Average Normal Wind Forces per unit area (psf)		
Tilt Angle	20°	35°	60°
Theory *	1.06	1.63	9.62
W.T. Test	1.03	2.46	4.92
Wind from Rear			
Theory *	1.63	2.22	11.21
W.T. Test	1.44	2.46	5.13

\* Dynamic factor of 1.5 removed from Table 6-2, reference 5

The array key wind parameters detailed in reference 5 are also shown in Figure 5-5. These parameters were verified by the wind tunnel test except for the dynamic pressure which is a fundamental parameter used in both test and theoretical methods. In general, the trends of all parameters, except ground clearance, were verified. However, the test results show that the parameters are all interrelated and cannot be separated as in Figure 5-5. As an example, angle of attack, ground clearance, and array spacing, are all affected by each other. Consequently, to predict the sensitivity precisely, a family of curves would be required varying only one parameter at a time. This would require an enormous amount of test data and results.

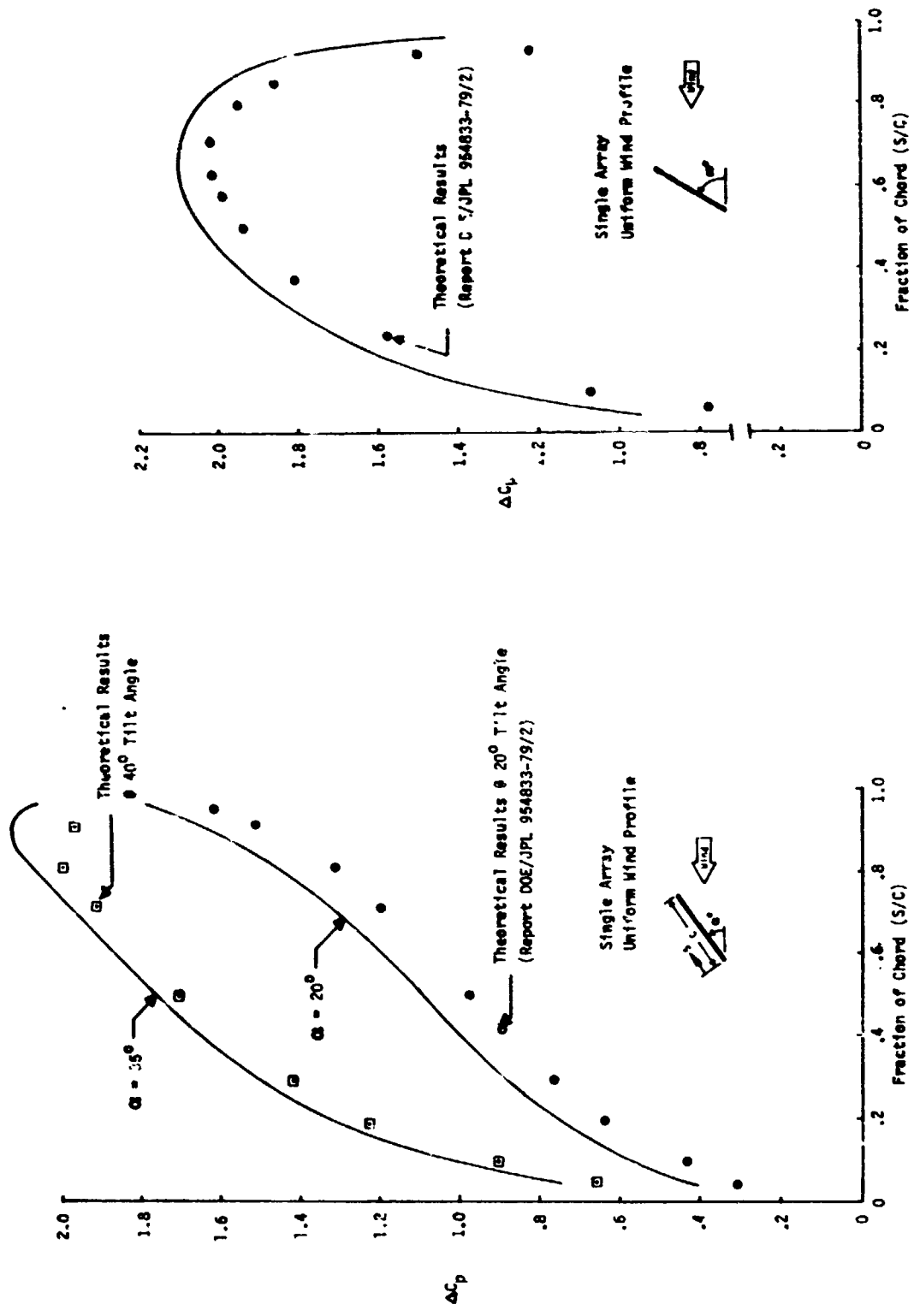


Figure 5-1. Array Pressure Coefficient Distribution Comparison Between Wind Tunnel Test and Theoretical Methods in Free Air

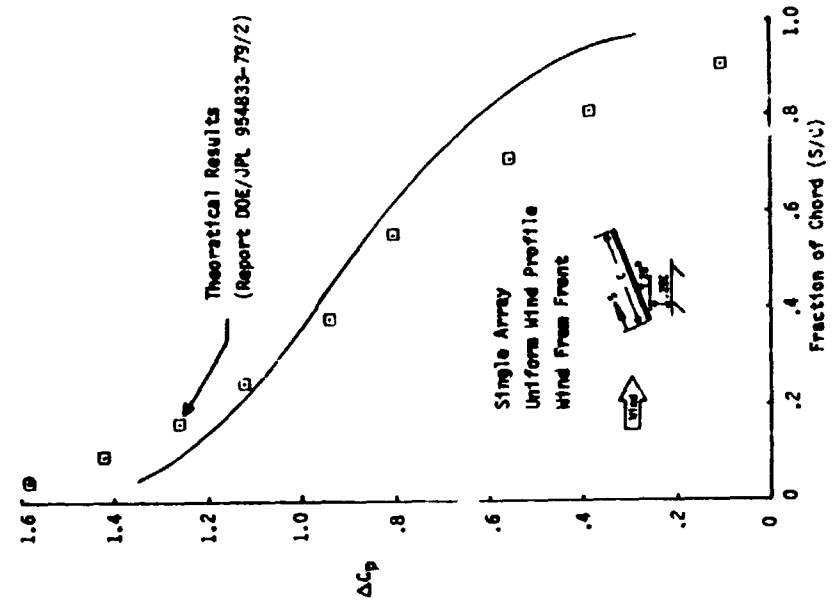
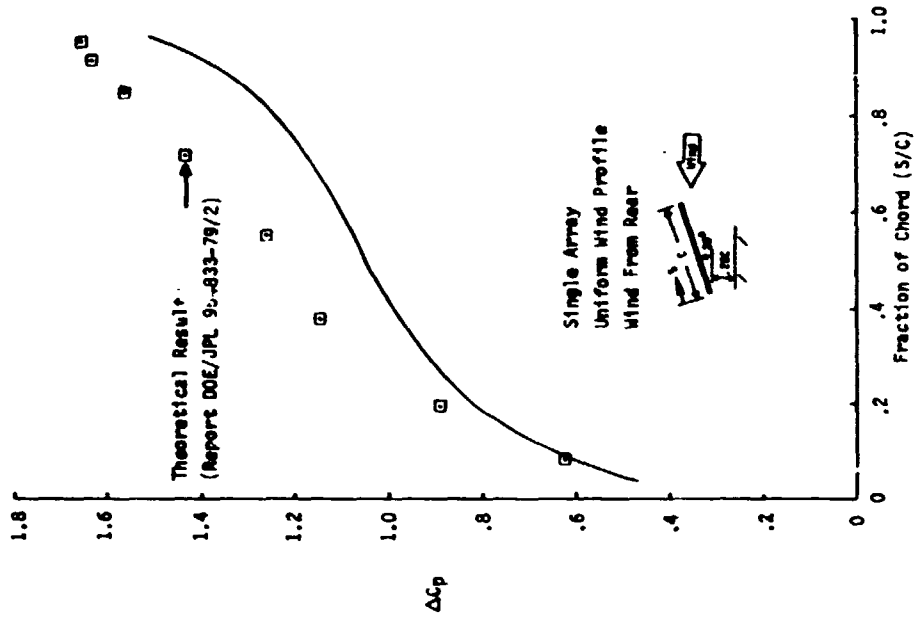


Figure 5-2a. Array Pressure Coefficient Distribution Comparison Between Wind Tunnel Test and Theoretical Methods in Close Ground Proximity (Tilt Angle = 20°)

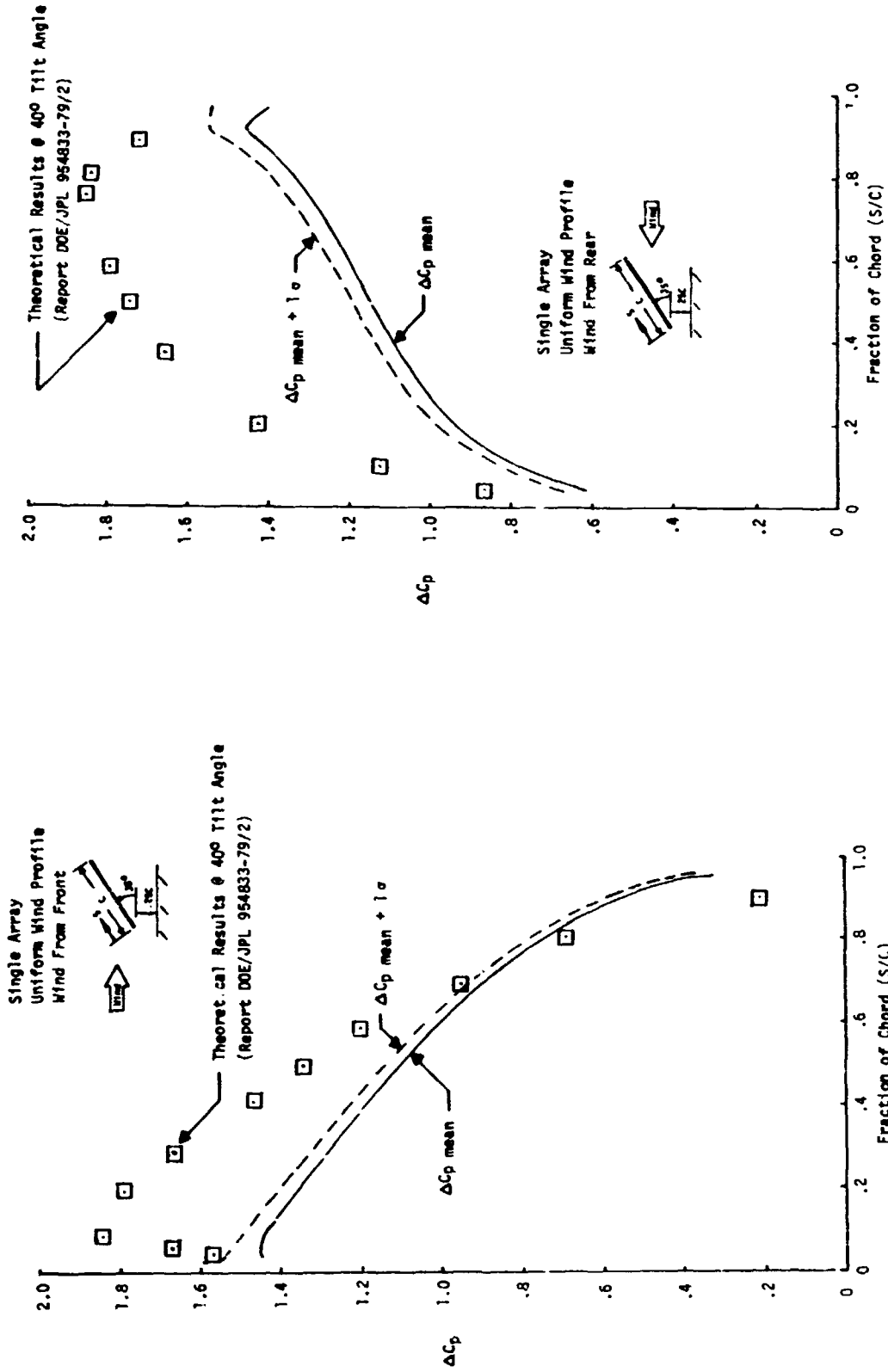


Figure 5-2b. Array Pressure Coefficient Distribution Comparison Between Wind Tunnel Test and Theoretical Methods In Close Ground Proximity (Tilt Angle = 35°)

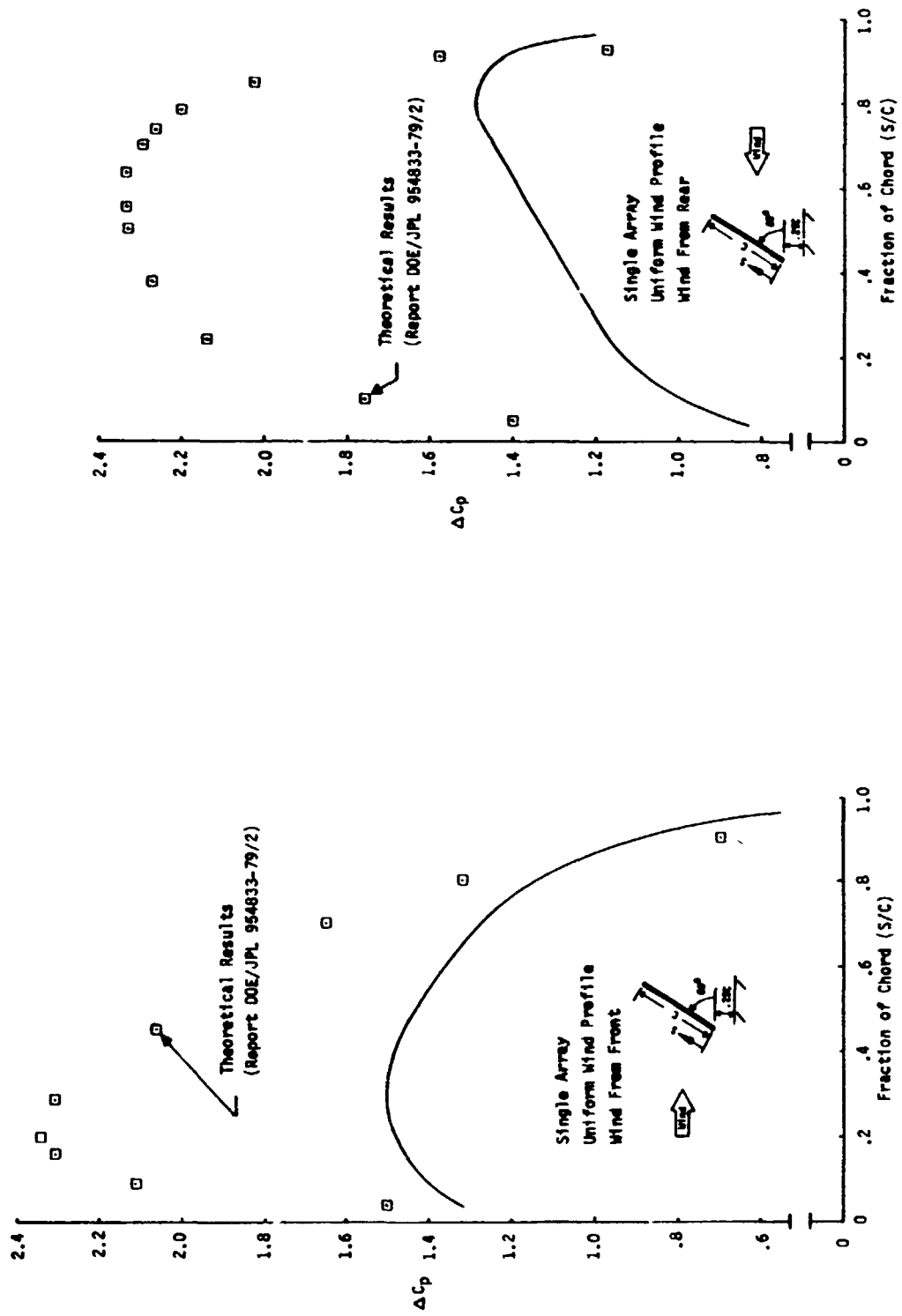
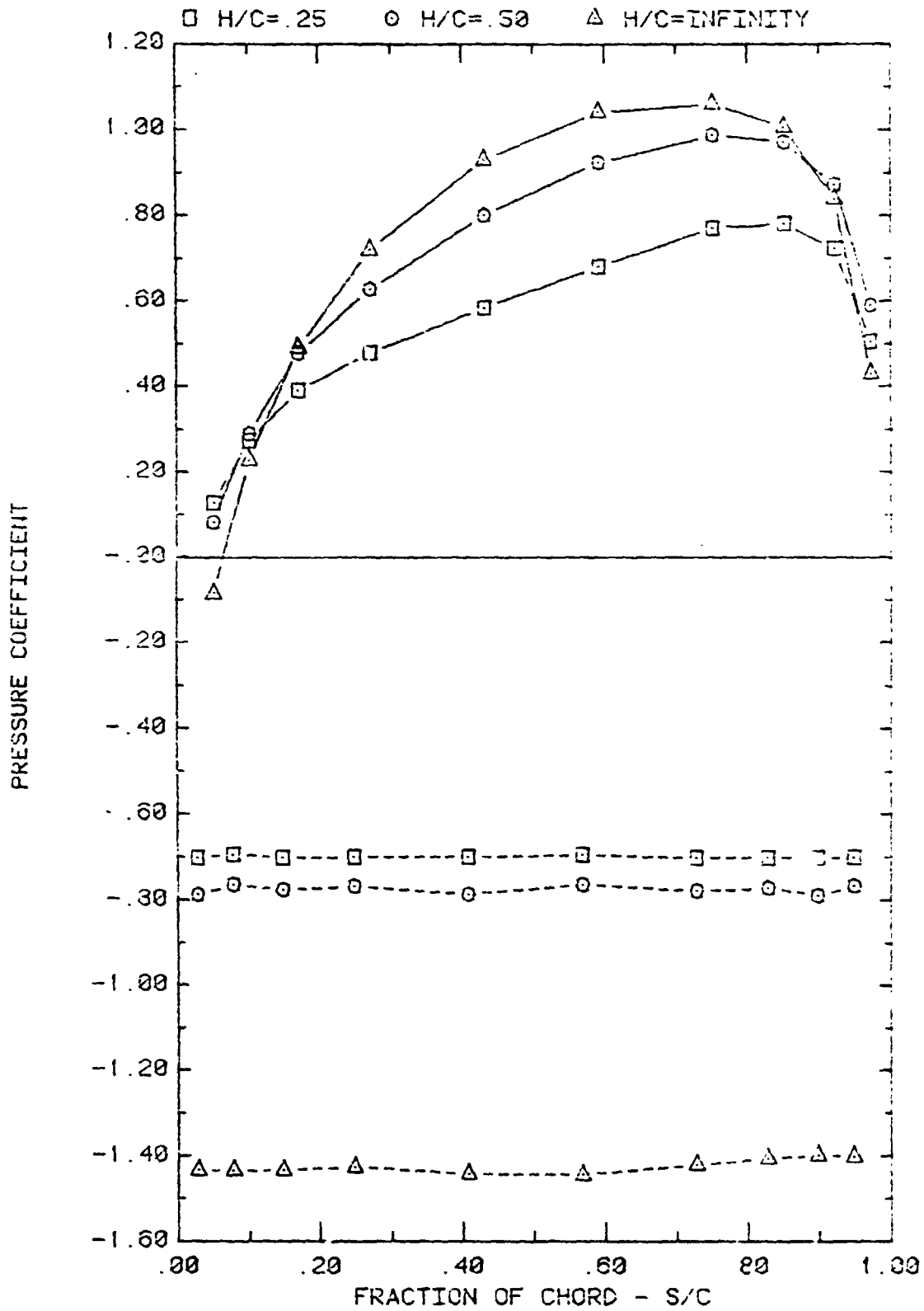


Figure 5-2c. Array Pressure Coefficient Distribution Comparison Between Wind Tunnel Test and Theoretical Methods in Close Ground Proximity (Tilt Angle = 60°)



FRONT AND BACK PRESSURES ON A SINGLE ARRAY IN UNIFORM FLOW  
EFFECT OF GROUND CLEARANCE FOR ATTACK ANGLE,  $\alpha = 60^\circ$

Figure 5-3. Effect of Ground Clearance on Front and Back Array Pressures in Uniform Flow (Tilt Angle =  $60^\circ$ , Wind from Back)

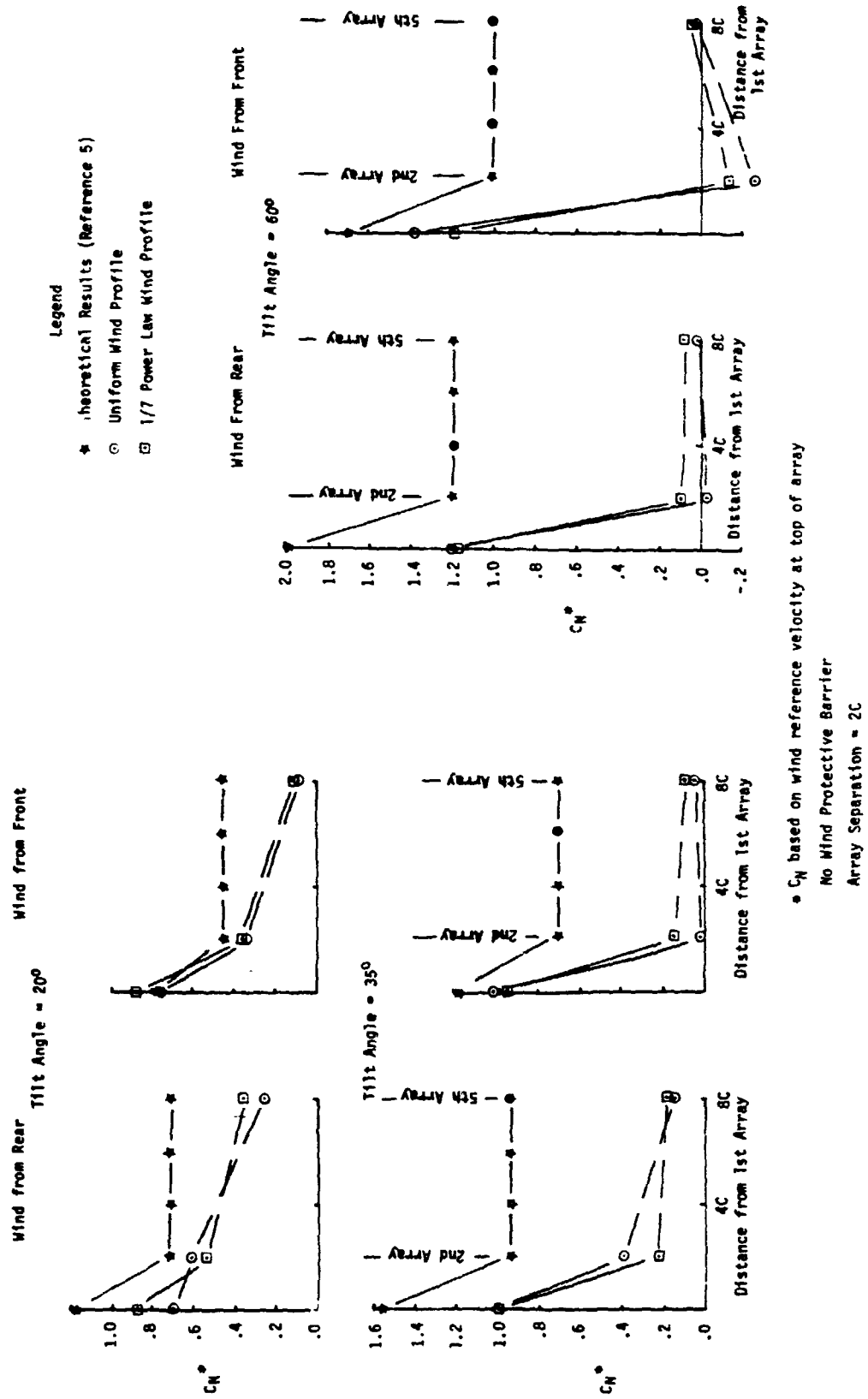


Figure 5-4. Array Normal Force Coefficient Comparison Between Wind Tunnel Test and Theoretical Methods

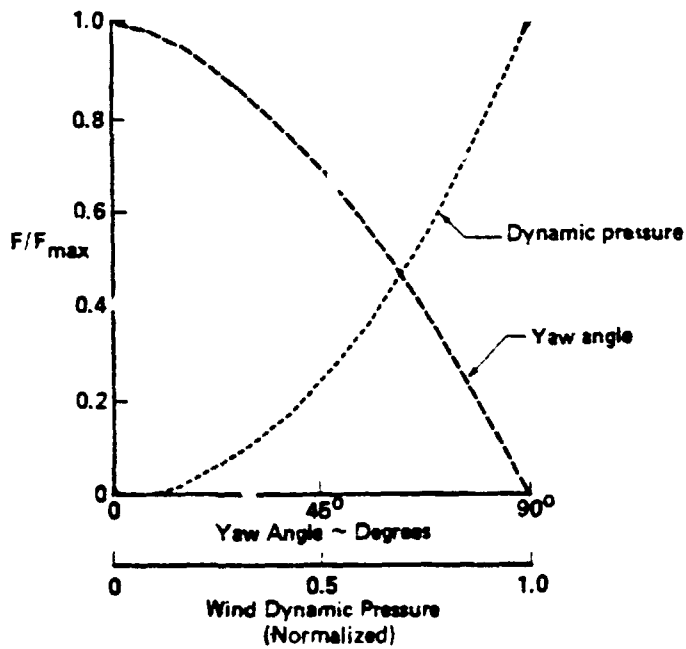
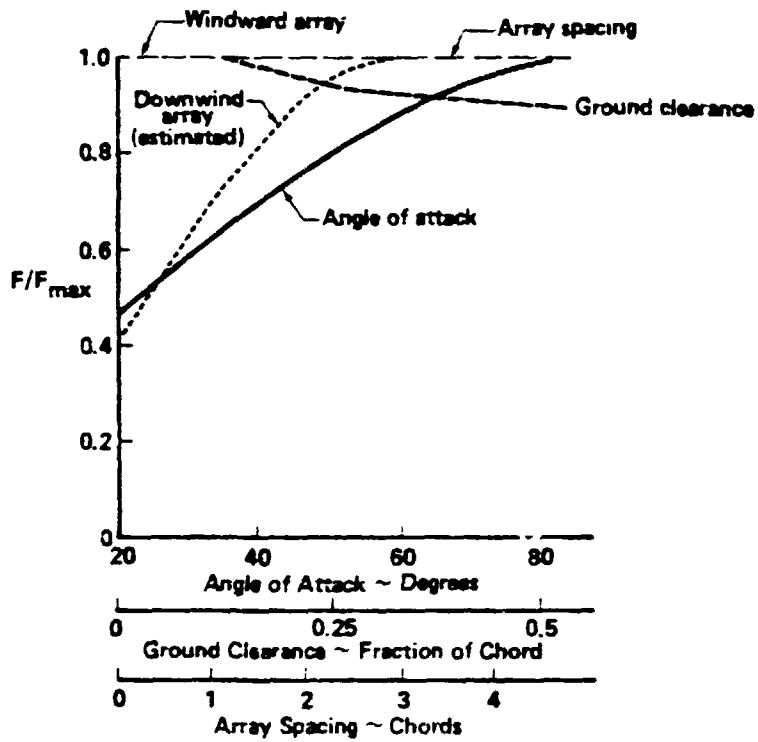


Figure 5-5. Theoretical Key Wind Loads Parameters and Their Sensitivity in Separated Flow Analyses (Reference 5)

## 6.0 DISCUSSION AND CONCLUSIONS

Currently, there are no known published data or results of wind loads from full sized photovoltaic arrays placed in the natural environment. The wind tunnel test utilizing the Meteorological Wind Tunnel and simulating the natural boundary layer wind as a  $1/7$  power law wind profile is the closest simulation compared to theoretical methods or uniform wind tunnel simulations of arrays placed in the natural environment. Therefore, all results from the different analyses were compared to the results obtained from the wind tunnel test that simulated the wind boundary layer.

Theoretical methods to calculate pressures and forces on arrays positioned at tilt angles greater than fifteen to twenty degrees require the use of separated flow analysis techniques that are directly applicable only to single arrays with infinite aspect ratios. Thus, the results must be extrapolated or modified for the array edges, arrays positioned behind fences, and interior arrays in an array field as performed in reference 5. The theoretical array pressure distribution and normal force results for the windward array and interior arrays were shown to be conservative (over designed) compared to the boundary layer wind tunnel test. The theoretical normal force results for arrays positioned behind fences are fairly close but conservative for tilt angles less than  $35^\circ$  and become much more conservative for tilt angles near  $60^\circ$ . As a result, if theoretical means are used for determining steady state wind loads on photovoltaic arrays and for sizing the array structural members, the arrays will be overstrength for steady state wind loading.

Most previous wind tunnel tests have been conducted for various shapes of structure in uniform wind profiles and out of the ground effect. Normal force coefficients for flat plates, cylinders, and spheres are readily available in the literature for this condition. If the flat plate coefficients for plates out of the ground effect are used for arrays close to the ground, they will yield normal wind forces that are ultra conservative. If test results are obtained for flat plate arrays in an array field and in a uniform flow wind tunnel with the influence of the ground effect, the results are variable, some conditions are conservative and others unconservative. Consequently, the results from a uniform flow wind tunnel for flat plate arrays would require a factor of safety to be applied to assure that the results are conservative if

used in an absolute sense for design values. However, the results are adequate to be used for trade studies in preliminary design such as using load alleviation devices, etc.

The boundary layer wind tunnel test for the flat plate photovoltaic array field produced some interesting results and conclusions. A fence (or the first windward array, if no fence exists) protects the downwind arrays except near the array edges from the wind. The wind normal forces and pressures of these downwind arrays are several times smaller than the first windward array when no fence protects it. In addition, as the tilt angles of the arrays increase, the greater the wind protection received by the downwind arrays and the smaller the normal forces and pressures on the arrays. Wind direction (frontal or rearward) does not significantly affect the results. The normal forces and pressures on arrays positioned as close as three to four rows from the front have the same magnitude whether a fence protects the field or not. A fence will significantly lower the loads on the first array and can even lower the first array loads below the loads on the arrays within the field. Thus, a fence can actually overprotect the arrays close to the fence. If the fence to protect the arrays from wind is properly designed, all arrays could be designed for the wind loads experienced by the interior arrays.

The pressure distribution on arrays protected by a fence and/or within the array field are essentially flat, resulting in no pitching moment on the array. In contrast to this, the first and second array without a protective fence have varying pressure distributions. The first array has a pressure distribution typical of a single flat plate. The second array is affected considerably by the downwash and turbulence of the first array and may have a pressure distribution along a chord that changes from positive to negative pressures. Another noteworthy observation is that the pressure on the base pressure side is flat for all conditions except near the edges.

The wind loads on the array edges are considerably different from the remainder of the array field. Vortices are produced by array corners and fence corners and can produce very high wind loads at and near the array edges, depending on the wind direction. Pressure coefficients tend to be especially high in the localized leading edge-side edge area of the array. The high wind loads diminish to the loads within the array field at approximately two slant height distances from the edge, again depending on the wind direction. Several means

to alleviate the wind loads at the edges were presented in Section 4 but even the reduced edge loads are still several times the array mid-span loads.

In the wind tunnel test, the fluctuating pressures were recorded for a finite time, averaged to obtain the steady state loads and the rms value of the variable loads calculated to obtain indications of the level of the pressures produced by the array generated turbulence. The actual rms values will be larger than those recorded because of the damping inherent in the data acquisition. However, the rms load values do give an indication of the turbulence. In general, from the test results, the front arrays received the most turbulence induced loads when a fence existed and the second arrays received the most when no fence existed.

For design purposes, envelopes of the normal force and pressure coefficients were developed, where applicable, to encompass the steady state loads for all tilt angles and wind directions. These design envelope loads are explained and presented in total in Section 7.0.



## 7.0 STEADY STATE WIND LOAD DESIGN GUIDELINES

Based on the results of the boundary layer wind tunnel test and the results of the theoretical study documented in reference 5, the following design guidelines are given for determining wind loading on photovoltaic flat plate arrays. The normal force and pressure coefficient guidelines were obtained by enveloping the results from the wind tunnel test and are valid for arrays with separations from 1.5C to 3.0C. Wind tunnel tests with the winds normal to the spanwise axis of the arrays were used for the guidelines. From the theoretical study and aerodynamic principles, winds normal to the spanwise axis will produce the maximum pressure loading on the arrays at locations at least two slant heights from the array side edges.

### 7.1 Wind Loads on Arrays Behind a Protective Wind Barrier

If a fence is used to protect the arrays in an array field, the steady state wind loading on the first arrays will be the same or less than the arrays within the field if the fence\* is properly designed for wind protection. Figure 7-1a presents normal force coefficients for conditions where the first array is protected from wind loading at least as well as the arrays interior to the field. This figure can be used to calculate steady state wind forces on arrays and array supporting structure in an array field. These loads are not applicable for the structure within two slant heights from the edge. The steady state normal wind force on the array is calculated by the equation:

$$F_N = q S C_{N1} \quad - - - (1)$$

\*The fence used in this study had a porosity of 30% and a height equal to three-quarters of the array slant height. Since this study did not investigate other fence configurations, it is the designer's responsibility to assure that his fence design produces as much wind protection as the fence used in this study. There are several papers referred to in reference 5 that investigate the effects of fence porosity on the wind velocity behind the fence. In general, a porosity of from 30% to 50% produces the best wind protection. A solid fence tends to increase the turbulence compared to a higher porosity fence and also causes reversed flow behind the fence. The height of the fence is less critical than fence porosity on array loads provided that the height of the fence is near or above the array height.

where:

$F_N$  = Steady state normal force (lbs)

$q$  = Dynamic pressure (psf) for reference design velocity at 10 meters

$S$  = Area of array (ft<sup>2</sup>)

$$C_{N1} = K_1 C_N$$

= Corrected normal force coefficient

$C_N$  = Normal force coefficient from figure 7-1a

$K_1$  = Scale factor to correct for array size

$$= \left( \frac{C \sin \alpha + H_0}{8 \sin \alpha + 2} \right)^{.28}$$

$C$  = Array slant height (ft)

$H_0$  = Ground clearance (ft)

$\alpha$  = Tilt angle (degrees)

The scale factor ( $K_1$ ) corrects (in an approximate manner) the wind forces for arrays whose slant height and ground clearance are different than the test array baseline size of 8 ft. slant height and 2 ft. ground clearance. This scale factor considers the difference in the wind velocity at the top of an array whose size and position is different from the baseline array relative to the wind velocity at the top of the baseline array.

Figure 7-1b presents steady state pressure coefficients normalized to the normal force coefficients at corresponding tilt angles. The steady state pressure distributions on the arrays behind a fence are essentially constant or vary linearly (increasing from the trailing edge to the leading edge) for all tilt angles. The pressures can be calculated by the equation:

$$P = qC_{p1} \text{ - - - - (2)}$$

where:

$p$  = Steady state local pressure loading (psf)

$q$  = Dynamic pressure (psf) for reference design velocity at 10 meters

$$C_{p1} = K_1 C_p$$

= Corrected pressure coefficient

$K_1$  = Scale factor to correct for array size and ground clearance

$$= \left( \frac{C \sin \alpha + H_0}{8 \sin \alpha + 2} \right)^{.27}$$

$C$  = Array slant height (ft)

$H_0$  = Ground clearance (ft)

$\alpha$  = Tilt angle (degrees)

$\frac{C_p}{C_N}$  = Normalized pressure coefficient from figure 7-1b

$C_N$  = Normal force coefficient from figure 7-1a

The steady state pressure loading is valid for all flat plate array panels in an array field except for panels within two slant heights from the edge. Where leading edge (L.E.) and trailing edge (T.E.) are given, the pressure loading is assumed as linearly increasing from the trailing edge value to the leading edge value. It should be noted that some conservatism is designed into the panel pressure loading by assuming a flat or linearly varying pressure coefficient. This conservatism can be seen in the normalized pressure coefficient shown in Figure 7-1. If the pressure coefficient distribution was matched exactly, the  $C_p/C_N$  curve would be equal to 1.0. Thus, conservatism of from 10 to 20% is built into the pressure loading by simplifying the distribution.

The use of these design guidelines can best be illustrated by the following example:

1. Determine the design normal force and pressure distribution on an array interior to an array field for a 90 mph wind approaching the front of the array and at sea level. The array slant height is 8 feet, ground clearance is 2 feet, span is 10 feet, and the tilt angle is 30 degrees.

$q$  = wind dynamic pressure at 10 meter height

$$= .5 \rho V^2$$

$$= .5 (.002378)(131.23)^2$$

$$= 20.5 \text{ psf}$$

$S$  = area of array

$$= 8 \times 10$$

$$= 80 \text{ ft}^2.$$

$$\begin{aligned}
 K_1 &= \text{Scale factor} \\
 &= \left( \frac{8 \sin(30^\circ) + 2}{8 \sin(30^\circ) + 2} \right) \cdot 28 \\
 &= 1.0
 \end{aligned}$$

$$C_N = .16 \text{ from figure 7-1a}$$

$$\begin{aligned}
 C_{N1} &= K_1 C_N \\
 &= .16
 \end{aligned}$$

To calculate the normal force

$$\begin{aligned}
 F_N &= q S C_{N1} \\
 &= 20.5 \times 80 \times .16 \\
 &= 262.4 \text{ lbs. force normal to the array (30}^\circ \text{ from vertical) and in downward} \\
 &\quad \text{direction per figure 7-1a}
 \end{aligned}$$

To calculate the pressure distribution along the chord

$$p = q C_{p1}$$

$$C_{p1} = K_1 \frac{C_p}{C_N} C_N$$

From figure 7-1b

$$\frac{C_p}{C_N} = 1.18 \text{ at trailing edge (top edge for wind from front)}$$

$$= 1.26 \text{ at leading edge (bottom edge for wind from front)}$$

$$C_N = .16 \text{ from figure 7-1a}$$

$$K_1 = 1.0$$

therefore

$$\begin{aligned}
 C_{p1} &= 1.18 \times .16 \\
 &= .19 \text{ trailing edge}
 \end{aligned}$$

$$\begin{aligned}
 \text{and } C_{p1} &= 1.26 \times .16 \\
 &= .20 \text{ leading edge}
 \end{aligned}$$

The local pressure is

$$\begin{aligned}
 p &= 20.5 (.19) \\
 &= 3.9 \text{ psf at trailing edge (downward direction per figure 7-1b)} \\
 p &= 20.5 (.20) \\
 &= 4.1 \text{ psf at leading edge (downward direction per figure 7-1b)}
 \end{aligned}$$

Therefore, the pressure varies on the panel from 4.1 psf at the leading edge (lower edge) to 3.9 psf at the trailing edge (upper edge) for a 90 mph wind approaching the front of the array field.

## 7.2 Wind Loads on Arrays Without a Protective Wind Barrier

If an array field is to be designed without a protective fence, the first two arrays from the front and back need to be designed for larger wind loads than in Section 7.1. All remaining arrays interior to these two front arrays can be designed to withstand wind loads given in Figure 7-1. The maximum normal wind forces on the first two arrays from the front and back of the array field can be calculated similarly to those in Section 7.1 using the normal force coefficient envelope and the delta pressure coefficient presented in Figure 7-2a and b. As an example:

- Calculate the normal force and pressure on the first array for the same conditions as in the example in 7.1.

To calculate the normal force:

From before

$$q = 20.5 \text{ psf}$$

$$S = 80. \text{ ft}^2$$

$$K_1 = 1.0$$

From figure 7-2a

$$C_N = .65$$

Therefore the normal force on the array is

$$F_N = 20.5 \times 80 \times .65$$

$$= 1066 \text{ lbs in downward direction per figure 7-2a}$$

C-2

To calculate the panel pressure

$$\begin{aligned} \frac{C_p}{C_N} &= 0.8 \text{ at trailing edge} \\ &= 1.28 \text{ at leading edge} \\ C_N &= .65 \\ p &= 20.5 \times 0.8 \times .65 \\ &= 10.7 \text{ psf at trailing edge} \\ &= 20.5 \times 1.28 \times .65 \\ &= 17.1 \text{ psf at leading edge} \end{aligned}$$

Therefore, the pressure varies from 17.1 psf at the leading edge to 10.7 psf at the trailing edge with the pressure in downward direction per figure 7-2b.

### 7.3 Array Edge Wind Loads

The wind loads within two slant heights from the side edges have a different character than those within the array field because of the corner vortices. This test program was primarily directed towards the wind loads within an array field and only a limited amount of testing was devoted to the edge loads. Consequently, a comprehensive set of wind load guidelines for the edge loads cannot be detailed from the test data. However, the following normal force coefficients and pressure coefficients are given as guidelines and can be used in the design of the edge arrays if the following design conditions are satisfied.

Array tilt angle  $\approx 35^\circ$

Fence design details, if applicable, as footnoted in Section 7.1

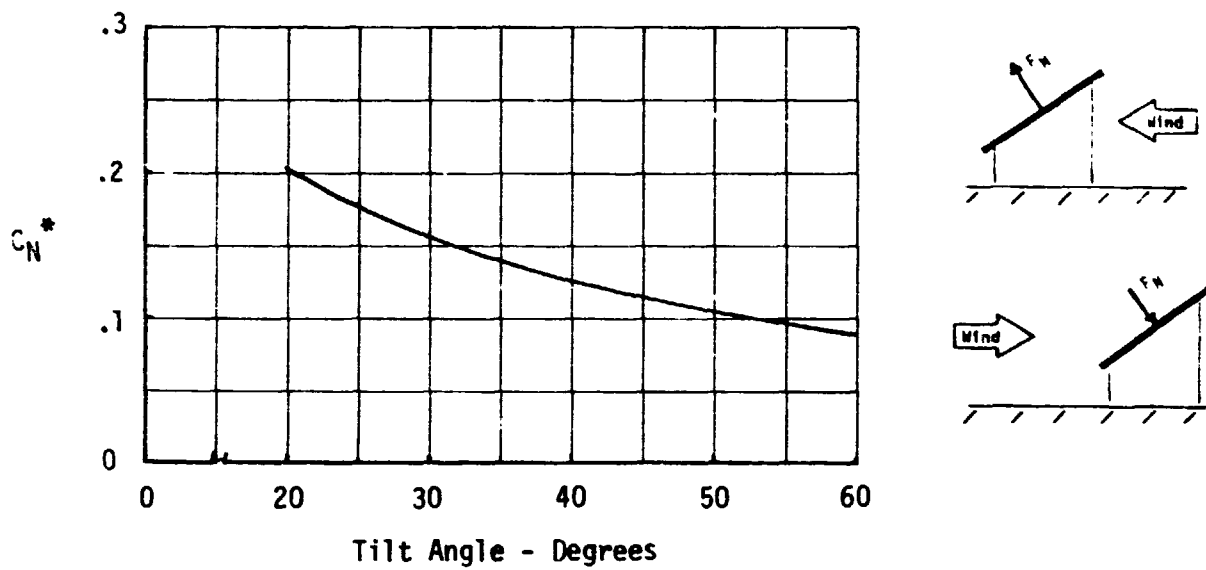
Fence corner modifications, if applicable, as shown in configuration 5,

Figure 4-16

The normal force coefficients and delta pressure coefficients for arrays within two slant heights from the side edge of the array field and for three field configurations - no fence, fence, and fence with the corners modified - are shown

in Figures 7-3a to 7-3c. These coefficients are based on the test data located .15 chord lengths from the side edge. Since the loads decrease with distance in from the edge, these coefficients are conservative if used over the two slant heights from the side edge. In addition, the pressure distributions show high pressure coefficients located within 5% to 10% from the upper edge. Since a structural support is likely to be located on the leading and trailing edges to support the arrays, these high pressure loads, within 10% of the top edge, may not be critical to the design of the panels and may not need to be considered in their design. The effect of this high pressure loading is in the normal force coefficient calculation which is a parameter used to size the supporting structure.

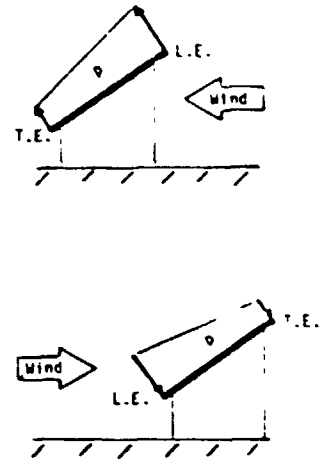
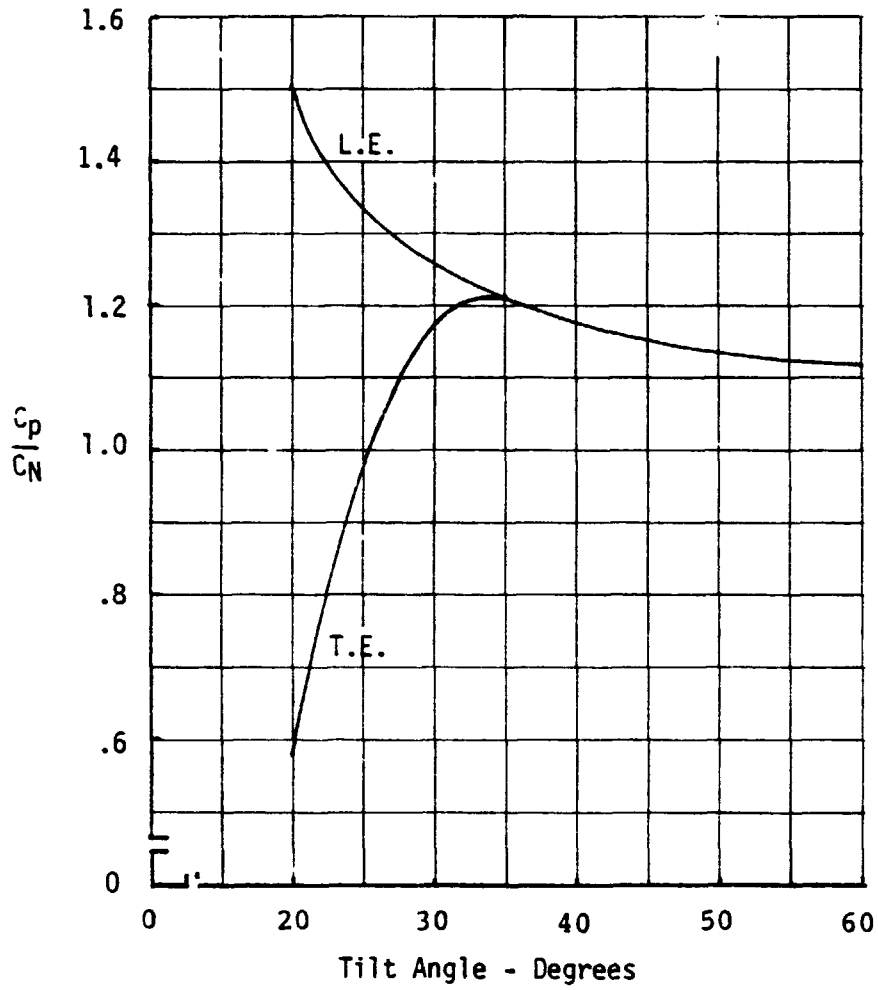
The application of these coefficients is similar to the examples shown in Section 7.1 and 7.2, except that  $C_p$  replaces  $\left(\frac{C_p}{C_N}\right)(C_N)$  in the examples.



•  $C_N$  based on wind reference velocity at 10 meters

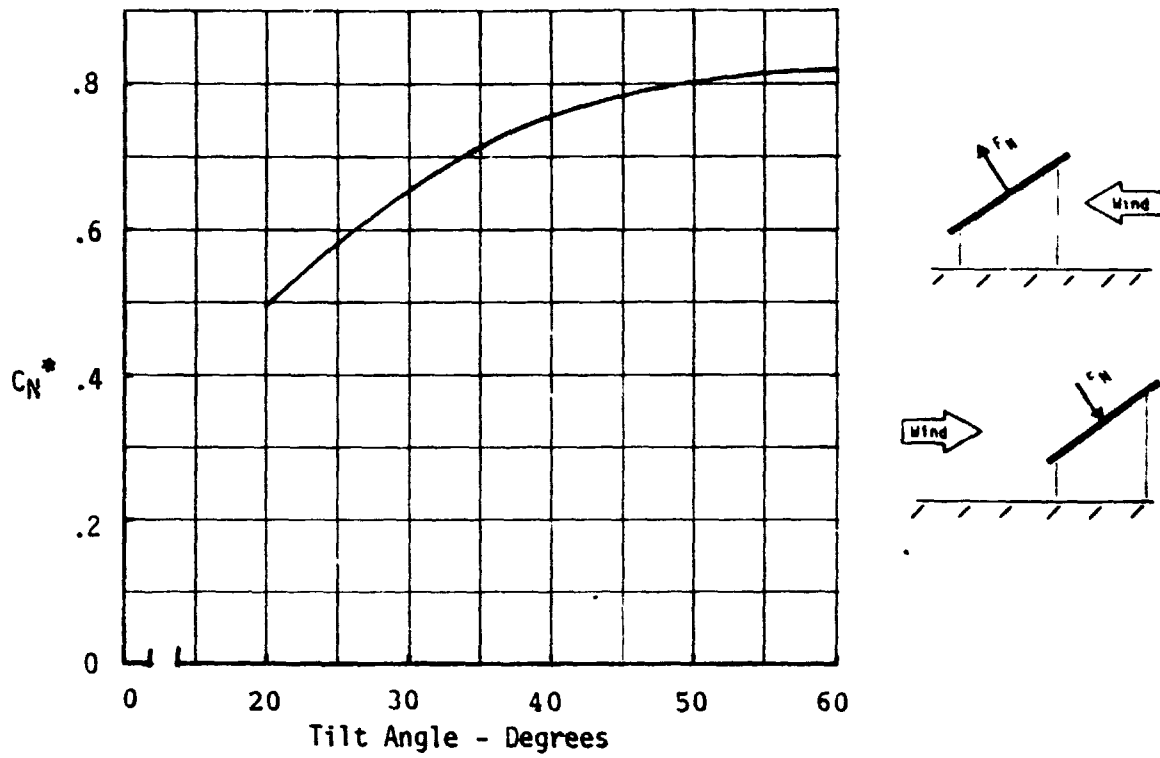
exception: not valid within two slant heights from the side edges

**Figure 7-1a. Steady State Wind Normal Force Coefficient Envelope for Arrays Within an Array Field or Behind a Protective Wind Barrier.**



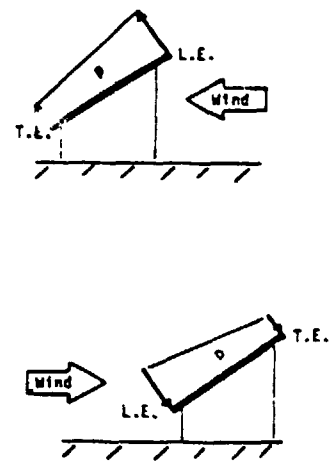
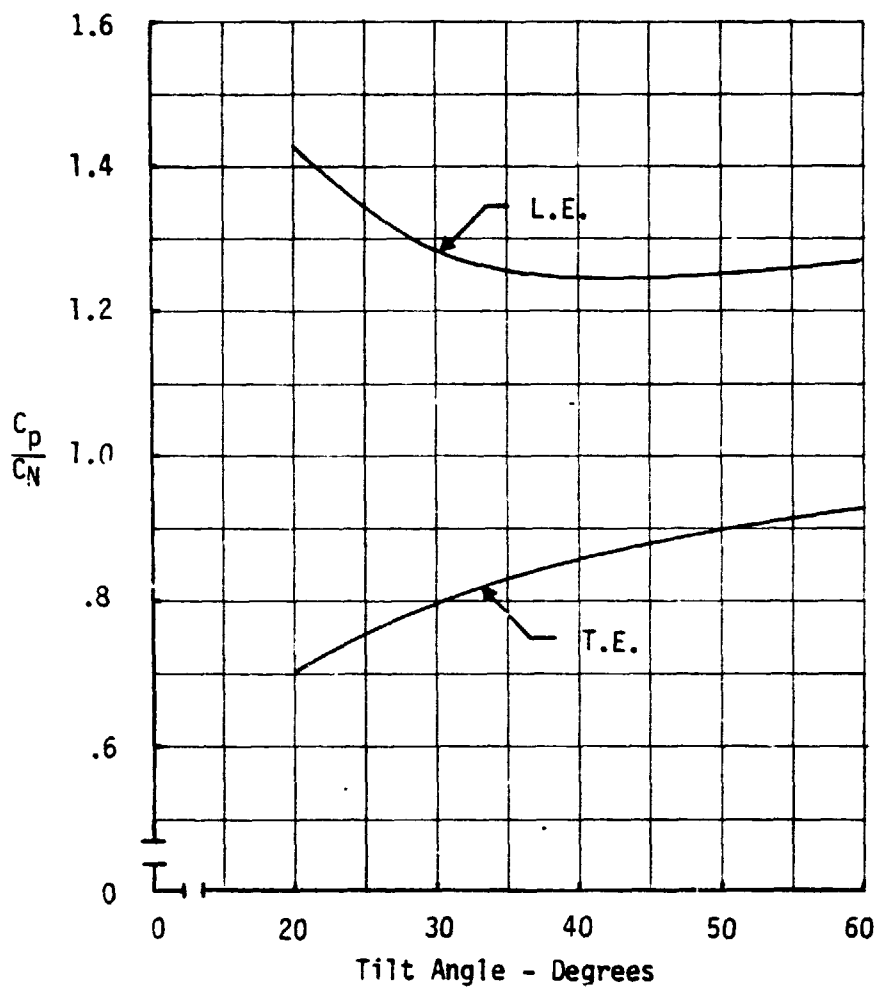
exception: not valid within two slant heights from the side edges

figure 7-1b. Steady State Wind Normalized Pressure Coefficient Envelope for Arrays Within an Array Field or Behind a Protective Wind Barrier



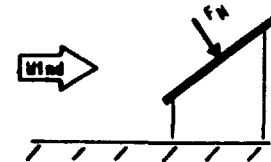
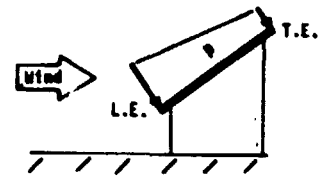
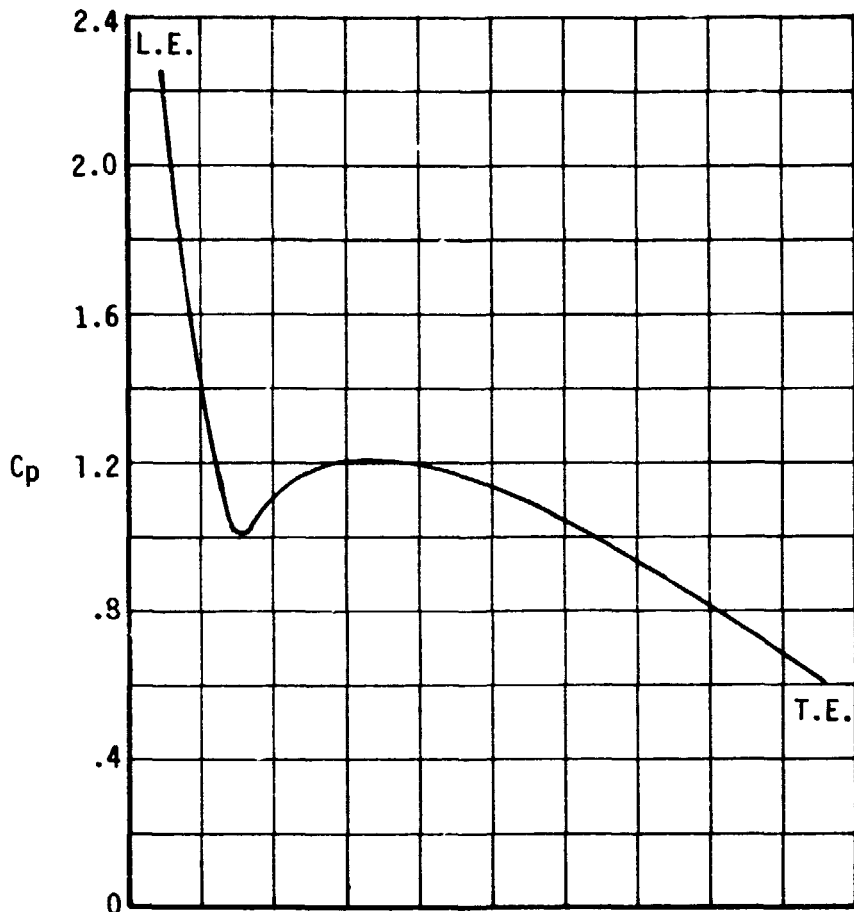
- $C_N$  based on wind reference velocity at 10 meters  
 exception: not valid within two slant heights from the side edges

**Figure 7-2a. Steady State Wind Normal Force Coefficient Envelope for the Two Outer Boundary Array Rows in an Array Field !Unprotected from the Wind**



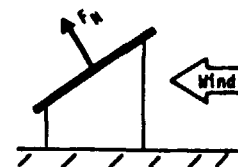
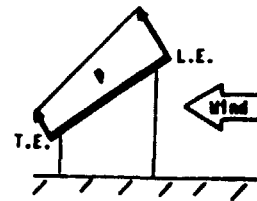
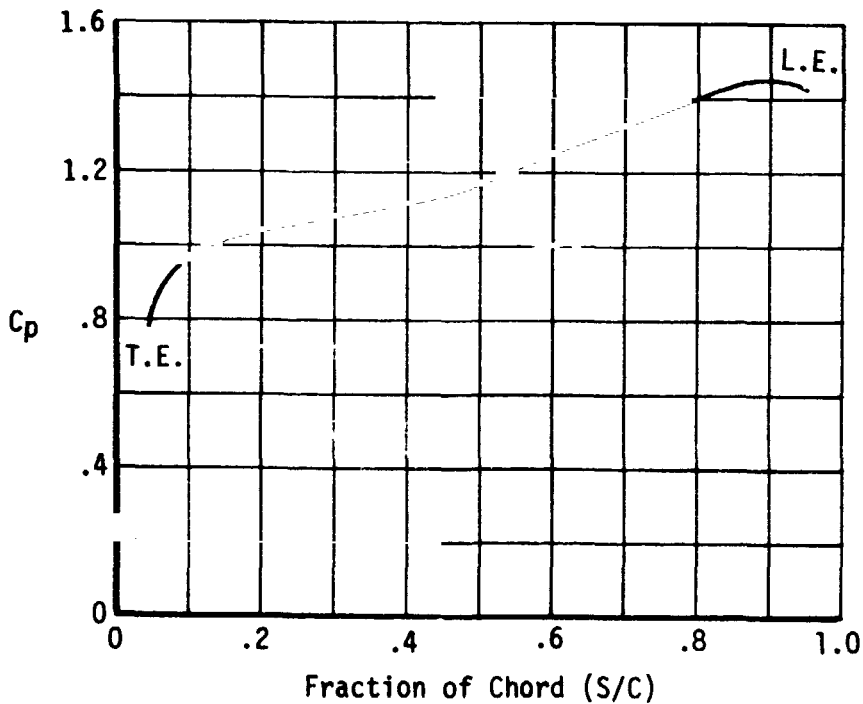
exception: not valid within two slant heights from the side edges

**Figure 7-2b. Steady State Wind Normalized Pressure Coefficient Envelope for the Two Outer Boundary Array Rows in an Array Field Unprotected from the Wind**



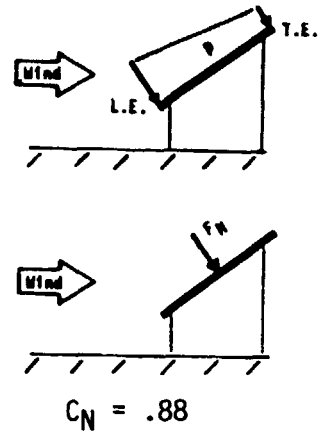
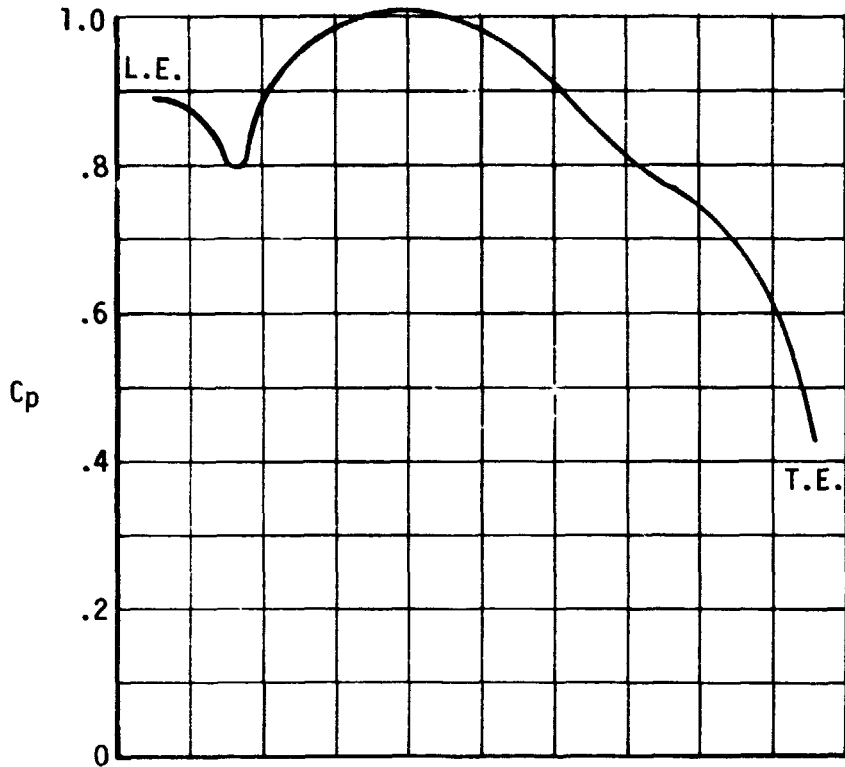
$$C_N = 1.12$$

Based on:  
Tilt Angle = 35°  
Wind reference velocity  
at 10 meters



$$C_N = 1.29$$

Figure 7-3a. Steady State Wind Pressure Coefficient and Normal Force Coefficient Guidelines for Edge Arrays in an Array Field (No Fence)



Based on:  
 Tilt Angle =  $35^\circ$   
 Wind reference velocity  
 at 10 meters

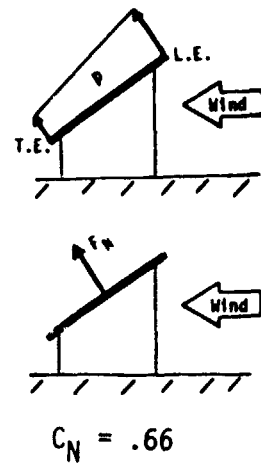
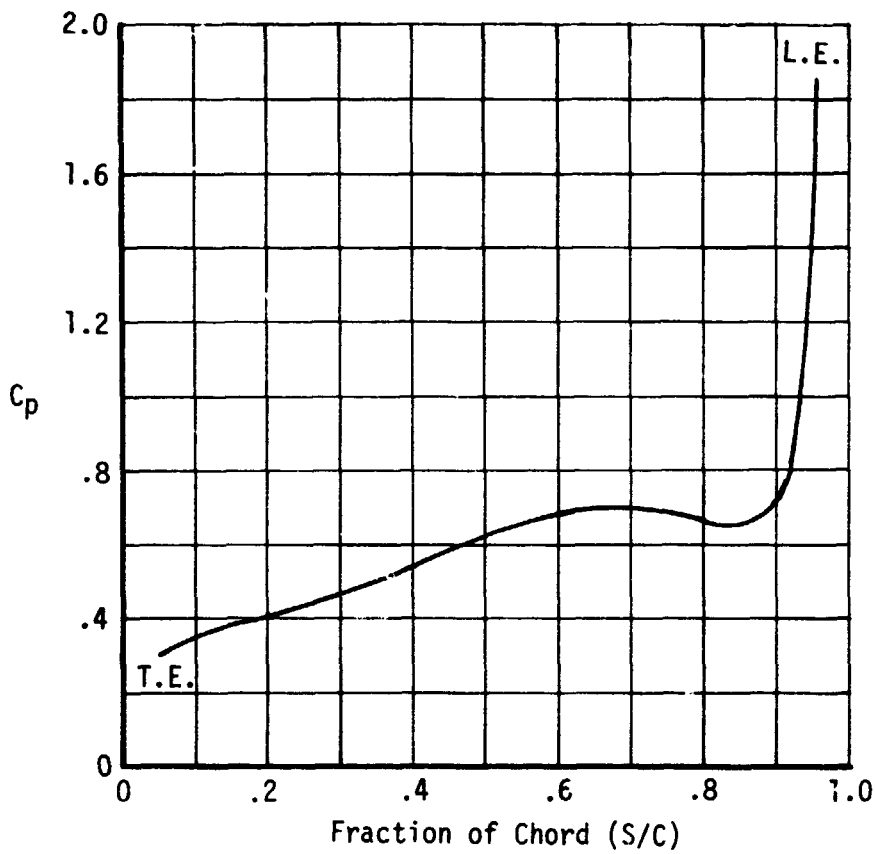
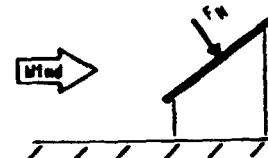
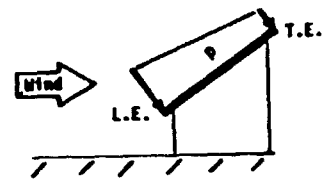
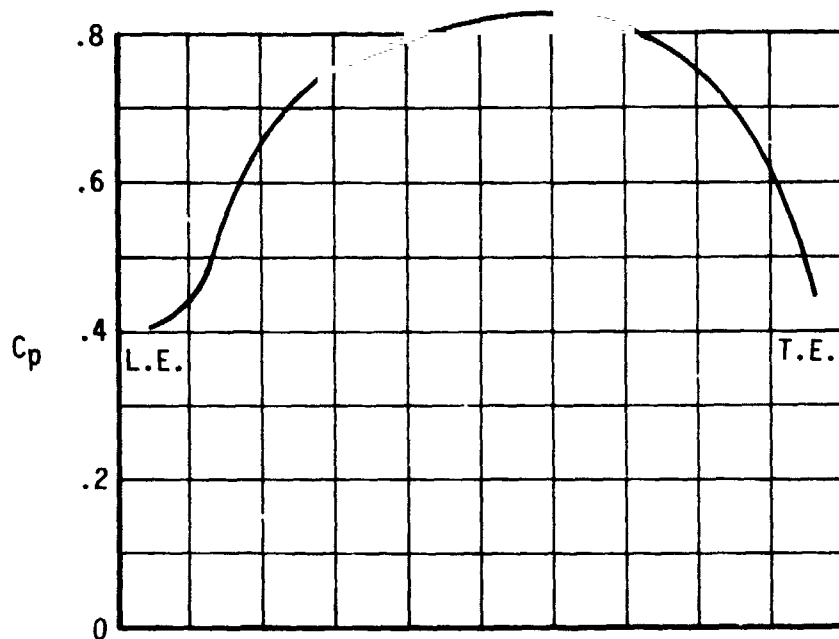
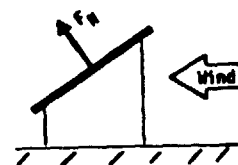
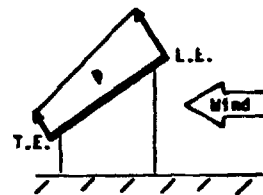
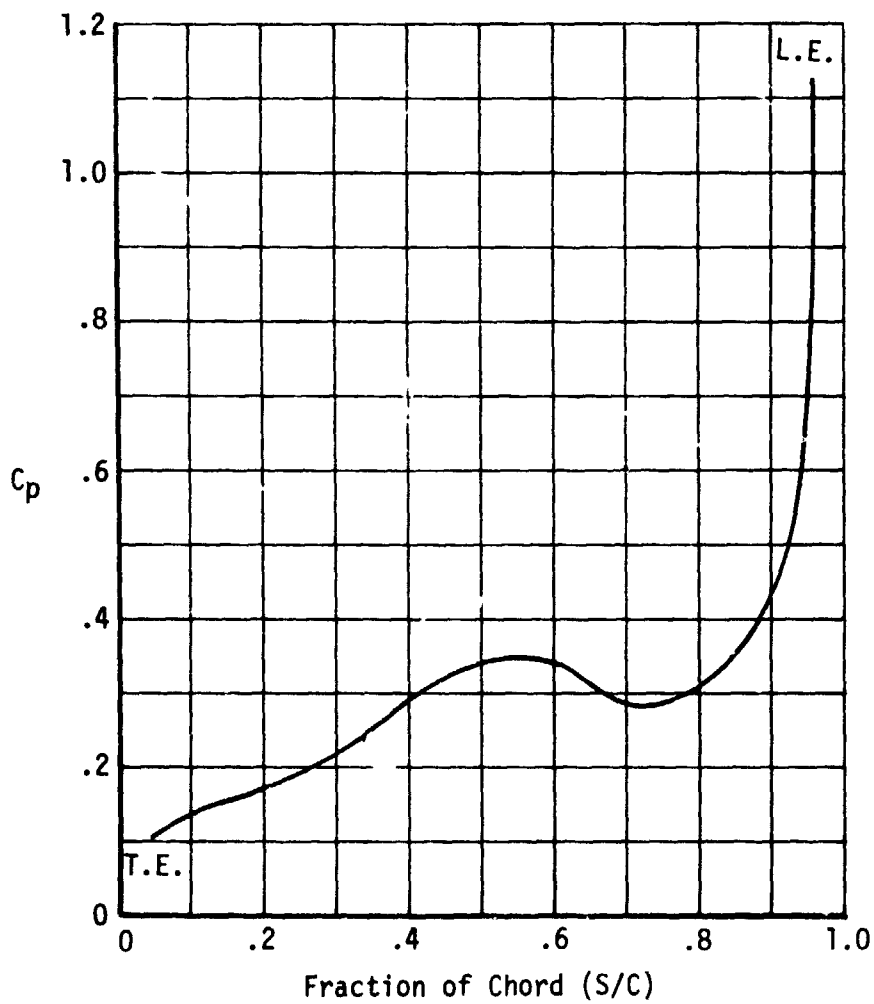


**Figure 7-3b. Steady State Wind Pressure Coefficient and Normal Force Coefficient Guidelines for Edge Arrays in an Array Field (Fence)**



$$C_N = .68$$

Based on:  
Tilt Angle =  $35^\circ$   
Wind reference velocity  
at 10 meters



$$C_N = .32$$

Figure 7-3c. Steady State Wind Pressure Coefficient and Normal Force Coefficient Guidelines for Edge Arrays in an Array Field (Fence with Modified Corners)

## 8.0 NEW TECHNOLOGY

No reportable items of new technology have been identified by Boeing during the contract of this work.

~~TOP SECRET~~

## 9.0 REFERENCES

1. National Photovoltaic Program, Program Plan, February 3, 1978, U.S. Department of Energy, Division of Solar Technology.
2. "Module/Array Interface Study," DOE/JPL-No. 954698-78/1, Bechtel National, Inc., Research and Engineering Operation, August, 1978.
3. "Feasibility Study of Solar Dome Encapsulation of Photovoltaic Arrays," DOE/JPL-No. 954833-78/1, Boeing Engineering and Construction Company, December, 1978.
4. A. G. Davenport, "Rationale for Determining Design Wind Velocities," Proceedings of the American Society of Civil Engineers, Vol. 86, No. ST5, May, 1960.
5. "Wind Loads on Flat Plate Photovoltaic Array Fields," DOE/JPL-No. 954833-79/2, Boeing Engineering and Construction, September, 1979.

**PRECEDING PAGE BLANK NOT FILMED**

PAGE \_\_\_\_\_ INTENCIONALES DEJAR

**APPENDIX**

**WIND LOADS ON FLAT PLATE  
PHOTOVOLTAIC ARRAY FIELDS**

**PHASE III - FINAL REPORT**

**WIND TUNNEL TEST REPORT**

**Prepared for Jet Propulsion Laboratory  
under Contract No. 9654833**

**Boeing Engineering and Construction Company  
A Division of The Boeing Company)  
Seattle, Washigton 98124**

**PRECEDING PAGE BLANK NOT FILMED**

~~CONFIDENTIAL~~ INTELLIGENCE REPORT

WIND PRESSURES AND FORCES ON  
FLAT-PLATE PHOTOVOLTAIC SOLAR ARRAYS

by

N. Hosoya,\* J. A. Peterka,\*\* M. Poreh,\*\*\*  
and J. E. Cermak\*\*\*\*

for

Boeing Engineering and Construction Company  
P. O. Box 3707  
Seattle, Washington 98124

Fluid Dynamics and Diffusion Laboratory  
Civil Engineering Department  
Colorado State University  
Fort Collins, Colorado 80523

September 1980

\*Graduate Research Assistant

\*\*Associate Professor

\*\*\*Professor

\*\*\*\*Professor-in-Charge, Fluid Mechanics  
and Wind Engineering Program

CER80-81NH-JAP-MP-JEC13

PRECEDING PAGE BLANK NOT FILMED

~~CONFIDENTIAL~~ UNRECORDED COPY

TABLE OF CONTENTS

	<u>Page</u>
LIST OF FIGURES . . . . .	v
LIST OF TABLES . . . . .	viii
LIST OF SYMBOLS . . . . .	x
1. INTRODUCTION . . . . .	A-1
2. EXPERIMENTAL CONFIGURATION . . . . .	A-3
2.1 Wind Tunnel . . . . .	A-3
2.2 Flow Simulation . . . . .	A-3
2.3 The Models . . . . .	A-6
3. INSTRUMENTATION AND DATA ACQUISITION . . . . .	A-8
3.1 Measurements of Flow Characteristics . . . . .	A-8
3.2 Pressure Measurements . . . . .	A-9
3.3 Normal Force Calculations . . . . .	A-9
4. PRESENTATION AND ANALYSIS OF THE EXPERIMENTAL DATA . . . . .	A-11
4.1 Single Array Tests . . . . .	A-11
4.2 Array Field Tests . . . . .	A-13
4.3 Flow Visualization . . . . .	A-14
5. CONCLUSIONS . . . . .	A-16
6. REFERENCES . . . . .	A-17
FIGURES . . . . .	A-18
TABLES . . . . .	A-58

PRECEDING PAGE BLANK NOT FILMED

~~CONFIDENTIAL~~ ~~CONFIDENTIAL~~ ~~CONFIDENTIAL~~

LIST OF FIGURES

<u>Figure</u>		<u>Page</u>
1	Meteorological Wind Tunnel . . . . .	A-19
2	Array Field Models in Meteorological Wind Tunnel . . . . .	A-20
3	Mean Velocity and Turbulence Distribution in Nonuniform Flow . . . . .	A-21
4	One Dimensional Velocity Spectra in Nonuniform Flow . . . . .	A-22
5	Turbulence Spectra in Nonuniform Flow (BL1) Compared to Atmospheric Spectra . . . . .	A-23
6	Mean Velocity and Turbulence Distribution in Uniform Flow . . . . .	A-24
7	Typical Horizontal Velocity Distribution across Meteorological Wind Tunnel . . . . .	A-25
8	1:12 Scale Models in Meteorological Wind Tunnel . . . . .	A-26
9	Photograph of Standard Corner Fence . . . . .	A-27
10	Position of Pressure Taps on Instrumented Model . . . . .	A-28
11	Schematic Description of Array Field . . . . .	A-29
12	Front and Back Pressures on a Single Array in Uniform Flow, $WD = 0^\circ$ , $H/c = 0.25$ , $\alpha = 20^\circ$ , $35^\circ$ , $60^\circ$ and $90^\circ$ . . . . .	A-30
13	Front and Back Pressures on a Single Array in Uniform Flow, $WD = 0^\circ$ , $H/c = 0.25$ , $\alpha = 120^\circ$ , $145^\circ$ and $160^\circ$ . . . . .	A-31
14	Front and Back Pressures on a Single Array in Uniform Flow, $WD = 0^\circ$ , $H/c = \text{infinity}$ , $\alpha = 20^\circ$ , $30^\circ$ , $60^\circ$ and $90^\circ$ . . . . .	A-32
15	Absolute Values of Normal Force Coefficients on a Single Array in Uniform Flow, $WD = 0^\circ$ . . . . .	A-33
16	Front and Back Pressures on a Single Array in Nonuniform Flow, $WD = 0^\circ$ , $H/c = 0.25$ , $\alpha = 20^\circ$ , $35^\circ$ , $60^\circ$ , and $90^\circ$ . . . . .	A-34

PRECEDING PAGE BLANK NOT FILMED

LIST OF FIGURES (Cont.)

<u>Figure</u>		<u>Page</u>
17	Front and Back Pressures on a Single Array in Nonuniform Flow, $WD = 0^\circ$ , $H/c = 0.25$ , $\alpha = 120^\circ$ , $145^\circ$ and $160^\circ$ . . . . .	A-35
18	Absolute Values of Normal Force Coefficient on a Single Array in Nonuniform and Uniform Flows, $WD = 0^\circ$ , $H/c = 0.25$ . . . . .	A-36
19	Normal Force Coefficients for an Array Field in Uniform Flow, $WD = 0$ , $x/c = 2.0$ , $H/c = 0.25$ , No Fence . . . . .	A-37
20	Normal Force Coefficients for an Array Field with a Fence of Various Height and Porosity, $WD = 0^\circ$ , $x/c = 2.0$ , $H/c = 0.25$ , $\alpha = 35^\circ$ . . . . .	A-38
21	Normal Force Coefficients for an Array Field with a Fence of Various Height and Porosity, $WD = 0^\circ$ , $x/c = 2.0$ , $H/c = 0.25$ , $\alpha = 145^\circ$ . . . . .	A-39
22	Corner Fence Configurations . . . . .	A-40
23	Normal Force Coefficients for an Array Field with Various Fence Configurations, $WD = 45^\circ$ , $x/c = 2.0$ , $H/c = 0.25$ , $MC = 0$ . . . . .	A-41
24	Model Configurations . . . . .	A-42
25	Normal Force Coefficients for an Array Field with Various Model Configurations, $WD = 45^\circ$ , $x/c = 2.0$ , $H/c = 0.25$ , $FC = 1$ . . . . .	A-43
26	Normal Force Coefficients for an Array Field in Nonuniform Flow, No Fence, $WD = 0^\circ$ , $H/c = 0.25$ , $\alpha = 20^\circ$ , $35^\circ$ , $60^\circ$ and $90^\circ$ . . . . .	A-44
27	Normal Force Coefficients for an Array Field in Nonuniform Flow, No Fence, $WD = 0^\circ$ , $H/C = 0.25$ , $\alpha = 120^\circ$ , $145^\circ$ and $160^\circ$ . . . . .	A-45
28	Normal Force Coefficients for an Array Field with Various Fences, $WD = 0^\circ$ , $x/c = 2.0$ , $H/c = 0.25$ , Nonuniform Flow . . . . .	A-46
29	Normal Force Coefficients for an Array Field, Edge and Corner Studies, $x/c = 2.0$ , $H/c = 0.25$ , Nonuniform Flow . . . . .	A-50

LIST OF FIGURES (Cont.)

<u>Figure</u>		<u>Page</u>
30	Normal Force Coefficients for an Array Field, Corner Study with Various Fence and Model Configurations, $x/c = 2.0$ , $H/c = 0.25$ , Nonuniform Flow . . . . .	A-52
31	Flow Visualization for an Array Field, $WD = 0^\circ$ . . . .	A-54
32	Flow Visualization for an Array Field, $WD = 45^\circ$ . . . .	A-57

LIST OF TABLES

<u>Table</u>		<u>Page</u>
1	Normal Force and Maximum Pressure Difference for a Single Array in Uniform Flow . . . . .	A-59
2	Normal Force and Maximum Pressure Difference for an Array Field in Uniform Flow, $x/c = 2.0$ . . . . .	A-60
3	Normal Force and Maximum Pressure Difference for an Array Field in Uniform Flow, $x/c = 1.5$ and $3.0$ . . . . .	A-61
4	Normal Force and Maximum Pressure Difference for a Single Array in Nonuniform Flow . . . . .	A-62
5	Normal Force and Maximum Pressure Difference for an Array Field in Nonuniform Flow, $x/c = 2.0$ . . . . .	A-63
6	Normal Force and Maximum Pressure Difference for an Array Field in Nonuniform Flow, $x/c = 1.5$ and $3.0$ . . . . .	A-64
7	Normal Force and Maximum Pressure Difference for an Array Field with a Fence, $H_f/c = 0.75$ , $P_f = 30\%$ , $x_f/c = 1.25$ . . . . .	A-65
8	Normal Force and Maximum Pressure Difference for an Array Field with a Fence, $H_f/c = 0.75$ , $P_f = 30\%$ , $x_f/c = 2.5$ . . . . .	A-66
9	Normal Force and Maximum Pressure Difference for an Array Field with a Fence, $H_f/c = 0.75$ , $P_f = 30\%$ , $x_f/c = 5.0$ . . . . .	A-67
10	Normal Force and Maximum Pressure Difference for an Array Field with a Fence of Various Height and Porosity . . . . .	A-68
11	Normal Force and Maximum Pressure Difference for an Array Field, Edge Study . . . . .	A-69
12	Normal Force and Maximum Pressure Difference for an Array Field, No Fence, Corner Study . . . . .	A-70
13	Normal Force and Maximum Pressure Difference for an Array Field with Various Fences, Corner Study . . . . .	A-71

LIST OF TABLES (continued)

<u>Table</u>	<u>Page</u>
14	Normal Force and Maximum Pressure Difference for an Array Field with Various Fences, MC = 1, Corner Study . . . . . A-72
15	Normal Force and Maximum Pressure Difference for an Array Field with Various Models, FC = 1 and 4, Corner Study . . . . . A-73
16	Normal Force and Maximum Pressure Difference for an Array Field with a Fence, $H_f/c = 1.0$ , $\alpha = 60^\circ$ and $120^\circ$ . . . . . A-74
17	Fence Configurations . . . . . A-75
18	List of Test Configurations . . . . . A-76

LIST OF SYMBOLS

<u>Symbol</u>	<u>Definition</u>
c	chord length of solar array
$C_N$	normal force coefficient
$C_p$	pressure coefficient
$\Delta C_{pmax}$	maximum pressure difference
D	characteristic length in Reynolds number
FC	fence configuration
F(N)	velocity spectrum
H	ground clearance of solar array
$H_{af}$	height of additional fence
$H_f$	height of fence
$H_s$	height of spoiler
MC	model configuration
N	frequency
P	pressure
$P_{af}$	porosity of additional fence
$P_f$	porosity of spoiler
$q_\infty$	dynamic pressure measured outside simulated boundary layer
$q_{ref}$	reference dynamic pressure
s	chordwise position--the edge where $s = 0$ corresponds to the leading edge for $\alpha \geq 90^\circ$ and the trailing edge for $\alpha < 90^\circ$
$s_{max}$	chordwise position where maximum pressure difference is observed
U	velocity of wind
$U_{ref}$	reference velocity of wind
$U_{rms}$	variance of fluctuating velocity

LIST OF SYMBOLS (Cont.)

<u>Symbol</u>	<u>Definition</u>
$U_{\delta}$	velocity of wind at simulated boundary layer height
$U_{\infty}$	velocity of wind measured outside simulated boundary layer
$x$	separation distance of solar array
$x_f$	separation distance between fence and solar array
$\alpha$	angle of attack of solar array
$\delta$	height of simulated boundary layer
$\nu$	kinematic viscosity of air
$\rho$	density of air



## 1. INTRODUCTION

An important factor influencing the design and subsequently cost of large photovoltaic power generating systems, which involve a large number of simple structural elements and supports, is the magnitude of wind-induced loads. It has been recognized that usual design procedures, like the ANSI code (A58.1 - 1972) for example [1], are not adequate for accurate wind design of these repetitive, photovoltaic arrays with their distinctive configuration, orientation and limited height. In fact, the information presently available in the technical literature is not sufficient even for an optimum design of the structure for supporting a single photovoltaic array. Wind loads on individual arrays at different locations in a large array field are more difficult to determine as they vary according to the array location in the field and wind direction in a complicated manner. Higher loads are expected to exist at the edges of the field, but those can be reduced by carefully designed fences or barriers.

A theoretical study of the aerodynamics of flat plate arrays was recently made by Ronald D. Miller and Donald Zimmerman [2] at the Boeing Engineering and Construction Company (BECC). The study identified the basic features of the flat plate array loading which can be used for design purposes. It has been recognized by the authors, however, that theoretically derived design criteria are conservative and a wind-tunnel study of the wind loadings of such arrays was therefore recommended.

This report describes the experimental study of wind loading on flat plate photovoltaic arrays and array fields performed in the Meteorological Wind Tunnel of the Fluid Dynamics and Diffusion Laboratory at Colorado State University for BECC. The experimental program was developed in cooperation with Ronald D. Miller (BECC). The program's objectives were to determine the pressure distribution and forces acting on photovoltaic arrays for different angles of attack, two wind directions, head on winds and cornering winds ( $WD = 0^\circ$  and  $45^\circ$  as defined in Figure 11) and two velocity profiles, as well as to investigate the effect of different fences and barriers on the wind loading at the edges and corners of an array field.

The wind-tunnel results were analyzed and the effect of the various parameters are presented in a form permitting calculation of the wind loading on prototype photovoltaic structures.

In view of the large number of data points collected in the report, it was found convenient to present most of the pressure measurements in a separate Appendix. The main report includes, however, a full description of the various runs and the calculated values of the normal force coefficient, the maximum local pressure coefficient and its location for each run in a tabulated form (Table 1 to 16) as well as a graphical representation of these data.

## 2. EXPERIMENTAL CONFIGURATION

### 2.1 Wind Tunnel

The Meteorological Wind Tunnel of the Fluid Dynamics and Diffusion Laboratory at Colorado State University (Figure 1) is characterized by a long (96 ft), slightly diverging test section, 6 ft-8 in. wide (at the turntable) and 6 ft high. The ceiling is adjustable to avoid pressure gradient along the test section. This facility is driven by a 400 HP variable pitch propeller with air flow velocity varying continuously from 0.5 fps up to 100 fps.

### 2.2 Flow Simulation

The primary consideration in modeling wind forces on structures in a wind tunnel is that the wind characteristics in the tunnel simulate natural boundary-layer winds at the actual site. In general this requires that the vertical distribution of mean velocity and turbulence in the wind tunnel boundary layer match those at the site and that the Reynolds numbers of the model and the prototype be equal. In addition, the small-scale model must be geometrically similar to its prototype. A detailed discussion of these requirements and their implementation in the wind-tunnel environment can be found in references 3, 4, and 5.

The construction of a 1:24 scale model of a prototype structure and its immediate surroundings (in this case, a flat, open area), submerged in a turbulent boundary layer of the Meteorological Wind Tunnel, shown in Figure 1, satisfies all the above criteria except those of equal Reynolds numbers and similarity of turbulence intensity and scale.

The kinematic viscosity  $\nu$  appearing in the Reynolds number  $UD/\nu$  is the same for both the tunnel and the full-scale structure. Because of this, the wind-tunnel air speed,  $U$ , would have to be 24 times the full-scale value if the model and prototype Reynolds numbers are to be equal. Testing at such high wind speeds is not feasible. However, for Reynolds numbers larger than  $2 \times 10^4$  for sharp-edged structures where the flow separation point is fixed, there is no significant change in the values of aerodynamic coefficients as the Reynolds number increases. Since typical Reynolds number values are  $10^6$ - $10^7$  for high-wind, full-scale flow and about  $5 \times 10^4$  for wind-tunnel flows, acceptable flow similarity is achieved without equality of Reynolds numbers.

At a model scale of 1:24, the larger scales of turbulence in the atmospheric boundary layer are not simulated in the wind-tunnel flow. However, because the integral scale of the turbulence in the wind tunnel was 2 to 3 times the largest dimension of the model collector, the influence of the scale of turbulence is not expected to be significant [6]. Evidence exists which demonstrates some influence of turbulence intensity on drag of flat plates [6,7,8]. Because the turbulence intensity difference between the current simulation and a simulation with complete similarity of turbulent structure is not large, the effects due to turbulence intensity should be small. For cases where an upstream collector disturbs the approach flow, turbulence characteristics are dominated by the wake characteristics of the upstream object and possible differences due to turbulence intensity should further decrease.

An important factor which affects the wind loadings is the structure of the atmospheric boundary layer near the ground. The boundary layer which develops over a flat terrain is usually characterized by a non-uniform velocity profile which is closely described by a 1/7th power law mean velocity distribution. It is impossible to simulate in a wind tunnel the entire atmospheric boundary layer at the desired model scale for this study (1:24). One can, however, simulate the lower part of the atmospheric boundary layer in a 45 in. deep wind tunnel boundary layer [3-5].

The shape of the 1/7th power law boundary layer, which will be referred to as the Nonuniform flow 1 was obtained by means of selected roughness on the wind-tunnel floor upstream of the model. Forty ft of test section length were covered with 1 in. cubes followed by a 40 ft length of pegboard with 0.25 in. diameter pegs projecting 0.5 in. above the pegboard base (see Figure 2). In addition to the floor roughness, four triangular spires were installed at the test section entrance in order to get a thicker boundary layer than would otherwise be obtained. The normalized velocity and turbulence profiles of this boundary layer are shown in Figure 3 and data is tabulated in the Appendix. Turbulence intensity is the root-mean-square of the longitudinal fluctuating velocity divided by the local mean velocity. The turbulence intensity reached values of 20 percent in the boundary layer.

The spectrum of longitudinal velocity fluctuations is shown in Figures 4 and 5, including two suggested analytical models of velocity spectra for the atmosphere by Harris (9) and Davenport (10).

The spectra were obtained at 4 and 8 in. above the wind-tunnel floor. In this plot  $N$  is frequency,  $F(N)$  is the velocity spectrum,  $U_{rms}^2$  is the variance of the fluctuating velocity,  $\delta$  is the simulated boundary layer height (900 ft full-scale), and  $U_\delta$  is the velocity at  $\delta$ . The region where turbulence structure may be important to the determination of mean loading ranges upward from abscissa values of about 20 for wind speeds up to about 30 mph at 30 ft. Thus, the simulation has a turbulence intensity somewhat too high in the frequency range affecting mean wind loading on the model and too low in the low-frequency gusts.

The "Uniform Flow" velocity profile was obtained by placing the model at the upstream end of the test section. The measured velocity profile at that station, shown in Figure 6, indicates that a very thin boundary layer has developed along the short upstream section. Its effect on the wind loading on elevated panels is expected, however, to be small. A typical velocity distribution across the tunnel is shown in Figure 7.

### 2.3 The Models

Aluminum models of the flat photovoltaic array field having a geometrical scaling of 1:24 (Figure 2) and 1:12 (Figure 8) were constructed. (The 1:12 model was used in a limited number of tests only).

The chord size of the 1:24 model was  $c = 4$  in., corresponding to a prototype value of 8 ft. Rows of pressure taps were drilled on each face of the array as shown in Figure 10. Each pressure tap represents the average pressure along a small section of the chord. The row at the edge of the array was used to study the wind loading at the side edge of the field.

To study the wind loadings on an array located in an array field, 1:24 scale models of array rows were constructed, which could be placed on the wind tunnel floor at desired locations to simulate the relative position in the field on the array with the pressure taps on which the wind loading was measured. Figure 2 shows a photograph of a 1:24 model of a photovoltaic array field in the wind tunnel. Figure 8 shows a photograph of the 1:12 model.

The fence was simulated in the model by perforated sheet metal, with holes of 3/16 in. diameter, having the same porosity (about 30 percent) as the prototype fence (see Figure 9).

### 3. INSTRUMENTATION AND DATA ACQUISITION

#### 3.1 Measurements of Flow Characteristics

Velocity and turbulence intensity profiles for the approach flow under test conditions were made at the locations of the model in the tunnel (turntable) with the model removed.

The measurements were made with a Thermosystems Model 1050 constant-temperature anemometer with a 0.001 in. diameter platinum film sensing element 0.02 in. long. The sensing probe was attached to a vertical traverse to measure velocities and turbulent intensities at different heights. Output was processed through the Laboratory on-line digital data acquisition system.

Tests were made at only one wind speed in the tunnel around 50 ft/sec. This wind was sufficiently high to ensure Reynolds number similarity between the model and prototype.

The reference velocity at each test was measured using a pitot-static tube which was connected to a Setra differential pressure transducer. The pitot tube was placed outside the simulated boundary layer and recorded the value of  $q_{\infty} = \rho U_{\infty}^2 / 2$ , where  $\rho$  is the mass density of the air. The ratio of the reference velocity  $U_{\text{ref}}$ , at a prototype height of 10 m above the ground, to  $U_{\infty}$  was determined from the velocity distribution of the boundary layer according to the scale of the model. The value

$$q_{\text{ref}} = \frac{\rho U_{\text{ref}}^2}{2} = \frac{\rho U_{\infty}^2}{2} \left( \frac{U_{\text{ref}}}{U_{\infty}} \right)^2 \quad (1)$$

at the height corresponding to 10 m above ground in the prototype was later used in calculating the dimensionless force and moment coefficients of the array, so that it was not necessary to measure the density of the air.

### 3.2 Pressure Measurements

Each pressure tap was connected through a pressure switch to a calibrated Setra differential transducer which measured the value of the local pressure above the ambient pressure at the test section away from the model. The output from the pressure transducers was recorded for 16 seconds at a 250 sample per second rate. The data was then analyzed by a Hewlett-Packard System 1000 minicomputer under program control and recorded. The minicomputer calculated the local pressure coefficients and using the reference total value  $q_{ref}$ , at 30 ft prototype height,

$$C_p = \frac{P}{q_{ref}} \quad (2)$$

### 3.3 Normal Force Calculations

The local force per unit area acting on each section of the array is equal to the difference in the pressures measured at the center of that section on the opposite faces of the array. The magnitude of this pressure difference is

$$\Delta p(s) = P(s)_{\text{lower face of array}} - P(s)_{\text{upper face of array}} \quad (3)$$

where  $s$  designates the position of the section as defined in Figure 11. A positive value of  $\Delta p(s)$  will thus correspond to a

normal net force per unit area with an upward component as shown schematically in Figure 11.

The dimensionless local pressure difference is defined as

$$\Delta C_p = \frac{\Delta P}{q_{\text{ref}}} . \quad (4)$$

The maximum value of this coefficient,  $\Delta C_{p_{\text{max}}}$  is of particular interest. The normal force  $N$  acting on the entire array can be calculated by integrating the value of  $\Delta p(s)$  over the cord. Similarly, the normal force coefficient  $C_N$  is given by

$$C_N = \frac{N}{c} = \frac{1}{c} \int_0^c \Delta C_p(s) ds \quad (5)$$

The direction of a positive normal force is shown in Figure 11. In most cases one would expect to find negative values of  $C_N$  for  $\alpha > 90^\circ$ .

## 4. PRESENTATION AND ANALYSIS OF THE EXPERIMENTAL DATA

4.1 Single Array Tests

Typical records of the pressure distribution on a single photovoltaic array for head-on winds ( $WD = 0^\circ$ ) in the uniform flow are shown in Figures 12-14.\* The solid lines in Figure 12 show the local pressure coefficient distributions on the upstream face of the panel. Positive values are usually recorded on the upstream face. The pressure coefficients on the downstream face, marked by dashed lines, are negative and hardly vary across the panel, indicating a flow separation, which was observed in the flow visualization study for both the single array and many of the arrays in an array field, see for example Figure 31. The shape of the pressure distribution curves on the upstream face of the panel is almost symmetric for  $\alpha = 90^\circ$ , but it becomes more and more skewed as the angle of attack decreases (Figure 12) or increases (Figure 13). Figure 14 shows the same data but for a large ground clearance,  $H/c = \infty$  (actually measured at  $H/c = 1.7$ ).

Comparing Figures 12 and 14 one finds that the pressure distribution on the upstream face of the panel is not affected to a large extent by the ground clearance. The back pressure, on the other hand, appears to change significantly. A value of  $C_p \approx -1.35$  was recorded for  $\alpha = 90^\circ$ ,  $H/c = \infty$ , whereas a value of  $C_p = -0.75$  was recorded for the same angle of attack with a ground clearance of  $H/c = 0.25$ . This reduction of the back pressure reduces significantly the normal force acting on the plate. Figure 15 shows the absolute values of

---

\*Unless explicitly stated, the data refers to the measurements at the center of the array (see Figure 10).

the normal force for all the single array tests in a uniform flow. Evidently, the same effect is apparent at all angles of attack.

The reduced drag at small ground clearances may be due to the changes in the wakes caused by the reduction in the eddy size downstream of the panel. It should be recalled that the approach velocities in these tests are independent of height. The complicated nature of the interaction between these eddies and the flow, which determine the base pressure, makes it difficult to predict the value of these pressures theoretically.

The pressure distributions on a single array ( $H/c = 0.25$ ) in a nonuniform flow are shown in Figures 16 and 17. A clear reduction of the pressure coefficients relative to those in the uniform flow is observed. The corresponding absolute values of the normal force for the two cases are shown in Figure 18. The average ratio  $C_N(\text{uniform})/C_N(\text{nonuniform})$  is  $1.43 \pm 5\%$  for these tests. This large reduction is primarily due to the relatively small wind speeds at the height of the array for the nonuniform velocity profile. It should be recalled that  $q_{\text{ref}}$  is measured at the height of 10 m above the ground whereas the center of the panel, for this value of ground clearance, varies from 3.36 ft for  $\alpha = 20^\circ$  to 6 ft for  $\alpha = 90^\circ$ . The corresponding ratios of  $q_{\text{ref}}/q_{\text{center of panel}}$  for these cases in a 1/7th power law velocity distribution are 1.89 and 1.61 respectively. Obviously, the difference in the dynamic pressure of the free stream at the height of the panel alone cannot fully explain the observed changes. Comparing the ratio of the back pressures in the two cases, for example, one finds an average ratio

of almost 2, whereas the ratio of the pressure coefficients on the upstream face of the panel is only around 1.5. The shape of the corresponding pressure distribution curves is also different for the two cases.

#### 4.2 Array Field Tests

A wide field of photovoltaic arrays is characterized by the separation distance,  $x/c$ , between the array (see Figure 11) and their angle of attack. The value of the normal force acting on each array depends, of course, on its position in the field. Figure 19 shows the values of  $C_N$  for the 1st, 2nd and 5th arrays (from the upstream edge of the field) for head-on uniform winds. The magnitudes of the normal force on array No. 1 are approximately equal to their values in a single array. A drastic reduction in the magnitude of the normal forces on the 2nd and 5th arrays is observed. In some cases the direction of the normal force is reversed.

The magnitude of the forces acting on the 1st array can be reduced by building a fence or a barrier (zero porosity fence) upstream of the field. The effect of the fence depends on its porosity, height and distance. Figure 20 shows the effect of a 30 percent porosity fence and a zero porosity fence on the magnitude of the normal forces acting on the 1st and 2nd rows for different fence heights, and for an angle of attack  $\alpha = 35^\circ$ . Similar results are obtained at different angles of attacks (see Figure 21).

The magnitude of the normal forces at the edge of an array, in case of head-on winds, is expected to be smaller than that of the forces acting on the center of the array. In case of side winds, however, the edges of the field and particularly the upstream corner will be exposed to higher loads. These forces can be reduced by a side fence and/or by different corner fence configurations. Figure 22 shows the corner fence configurations tested in this study. Their effect on the magnitude of the normal force for cornering winds is shown in Figure 23, which clearly exhibits the effect of properly designed fences on the normal forces at the field edges and corners.

Another way to reduce forces at the edge of the array field is to extend the array by an inexpensive stronger structure or by modifying the shape of the array edges. Several configurations, shown in Figure 24, have been studied. The fence configurations are also tabulated in Table 17. Their effect on the normal forces at the corner for  $WD = 45^\circ$  is shown in Figure 25 for  $\alpha = 35^\circ$  and  $\alpha = 145^\circ$ .

An overall view of the results and the effect of the various parameters on the normal forces is shown in Figures 26-30. Figures 26 and 27 show the effect of the distance between the arrays for different angles of attack. Figure 28 summarizes the fence study for head-on winds. Figures 29-30 show the effect of the corner fences and the modifications of the array edges. All test configurations investigated for this study are listed in Table 18.

#### 4.3 Flow Visualization

Flow visualization was used in this study to explore the structure of the flow in the array field and to obtain a better understanding of the force and pressure measurements.

Figure 31a shows the wake behind the first array in the field and behind an array in the center of the field. Clear flow separation is observed for this angle of attack and spacing. Figures 31b and 31c show the structure and the nature of the flow at different points between the arrays.

Figure 32 shows two corner fence configurations and their effect on the flow structure near the fence.

5. CONCLUSIONS

Wind loadings on photovoltaic arrays in a large array field were measured on 1:24 and 1:12 scale wind-tunnel models. The dimensionless pressure and force coefficients measured are independent of the Reynolds number and can therefore be used for the design of prototype arrays.

Considerable differences were found between the normal force coefficients for uniform and nonuniform velocity fields. The arrays at the edges and corners of the field will usually be exposed to much larger forces than the arrays in the interior of the field. These forces can be considerably reduced, however, by fences and barriers. Data is presented which make it possible to design the prototype array field and fences for given atmospheric winds.

## 6. REFERENCES

1. American National Standards Institute, American National Standard Building Code Requirements for Minimum Design Loads in Buildings and Other Structures, ANSI Standard A58.1, 1972.
2. Miller, R. D. and Zimmerman, D., Wind Loads on Flat Plate Photovoltaic Array Fields, Boeing Engineering and Construction Report No. DOE/JPLG54833-79/2, Seattle, Washington 98124, September 1979.
3. Cermak, J. E., Aerodynamics of Buildings, Annual Review of Fluid Mechanics, Vol. 8, 1976.
4. Cermak, J. E., Laboratory Simulation of the Atmospheric Boundary Layer, AIAA J1., Vol. 9, September 1971.
5. Cermak, J. E., Applications of Fluid Mechanics to Wind Engineering, A Freeman Scholar Lecture, ASME J1. of Fluids Engineering, Vol. 97, No. 1, March 1975.
6. Bearman, P. W., Turbulence Effects on Bluff Body Mean Flow, Third U.S. National Conference on Wind Engineering Research, pp. 265-272, 1978.
7. Bearman, P. W., An Investigation of the Forces on Flat Plates Normal to a Turbulent Flow, J1. Fluid Mechanics, Vol. 46, pp. 177-198, 1971.
8. Nakamura, Y. and Tomonari, Y., The Effect of Turbulence on the Drag of Rectangular Prisms, Transactions Japan Society of Aeronautical and Space Science, Vol. 19, pp. 81-86, 1976.
9. Harris, R. I., The Nature of the Wind, Modern Design for Wind Sensitive Structures, Paper 3, 1971.
10. Davenport, A. G., The Spectrum of Horizontal Gustiness Near the Ground, Quarterly J1., Royal Meteorological Society, Vol. 81, pp. 194-211, 1961.

**A-18**

**FIGURES**

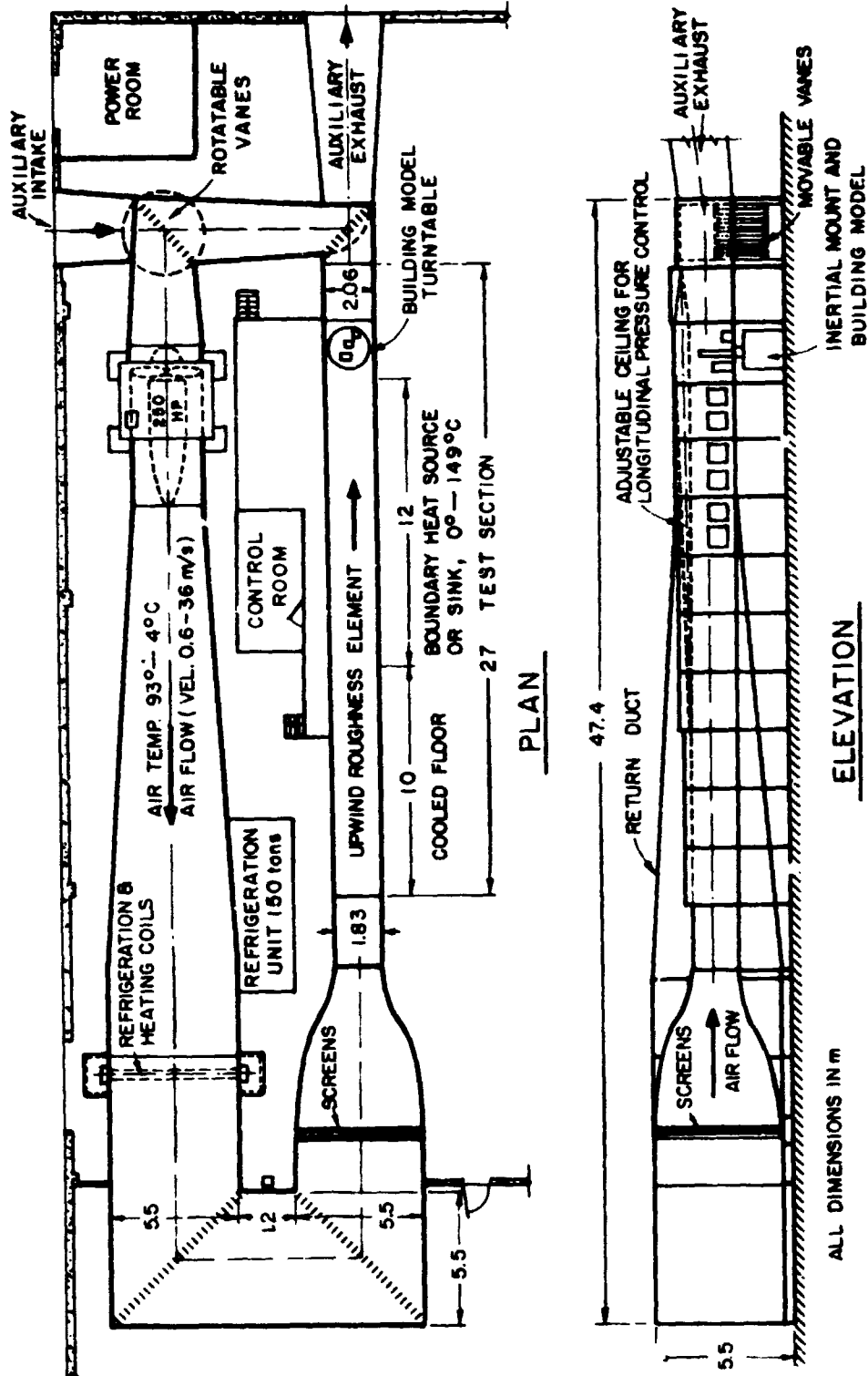
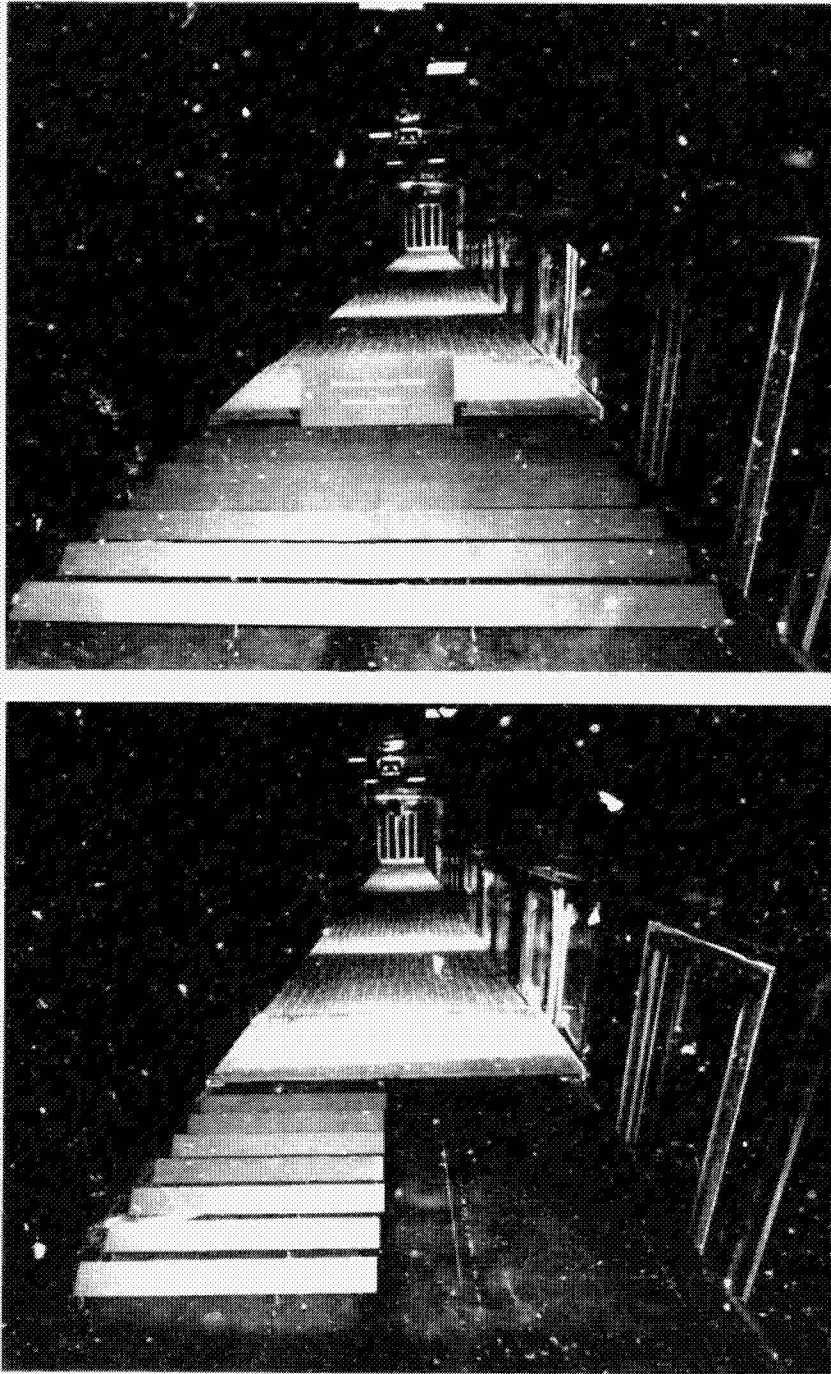


Figure 1. Meteorological Wind Tunnel



*Figure 2. Array Field Models in Meteorological Wind Tunnel*

ORIGINAL PAGE IS  
OF POOR QUALITY

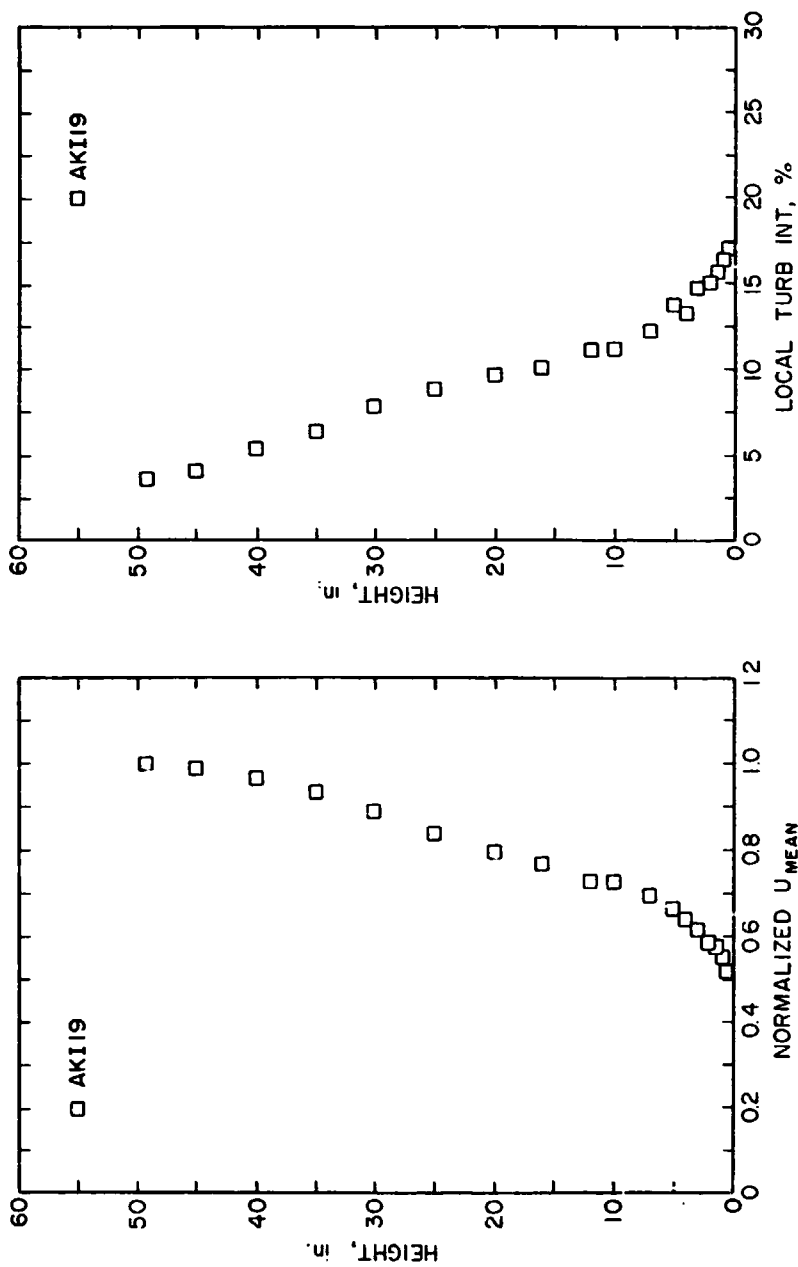


Figure 3. Mean Velocity and Turbulence Distribution in Nonuniform Flow

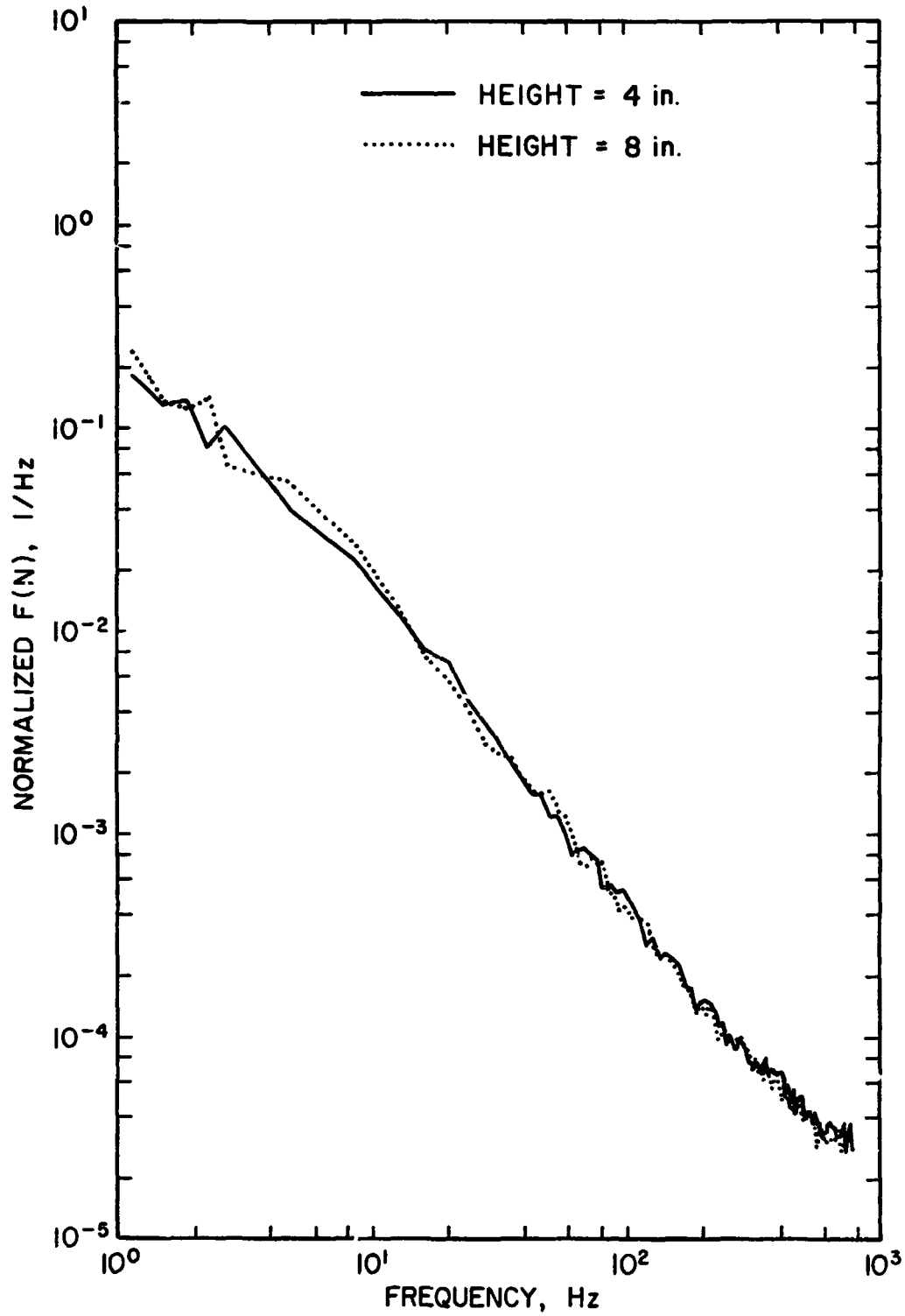


Figure 4. One Dimensional Velocity Spectra in Nonuniform Flow

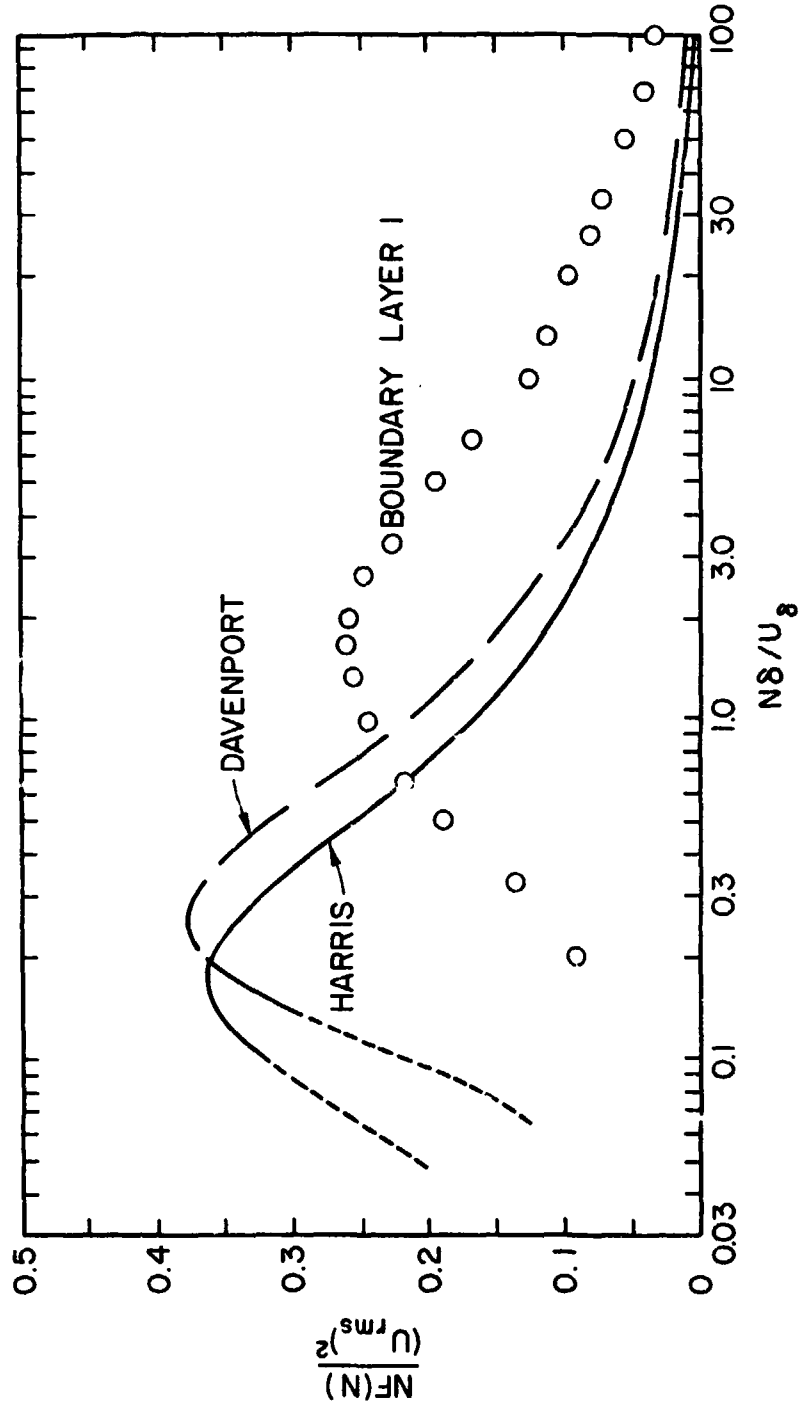


Figure 5. Turbulence Spectra in Nonuniform Flow (BL1) Compared to Atmospheric Spectra

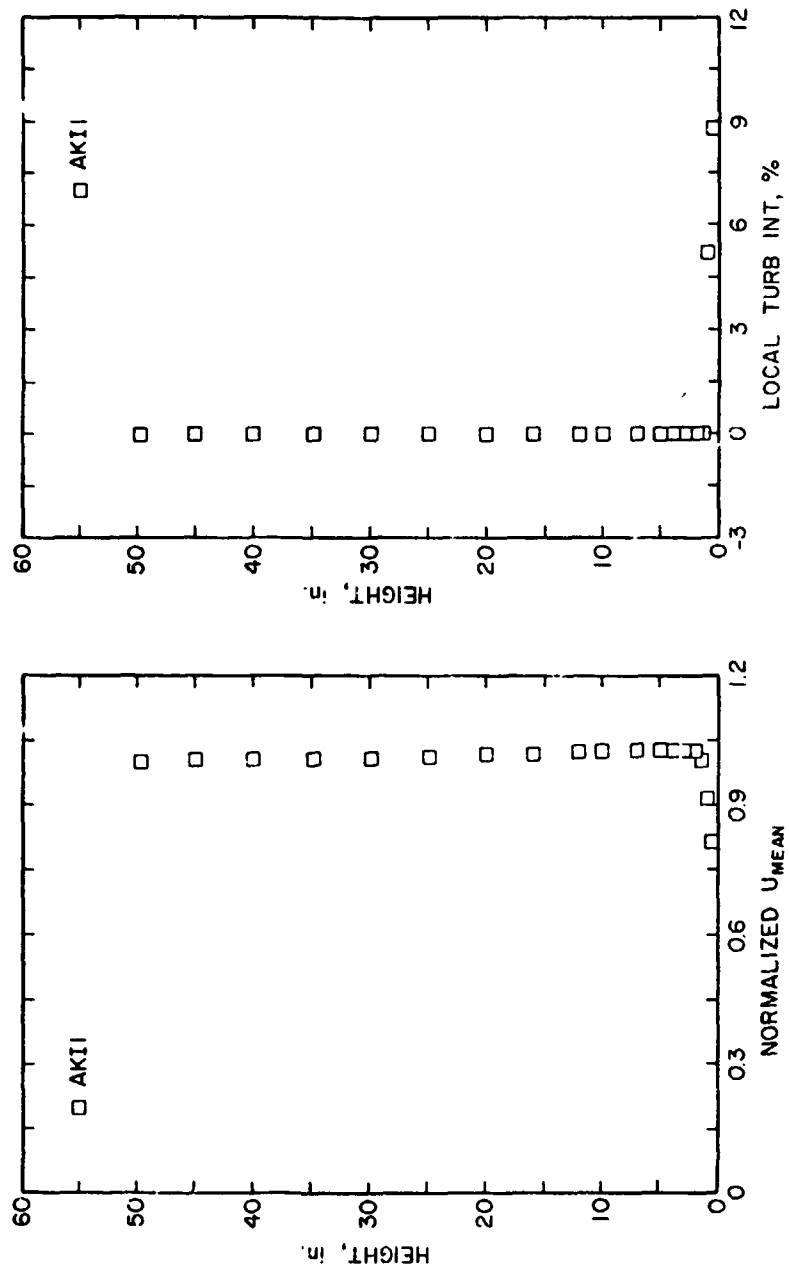


Figure 6. Mean Velocity and Turbulence Distribution in Uniform Flow

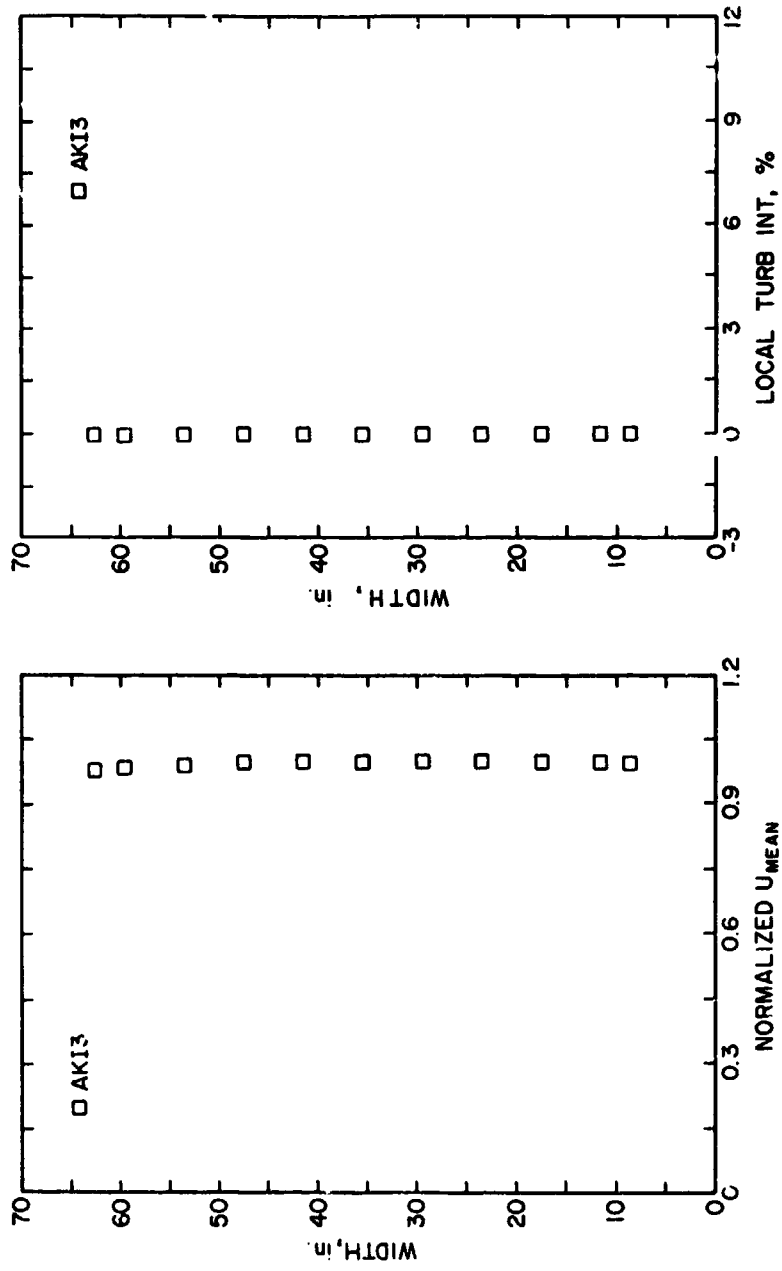
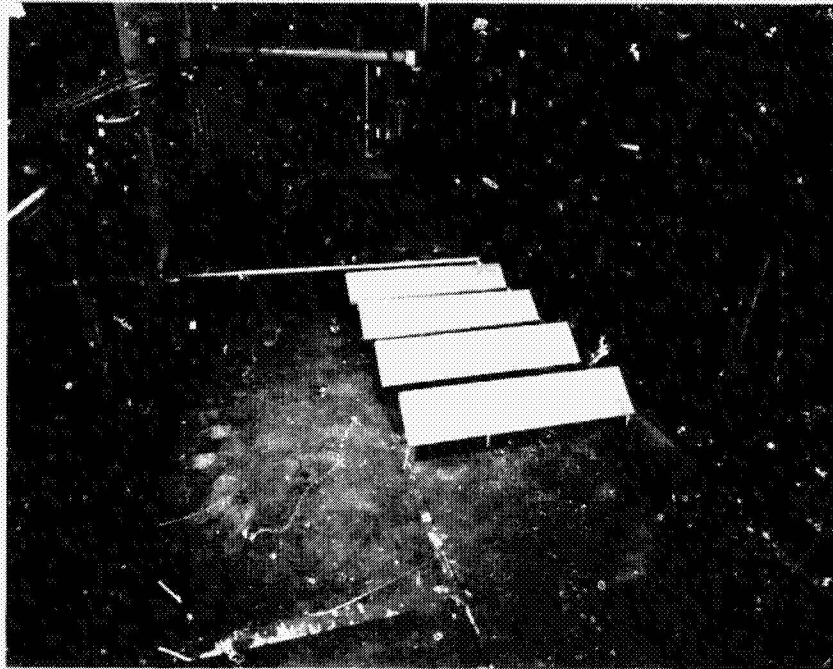
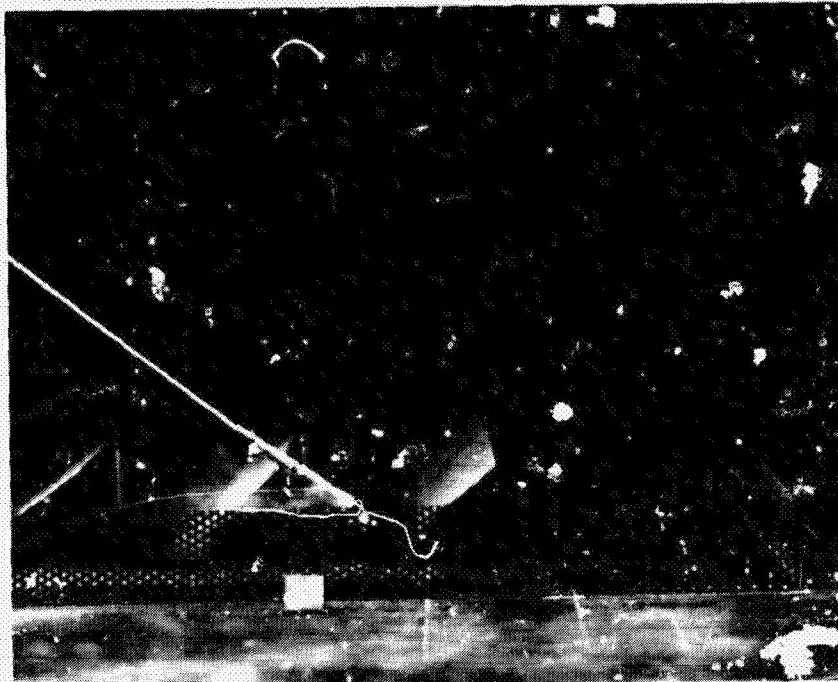


Figure 7. Typical Horizontal Velocity Distribution across Meteorological Wind Tunnel



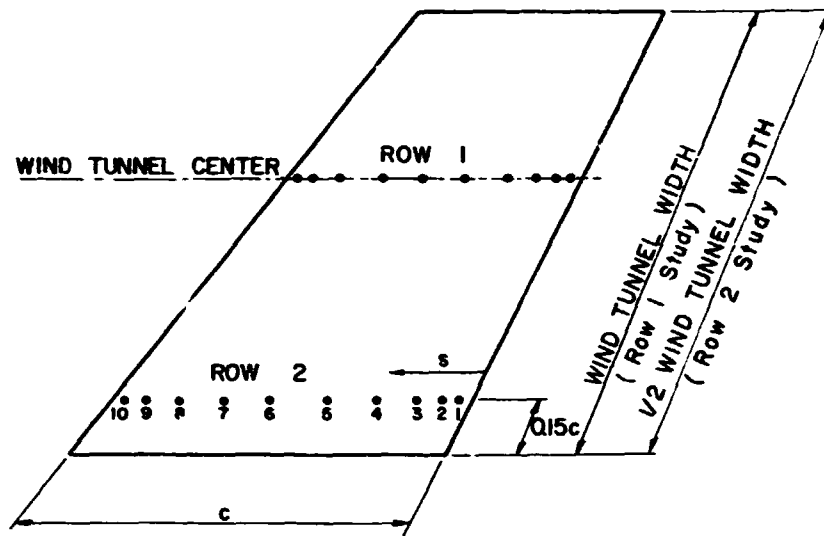
*Figure 8. 1:12 Scale Models in Meteorological Wind Tunnel*

ORIGINAL PAGE IS  
OF POOR QUALITY



*Figure 9. Photograph of Standard Corner Fence*

ORIGINAL PAGE IS  
OF FOUR QUALITY



TAP LOCATIONS - FRACTION OF CHORD  $s/c$

	1	2	3	4	5	6	7	8	9	10
UPSTREAM SURFACE	0.052	0.102	0.172	0.272	0.432	0.592	0.752	0.852	0.922	0.972
DOWNSTREAM SURFACE	0.028	0.078	0.148	0.248	0.408	0.568	0.728	0.828	0.898	0.948

Figure 10. Position of Pressure Taps on Instrumented Model

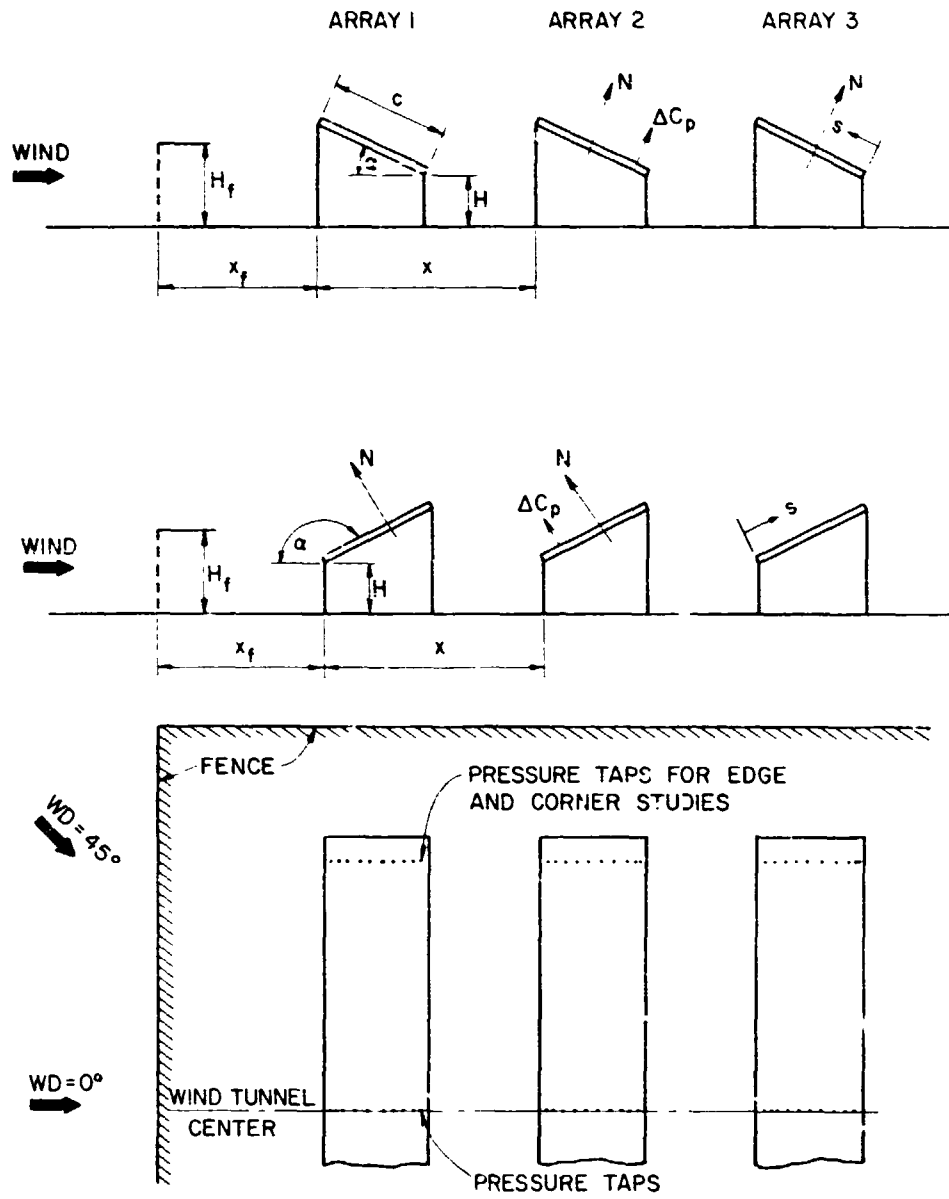


Figure 11. Schematic Description of Array Field

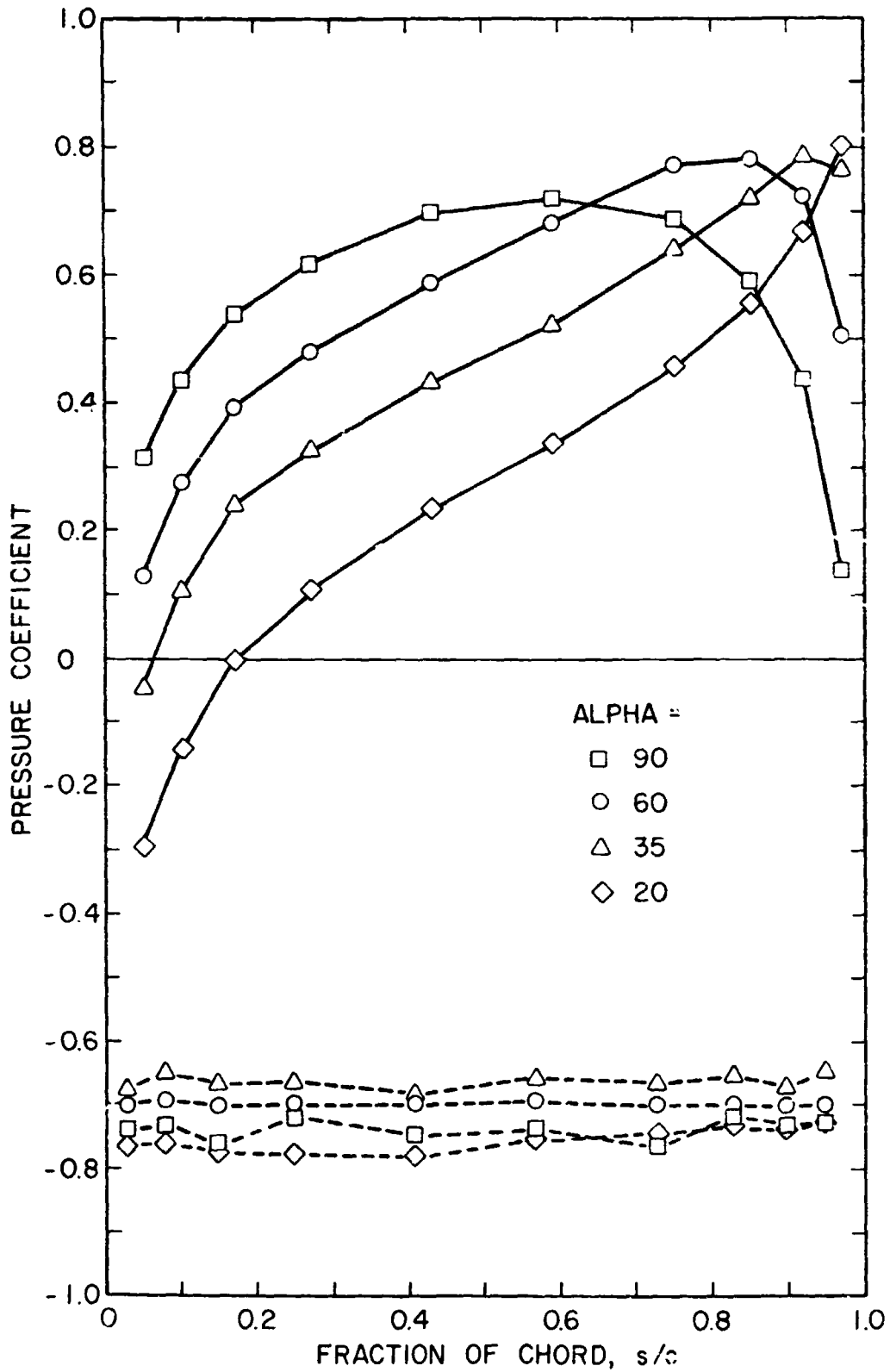


Figure 12. Front and Back Pressures on a Single Array in Uniform Flow,  $WD = 0^\circ$ ,  $H/c = 0.25$ ,  $\alpha = 20^\circ, 35^\circ, 60^\circ$  and  $90^\circ$

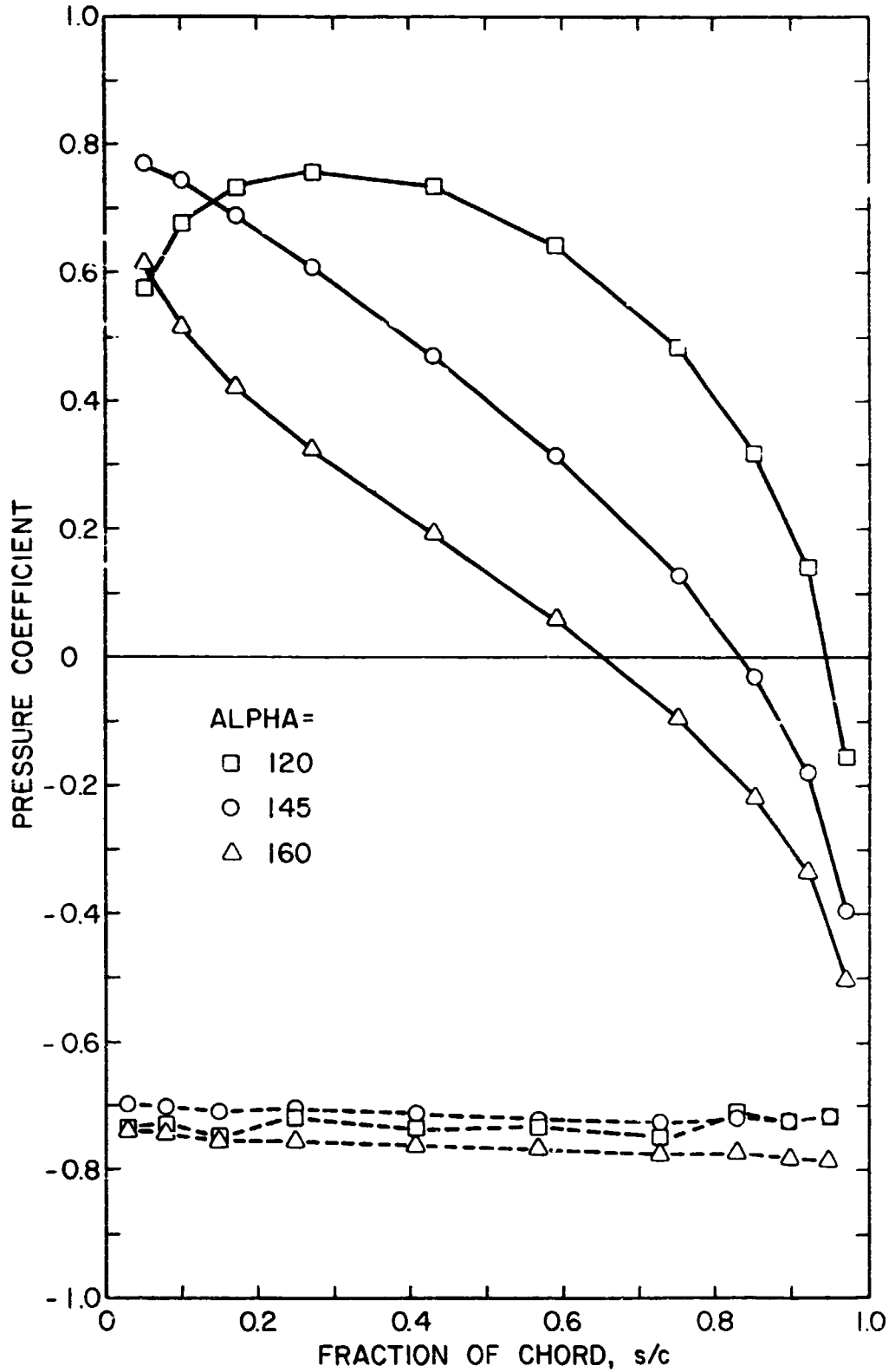


Figure 13. Front and Back Pressures on a Single Array in Uniform Flow,  $WD = 0^\circ$ ,  $H/c = 0.25$ ,  $\alpha = 120^\circ$ ,  $145^\circ$  and  $160^\circ$

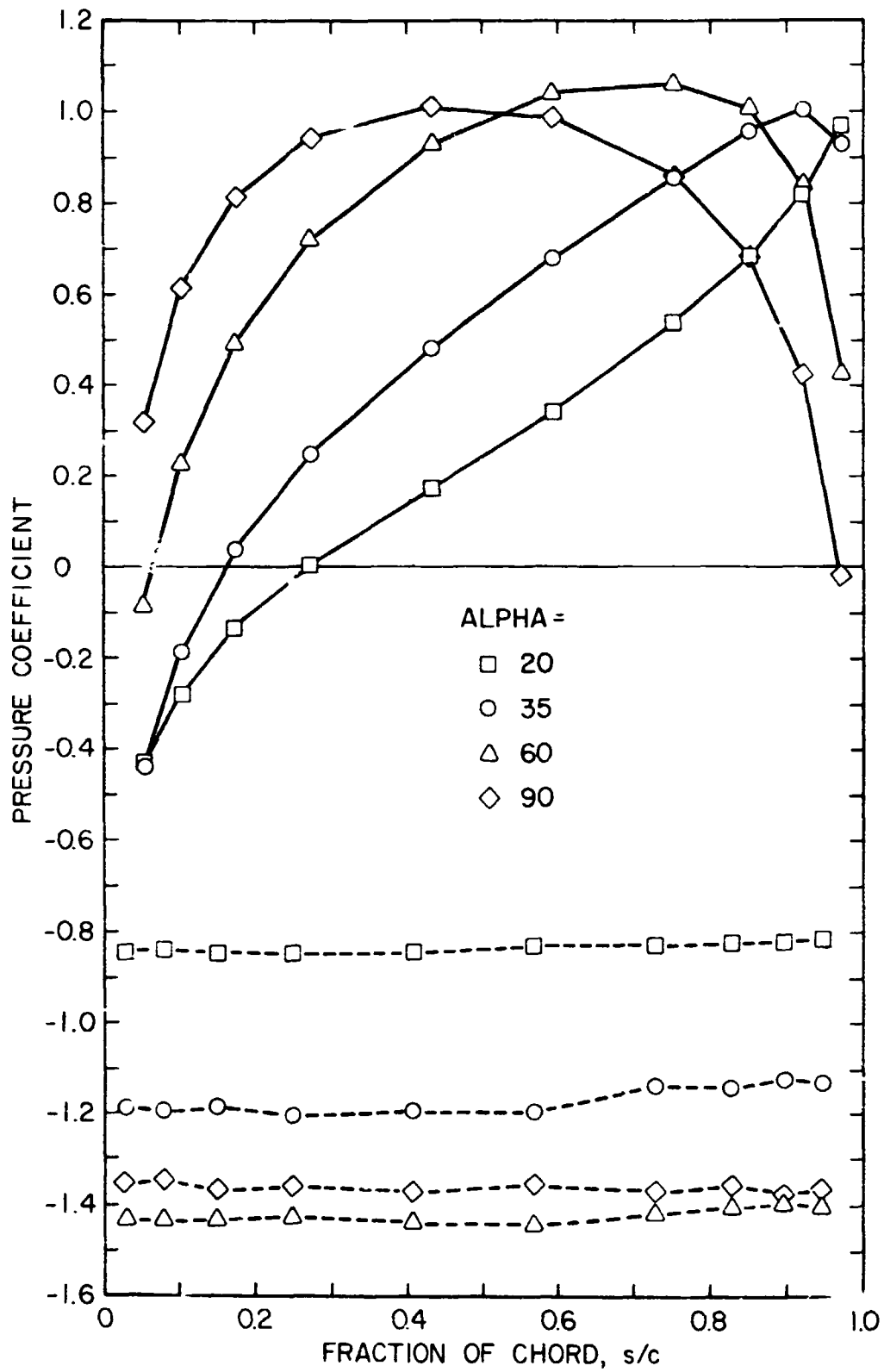


Figure 14. Front and Back Pressures on a Single Array in Uniform Flow,  $WD = 0^\circ$ ,  $H/c = \text{infinity}$ ,  $\alpha = 20^\circ$ ,  $30^\circ$ ,  $60^\circ$ , and  $90^\circ$

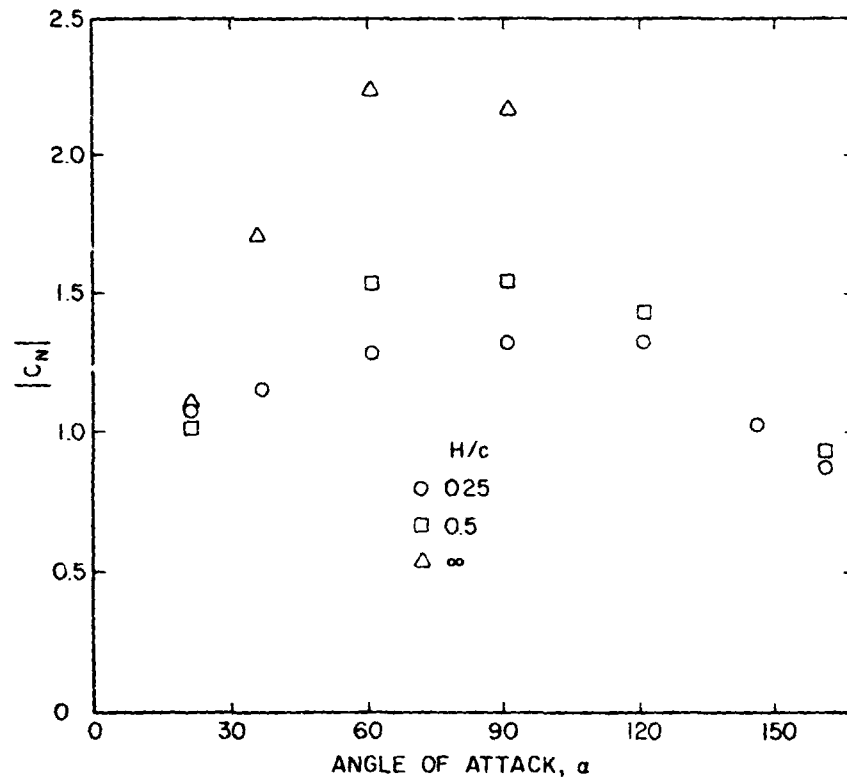


Figure 15. Absolute Values of Normal Force Coefficients on a Single Array in Uniform Flow,  $WD = 0^\circ$

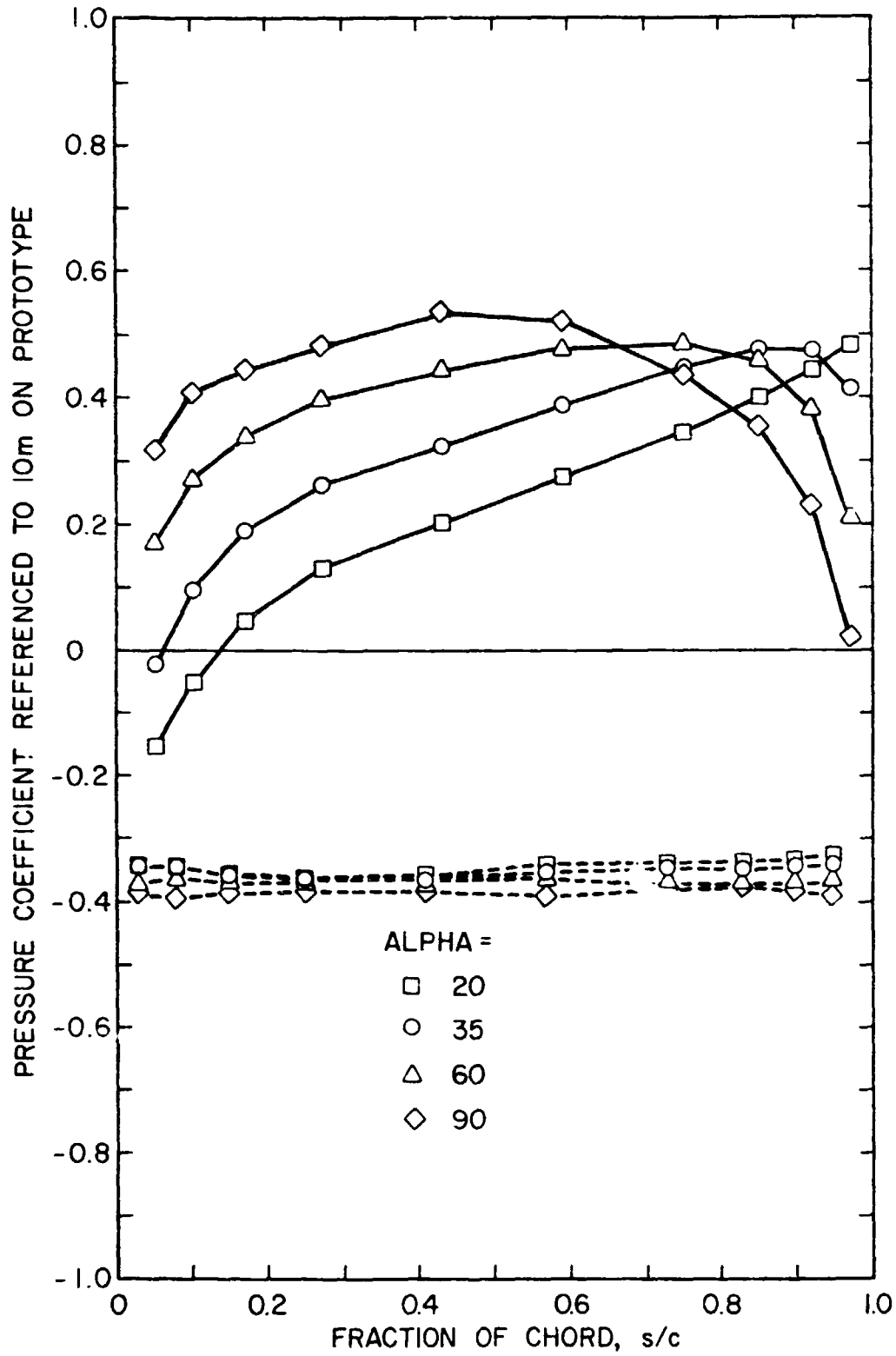


Figure 16. Front and Back Pressures on a Single Array in Nonuniform Flow,  $WD = 0^\circ$ ,  $H/c = 0.25$ ,  $\alpha = 20^\circ$ ,  $30^\circ$ ,  $60^\circ$  and  $90^\circ$

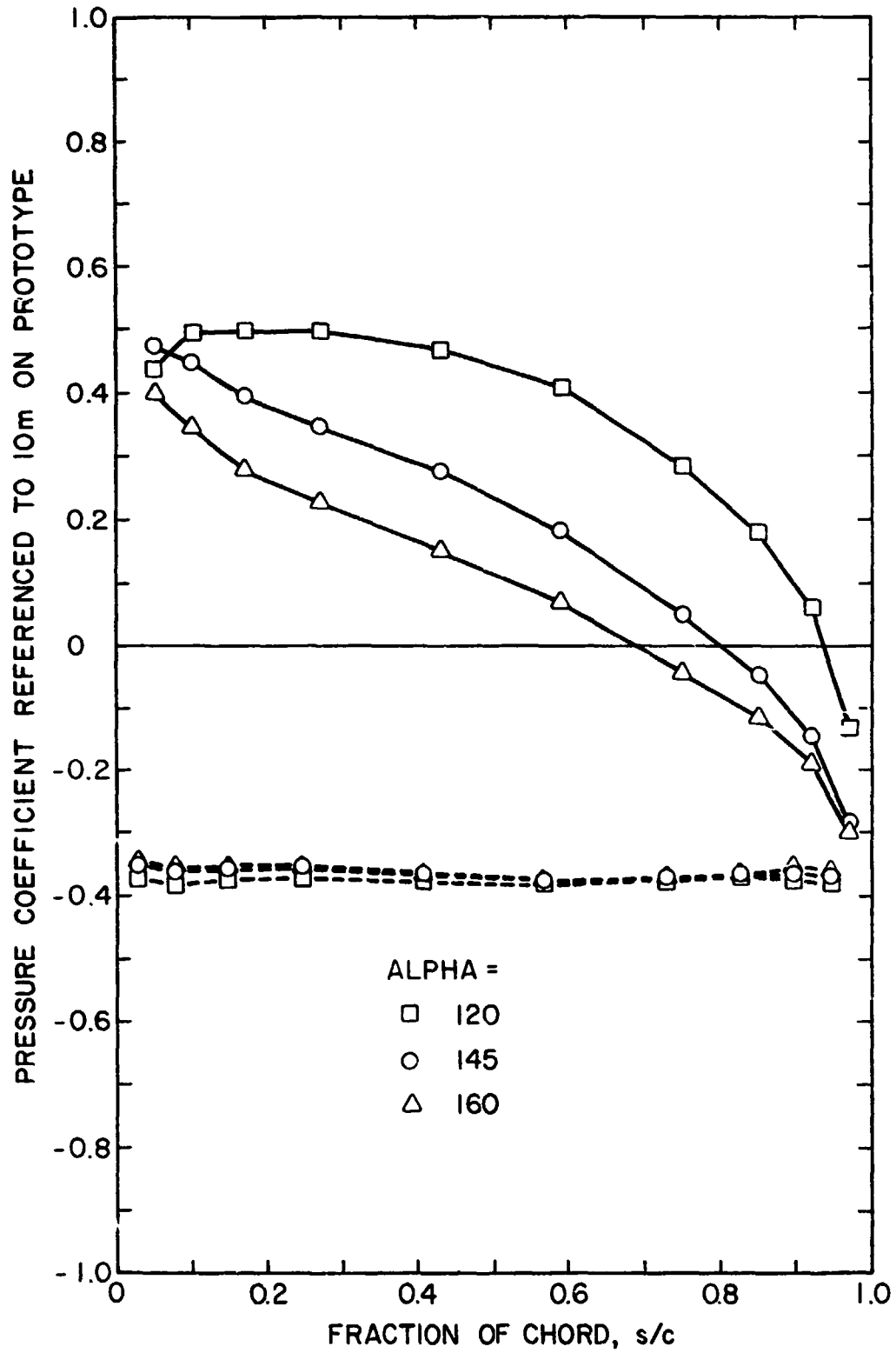


Figure 17. Front and Back Pressures on a Single Array in Nonuniform Flow,  $WD = 0^\circ$ ,  $H/c = 0.25$ ,  $\alpha = 120^\circ$ ,  $145^\circ$  and  $160^\circ$

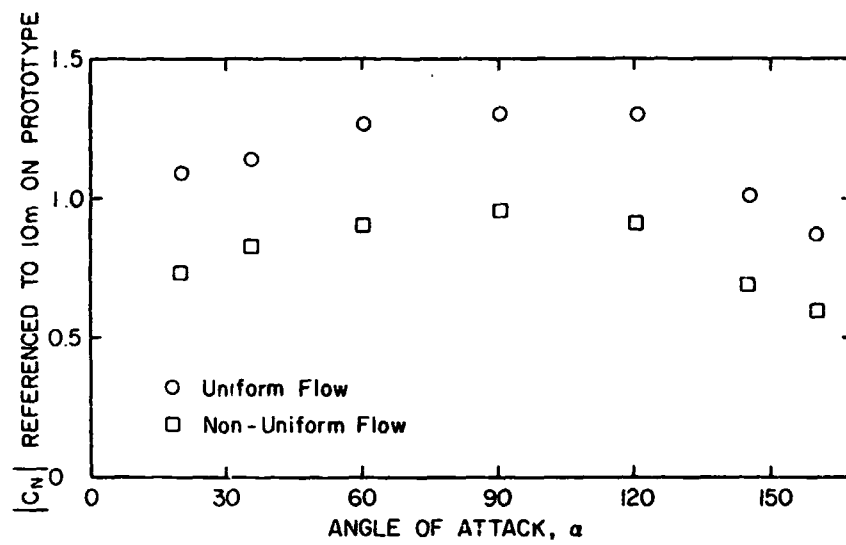


Figure 13. Absolute Values of Normal Force Coefficients on a Single Array in Nonuniform and Uniform Flows,  $WD = 0^\circ$ ,  $H/c = 0.25$

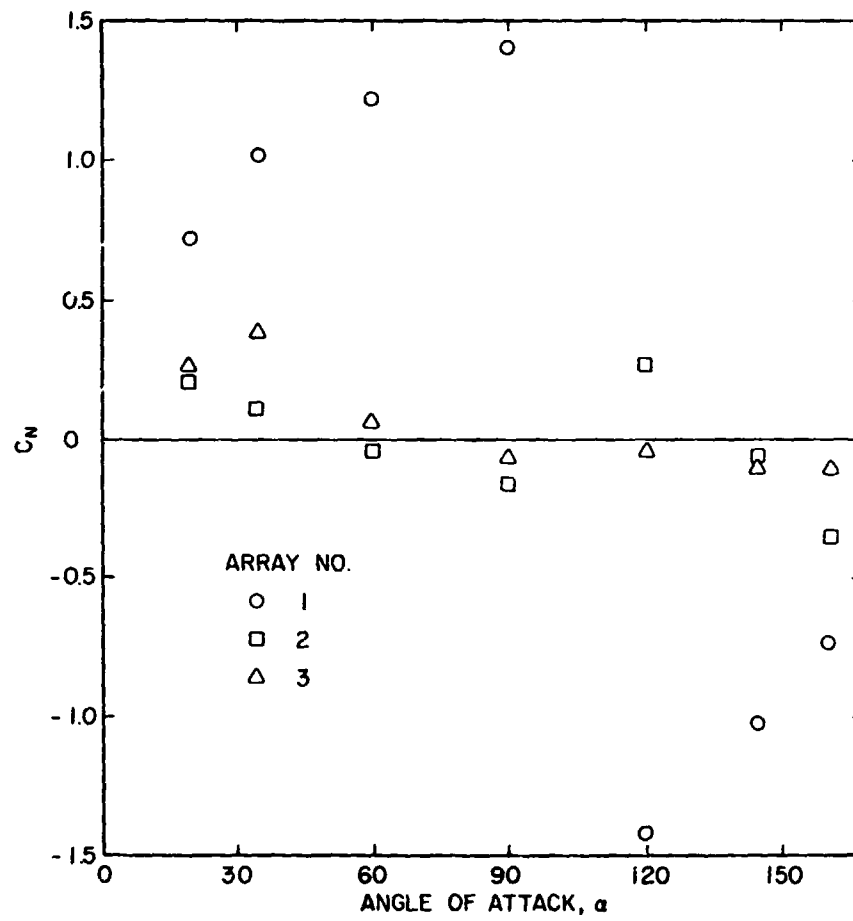


Figure 19. Normal Force Coefficients for an Array Field in Uniform Flow,  $WD = 0^\circ$ ,  $x/c = 2.0$ ,  $H/c = 0.25$ , No Fence

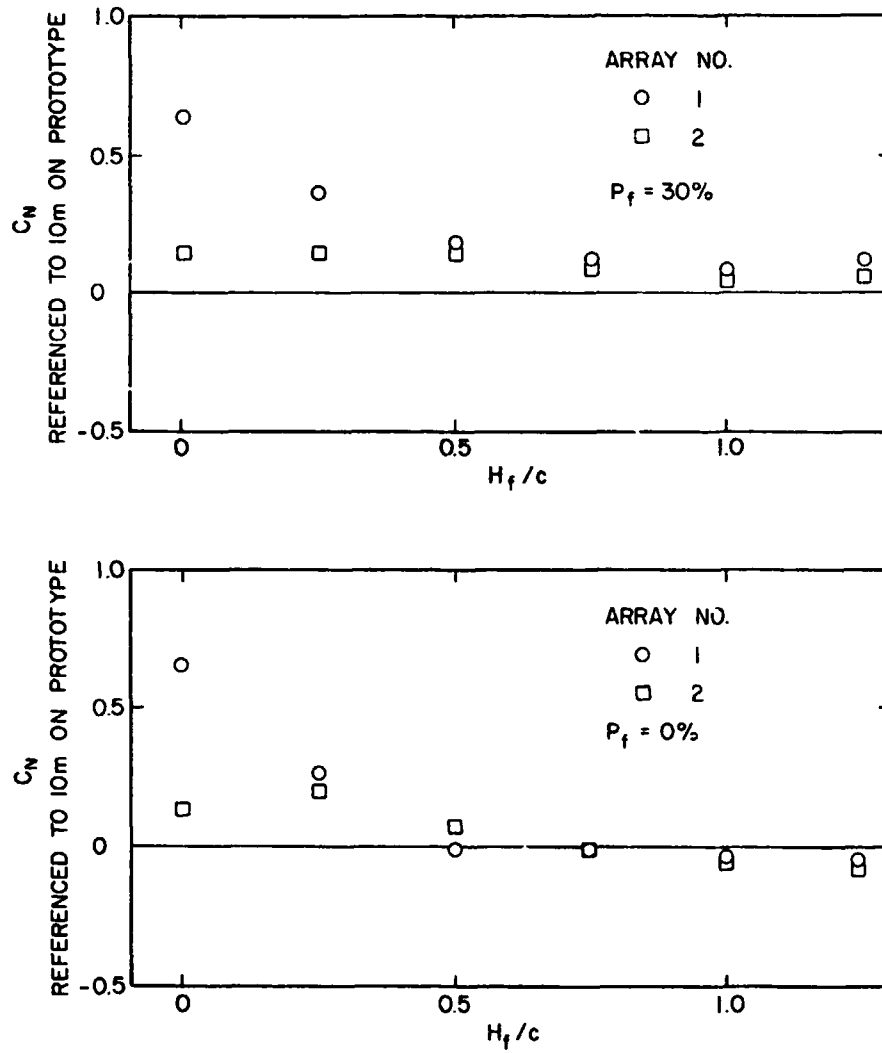


Figure 20. Normal Force Coefficients for an Array Field with a Fence of Various Height and Porosity,  $WD = 0^\circ$ ,  $x/c = 2.0$ ,  $H/c = 0.25$ ,  $\alpha = 35^\circ$

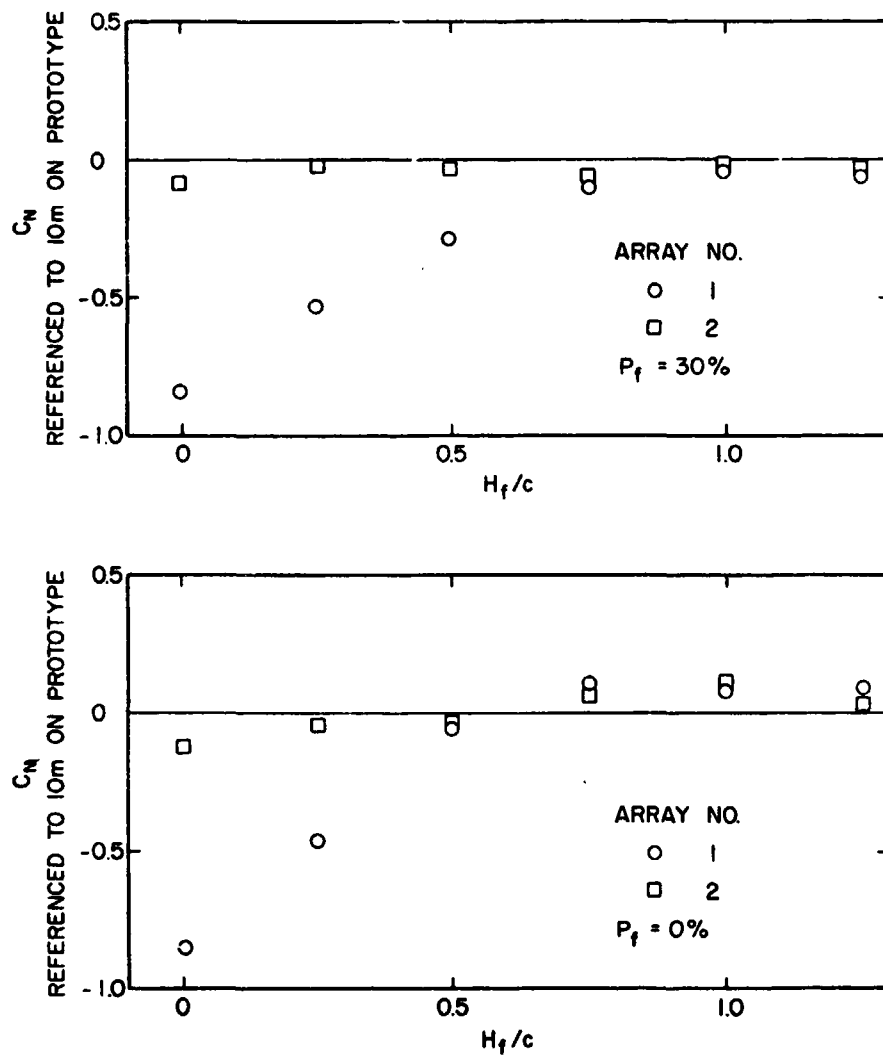


Figure 21. Normal Force Coefficients for an Array Field with a Fence of various Height and Porosity,  $WD = 0^\circ$ ,  $x/c = 2-0$ ,  $H/c = 0.25$ ,  $\alpha = 145^\circ$

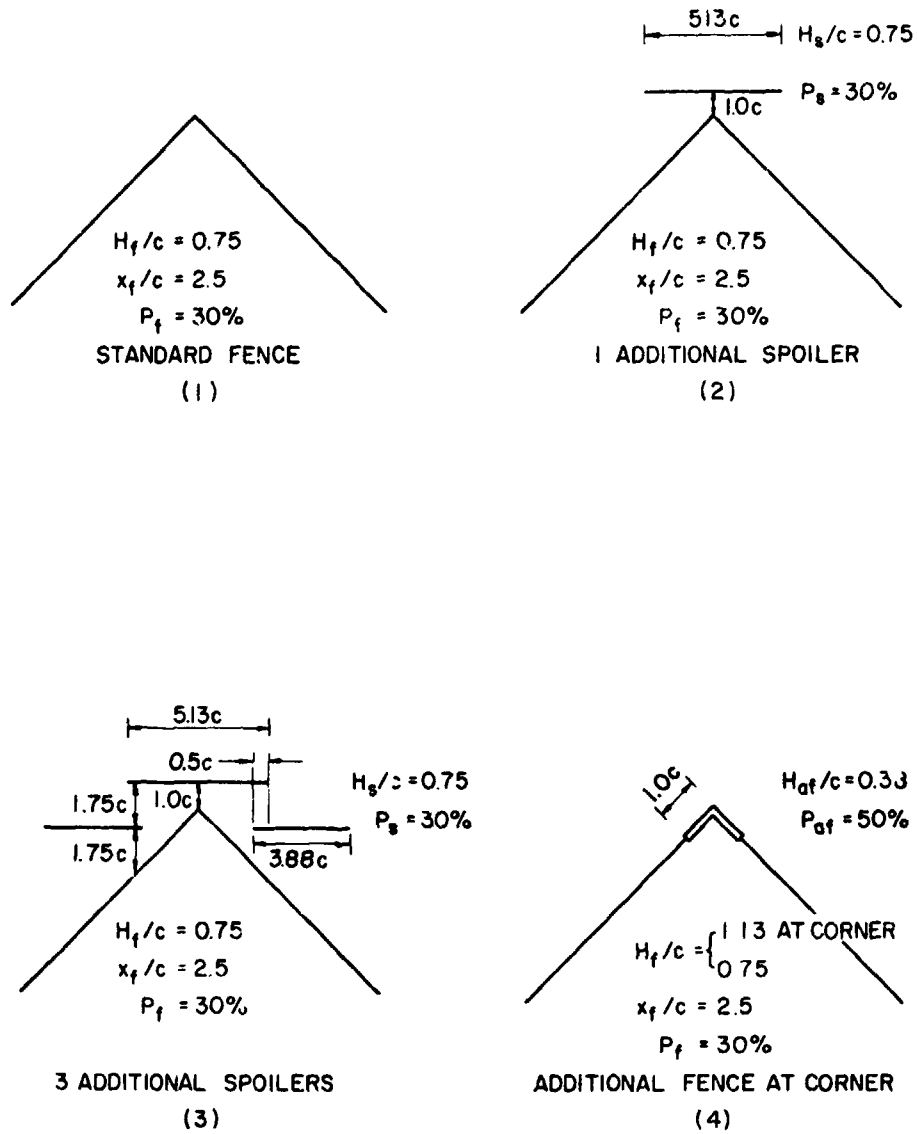


Figure 22. Corner Fence Configurations

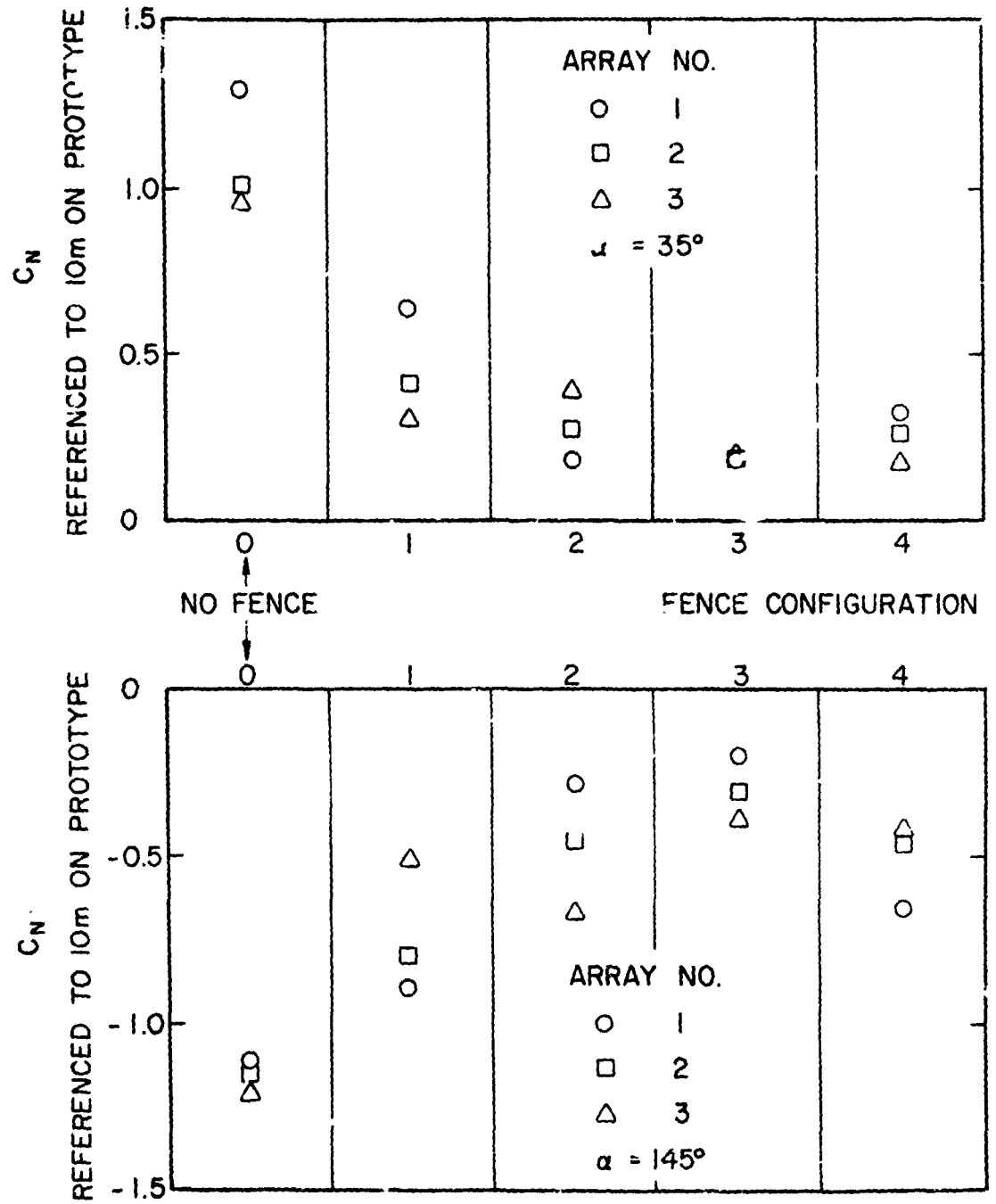


Figure 23. Normal Force Coefficients for an Array Field with Various Fence Configurations;  $WD = 45^\circ$ ,  $x/c = 2.0$ ,  $h/c = 0.25$ ,  $MC = 0$

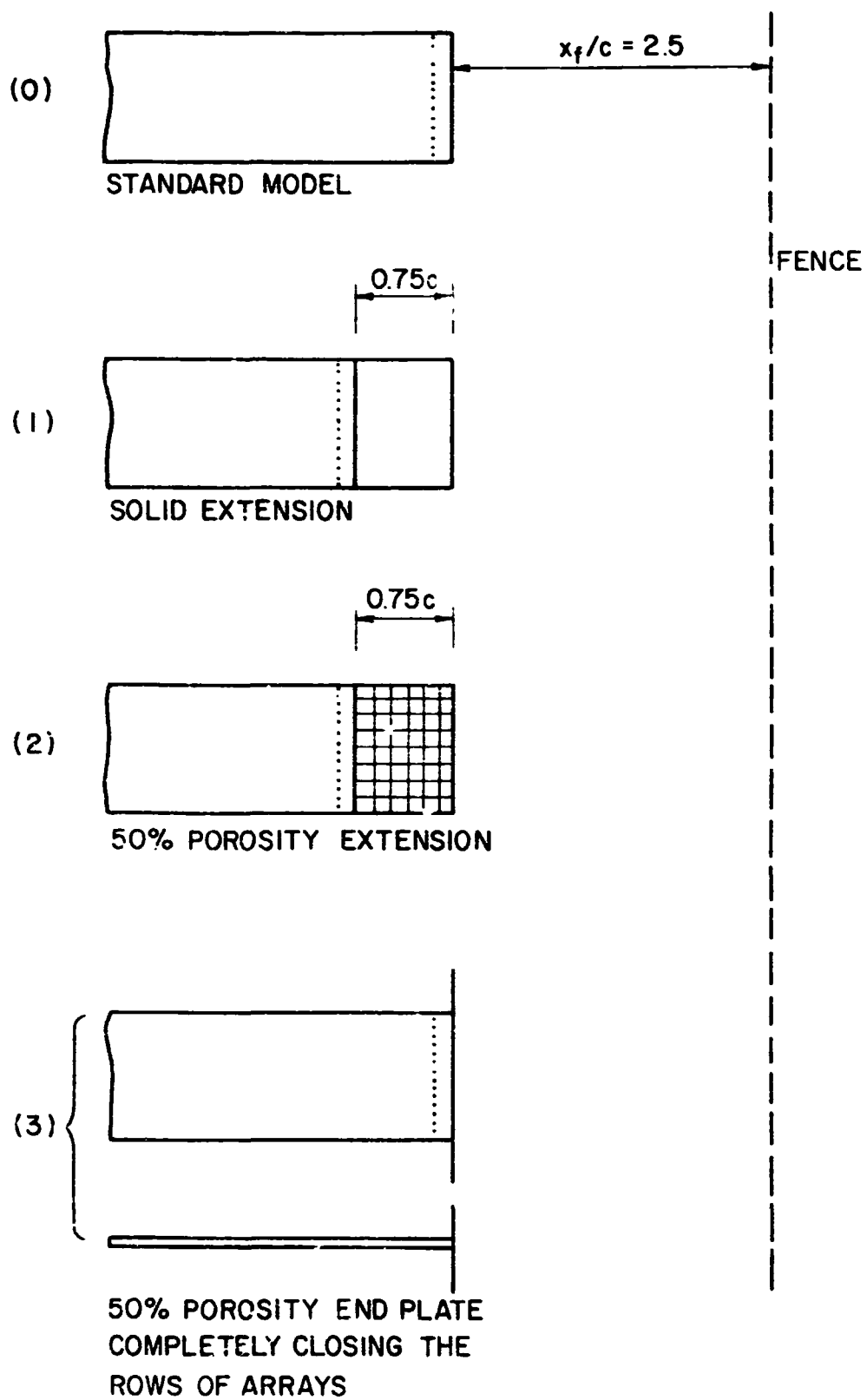


Figure 24. Model Configurations

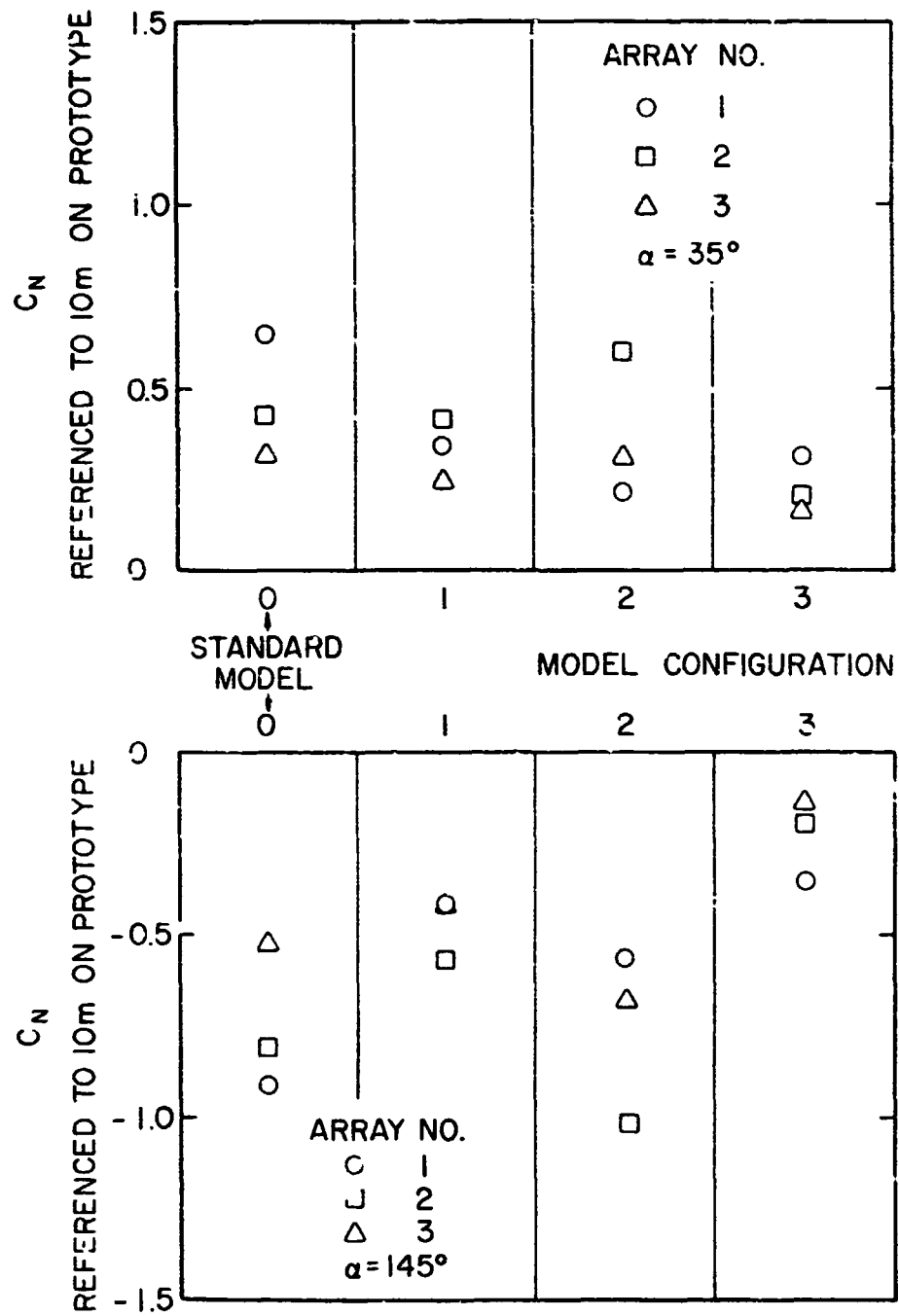


Figure 25. Normal Force Coefficients for an Array Field with Various Model Configurations,  $WD = 45^\circ$ ,  $x/c = 2.0$ ,  $H/c = 0.25$ ,  $FC = 1$

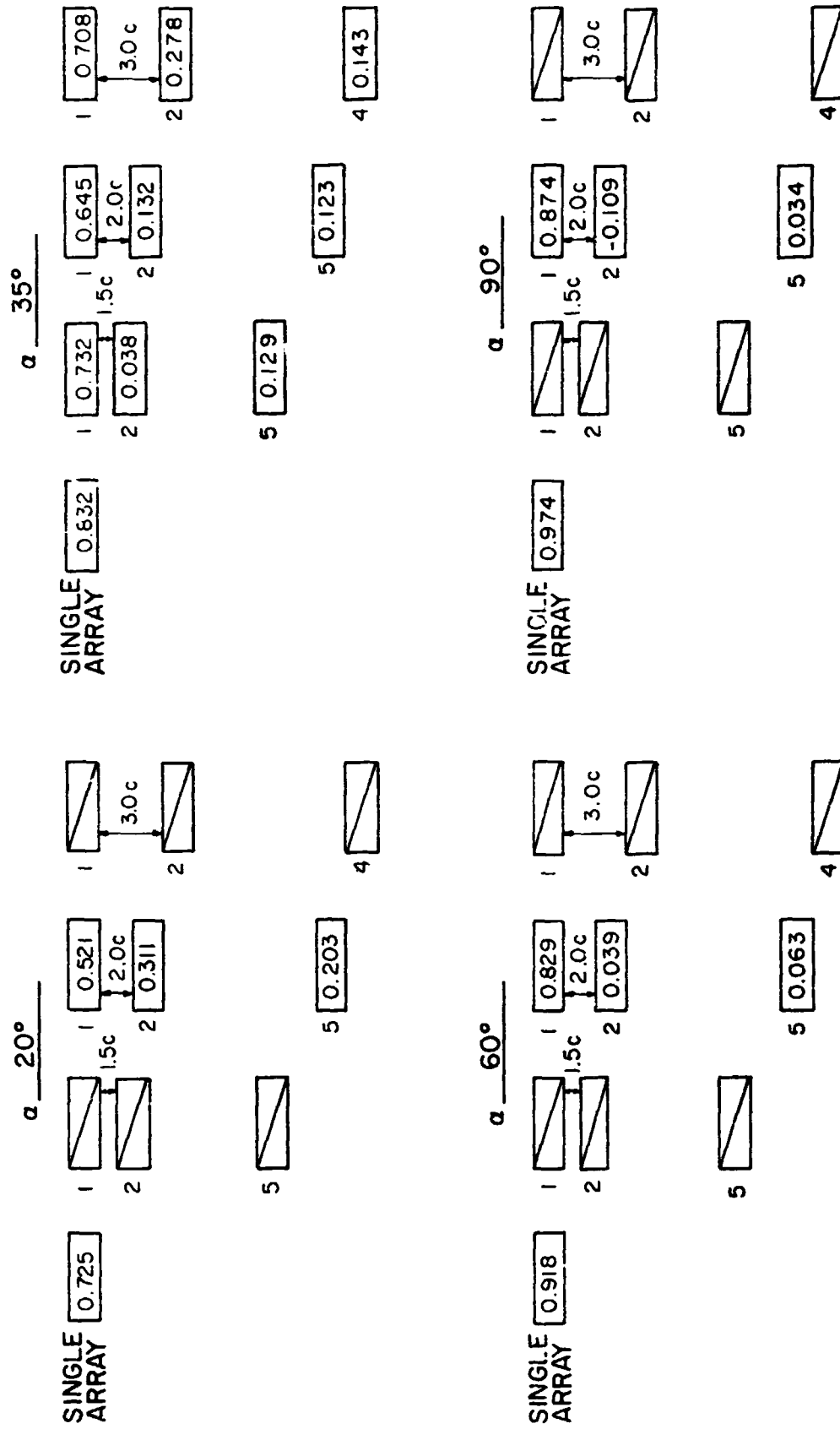


Figure 26. Normal Force Coefficients for an Array Field in Nonuniform Flow, No Fence,  $WD = 0^\circ$ ,  $H/c = 0.25$ ,  $\alpha = 20^\circ, 35^\circ, 60^\circ$  and  $90^\circ$

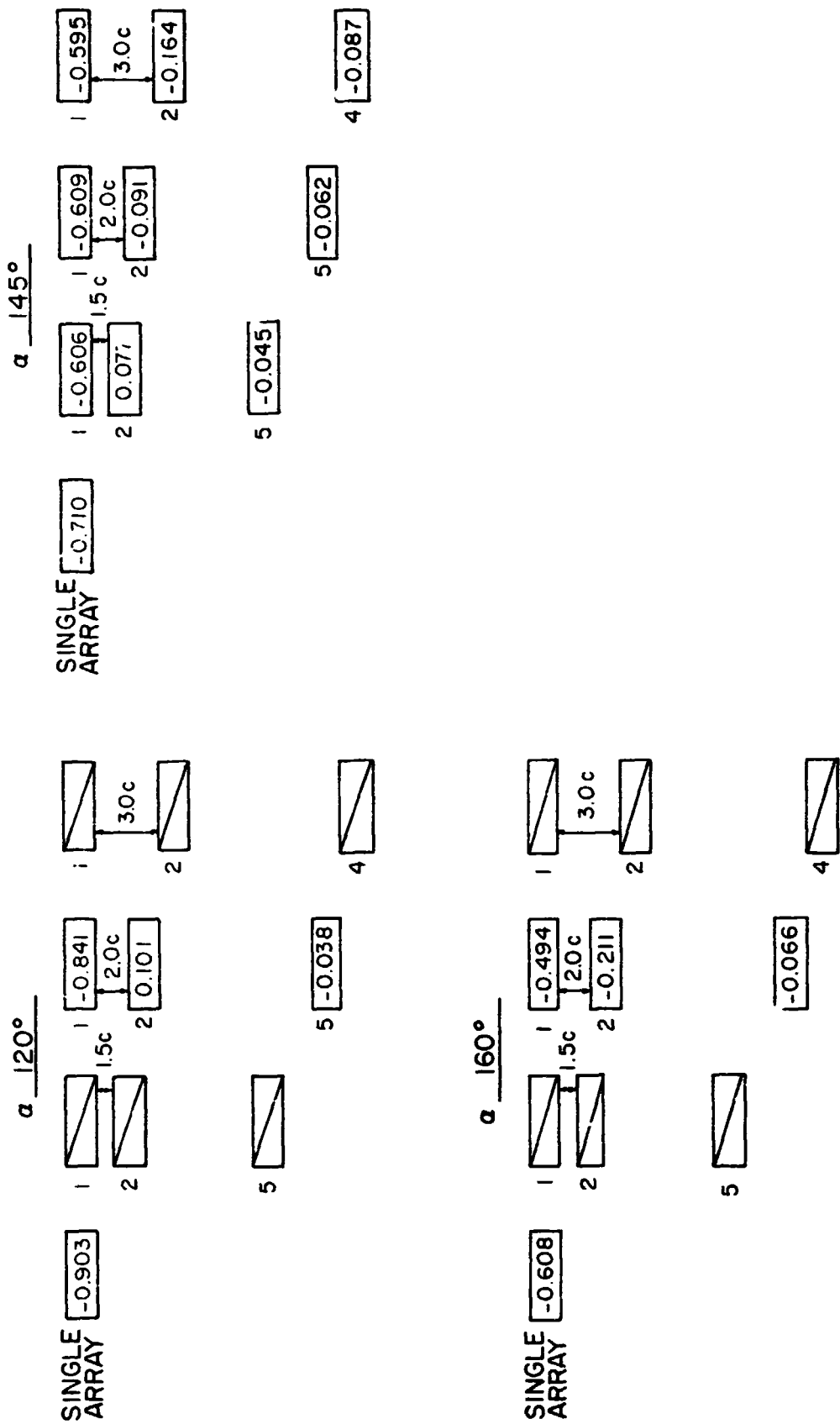


Figure 27. Normal Force Coefficients for an Array Field in Nonuniform Flow, No Fence,  $WD = 0^\circ$ ,  $H/c = 0.25$ ,  $\alpha = 120^\circ$ ,  $145^\circ$  and  $160^\circ$

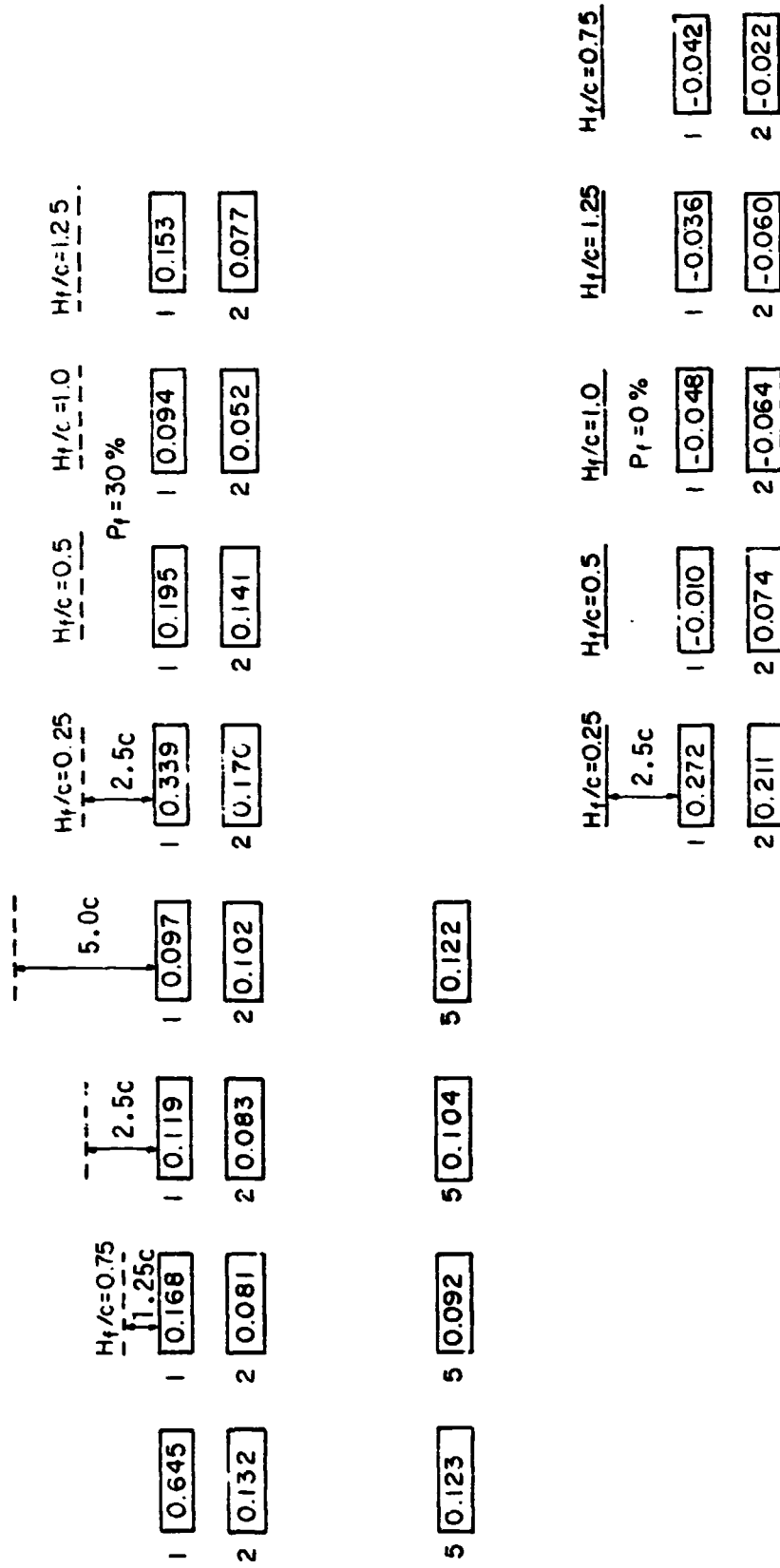


Figure 28a. Normal Force Coefficients for an Array Field with Various Fences,  $WD = 0^\circ$ ,  $x/c = 2.0$ ,  $H/c = 0.25$ ,  $\alpha = 35^\circ$ , Nonuniform Flow

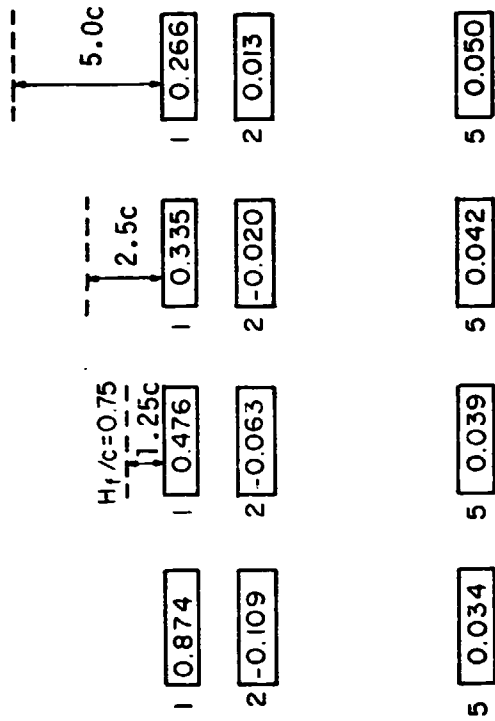


Figure 28b. Normal Force Coefficients for an Array Field with Various Fences,  $WD = 0^\circ$ ,  $x/c = 2.0$ ,  $H/c = 0.25$ ,  $\alpha = 90^\circ$ , Nonuniform Flow

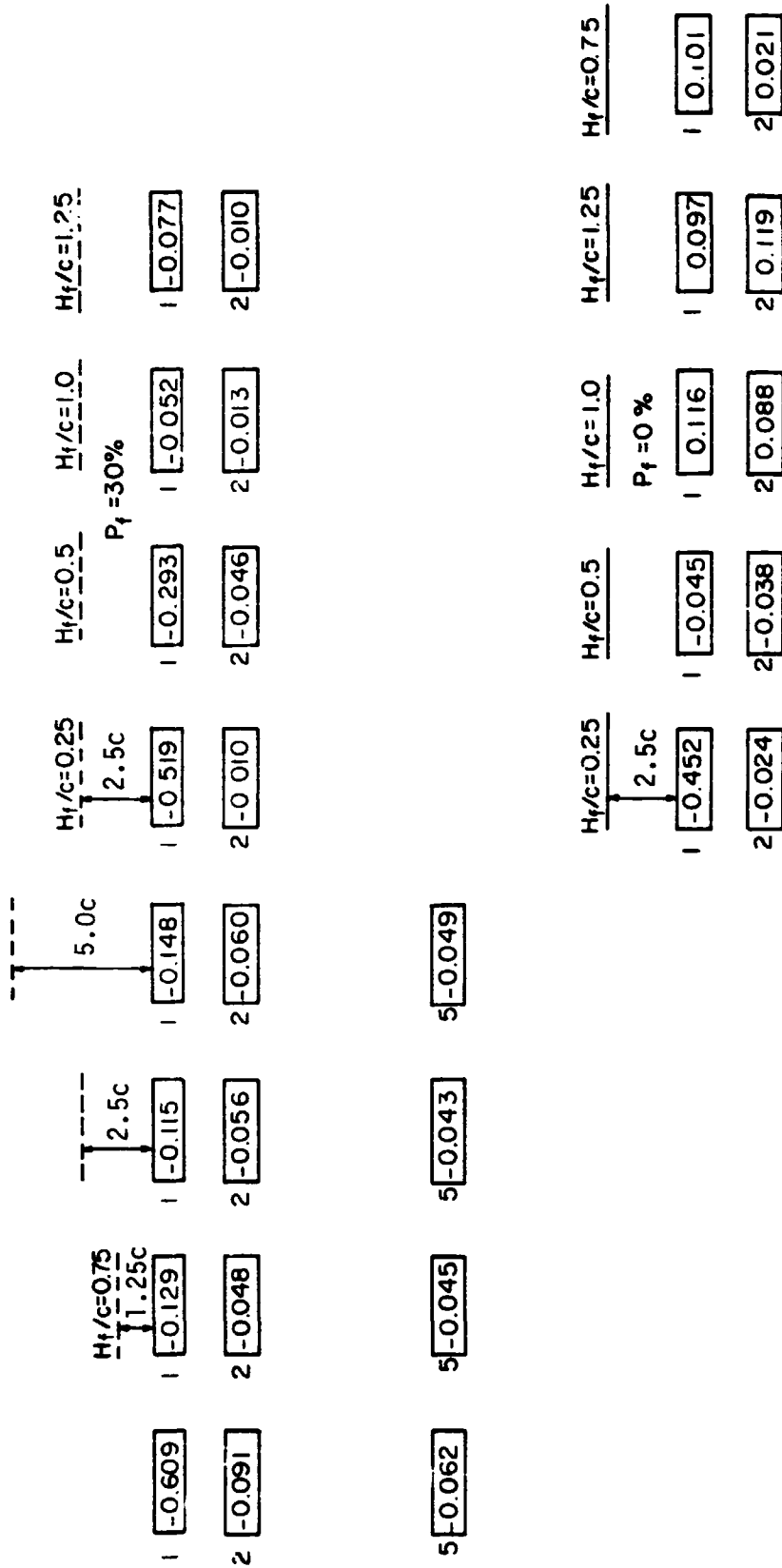


Figure 28c. Normal Force Coefficients for an Array Field with Various Fences,  $WD = 0^\circ$ ,  $x/c = 2.0$ ,  $H/c = 0.25$ ,  $\alpha = 145^\circ$ , Nonuniform Flow

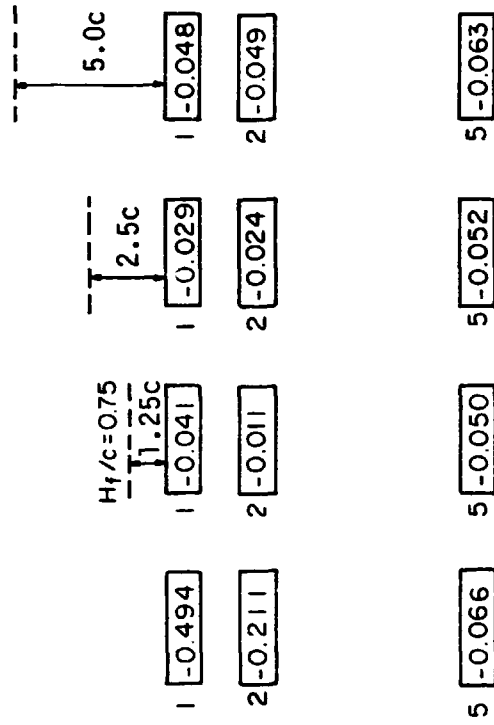


Figure 28d. Normal Force Coefficients for an Array Field with Various Fences,  $\omega D = 0^\circ$ ,  $x/c = 2.0$ ,  $H/c = 0.25$ ,  $\alpha = 160^\circ$ , Nonuniform Flow

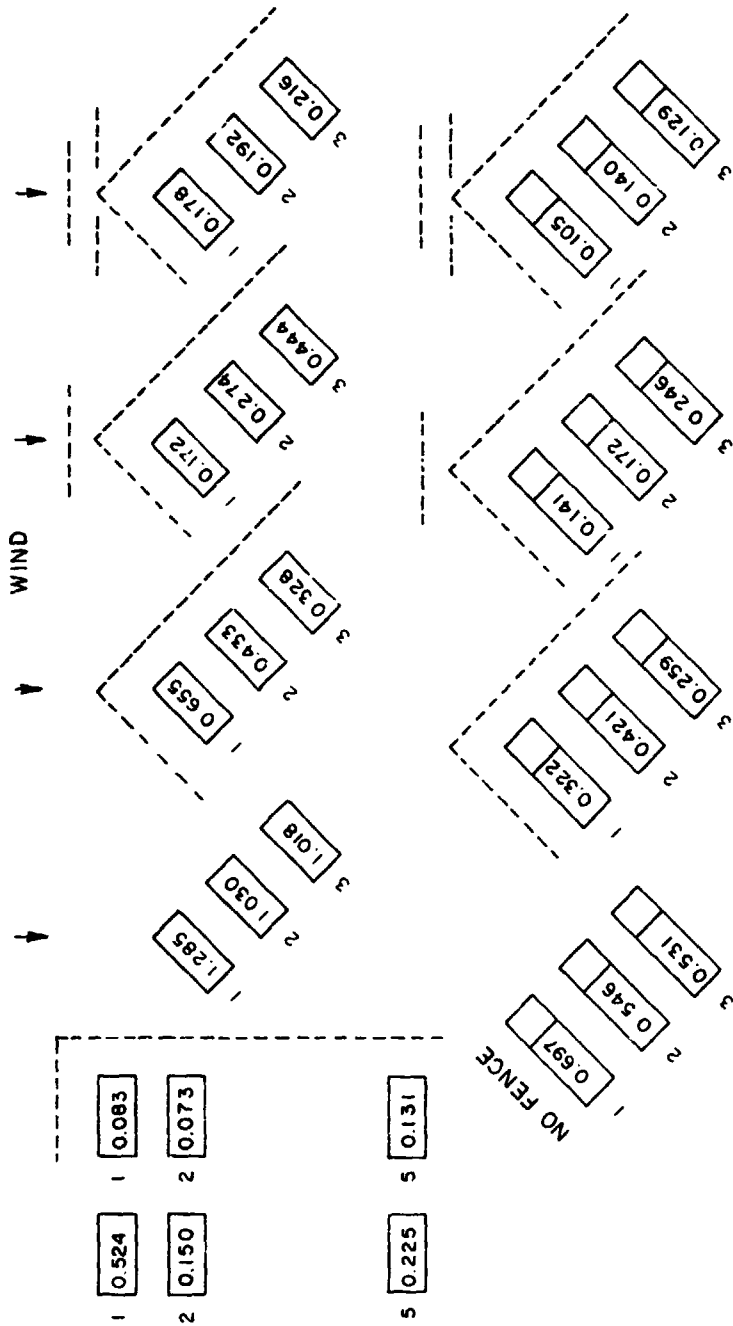


Figure 29a. Normal Force Coefficients for an Array Field, Edge and Corner Studies,  $x/c = 2.0$ ,  $H/c = 0.25$ ,  $\alpha = 35^\circ$ , Nonuniform Flow

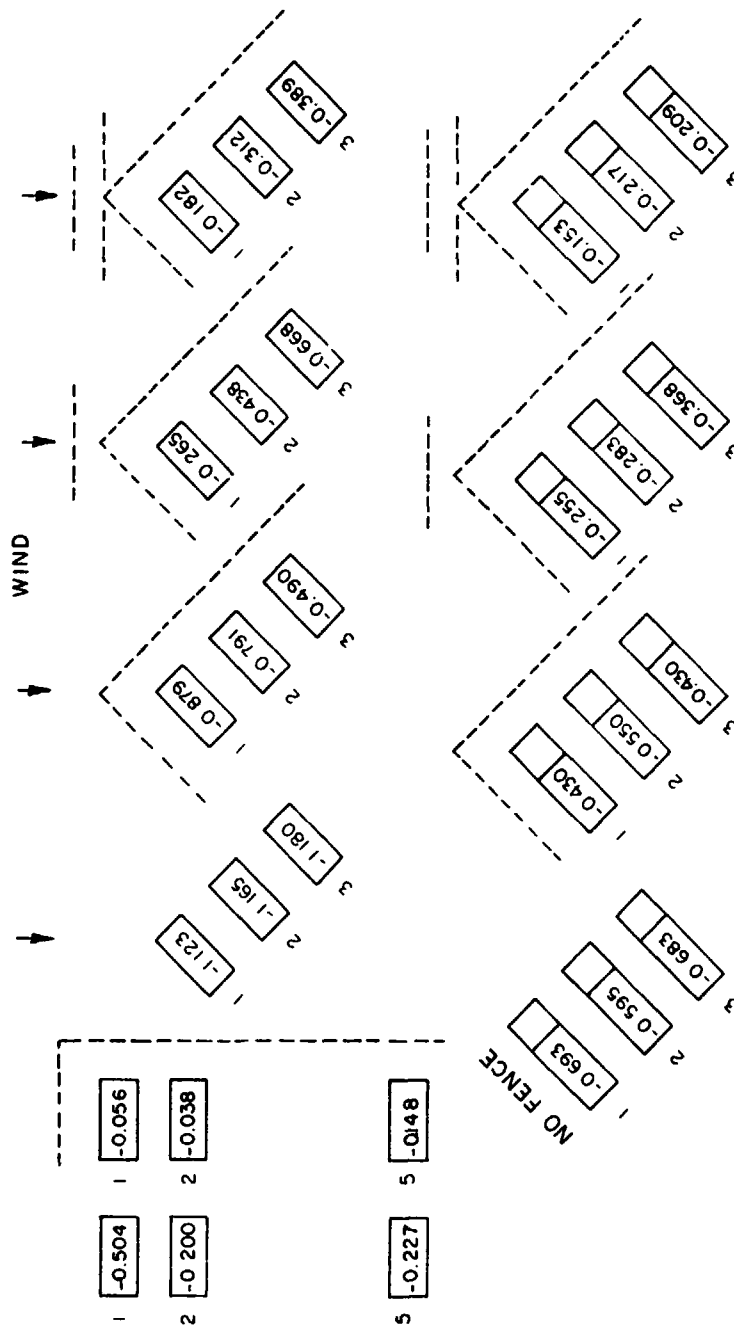


Figure 29b. Normal Force Coefficients for an Array Field, Edge and Corner Studies,  $x/c = 2.0$ ,  $H/c = 0.25$ ,  $\alpha = 145^\circ$ , Nonuniform Flow

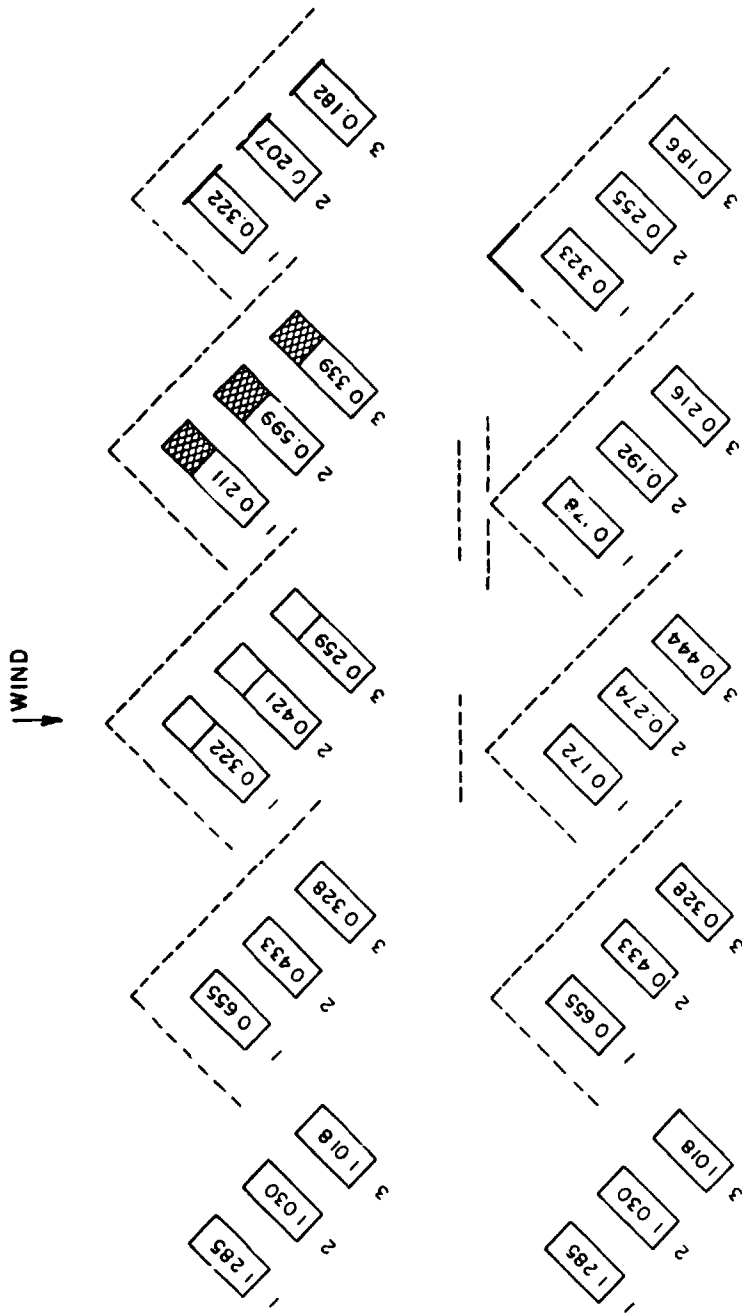


Figure 30a. Normal Force Coefficients for an Array Field, Corner Study with Various Fence and Model Configurations,  $x/c = 2.0$ ,  $H/c = 0.25$ ,  $\alpha = 35^\circ$ , Nonuniform Flow

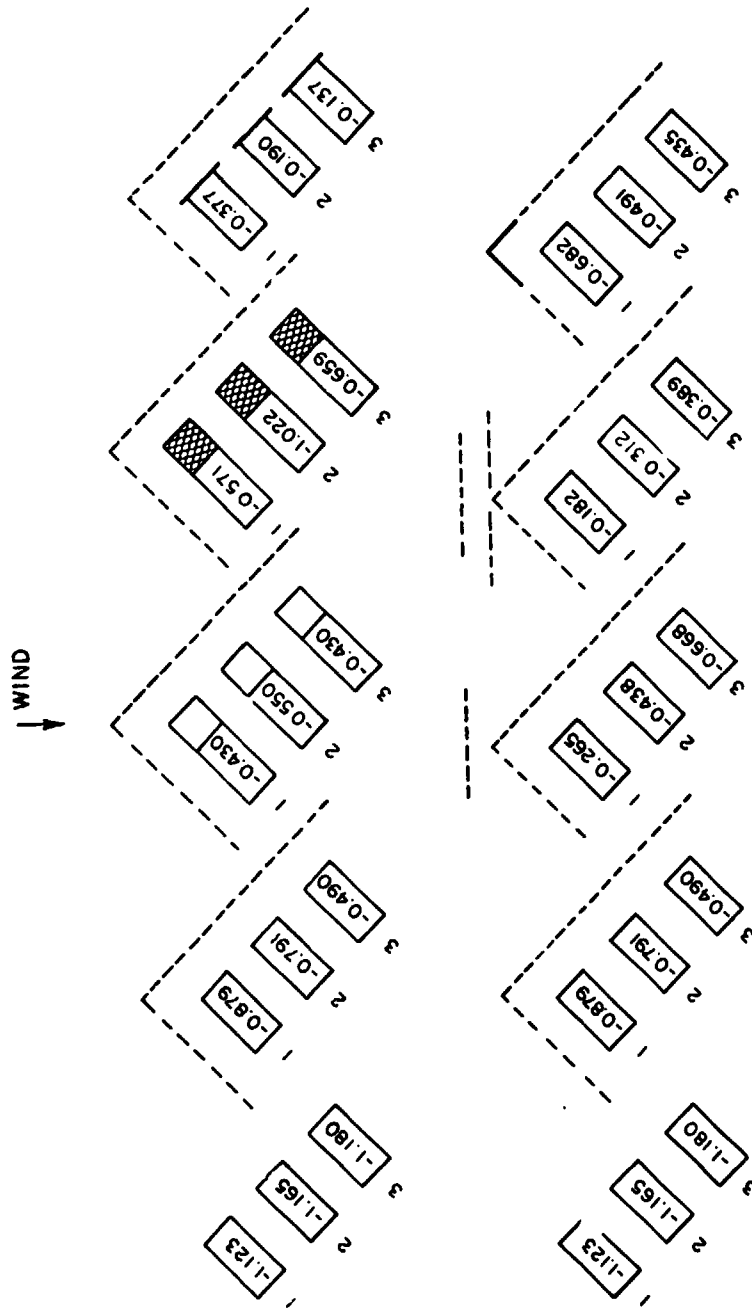
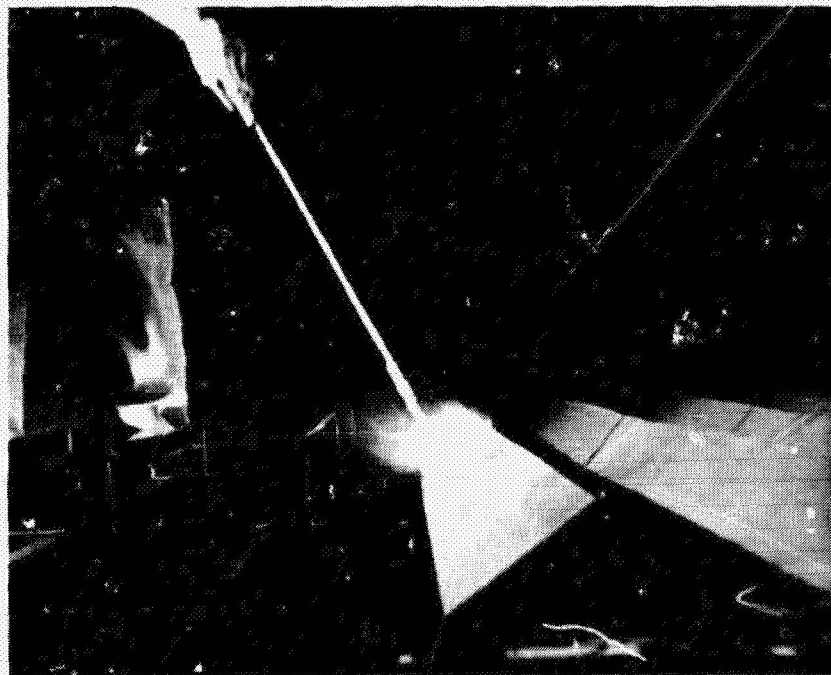
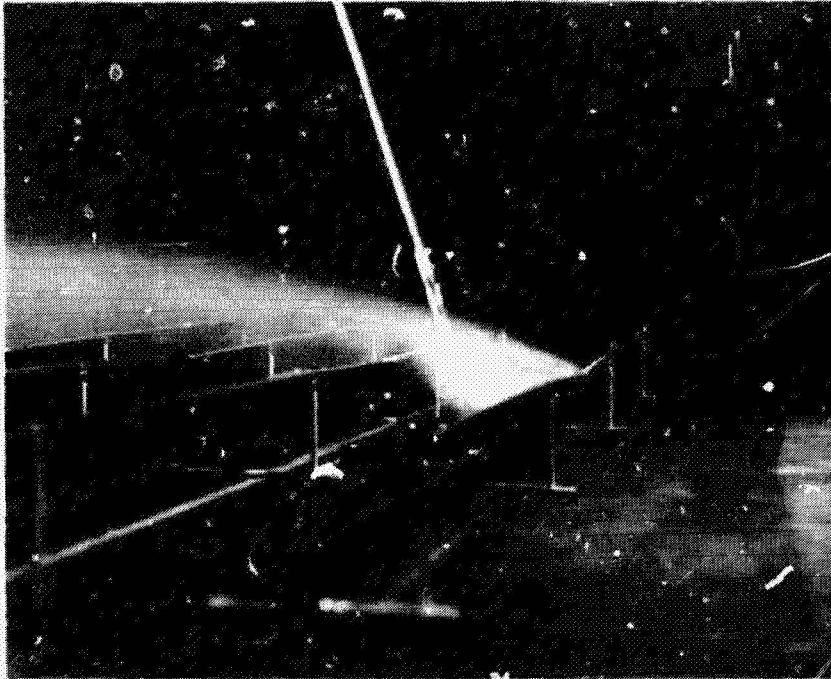


Figure 30b. Normal Force Coefficients for an Array Field, Corner Study with Various Fence and Model Configurations,  $x/c = 2.0$ ,  $H/c = 0.25$ ,  $\alpha = 145^\circ$ , Nonuniform flow



*Figure 31a. Flow visualization for an Array Field,  $WD = 0^\circ$*

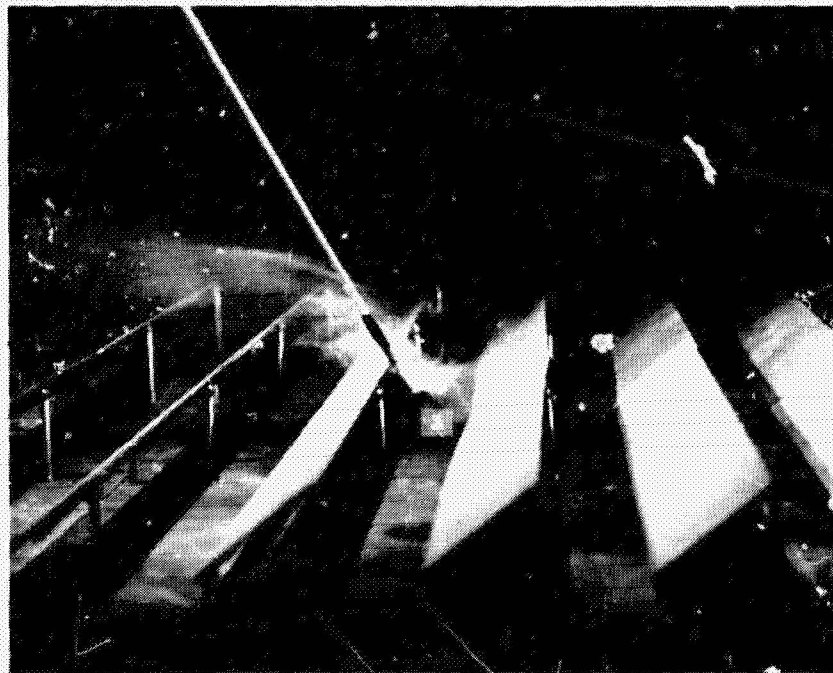
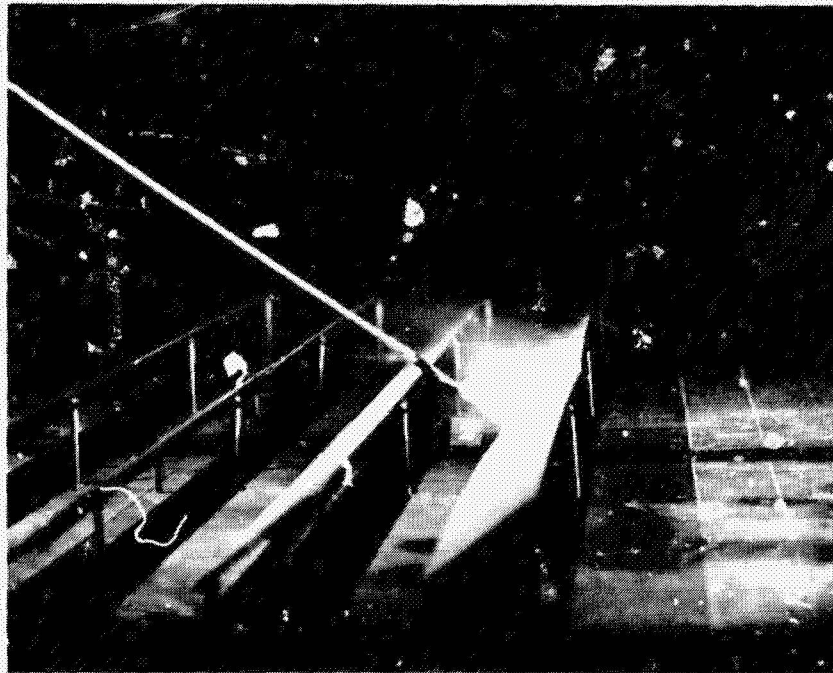


Figure 31b. Flow Visualization for an Array Field,  $WD = 0^\circ$

ORIGINAL PAGE IS  
OF POOR QUALITY



*Figure 31c. Flow Visualization for an Array Field,  $WD = 0^\circ$*



*Figure 32. Flow Visualization for an Array Field,  $WD = 45^\circ$*

ORIGINAL PAGE IS  
OF POOR QUALITY

**A-58**

**TABLES**

Table 1. Normal Force and Maximum Pressure Difference  
for a Single Array in Uniform Flow

File Name	H/c	$\alpha$	$C_N$	$\Delta C_{p \max}$	$s_{\max}/c$
A02001	0.25	20	1.086	1.53	0.98
A03501	0.25	35	1.145	1.45	0.89
A06001	0.25	60	1.283	1.48	0.83
A09001	0.25	90	1.320	1.46	0.59
A12001	0.25	120	-1.320	-1.48	0.29
A14501	0.25	145	-1.024	-1.46	0.06
A16001	0.25	160	-0.885	-1.37	0.05
B02001	0.5	20	1.015	1.66	0.96
B06001	0.5	60	1.523	1.76	0.74
B09001	0.5	90	1.534	1.74	0.42
B12001	0.5	120	-1.440	-1.73	0.18
B16001	0.5	160	-0.936	-1.49	0.04
C02001	$\infty$	20	1.133	1.79	0.97
C03501	$\infty$	35	1.715	2.13	0.91
C06001	$\infty$	60	2.228	2.48	0.71
C09001	$\infty$	90	2.168	2.35	0.42

Table 2. Normal Force and Maximum Pressure Difference  
for an Array Field in Uniform Flow,  $x/c = 2.0$

File Name	Array #	$\alpha$	$C_N$	$\Delta C_{p \text{ max}}$	$s_{\text{max}}/c$
E02001	1	20	0.717	1.06	0.96
E02101	2	20	0.210	0.82	0.73
E02201	5	20	0.267	0.91	0.86
E03501	1	35	1.006	1.24	0.91
E03601	2	35	0.383	0.75	0.26
E03701	5	35	0.100	0.20	0.45
E06001	1	60	1.220	1.39	0.84
E06101	2	60	-0.055	0.32	0.05
E06201	5	60	0.011	-0.04	0.46
E09001	1	90	1.400	1.56	0.58
E09101	2	90	-0.156	-0.28	0.59
E09201	5	90	-0.056	-0.07	0.42
E12001	1	120	-1.419	-1.60	0.27
E12101	2	120	0.277	0.38	0.28
E12201	5	120	-0.026	-0.10	0.92
E14501	1	145	-1.021	-1.38	0.04
E14601	2	145	-0.031	-0.11	0.74
E14701	5	145	-0.072	-0.10	0.83
E16001	1	160	-0.734	-1.10	0.05
E16101	2	160	-0.348	-0.48	0.05
E16201	5	160	-0.084	-0.10	0.59

Table 3. Normal Force and Maximum Pressure Difference  
for an Array Field in Uniform Flow,  
 $x/c = 1.5$  and  $3.0$

File Name	$x/c$	Array #	$\alpha$	$C_N$	$\Delta C_{p \max}$	$s_{\max}/c$
D03501	1.5	1	35	1.065	1.32	0.92
D03601	1.5	2	35	0.034	0.43	0.97
D03701	1.5	5	35	0.123	0.25	0.19
D14501	1.5	1	145	-1.076	-1.44	0.05
D14601	1.5	2	145	0.168	0.30	0.08
F03501	3.0	1	35	0.925	1.13	0.97
F03601	3.0	2	35	0.326	0.48	0.26
F03701	3.0	4	35	0.081	0.12	0.95
F14501	3.0	1	145	-0.937	-1.38	0.06
F14601	3.0	2	145	-0.063	-0.08	0.56
F14701	3.0	4	145	-0.116	-0.14	0.74

Table 4. Normal Force and Maximum Pressure Difference  
for a Single Array in Nonuniform Flow

File Name	$H_f/c$	$\alpha$	$C_N^*$	$\Delta C_{p \max}^*$	$s_{\max}/c$
G02001	---	20	0.725	0.96	0.96
G03501	---	35	0.832	0.98	0.85
G06001	---	60	0.918	1.02	0.74
G09001	---	90	0.974	1.05	0.44
G12001	---	120	-0.903	-1.04	0.16
G14501	---	145	-0.710	-0.99	0.05
G16001	---	160	-0.608	-0.87	0.05
G01101	0.25	35	0.504	0.71	0.96
G01201	0.5	35	0.295	0.41	0.96
G01301	0.75	35	0.143	0.18	0.82
G01401	1.0	35	0.099	0.11	0.81
G01501	1.25	35	0.286	0.34	0.85
G02101	0.25	145	-0.577	-0.66	0.32
G02201	0.5	145	-0.309	-0.38	0.56
G02301	0.75	145	-0.120	-0.14	0.54
G02401	1.0	145	-0.066	-0.08	0.08
G02501	1.25	145	-0.196	-0.28	0.06

\*referenced to 10 m on prototype

Table 5. Normal Force and Maximum Pressure Difference  
for an Array Field in Nonuniform Flow,  
 $x/c = 2.0$

File Name	Array #	$\alpha$	$C_N^*$	$\Delta C_{p \max}^*$	$s_{\max}/c$
I02001	1	20	0.521	0.73	0.95
I02101	2	20	0.311	0.38	0.74
I02201	5	20	0.203	0.31	0.90
I03501	1	35	0.645	0.76	0.91
I03601	2	35	0.132	0.29	0.20
I03701	5	35	0.123	0.15	0.74
I06001	1	60	0.829	0.90	0.75
I06101	2	60	0.039	0.34	0.06
I06201	5	60	0.063	0.08	0.83
I09001	1	90	0.874	0.97	0.28
I09101	2	90	-0.109	-0.20	0.57
I09201	5	90	0.034	0.08	0.96
I12001	1	120	-0.841	-0.94	0.17
I12101	2	120	0.101	0.17	0.42
I12201	5	120	-0.031	-0.08	0.92
I14501	1	145	-0.609	-0.83	0.05
I14601	2	145	-0.091	-0.11	0.13
I14701	5	145	-0.062	-0.08	0.78
I16001	1	150	-0.494	-0.71	0.05
I16101	2	160	-0.211	-0.32	0.05
I16201	5	160	-0.066	-0.08	0.59

\*referenced to 10 m on prototype

Table 6. Normal Force and Maximum Pressure Difference  
for an Array Field in Nonuniform Flow,  
 $x/c = 1.5$  and  $3.0$

File Name	$x/c$	Array #	$\alpha$	$C_N^*$	$\wedge C_{p \max}^*$	$s_{\max}/c$
H03501	1.5	1	35	0.732	0.85	0.93
H03601	1.5	2	35	0.038	0.29	0.16
H03701	1.5	5	35	0.129	0.18	0.43
H14501	1.5	1	145	-0.606	-0.81	0.05
H14601	1.5	2	145	0.077	0.17	0.05
H14701	1.5	5	145	-0.045	-0.11	0.82
J03501	3.0	1	35	0.708	0.83	0.93
J03601	3.0	2	35	0.278	0.42	0.40
J03701	3.0	4	35	0.143	0.21	0.82
J14501	3.0	1	145	-0.595	-0.78	0.05
J14601	3.0	2	145	-0.164	-0.18	0.56
J14701	3.0	4	145	-0.087	-0.10	0.63

\*referenced to 10 m on prototype

Table 7. Normal Force and Maximum Pressure Difference  
for an Array Field with a Fence,  $H_f/c = 0.75$ ,  
 $P_f = 30\%$ ,  $x_f/c = 1.25$

File Name	Array #	$\alpha$	$C_N^*$	$\Delta C_{p \max}^*$	$s_{\max}'/c$
K03501	1	35	0.168	0.20	0.82
K03601	2	35	0.081	0.10	0.53
K03701	5	35	0.092	0.14	0.90
K09001	1	90	0.476	0.53	0.84
K09101	2	90	-0.063	-0.13	0.46
K09201	5	90	0.039	0.08	0.86
K14501	1	145	-0.129	-0.15	0.17
K14601	2	145	-0.048	-0.06	0.76
K14701	5	145	-0.045	-0.07	0.77
K16001	1	160	-0.041	-0.06	0.11
K16101	2	160	-0.011	-0.03	0.82
K16201	5	160	-0.050	-0.07	0.61

\*referenced to 10 m on prototype

Table 8. Normal Force and Maximum Pressure Difference  
for an Array Field with a Fence,  $H_f/c = 0.75$ ,  
 $P_f = 30\%$ ,  $x_f/c = 2.5$

File Name	Array #	$\alpha$	$C_N^*$	$\Delta C_{p \max}^*$	$s_{\max}/c$
L03501	1	35	0.119	0.13	0.58
L03601	2	35	0.083	0.11	0.83
L03701	5	35	0.104	0.13	0.84
L09001	1	90	0.335	0.38	0.83
L09101	2	90	-0.020	-0.04	0.44
L09201	5	90	0.042	0.08	0.92
L14501	1	145	-0.115	-0.13	0.73
L14601	2	145	-0.056	-0.08	0.77
L14701	5	145	-0.043	-0.08	0.85
L16001	1	160	-0.029	-0.06	0.12
L16101	2	160	-0.024	-0.03	0.58
L16201	5	160	-0.052	-0.08	0.58

\*referenced to 10 m on prototype

Table 9. Normal Force and Maximum Pressure Difference  
for an Array Field with a Fence,  $H_f/c = 0.75$ ,  
 $P_f = 30\%$ ,  $x_f/c = 5.0$

File Name	Array #	$\alpha$	$C_N^*$	$\Delta C_{P \max}^*$	$s_{\max}/c$
M03501	1	35	0.097	0.13	0.83
M03601	2	35	0.102	0.14	0.84
M03701	5	35	0.122	0.17	0.95
M09001	1	90	0.266	0.34	0.82
M09101	2	90	0.013	0.03	0.24
M09201	5	90	0.050	0.08	0.96
M14501	1	145	-0.148	-0.27	0.44
M14601	2	145	-0.060	-0.10	0.77
M14701	5	145	-0.049	-0.08	0.76
M16001	1	160	-0.048	-0.06	0.28
M16101	2	160	-0.049	-0.07	0.60
M16201	5	160	-0.063	-0.08	0.55

\*referenced to 10 m on prototype

Table 10. Normal Force and Maximum Pressure Difference for an Array Field with a Fence of Various Height and Porosity

File Name	$P_f$	$H_f/c$	Array #	$\alpha$	$C_N$	$\Delta C_{p \max}^*$	$s_{\max}/c$
N11101	30%	0.25	1	35	0.339	0.49	0.96
O11101	30%	0.25	2	35	0.170	0.22	0.41
N11201	30%	0.5	1	35	0.195	0.27	0.95
O11201	30%	0.5	2	35	0.141	0.20	0.89
N11401	30%	1.0	1	35	0.094	0.11	0.42
O11401	30%	1.0	2	35	0.052	0.08	0.43
N11501	30%	1.25	1	35	0.153	0.20	0.91
O11501	30%	1.25	2	35	0.077	0.13	0.42
N12101	30%	0.25	1	145	-0.519	-0.64	0.15
O12101	30%	0.25	2	145	-0.010	-0.06	0.76
N12201	30%	0.5	1	145	-0.293	-0.34	0.71
O12201	30%	0.5	2	145	-0.046	-0.10	0.78
N12401	30%	1.0	1	145	-0.052	-0.07	0.18
O12401	30%	1.0	2	145	-0.013	-0.06	0.74
N12501	30%	1.25	1	145	-0.077	-0.13	0.14
O12501	30%	1.25	2	145	-0.010	-0.03	0.74
N01301	0%	0.75	1	35	-0.042	-0.06	0.26
O01301	0%	0.75	2	35	-0.022	-0.04	0.26
N02301	0%	0.75	1	145	0.101	0.15	0.41
O02301	0%	0.75	2	145	0.021	0.06	0.26

\*referenced to 10 m on prototype

Table 11. Normal Force and Maximum Pressure Difference for an Array Field, Edge Study

File Name	Fence	Array #	$\alpha$	$C_N^*$	$\Delta C_{p \max}^*$	$s_{\max}/c$
P03501	✓	1	35	0.083	0.18	0.91
P03601	✓	2	35	0.073	0.17	0.92
P03701	✓	5	35	0.137	0.29	0.94
P14501	✓	1	145	-0.056	-0.08	0.83
P14601	✓	2	145	-0.038	-0.08	0.83
P14701	✓	5	145	-0.108	-0.17	0.73
Q03501	---	1	35	0.524	0.78	0.95
Q03601	---	2	35	0.150	0.32	0.92
Q03701	---	5	35	0.225	0.46	0.95
Q14501	---	1	145	-0.504	-0.71	0.05
Q14601	---	2	145	-0.200	-0.34	0.06
Q14701	---	5	145	-0.227	-0.36	0.06

\*referenced to 10 m on prototype

Table 12. Normal Force and Maximum Pressure Difference  
for an Array Field, No Fence, Corner Study

File Name	MC	Array #	$\alpha$	$C_N^*$	$\Delta C_{p \max}^*$	$s_{\max}/c$
U03501	0	1	35	1.285	1.48	0.90
U03601	0	2	35	1.030	1.27	0.90
U03701	0	3	35	1.018	1.26	0.90
U14501	0	1	145	-1.123	-2.34	0.03
U14601	0	2	145	-1.165	-2.04	0.03
U14701	0	3	145	-1.180	-2.03	0.03
V03501	1	1	35	0.697	1.36	0.83
V03601	1	2	35	0.546	0.76	0.81
V03701	1	3	35	0.531	0.76	0.81
V14501	1	1	145	-0.693	-1.13	0.24
V14601	1	2	145	-0.595	-0.90	0.21
V14701	1	3	145	-0.638	-0.97	0.21

\*referenced to 10 m on prototype

Table 13. Normal Force and Maximum Pressure Difference for  
an Array Field with Various Fences, Corner Study

File Name	FC	Array #	$\alpha$	$C_N^*$	$\Delta C_p^*_{max}$	$s_{max}/c$
R01101	1	1	35	0.655	1.93	0.96
S01101	1	2	35	0.433	1.09	0.96
T01101	1	3	35	0.328	0.62	0.96
R02101	1	1	145	0.879	-1.04	0.41
S02101	1	2	145	-0.791	-1.02	0.04
T02101	1	3	145	-0.490	-0.53	0.46
R01201	2	1	35	0.172	0.52	0.96
S01201	2	2	35	0.274	0.71	0.96
T01201	2	3	35	0.444	1.22	0.96
R02201	2	1	145	-0.265	-0.28	0.56
S02201	2	2	145	-0.438	-0.49	0.43
T02201	2	3	145	-0.668	-0.76	0.39
R01301	3	1	35	0.178	0.52	0.96
S01301	3	2	35	0.192	0.52	0.96
T01301	3	3	35	0.216	0.67	0.96
R02301	3	1	145	-0.182	-0.20	0.73
S02301	3	2	145	-0.312	-0.34	0.58
T02301	3	3	145	-0.389	-0.43	0.42

\*referenced to 10 m on prototype

Table 14. Normal Force and Maximum Pressure Difference  
for an Array Field with Various Fences,  
MC = 1, Corner Study

File Name	FC	Array #	$\alpha$	$C_N^*$	$\Delta C_{p \max}^*$	$s_{\max}/c$
R11101	1	1	35	0.322	0.77	0.96
S11101	1	2	35	0.421	0.78	0.96
T11101	1	3	35	0.259	0.34	0.84
R12101	1	1	145	-0.430	-0.50	0.43
S12101	1	2	145	-0.550	-0.64	0.40
T12101	1	3	145	-0.430	-0.50	0.27
R11201	2	1	35	0.141	0.27	0.97
S11201	2	2	35	0.172	0.31	0.97
T11201	2	3	35	0.246	0.50	0.97
R12201	2	1	145	-0.255	-0.29	0.43
S12201	2	2	145	-0.283	-0.34	0.38
T12201	2	3	145	-0.368	-0.43	0.29
R11301	3	1	35	0.105	0.20	0.96
S11301	3	2	35	0.140	0.27	0.96
T11301	3	3	35	0.129	0.22	0.96
R12301	3	1	145	-0.153	-0.17	0.43
S12301	3	2	145	-0.217	-0.27	0.43
T12301	3	3	145	-0.209	-0.25	0.43

\*referenced to 10 m on prototype

Table 15. Normal Force and Maximum Pressure Difference  
for an Array Field with Various Models, FC = 1  
and 4, Corner Study

File Name	MC	FC	$\alpha$	Array #	$C_N^*$	$\Delta C_{p \max}^*$	$s_{\max}/c$
R21101	2	1	35	1	0.211	0.67	0.96
S21101	2	1	35	2	0.599	1.64	0.96
T21101	2	1	35	3	0.339	0.53	0.96
R22101	2	1	145	1	-0.571	-0.67	0.72
S22101	2	1	145	2	-1.022	-1.19	0.16
T22101	2	1	145	3	-0.659	-0.74	0.42
R31101	3	1	35	1	0.322	0.85	0.96
S31101	3	1	35	2	0.207	0.36	0.96
T31101	3	1	35	3	0.182	0.25	0.96
R32101	3	1	145	1	-0.377	-0.45	0.04
S32101	3	1	145	2	-0.190	-0.21	0.74
T32101	3	1	145	3	-0.137	-0.15	0.61
R01401	0	4	35	1	0.323	0.14	0.82
S01401	0	4	35	2	0.255	0.13	0.83
T01401	0	4	35	3	0.186	0.15	0.83
R02401	0	4	145	1	-0.682	-0.14	0.73
S02401	0	4	145	2	-0.491	-0.10	0.77
T02401	0	4	145	3	-0.435	-0.09	0.76

\*referenced to 10 m on prototype

Table 16. Normal Force and Maximum Pressure Difference  
for an Array Field with a Fence,  $H_f/c = 1.0$ ,  
 $\alpha = 60^\circ$  and  $120^\circ$

File Name	$\alpha$	Array #	$C_N^*$	$\Delta C_{p \max}^*$	$s_{\max}/c$
N23401	60	1	0.183	0.12	0.54
N24401	60	2	0.025	0.04	0.72
N25401	60	5	0.053	0.05	0.94
N33401	120	1	-0.165	-0.10	0.18
N34401	120	2	-0.015	-0.06	0.28
N35401	120	5	-0.048	-0.05	0.79

\*referenced to 10 m on prototype

Table 17. Fence Configurations

FC	$H_f/c$	$x_f/c$	$P_f$
1	0.75	2.5	30%
2	0.75	2.5	30%
3	0.75	2.5	30%
4	0.75	2.5	30%
5	0.75	1.25	30%
6	0.75	5.0	30%
7	0.25	2.5	30%
8	0.5	2.5	30%
9	1.0	2.5	30%
10	1.25	2.5	30%
11	0.25	2.5	0%
12	0.5	2.5	0%
13	0.75	2.5	0%
14	1.0	2.5	0%
15	1.25	2.5	0%

} see Figure 22

Table 18. List of Test Configurations

File Name	Flow Profile		WD	Array		H/c	x	α	Array #	FC <sup>1</sup>	M <sup>2</sup>
	Uniform	1/7 th		Single	Multiple						
A02001	✓		0	✓		0.25	-	20	-	-	0
A03501	✓		0	✓		0.25	-	35	-	-	0
A06001	✓		0	✓		0.25	-	60	-	-	0
A09001	✓		0	✓		0.25	-	90	-	-	0
A12001	✓		0	✓		0.25	-	120	-	-	0
A14501	✓		0	✓		0.25	-	145	-	-	0
A16001	✓		0	✓		0.25	-	160	-	-	0
B02001	✓		0	✓		0.5	-	20	-	-	0
B06001	✓		0	✓		0.5	-	60	-	-	0
B09001	✓		0	✓		0.5	-	90	-	-	0
B12001	✓		0	✓		0.5	-	120	-	-	0
E16001	✓		0	✓		0.5	-	160	-	-	0
C02001	✓		0	✓		-	-	20	-	-	0
C03501	✓		0	✓		-	-	35	-	-	0
C06001	✓		0	✓		-	-	60	-	-	0
C09001	✓		0	✓		-	-	90	-	-	0
D02001	✓		0		✓	0.25	1.5c	20	1	-	0
D02101	✓		0		✓	0.25	1.5c	20	2	-	0
D02201	✓		0		✓	0.25	1.5c	20	5	-	0
D03501	✓		0		✓	0.25	1.5c	35	1	-	0
D03601	✓		0		✓	0.25	1.5c	35	2	-	0
D03701	✓		0		✓	0.25	1.5c	35	5	-	0
D14501	✓		0		✓	0.25	1.5c	145	1	-	0
D14601	✓		0		✓	0.25	1.5c	145	2	-	0
D16001	✓		0		✓	0.25	1.5c	160	1	-	0
D16101	✓		0		✓	0.25	1.5c	160	2	-	0
E02001	✓		0		✓	0.25	2.0c	20	1	-	0
E02101	✓		0		✓	0.25	2.0c	20	2	-	0
E02201	✓		0		✓	0.25	2.0c	20	5	-	0
E03501	✓		0		✓	0.25	2.0c	35	1	-	0
E03601	✓		0		✓	0.25	2.0c	35	2	-	0
E03701	✓		0		✓	0.25	2.0c	35	5	-	0
E06001	✓		0		✓	0.25	2.0c	60	1	-	0
E06101	✓		0		✓	0.25	2.0c	60	2	-	0
E06201	✓		0		✓	0.25	2.0c	60	5	-	0
E09001	✓		0		✓	0.25	2.0c	90	1	-	0
E09101	✓		0		✓	0.25	2.0c	90	2	-	0
E09201	✓		0		✓	0.25	2.0c	90	5	-	0
E12001	✓		0		✓	0.25	2.0c	120	1	-	0
E12101	✓		0		✓	0.25	2.0c	120	2	-	0
E12201	✓		0		✓	0.25	2.0c	120	5	-	0
E14501	✓		0		✓	0.25	2.0c	145	1	-	0
E14601	✓		0		✓	0.25	2.0c	145	2	-	0
E14701	✓		0		✓	0.25	2.0c	145	5	-	0
E16001	✓		0		✓	0.25	2.0c	160	1	-	0
E16101	✓		0		✓	0.25	2.0c	160	2	-	0
E16201	✓		0		✓	0.25	2.0c	160	5	-	0
F03501	✓		0		✓	0.25	3.0c	35	1	-	0

<sup>1</sup>defined in Table 17<sup>2</sup>defined in Figure 24

Table 18. (continued)

File Name	Flow Profile		WD	Array		H/c	x	a	Array #	FC	MC
	Uniform	1/7 th		Single	Multiple						
F03601	/		0		/	0.25	3.0c	35	2	-	0
F03701	/		0		/	0.25	3.0c	35	4	-	0
F06001	/		0		/	0.25	3.0c	60	1	-	0
F06101	/		0		/	0.25	3.0c	60	2	-	0
F06201	/		0		/	0.25	3.0c	60	4	-	0
F12001	/		0		/	0.25	3.0c	120	1	-	0
F12101	/		0		/	0.25	3.0c	120	2	-	0
F12201	/		0		/	0.25	3.0c	120	4	-	0
F14501	/		0		/	0.25	3.0c	145	1	-	0
F14601	/		0		/	0.25	3.0c	145	2	-	0
F14701	/		0		/	0.25	3.0c	145	4	-	0
G02001		/	0	/		0.25	-	20	-	-	0
G03501		/	0	/		0.25	-	35	-	-	0
G06001		/	0	/		0.25	-	60	-	-	0
G09001		/	0	/		0.25	-	90	-	-	0
G12001		/	0	/		0.25	-	120	-	-	0
G14501		/	0	/		0.25	-	145	-	-	0
G16001		/	0	/		0.25	-	160	-	-	0
G01101		/	0	/		0.25	-	35	-	7	0
G01201		/	0	/		0.25	-	35	-	8	0
G01301		/	0	/		0.25	-	35	-	1	0
G01401		/	0	/		0.25	-	35	-	9	0
G01501		/	0	/		0.25	-	35	-	10	0
G02101		/	0	/		0.25	-	145	-	7	0
G02201		/	0	/		0.25	-	145	-	8	0
G02301		/	0	/		0.25	-	145	-	1	0
G02401		/	0	/		0.25	-	145	-	9	0
G02501		/	0	/		0.25	-	145	-	10	0
H02001		/	0		/	0.25	1.5c	20	1	-	0
H02101		/	0		/	0.25	1.5c	20	2	-	0
H02201		/	0		/	0.25	1.5c	20	5	-	0
H03501		/	0		/	0.25	1.5c	35	1	-	0
H03601		/	0		/	0.25	1.5c	35	2	-	0
H03701		/	0		/	0.25	1.5c	35	5	-	0
H14501		/	0		/	0.25	1.5c	145	1	-	0
H14601		/	0		/	0.25	1.5c	145	2	-	0
H14701		/	0		/	0.25	1.5c	145	5	-	0
H16001		/	0		/	0.25	1.5c	160	1	-	0
H16101		/	0		/	0.25	1.5c	160	2	-	0
H16201		/	0		/	0.25	1.5c	160	5	-	0
I02001		/	0		/	0.25	2.0c	20	1	-	0
I02101		/	0		/	0.25	2.0c	20	2	-	0
I02201		/	0		/	0.25	2.0c	20	5	-	0
I03501		/	0		/	0.25	2.0c	35	1	-	0
I03601		/	0		/	0.25	2.0c	35	2	-	0
I03701		/	0		/	0.25	2.0c	35	5	-	0
I06001		/	0		/	0.25	2.0c	60	1	-	0
I06101		/	0		/	0.25	2.0c	60	2	-	0

Table 18. (continued)

File Name	Flow Profile		WD	Array		H/c	x	a	Array #	FC	NC
	Uniform	1/7 th		Single	Multiple						
I06201	✓		0	✓		0.25	2.0c	60	5	-	0
I09001	✓		0	✓		0.25	2.0c	90	1	-	0
I09101	✓		0	✓		0.25	2.0c	90	2	-	0
I09201	✓		0	✓		0.25	2.0c	90	5	-	0
I12001	✓		0	✓		0.25	2.0c	120	1	-	0
I12101	✓		0	✓		0.25	2.0c	120	2	-	0
I12201	✓		0	✓		0.25	2.0c	120	5	-	0
I14501	✓		0	✓		0.25	2.0c	145	1	-	0
I14601	✓		0	✓		0.25	2.0c	145	2	-	0
I14701	✓		0	✓		0.25	2.0c	145	5	-	0
I16001	✓		0	✓		0.25	2.0c	160	1	-	0
I16101	✓		0	✓		0.25	2.0c	160	2	-	0
I16201	✓		0	✓		0.25	2.0c	160	5	-	0
J03501	✓		0	✓		0.25	3.0c	35	1	-	0
J03601	✓		0	✓		0.25	3.0c	35	2	-	0
J03701	✓		0	✓		0.25	3.0c	35	4	-	0
J06001	✓		0	✓		0.25	3.0c	60	1	-	0
J06101	✓		0	✓		0.25	3.0c	60	2	-	0
J06201	✓		0	✓		0.25	3.0c	60	4	-	0
J12001	✓		0	✓		0.25	3.0c	120	1	-	0
J12101	✓		0	✓		0.25	3.0c	120	2	-	0
J12201	✓		0	✓		0.25	3.0c	120	4	-	0
J14501	✓		0	✓		0.25	3.0c	145	1	-	0
J14601	✓		0	✓		0.25	3.0c	145	2	-	0
J14701	✓		0	✓		0.25	3.0c	145	4	-	0
K03501	✓		0	✓		0.25	2.0c	35	1	5	0
K03601	✓		0	✓		0.25	2.0c	35	2	5	0
K03701	✓		0	✓		0.25	2.0c	35	5	5	0
K09001	✓		0	✓		0.25	2.0c	90	1	5	0
K09101	✓		0	✓		0.25	2.0c	90	2	5	0
K09201	✓		0	✓		0.25	2.0c	90	5	5	0
K14501	✓		0	✓		0.25	2.0c	145	1	5	0
K14601	✓		0	✓		0.25	2.0c	145	2	5	0
K14701	✓		0	✓		0.25	2.0c	145	5	5	0
K16001	✓		0	✓		0.25	2.0c	160	1	5	0
K16101	✓		0	✓		0.25	2.0c	160	2	5	0
K16201	✓		0	✓		0.25	2.0c	160	5	5	0
L03501	✓		0	✓		0.25	2.0c	35	1	1	0
L03601	✓		0	✓		0.25	2.0c	35	2	1	0
L03701	✓		0	✓		0.25	2.0c	35	5	1	0
L09001	✓		0	✓		0.25	2.0c	90	1	1	0
L09101	✓		0	✓		0.25	2.0c	90	2	1	0
L09201	✓		0	✓		0.25	2.0c	90	5	1	0
L14501	✓		0	✓		0.25	2.0c	145	1	1	0
L14601	✓		0	✓		0.25	2.0c	145	2	1	0
L14701	✓		0	✓		0.25	2.0c	145	5	1	0
L16001	✓		0	✓		0.25	2.0c	160	1	1	0
L16101	✓		0	✓		0.25	2.0c	160	2	1	0

Table 18. (continued)

File Name	Flow Profile		WD	Array		H/c	x	a	Array #	FC	MC
	Uniform	1/7 ch		Single	Multiple						
L16201	/		0		/	0.25	2.0c	160	5	1	0
M03501	/		0		/	0.25	2.0c	35	1	6	0
M03601	/		0		/	0.25	2.0c	35	2	6	0
M03701	/		0		/	0.25	2.0c	35	5	6	0
M09001	/		0		/	0.25	2.0c	90	1	6	0
M09101	/		0		/	0.25	2.0c	90	2	6	0
M09201	/		0		/	0.25	2.0c	90	5	6	0
M14501	/		0		/	0.25	2.0c	145	1	6	0
M14601	/		0		/	0.25	2.0c	145	2	6	0
M14701	/		0		/	0.25	2.0c	145	5	6	0
M16001	/		0		/	0.25	2.0c	160	1	6	0
M15101	/		0		/	0.25	2.0c	160	2	6	0
M16201	/		0		/	0.25	2.0c	160	5	6	0
N01101	/		0		/	0.25	2.0c	35	1	11	0
N01201	/		0		/	0.25	2.0c	35	1	12	0
N01301	/		0		/	0.25	2.0c	35	1	13	0
N01401	/		0		/	0.25	2.0c	35	1	14	0
N01501	/		0		/	0.25	2.0c	35	1	15	0
N02101	/		0		/	0.25	2.0c	145	1	11	0
N02201	/		0		/	0.25	2.0c	145	1	12	0
N02301	/		0		/	0.25	2.0c	145	1	13	0
N02401	/		0		/	0.25	2.0c	145	1	14	0
N02501	/		0		/	0.25	2.0c	145	1	15	0
N11101	/		0		/	0.25	2.0c	35	1	7	0
N11201	/		0		/	0.25	2.0c	35	1	8	0
N11401	/		0		/	0.25	2.0c	35	1	9	0
N11501	/		0		/	0.25	2.0c	35	1	10	0
N12101	/		0		/	0.25	2.0c	145	1	7	0
N12201	/		0		/	0.25	2.0c	145	1	8	0
N12401	/		0		/	0.25	2.0c	145	1	9	0
N12501	/		0		/	0.25	2.0c	145	1	10	0
N23401	/		0		/	0.25	2.0c	60	1	9	0
N24401	/		0		/	0.25	2.0c	60	2	9	0
N25401	/		0		/	0.25	2.0c	60	5	9	0
N33401	/		0		/	0.25	2.0c	120	1	9	0
N34401	/		0		/	0.25	2.0c	120	2	9	0
N35401	/		0		/	0.25	2.0c	120	5	9	0
001101	/		0		/	0.25	2.0c	35	2	11	0
001201	/		0		/	0.25	2.0c	35	2	12	0
001301	/		0		/	0.25	2.0c	35	2	13	0
001401	/		0		/	0.25	2.0c	35	2	14	0
001501	/		0		/	0.25	2.0c	35	2	15	0
002101	/		0		/	0.25	2.0c	145	2	11	0
002201	/		0		/	0.25	2.0c	145	2	12	0
002301	/		0		/	0.25	2.0c	145	2	13	0
002401	/		0		/	0.25	2.0c	145	2	14	0
002501	/		0		/	0.25	2.0c	145	2	15	0
C11101	/		0		/	0.25	2.0c	35	2	7	0

Table 18. (continued)

File Name	Flow Profile		WD	Array		H/c	x	a	Array #	FC	MC
	Uniform	1/7 th		Single	Multiple						
O11201	✓		0		✓	0.25	2.0c	35	2	8	0
O11401	✓		0		✓	0.25	2.0c	35	2	9	0
O11501	✓		0		✓	0.25	2.0c	35	2	10	0
O12101	✓		0		✓	0.25	2.0c	145	2	7	0
O12201	✓		0		✓	0.25	2.0c	145	2	8	0
O12401	✓		0		✓	0.25	2.0c	145	2	9	0
O12501	✓		0		✓	0.25	2.0c	145	2	10	0
P03501	✓		0		(edge)	0.25	2.0c	35	1	1	0
P03601	✓		0		(edge)	0.25	2.0c	35	2	1	0
P03701	✓		0		(edge)	0.25	2.0c	35	5	1	0
P14501	✓		0		(edge)	0.25	2.0c	145	1	1	0
P14601	✓		0		(edge)	0.25	2.0c	145	2	1	0
P14701	✓		0		(edge)	0.25	2.0c	145	5	1	0
Q03501	✓		0		(edge)	0.25	2.0c	35	1	-	0
Q03601	✓		0		(edge)	0.25	2.0c	35	2	-	0
Q03701	✓		0		(edge)	0.25	2.0c	35	5	-	0
Q14501	✓		0		(edge)	0.25	2.0c	145	1	-	0
Q14601	✓		0		(edge)	0.25	2.0c	145	2	-	0
Q14701	✓		0		(edge)	0.25	2.0c	145	5	-	0
R01101	✓		45		✓	0.25	2.0c	35	1	1	0
R02101	✓		45		✓	0.25	2.0c	145	1	1	0
R01201	✓		45		✓	0.25	2.0c	35	1	2	0
R02201	✓		45		✓	0.25	2.0c	145	1	2	0
R01301	✓		45		✓	0.25	2.0c	35	1	3	0
R02301	✓		45		✓	0.25	2.0c	145	1	3	0
R01401	✓		45		✓	0.25	2.0c	35	1	4	0
R02401	✓		45		✓	0.25	2.0c	145	1	4	0
R11101	✓		45		✓	0.25	2.0c	35	1	1	1
R12101	✓		45		✓	0.25	2.0c	145	1	1	1
R11201	✓		45		✓	0.25	2.0c	35	1	2	1
R12201	✓		45		✓	0.25	2.0c	145	1	2	1
R11301	✓		45		✓	0.25	2.0c	35	1	3	1
R12301	✓		45		✓	0.25	2.0c	145	1	3	1
R21101	✓		45		✓	0.25	2.0c	35	1	1	2
R22101	✓		45		✓	0.25	2.0c	145	1	1	2
R31101	✓		45		✓	0.25	2.0c	35	1	1	3
R32101	✓		45		✓	0.25	2.0c	145	1	1	3
S01101	✓		45		✓	0.25	2.0c	35	2	1	0
S02101	✓		45		✓	0.25	2.0c	145	2	1	0
S01201	✓		45		✓	0.25	2.0c	35	2	2	0
S02201	✓		45		✓	0.25	2.0c	145	2	2	0
S01301	✓		45		✓	0.25	2.0c	35	2	3	0
S02301	✓		45		✓	0.25	2.0c	145	2	3	0
S01401	✓		45		✓	0.25	2.0c	35	2	4	0
S02401	✓		45		✓	0.25	2.0c	145	2	4	0
S11101	✓		45		✓	0.25	2.0c	35	2	1	1
S12101	✓		45		✓	0.25	2.0c	145	2	1	1
S11201	✓		45		✓	0.25	2.0c	35	2	2	1

Table 18. (continued)

File Name	Flow Profile		WD	Array		H/c	x	a	Array #	FC	MC
	Uniform	1/7 th		Single	Multiple						
S12201	✓		45		✓	0.25	2.0c	145	2	2	1
S11301	✓		45		✓	0.25	2.0c	35	2	3	1
S12301	✓		45		✓	0.25	2.0c	145	2	3	1
S21101	✓		45		✓	0.25	2.0c	35	2	1	2
S22101	✓		45		✓	0.25	2.0c	145	2	1	2
S31101	✓		45		✓	0.25	2.0c	35	2	1	3
S32101	✓		45		✓	0.25	2.0c	145	2	1	3
T01101	✓		45		✓	0.25	2.0c	35	3	1	0
T02101	✓		45		✓	0.25	2.0c	145	3	1	0
T01201	✓		45		✓	0.25	2.0c	35	3	2	0
T02201	✓		45		✓	0.25	2.0c	145	3	2	0
T01301	✓		45		✓	0.25	2.0c	35	3	3	0
T02301	✓		45		✓	0.25	2.0c	145	3	3	0
T01401	✓		45		✓	0.25	2.0c	35	3	4	0
T02401	✓		45		✓	0.25	2.0c	145	3	4	0
T11101	✓		45		✓	0.25	2.0c	35	3	1	1
T12101	✓		45		✓	0.25	2.0c	145	3	1	1
T11201	✓		45		✓	0.25	2.0c	35	3	2	1
T12201	✓		45		✓	0.25	2.0c	145	3	2	1
T11301	✓		45		✓	0.25	2.0c	35	3	3	1
T12301	✓		45		✓	0.25	2.0c	145	3	3	1
T21101	✓		45		✓	0.25	2.0c	35	3	1	2
T22101	✓		45		✓	0.25	2.0c	145	3	1	2
T31101	✓		45		✓	0.25	2.0c	35	3	1	3
T32101	✓		45		✓	0.25	2.0c	145	3	1	3
U03501	✓		45		✓	0.25	2.0c	35	1	-	0
U03601	✓		45		✓	0.25	2.0c	35	2	-	0
U03701	✓		45		✓	0.25	2.0c	35	3	-	0
U14501	✓		45		✓	0.25	2.0c	145	1	-	0
U14601	✓		45		✓	0.25	2.0c	145	2	-	0
U14701	✓		45		✓	0.25	2.0c	145	3	-	0
V03501	✓		45		✓	0.25	2.0c	35	1	-	1
V03601	✓		45		✓	0.25	2.0c	35	2	-	1
V03701	✓		45		✓	0.25	2.0c	35	3	-	1
V14501	✓		45		✓	0.25	2.0c	145	1	-	1
V14601	✓		45		✓	0.25	2.0c	145	2	-	1
V14701	✓		45		✓	0.25	2.0c	145	3	-	1
W03501	✓		0		(edge)	0.25	2.0c	35	1	-	(1:12) <sup>0</sup>
W03601	✓		0		(edge)	0.25	2.0c	35	2	-	(1:12) <sup>0</sup>
W03701	✓		0		(edge)	0.25	2.0c	35	5	-	(1:12) <sup>0</sup>
W14501	✓		0		(edge)	0.25	2.0c	145	1	-	(1:12) <sup>0</sup>
W14601	✓		0		(edge)	0.25	2.0c	145	2	-	(1:12) <sup>0</sup>
W14701	✓		0		(edge)	0.25	2.0c	145	5	-	(1:12) <sup>0</sup>
X03501	✓		0		(edge)	0.25	2.0c	35	1	1	(1:12) <sup>0</sup>
X03601	✓		0		(edge)	0.25	2.0c	35	2	1	(1:12) <sup>0</sup>
X14501	✓		0		(edge)	0.25	2.0c	145	1	1	(1:12) <sup>0</sup>
X14601	✓		0		(edge)	0.25	2.0c	145	2	1	(1:12) <sup>0</sup>
Z03501	✓		0		✓	0.25	-	35	-	-	(1:12) <sup>0</sup>

A-82



**B-1**

**APPENDIX B**

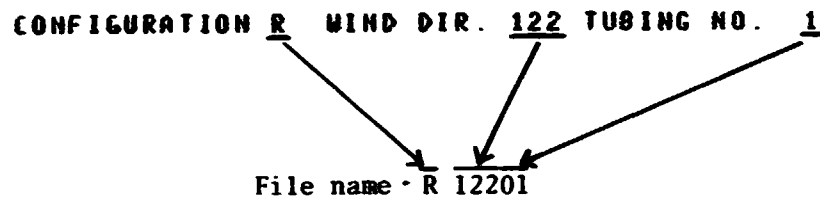
**Pressure Data Referenced to 10 m on Prototype**

**This Page Left  
Blank Intentionally**

## B-1a

This appendix presents the data supplement consisting of the velocity and turbulent profile of the nonuniform flow, the digitized pressure data referenced to 10 m on prototype and the various plots of pressure distribution along the chord of the solar array.

Pressure coefficients are defined in Section 3.2 on the main report. The pressure tap numbers shown in Appendix B are defined that; on the upstream surface of the solar array, the number runs 1 through 10 from the edge where  $s/c = 0$ , and on the downstream surface, 20 through 11. The file name for each test configuration is formulated as follows.



Force and model configurations are schematically explained in Figures 22 and 24 of the main report, respectively. Fence configurations are also tabulated in Table 17 of that report.

## List of Run Configurations

File Name	Flow Profile		WD	Array		H/c	x	a	Array #	FC	MC
	Uniform	1/7 th		Single	Multiple						
A02001	✓		0	✓		0.25	-	20	-	-	0
A03501	✓		0	✓		0.25	-	35	-	-	0
A06001	✓		0	✓		0.25	-	60	-	-	0
A09001	✓		0	✓		0.25	-	90	-	-	0
A12001	✓		0	✓		0.25	-	120	-	-	0
A14501	✓		0	✓		0.25	-	145	-	-	0
A16001	✓		0	✓		0.25	-	160	-	-	0
B02001	✓		0	✓		0.5	-	20	-	-	0
B06001	✓		0	✓		0.5	-	60	-	-	0
B09001	✓		0	✓		0.5	-	90	-	-	0
B12001	✓		0	✓		0.5	-	120	-	-	0
B16001	✓		0	✓		0.5	-	160	-	-	0
C02001	✓		0	✓		"	-	20	-	-	0
C03501	✓		0	✓		"	-	35	-	-	0
C06001	✓		0	✓		"	-	60	-	-	0
C09001	✓		0	✓		"	-	90	-	-	0
D02001	✓		0		✓	0.25	1.5c	20	1	-	0
D02101	✓		0		✓	0.25	1.5c	20	2	-	0
D02201	✓		0		✓	0.25	1.5c	20	5	-	0
D03501	✓		0		✓	0.25	1.5c	35	1	-	0
D03601	✓		0		✓	0.25	1.5c	35	2	-	0
D03701	✓		0		✓	0.25	1.5c	35	5	-	0
D14501	✓		0		✓	0.25	1.5c	145	1	-	0
D14601	✓		0		✓	0.25	1.5c	145	2	-	0
D16001	✓		0		✓	0.25	1.5c	160	1	-	0
D16101	✓		0		✓	0.25	1.5c	160	2	-	0
E02001	✓		0		✓	0.25	2.0c	20	1	-	0
E02101	✓		0		✓	0.25	2.0c	20	2	-	0
E02201	✓		0		✓	0.25	2.0c	20	5	-	0
E03501	✓		0		✓	0.25	2.0c	35	1	-	0
E03601	✓		0		✓	0.25	2.0c	35	2	-	0
E03701	✓		0		✓	0.25	2.0c	35	5	-	0
E06001	✓		0		✓	0.25	2.0c	60	1	-	0
E06101	✓		0		✓	0.25	2.0c	60	2	-	0
E06201	✓		0		✓	0.25	2.0c	60	5	-	0
E09001	✓		0		✓	0.25	2.0c	90	1	-	0
E09101	✓		0		✓	0.25	2.0c	90	2	-	0
E09201	✓		0		✓	0.25	2.0c	90	5	-	0
E12001	✓		0		✓	0.25	2.0c	120	1	-	0
E12101	✓		0		✓	0.25	2.0c	120	2	-	0
E12201	✓		0		✓	0.25	2.0c	120	5	-	0
E14501	✓		0		✓	0.25	2.0c	145	1	-	0
E14601	✓		0		✓	0.25	2.0c	145	2	-	0
E14701	✓		0		✓	0.25	2.0c	145	5	-	0
E16001	✓		0		✓	0.25	2.0c	160	1	-	0
E16101	✓		0		✓	0.25	2.0c	160	2	-	0
E16201	✓		0		✓	0.25	2.0c	160	5	-	0
F03501	✓		0		✓	0.25	3.0c	35	1	-	0

B-3

File Name	Flow Profile		WD	Array		H/c	x	a	Array #	FC	MC
	Uniform	1/7 th		Single	Multiple						
F03601	✓		0		✓	0.25	3.0c	35	2	-	0
F03701	✓		0		✓	0.25	3.0c	35	4	-	0
F06001	✓		0		✓	0.25	3.0c	60	1	-	0
F06101	✓		0		✓	0.25	3.0c	60	2	-	0
F06201	✓		0		✓	0.25	3.0c	60	4	-	0
F12001	✓		0		✓	0.25	3.0c	120	1	-	0
F12101	✓		0		✓	0.25	3.0c	120	2	-	0
F12201	✓		0		✓	0.25	3.0c	120	4	-	0
F14001	✓		0		✓	0.25	3.0c	145	1	-	0
F14601	✓		0		✓	0.25	3.0c	145	2	-	0
F14701	✓		0		✓	0.25	3.0c	145	4	-	0
G02001		✓	0	✓		0.25	-	20	-	-	0
G03501		✓	0	✓		0.25	-	35	-	-	0
G06001		✓	0	✓		0.25	-	60	-	-	0
G09001		✓	0	✓		0.25	-	90	-	-	0
G12001		✓	0	✓		0.25	-	120	-	-	0
G14001		✓	0	✓		0.25	-	145	-	-	0
G16001		✓	0	✓		0.25	-	160	-	-	0
G01101		✓	0	✓		0.25	-	35	-	7	0
G01201		✓	0	✓		0.25	-	35	-	8	0
G01301		✓	0	✓		0.25	-	35	-	1	0
G01401		✓	0	✓		0.25	-	35	-	9	0
G01501		✓	0	✓		0.25	-	35	-	10	0
G02101		✓	0	✓		0.25	-	145	-	7	0
G02201		✓	0	✓		0.25	-	145	-	8	0
G02301		✓	0	✓		0.25	-	145	-	1	0
G02401		✓	0	✓		0.25	-	145	-	9	0
G02501		✓	0	✓		0.25	-	145	-	10	0
H02001		✓	0		✓	0.25	1.5c	20	1	-	0
H02101		✓	0		✓	0.25	1.5c	20	2	-	0
H02201		✓	0		✓	0.25	1.5c	20	5	-	0
H03501		✓	0		✓	0.25	1.5c	35	1	-	0
H03601		✓	0		✓	0.25	1.5c	35	2	-	0
H03701		✓	0		✓	0.25	1.5c	35	5	-	0
H14501		✓	0		✓	0.25	1.5c	145	1	-	0
H14601		✓	0		✓	0.25	1.5c	145	2	-	0
H14701		✓	0		✓	0.25	1.5c	145	5	-	0
H16001		✓	0		✓	0.25	1.5c	160	1	-	0
H16101		✓	0		✓	0.25	1.5c	160	2	-	0
H16201		✓	0		✓	0.25	1.5c	160	5	-	0
I02001		✓	0		✓	0.25	2.0c	20	1	-	0
I02101		✓	0		✓	0.25	2.0c	20	2	-	0
I02201		✓	0		✓	0.25	2.0c	20	5	-	0
I03001		✓	0		✓	0.25	2.0c	35	1	-	0
I03101		✓	0		✓	0.25	2.0c	35	2	-	0
I03201		✓	0		✓	0.25	2.0c	35	5	-	0
I06001		✓	0		✓	0.25	2.0c	60	1	-	0
I06101		✓	0		✓	0.25	2.0c	60	2	-	0

File Name	Flow Profile		WD	Array		H/c	x	a	Array #	FC	MC
	Uniform	1/7 th		Single	Multiple						
I06201	/		0	/		0.25	2.0c	60	5	-	0
I09001	/		0	/		0.25	2.0c	90	1	-	0
I09101	/		0	/		0.25	2.0c	90	2	-	0
I09201	/		0	/		0.25	2.0c	90	5	-	0
I12001	/		0	/		0.25	2.0c	120	1	-	0
I12101	/		0	/		0.25	2.0c	120	2	-	0
I12201	/		0	/		0.25	2.0c	120	5	-	0
I14501	/		0	/		0.25	2.0c	145	1	-	0
I14601	/		0	/		0.25	2.0c	145	2	-	0
I14701	/		0	/		0.25	2.0c	145	5	-	0
I16001	/		0	/		0.25	2.0c	160	1	-	0
I16101	/		0	/		0.25	2.0c	160	2	-	0
I16201	/		0	/		0.25	2.0c	160	5	-	0
J03501	/		0	/		0.25	3.0c	35	1	-	0
J03601	/		0	/		0.25	3.0c	35	2	-	0
J03701	/		0	/		0.25	3.0c	35	4	-	0
J06001	/		0	/		0.25	3.0c	60	1	-	0
J06101	/		0	/		0.25	3.0c	60	2	-	0
J06201	/		0	/		0.25	3.0c	60	4	-	0
J12001	/		0	/		0.25	3.0c	120	1	-	0
J12101	/		0	/		0.25	3.0c	120	2	-	0
J12201	/		0	/		0.25	3.0c	120	4	-	0
J14501	/		0	/		0.25	3.0c	145	1	-	0
J14601	/		0	/		0.25	3.0c	145	2	-	0
J14701	/		0	/		0.25	3.0c	145	4	-	0
K03501	/		0	/		0.25	2.0c	35	1	5	0
K03601	/		0	/		0.25	2.0c	35	2	5	0
K03701	/		0	/		0.25	2.0c	35	5	5	0
K09001	/		0	/		0.25	2.0c	90	1	5	0
K09101	/		0	/		0.25	2.0c	90	2	5	0
K09201	/		0	/		0.25	2.0c	90	5	5	0
K14501	/		0	/		0.25	2.0c	145	1	5	0
K14601	/		0	/		0.25	2.0c	145	2	5	0
K14701	/		0	/		0.25	2.0c	145	5	5	0
K16001	/		0	/		0.25	2.0c	160	1	5	0
K16101	/		0	/		0.25	2.0c	160	2	5	0
K16201	/		0	/		0.25	2.0c	160	5	5	0
L03501	/		0	/		0.25	2.0c	35	1	1	0
L03601	/		0	/		0.25	2.0c	35	2	1	0
L03701	/		0	/		0.25	2.0c	35	5	1	0
L09001	/		0	/		0.25	2.0c	90	1	1	0
L09101	/		0	/		0.25	2.0c	90	2	1	0
L09201	/		0	/		0.25	2.0c	90	5	1	0
L14501	/		0	/		0.25	2.0c	145	1	1	0
L14601	/		0	/		0.25	2.0c	145	2	1	0
L14701	/		0	/		0.25	2.0c	145	5	1	0
L16001	/		0	/		0.25	2.0c	160	1	1	0
L16101	/		0	/		0.25	2.0c	160	2	1	0

## B-5

File Name	Flow Profile		WD	Array		H/c	x	a	Array #	FC	MC
	Uniform	1/7 th		Single	Multiple						
L16201	✓		0		✓	0.25	2.0c	160	5	1	0
M03501	✓		0		✓	0.25	2.0c	35	1	6	0
M03601	✓		0		✓	0.25	2.0c	35	2	6	0
M03701	✓		0		✓	0.25	2.0c	35	5	6	0
M09001	✓		0		✓	0.25	2.0c	90	1	6	0
M09101	✓		0		✓	0.25	2.0c	90	2	6	0
M09201	✓		0		✓	0.25	2.0c	90	5	6	0
M14501	✓		0		✓	0.25	2.0c	145	1	6	0
M14601	✓		0		✓	0.25	2.0c	145	2	6	0
M14701	✓		0		✓	0.25	2.0c	145	5	6	0
M16001	✓		0		✓	0.25	2.0c	160	1	6	0
M16101	✓		0		✓	0.25	2.0c	160	2	6	0
M16201	✓		0		✓	0.25	2.0c	160	5	6	0
N01101	✓		0		✓	0.25	2.0c	35	1	11	0
N01201	✓		0		✓	0.25	2.0c	35	1	12	0
N01301	✓		0		✓	0.25	2.0c	35	1	13	0
N01401	✓		0		✓	0.25	2.0c	35	1	14	0
N01501	✓		0		✓	0.25	2.0c	35	1	15	0
N02101	✓		0		✓	0.25	2.0c	145	1	11	0
N02201	✓		0		✓	0.25	2.0c	145	1	12	0
N02301	✓		0		✓	0.25	2.0c	145	1	13	0
N02401	✓		0		✓	0.25	2.0c	145	1	14	0
N02501	✓		0		✓	0.25	2.0c	145	1	15	0
N11101	✓		0		✓	0.25	2.0c	35	1	7	0
N11201	✓		0		✓	0.25	2.0c	35	1	8	0
N11401	✓		0		✓	0.25	2.0c	35	1	9	0
N11501	✓		0		✓	0.25	2.0c	35	1	10	0
N12101	✓		0		✓	0.25	2.0c	145	1	7	0
N12201	✓		0		✓	0.25	2.0c	145	1	8	0
N12401	✓		0		✓	0.25	2.0c	145	1	9	0
N12501	✓		0		✓	0.25	2.0c	145	1	10	0
N23401	✓		0		✓	0.25	2.0c	60	1	9	0
N24401	✓		0		✓	0.25	2.0c	60	2	9	0
N25401	✓		0		✓	0.25	2.0c	60	5	9	0
N33401	✓		0		✓	0.25	2.0c	120	1	9	0
N34401	✓		0		✓	0.25	2.0c	120	2	9	0
N35401	✓		0		✓	0.25	2.0c	120	5	9	0
O01101	✓		0		✓	0.25	2.0c	35	2	11	0
O01201	✓		0		✓	0.25	2.0c	35	2	12	0
O01301	✓		0		✓	0.25	2.0c	35	2	13	0
O01401	✓		0		✓	0.25	2.0c	35	2	14	0
O01501	✓		0		✓	0.25	2.0c	35	2	15	0
O02101	✓		0		✓	0.25	2.0c	145	2	11	0
O02201	✓		0		✓	0.25	2.0c	145	2	12	0
O02301	✓		0		✓	0.25	2.0c	145	2	13	0
O02401	✓		0		✓	0.25	2.0c	145	2	14	0
O02501	✓		0		✓	0.25	2.0c	145	2	15	0
O11101	✓		0		✓	0.25	2.0c	35	2	7	0

B-6

File Name	Flow Profile		WD	Array		H/c	x	a	Array #	FC	MC
	Uniform	1/7 ch		Single	Multiple						
O11201	✓		0		✓	0.25	2.0c	35	2	8	0
O11401	✓		0		✓	0.25	2.0c	35	2	9	0
O11501	✓		0		✓	0.25	2.0c	35	2	10	0
O12101	✓		0		✓	0.25	2.0c	145	2	7	0
O12201	✓		0		✓	0.25	2.0c	145	2	8	0
O12401	✓		0		✓	0.25	2.0c	145	2	9	0
O12501	✓		0		✓	0.25	2.0c	145	2	10	0
P03501	✓		0		(edge)	0.25	2.0c	35	1	1	0
P03601	✓		0		(edge)	0.25	2.0c	35	2	1	0
P03701	✓		0		(edge)	0.25	2.0c	35	5	1	0
P14501	✓		0		(edge)	0.25	2.0c	145	1	1	0
P14601	✓		0		(edge)	0.25	2.0c	145	2	1	0
P14701	✓		0		(edge)	0.25	2.0c	145	5	1	0
Q03501	✓		0		(edge)	0.25	2.0c	35	1	-	0
Q03601	✓		0		(edge)	0.25	2.0c	35	2	-	0
Q03701	✓		0		(edge)	0.25	2.0c	35	5	-	0
Q14501	✓		0		(edge)	0.25	2.0c	145	1	-	0
Q14601	✓		0		(edge)	0.25	2.0c	145	2	-	0
Q14701	✓		0		(edge)	0.25	2.0c	145	5	-	0
R01101	✓		45		✓	0.25	2.0c	35	1	1	0
R02101	✓		45		✓	0.25	2.0c	145	1	1	0
R01201	✓		45		✓	0.25	2.0c	35	1	2	0
R02201	✓		45		✓	0.25	2.0c	145	1	2	0
R01301	✓		45		✓	0.25	2.0c	35	1	3	0
R02301	✓		45		✓	0.25	2.0c	145	1	3	0
R01401	✓		45		✓	0.25	2.0c	35	1	4	0
R02401	✓		45		✓	0.25	2.0c	145	1	4	0
R11101	✓		45		✓	0.25	2.0c	35	1	1	1
R12101	✓		45		✓	0.25	2.0c	145	1	1	1
R11201	✓		45		✓	0.25	2.0c	35	1	2	1
R12201	✓		45		✓	0.25	2.0c	145	1	2	1
R11301	✓		45		✓	0.25	2.0c	35	1	3	1
R12301	✓		45		✓	0.25	2.0c	145	1	3	1
R21101	✓		45		✓	0.25	2.0c	35	1	1	2
R22101	✓		45		✓	0.25	2.0c	145	1	1	2
R31101	✓		45		✓	0.25	2.0c	35	1	1	3
R32101	✓		45		✓	0.25	2.0c	145	1	1	3
S01101	✓		45		✓	0.25	2.0c	35	2	1	0
S02101	✓		45		✓	0.25	2.0c	145	2	1	0
S01201	✓		45		✓	0.25	2.0c	35	2	2	0
S02201	✓		45		✓	0.25	2.0c	145	2	2	0
S01301	✓		45		✓	0.25	2.0c	35	2	3	0
S02301	✓		45		✓	0.25	2.0c	145	2	3	0
S01401	✓		45		✓	0.25	2.0c	35	2	4	0
S02401	✓		45		✓	0.25	2.0c	145	2	4	0
S11101	✓		45		✓	0.25	2.0c	35	2	1	1
S12101	✓		45		✓	0.25	2.0c	145	2	1	1
S11201	✓		45		✓	0.25	2.0c	35	2	2	1

B-7

File Name	Flow Profile		WD	Array		H/c	x	a	Array #	FC	MC
	Uniform	1/7 th		Single	Multiple						
S12201	✓		45	✓		0.25	2.0c	145	2	2	1
S11301	✓		45	✓		0.25	2.0c	35	2	3	1
S12301	✓		45	✓		0.25	2.0c	145	2	3	1
S21101	✓		45	✓		0.25	2.0c	35	2	1	2
S22101	✓		45	✓		0.25	2.0c	145	2	1	2
S31101	✓		45	✓		0.25	2.0c	35	2	1	3
S32101	✓		45	✓		0.25	2.0c	145	2	1	3
T01101	✓		45	✓		0.25	2.0c	35	3	1	0
T02101	✓		45	✓		0.25	2.0c	145	3	1	0
T01201	✓		45	✓		0.25	2.0c	35	3	2	0
TC2201	✓		45	✓		0.25	2.0c	145	3	2	0
T01301	✓		45	✓		0.25	2.0c	35	3	3	0
T02301	✓		45	✓		0.25	2.0c	145	3	3	0
T01401	✓		45	✓		0.25	2.0c	35	3	4	0
T02401	✓		45	✓		0.25	2.0c	145	3	4	0
T11101	✓		45	✓		0.25	2.0c	35	3	1	1
T12101	✓		45	✓		0.25	2.0c	145	3	1	1
T11201	✓		45	✓		0.25	2.0c	35	3	2	1
T12201	✓		45	✓		0.25	2.0c	145	3	2	1
T11301	✓		45	✓		0.25	2.0c	35	3	3	1
T12301	✓		45	✓		0.25	2.0c	145	3	3	1
T21101	✓		45	✓		0.25	2.0c	35	3	1	2
T2101	✓		45	✓		0.25	2.0c	145	3	1	2
T31101	✓		45	✓		0.25	2.0c	35	3	1	3
T32101	✓		45	✓		0.25	2.0c	145	3	1	3
U03501	✓		45	✓		0.25	2.0c	35	1	-	0
U03601	✓		45	✓		0.25	2.0c	35	2	-	0
U03701	✓		45	✓		0.25	2.0c	35	3	-	0
U14501	✓		45	✓		0.25	2.0c	145	1	-	0
U14601	✓		45	✓		0.25	2.0c	145	2	-	0
U14701	✓		45	✓		0.25	2.0c	145	3	-	0
V03501	✓		45	✓		0.25	2.0c	35	1	-	1
V03601	✓		45	✓		0.25	2.0c	35	2	-	1
V03701	✓		45	✓		0.25	2.0c	35	3	-	1
V14501	✓		45	✓		0.25	2.0c	145	1	-	1
V14601	✓		45	✓		0.25	2.0c	145	2	-	1
V14701	✓		45	✓		0.25	2.0c	145	3	-	1
W03501	✓		0	(edge)		0.25	2.0c	35	1	-	0 (1:12)
W03601	✓		0	(edge)		0.25	2.0c	35	2	-	0 (1:12)
W03701	✓		0	(edge)		0.25	2.0c	35	5	-	0 (1:12)
W14501	✓		0	(edge)		0.25	2.0c	145	1	-	0 (1:12)
W14601	✓		0	(edge)		0.25	2.0c	145	2	-	0 (1:12)
W14701	✓		0	(edge)		0.25	2.0c	145	5	-	0 (1:12)
X03501	✓		0	(edge)		0.25	2.0c	35	1	1	0 (1:12)
X03601	✓		0	(edge)		0.25	2.0c	35	2	1	0 (1:12)
X14501	✓		0	(edge)		0.25	2.0c	145	1	1	0 (1:12)
X14601	✓		0	(edge)		0.25	2.0c	145	2	1	0 (1:12)
Z03501	✓		0	✓		0.25	-	35	-	-	0 (1:12)



DATA FOR PROJECT 6022 CONFIG. 8 WIND DIR. 160 TUBING NO. 1

TAP	MEAN	RMS	MAX	MIN	TAP	MEAN	RMS	MAX	MIN	TAP	MEAN	RMS	MAX	MIN
1	379	040	150	25	1	714	039	576	879	1	714	039	576	879
2	248	022	110	27	2	725	027	504	885	2	725	027	504	885
3	104	025	89	10	3	725	025	505	879	3	725	025	505	879
4	153	020	119	2	4	725	020	516	875	4	725	020	516	875
5	288	019	154	2	5	757	033	522	898	5	757	033	522	898
6	615	017	170	1	6	761	040	522	898	6	761	040	522	898
7	759	016	159	1	7	777	060	526	911	7	777	060	526	911
8	929	016	159	1	8	777	060	526	911	8	777	060	526	911
10					10					10				

DATA FOR PROJECT 6022 CONFIG. 8 WIND DIR. 90 TUBING NO. 1

TAP	MEAN	RMS	MAX	MIN	TAP	MEAN	RMS	MAX	MIN	TAP	MEAN	RMS	MAX	MIN
1	497	074	654	11	1	750	050	555	880	1	750	050	555	880
2	700	050	863	2	2	733	038	523	880	2	733	038	523	880
3	837	041	1059	3	3	722	038	523	880	3	722	038	523	880
4	931	039	1111	4	4	722	038	523	880	4	722	038	523	880
5	937	035	1111	5	5	722	038	523	880	5	722	038	523	880
6	802	024	1085	6	6	722	038	523	880	6	722	038	523	880
7	637	024	1085	7	7	722	038	523	880	7	722	038	523	880
8	439	035	1013	8	8	722	038	523	880	8	722	038	523	880
10					10					10				

DATA FOR PROJECT 6022 CONFIG. 8 WIND DIR. 160 TUBING NO. 1

TAP	MEAN	RMS	MAX	MIN	TAP	MEAN	RMS	MAX	MIN	TAP	MEAN	RMS	MAX	MIN
1	887	015	159	31	1	855	020	159	31	1	855	020	159	31
2	657	014	155	31	2	855	020	159	31	2	855	020	159	31
3	477	013	155	31	3	855	020	159	31	3	855	020	159	31
4	477	012	155	31	4	855	020	159	31	4	855	020	159	31
5	134	013	155	31	5	855	020	159	31	5	855	020	159	31
6	157	013	155	31	6	855	020	159	31	6	855	020	159	31
7	156	013	155	31	7	855	020	159	31	7	855	020	159	31
10					10					10				

DATA FOR PROJECT 6022 CONFIG. C				WIND DIR. C				WIND DIR. 35 TUBING NO. 1						
TAP	MEAN	RMS	MAX	MIN	TAP	MEAN	RMS	MAX	MIN	TAP	MEAN	RMS	MAX	MIN
1	1025	0202	1025	1025	1	123	0174	123	123	1	123	0174	123	123
2	1025	0202	1025	1025	2	123	0174	123	123	2	123	0174	123	123
3	1025	0202	1025	1025	3	123	0174	123	123	3	123	0174	123	123
4	1025	0202	1025	1025	4	123	0174	123	123	4	123	0174	123	123
5	1025	0202	1025	1025	5	123	0174	123	123	5	123	0174	123	123
6	1025	0202	1025	1025	6	123	0174	123	123	6	123	0174	123	123
7	1025	0202	1025	1025	7	123	0174	123	123	7	123	0174	123	123
8	1025	0202	1025	1025	8	123	0174	123	123	8	123	0174	123	123
9	1025	0202	1025	1025	9	123	0174	123	123	9	123	0174	123	123
10	1025	0202	1025	1025	10	123	0174	123	123	10	123	0174	123	123

DATA FOR PROJECT 6022 CONFIG. C				WIND DIR. C				WIND DIR. 90 TUBING NO. 1						
TAP	MEAN	RMS	MAX	MIN	TAP	MEAN	RMS	MAX	MIN	TAP	MEAN	RMS	MAX	MIN
1	1025	0202	1025	1025	1	123	0174	123	123	1	123	0174	123	123
2	1025	0202	1025	1025	2	123	0174	123	123	2	123	0174	123	123
3	1025	0202	1025	1025	3	123	0174	123	123	3	123	0174	123	123
4	1025	0202	1025	1025	4	123	0174	123	123	4	123	0174	123	123
5	1025	0202	1025	1025	5	123	0174	123	123	5	123	0174	123	123
6	1025	0202	1025	1025	6	123	0174	123	123	6	123	0174	123	123
7	1025	0202	1025	1025	7	123	0174	123	123	7	123	0174	123	123
8	1025	0202	1025	1025	8	123	0174	123	123	8	123	0174	123	123
9	1025	0202	1025	1025	9	123	0174	123	123	9	123	0174	123	123
10	1025	0202	1025	1025	10	123	0174	123	123	10	123	0174	123	123

DATA FOR PROJECT 6022 CONFIG. D				WIND DIR. D				WIND DIR. 21 TUBING NO. 1						
TAP	MEAN	RMS	MAX	MIN	TAP	MEAN	RMS	MAX	MIN	TAP	MEAN	RMS	MAX	MIN
1	1025	0202	1025	1025	1	123	0174	123	123	1	123	0174	123	123
2	1025	0202	1025	1025	2	123	0174	123	123	2	123	0174	123	123
3	1025	0202	1025	1025	3	123	0174	123	123	3	123	0174	123	123
4	1025	0202	1025	1025	4	123	0174	123	123	4	123	0174	123	123
5	1025	0202	1025	1025	5	123	0174	123	123	5	123	0174	123	123
6	1025	0202	1025	1025	6	123	0174	123	123	6	123	0174	123	123
7	1025	0202	1025	1025	7	123	0174	123	123	7	123	0174	123	123
8	1025	0202	1025	1025	8	123	0174	123	123	8	123	0174	123	123
9	1025	0202	1025	1025	9	123	0174	123	123	9	123	0174	123	123
10	1025	0202	1025	1025	10	123	0174	123	123	10	123	0174	123	123



DATA FOR PROJECT 6022 CONFIG. D WIND DIR. 160 TUBING NO. 1									
TAP	MEAN	RMS	MAX	MIN	TAP	MEAN	RMS	MAX	MIN
1	594	027	44	37	1	555	025	47	37
2	400	020	31	29	2	334	025	37	29
3	314	020	31	29	3	334	025	37	29
4	202	015	20	19	4	202	025	37	29
5	202	015	20	19	5	202	025	37	29
6	152	015	20	19	6	152	025	37	29
7	152	015	20	19	7	152	025	37	29
8	152	015	20	19	8	152	025	37	29
9	152	015	20	19	9	152	025	37	29
10	152	015	20	19	10	152	025	37	29

DATA FOR PROJECT 6022 CONFIG. E WIND DIR. 20 TUBING NO. 1									
TAP	MEAN	RMS	MAX	MIN	TAP	MEAN	RMS	MAX	MIN
1	107	018	15	15	1	107	025	37	29
2	107	018	15	15	2	107	025	37	29
3	107	018	15	15	3	107	025	37	29
4	107	018	15	15	4	107	025	37	29
5	107	018	15	15	5	107	025	37	29
6	107	018	15	15	6	107	025	37	29
7	107	018	15	15	7	107	025	37	29
8	107	018	15	15	8	107	025	37	29
9	107	018	15	15	9	107	025	37	29
10	107	018	15	15	10	107	025	37	29

DATA FOR PROJECT 6022 CONFIG. E WIND DIR. 22 TUBING NO. 1									
TAP	MEAN	RMS	MAX	MIN	TAP	MEAN	RMS	MAX	MIN
1	107	027	44	37	1	107	025	37	29
2	107	027	44	37	2	107	025	37	29
3	107	027	44	37	3	107	025	37	29
4	107	027	44	37	4	107	025	37	29
5	107	027	44	37	5	107	025	37	29
6	107	027	44	37	6	107	025	37	29
7	107	027	44	37	7	107	025	37	29
8	107	027	44	37	8	107	025	37	29
9	107	027	44	37	9	107	025	37	29
10	107	027	44	37	10	107	025	37	29

DATA FOR PROJECT 6022 CONFIG. D WIND DIR. 161 TUBING NO. 1									
TAP	MEAN	RMS	MAX	MIN	TAP	MEAN	RMS	MAX	MIN
1	455	025	32	31	1	455	025	32	31
2	355	025	32	31	2	355	025	32	31
3	355	025	32	31	3	355	025	32	31
4	355	025	32	31	4	355	025	32	31
5	355	025	32	31	5	355	025	32	31
6	355	025	32	31	6	355	025	32	31
7	355	025	32	31	7	355	025	32	31
8	355	025	32	31	8	355	025	32	31
9	355	025	32	31	9	355	025	32	31
10	355	025	32	31	10	355	025	32	31

DATA FOR PROJECT 6022 CONFIG. E WIND DIR. 21 TUBING NO. 1									
TAP	MEAN	RMS	MAX	MIN	TAP	MEAN	RMS	MAX	MIN
1	455	025	32	31	1	455	025	32	31
2	355	025	32	31	2	355	025	32	31
3	355	025	32	31	3	355	025	32	31
4	355	025	32	31	4	355	025	32	31
5	355	025	32	31	5	355	025	32	31
6	355	025	32	31	6	355	025	32	31
7	355	025	32	31	7	355	025	32	31
8	355	025	32	31	8	355	025	32	31
9	355	025	32	31	9	355	025	32	31
10	355	025	32	31	10	355	025	32	31

DATA FOR PROJECT 6022 CONFIG. E WIND DIR. 25 TUBING NO. 1									
TAP	MEAN	RMS	MAX	MIN	TAP	MEAN	RMS	MAX	MIN
1	455	025	32	31	1	455	025	32	31
2	355	025	32	31	2	355	025	32	31
3	355	025	32	31	3	355	025	32	31
4	355	025	32	31	4	355	025	32	31
5	355	025	32	31	5	355	025	32	31
6	355	025	32	31	6	355	025	32	31
7	355	025	32	31	7	355	025	32	31
8	355	025	32	31	8	355	025	32	31
9	355	025	32	31	9	355	025	32	31
10	355	025	32	31	10	355	025	32	31

DATA FOR PROJECT 6022													
TAP		MEAN	RMS	MAX	MIN	WIND DIR		WIND DIR		TUBING NO			
TAP	MEAN	RMS	MAX	MIN	TAP	MEAN	RMS	MAX	MIN	TAP	RMS	MAX	MIN
1	112	0.45	1.25	1.25	1	112	0.45	1.25	1.25	1	0.45	1.25	1.25
2	113	0.45	1.25	1.25	2	113	0.45	1.25	1.25	2	0.45	1.25	1.25
3	114	0.45	1.25	1.25	3	114	0.45	1.25	1.25	3	0.45	1.25	1.25
4	115	0.45	1.25	1.25	4	115	0.45	1.25	1.25	4	0.45	1.25	1.25
5	116	0.45	1.25	1.25	5	116	0.45	1.25	1.25	5	0.45	1.25	1.25
6	117	0.45	1.25	1.25	6	117	0.45	1.25	1.25	6	0.45	1.25	1.25
7	118	0.45	1.25	1.25	7	118	0.45	1.25	1.25	7	0.45	1.25	1.25
8	119	0.45	1.25	1.25	8	119	0.45	1.25	1.25	8	0.45	1.25	1.25
9	120	0.45	1.25	1.25	9	120	0.45	1.25	1.25	9	0.45	1.25	1.25
10	121	0.45	1.25	1.25	10	121	0.45	1.25	1.25	10	0.45	1.25	1.25

DATA FOR PROJECT 6022													
TAP		MEAN	RMS	MAX	MIN	WIND DIR		WIND DIR		TUBING NO			
TAP	MEAN	RMS	MAX	MIN	TAP	MEAN	RMS	MAX	MIN	TAP	RMS	MAX	MIN
1	112	0.45	1.25	1.25	1	112	0.45	1.25	1.25	1	0.45	1.25	1.25
2	113	0.45	1.25	1.25	2	113	0.45	1.25	1.25	2	0.45	1.25	1.25
3	114	0.45	1.25	1.25	3	114	0.45	1.25	1.25	3	0.45	1.25	1.25
4	115	0.45	1.25	1.25	4	115	0.45	1.25	1.25	4	0.45	1.25	1.25
5	116	0.45	1.25	1.25	5	116	0.45	1.25	1.25	5	0.45	1.25	1.25
6	117	0.45	1.25	1.25	6	117	0.45	1.25	1.25	6	0.45	1.25	1.25
7	118	0.45	1.25	1.25	7	118	0.45	1.25	1.25	7	0.45	1.25	1.25
8	119	0.45	1.25	1.25	8	119	0.45	1.25	1.25	8	0.45	1.25	1.25
9	120	0.45	1.25	1.25	9	120	0.45	1.25	1.25	9	0.45	1.25	1.25
10	121	0.45	1.25	1.25	10	121	0.45	1.25	1.25	10	0.45	1.25	1.25

DATA FOR PROJECT 6022													
TAP		MEAN	RMS	MAX	MIN	WIND DIR		WIND DIR		TUBING NO			
TAP	MEAN	RMS	MAX	MIN	TAP	MEAN	RMS	MAX	MIN	TAP	RMS	MAX	MIN
1	112	0.45	1.25	1.25	1	112	0.45	1.25	1.25	1	0.45	1.25	1.25
2	113	0.45	1.25	1.25	2	113	0.45	1.25	1.25	2	0.45	1.25	1.25
3	114	0.45	1.25	1.25	3	114	0.45	1.25	1.25	3	0.45	1.25	1.25
4	115	0.45	1.25	1.25	4	115	0.45	1.25	1.25	4	0.45	1.25	1.25
5	116	0.45	1.25	1.25	5	116	0.45	1.25	1.25	5	0.45	1.25	1.25
6	117	0.45	1.25	1.25	6	117	0.45	1.25	1.25	6	0.45	1.25	1.25
7	118	0.45	1.25	1.25	7	118	0.45	1.25	1.25	7	0.45	1.25	1.25
8	119	0.45	1.25	1.25	8	119	0.45	1.25	1.25	8	0.45	1.25	1.25
9	120	0.45	1.25	1.25	9	120	0.45	1.25	1.25	9	0.45	1.25	1.25
10	121	0.45	1.25	1.25	10	121	0.45	1.25	1.25	10	0.45	1.25	1.25



DATA FOR PROJECT 6022 CONFIG. E WIND DIR 147 TUBING NO. 1									
TAP	MEAN	RMS	MAX	MIN	TAP	MEAN	RMS	MAX	MIN
1	1.4	0.000	0.000	0.000	1	0.000	0.000	0.000	0.000
2	1.4	0.000	0.000	0.000	2	0.000	0.000	0.000	0.000
3	1.4	0.000	0.000	0.000	3	0.000	0.000	0.000	0.000
4	1.4	0.000	0.000	0.000	4	0.000	0.000	0.000	0.000
5	1.4	0.000	0.000	0.000	5	0.000	0.000	0.000	0.000
6	1.4	0.000	0.000	0.000	6	0.000	0.000	0.000	0.000
7	1.4	0.000	0.000	0.000	7	0.000	0.000	0.000	0.000
8	1.4	0.000	0.000	0.000	8	0.000	0.000	0.000	0.000
9	1.4	0.000	0.000	0.000	9	0.000	0.000	0.000	0.000
10	1.4	0.000	0.000	0.000	10	0.000	0.000	0.000	0.000

DATA FOR PROJECT 6022 CONFIG. E WIND DIR 161 TUBING NO. 1									
TAP	MEAN	RMS	MAX	MIN	TAP	MEAN	RMS	MAX	MIN
1	1.4	0.000	0.000	0.000	1	0.000	0.000	0.000	0.000
2	1.4	0.000	0.000	0.000	2	0.000	0.000	0.000	0.000
3	1.4	0.000	0.000	0.000	3	0.000	0.000	0.000	0.000
4	1.4	0.000	0.000	0.000	4	0.000	0.000	0.000	0.000
5	1.4	0.000	0.000	0.000	5	0.000	0.000	0.000	0.000
6	1.4	0.000	0.000	0.000	6	0.000	0.000	0.000	0.000
7	1.4	0.000	0.000	0.000	7	0.000	0.000	0.000	0.000
8	1.4	0.000	0.000	0.000	8	0.000	0.000	0.000	0.000
9	1.4	0.000	0.000	0.000	9	0.000	0.000	0.000	0.000
10	1.4	0.000	0.000	0.000	10	0.000	0.000	0.000	0.000

DATA FOR PROJECT 6022 CONFIG. F WIND DIR 35 TUBING NO. 1									
TAP	MEAN	RMS	MAX	MIN	TAP	MEAN	RMS	MAX	MIN
1	1.4	0.000	0.000	0.000	1	0.000	0.000	0.000	0.000
2	1.4	0.000	0.000	0.000	2	0.000	0.000	0.000	0.000
3	1.4	0.000	0.000	0.000	3	0.000	0.000	0.000	0.000
4	1.4	0.000	0.000	0.000	4	0.000	0.000	0.000	0.000
5	1.4	0.000	0.000	0.000	5	0.000	0.000	0.000	0.000
6	1.4	0.000	0.000	0.000	6	0.000	0.000	0.000	0.000
7	1.4	0.000	0.000	0.000	7	0.000	0.000	0.000	0.000
8	1.4	0.000	0.000	0.000	8	0.000	0.000	0.000	0.000
9	1.4	0.000	0.000	0.000	9	0.000	0.000	0.000	0.000
10	1.4	0.000	0.000	0.000	10	0.000	0.000	0.000	0.000





DATA FOR PROJECT 6022 CONFIG. F WIND DIR. 147 TUBING NO. 1										DATA FOR PROJECT 6022 CONFIG. G WIND DIR. 20 TUBING NO. 1									
TAP	MEAN	RMS	MAX	MIN	TAP	MEAN	RMS	MAX	MIN	TAP	MEAN	RMS	MAX	MIN	TAP	MEAN	RMS	MAX	MIN
1	107	0.69	147	427	120	222	0.27	120	394	1	107	0.69	147	427	1	107	0.69	147	427
2	107	0.87	147	509	120	222	0.27	120	394	2	107	0.87	147	509	2	107	0.87	147	509
3	107	1.07	147	549	120	222	0.27	120	394	3	107	1.07	147	549	3	107	1.07	147	549
4	107	1.16	147	549	120	222	0.27	120	394	4	107	1.16	147	549	4	107	1.16	147	549
5	107	1.16	147	549	120	222	0.27	120	394	5	107	1.16	147	549	5	107	1.16	147	549
6	107	1.16	147	549	120	222	0.27	120	394	6	107	1.16	147	549	6	107	1.16	147	549
7	107	1.16	147	549	120	222	0.27	120	394	7	107	1.16	147	549	7	107	1.16	147	549
8	107	1.16	147	549	120	222	0.27	120	394	8	107	1.16	147	549	8	107	1.16	147	549
9	107	1.16	147	549	120	222	0.27	120	394	9	107	1.16	147	549	9	107	1.16	147	549
10	107	1.16	147	549	120	222	0.27	120	394	10	107	1.16	147	549	10	107	1.16	147	549

DATA FOR PROJECT 6022 CONFIG. G WIND DIR. 35 TUBING NO. 1										DATA FOR PROJECT 6022 CONFIG. G WIND DIR. 60 TUBING NO. 1									
TAP	MEAN	RMS	MAX	MIN	TAP	MEAN	RMS	MAX	MIN	TAP	MEAN	RMS	MAX	MIN	TAP	MEAN	RMS	MAX	MIN
1	107	0.51	156	208	120	222	0.27	120	394	1	107	0.51	156	208	1	107	0.51	156	208
2	107	0.57	156	208	120	222	0.27	120	394	2	107	0.57	156	208	2	107	0.57	156	208
3	107	0.65	156	208	120	222	0.27	120	394	3	107	0.65	156	208	3	107	0.65	156	208
4	107	0.65	156	208	120	222	0.27	120	394	4	107	0.65	156	208	4	107	0.65	156	208
5	107	0.65	156	208	120	222	0.27	120	394	5	107	0.65	156	208	5	107	0.65	156	208
6	107	0.65	156	208	120	222	0.27	120	394	6	107	0.65	156	208	6	107	0.65	156	208
7	107	0.65	156	208	120	222	0.27	120	394	7	107	0.65	156	208	7	107	0.65	156	208
8	107	0.65	156	208	120	222	0.27	120	394	8	107	0.65	156	208	8	107	0.65	156	208
9	107	0.65	156	208	120	222	0.27	120	394	9	107	0.65	156	208	9	107	0.65	156	208
10	107	0.65	156	208	120	222	0.27	120	394	10	107	0.65	156	208	10	107	0.65	156	208

DATA FOR PROJECT 6022 CONFIG. G WIND DIR. 90 TUBING NO. 1										DATA FOR PROJECT 6022 CONFIG. G WIND DIR. 120 TUBING NO. 1									
TAP	MEAN	RMS	MAX	MIN	TAP	MEAN	RMS	MAX	MIN	TAP	MEAN	RMS	MAX	MIN	TAP	MEAN	RMS	MAX	MIN
1	107	0.96	186	267	120	222	0.27	120	394	1	107	0.96	186	267	1	107	0.96	186	267
2	107	1.05	186	267	120	222	0.27	120	394	2	107	1.05	186	267	2	107	1.05	186	267
3	107	1.15	186	267	120	222	0.27	120	394	3	107	1.15	186	267	3	107	1.15	186	267
4	107	1.15	186	267	120	222	0.27	120	394	4	107	1.15	186	267	4	107	1.15	186	267
5	107	1.15	186	267	120	222	0.27	120	394	5	107	1.15	186	267	5	107	1.15	186	267
6	107	1.15	186	267	120	222	0.27	120	394	6	107	1.15	186	267	6	107	1.15	186	267
7	107	1.15	186	267	120	222	0.27	120	394	7	107	1.15	186	267	7	107	1.15	186	267
8	107	1.15	186	267	120	222	0.27	120	394	8	107	1.15	186	267	8	107	1.15	186	267
9	107	1.15	186	267	120	222	0.27	120	394	9	107	1.15	186	267	9	107	1.15	186	267
10	107	1.15	186	267	120	222	0.27	120	394	10	107	1.15	186	267	10	107	1.15	186	267

DATA FOR PROJECT 6022 CONFIG. G WIND DIR. 145 TUBING NO. 1											
TAP	MEAN	RMS	MAX	MIN	TAP	MEAN	RMS	MAX	MIN	TAP	MEAN
1	12.4	0.73	9.0	1.5	1	12.4	0.73	9.0	1.5	1	12.4
2	13.5	0.73	9.0	1.5	2	13.5	0.73	9.0	1.5	2	13.5
3	14.6	0.73	9.0	1.5	3	14.6	0.73	9.0	1.5	3	14.6
4	15.7	0.73	9.0	1.5	4	15.7	0.73	9.0	1.5	4	15.7
5	16.8	0.73	9.0	1.5	5	16.8	0.73	9.0	1.5	5	16.8
6	17.9	0.73	9.0	1.5	6	17.9	0.73	9.0	1.5	6	17.9
7	19.0	0.73	9.0	1.5	7	19.0	0.73	9.0	1.5	7	19.0
8	20.1	0.73	9.0	1.5	8	20.1	0.73	9.0	1.5	8	20.1
9	21.2	0.73	9.0	1.5	9	21.2	0.73	9.0	1.5	9	21.2
10	22.3	0.73	9.0	1.5	10	22.3	0.73	9.0	1.5	10	22.3

DATA FOR PROJECT 6022 CONFIG. G WIND DIR. 12 TUBING NO. 1											
TAP	MEAN	RMS	MAX	MIN	TAP	MEAN	RMS	MAX	MIN	TAP	MEAN
1	12.4	0.83	9.5	1.5	1	12.4	0.83	9.5	1.5	1	12.4
2	13.5	0.83	9.5	1.5	2	13.5	0.83	9.5	1.5	2	13.5
3	14.6	0.83	9.5	1.5	3	14.6	0.83	9.5	1.5	3	14.6
4	15.7	0.83	9.5	1.5	4	15.7	0.83	9.5	1.5	4	15.7
5	16.8	0.83	9.5	1.5	5	16.8	0.83	9.5	1.5	5	16.8
6	17.9	0.83	9.5	1.5	6	17.9	0.83	9.5	1.5	6	17.9
7	19.0	0.83	9.5	1.5	7	19.0	0.83	9.5	1.5	7	19.0
8	20.1	0.83	9.5	1.5	8	20.1	0.83	9.5	1.5	8	20.1
9	21.2	0.83	9.5	1.5	9	21.2	0.83	9.5	1.5	9	21.2
10	22.3	0.83	9.5	1.5	10	22.3	0.83	9.5	1.5	10	22.3

DATA FOR PROJECT 6022 CONFIG. G WIND DIR. 14 TUBING NO. 1											
TAP	MEAN	RMS	MAX	MIN	TAP	MEAN	RMS	MAX	MIN	TAP	MEAN
1	12.4	0.61	8.5	1.5	1	12.4	0.61	8.5	1.5	1	12.4
2	13.5	0.61	8.5	1.5	2	13.5	0.61	8.5	1.5	2	13.5
3	14.6	0.61	8.5	1.5	3	14.6	0.61	8.5	1.5	3	14.6
4	15.7	0.61	8.5	1.5	4	15.7	0.61	8.5	1.5	4	15.7
5	16.8	0.61	8.5	1.5	5	16.8	0.61	8.5	1.5	5	16.8
6	17.9	0.61	8.5	1.5	6	17.9	0.61	8.5	1.5	6	17.9
7	19.0	0.61	8.5	1.5	7	19.0	0.61	8.5	1.5	7	19.0
8	20.1	0.61	8.5	1.5	8	20.1	0.61	8.5	1.5	8	20.1
9	21.2	0.61	8.5	1.5	9	21.2	0.61	8.5	1.5	9	21.2
10	22.3	0.61	8.5	1.5	10	22.3	0.61	8.5	1.5	10	22.3



DATA FOR PROJECT 6022										DATA FOR PROJECT 6022																			
CONFIG. H					WIND DIR.					TUBING NO. 1					CONFIG. H					WIND DIR.					TUBING NO. 1				
TAP	MEAN	RMS	MAX	MIN	TAP	MEAN	RMS	MAX	MIN	TAP	MEAN	RMS	MAX	MIN	TAP	MEAN	RMS	MAX	MIN	TAP	MEAN	RMS	MAX	MIN					
1	002	002	171	52	1	002	002	002	002	1	002	002	002	002	1	002	002	002	002	1	002	002	002	002					
2	003	003	200	53	2	003	003	003	003	2	003	003	003	003	2	003	003	003	003	2	003	003	003	003					
3	004	004	230	54	3	004	004	004	004	3	004	004	004	004	3	004	004	004	004	3	004	004	004	004					
4	005	005	260	55	4	005	005	005	005	4	005	005	005	005	4	005	005	005	005	4	005	005	005	005					
5	006	006	290	56	5	006	006	006	006	5	006	006	006	006	5	006	006	006	006	5	006	006	006	006					
6	007	007	320	57	6	007	007	007	007	6	007	007	007	007	6	007	007	007	007	6	007	007	007	007					
7	008	008	350	58	7	008	008	008	008	7	008	008	008	008	7	008	008	008	008	7	008	008	008	008					
8	009	009	380	59	8	009	009	009	009	8	009	009	009	009	8	009	009	009	009	8	009	009	009	009					
9	010	010	410	60	9	010	010	010	010	9	010	010	010	010	9	010	010	010	010	9	010	010	010	010					
10	011	011	440	61	10	011	011	011	011	10	011	011	011	011	10	011	011	011	011	10	011	011	011	011					

DATA FOR PROJECT 6022										DATA FOR PROJECT 6022																			
CONFIG. H					WIND DIR.					TUBING NO. 1					CONFIG. H					WIND DIR.					TUBING NO. 1				
TAP	MEAN	RMS	MAX	MIN	TAP	MEAN	RMS	MAX	MIN	TAP	MEAN	RMS	MAX	MIN	TAP	MEAN	RMS	MAX	MIN	TAP	MEAN	RMS	MAX	MIN					
1	025	025	222	70	1	025	025	025	025	1	025	025	025	025	1	025	025	025	025	1	025	025	025	025					
2	026	026	252	71	2	026	026	026	026	2	026	026	026	026	2	026	026	026	026	2	026	026	026	026					
3	027	027	282	72	3	027	027	027	027	3	027	027	027	027	3	027	027	027	027	3	027	027	027	027					
4	028	028	312	73	4	028	028	028	028	4	028	028	028	028	4	028	028	028	028	4	028	028	028	028					
5	029	029	342	74	5	029	029	029	029	5	029	029	029	029	5	029	029	029	029	5	029	029	029	029					
6	030	030	372	75	6	030	030	030	030	6	030	030	030	030	6	030	030	030	030	6	030	030	030	030					
7	031	031	402	76	7	031	031	031	031	7	031	031	031	031	7	031	031	031	031	7	031	031	031	031					
8	032	032	432	77	8	032	032	032	032	8	032	032	032	032	8	032	032	032	032	8	032	032	032	032					
9	033	033	462	78	9	033	033	033	033	9	033	033	033	033	9	033	033	033	033	9	033	033	033	033					
10	034	034	492	79	10	034	034	034	034	10	034	034	034	034	10	034	034	034	034	10	034	034	034	034					

DATA FOR PROJECT 6022										DATA FOR PROJECT 6022																			
CONFIG. H					WIND DIR.					TUBING NO. 1					CONFIG. H					WIND DIR.					TUBING NO. 1				
TAP	MEAN	RMS	MAX	MIN	TAP	MEAN	RMS	MAX	MIN	TAP	MEAN	RMS	MAX	MIN	TAP	MEAN	RMS	MAX	MIN	TAP	MEAN	RMS	MAX	MIN					
1	035	035	522	80	1	035	035	035	035	1	035	035	035	035	1	035	035	035	035	1	035	035	035	035					
2	036	036	552	81	2	036	036	036	036	2	036	036	036	036	2	036	036	036	036	2	036	036	036	036					
3	037	037	582	82	3	037	037	037	037	3	037	037	037	037	3	037	037	037	037	3	037	037	037	037					
4	038	038	612	83	4	038	038	038	038	4	038	038	038	038	4	038	038	038	038	4	038	038	038	038					
5	039	039	642	84	5	039	039	039	039	5	039	039	039	039	5	039	039	039	039	5	039	039	039	039					
6	040	040	672	85	6	040	040	040	040	6	040	040	040	040	6	040	040	040	040	6	040	040	040	040					
7	041	041	702	86	7	041	041	041	041	7	041	041	041	041	7	041	041	041	041	7	041	041	041	041					
8	042	042	732	87	8	042	042	042	042	8	042	042	042	042	8	042	042	042	042	8	042	042	042	042					
9	043	043	762	88	9	043	043	043	043	9	043	043	043	043	9	043	043	043	043	9	043	043	043	043					
10	044	044	792	89	10	044	044	044	044	10	044	044	044	044	10	044	044	044	044	10	044	044	044	044					

DATA FOR PROJECT 6022 CONFIG. H WIND DIR. 145 TUBING NO. 1

TAP	MEAN	RMS	MAX	MIN	TAP	MEAN	RMS	MAX	MIN	TAP	MEAN	RMS	MAX	MIN
10M456789	42	106	63	33	12	42	08	60	6	10M456789	28	102	58	15
1	41	105	62	32	13	41	09	59	5	1	29	101	57	14
	40	104	61	31	14	40	09	58	4		30	100	56	13
	39	103	60	30	15	39	09	57	3		31	99	55	12
	38	102	59	29	16	38	09	56	2		32	98	54	11
	37	101	58	28	17	37	09	55	1		33	97	53	10
	36	100	57	27	18	36	09	54	0		34	96	52	9
	35	99	56	26	19	35	09	53	0		35	95	51	8
	34	98	55	25	20	34	09	52	0		36	94	50	7
	33	97	54	24	21	33	09	51	0		37	93	49	6
	32	96	53	23	22	32	09	50	0		38	92	48	5
	31	95	52	22	23	31	09	49	0		39	91	47	4
	30	94	51	21	24	30	09	48	0		40	90	46	3
	29	93	50	20	25	29	09	47	0		41	89	45	2
	28	92	49	19	26	28	09	46	0		42	88	44	1
	27	91	48	18	27	27	09	45	0		43	87	43	0
	26	90	47	17	28	26	09	44	0		44	86	42	0
	25	89	46	16	29	25	09	43	0		45	85	41	0
	24	88	45	15	30	24	09	42	0		46	84	40	0
	23	87	44	14	31	23	09	41	0		47	83	39	0
	22	86	43	13	32	22	09	40	0		48	82	38	0
	21	85	42	12	33	21	09	39	0		49	81	37	0
	20	84	41	11	34	20	09	38	0		50	80	36	0
	19	83	40	10	35	19	09	37	0		51	79	35	0
	18	82	39	9	36	18	09	36	0		52	78	34	0
	17	81	38	8	37	17	09	35	0		53	77	33	0
	16	80	37	7	38	16	09	34	0		54	76	32	0
	15	79	36	6	39	15	09	33	0		55	75	31	0
	14	78	35	5	40	14	09	32	0		56	74	30	0
	13	77	34	4	41	13	09	31	0		57	73	29	0
	12	76	33	3	42	12	09	30	0		58	72	28	0
	11	75	32	2	43	11	09	29	0		59	71	27	0
	10	74	31	1	44	10	09	28	0		60	70	26	0
	9	73	30	0	45	9	09	27	0		61	69	25	0
	8	72	29	0	46	8	09	26	0		62	68	24	0
	7	71	28	0	47	7	09	25	0		63	67	23	0
	6	70	27	0	48	6	09	24	0		64	66	22	0
	5	69	26	0	49	5	09	23	0		65	65	21	0
	4	68	25	0	50	4	09	22	0		66	64	20	0
	3	67	24	0	51	3	09	21	0		67	63	19	0
	2	66	23	0	52	2	09	20	0		68	62	18	0
	1	65	22	0	53	1	09	19	0		69	61	17	0
	0	64	21	0	54	0	09	18	0		70	60	16	0

DATA FOR PROJECT 6022 CONFIG. H WIND DIR. 147 TUBING NO. 1

TAP	MEAN	RMS	MAX	MIN	TAP	MEAN	RMS	MAX	MIN	TAP	MEAN	RMS	MAX	MIN
10M456789	110	049	78	77	12	110	04	70	76	10M456789	32	08	62	75
1	109	048	77	76	13	109	04	69	75	1	33	08	61	74
	108	047	76	75	14	108	04	68	74		34	08	60	73
	107	046	75	74	15	107	04	67	73		35	08	59	72
	106	045	74	73	16	106	04	66	72		36	08	58	71
	105	044	73	72	17	105	04	65	71		37	08	57	70
	104	043	72	71	18	104	04	64	70		38	08	56	69
	103	042	71	70	19	103	04	63	69		39	08	55	68
	102	041	70	69	20	102	04	62	68		40	08	54	67
	101	040	69	68	21	101	04	61	67		41	08	53	66
	100	039	68	67	22	100	04	60	66		42	08	52	65
	99	038	67	66	23	99	04	59	65		43	08	51	64
	98	037	66	65	24	98	04	58	64		44	08	50	63
	97	036	65	64	25	97	04	57	63		45	08	49	62
	96	035	64	63	26	96	04	56	62		46	08	48	61
	95	034	63	62	27	95	04	55	61		47	08	47	60
	94	033	62	61	28	94	04	54	60		48	08	46	59
	93	032	61	60	29	93	04	53	59		49	08	45	58
	92	031	60	59	30	92	04	52	58		50	08	44	57
	91	030	59	58	31	91	04	51	57		51	08	43	56
	90	029	58	57	32	90	04	50	56		52	08	42	55
	89	028	57	56	33	89	04	49	55		53	08	41	54
	88	027	56	55	34	88	04	48	54		54	08	40	53
	87	026	55	54	35	87	04	47	53		55	08	39	52
	86	025	54	53	36	86	04	46	52		56	08	38	51
	85	024	53	52	37	85	04	45	51		57	08	37	50
	84	023	52	51	38	84	04	44	50		58	08	36	49
	83	022	51	50	39	83	04	43	49		59	08	35	48
	82	021	50	49	40	82	04	42	48		60	08	34	47
	81	020	49	48	41	81	04	41	47		61	08	33	46
	80	019	48	47	42	80	04	40	46		62	08	32	45
	79	018	47	46	43	79	04	39	45		63	08	31	44
	78	017	46	45	44	78	04	38	44		64	08	30	43
	77	016	45	44	45	77	04	37	43		65	08	29	42
	76	015	44	43	46	76	04	36	42		66	08	28	41
	75	014	43	42	47	75	04	35	41		67	08	27	40
	74	013	42	41	48	74	04	34	40		68	08	26	39
	73	012	41	40	49	73	04	33	39		69	08	25	38
	72	011	40	39	50	72	04	32	38		70	08	24	37
	71	010	39	38	51	71	04	31	37		71	08	23	36
	70	009	38	37	52	70	04	30	36		72	08	22	35
	69	008	37	36	53	69	04	29	35		73	08	21	34
	68	007	36	35	54	68	04	28	34		74	08	20	33
	67	006	35	34	55	67	04	27	33		75	08	19	32
	66	005	34	33	56	66	04	26	32		76	08	18	31
	65	004	33	32	57	65	04	25	31		77	08	17	30
	64	003	32	31	58	64	04	24	30		78	08	16	29
	63	002	31	30	59	63	04	23	29		79	08	15	28
	62	001	30	29	60	62	04	22	28		80	08	14	27
	61	000	29	28	61	61	04	21	27		81	08	13	26
	60	000	28	27	62	60	04	20	26		82	08	12	25
	59	000	27	26	63	59	04	19	25		83	08	11	24
	58	000	26	25	64	58	04	18	24		84	08	10	23
	57	000	25	24	65	57	04	17	23		85	08	9	22
	56	000	24	23	66	56	04	16	22		86	08	8	21
	55	000	23	22	67	55	04	15	21					



DATA FOR PROJECT 6022 CONFIG. 1 WIND DIR. 1 WIND DIR. 61 TUBING NO. 1									
TAP	MEAN	RMS	MAX	MIN	TAP	MEAN	RMS	MAX	MIN
1	1275	072	427	023	1	3296	106	968	012
2	3395	087	1271	045	2	2286	083	000	116
3	4742	096	824	138	3	2286	087	000	116
4	4850	096	824	138	4	2286	087	000	116
5	4850	096	824	138	5	2286	087	000	116
6	4850	096	824	138	6	2286	087	000	116
7	4850	096	824	138	7	2286	087	000	116
8	4850	096	824	138	8	2286	087	000	116
9	4850	096	824	138	9	2286	087	000	116
10	4850	096	824	138	10	2286	087	000	116

DATA FOR PROJECT 6022 CONFIG. 1 WIND DIR. 1 WIND DIR. 90 TUBING NO. 1									
TAP	MEAN	RMS	MAX	MIN	TAP	MEAN	RMS	MAX	MIN
1	0288	078	159	028	1	4239	054	3887	009
2	0684	087	159	045	2	4239	054	3887	009
3	0684	087	159	045	3	4239	054	3887	009
4	0684	087	159	045	4	4239	054	3887	009
5	0684	087	159	045	5	4239	054	3887	009
6	0684	087	159	045	6	4239	054	3887	009
7	0684	087	159	045	7	4239	054	3887	009
8	0684	087	159	045	8	4239	054	3887	009
9	0684	087	159	045	9	4239	054	3887	009
10	0684	087	159	045	10	4239	054	3887	009

DATA FOR PROJECT 6022 CONFIG. 1 WIND DIR. 1 WIND DIR. 92 TUBING NO. 1									
TAP	MEAN	RMS	MAX	MIN	TAP	MEAN	RMS	MAX	MIN
1	0708	072	026	023	1	0652	055	026	000
2	0708	072	026	023	2	0652	055	026	000
3	0708	072	026	023	3	0652	055	026	000
4	0708	072	026	023	4	0652	055	026	000
5	0708	072	026	023	5	0652	055	026	000
6	0708	072	026	023	6	0652	055	026	000
7	0708	072	026	023	7	0652	055	026	000
8	0708	072	026	023	8	0652	055	026	000
9	0708	072	026	023	9	0652	055	026	000
10	0708	072	026	023	10	0652	055	026	000

DATA FOR PROJECT 6022 CONFIG. I WIND DIR. 120 TUBING NO. 1									
TAP	MEAN	RMS	MAX	MIN	TAP	MEAN	RMS	MAX	MIN
1	297	116	60	136	1	127	054	277	557
2	477	111	82	170	2	128	055	287	557
3	477	111	82	170	3	129	055	294	557
4	477	111	82	170	4	129	055	294	557
5	477	111	82	170	5	129	055	294	557
6	477	111	82	170	6	129	055	294	557
7	477	111	82	170	7	129	055	294	557
8	477	111	82	170	8	129	055	294	557
9	477	111	82	170	9	129	055	294	557
10	477	111	82	170	10	129	055	294	557

DATA FOR PROJECT 6022 CONFIG. I WIND DIR. 145 TUBING NO. 1									
TAP	MEAN	RMS	MAX	MIN	TAP	MEAN	RMS	MAX	MIN
1	627	107	110	220	1	127	054	277	557
2	100	107	110	220	2	128	055	287	557
3	100	107	110	220	3	129	055	294	557
4	100	107	110	220	4	129	055	294	557
5	100	107	110	220	5	129	055	294	557
6	100	107	110	220	6	129	055	294	557
7	100	107	110	220	7	129	055	294	557
8	100	107	110	220	8	129	055	294	557
9	100	107	110	220	9	129	055	294	557
10	100	107	110	220	10	129	055	294	557

DATA FOR PROJECT 6022 CONFIG. I WIND DIR. 147 TUBING NO. 1									
TAP	MEAN	RMS	MAX	MIN	TAP	MEAN	RMS	MAX	MIN
1	707	107	110	220	1	127	054	277	557
2	100	107	110	220	2	128	055	287	557
3	100	107	110	220	3	129	055	294	557
4	100	107	110	220	4	129	055	294	557
5	100	107	110	220	5	129	055	294	557
6	100	107	110	220	6	129	055	294	557
7	100	107	110	220	7	129	055	294	557
8	100	107	110	220	8	129	055	294	557
9	100	107	110	220	9	129	055	294	557
10	100	107	110	220	10	129	055	294	557

DATA FOR PROJECT 6022 CONFIG. I WIND DIR. 161 TUBING NO. 1

TAP	MEAN	RMS	MAX	MIN	TAP	MEAN	RMS	MAX	MIN
1	0.000	0.000	0.000	0.000	1	0.000	0.000	0.000	0.000
2	0.000	0.000	0.000	0.000	2	0.000	0.000	0.000	0.000
3	0.000	0.000	0.000	0.000	3	0.000	0.000	0.000	0.000
4	0.000	0.000	0.000	0.000	4	0.000	0.000	0.000	0.000
5	0.000	0.000	0.000	0.000	5	0.000	0.000	0.000	0.000
6	0.000	0.000	0.000	0.000	6	0.000	0.000	0.000	0.000
7	0.000	0.000	0.000	0.000	7	0.000	0.000	0.000	0.000
8	0.000	0.000	0.000	0.000	8	0.000	0.000	0.000	0.000
9	0.000	0.000	0.000	0.000	9	0.000	0.000	0.000	0.000
10	0.000	0.000	0.000	0.000	10	0.000	0.000	0.000	0.000

DATA FOR PROJECT 6022 CONFIG. J WIND DIR. 35 TUBING NO. 1

TAP	MEAN	RMS	MAX	MIN	TAP	MEAN	RMS	MAX	MIN
1	0.000	0.000	0.000	0.000	1	0.000	0.000	0.000	0.000
2	0.000	0.000	0.000	0.000	2	0.000	0.000	0.000	0.000
3	0.000	0.000	0.000	0.000	3	0.000	0.000	0.000	0.000
4	0.000	0.000	0.000	0.000	4	0.000	0.000	0.000	0.000
5	0.000	0.000	0.000	0.000	5	0.000	0.000	0.000	0.000
6	0.000	0.000	0.000	0.000	6	0.000	0.000	0.000	0.000
7	0.000	0.000	0.000	0.000	7	0.000	0.000	0.000	0.000
8	0.000	0.000	0.000	0.000	8	0.000	0.000	0.000	0.000
9	0.000	0.000	0.000	0.000	9	0.000	0.000	0.000	0.000
10	0.000	0.000	0.000	0.000	10	0.000	0.000	0.000	0.000

DATA FOR PROJECT 6022 CONFIG. J WIND DIR. 37 TUBING NO. 1

TAP	MEAN	RMS	MAX	MIN	TAP	MEAN	RMS	MAX	MIN
1	0.000	0.000	0.000	0.000	1	0.000	0.000	0.000	0.000
2	0.000	0.000	0.000	0.000	2	0.000	0.000	0.000	0.000
3	0.000	0.000	0.000	0.000	3	0.000	0.000	0.000	0.000
4	0.000	0.000	0.000	0.000	4	0.000	0.000	0.000	0.000
5	0.000	0.000	0.000	0.000	5	0.000	0.000	0.000	0.000
6	0.000	0.000	0.000	0.000	6	0.000	0.000	0.000	0.000
7	0.000	0.000	0.000	0.000	7	0.000	0.000	0.000	0.000
8	0.000	0.000	0.000	0.000	8	0.000	0.000	0.000	0.000
9	0.000	0.000	0.000	0.000	9	0.000	0.000	0.000	0.000
10	0.000	0.000	0.000	0.000	10	0.000	0.000	0.000	0.000



DATA FOR PROJECT 6022 CONFIG. J WIND DIR. 146 TUBING NO. 1

TAP	MEAN	RMS	MAX	MIN	TAP	MEAN	RMS	MAX	MIN
1	0000000000	0000000000	0000000000	0000000000	1	0000000000	0000000000	0000000000	0000000000

DATA FOR PROJECT 6022 CONFIG. K WIND DIR. 35 TUBING NO. 1

TAP	MEAN	RMS	MAX	MIN	TAP	MEAN	RMS	MAX	MIN
1	0000000000	0000000000	0000000000	0000000000	1	0000000000	0000000000	0000000000	0000000000

DATA FOR PROJECT 6022 CONFIG. K WIND DIR. 37 TUBING NO. 1

TAP	MEAN	RMS	MAX	MIN	TAP	MEAN	RMS	MAX	MIN
1	0000000000	0000000000	0000000000	0000000000	1	0000000000	0000000000	0000000000	0000000000

DATA FOR PROJECT 6022 CONFIG. J WIND DIR. 145 TUBING NO. 1

TAP	MEAN	RMS	MAX	MIN	TAP	MEAN	RMS	MAX	MIN
1	0000000000	0000000000	0000000000	0000000000	1	0000000000	0000000000	0000000000	0000000000

DATA FOR PROJECT 6022 CONFIG. J WIND DIR. 147 TUBING NO. 1

TAP	MEAN	RMS	MAX	MIN	TAP	MEAN	RMS	MAX	MIN
1	0000000000	0000000000	0000000000	0000000000	1	0000000000	0000000000	0000000000	0000000000

DATA FOR PROJECT 6022 CONFIG. K WIND DIR. 36 TUBING NO. 1

TAP	MEAN	RMS	MAX	MIN	TAP	MEAN	RMS	MAX	MIN
1	0000000000	0000000000	0000000000	0000000000	1	0000000000	0000000000	0000000000	0000000000





DATA FOR PROJECT 6022 CONFIG. L WIND DIR. 91 TUBING NO. 1

TAP	MEAN	RMS	MAX	MIN	TAP	MEAN	RMS	MAX	MIN
1	078	056	245	000	1	123	065	523	000
2	074	054	245	000	2	123	065	523	000
3	074	054	245	000	3	123	065	523	000
4	087	054	245	000	4	123	065	523	000
5	106	054	245	000	5	123	065	523	000
6	107	054	245	000	6	123	065	523	000
7	107	054	245	000	7	123	065	523	000
8	107	054	245	000	8	123	065	523	000
9	107	054	245	000	9	123	065	523	000
10	107	054	245	000	10	123	065	523	000

DATA FOR PROJECT 6022 CONFIG. L WIND DIR. 145 TUBING NO. 1

TAP	MEAN	RMS	MAX	MIN	TAP	MEAN	RMS	MAX	MIN
1	078	056	245	000	1	123	065	523	000
2	074	054	245	000	2	123	065	523	000
3	074	054	245	000	3	123	065	523	000
4	087	054	245	000	4	123	065	523	000
5	106	054	245	000	5	123	065	523	000
6	107	054	245	000	6	123	065	523	000
7	107	054	245	000	7	123	065	523	000
8	107	054	245	000	8	123	065	523	000
9	107	054	245	000	9	123	065	523	000
10	107	054	245	000	10	123	065	523	000

DATA FOR PROJECT 6022 CONFIG. L WIND DIR. 147 TUBING NO. 1

TAP	MEAN	RMS	MAX	MIN	TAP	MEAN	RMS	MAX	MIN
1	078	056	245	000	1	123	065	523	000
2	074	054	245	000	2	123	065	523	000
3	074	054	245	000	3	123	065	523	000
4	087	054	245	000	4	123	065	523	000
5	106	054	245	000	5	123	065	523	000
6	107	054	245	000	6	123	065	523	000
7	107	054	245	000	7	123	065	523	000
8	107	054	245	000	8	123	065	523	000
9	107	054	245	000	9	123	065	523	000
10	107	054	245	000	10	123	065	523	000

DATA FOR PROJECT 6022 CONFIG. L WIND DIR. 161 TUBING NO. 1									
TAP	MEAN	RMS	MAX	MIN	TAP	MEAN	RMS	MAX	MIN
1	0.02	0.32	0.8	0.1	1	0.73	0.39	0.93	0.29
2	0.02	0.32	0.8	0.1	2	0.81	0.39	0.93	0.29
3	0.02	0.32	0.8	0.1	3	0.78	0.39	0.93	0.29
4	0.02	0.32	0.8	0.1	4	0.78	0.39	0.93	0.29
5	0.02	0.32	0.8	0.1	5	0.88	0.44	0.93	0.29
6	0.02	0.32	0.8	0.1	6	0.88	0.44	0.93	0.29
7	0.02	0.32	0.8	0.1	7	0.88	0.44	0.93	0.29
8	0.02	0.32	0.8	0.1	8	0.88	0.44	0.93	0.29
9	0.02	0.32	0.8	0.1	9	0.88	0.44	0.93	0.29
10	0.02	0.32	0.8	0.1	10	0.88	0.44	0.93	0.29

DATA FOR PROJECT 6022 CONFIG. M WIND DIR. 35 TUBING NO. 1									
TAP	MEAN	RMS	MAX	MIN	TAP	MEAN	RMS	MAX	MIN
1	0.00	0.50	1.2	0.2	1	0.97	0.62	1.2	0.2
2	0.00	0.50	1.2	0.2	2	1.00	0.62	1.2	0.2
3	0.00	0.50	1.2	0.2	3	1.00	0.62	1.2	0.2
4	0.00	0.50	1.2	0.2	4	1.00	0.62	1.2	0.2
5	0.00	0.50	1.2	0.2	5	1.00	0.62	1.2	0.2
6	0.00	0.50	1.2	0.2	6	1.00	0.62	1.2	0.2
7	0.00	0.50	1.2	0.2	7	1.00	0.62	1.2	0.2
8	0.00	0.50	1.2	0.2	8	1.00	0.62	1.2	0.2
9	0.00	0.50	1.2	0.2	9	1.00	0.62	1.2	0.2
10	0.00	0.50	1.2	0.2	10	1.00	0.62	1.2	0.2

DATA FOR PROJECT 6022 CONFIG. N WIND DIR. 37 TUBING NO. 1									
TAP	MEAN	RMS	MAX	MIN	TAP	MEAN	RMS	MAX	MIN
1	0.00	0.50	1.2	0.2	1	1.00	0.62	1.2	0.2
2	0.00	0.50	1.2	0.2	2	1.00	0.62	1.2	0.2
3	0.00	0.50	1.2	0.2	3	1.00	0.62	1.2	0.2
4	0.00	0.50	1.2	0.2	4	1.00	0.62	1.2	0.2
5	0.00	0.50	1.2	0.2	5	1.00	0.62	1.2	0.2
6	0.00	0.50	1.2	0.2	6	1.00	0.62	1.2	0.2
7	0.00	0.50	1.2	0.2	7	1.00	0.62	1.2	0.2
8	0.00	0.50	1.2	0.2	8	1.00	0.62	1.2	0.2
9	0.00	0.50	1.2	0.2	9	1.00	0.62	1.2	0.2
10	0.00	0.50	1.2	0.2	10	1.00	0.62	1.2	0.2

DATA FOR PROJECT 6022 CONFIG. H WIND DIR. 91 TUBING NO. 1									
TAP	MEAN	RMS	MAX	MIN	TAP	MEAN	RMS	MAX	MIN
1	0.22	0.61	2.15	0.71	1	0.95	0.58	1.74	0.70
2	0.26	0.62	2.22	0.77	2	0.99	0.55	1.81	0.95
3	0.45	0.74	2.39	0.99	3	1.02	0.51	1.81	1.02
4	0.28	0.72	2.59	0.85	4	1.05	0.46	1.82	1.04
5	0.98	0.92	2.87	1.25	5	1.08	0.38	1.82	1.09
6	1.16	1.13	2.95	1.29	6	1.16	0.44	1.82	1.16
7	1.15	1.16	2.71	1.34	7	1.06	0.46	1.82	1.06
8	0.85	1.16	2.90	1.34	8	1.18	0.44	1.82	1.18
9	0.85	1.16	2.90	1.34	9	1.18	0.44	1.82	1.18
10	0.85	1.16	2.90	1.34	10	1.18	0.44	1.82	1.18

DATA FOR PROJECT 6022 CONFIG. H WIND DIR. 145 TUBING NO. 1									
TAP	MEAN	RMS	MAX	MIN	TAP	MEAN	RMS	MAX	MIN
1	0.55	0.75	1.62	0.86	1	1.23	0.42	1.62	0.86
2	0.55	0.75	1.62	0.86	2	1.23	0.42	1.62	0.86
3	0.55	0.75	1.62	0.86	3	1.23	0.42	1.62	0.86
4	0.55	0.75	1.62	0.86	4	1.23	0.42	1.62	0.86
5	0.55	0.75	1.62	0.86	5	1.23	0.42	1.62	0.86
6	0.55	0.75	1.62	0.86	6	1.23	0.42	1.62	0.86
7	0.55	0.75	1.62	0.86	7	1.23	0.42	1.62	0.86
8	0.55	0.75	1.62	0.86	8	1.23	0.42	1.62	0.86
9	0.55	0.75	1.62	0.86	9	1.23	0.42	1.62	0.86
10	0.55	0.75	1.62	0.86	10	1.23	0.42	1.62	0.86

DATA FOR PROJECT 6022 CONFIG. H WIND DIR. 147 TUBING NO. 1									
TAP	MEAN	RMS	MAX	MIN	TAP	MEAN	RMS	MAX	MIN
1	0.28	0.48	1.65	0.93	1	0.28	0.38	1.65	0.93
2	0.24	0.55	2.04	0.93	2	0.27	0.38	1.65	0.93
3	0.24	0.55	2.04	0.93	3	0.27	0.38	1.65	0.93
4	0.24	0.55	2.04	0.93	4	0.27	0.38	1.65	0.93
5	0.24	0.55	2.04	0.93	5	0.27	0.38	1.65	0.93
6	0.24	0.55	2.04	0.93	6	0.27	0.38	1.65	0.93
7	0.24	0.55	2.04	0.93	7	0.27	0.38	1.65	0.93
8	0.24	0.55	2.04	0.93	8	0.27	0.38	1.65	0.93
9	0.24	0.55	2.04	0.93	9	0.27	0.38	1.65	0.93
10	0.24	0.55	2.04	0.93	10	0.27	0.38	1.65	0.93



DATA FOR PROJECT 6022 CONFIG. N WIND DIR. 14 TUBING NO. 1										DATA FOR PROJECT 6022 CONFIG. N WIND DIR. 15 TUBING NO. 1									
TAP	MEAN	RMS	MAX	MIN	TAP	MEAN	RMS	MAX	MIN	TAP	MEAN	RMS	MAX	MIN	TAP	MEAN	RMS	MAX	MIN
1	326	065	146	887	123	311	044	055	604	1	390	063	94	88	1	368	053	182	57
2	325	065	147	887	123	301	045	052	604	2	391	061	100	88	2	369	053	173	57
3	325	065	147	887	123	298	045	047	604	3	392	056	100	88	3	369	053	173	57
4	325	065	147	887	123	296	045	041	604	4	378	047	77	88	4	346	056	170	57
5	325	065	147	887	123	290	045	044	604	5	384	048	72	88	5	335	053	150	57
6	325	065	147	887	123	285	045	044	604	6	357	047	72	88	6	335	053	150	57
7	325	065	147	887	123	285	045	044	604	7	357	047	72	88	7	335	053	150	57
8	325	065	147	887	123	285	045	044	604	8	357	047	72	88	8	335	053	150	57
9	325	065	147	887	123	285	045	044	604	9	357	047	72	88	9	335	053	150	57
10	325	065	147	887	123	285	045	044	604	10	357	047	72	88	10	335	053	150	57

DATA FOR PROJECT 6022 CONFIG. N WIND DIR. 21 TUBING NO. 1										DATA FOR PROJECT 6022 CONFIG. N WIND DIR. 22 TUBING NO. 1									
TAP	MEAN	RMS	MAX	MIN	TAP	MEAN	RMS	MAX	MIN	TAP	MEAN	RMS	MAX	MIN	TAP	MEAN	RMS	MAX	MIN
1	300	076	248	210	123	209	069	129	46	1	309	043	94	16	1	309	043	94	16
2	300	076	248	210	123	288	069	129	46	2	189	071	100	16	2	189	071	100	16
3	300	076	248	210	123	296	069	129	46	3	171	085	100	16	3	182	074	100	16
4	300	076	248	210	123	275	069	129	46	4	131	105	100	16	4	158	074	100	16
5	300	076	248	210	123	281	069	129	46	5	108	119	100	16	5	158	074	100	16
6	300	076	248	210	123	249	069	129	46	6	064	119	100	16	6	158	074	100	16
7	300	076	248	210	123	249	069	129	46	7	064	119	100	16	7	158	074	100	16
8	300	076	248	210	123	249	069	129	46	8	064	119	100	16	8	158	074	100	16
9	300	076	248	210	123	249	069	129	46	9	064	119	100	16	9	158	074	100	16
10	300	076	248	210	123	249	069	129	46	10	064	119	100	16	10	158	074	100	16

DATA FOR PROJECT 6022 CONFIG. N WIND DIR. 23 TUBING NO. 1										DATA FOR PROJECT 6022 CONFIG. N WIND DIR. 24 TUBING NO. 1									
TAP	MEAN	RMS	MAX	MIN	TAP	MEAN	RMS	MAX	MIN	TAP	MEAN	RMS	MAX	MIN	TAP	MEAN	RMS	MAX	MIN
1	327	057	205	623	123	407	052	498	18	1	407	052	498	18	1	326	057	185	56
2	327	057	205	623	123	448	057	205	623	2	408	054	511	18	2	326	057	185	56
3	327	057	205	623	123	420	057	205	623	3	413	054	511	18	3	326	057	185	56
4	327	057	205	623	123	420	057	205	623	4	409	056	522	18	4	326	057	185	56
5	327	057	205	623	123	412	056	522	18	5	412	056	522	18	5	326	057	185	56
6	327	057	205	623	123	404	056	522	18	6	414	054	511	18	6	326	057	185	56
7	327	057	205	623	123	404	056	522	18	7	414	054	511	18	7	326	057	185	56
8	327	057	205	623	123	404	056	522	18	8	414	054	511	18	8	326	057	185	56
9	327	057	205	623	123	404	056	522	18	9	414	054	511	18	9	326	057	185	56
10	327	057	205	623	123	404	056	522	18	10	414	054	511	18	10	326	057	185	56

DATA FOR PROJECT 6022 CONFIG. N WIND DIR. 111 TUBING NO. 1									
TAP	MEAN	RMS	MAX	MIN	TAP	MEAN	RMS	MAX	MIN
1	151	047	229	147	1	173	066	050	499
2	092	055	232	108	2	188	069	046	513
3	141	057	239	107	3	185	069	039	489
4	148	067	234	096	4	185	069	004	453
5	227	067	234	065	5	207	056	002	398
6	227	091	234	069	6	184	056	002	397
7	227	091	234	069	7	185	054	002	397
8	227	091	234	069	8	185	054	002	397
9	227	091	234	069	9	185	054	002	397
10	227	091	234	069	10	185	054	002	397

DATA FOR PROJECT 6022 CONFIG. N WIND DIR. 114 TUBING NO. 1									
TAP	MEAN	RMS	MAX	MIN	TAP	MEAN	RMS	MAX	MIN
1	113	046	239	058	1	182	078	040	907
2	107	045	242	058	2	182	068	046	831
3	098	044	242	058	3	182	068	046	831
4	074	044	242	058	4	187	068	046	691
5	079	044	242	058	5	187	068	046	691
6	085	044	242	058	6	177	068	046	455
7	084	044	242	058	7	177	068	046	455
8	084	044	242	058	8	190	068	046	499
9	084	044	242	058	9	190	068	046	499
10	084	044	242	058	10	190	068	046	499

DATA FOR PROJECT 6022 CONFIG. N WIND DIR. 121 TUBING NO. 1									
TAP	MEAN	RMS	MAX	MIN	TAP	MEAN	RMS	MAX	MIN
1	209	137	342	103	1	295	99	147	553
2	209	137	342	103	2	302	99	164	553
3	209	137	342	103	3	302	99	180	553
4	209	137	342	103	4	302	99	185	553
5	209	137	342	103	5	302	99	185	553
6	209	137	342	103	6	302	99	185	553
7	209	137	342	103	7	302	99	185	553
8	209	137	342	103	8	302	99	185	553
9	209	137	342	103	9	302	99	185	553
10	209	137	342	103	10	302	99	185	553

DATA FOR PROJECT 6022										WIND DIR. 122 TUBING NO. 1										WIND DIR. 124 TUBING NO. 1									
TAP	MEAN	RMS	MAX	CONFIG.	H	TAP	MEAN	RMS	MAX	MIN	TAP	MEAN	RMS	MAX	CONFIG.	H	TAP	MEAN	RMS	MAX	MIN								
1	0.4	0.81	5.72	1	1	1	0.1	0.41	0.72	3.52	1	1.5	0.49	0.88	3	1	1.8	0.40	0.70	3.0	1	1.8							
2	0.7	0.91	6.72	1	2	1	0.2	0.45	0.84	3.59	1	1.3	0.49	0.88	3	1	1.8	0.40	0.70	3.0	1	1.8							
3	0.7	1.01	7.12	1	3	1	0.2	0.47	0.86	3.57	1	1.3	0.49	0.88	3	1	1.8	0.40	0.70	3.0	1	1.8							
4	0.9	1.08	6.80	1	4	1	0.2	0.47	0.86	3.58	1	1.4	0.52	0.94	4	1	1.9	0.40	0.70	3.0	1	1.8							
5	0.9	1.14	6.89	1	5	1	0.2	0.50	0.87	3.56	1	1.5	0.56	1.04	5	1	2.0	0.40	0.70	3.0	1	1.8							
6	0.9	1.04	6.59	1	6	1	0.2	0.53	0.87	3.54	1	1.8	0.57	1.06	6	1	2.0	0.40	0.70	3.0	1	1.8							
7	0.9	1.04	6.59	1	7	1	0.2	0.53	0.87	3.54	1	1.8	0.57	1.06	6	1	2.0	0.40	0.70	3.0	1	1.8							
8	0.9	1.04	6.59	1	8	1	0.2	0.53	0.87	3.54	1	1.8	0.57	1.06	6	1	2.0	0.40	0.70	3.0	1	1.8							
9	0.9	1.04	6.59	1	9	1	0.2	0.53	0.87	3.54	1	1.8	0.57	1.06	6	1	2.0	0.40	0.70	3.0	1	1.8							
10	0.9	1.04	6.59	1	10	1	0.2	0.53	0.87	3.54	1	1.8	0.57	1.06	6	1	2.0	0.40	0.70	3.0	1	1.8							

DATA FOR PROJECT 6022										WIND DIR. 125 TUBING NO. 1										WIND DIR. 234 TUBING NO. 1									
TAP	MEAN	RMS	MAX	CONFIG.	H	TAP	MEAN	RMS	MAX	MIN	TAP	MEAN	RMS	MAX	CONFIG.	H	TAP	MEAN	RMS	MAX	MIN								
1	0.4	0.51	0.76	1	1	1	0.5	0.41	0.71	3.2	1	2.9	0.44	0.66	2	1	1.3	0.44	0.71	3.4	1	2.9							
2	0.5	0.59	0.84	1	2	1	0.5	0.42	0.72	3.2	1	2.9	0.44	0.66	2	1	1.3	0.44	0.71	3.4	1	2.9							
3	0.5	0.67	0.92	1	3	1	0.5	0.43	0.73	3.2	1	2.9	0.44	0.66	2	1	1.3	0.44	0.71	3.4	1	2.9							
4	0.5	0.75	1.00	1	4	1	0.5	0.44	0.74	3.2	1	2.9	0.44	0.66	2	1	1.3	0.44	0.71	3.4	1	2.9							
5	0.5	0.83	1.08	1	5	1	0.5	0.45	0.75	3.2	1	2.9	0.44	0.66	2	1	1.3	0.44	0.71	3.4	1	2.9							
6	0.5	0.91	1.16	1	6	1	0.5	0.46	0.76	3.2	1	2.9	0.44	0.66	2	1	1.3	0.44	0.71	3.4	1	2.9							
7	0.5	0.99	1.24	1	7	1	0.5	0.47	0.77	3.2	1	2.9	0.44	0.66	2	1	1.3	0.44	0.71	3.4	1	2.9							
8	0.5	1.07	1.32	1	8	1	0.5	0.48	0.78	3.2	1	2.9	0.44	0.66	2	1	1.3	0.44	0.71	3.4	1	2.9							
9	0.5	1.15	1.40	1	9	1	0.5	0.49	0.79	3.2	1	2.9	0.44	0.66	2	1	1.3	0.44	0.71	3.4	1	2.9							
10	0.5	1.23	1.48	1	10	1	0.5	0.50	0.80	3.2	1	2.9	0.44	0.66	2	1	1.3	0.44	0.71	3.4	1	2.9							

DATA FOR PROJECT 6022										WIND DIR. 244 TUBING NO. 1										WIND DIR. 254 TUBING NO. 1									
TAP	MEAN	RMS	MAX	CONFIG.	H	TAP	MEAN	RMS	MAX	MIN	TAP	MEAN	RMS	MAX	CONFIG.	H	TAP	MEAN	RMS	MAX	MIN								
1	0.4	0.49	0.74	1	1	1	0.9	0.33	0.62	2.5	1	1.2	0.50	0.84	1	1	1.2	0.50	0.84	1	1.2								
2	0.4	0.57	0.82	1	2	1	0.9	0.34	0.64	2.5	1	1.2	0.50	0.84	1	1	1.2	0.50	0.84	1	1.2								
3	0.4	0.65	0.90	1	3	1	0.9	0.35	0.66	2.5	1	1.2	0.50	0.84	1	1	1.2	0.50	0.84	1	1.2								
4	0.4	0.73	0.98	1	4	1	0.9	0.36	0.68	2.5	1	1.2	0.50	0.84	1	1	1.2	0.50	0.84	1	1.2								
5	0.4	0.81	1.06	1	5	1	0.9	0.37	0.70	2.5	1	1.2	0.50	0.84	1	1	1.2	0.50	0.84	1	1.2								
6	0.4	0.89	1.14	1	6	1	0.9	0.38	0.72	2.5	1	1.2	0.50	0.84	1	1	1.2	0.50	0.84	1	1.2								
7	0.4	0.97	1.22	1	7	1	0.9	0.39	0.74	2.5	1	1.2	0.50	0.84	1	1	1.2	0.50	0.84	1	1.2								
8	0.4	1.05	1.30	1	8	1	0.9	0.40	0.76	2.5	1	1.2	0.50	0.84	1	1	1.2	0.50	0.84	1	1.2								
9	0.4	1.13	1.38	1	9	1	0.9	0.41	0.78	2.5	1	1.2	0.50	0.84	1	1	1.2	0.50	0.84	1	1.2								
10	0.4	1.21	1.46	1	10	1	0.9	0.42	0.80	2.5	1	1.2	0.50	0.84	1	1	1.2	0.50	0.84	1	1.2								

DATA FOR PROJECT 6022 CONFIG. 0 WIND DIR. 0 WIND DIR. 344 TUBING NO. 1

TAP	MEAN	RMS	MAX	MIN	TAP	MEAN	RMS	MAX	MIN
1	105	048	039	287	1	197	049	028	18
2	106	050	039	287	2	201	047	027	18
3	106	050	039	287	3	201	047	027	18
4	106	050	039	287	4	201	047	027	18
5	106	050	039	287	5	201	047	027	18
6	106	050	039	287	6	201	047	027	18
7	106	050	039	287	7	201	047	027	18
8	106	050	039	287	8	201	047	027	18
9	106	050	039	287	9	201	047	027	18
10	106	050	039	287	10	201	047	027	18

DATA FOR PROJECT 6022 CONFIG. 0 WIND DIR. 0 WIND DIR. 344 TUBING NO. 1

TAP	MEAN	RMS	MAX	MIN	TAP	MEAN	RMS	MAX	MIN
1	105	048	039	287	1	201	047	027	18
2	106	050	039	287	2	201	047	027	18
3	106	050	039	287	3	201	047	027	18
4	106	050	039	287	4	201	047	027	18
5	106	050	039	287	5	201	047	027	18
6	106	050	039	287	6	201	047	027	18
7	106	050	039	287	7	201	047	027	18
8	106	050	039	287	8	201	047	027	18
9	106	050	039	287	9	201	047	027	18
10	106	050	039	287	10	201	047	027	18

DATA FOR PROJECT 6022 CONFIG. 0 WIND DIR. 0 WIND DIR. 344 TUBING NO. 1

TAP	MEAN	RMS	MAX	MIN	TAP	MEAN	RMS	MAX	MIN
1	105	048	039	287	1	201	047	027	18
2	106	050	039	287	2	201	047	027	18
3	106	050	039	287	3	201	047	027	18
4	106	050	039	287	4	201	047	027	18
5	106	050	039	287	5	201	047	027	18
6	106	050	039	287	6	201	047	027	18
7	106	050	039	287	7	201	047	027	18
8	106	050	039	287	8	201	047	027	18
9	106	050	039	287	9	201	047	027	18
10	106	050	039	287	10	201	047	027	18

DATA FOR PROJECT 6022 CONFIG. 0 WIND DIR. 15 TUBING NO. 1									
TAP	MEAN	RMS	MAX	MIN	TAP	MEAN	RMS	MAX	MIN
1	277	091	050	746	1	289	070	062	686
2	280	082	041	736	2	291	022	060	690
3	285	082	012	736	3	273	023	052	640
4	282	087	028	726	4	267	000	015	545
5	286	085	018	726	5	259	000	022	533
6	282	085	019	726	6	240	007	013	492
7	282	085	011	726	7	236	053	012	492
8	283	083	041	726	8	227	008	019	636
9	283	083	041	726	9	224	008	019	636
10	283	083	041	726	10	224	008	019	636

DATA FOR PROJECT 6022 CONFIG. 0 WIND DIR. 22 TUBING NO. 1									
TAP	MEAN	RMS	MAX	MIN	TAP	MEAN	RMS	MAX	MIN
1	124	088	038	322	1	081	088	034	225
2	125	087	027	322	2	082	088	034	225
3	112	087	025	322	3	082	088	034	225
4	114	087	024	322	4	082	088	034	225
5	114	087	024	322	5	082	088	034	225
6	104	087	024	322	6	082	088	034	225
7	056	087	024	322	7	082	088	034	225
8	044	087	024	322	8	082	088	034	225
9	069	087	024	322	9	082	088	034	225
10	069	087	024	322	10	082	088	034	225

DATA FOR PROJECT 6022 CONFIG. 0 WIND DIR. 24 TUBING NO. 1									
TAP	MEAN	RMS	MAX	MIN	TAP	MEAN	RMS	MAX	MIN
1	178	074	048	383	1	158	051	036	250
2	175	068	045	407	2	125	032	036	250
3	165	068	045	407	3	165	032	036	250
4	165	068	045	407	4	165	032	036	250
5	165	068	045	407	5	165	032	036	250
6	165	068	045	407	6	165	032	036	250
7	165	068	045	407	7	165	032	036	250
8	165	068	045	407	8	165	032	036	250
9	165	068	045	407	9	165	032	036	250
10	165	068	045	407	10	165	032	036	250

DATA FOR PROJECT 6022										DATA FOR PROJECT 6022																			
CONFIG. 0					WIND DIR. 1					TUBING NO. 1					CONFIG. 0					WIND DIR. 1					TUBING NO. 1				
TAP	MEAN	RMS	MAX	MIN	TAP	MEAN	RMS	MAX	MIN	TAP	MEAN	RMS	MAX	MIN	TAP	MEAN	RMS	MAX	MIN	TAP	MEAN	RMS	MAX	MIN	TAP	MEAN	RMS	MAX	MIN
1	332	0.55	120	60	1	250	0.55	120	60	1	123	0.65	369	204	1	176	0.55	295	175	1	176	0.55	295	175	1	176	0.55	295	175
2	332	0.55	120	60	2	250	0.55	120	60	2	123	0.65	369	204	2	176	0.55	295	175	2	176	0.55	295	175	2	176	0.55	295	175
3	332	0.55	120	60	3	250	0.55	120	60	3	123	0.65	369	204	3	176	0.55	295	175	3	176	0.55	295	175	3	176	0.55	295	175
4	332	0.55	120	60	4	250	0.55	120	60	4	123	0.65	369	204	4	176	0.55	295	175	4	176	0.55	295	175	4	176	0.55	295	175
5	332	0.55	120	60	5	250	0.55	120	60	5	123	0.65	369	204	5	176	0.55	295	175	5	176	0.55	295	175	5	176	0.55	295	175
6	332	0.55	120	60	6	250	0.55	120	60	6	123	0.65	369	204	6	176	0.55	295	175	6	176	0.55	295	175	6	176	0.55	295	175
7	332	0.55	120	60	7	250	0.55	120	60	7	123	0.65	369	204	7	176	0.55	295	175	7	176	0.55	295	175	7	176	0.55	295	175
8	332	0.55	120	60	8	250	0.55	120	60	8	123	0.65	369	204	8	176	0.55	295	175	8	176	0.55	295	175	8	176	0.55	295	175
9	332	0.55	120	60	9	250	0.55	120	60	9	123	0.65	369	204	9	176	0.55	295	175	9	176	0.55	295	175	9	176	0.55	295	175
10	332	0.55	120	60	10	250	0.55	120	60	10	123	0.65	369	204	10	176	0.55	295	175	10	176	0.55	295	175	10	176	0.55	295	175

DATA FOR PROJECT 6022										DATA FOR PROJECT 6022																			
CONFIG. 0					WIND DIR. 1					TUBING NO. 1					CONFIG. 0					WIND DIR. 1					TUBING NO. 1				
TAP	MEAN	RMS	MAX	MIN	TAP	MEAN	RMS	MAX	MIN	TAP	MEAN	RMS	MAX	MIN	TAP	MEAN	RMS	MAX	MIN	TAP	MEAN	RMS	MAX	MIN	TAP	MEAN	RMS	MAX	MIN
1	021	0.25	200	100	1	180	0.43	60	30	1	123	0.43	60	30	1	158	0.43	60	30	1	158	0.43	60	30	1	158	0.43	60	30
2	021	0.25	200	100	2	180	0.43	60	30	2	123	0.43	60	30	2	158	0.43	60	30	2	158	0.43	60	30	2	158	0.43	60	30
3	021	0.25	200	100	3	180	0.43	60	30	3	123	0.43	60	30	3	158	0.43	60	30	3	158	0.43	60	30	3	158	0.43	60	30
4	021	0.25	200	100	4	180	0.43	60	30	4	123	0.43	60	30	4	158	0.43	60	30	4	158	0.43	60	30	4	158	0.43	60	30
5	021	0.25	200	100	5	180	0.43	60	30	5	123	0.43	60	30	5	158	0.43	60	30	5	158	0.43	60	30	5	158	0.43	60	30
6	021	0.25	200	100	6	180	0.43	60	30	6	123	0.43	60	30	6	158	0.43	60	30	6	158	0.43	60	30	6	158	0.43	60	30
7	021	0.25	200	100	7	180	0.43	60	30	7	123	0.43	60	30	7	158	0.43	60	30	7	158	0.43	60	30	7	158	0.43	60	30
8	021	0.25	200	100	8	180	0.43	60	30	8	123	0.43	60	30	8	158	0.43	60	30	8	158	0.43	60	30	8	158	0.43	60	30
9	021	0.25	200	100	9	180	0.43	60	30	9	123	0.43	60	30	9	158	0.43	60	30	9	158	0.43	60	30	9	158	0.43	60	30
10	021	0.25	200	100	10	180	0.43	60	30	10	123	0.43	60	30	10	158	0.43	60	30	10	158	0.43	60	30	10	158	0.43	60	30

DATA FOR PROJECT 6022										DATA FOR PROJECT 6022																			
CONFIG. 0					WIND DIR. 1					TUBING NO. 1					CONFIG. 0					WIND DIR. 1					TUBING NO. 1				
TAP	MEAN	RMS	MAX	MIN	TAP	MEAN	RMS	MAX	MIN	TAP	MEAN	RMS	MAX	MIN	TAP	MEAN	RMS	MAX	MIN	TAP	MEAN	RMS	MAX	MIN	TAP	MEAN	RMS	MAX	MIN
1	021	0.25	200	100	1	180	0.43	60	30	1	123	0.43	60	30	1	158	0.43	60	30	1	158	0.43	60	30	1	158	0.43	60	30
2	021	0.25	200	100	2	180	0.43	60	30	2	123	0.43	60	30	2	158	0.43	60	30	2	158	0.43	60	30	2	158	0.43	60	30
3	021	0.25	200	100	3	180	0.43	60	30	3	123	0.43	60	30	3	158	0.43	60	30	3	158	0.43	60	30	3	158	0.43	60	30
4	021	0.25	200	100	4	180	0.43	60	30	4	123	0.43	60	30	4	158	0.43	60	30	4	158	0.43	60	30	4	158	0.43	60	30
5	021	0.25	200	100	5	180	0.43	60	30	5	123	0.43	60	30	5	158	0.43	60	30	5	158	0.43	60	30	5	158	0.43	60	30
6	021	0.25	200	100	6	180	0.43	60	30	6	123	0.43	60	30	6	158	0.43	60	30	6	158	0.43	60	30	6	158	0.43	60	30
7	021	0.25	200	100	7	180	0.43	60	30	7	123	0.43	60	30	7	158	0.43	60	30	7	158	0.43	60	30	7	158	0.43	60	30
8	021	0.25	200	100	8	180	0.43	60	30	8	123	0.43	60	30	8	158	0.43	60	30	8	158	0.43	60	30	8	158	0.43	60	30
9	021	0.25	200	100	9	180	0.43	60	30	9	123	0.43	60	30	9	158	0.43	60	30	9	158	0.43	60	30	9	158	0.43	60	30
10	021	0.25	200	100	10	180	0.43	60	30	10	123	0.43	60	30	10	158	0.43	60	30	10	158	0.43	60	30	10	158	0.43	60	30

DATA FOR PROJECT 6022 CONFIG. 0 WIND DIR. 0 WIND DIR. 124 TUBING NO. 1									
TAP	MEAN	RMS	MAX	MIN	TAP	MEAN	RMS	MAX	MIN
1	0.4750000000	0.4462250000	0.7517400000	0.2244400000	1	0.9544000000	0.9390000000	1.5523000000	0.7225000000
10	1.0000000000	0.0000000000	0.0000000000	0.0000000000	10	0.0000000000	0.0000000000	0.0000000000	0.0000000000
100	0.0000000000	0.0000000000	0.0000000000	0.0000000000	100	0.0000000000	0.0000000000	0.0000000000	0.0000000000
1000	0.0000000000	0.0000000000	0.0000000000	0.0000000000	1000	0.0000000000	0.0000000000	0.0000000000	0.0000000000
10000	0.0000000000	0.0000000000	0.0000000000	0.0000000000	10000	0.0000000000	0.0000000000	0.0000000000	0.0000000000

DATA FOR PROJECT 6022 CONFIG. P WIND DIR. 35 TUBING NO. 1									
TAP	MEAN	RMS	MAX	MIN	TAP	MEAN	RMS	MAX	MIN
1	1.2140000000	0.4780000000	0.1000000000	0.0000000000	1	2.2240000000	1.1000000000	0.0000000000	0.0000000000
10	1.1140000000	0.0000000000	0.0000000000	0.0000000000	10	1.1000000000	0.0000000000	0.0000000000	0.0000000000
100	0.0000000000	0.0000000000	0.0000000000	0.0000000000	100	0.0000000000	0.0000000000	0.0000000000	0.0000000000
1000	0.0000000000	0.0000000000	0.0000000000	0.0000000000	1000	0.0000000000	0.0000000000	0.0000000000	0.0000000000
10000	0.0000000000	0.0000000000	0.0000000000	0.0000000000	10000	0.0000000000	0.0000000000	0.0000000000	0.0000000000

DATA FOR PROJECT 6022 CONFIG. P WIND DIR. 37 TUBING NO. 1									
TAP	MEAN	RMS	MAX	MIN	TAP	MEAN	RMS	MAX	MIN
1	0.9250000000	0.5740000000	0.2222400000	0.0000000000	1	0.9544000000	0.9390000000	1.5523000000	0.7225000000
10	0.0000000000	0.0000000000	0.0000000000	0.0000000000	10	0.0000000000	0.0000000000	0.0000000000	0.0000000000
100	0.0000000000	0.0000000000	0.0000000000	0.0000000000	100	0.0000000000	0.0000000000	0.0000000000	0.0000000000
1000	0.0000000000	0.0000000000	0.0000000000	0.0000000000	1000	0.0000000000	0.0000000000	0.0000000000	0.0000000000
10000	0.0000000000	0.0000000000	0.0000000000	0.0000000000	10000	0.0000000000	0.0000000000	0.0000000000	0.0000000000

DATA FOR PROJECT 6022 CONFIG. P WIND DIR. 146 TUBING NO. 1									
TAP	MEAN	RMS	MAX	MIN	TAP	MEAN	RMS	MAX	MIN
1	1207	0000	0500	0000	1	1207	0000	0500	0000
2	1207	0000	0500	0000	2	1207	0000	0500	0000
3	1207	0000	0500	0000	3	1207	0000	0500	0000
4	1207	0000	0500	0000	4	1207	0000	0500	0000
5	1207	0000	0500	0000	5	1207	0000	0500	0000
6	1207	0000	0500	0000	6	1207	0000	0500	0000
7	1207	0000	0500	0000	7	1207	0000	0500	0000
8	1207	0000	0500	0000	8	1207	0000	0500	0000
9	1207	0000	0500	0000	9	1207	0000	0500	0000
10	1207	0000	0500	0000	10	1207	0000	0500	0000

DATA FOR PROJECT 6022 CONFIG. 0 WIND DIR. 35 TUBING NO. 1									
TAP	MEAN	RMS	MAX	MIN	TAP	MEAN	RMS	MAX	MIN
1	1207	0000	0500	0000	1	1207	0000	0500	0000
2	1207	0000	0500	0000	2	1207	0000	0500	0000
3	1207	0000	0500	0000	3	1207	0000	0500	0000
4	1207	0000	0500	0000	4	1207	0000	0500	0000
5	1207	0000	0500	0000	5	1207	0000	0500	0000
6	1207	0000	0500	0000	6	1207	0000	0500	0000
7	1207	0000	0500	0000	7	1207	0000	0500	0000
8	1207	0000	0500	0000	8	1207	0000	0500	0000
9	1207	0000	0500	0000	9	1207	0000	0500	0000
10	1207	0000	0500	0000	10	1207	0000	0500	0000

DATA FOR PROJECT 6022 CONFIG. 0 WIND DIR. 37 TUBING NO. 1									
TAP	MEAN	RMS	MAX	MIN	TAP	MEAN	RMS	MAX	MIN
1	1207	0000	0500	0000	1	1207	0000	0500	0000
2	1207	0000	0500	0000	2	1207	0000	0500	0000
3	1207	0000	0500	0000	3	1207	0000	0500	0000
4	1207	0000	0500	0000	4	1207	0000	0500	0000
5	1207	0000	0500	0000	5	1207	0000	0500	0000
6	1207	0000	0500	0000	6	1207	0000	0500	0000
7	1207	0000	0500	0000	7	1207	0000	0500	0000
8	1207	0000	0500	0000	8	1207	0000	0500	0000
9	1207	0000	0500	0000	9	1207	0000	0500	0000
10	1207	0000	0500	0000	10	1207	0000	0500	0000

DATA FOR PROJECT 6022 CONFIG. 0 WIND DIR. 146 TUBING NO. 1									
TAP	MEAN	RMS	MAX	MIN	TAP	MEAN	RMS	MAX	MIN
1	2266	1217	8788	1692	1	1588	234	31	45
2	2266	1217	8788	1692	2	1588	234	31	45
3	2266	1217	8788	1692	3	1588	234	31	45
4	2266	1217	8788	1692	4	1588	234	31	45
5	2266	1217	8788	1692	5	1588	234	31	45
6	2266	1217	8788	1692	6	1588	234	31	45
7	2266	1217	8788	1692	7	1588	234	31	45
8	2266	1217	8788	1692	8	1588	234	31	45
9	2266	1217	8788	1692	9	1588	234	31	45
10	2266	1217	8788	1692	10	1588	234	31	45

DATA FOR PROJECT 6022 CONFIG. 0 WIND DIR. 147 TUBING NO. 1									
TAP	MEAN	RMS	MAX	MIN	TAP	MEAN	RMS	MAX	MIN
1	1024	455	2755	222	1	1024	455	2755	222
2	1024	455	2755	222	2	1024	455	2755	222
3	1024	455	2755	222	3	1024	455	2755	222
4	1024	455	2755	222	4	1024	455	2755	222
5	1024	455	2755	222	5	1024	455	2755	222
6	1024	455	2755	222	6	1024	455	2755	222
7	1024	455	2755	222	7	1024	455	2755	222
8	1024	455	2755	222	8	1024	455	2755	222
9	1024	455	2755	222	9	1024	455	2755	222
10	1024	455	2755	222	10	1024	455	2755	222

DATA FOR PROJECT 6022 CONFIG. 0 WIND DIR. 12 TUBING NO. 1									
TAP	MEAN	RMS	MAX	MIN	TAP	MEAN	RMS	MAX	MIN
1	1281	575	3402	445	1	1281	575	3402	445
2	1281	575	3402	445	2	1281	575	3402	445
3	1281	575	3402	445	3	1281	575	3402	445
4	1281	575	3402	445	4	1281	575	3402	445
5	1281	575	3402	445	5	1281	575	3402	445
6	1281	575	3402	445	6	1281	575	3402	445
7	1281	575	3402	445	7	1281	575	3402	445
8	1281	575	3402	445	8	1281	575	3402	445
9	1281	575	3402	445	9	1281	575	3402	445
10	1281	575	3402	445	10	1281	575	3402	445

DATA FOR PROJECT 6022 CONFIG. R WIND DIR. 22 TUBING NO. 1

TAP	MEAN	RMS	MAX	MIN	TAP	MEAN	RMS	MAX	MIN
1	0300	0920	1800	7	1	0300	0920	1800	7
2	0000	1050	1900	0	2	0000	1050	1900	0
3	0000	1050	1900	0	3	0000	1050	1900	0
4	0000	1050	1900	0	4	0000	1050	1900	0
5	0000	1050	1900	0	5	0000	1050	1900	0
6	0000	1050	1900	0	6	0000	1050	1900	0
7	0000	1050	1900	0	7	0000	1050	1900	0
8	0000	1050	1900	0	8	0000	1050	1900	0
9	0000	1050	1900	0	9	0000	1050	1900	0
10	0000	1050	1900	0	10	0000	1050	1900	0

DATA FOR PROJECT 6022 CONFIG. R WIND DIR. 23 TUBING NO. 1

TAP	MEAN	RMS	MAX	MIN	TAP	MEAN	RMS	MAX	MIN
1	0500	0800	1500	0	1	0500	0800	1500	0
2	0000	0900	1600	0	2	0000	0900	1600	0
3	0000	0900	1600	0	3	0000	0900	1600	0
4	0000	0900	1600	0	4	0000	0900	1600	0
5	0000	0900	1600	0	5	0000	0900	1600	0
6	0000	0900	1600	0	6	0000	0900	1600	0
7	0000	0900	1600	0	7	0000	0900	1600	0
8	0000	0900	1600	0	8	0000	0900	1600	0
9	0000	0900	1600	0	9	0000	0900	1600	0
10	0000	0900	1600	0	10	0000	0900	1600	0

DATA FOR PROJECT 6022 CONFIG. R WIND DIR. 24 TUBING NO. 1

TAP	MEAN	RMS	MAX	MIN	TAP	MEAN	RMS	MAX	MIN
1	0400	0700	1400	0	1	0400	0700	1400	0
2	0000	0800	1500	0	2	0000	0800	1500	0
3	0000	0800	1500	0	3	0000	0800	1500	0
4	0000	0800	1500	0	4	0000	0800	1500	0
5	0000	0800	1500	0	5	0000	0800	1500	0
6	0000	0800	1500	0	6	0000	0800	1500	0
7	0000	0800	1500	0	7	0000	0800	1500	0
8	0000	0800	1500	0	8	0000	0800	1500	0
9	0000	0800	1500	0	9	0000	0800	1500	0
10	0000	0800	1500	0	10	0000	0800	1500	0

DATA FOR PROJECT 6022 CONFIG. R WIND DIR. 13 TUBING NO. 1

TAP	MEAN	RMS	MAX	MIN	TAP	MEAN	RMS	MAX	MIN
1	0500	0900	1700	0	1	0500	0900	1700	0
2	0000	1000	1800	0	2	0000	1000	1800	0
3	0000	1000	1800	0	3	0000	1000	1800	0
4	0000	1000	1800	0	4	0000	1000	1800	0
5	0000	1000	1800	0	5	0000	1000	1800	0
6	0000	1000	1800	0	6	0000	1000	1800	0
7	0000	1000	1800	0	7	0000	1000	1800	0
8	0000	1000	1800	0	8	0000	1000	1800	0
9	0000	1000	1800	0	9	0000	1000	1800	0
10	0000	1000	1800	0	10	0000	1000	1800	0

DATA FOR PROJECT 6022 CONFIG. R WIND DIR. 14 TUBING NO. 1

TAP	MEAN	RMS	MAX	MIN	TAP	MEAN	RMS	MAX	MIN
1	0500	0900	1700	0	1	0500	0900	1700	0
2	0000	1000	1800	0	2	0000	1000	1800	0
3	0000	1000	1800	0	3	0000	1000	1800	0
4	0000	1000	1800	0	4	0000	1000	1800	0
5	0000	1000	1800	0	5	0000	1000	1800	0
6	0000	1000	1800	0	6	0000	1000	1800	0
7	0000	1000	1800	0	7	0000	1000	1800	0
8	0000	1000	1800	0	8	0000	1000	1800	0
9	0000	1000	1800	0	9	0000	1000	1800	0
10	0000	1000	1800	0	10	0000	1000	1800	0

DATA FOR PROJECT 6022 CONFIG. R WIND DIR. 111 TUBING NO. 1

TAP	MEAN	RMS	MAX	MIN	TAP	MEAN	RMS	MAX	MIN
1	0500	0900	1700	0	1	0500	0900	1700	0
2	0000	1000	1800	0	2	0000	1000	1800	0
3	0000	1000	1800	0	3	0000	1000	1800	0
4	0000	1000	1800	0	4	0000	1000	1800	0
5	0000	1000	1800	0	5	0000	1000	1800	0
6	0000	1000	1800	0	6	0000	1000	1800	0
7	0000	1000	1800	0	7	0000	1000	1800	0
8	0000	1000	1800	0	8	0000	1000	1800	0
9	0000	1000	1800	0	9	0000	1000	1800	0
10	0000	1000	1800	0	10	0000	1000	1800	0

DATA FOR PROJECT 6022 CONFIG. R WIND DIR. 121 TUBING NO. 1

TAP	MEAN	RMS	MAX	MIN	TAP	MEAN	RMS	MAX	MIN	TAP	MEAN	RMS	MAX	MIN
1	0.27	1.19	2.28	0.06	1	0.27	0.67	1.23	0.00					
2	0.27	1.19	2.28	0.06	2	0.27	0.77	1.23	0.00					
3	0.27	1.19	2.28	0.06	3	0.27	0.85	1.23	0.00					
4	0.27	1.19	2.28	0.06	4	0.27	1.00	1.23	0.00					
5	0.27	1.19	2.28	0.06	5	0.27	1.07	1.23	0.00					
6	0.27	1.19	2.28	0.06	6	0.27	1.17	1.23	0.00					
7	0.27	1.19	2.28	0.06	7	0.27	1.24	1.23	0.00					
8	0.27	1.19	2.28	0.06	8	0.27	1.31	1.23	0.00					
9	0.27	1.19	2.28	0.06	9	0.27	1.38	1.23	0.00					
10	0.27	1.19	2.28	0.06	10	0.27	1.45	1.23	0.00					

DATA FOR PROJECT 6022 CONFIG. R WIND DIR. 112 TUBING NO. 1

TAP	MEAN	RMS	MAX	MIN	TAP	MEAN	RMS	MAX	MIN
1	0.27	1.19	2.28	0.06	1	0.27	1.35	2.28	0.00
2	0.27	1.19	2.28	0.06	2	0.27	1.23	2.28	0.00
3	0.27	1.19	2.28	0.06	3	0.27	1.11	2.28	0.00
4	0.27	1.19	2.28	0.06	4	0.27	0.99	2.28	0.00
5	0.27	1.19	2.28	0.06	5	0.27	0.87	2.28	0.00
6	0.27	1.19	2.28	0.06	6	0.27	0.75	2.28	0.00
7	0.27	1.19	2.28	0.06	7	0.27	0.63	2.28	0.00
8	0.27	1.19	2.28	0.06	8	0.27	0.51	2.28	0.00
9	0.27	1.19	2.28	0.06	9	0.27	0.39	2.28	0.00
10	0.27	1.19	2.28	0.06	10	0.27	0.27	2.28	0.00

DATA FOR PROJECT 6022 CONFIG. R WIND DIR. 122 TUBING NO. 1

TAP	MEAN	RMS	MAX	MIN	TAP	MEAN	RMS	MAX	MIN
1	0.27	1.19	2.28	0.06	1	0.27	0.49	0.67	0.00
2	0.27	1.19	2.28	0.06	2	0.27	0.59	0.67	0.00
3	0.27	1.19	2.28	0.06	3	0.27	0.69	0.67	0.00
4	0.27	1.19	2.28	0.06	4	0.27	0.79	0.67	0.00
5	0.27	1.19	2.28	0.06	5	0.27	0.89	0.67	0.00
6	0.27	1.19	2.28	0.06	6	0.27	0.99	0.67	0.00
7	0.27	1.19	2.28	0.06	7	0.27	1.09	0.67	0.00
8	0.27	1.19	2.28	0.06	8	0.27	1.19	0.67	0.00
9	0.27	1.19	2.28	0.06	9	0.27	1.29	0.67	0.00
10	0.27	1.19	2.28	0.06	10	0.27	1.39	0.67	0.00

DATA FOR PROJECT 6022 CONFIG. R WIND DIR. 113 TUBING NO. 1

TAP	MEAN	RMS	MAX	MIN	TAP	MEAN	RMS	MAX	MIN
1	0.27	1.19	2.28	0.06	1	0.27	1.35	2.28	0.00
2	0.27	1.19	2.28	0.06	2	0.27	1.23	2.28	0.00
3	0.27	1.19	2.28	0.06	3	0.27	1.11	2.28	0.00
4	0.27	1.19	2.28	0.06	4	0.27	0.99	2.28	0.00
5	0.27	1.19	2.28	0.06	5	0.27	0.87	2.28	0.00
6	0.27	1.19	2.28	0.06	6	0.27	0.75	2.28	0.00
7	0.27	1.19	2.28	0.06	7	0.27	0.63	2.28	0.00
8	0.27	1.19	2.28	0.06	8	0.27	0.51	2.28	0.00
9	0.27	1.19	2.28	0.06	9	0.27	0.39	2.28	0.00
10	0.27	1.19	2.28	0.06	10	0.27	0.27	2.28	0.00

DATA FOR PROJECT 6022 CONFIG. R WIND DIR. 123 TUBING NO. 1

TAP	MEAN	RMS	MAX	MIN	TAP	MEAN	RMS	MAX	MIN
1	0.27	1.19	2.28	0.06	1	0.27	0.45	0.67	0.00
2	0.27	1.19	2.28	0.06	2	0.27	0.55	0.67	0.00
3	0.27	1.19	2.28	0.06	3	0.27	0.65	0.67	0.00
4	0.27	1.19	2.28	0.06	4	0.27	0.75	0.67	0.00
5	0.27	1.19	2.28	0.06	5	0.27	0.85	0.67	0.00
6	0.27	1.19	2.28	0.06	6	0.27	0.95	0.67	0.00
7	0.27	1.19	2.28	0.06	7	0.27	1.05	0.67	0.00
8	0.27	1.19	2.28	0.06	8	0.27	1.15	0.67	0.00
9	0.27	1.19	2.28	0.06	9	0.27	1.25	0.67	0.00
10	0.27	1.19	2.28	0.06	10	0.27	1.35	0.67	0.00

DATA FOR PROJECT 6022 CONFIG. R WIND DIR. 211 TUBING NO. 1

TAP	MEAN	RMS	MAX	MIN	TAP	MEAN	RMS	MAX	MIN
1	0.27	1.19	2.28	0.06	1	0.27	0.68	0.67	0.00
2	0.27	1.19	2.28	0.06	2	0.27	0.78	0.67	0.00
3	0.27	1.19	2.28	0.06	3	0.27	0.88	0.67	0.00
4	0.27	1.19	2.28	0.06	4	0.27	0.98	0.67	0.00
5	0.27	1.19	2.28	0.06	5	0.27	1.08	0.67	0.00
6	0.27	1.19	2.28	0.06	6	0.27	1.18	0.67	0.00
7	0.27	1.19	2.28	0.06	7	0.27	1.28	0.67	0.00
8	0.27	1.19	2.28	0.06	8	0.27	1.38	0.67	0.00
9	0.27	1.19	2.28	0.06	9	0.27	1.48	0.67	0.00
10	0.27	1.19	2.28	0.06	10	0.27	1.58	0.67	0.00

DATA FOR PROJECT 6022 CONFIG. R WIND DIR. 221 TUBING NO. 1									
TAP	MEAN	RMS	MAX	MIN	TAP	MEAN	RMS	MAX	MIN
1	0.22	0.15	0.37	0.00	1	0.17	0.12	0.49	0.00
2	0.17	0.12	0.30	0.00	2	0.13	0.09	0.43	0.00
3	0.17	0.12	0.30	0.00	3	0.13	0.09	0.43	0.00
4	0.17	0.12	0.30	0.00	4	0.13	0.09	0.43	0.00
5	0.17	0.12	0.30	0.00	5	0.13	0.09	0.43	0.00
6	0.17	0.12	0.30	0.00	6	0.13	0.09	0.43	0.00
7	0.17	0.12	0.30	0.00	7	0.13	0.09	0.43	0.00
8	0.17	0.12	0.30	0.00	8	0.13	0.09	0.43	0.00
9	0.17	0.12	0.30	0.00	9	0.13	0.09	0.43	0.00
10	0.17	0.12	0.30	0.00	10	0.13	0.09	0.43	0.00

DATA FOR PROJECT 6022 CONFIG. S WIND DIR. 311 TUBING NO. 1									
TAP	MEAN	RMS	MAX	MIN	TAP	MEAN	RMS	MAX	MIN
1	0.15	0.10	0.25	0.00	1	0.12	0.08	0.35	0.00
2	0.15	0.10	0.25	0.00	2	0.12	0.08	0.35	0.00
3	0.15	0.10	0.25	0.00	3	0.12	0.08	0.35	0.00
4	0.15	0.10	0.25	0.00	4	0.12	0.08	0.35	0.00
5	0.15	0.10	0.25	0.00	5	0.12	0.08	0.35	0.00
6	0.15	0.10	0.25	0.00	6	0.12	0.08	0.35	0.00
7	0.15	0.10	0.25	0.00	7	0.12	0.08	0.35	0.00
8	0.15	0.10	0.25	0.00	8	0.12	0.08	0.35	0.00
9	0.15	0.10	0.25	0.00	9	0.12	0.08	0.35	0.00
10	0.15	0.10	0.25	0.00	10	0.12	0.08	0.35	0.00

DATA FOR PROJECT 6022 CONFIG. S WIND DIR. 321 TUBING NO. 1									
TAP	MEAN	RMS	MAX	MIN	TAP	MEAN	RMS	MAX	MIN
1	0.15	0.10	0.25	0.00	1	0.12	0.08	0.35	0.00
2	0.15	0.10	0.25	0.00	2	0.12	0.08	0.35	0.00
3	0.15	0.10	0.25	0.00	3	0.12	0.08	0.35	0.00
4	0.15	0.10	0.25	0.00	4	0.12	0.08	0.35	0.00
5	0.15	0.10	0.25	0.00	5	0.12	0.08	0.35	0.00
6	0.15	0.10	0.25	0.00	6	0.12	0.08	0.35	0.00
7	0.15	0.10	0.25	0.00	7	0.12	0.08	0.35	0.00
8	0.15	0.10	0.25	0.00	8	0.12	0.08	0.35	0.00
9	0.15	0.10	0.25	0.00	9	0.12	0.08	0.35	0.00
10	0.15	0.10	0.25	0.00	10	0.12	0.08	0.35	0.00

DATA FOR PROJECT 6022 CONFIG. S WIND DIR. 331 TUBING NO. 1									
TAP	MEAN	RMS	MAX	MIN	TAP	MEAN	RMS	MAX	MIN
1	0.15	0.10	0.25	0.00	1	0.12	0.08	0.35	0.00
2	0.15	0.10	0.25	0.00	2	0.12	0.08	0.35	0.00
3	0.15	0.10	0.25	0.00	3	0.12	0.08	0.35	0.00
4	0.15	0.10	0.25	0.00	4	0.12	0.08	0.35	0.00
5	0.15	0.10	0.25	0.00	5	0.12	0.08	0.35	0.00
6	0.15	0.10	0.25	0.00	6	0.12	0.08	0.35	0.00
7	0.15	0.10	0.25	0.00	7	0.12	0.08	0.35	0.00
8	0.15	0.10	0.25	0.00	8	0.12	0.08	0.35	0.00
9	0.15	0.10	0.25	0.00	9	0.12	0.08	0.35	0.00
10	0.15	0.10	0.25	0.00	10	0.12	0.08	0.35	0.00

DATA FOR PROJECT 6022 CONFIG. 8 WIND DIR. 13 TUBING NO. 1									
TAP	MEAN	RMS	MAX	MIN	TAP	MEAN	RMS	MAX	MIN
1	0620	1113	709	0	1	0620	1113	709	0
2	1005	1218	729	2384	2	1005	1218	729	2384
3	1359	1331	894	1928	3	1359	1331	894	1928
4	1357	1334	900	1928	4	1357	1334	900	1928
5	1175	1326	875	2050	5	1175	1326	875	2050
6	1151	1326	875	2050	6	1151	1326	875	2050
7	0601	1101	709	0	7	0601	1101	709	0
8	0601	1101	709	0	8	0601	1101	709	0
9	0601	1101	709	0	9	0601	1101	709	0
10	0601	1101	709	0	10	0601	1101	709	0

DATA FOR PROJECT 6022 CONFIG. 9 WIND DIR. 14 TUBING NO. 1									
TAP	MEAN	RMS	MAX	MIN	TAP	MEAN	RMS	MAX	MIN
1	0423	1109	735	0	1	0423	1109	735	0
2	0645	1208	809	0	2	0645	1208	809	0
3	0725	1120	787	0	3	0725	1120	787	0
4	0925	1111	787	0	4	0925	1111	787	0
5	0559	1109	735	0	5	0559	1109	735	0
6	0559	1109	735	0	6	0559	1109	735	0
7	0559	1109	735	0	7	0559	1109	735	0
8	0559	1109	735	0	8	0559	1109	735	0
9	0559	1109	735	0	9	0559	1109	735	0
10	0559	1109	735	0	10	0559	1109	735	0

DATA FOR PROJECT 6022 CONFIG. 5 WIND DIR. 111 TUBING NO. 1									
TAP	MEAN	RMS	MAX	MIN	TAP	MEAN	RMS	MAX	MIN
1	0908	1284	880	0	1	0908	1284	880	0
2	1105	1314	920	0	2	1105	1314	920	0
3	1119	1314	920	0	3	1119	1314	920	0
4	1144	1314	920	0	4	1144	1314	920	0
5	1144	1314	920	0	5	1144	1314	920	0
6	1063	1314	920	0	6	1063	1314	920	0
7	0908	1284	880	0	7	0908	1284	880	0
8	0908	1284	880	0	8	0908	1284	880	0
9	0908	1284	880	0	9	0908	1284	880	0
10	0908	1284	880	0	10	0908	1284	880	0

DATA FOR PROJECT 6022 CONFIG. 5 WIND DIR. 121 TUBING NO. 1									
TAP	MEAN	RMS	MAX	MIN	TAP	MEAN	RMS	MAX	MIN
1	126	116	607	276	1	202	089	042	587
2	126	114	622	274	2	235	085	024	592
3	126	114	625	274	3	235	085	024	592
4	126	114	625	274	4	235	085	024	592
5	126	114	625	274	5	235	085	024	592
6	126	114	625	274	6	235	085	024	592
7	126	114	625	274	7	235	085	024	592
8	126	114	625	274	8	235	085	024	592
9	126	114	625	274	9	235	085	024	592
10	126	114	625	274	10	235	085	024	592

DATA FOR PROJECT 6022 CONFIG. 5 WIND DIR. 122 TUBING NO. 1									
TAP	MEAN	RMS	MAX	MIN	TAP	MEAN	RMS	MAX	MIN
1	105	105	459	244	1	170	091	170	222
2	109	109	459	244	2	170	091	170	222
3	109	109	459	244	3	170	091	170	222
4	109	109	459	244	4	170	091	170	222
5	109	109	459	244	5	170	091	170	222
6	109	109	459	244	6	170	091	170	222
7	109	109	459	244	7	170	091	170	222
8	109	109	459	244	8	170	091	170	222
9	109	109	459	244	9	170	091	170	222
10	109	109	459	244	10	170	091	170	222

DATA FOR PROJECT 6022 CONFIG. 5 WIND DIR. 123 TUBING NO. 1									
TAP	MEAN	RMS	MAX	MIN	TAP	MEAN	RMS	MAX	MIN
1	105	105	459	244	1	150	086	024	586
2	109	109	459	244	2	150	086	024	586
3	109	109	459	244	3	150	086	024	586
4	109	109	459	244	4	150	086	024	586
5	109	109	459	244	5	150	086	024	586
6	109	109	459	244	6	150	086	024	586
7	109	109	459	244	7	150	086	024	586
8	109	109	459	244	8	150	086	024	586
9	109	109	459	244	9	150	086	024	586
10	109	109	459	244	10	150	086	024	586

DATA FOR PROJECT 6022 CONFIG. 5 WIND DIR. 112 TUBING NO. 1									
TAP	MEAN	RMS	MAX	MIN	TAP	MEAN	RMS	MAX	MIN
1	021	021	059	021	1	274	130	108	135
2	021	021	059	021	2	274	130	108	135
3	021	021	059	021	3	274	130	108	135
4	021	021	059	021	4	274	130	108	135
5	021	021	059	021	5	274	130	108	135
6	021	021	059	021	6	274	130	108	135
7	021	021	059	021	7	274	130	108	135
8	021	021	059	021	8	274	130	108	135
9	021	021	059	021	9	274	130	108	135
10	021	021	059	021	10	274	130	108	135

DATA FOR PROJECT 6022 CONFIG. 5 WIND DIR. 113 TUBING NO. 1									
TAP	MEAN	RMS	MAX	MIN	TAP	MEAN	RMS	MAX	MIN
1	019	019	047	019	1	222	110	091	111
2	019	019	047	019	2	222	110	091	111
3	019	019	047	019	3	222	110	091	111
4	019	019	047	019	4	222	110	091	111
5	019	019	047	019	5	222	110	091	111
6	019	019	047	019	6	222	110	091	111
7	019	019	047	019	7	222	110	091	111
8	019	019	047	019	8	222	110	091	111
9	019	019	047	019	9	222	110	091	111
10	019	019	047	019	10	222	110	091	111

DATA FOR PROJECT 6022 CONFIG. 5 WIND DIR. 211 TUBING NO. 1									
TAP	MEAN	RMS	MAX	MIN	TAP	MEAN	RMS	MAX	MIN
1	022	022	084	022	1	000	000	000	000
2	022	022	084	022	2	000	000	000	000
3	022	022	084	022	3	000	000	000	000
4	022	022	084	022	4	000	000	000	000
5	022	022	084	022	5	000	000	000	000
6	022	022	084	022	6	000	000	000	000
7	022	022	084	022	7	000	000	000	000
8	022	022	084	022	8	000	000	000	000
9	022	022	084	022	9	000	000	000	000
10	022	022	084	022	10	000	000	000	000

DATA FOR PROJECT 6022 CONFIG. S WIND DIR. 221 TUBING NO. 1									
TAP	MEAN	RMS	MAX	MIN	TAP	MEAN	RMS	MAX	MIN
1	407	135	922	477	1	624	124	925	235
2	493	133	927	537	2	629	118	925	235
3	432	117	940	511	3	620	122	925	235
4	436	128	944	597	4	609	134	925	235
5	380	110	912	597	5	625	124	925	235
6	165	106	889	114	6	726	120	925	235
7	141	104	854	121	7	713	117	925	235
8	160	107	854	146	8	713	117	925	235
10					10				

DATA FOR PROJECT 6022 CONFIG. S WIND DIR. 311 TUBING NO. 1									
TAP	MEAN	RMS	MAX	MIN	TAP	MEAN	RMS	MAX	MIN
1	137	041	093	206	1	123	036	093	685
2	105	041	093	206	2	123	036	093	685
3	089	041	093	206	3	123	036	093	685
4	089	041	093	206	4	123	036	093	685
5	089	041	093	206	5	123	036	093	685
6	089	041	093	206	6	123	036	093	685
7	089	041	093	206	7	123	036	093	685
8	089	041	093	206	8	123	036	093	685
10					10				

DATA FOR PROJECT 6022 CONFIG. S WIND DIR. 321 TUBING NO. 1									
TAP	MEAN	RMS	MAX	MIN	TAP	MEAN	RMS	MAX	MIN
1	102	186	678	237	1	123	047	475	235
2	108	186	678	237	2	123	047	475	235
3	105	186	678	237	3	123	047	475	235
4	105	186	678	237	4	123	047	475	235
5	105	186	678	237	5	123	047	475	235
6	105	186	678	237	6	123	047	475	235
7	105	186	678	237	7	123	047	475	235
8	105	186	678	237	8	123	047	475	235
10					10				

DATA FOR PROJECT 6022 CONFIG. T WIND DIR. 11 TUBING NO. 1									
TAP	MEAN	RMS	MAX	MIN	TAP	MEAN	RMS	MAX	MIN
1	120	082	170	487	1	123	080	170	399
2	120	082	170	487	2	123	080	170	399
3	120	082	170	487	3	123	080	170	399
4	120	082	170	487	4	123	080	170	399
5	120	082	170	487	5	123	080	170	399
6	120	082	170	487	6	123	080	170	399
7	120	082	170	487	7	123	080	170	399
8	120	082	170	487	8	123	080	170	399
10					10				

DATA FOR PROJECT 6022 CONFIG. T WIND DIR. 21 TUBING NO. 1									
TAP	MEAN	RMS	MAX	MIN	TAP	MEAN	RMS	MAX	MIN
1	137	080	170	487	1	123	080	170	399
2	137	080	170	487	2	123	080	170	399
3	137	080	170	487	3	123	080	170	399
4	137	080	170	487	4	123	080	170	399
5	137	080	170	487	5	123	080	170	399
6	137	080	170	487	6	123	080	170	399
7	137	080	170	487	7	123	080	170	399
8	137	080	170	487	8	123	080	170	399
10					10				

DATA FOR PROJECT 6022 CONFIG. T WIND DIR. 31 TUBING NO. 1									
TAP	MEAN	RMS	MAX	MIN	TAP	MEAN	RMS	MAX	MIN
1	137	080	170	487	1	123	080	170	399
2	137	080	170	487	2	123	080	170	399
3	137	080	170	487	3	123	080	170	399
4	137	080	170	487	4	123	080	170	399
5	137	080	170	487	5	123	080	170	399
6	137	080	170	487	6	123	080	170	399
7	137	080	170	487	7	123	080	170	399
8	137	080	170	487	8	123	080	170	399
10					10				

DATA FOR PROJECT 6022 CONFIG. T WIND DIR. 22 TUBING NO. 1

TAP	MEAN	RMS	MAX	MIN	TAP	MEAN	RMS	MAX	MIN
1	168	140	783	40	1	326	82	502	752
2	216	142	772	506	2	361	89	520	782
3	227	144	829	375	3	374	93	570	820
4	220	144	847	183	4	489	103	623	852
5	224	142	849	103	5	443	108	696	841
6	224	121	727	124	6	419	105	642	812
7	234	119	585	33	7	548	105	642	812
8	24	89	401	33	8	548	105	642	812
10	024	089	401	33	10	548	105	642	812

DATA FOR PROJECT 6022 CONFIG. T WIND DIR. 23 TUBING NO. 1

TAP	MEAN	RMS	MAX	MIN	TAP	MEAN	RMS	MAX	MIN
1	173	142	814	50	1	326	82	502	752
2	216	142	814	50	2	361	89	520	782
3	227	144	829	50	3	374	93	570	820
4	220	144	847	50	4	489	103	623	852
5	224	142	849	50	5	443	108	696	841
6	224	121	727	50	6	419	105	642	812
7	234	119	585	50	7	548	105	642	812
8	24	89	401	50	8	548	105	642	812
10	024	089	401	50	10	548	105	642	812

DATA FOR PROJECT 6022 CONFIG. T WIND DIR. 24 TUBING NO. 1

TAP	MEAN	RMS	MAX	MIN	TAP	MEAN	RMS	MAX	MIN
1	173	142	814	50	1	326	82	502	752
2	216	142	814	50	2	361	89	520	782
3	227	144	829	50	3	374	93	570	820
4	220	144	847	50	4	489	103	623	852
5	224	142	849	50	5	443	108	696	841
6	224	121	727	50	6	419	105	642	812
7	234	119	585	50	7	548	105	642	812
8	24	89	401	50	8	548	105	642	812
10	024	089	401	50	10	548	105	642	812

DATA FOR PROJECT 6022 CONFIG. T WIND DIR. 13 TUBING NO. 1

TAP	MEAN	RMS	MAX	MIN	TAP	MEAN	RMS	MAX	MIN
1	073	061	164	93	1	634	385	166	592
2	077	064	222	232	2	632	126	190	628
3	059	064	227	55	3	632	126	190	628
4	074	074	237	0	4	632	126	190	628
5	023	097	247	35	5	632	126	190	628
6	029	097	247	35	6	632	126	190	628
7	019	114	266	39	7	632	126	190	628
10	019	114	266	39	10	632	126	190	628

DATA FOR PROJECT 6022 CONFIG. T WIND DIR. 14 TUBING NO. 1

TAP	MEAN	RMS	MAX	MIN	TAP	MEAN	RMS	MAX	MIN
1	167	060	40	33	1	634	385	166	592
2	145	060	88	33	2	632	126	190	628
3	126	067	132	33	3	632	126	190	628
4	108	085	240	33	4	632	126	190	628
5	105	112	373	33	5	632	126	190	628
6	105	112	373	33	6	632	126	190	628
7	105	112	373	33	7	632	126	190	628
10	105	112	373	33	10	632	126	190	628

DATA FOR PROJECT 6022 CONFIG. T WIND DIR. 111 TUBING NO. 1

TAP	MEAN	RMS	MAX	MIN	TAP	MEAN	RMS	MAX	MIN
1	024	067	84	31	1	634	385	166	592
2	038	085	226	31	2	632	126	190	628
3	037	085	226	31	3	632	126	190	628
4	037	085	226	31	4	632	126	190	628
5	037	085	226	31	5	632	126	190	628
6	037	085	226	31	6	632	126	190	628
7	037	085	226	31	7	632	126	190	628
8	037	085	226	31	8	632	126	190	628
10	037	085	226	31	10	632	126	190	628

DATA FOR PROJECT 6022 CONFIG. T WIND DIR. 121 TUBING NO. 1									
TAP	MEAN	RMS	MAX	MIN	TAP	MEAN	RMS	MAX	MIN
1	157	114	639	150	1	192	061	053	4
2	137	126	584	154	2	200	060	023	4
3	137	126	584	154	3	200	060	023	4
4	137	126	584	154	4	200	060	023	4
5	137	126	584	154	5	200	060	023	4
6	137	126	584	154	6	200	060	023	4
7	137	126	584	154	7	200	060	023	4
8	137	126	584	154	8	200	060	023	4
9	137	126	584	154	9	200	060	023	4
10	137	126	584	154	10	200	060	023	4

DATA FOR PROJECT 6022 CONFIG. T WIND DIR. 122 TUBING NO. 1									
TAP	MEAN	RMS	MAX	MIN	TAP	MEAN	RMS	MAX	MIN
1	123	105	622	122	1	123	052	091	23
2	123	105	622	122	2	123	052	091	23
3	123	105	622	122	3	123	052	091	23
4	123	105	622	122	4	123	052	091	23
5	123	105	622	122	5	123	052	091	23
6	123	105	622	122	6	123	052	091	23
7	123	105	622	122	7	123	052	091	23
8	123	105	622	122	8	123	052	091	23
9	123	105	622	122	9	123	052	091	23
10	123	105	622	122	10	123	052	091	23

DATA FOR PROJECT 6022 CONFIG. T WIND DIR. 123 TUBING NO. 1									
TAP	MEAN	RMS	MAX	MIN	TAP	MEAN	RMS	MAX	MIN
1	157	114	639	150	1	192	061	053	4
2	137	126	584	154	2	200	060	023	4
3	137	126	584	154	3	200	060	023	4
4	137	126	584	154	4	200	060	023	4
5	137	126	584	154	5	200	060	023	4
6	137	126	584	154	6	200	060	023	4
7	137	126	584	154	7	200	060	023	4
8	137	126	584	154	8	200	060	023	4
9	137	126	584	154	9	200	060	023	4
10	137	126	584	154	10	200	060	023	4

DATA FOR PROJECT 6022 CONFIG. T WIND DIR. 112 TUBING NO. 1									
TAP	MEAN	RMS	MAX	MIN	TAP	MEAN	RMS	MAX	MIN
1	157	114	639	150	1	192	061	053	4
2	137	126	584	154	2	200	060	023	4
3	137	126	584	154	3	200	060	023	4
4	137	126	584	154	4	200	060	023	4
5	137	126	584	154	5	200	060	023	4
6	137	126	584	154	6	200	060	023	4
7	137	126	584	154	7	200	060	023	4
8	137	126	584	154	8	200	060	023	4
9	137	126	584	154	9	200	060	023	4
10	137	126	584	154	10	200	060	023	4

DATA FOR PROJECT 6022 CONFIG. T WIND DIR. 113 TUBING NO. 1									
TAP	MEAN	RMS	MAX	MIN	TAP	MEAN	RMS	MAX	MIN
1	123	105	622	122	1	123	052	091	23
2	123	105	622	122	2	123	052	091	23
3	123	105	622	122	3	123	052	091	23
4	123	105	622	122	4	123	052	091	23
5	123	105	622	122	5	123	052	091	23
6	123	105	622	122	6	123	052	091	23
7	123	105	622	122	7	123	052	091	23
8	123	105	622	122	8	123	052	091	23
9	123	105	622	122	9	123	052	091	23
10	123	105	622	122	10	123	052	091	23

DATA FOR PROJECT 6022 CONFIG. T WIND DIR. 211 TUBING NO. 1									
TAP	MEAN	RMS	MAX	MIN	TAP	MEAN	RMS	MAX	MIN
1	157	114	639	150	1	192	061	053	4
2	137	126	584	154	2	200	060	023	4
3	137	126	584	154	3	200	060	023	4
4	137	126	584	154	4	200	060	023	4
5	137	126	584	154	5	200	060	023	4
6	137	126	584	154	6	200	060	023	4
7	137	126	584	154	7	200	060	023	4
8	137	126	584	154	8	200	060	023	4
9	137	126	584	154	9	200	060	023	4
10	137	126	584	154	10	200	060	023	4

DATA FOR PROJECT 6022 CONFIG. T WIND DIR. 221 TUBING NO. 1									
TAP	MEAN	RMS	MAX	MIN	TAP	MEAN	RMS	MAX	MIN
1	167	145	776	305	1	357	078	093	706
2	227	160	868	250	2	390	079	124	734
3	273	162	908	138	3	397	075	120	727
4	299	141	934	148	4	401	065	120	627
5	204	125	742	178	5	438	068	166	574
6	225	100	525	189	6	493	121	114	133
7	144	100	414	277	7	489	145	100	124
8	186	083	271	390	8	519	151	041	148
10	-	-	-	-	10	-	-	-	-

DATA FOR PROJECT 6022 CONFIG. U WIND DIR. 321 TUBING NO. 1									
TAP	MEAN	RMS	MAX	MIN	TAP	MEAN	RMS	MAX	MIN
1	114	041	012	310	1	267	049	133	403
2	143	042	015	275	2	264	039	109	380
3	133	043	023	310	3	261	039	127	386
4	133	048	022	290	4	264	040	112	384
5	133	052	029	296	5	269	041	096	420
6	136	054	029	374	6	271	041	146	413
7	136	054	055	371	7	273	041	150	413
8	130	054	000	413	8	273	041	150	413
10	-	-	-	-	10	-	-	-	-

DATA FOR PROJECT 6022 CONFIG. U WIND DIR. 36 TUBING NO. 1									
TAP	MEAN	RMS	MAX	MIN	TAP	MEAN	RMS	MAX	MIN
1	97	067	234	244	1	827	295	168	308
2	102	069	250	208	2	815	224	170	347
3	122	072	259	181	3	809	226	189	349
4	122	085	272	181	4	724	190	211	358
5	122	092	272	150	5	652	180	220	329
6	122	093	272	150	6	571	180	192	329
7	122	093	272	150	7	571	180	192	329
8	122	093	272	150	8	571	180	192	329
10	-	-	-	-	10	-	-	-	-

DATA FOR PROJECT 6022 CONFIG. T WIND DIR. 311 TUBING NO. 1									
TAP	MEAN	RMS	MAX	MIN	TAP	MEAN	RMS	MAX	MIN
1	113	043	104	99	1	369	076	126	767
2	103	044	102	225	2	357	065	126	687
3	084	042	047	225	3	321	056	127	508
4	075	047	027	225	4	265	056	061	465
5	096	047	020	225	5	265	047	031	379
6	093	049	014	225	6	219	047	031	387
7	093	051	014	225	7	219	049	056	405
8	132	058	014	225	8	232	050	056	472
10	-	-	-	-	10	-	-	-	-

DATA FOR PROJECT 6022 CONFIG. U WIND DIR. 35 TUBING NO. 1									
TAP	MEAN	RMS	MAX	MIN	TAP	MEAN	RMS	MAX	MIN
1	007	074	26	368	1	983	404	141	94
2	127	078	23	270	2	974	378	237	000
3	282	088	33	007	3	954	365	237	000
4	398	096	34	081	4	935	345	235	000
5	449	108	31	109	5	893	314	219	000
6	485	123	31	124	6	834	323	188	000
7	509	136	30	132	7	834	323	188	000
8	471	170	11	104	8	798	326	188	000
10	-	-	-	-	10	-	-	-	-

DATA FOR PROJECT 6022 CONFIG. U WIND DIR. 37 TUBING NO. 1									
TAP	MEAN	RMS	MAX	MIN	TAP	MEAN	RMS	MAX	MIN
1	006	057	00	222	1	829	292	181	44
2	193	071	13	222	2	819	222	191	66
3	224	082	33	222	3	806	222	226	62
4	229	089	31	222	4	806	222	226	62
5	271	100	27	222	5	737	164	181	53
6	271	102	27	222	6	677	189	181	53
7	443	120	10	222	7	624	222	189	53
8	409	146	10	222	8	624	222	189	53
10	-	-	-	-	10	-	-	-	-

DATA FOR PROJECT 6022 CONFIG. U WIND DIR. 146 TUBING NO. 1									
TAP	MEAN	RMS	MAX	MIN	TAP	MEAN	RMS	MAX	MIN
1	16	126	969	090	1	529	147	96	1
2	3887	1122	9823	180	12	572	170	99	2
3	3331	1122	8237	064	13	626	182	222	3
4	3331	1122	7779	020	14	626	217	220	4
5	3331	1122	7779	020	15	849	243	280	5
6	3331	1122	6949	075	16	849	243	280	6
7	3331	1122	6949	075	17	849	243	280	7
8	3331	1122	6949	075	18	849	243	280	8
9	3331	1122	6949	075	19	849	243	280	9
10	3331	1122	6949	075	20	849	243	280	10

DATA FOR PROJECT 6022 CONFIG. V WIND DIR. 35 TUBING NO. 1									
TAP	MEAN	RMS	MAX	MIN	TAP	MEAN	RMS	MAX	MIN
1	235	146	969	025	1	596	155	101	1
2	3331	1122	969	044	2	691	172	101	2
3	3331	1122	8237	038	3	725	182	101	3
4	3331	1122	7779	055	4	857	205	101	4
5	3331	1122	7779	055	5	857	205	101	5
6	3331	1122	6949	022	6	957	225	101	6
7	3331	1122	6949	022	7	957	225	101	7
8	3331	1122	6949	022	8	957	225	101	8
9	3331	1122	6949	022	9	957	225	101	9
10	3331	1122	6949	022	10	957	225	101	10

DATA FOR PROJECT 6022 CONFIG. V WIND DIR. 37 TUBING NO. 1									
TAP	MEAN	RMS	MAX	MIN	TAP	MEAN	RMS	MAX	MIN
1	148	66	433	085	1	457	140	5	1
2	185	67	433	281	2	457	140	5	2
3	250	68	433	182	3	457	140	5	3
4	250	68	433	182	4	457	140	5	4
5	250	68	433	182	5	457	140	5	5
6	250	68	433	182	6	457	140	5	6
7	250	68	433	182	7	457	140	5	7
8	250	68	433	182	8	457	140	5	8
9	250	68	433	182	9	457	140	5	9
10	250	68	433	182	10	457	140	5	10

DATA FOR PROJECT 6022 CONFIG. V WIND DIR. 145 TUBING NO. 1									
TAP	MEAN	RMS	MAX	MIN	MEAN	RMS	MAX	MIN	TAP
1	323	132	525	017	107	077	148	452	1
2	334	111	512	043	114	073	130	452	2
3	308	113	515	043	117	073	130	452	3
4	240	105	515	017	107	073	130	452	4
5	192	095	501	049	119	073	130	452	5
6	173	095	407	090	119	073	130	452	6
7	194	096	408	090	119	073	130	452	7
8	194	096	408	090	119	073	130	452	8
9	194	096	408	090	119	073	130	452	9
10	194	096	408	090	119	073	130	452	10

DATA FOR PROJECT 6022 CONFIG. U WIND DIR. 35 TUBING NO. 1									
TAP	MEAN	RMS	MAX	MIN	MEAN	RMS	MAX	MIN	TAP
1	335	107	688	784	125	053	125	975	1
2	333	103	682	844	125	055	125	975	2
3	337	103	674	844	125	055	125	975	3
4	337	103	674	844	125	055	125	975	4
5	337	103	674	844	125	055	125	975	5
6	337	103	674	844	125	055	125	975	6
7	337	103	674	844	125	055	125	975	7
8	337	103	674	844	125	055	125	975	8
9	337	103	674	844	125	055	125	975	9
10	337	103	674	844	125	055	125	975	10

DATA FOR PROJECT 6022 CONFIG. W WIND DIR. 37 TUBING NO. 1									
TAP	MEAN	RMS	MAX	MIN	MEAN	RMS	MAX	MIN	TAP
1	327	136	525	017	107	077	148	452	1
2	334	111	512	043	114	073	130	452	2
3	308	113	515	043	117	073	130	452	3
4	240	105	515	017	107	073	130	452	4
5	192	095	501	049	119	073	130	452	5
6	173	095	407	090	119	073	130	452	6
7	194	096	408	090	119	073	130	452	7
8	194	096	408	090	119	073	130	452	8
9	194	096	408	090	119	073	130	452	9
10	194	096	408	090	119	073	130	452	10

DATA FOR PROJECT 6022 CONFIG. U WIND DIR. 146 TUBING NO. 1										
TAP	MEAN	RMS	MAX	MIN	TAP	MEAN	RMS	MAX	MIN	TAP
1	103	0.085	0.230	0.022	1	123	0.085	0.230	0.022	1
2	103	0.085	0.230	0.022	2	123	0.085	0.230	0.022	2
3	103	0.085	0.230	0.022	3	123	0.085	0.230	0.022	3
4	103	0.085	0.230	0.022	4	123	0.085	0.230	0.022	4
5	103	0.085	0.230	0.022	5	123	0.085	0.230	0.022	5
6	103	0.085	0.230	0.022	6	123	0.085	0.230	0.022	6
7	103	0.085	0.230	0.022	7	123	0.085	0.230	0.022	7
8	103	0.085	0.230	0.022	8	123	0.085	0.230	0.022	8
9	103	0.085	0.230	0.022	9	123	0.085	0.230	0.022	9
10	103	0.085	0.230	0.022	10	123	0.085	0.230	0.022	10

DATA FOR PROJECT 6022 CONFIG. X WIND DIR. 35 TUBING NO. 1										
TAP	MEAN	RMS	MAX	MIN	TAP	MEAN	RMS	MAX	MIN	TAP
1	127	0.092	0.245	0.025	1	147	0.092	0.245	0.025	1
2	127	0.092	0.245	0.025	2	147	0.092	0.245	0.025	2
3	127	0.092	0.245	0.025	3	147	0.092	0.245	0.025	3
4	127	0.092	0.245	0.025	4	147	0.092	0.245	0.025	4
5	127	0.092	0.245	0.025	5	147	0.092	0.245	0.025	5
6	127	0.092	0.245	0.025	6	147	0.092	0.245	0.025	6
7	127	0.092	0.245	0.025	7	147	0.092	0.245	0.025	7
8	127	0.092	0.245	0.025	8	147	0.092	0.245	0.025	8
9	127	0.092	0.245	0.025	9	147	0.092	0.245	0.025	9
10	127	0.092	0.245	0.025	10	147	0.092	0.245	0.025	10

DATA FOR PROJECT 6022 CONFIG. X WIND DIR. 145 TUBING NO. 1										
TAP	MEAN	RMS	MAX	MIN	TAP	MEAN	RMS	MAX	MIN	TAP
1	123	0.085	0.230	0.022	1	143	0.085	0.230	0.022	1
2	123	0.085	0.230	0.022	2	143	0.085	0.230	0.022	2
3	123	0.085	0.230	0.022	3	143	0.085	0.230	0.022	3
4	123	0.085	0.230	0.022	4	143	0.085	0.230	0.022	4
5	123	0.085	0.230	0.022	5	143	0.085	0.230	0.022	5
6	123	0.085	0.230	0.022	6	143	0.085	0.230	0.022	6
7	123	0.085	0.230	0.022	7	143	0.085	0.230	0.022	7
8	123	0.085	0.230	0.022	8	143	0.085	0.230	0.022	8
9	123	0.085	0.230	0.022	9	143	0.085	0.230	0.022	9
10	123	0.085	0.230	0.022	10	143	0.085	0.230	0.022	10

DATA FOR PROJECT 6022 CONFIG X WIND DIR. 146 TUBING NO. 1										DATA FOR PROJECT 6022 CONFIG. 2 WIND DIR. 35 TUBING NO. 1									
TAP	MEAN	RMS	MAX	MIN	TAP	MEAN	RMS	MAX	MIN	TAP	MEAN	RMS	MAX	MIN	TAP	MEAN	RMS	MAX	MIN
1	107	044	199	77	1	210	024	167	119	1	727	026	167	119	1	727	026	167	119
2	107	044	199	77	2	210	024	167	119	2	727	026	167	119	2	727	026	167	119
3	107	044	199	77	3	210	024	167	119	3	727	026	167	119	3	727	026	167	119
4	107	044	199	77	4	210	024	167	119	4	727	026	167	119	4	727	026	167	119
5	107	044	199	77	5	210	024	167	119	5	727	026	167	119	5	727	026	167	119
6	107	044	199	77	6	210	024	167	119	6	727	026	167	119	6	727	026	167	119
7	107	044	199	77	7	210	024	167	119	7	727	026	167	119	7	727	026	167	119
8	107	044	199	77	8	210	024	167	119	8	727	026	167	119	8	727	026	167	119
9	107	044	199	77	9	210	024	167	119	9	727	026	167	119	9	727	026	167	119
10	107	044	199	77	10	210	024	167	119	10	727	026	167	119	10	727	026	167	119

C-1

APPENDIX C

Plots of Pressure Distribution along Chord of Solar Array

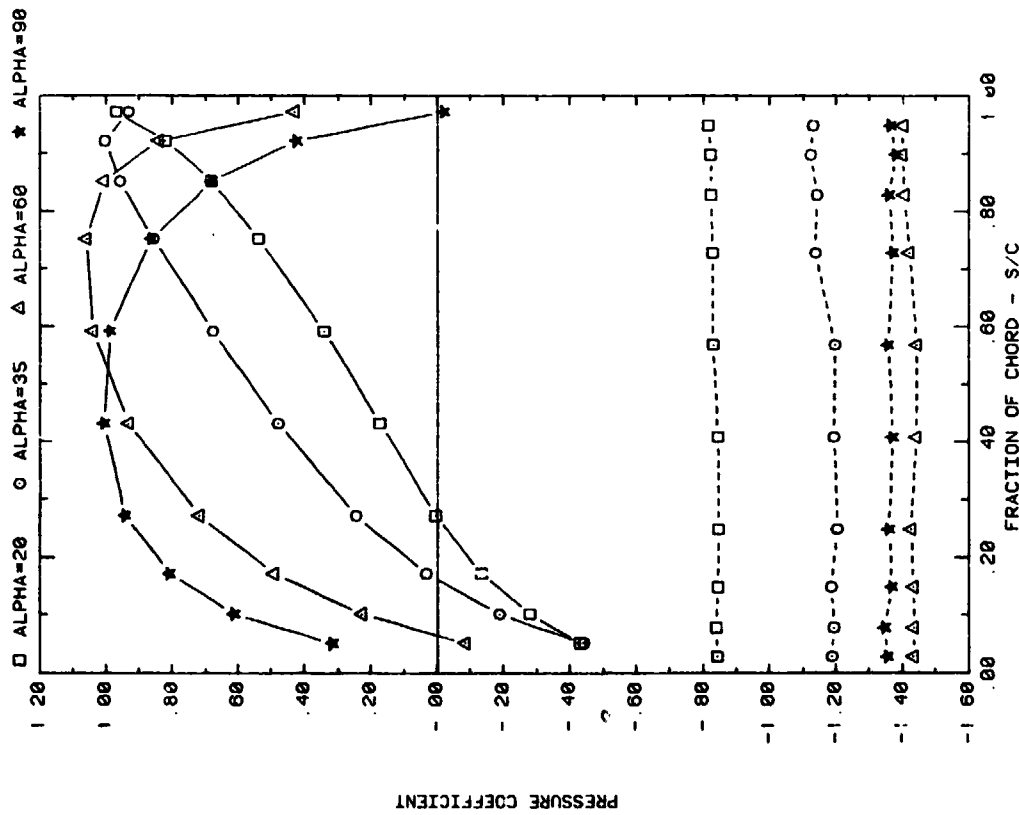
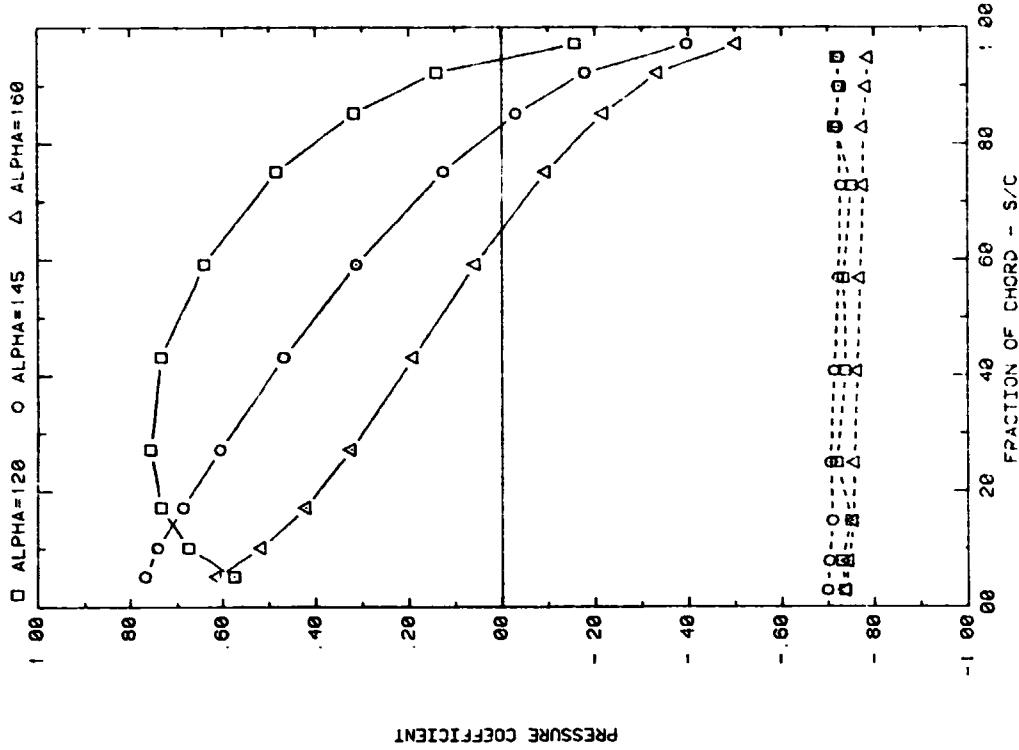


## LIST OF PLOTS

<u>Plot</u>	<u>Page</u>
1-1      Single Array, Uniform Flow Study Effects of Angle of Attack and Ground Clearance . . . . .	C-3
1-2      Single Array, Nonuniform Flow Study Effects of Angle of Attack and Fence Height . . . . .	C-9
2-1-1    Multiple Arrays without Fence, Uniform Flow Study Effect of Angle of Attack . . . . .	C-11
2-1-2    Multiple Arrays without Fence, Uniform Flow Study Effect of Separation Distance . . . . .	C-20
2-1-3    Multiple Arrays without Fence, Uniform Flow Study Effect of Array Position . . . . .	C-31
2-2-1    Multiple Arrays without Fence, Nonuniform Flow Study Effect of Angle of Attack . . . . .	C-39
2-2-2    Multiple Arrays without Fence, Nonuniform Flow Study Effect of Separation Distance . . . . .	C-48
2-2-3    Multiple Arrays without Fence, Nonuniform Flow Study Effect of Array Position . . . . .	C-59
3-1      Multiple Arrays with Fence, $WD = 0^\circ$ Effect of Angle of Attack. . . . .	C-67
3-2      Multiple Arrays with Fence, $WD = 0^\circ$ Effect of Array Position . . . . .	C-72
3-3      Multiple Arrays with Fence, $WD = 0^\circ$ Effect of Fence Distance . . . . .	C-78
3-4      Multiple Arrays with Fence, $WD = 0^\circ$ Effect of Fence Height . . . . .	C-84
3-5      Multiple Arrays with Fence, $WD = 0^\circ$ Effect of Fence Porosity . . . . .	C-92
4-1      Edge Study, $WD = 0^\circ$ Effect of Fence . . . . .	C-93
5-1-1    Corner Study, $WD = 45^\circ$ , Standard Model Effect of Array Position . . . . .	C-96
5-1-2    Corner Study, $WD = 45^\circ$ , Standard Model Effect of Fence Configuration . . . . .	C-101
5-2-1    Corner Study, $WD = 45^\circ$ , Modified Model with Solid Extension Effect of Array Position . . . . .	C-104

C-2b

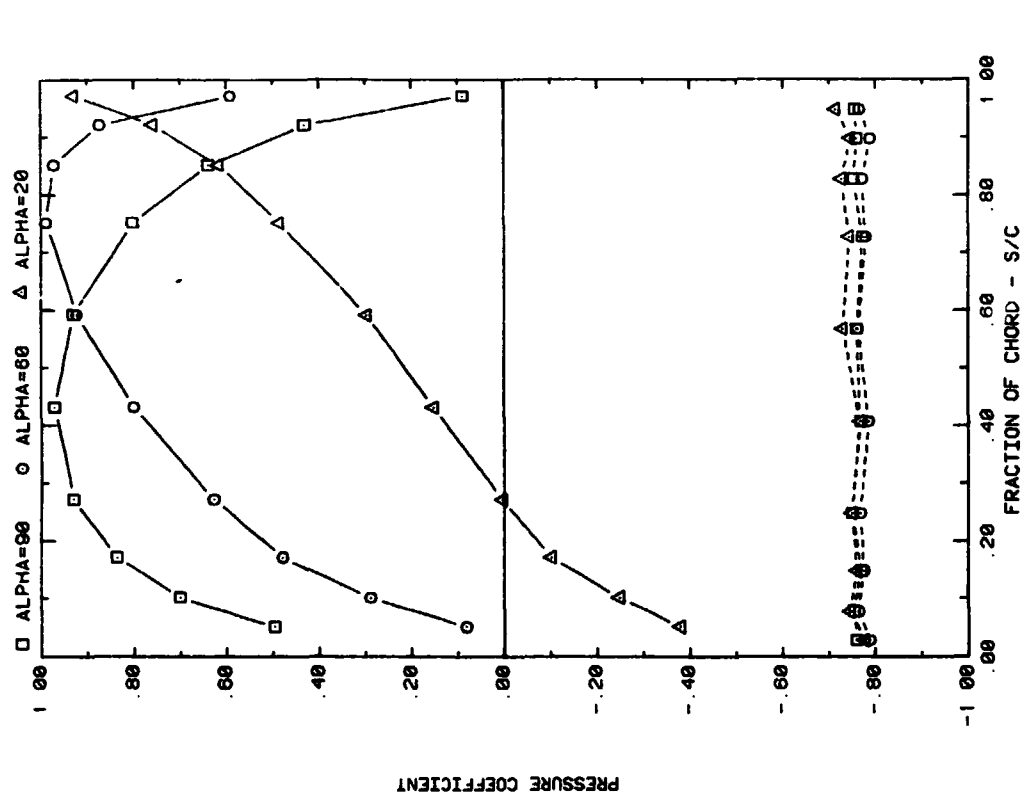
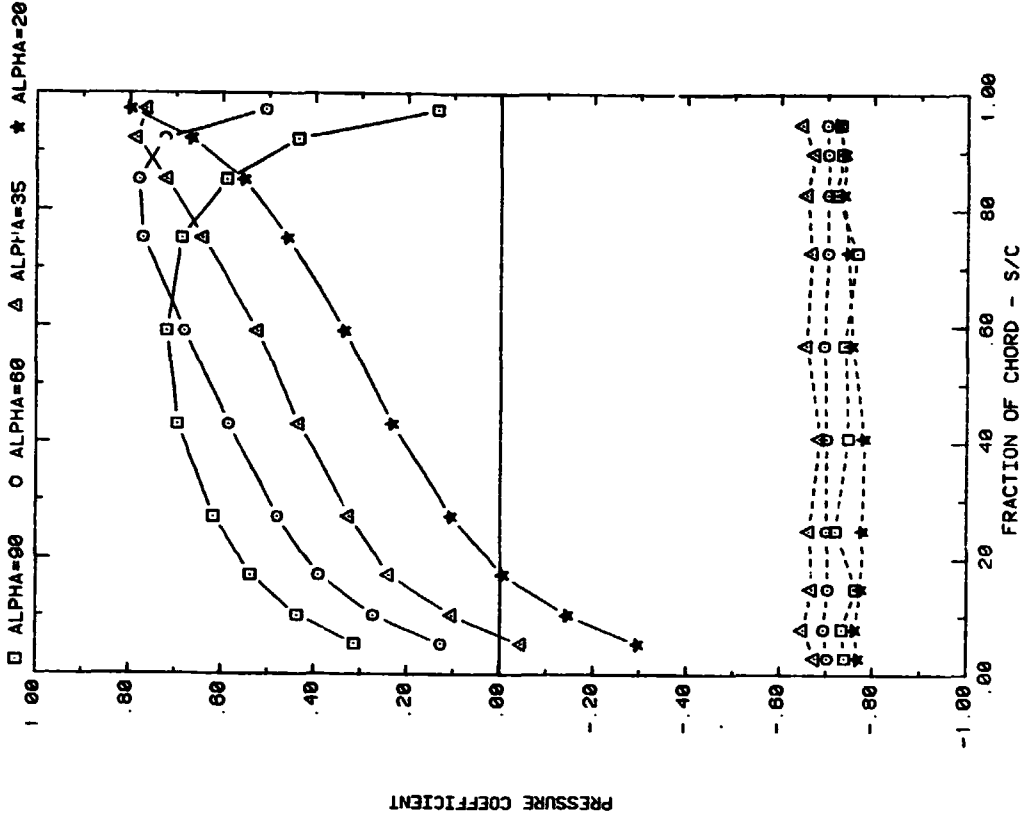
<u>Plot</u>		<u>Page</u>
5-2-2	Corner Study, WD = 45°, Modified Model with Solid Extension Effect of Model Modification . . . . .	C-108
5-2-3	Corner Study, WD = 45°, Modified Model with Solid Extension Effect of Fence Configuration . . . . .	C-117
5-3-1	Corner Study, WD = 45°, Modified Model with Various Extension Effect of Array Position . . . . .	C-120
5-3-2	Corner Study, WD = 45°, Modified Model with Various Extension Effect of Model Configuration . . . . .	C-122



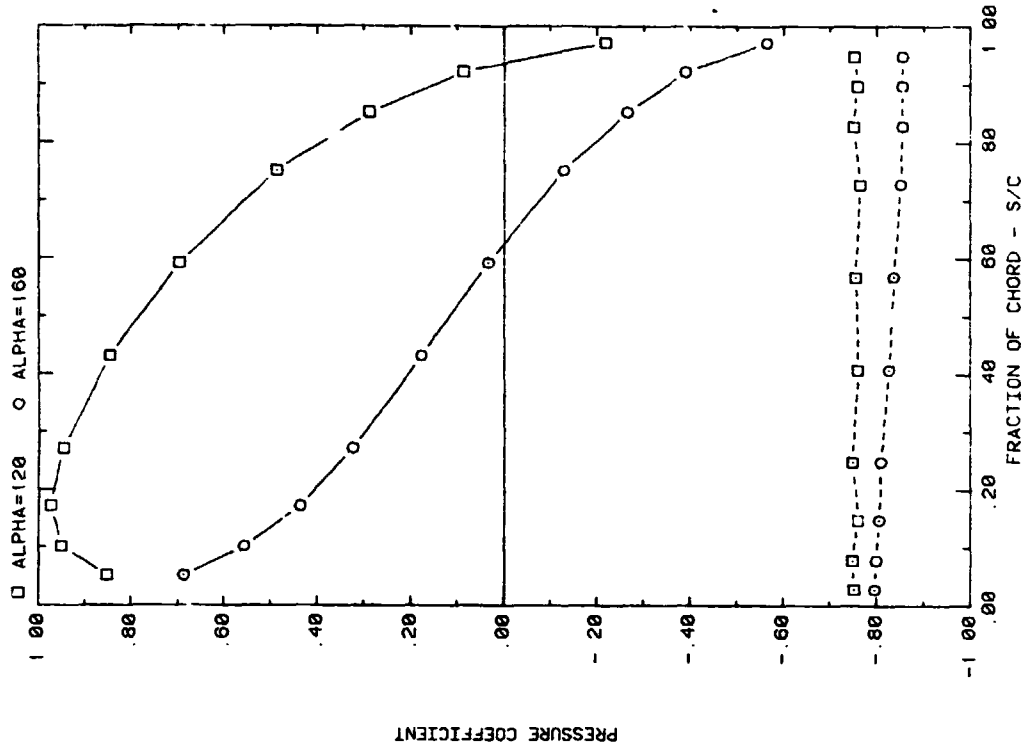
FRONT AND BACK PRESSURES ON A SINGLE ARRAY IN UNIFORM FLOW  
EFFECT OF ATTACK ANGLE FOR GROUND CLEARANCE, H/C = 0.25

FRONT AND BACK PRESSURES ON A SINGLE ARRAY IN UNIFORM FLOW  
EFFECT OF ATTACK ANGLE FOR GROUND CLEARANCE, H/C = INFINITY

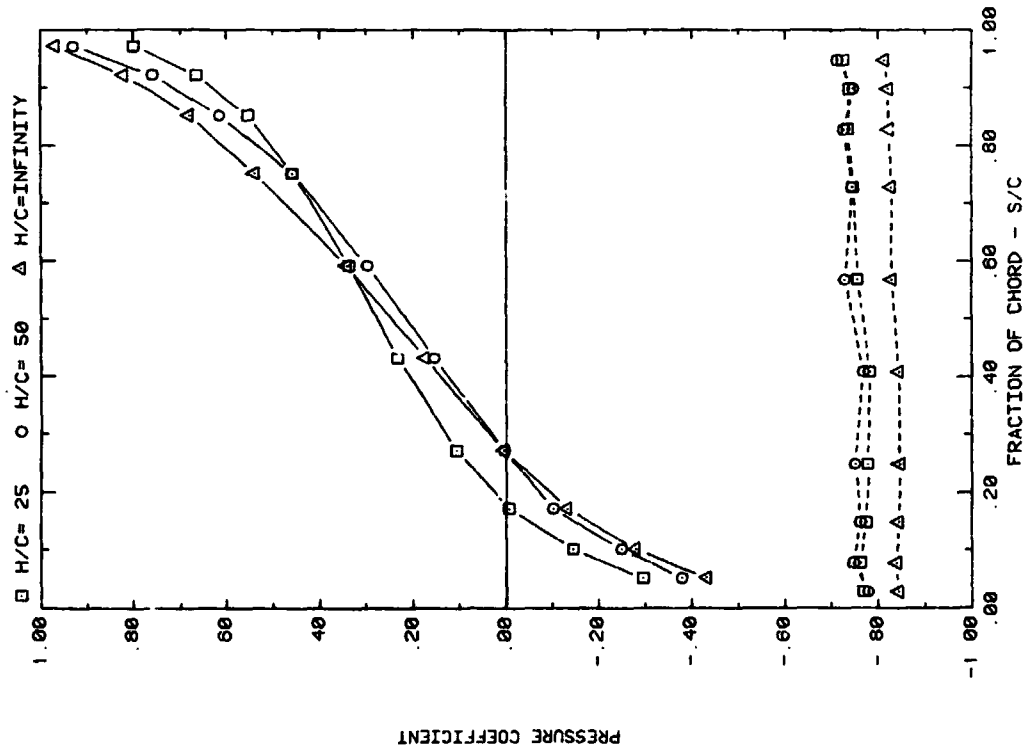
Plot 1-1. Single Array, Uniform Flow Study Effects of  
Angle of Attack and Ground Clearance



Plot 1-1. (Continued)

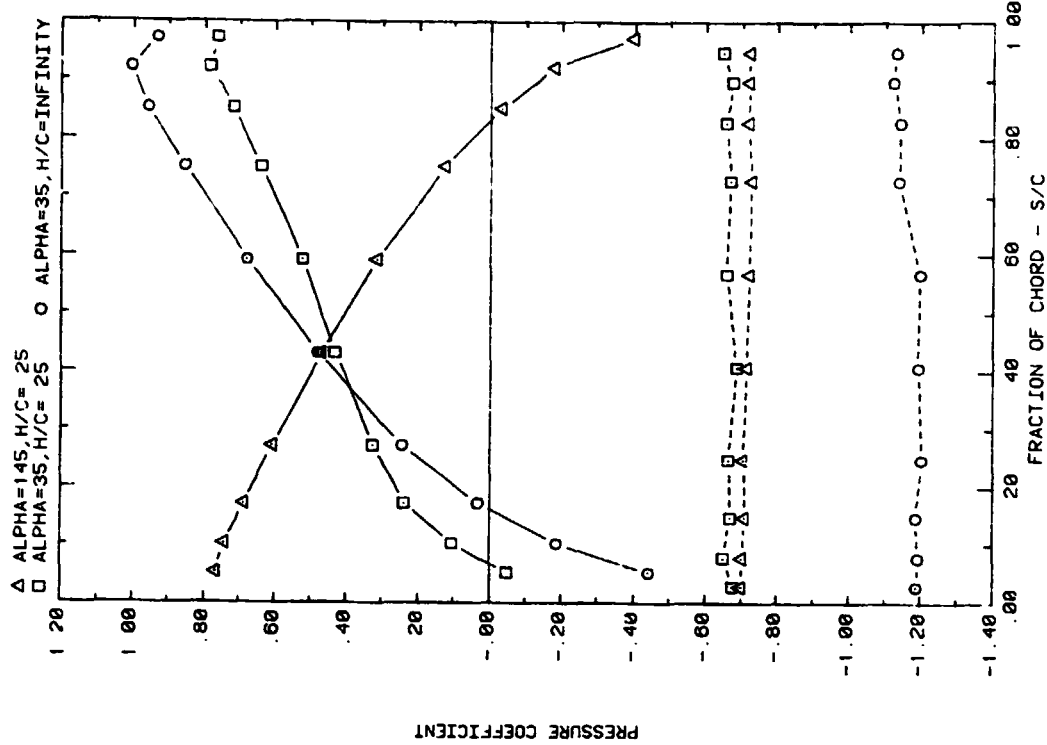


FRONT AND BACK PRESSURES ON A SINGLE ARRAY IN UNIFORM FLOW  
EFFECT ON ATTACK ANGLE FOR GROUND CLEARANCE, H/C = 0.50

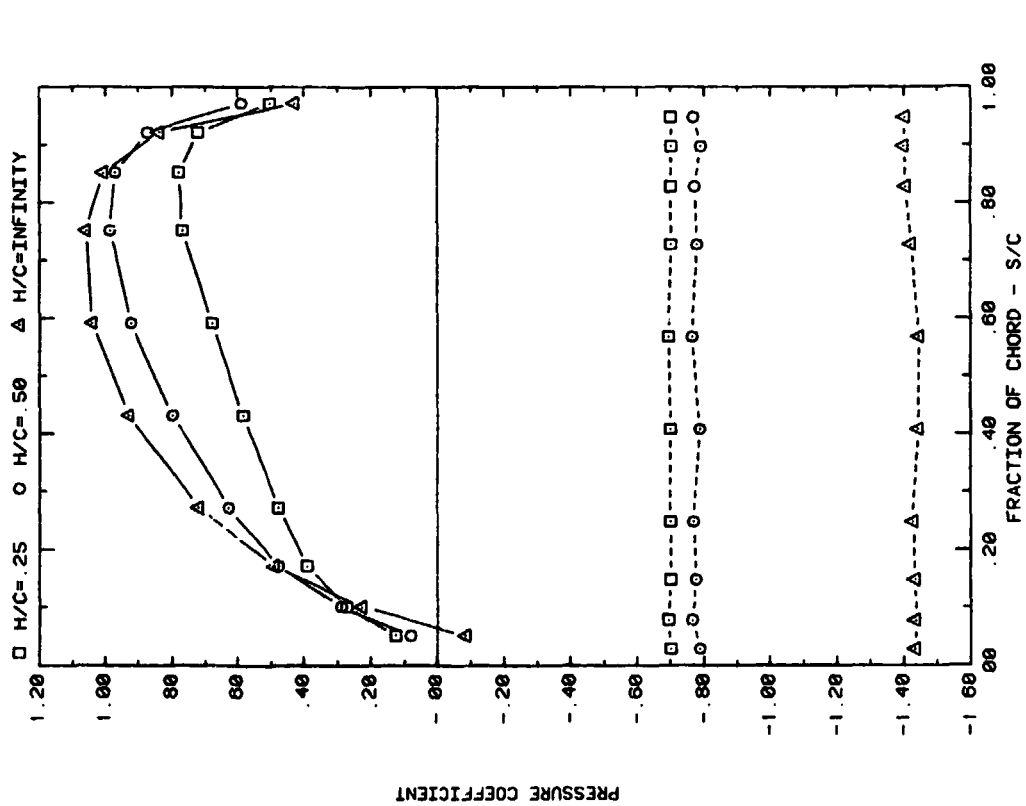


FRONT AND BACK PRESSURES ON A SINGLE ARRAY IN UNIFORM FLOW  
EFFECT OF GROUND CLEARANCE FOR ATTACK ANGLE, ALPHA = 20

Plot 1-1. (Continued)

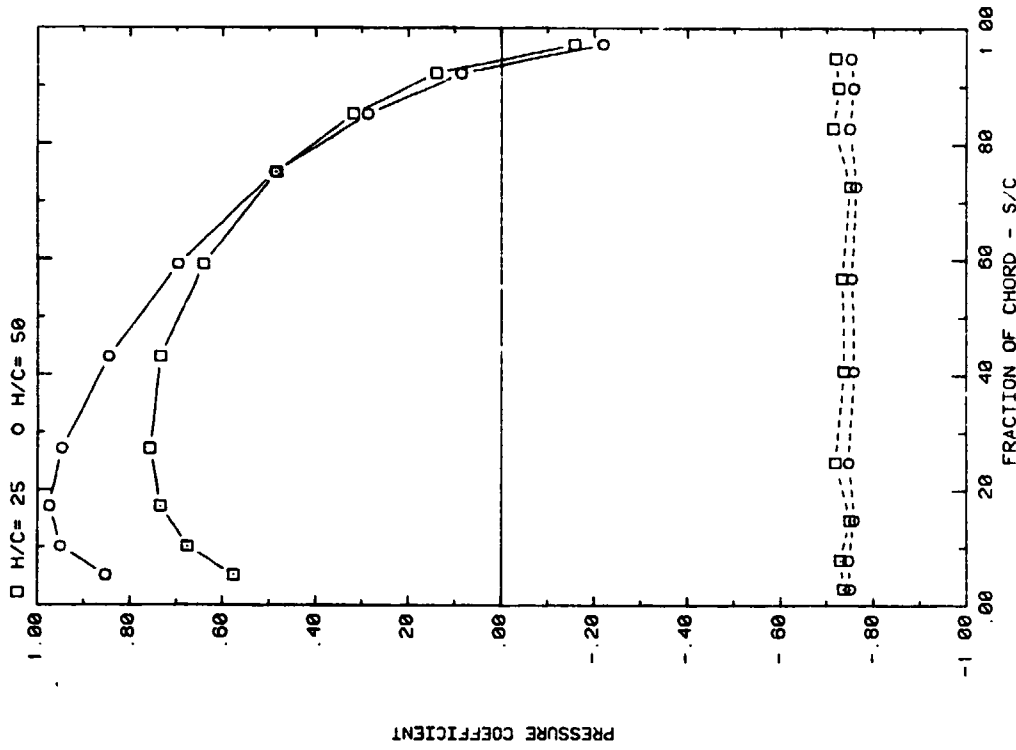


FRONT AND BACK PRESSURES ON A SINGLE ARRAY IN UNIFORM FLOW  
EFFECT OF GROUND CLEARANCE FOR ATTACK ANGLES

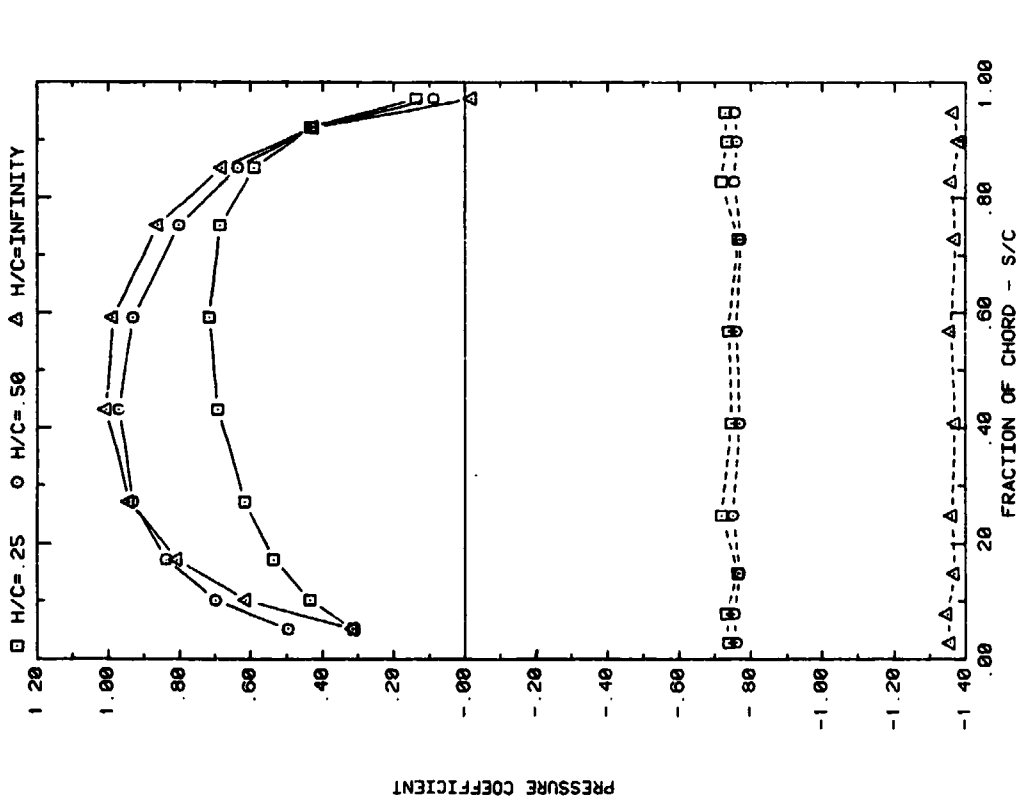


FRONT AND BACK PRESSURES ON A SINGLE ARRAY IN UNIFORM FLOW  
EFFECT OF GROUND CLEARANCE FOR ATTACK ANGLE, ALPHA = 60

Plot 1-1. (Continued)

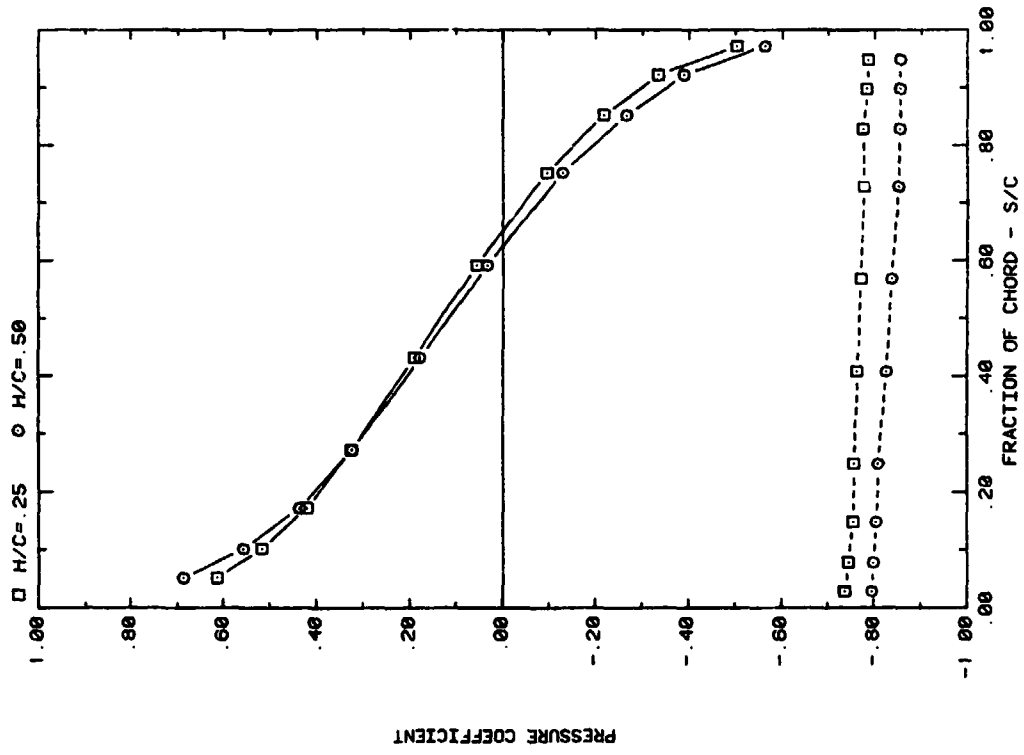


FRONT AND BACK PRESSURES ON A SINGLE ARRAY IN UNIFORM FLOW  
EFFECT OF GROUND CLEARANCE FOR ATTACK ANGLE, ALPHA = 120



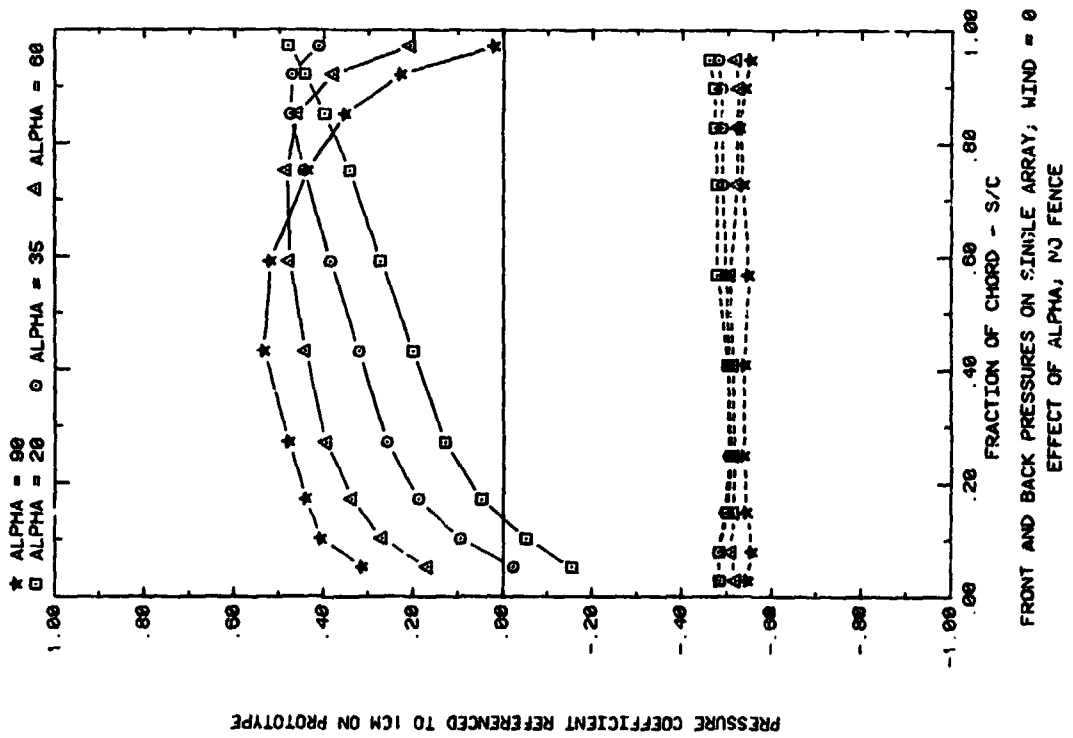
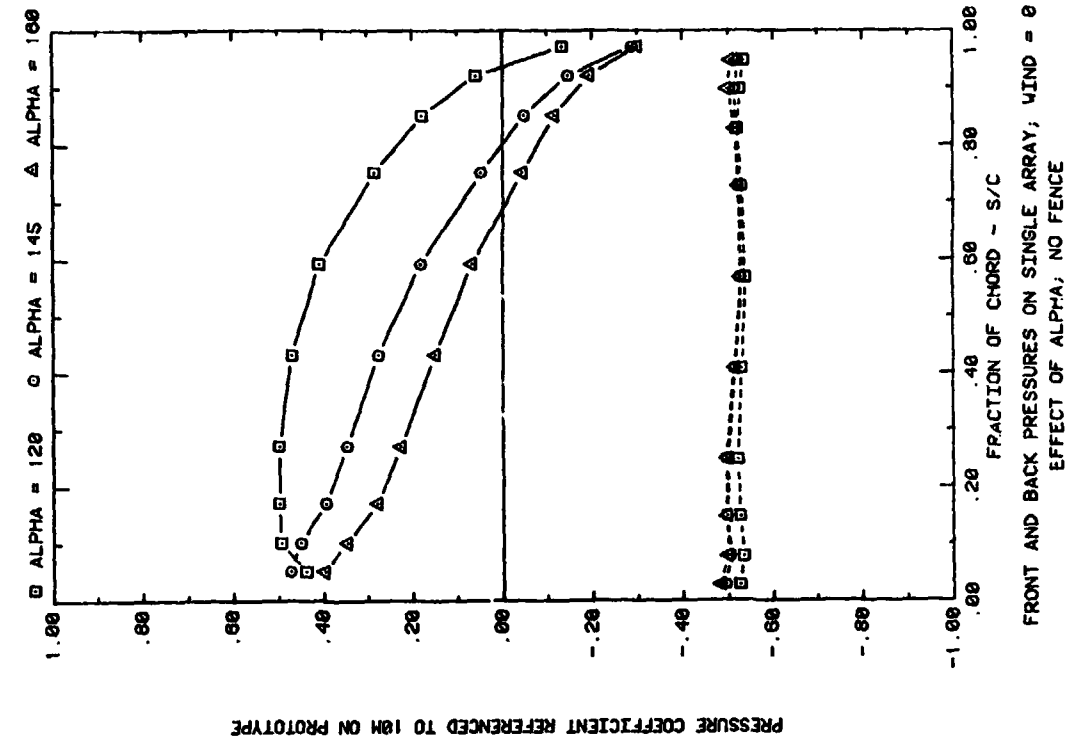
FRONT AND BACK PRESSURES ON A SINGLE ARRAY IN UNIFORM FLOW  
EFFECT OF GROUND CLEARANCE FOR ATTACK ANGLE, ALPHA = 90

Plot 1-1. (Continued)

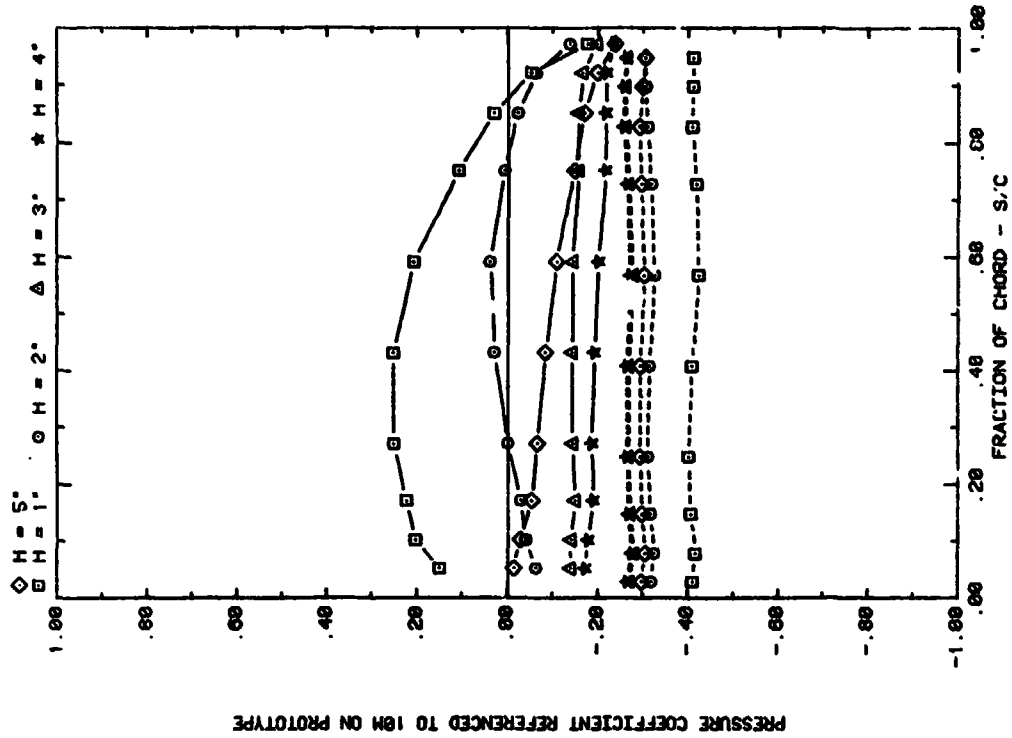


FRONT AND BACK PRESSURES ON A SINGLE ARRAY IN UNIFORM FLOW  
EFFECT OF GROUND CLEARANCE FOR ATTACK ANGLE, ALPHA = 160

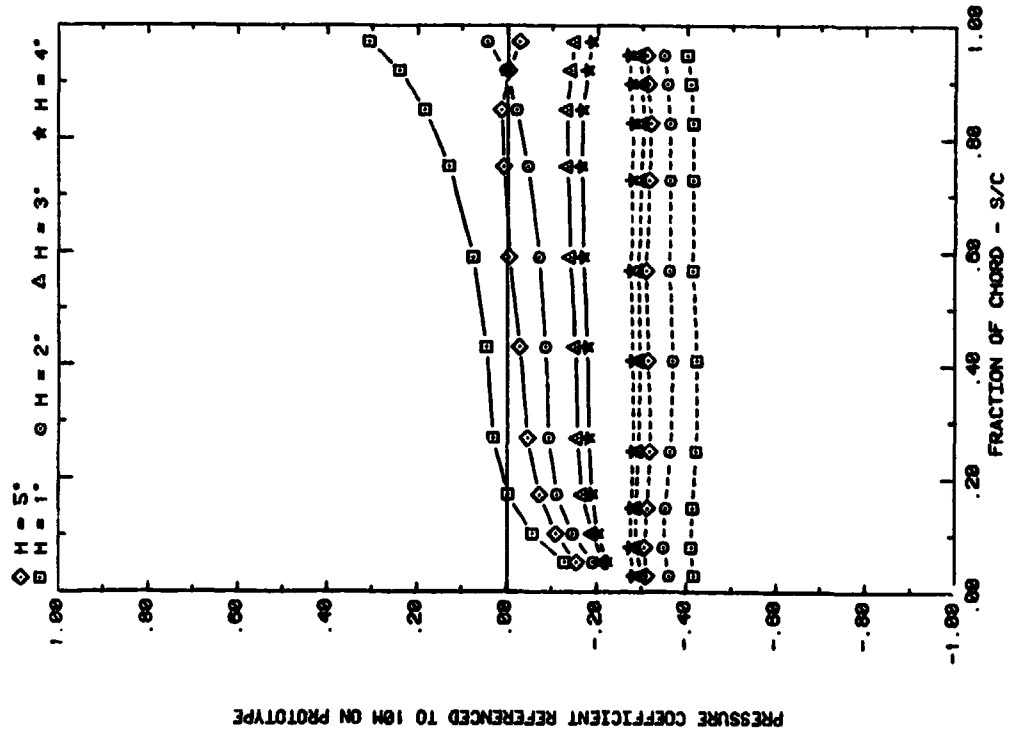
Plot 1-1. (Concluded)



Plot 1-2. Single Array, Nonuniform Flow Study Effects of Angle of Attack and Fence Height

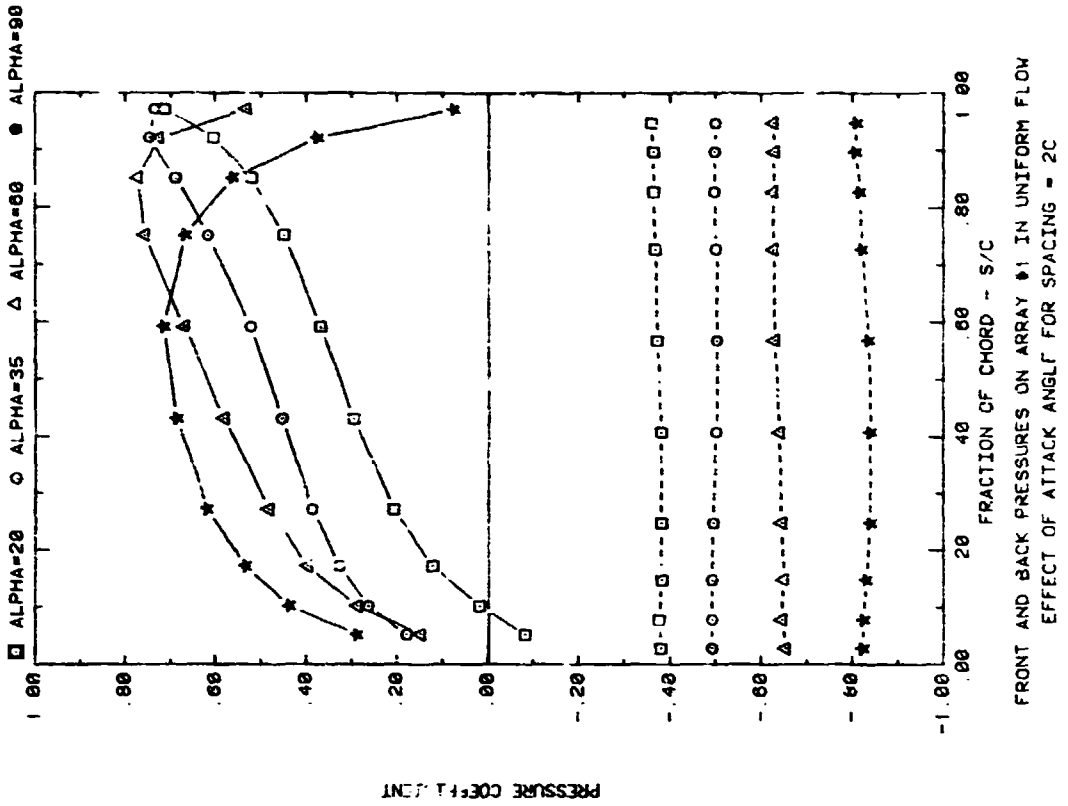


FRONT AND BACK PRESSURES ON SINGLE ARRAY; WIND = 0  
EFFECT OF FENCE HEIGHT; ALPHA = 145, D = 10, P = 30%

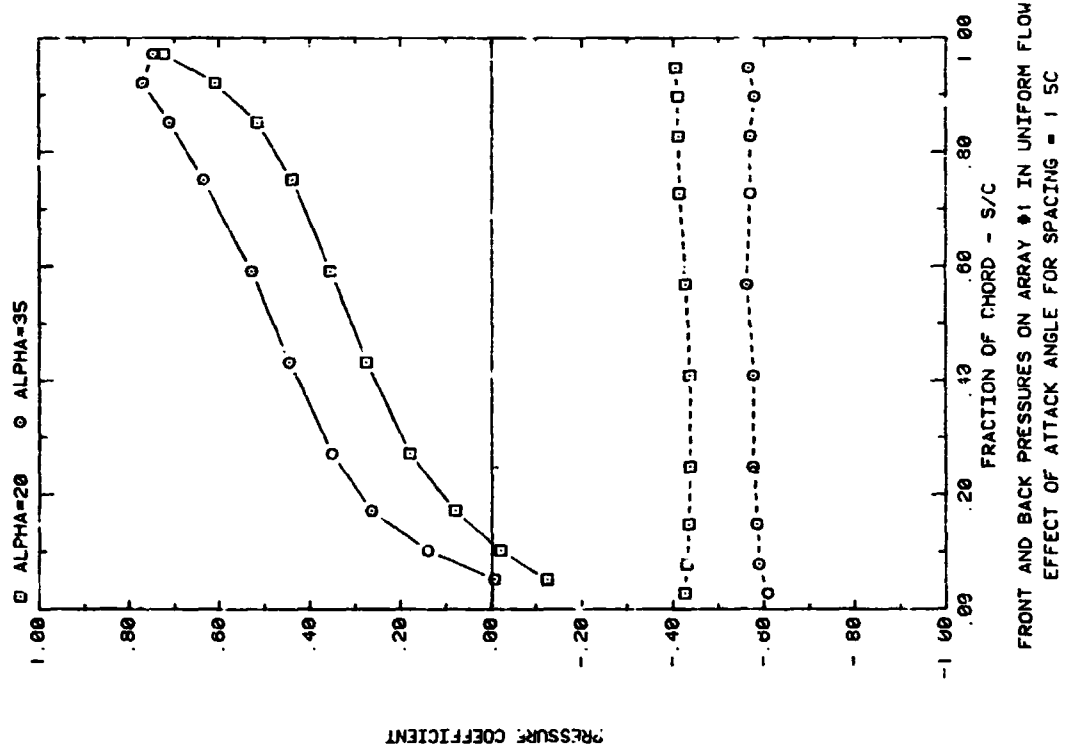


FRONT AND BACK PRESSURES ON SINGLE ARRAY; WIND = 0  
EFFECT OF FENCE HEIGHT; ALPHA = 35, D = 10, P = 30%

Plot 1-2. (Concluded)

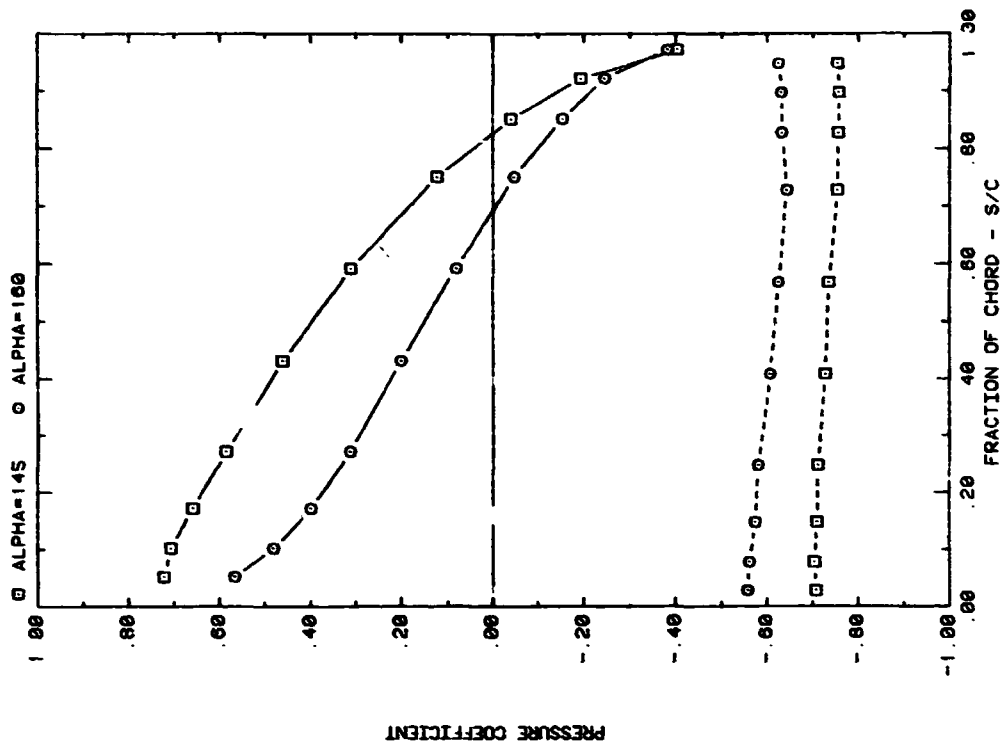


FRONT AND BACK PRESSURES ON ARRAY #1 IN UNIFORM FLOW  
EFFECT OF ATTACK ANGLE FOR SPACING = 2C

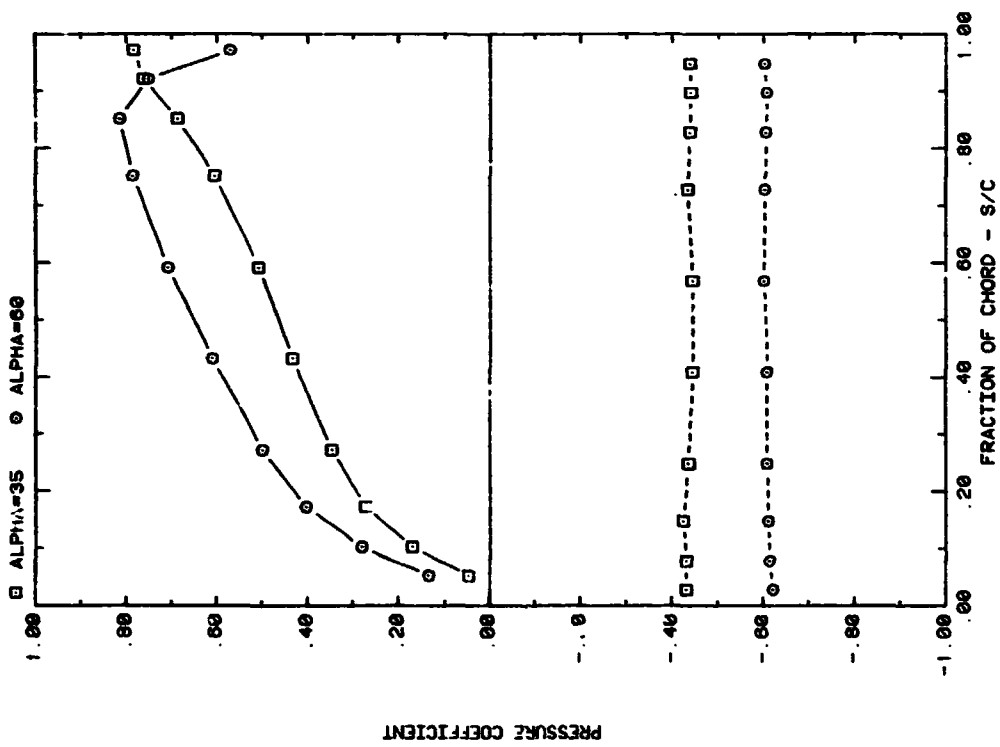


FRONT AND BACK PRESSURES ON ARRAY #1 IN UNIFORM FLOW  
EFFECT OF ATTACK ANGLE FOR SPACING = 1.5C

Plot 2-1-1. Multiple Arrays without Fence, Uniform Flow Study  
Effect of Angle of Attack

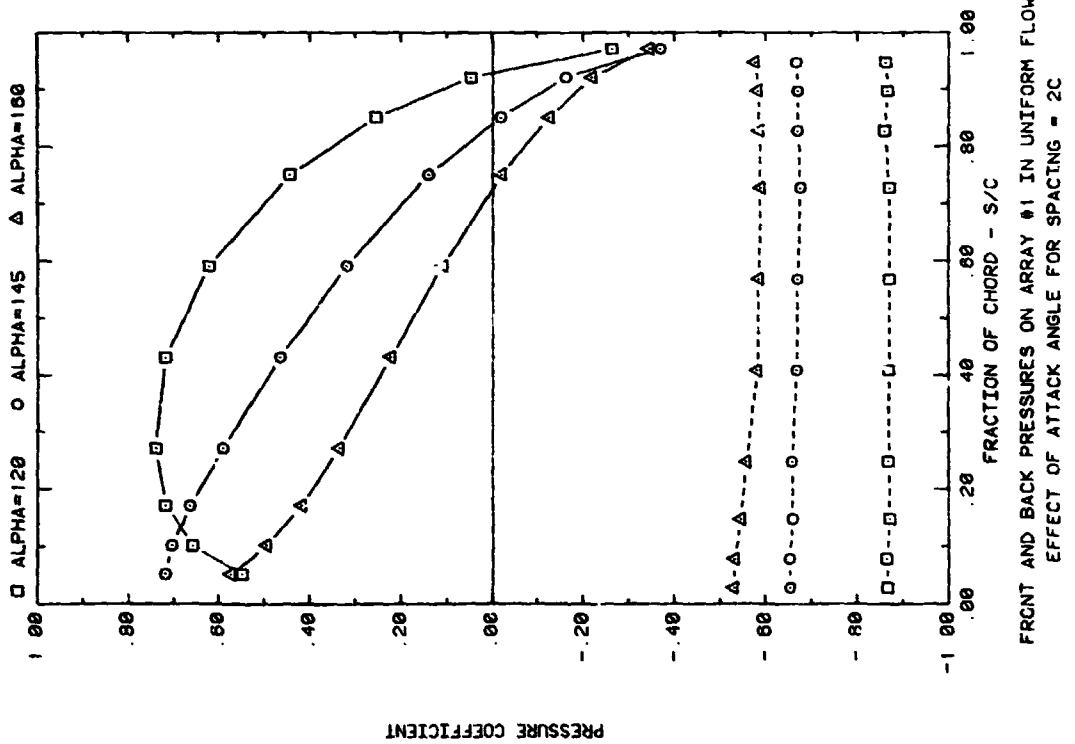
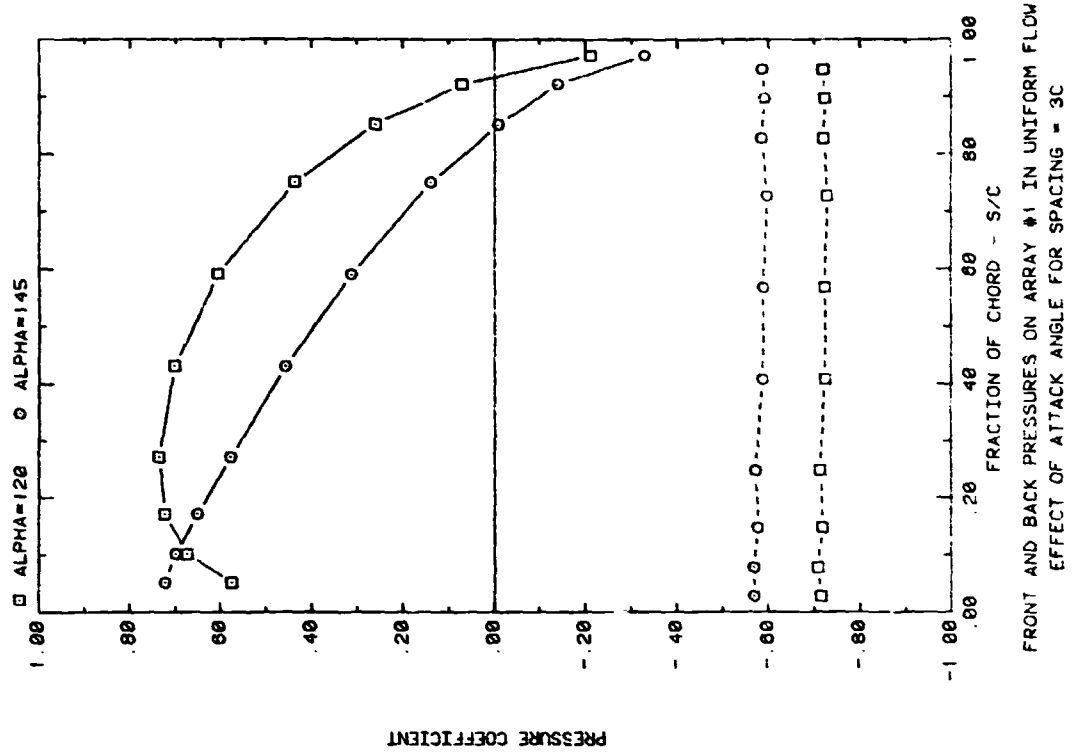


FRONT AND BACK PRESSURES ON ARRAY #1 IN UNIFORM FLOW  
EFFECT OF ATTACK ANGLE FOR SPACING = 1 SC

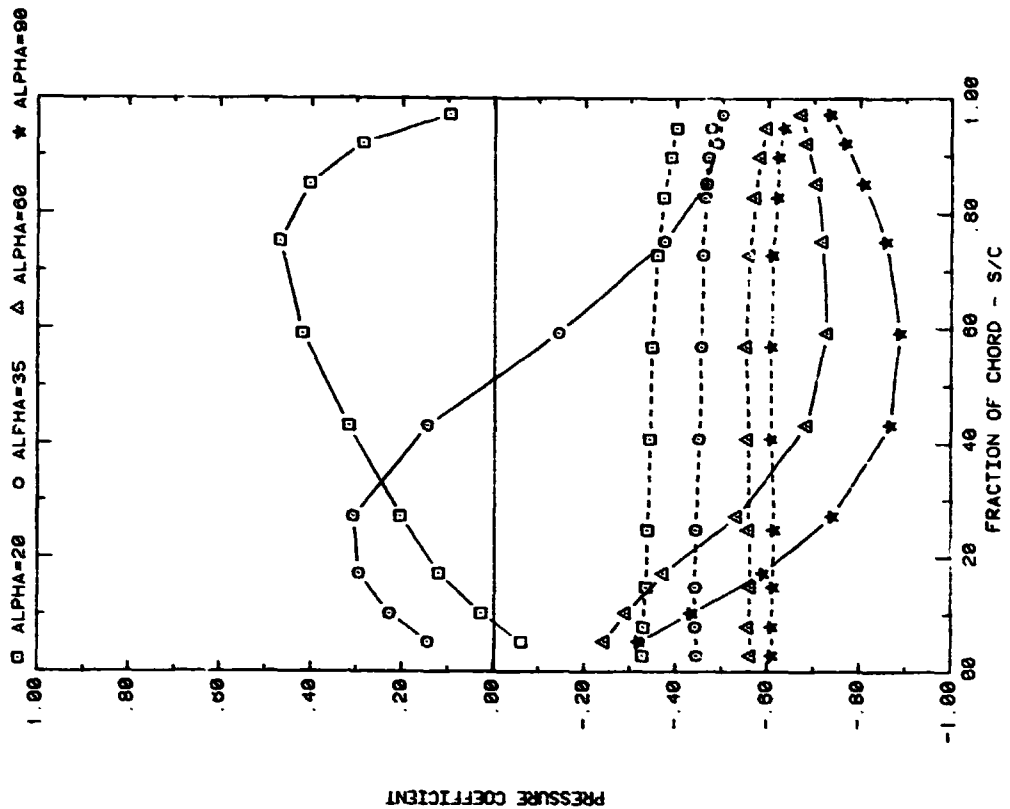


FRONT AND BACK PRESSURES ON ARRAY #1 IN UNIFORM FLOW  
EFFECT OF ATTACK ANGLE FOR SPACING = 3C

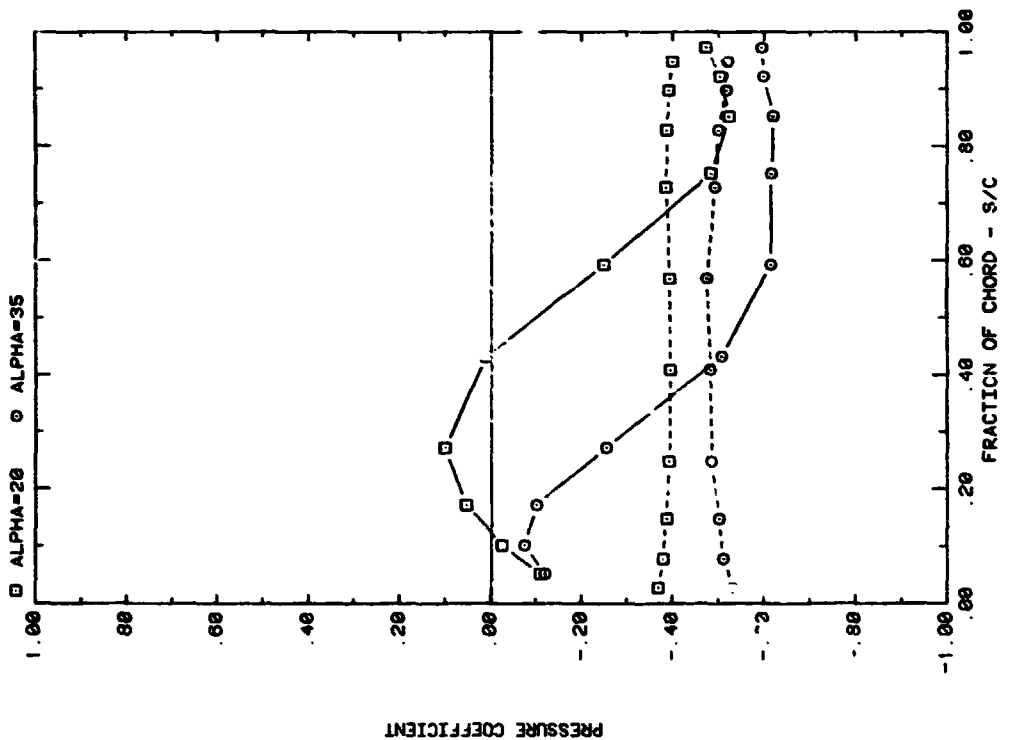
Plot 2-1-1. (Continued)



Plot 2-1-1. (Continued)

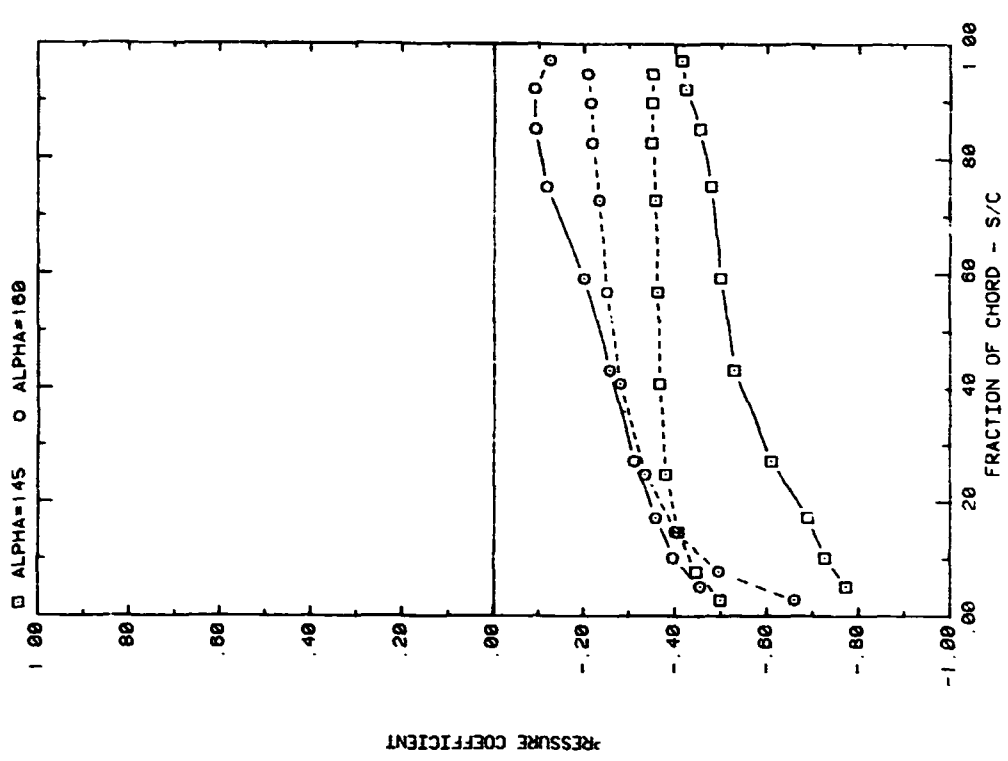


FRONT AND BACK PRESSURES ON ARRAY #2 IN UNIFORM FLOW  
EFFECT OF ATTACK ANGLE FOR SPACING = 2C

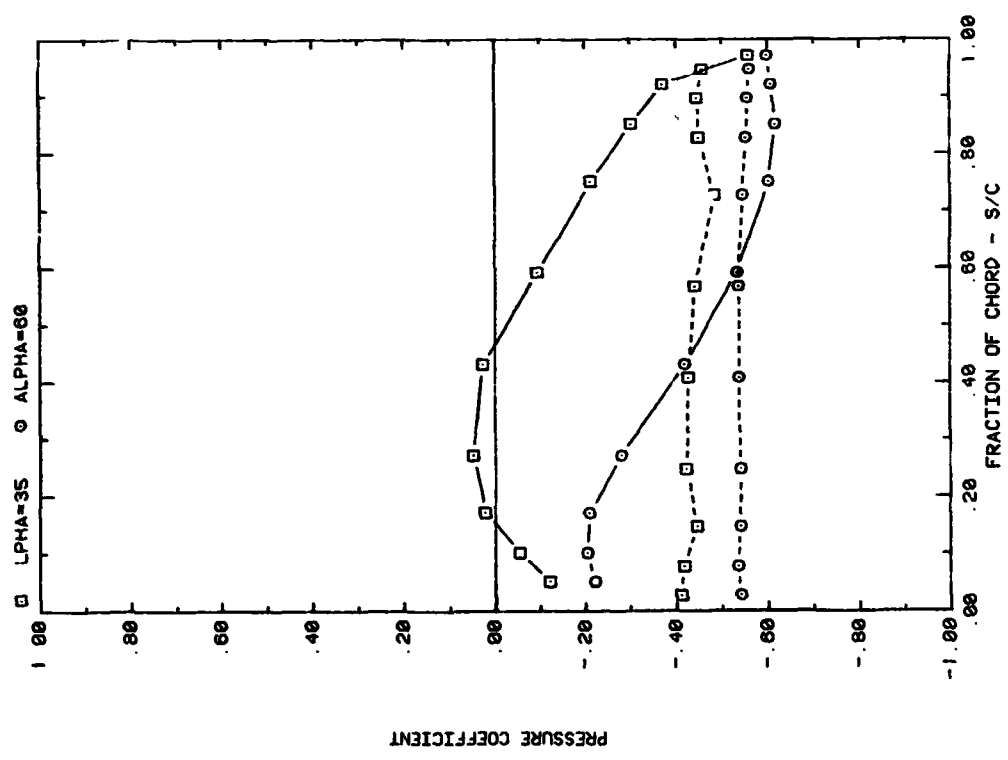


FRONT AND BACK PRESSURES ON ARRAY #2 IN UNIFORM FLOW  
EFFECT OF ATTACK ANGLE FOR SPACING = 1.5C

Plot 2-1-1. (Continued)

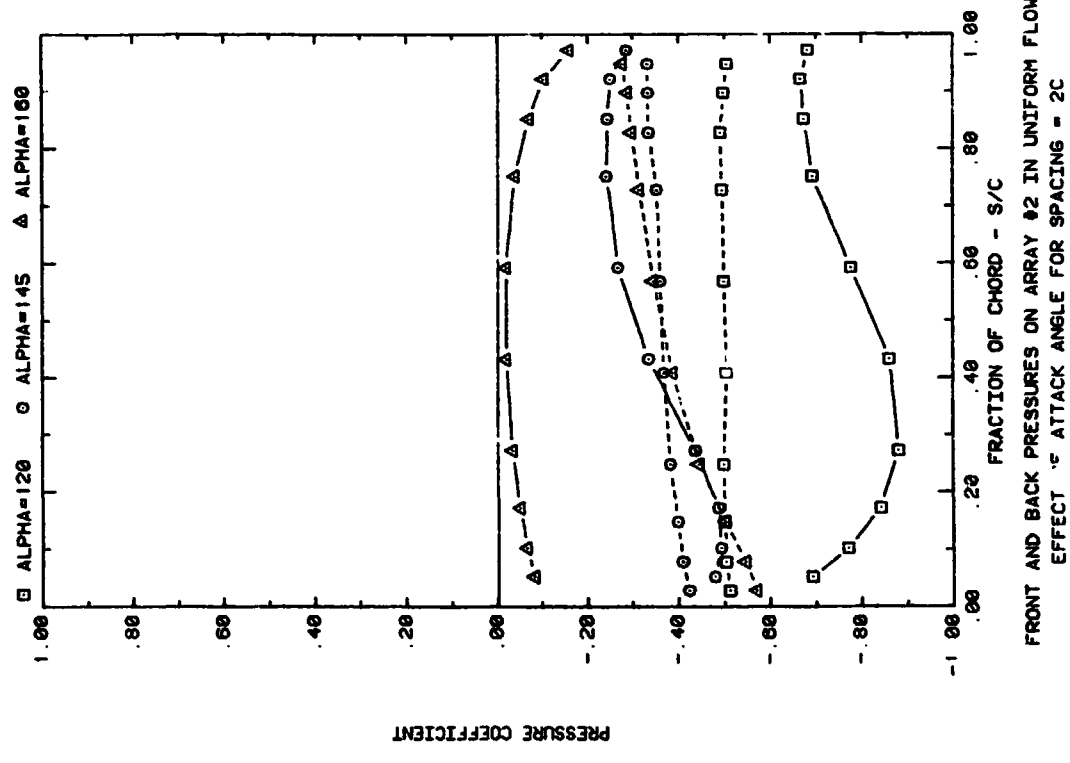
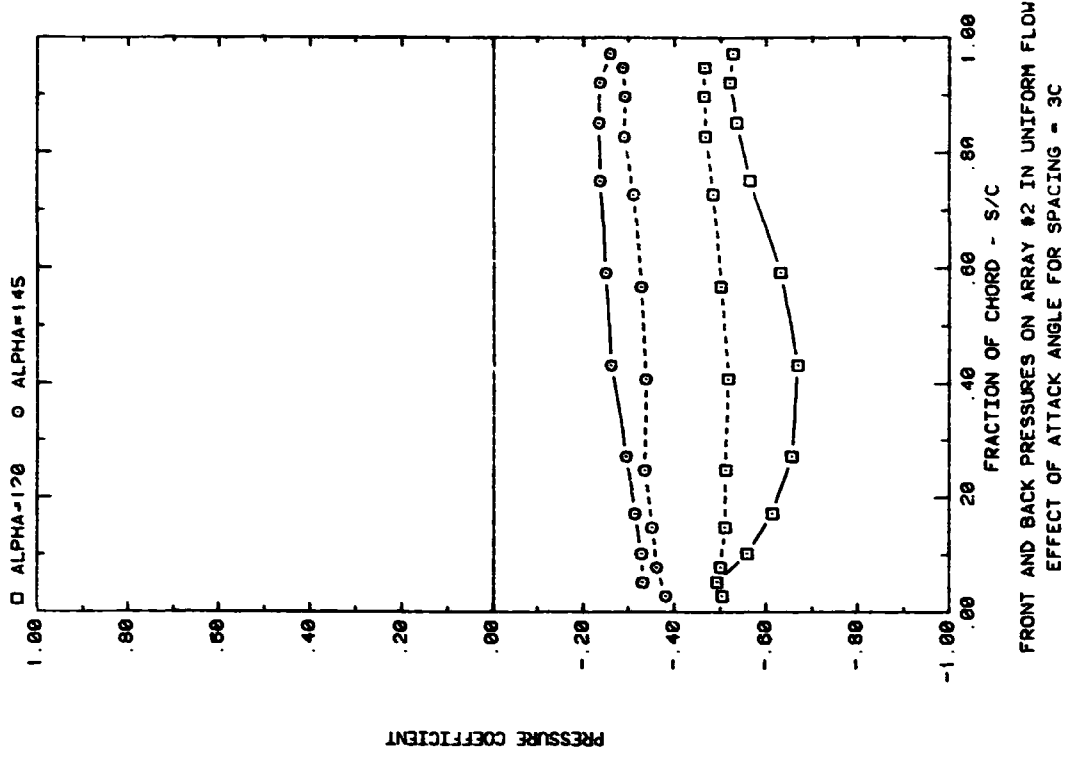


FRONT AND BACK PRESSURES ON ARRAY #2 IN UNIFORM FLOW  
EFFECT OF ATTACK ANGLE FOR SPACING = 1.5C

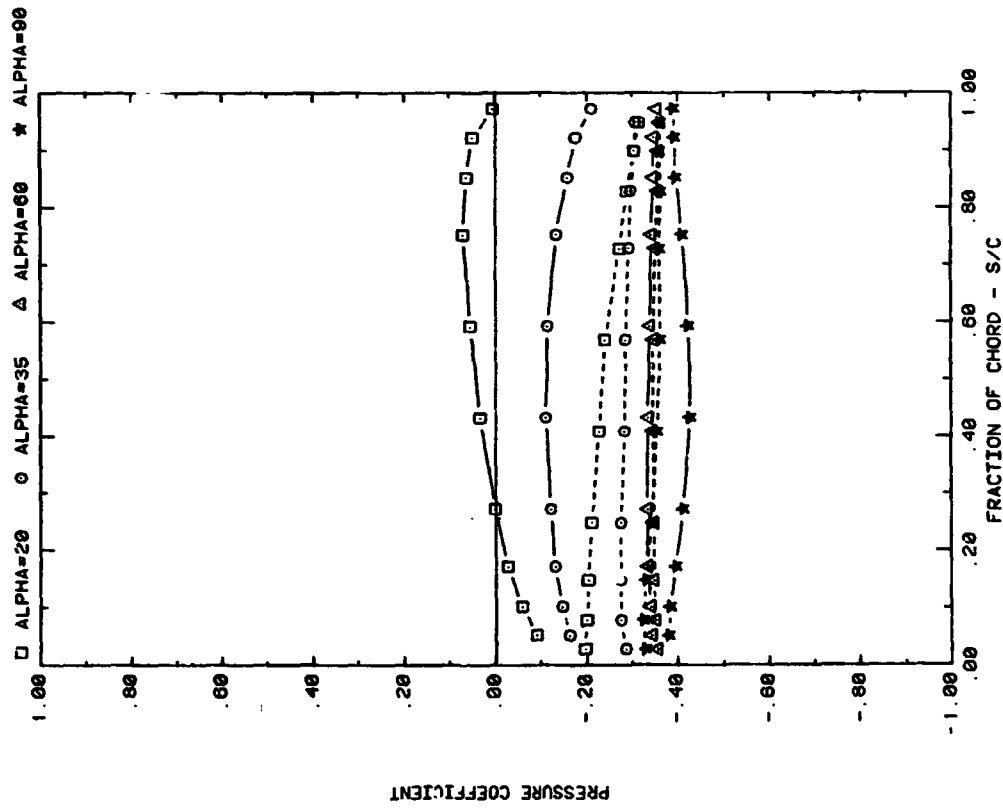
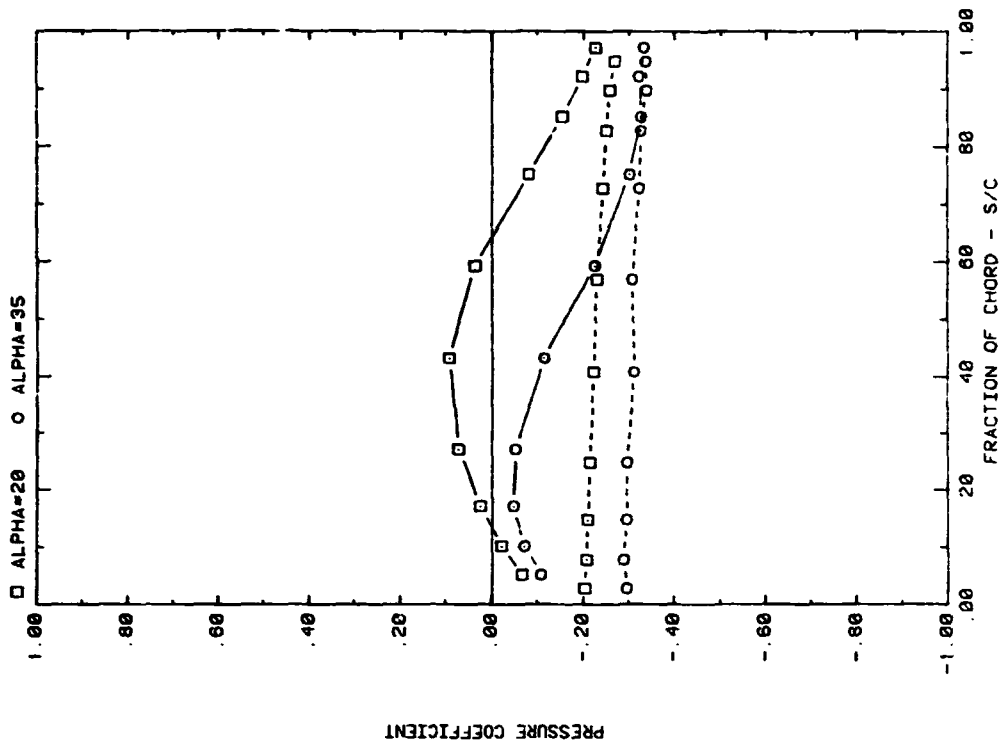


FRONT AND BACK PRESSURES ON ARRAY #2 IN UNIFORM FLOW  
EFFECT OF ATTACK ANGLE FOR SPACING = 3C

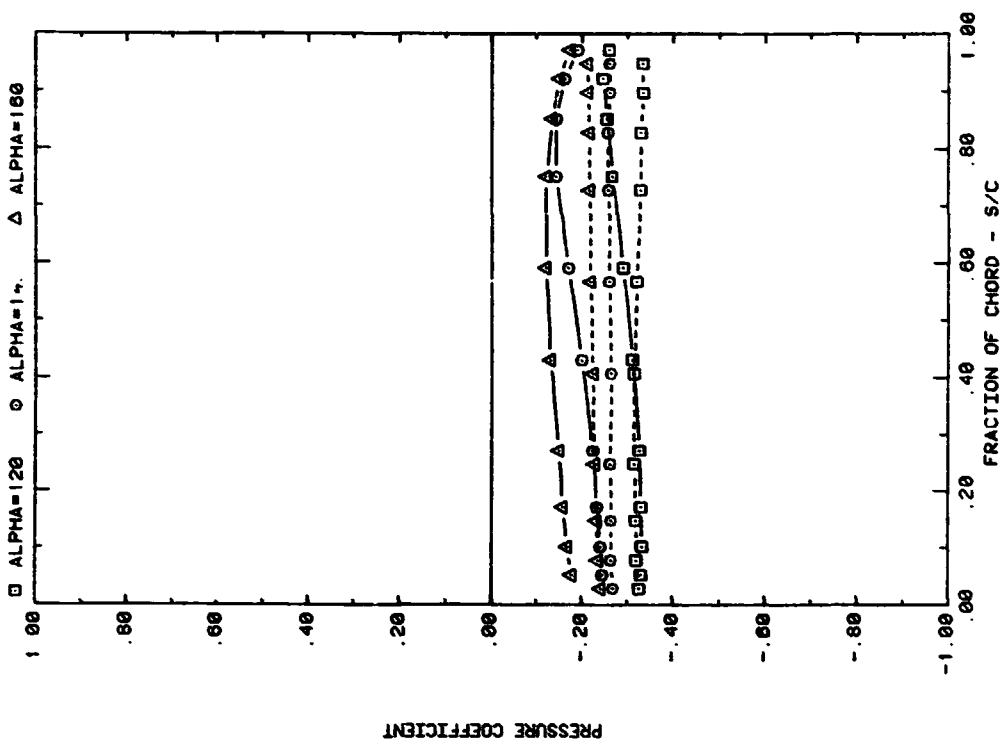
Plot 2-1-1. (Continued)



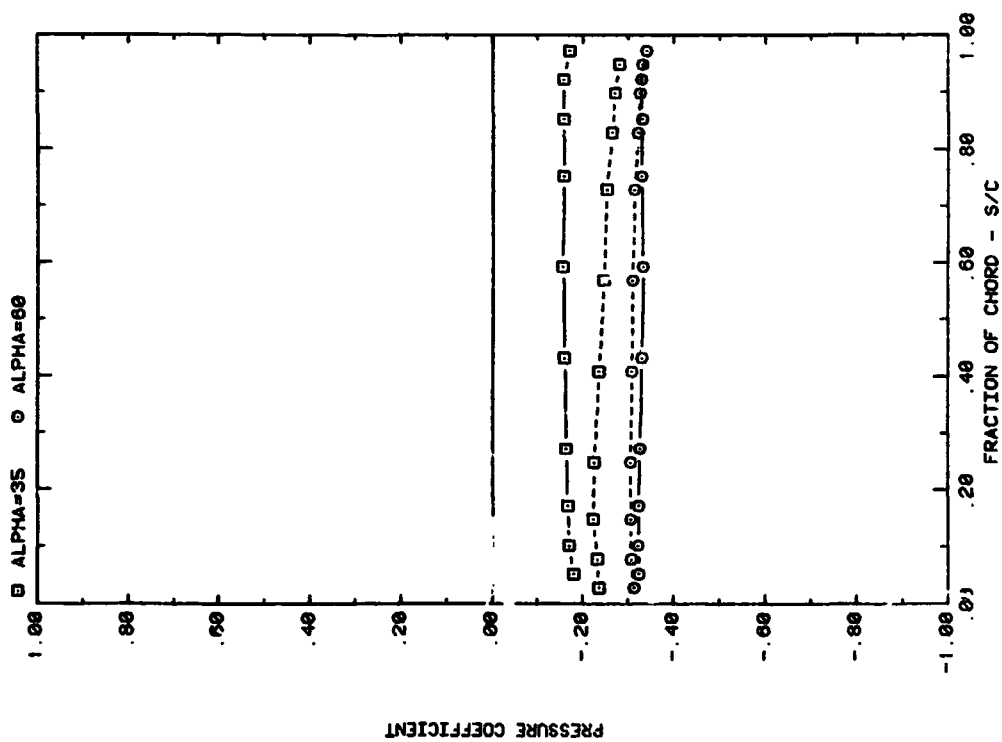
Plot 2-1-1. (Continued)



Plot 2-1-1. (Continued)

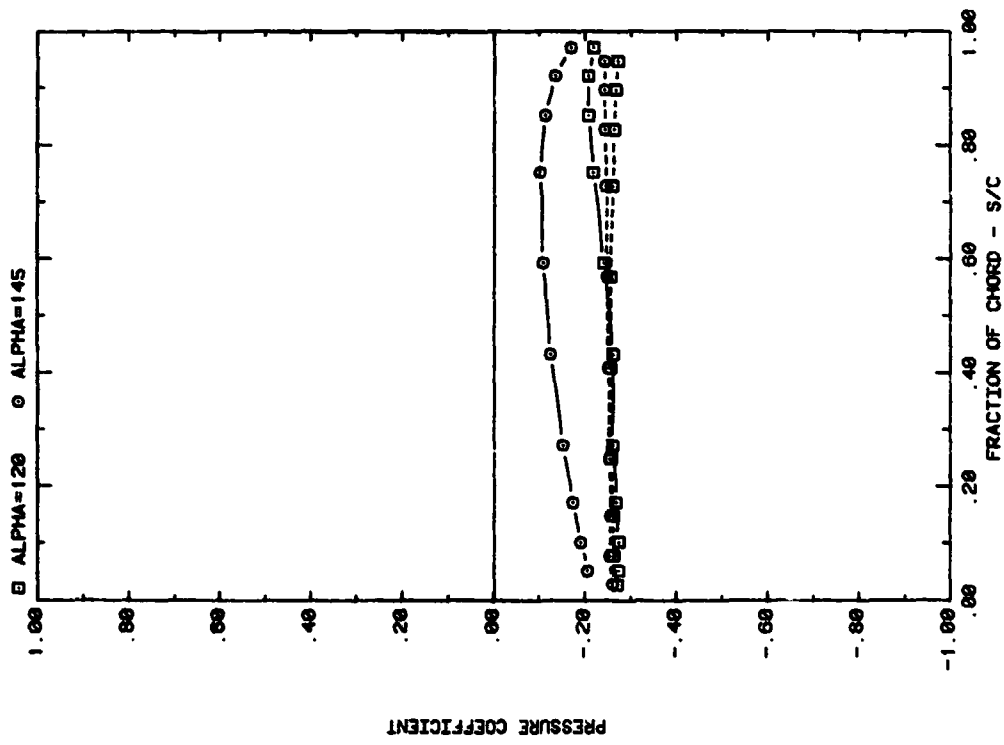


FRONT AND BACK PRESSURES ON ARRAY #5 IN UNIFORM FLOW  
EFFECT OF ATTACK ANGLE FOR SPACING = 2C



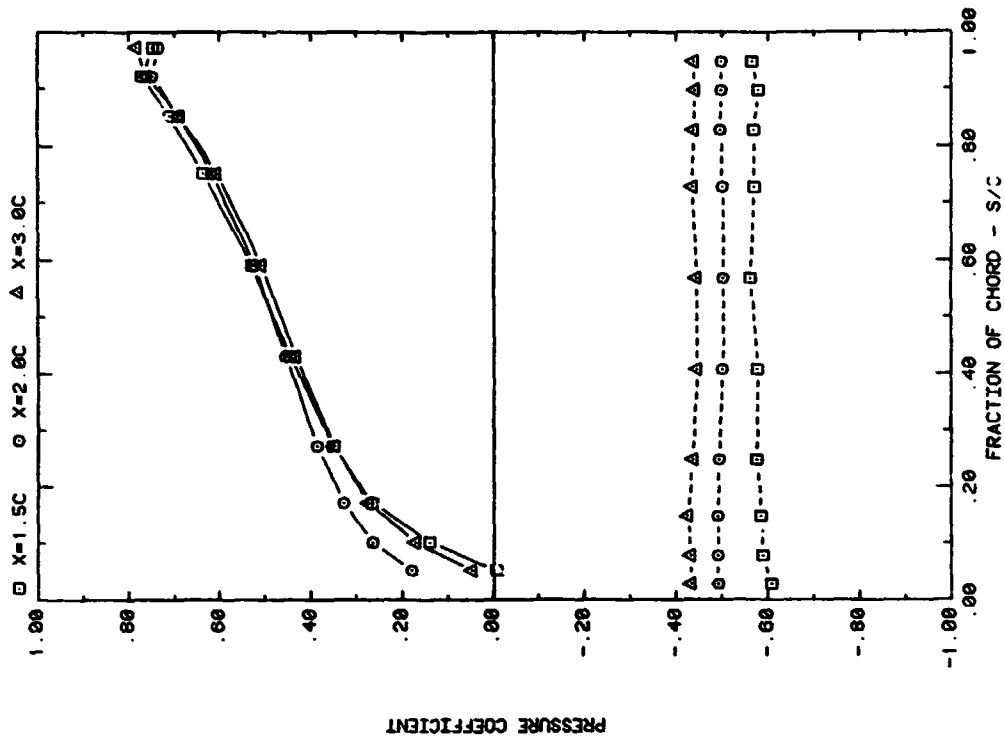
FRONT AND BACK PRESSURES ON ARRAY #4 IN UNIFORM FLOW  
EFFECT OF ATTACK ANGLE FOR SPACING = 3C

Plot 2-1-1. (Continued)

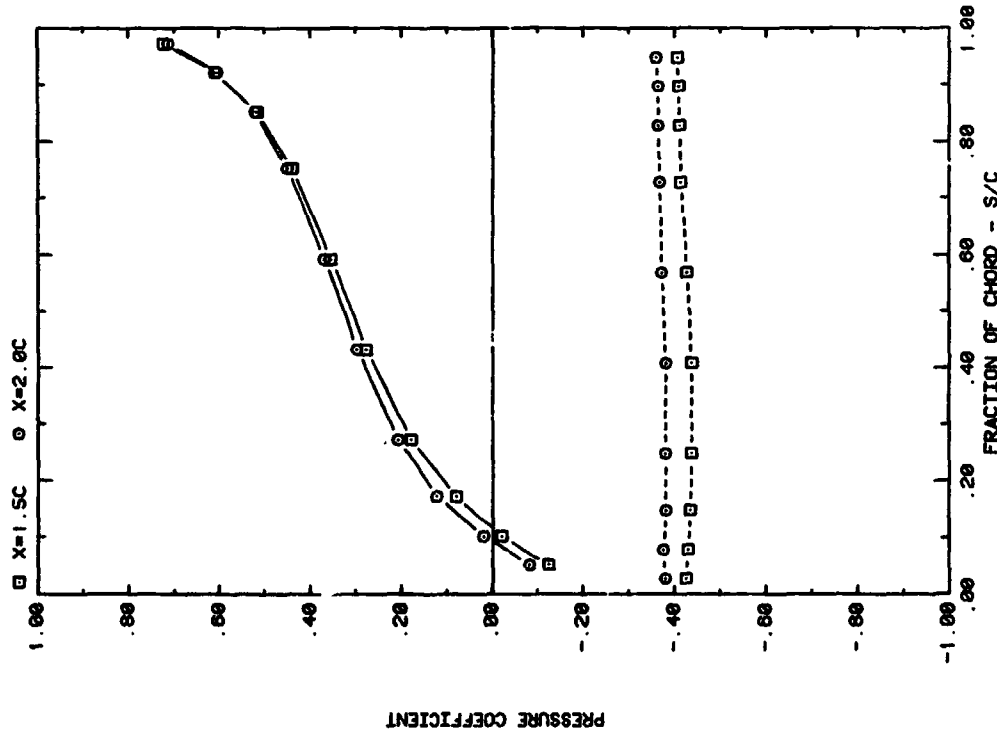


FRONT AND BACK PRESSURES ON ARRAY #4 IN UNIFORM FLOW  
EFFECT OF ATTACK ANGLE FOR SPACING = 3C

Plot 2-1-1. (Concluded)

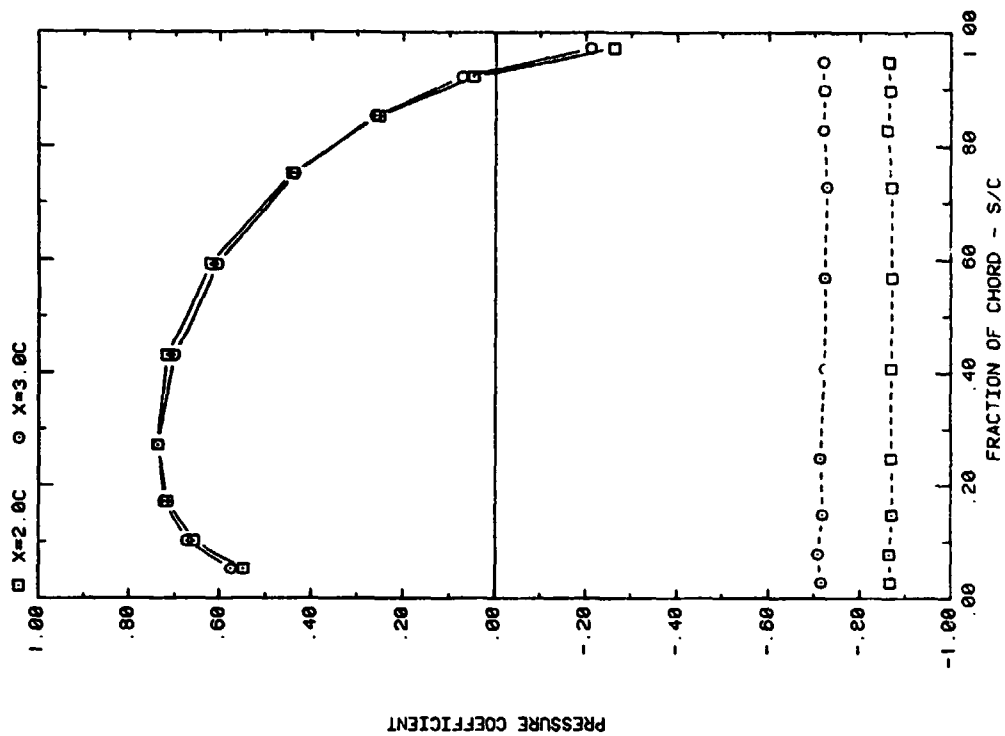


FRONT AND BACK PRESSURES ON ARRAY #1 IN UNIFORM FLOW  
EFFECT OF SEPARATION (X) ON ATTACK ANGLE 35, H/C = 0.25

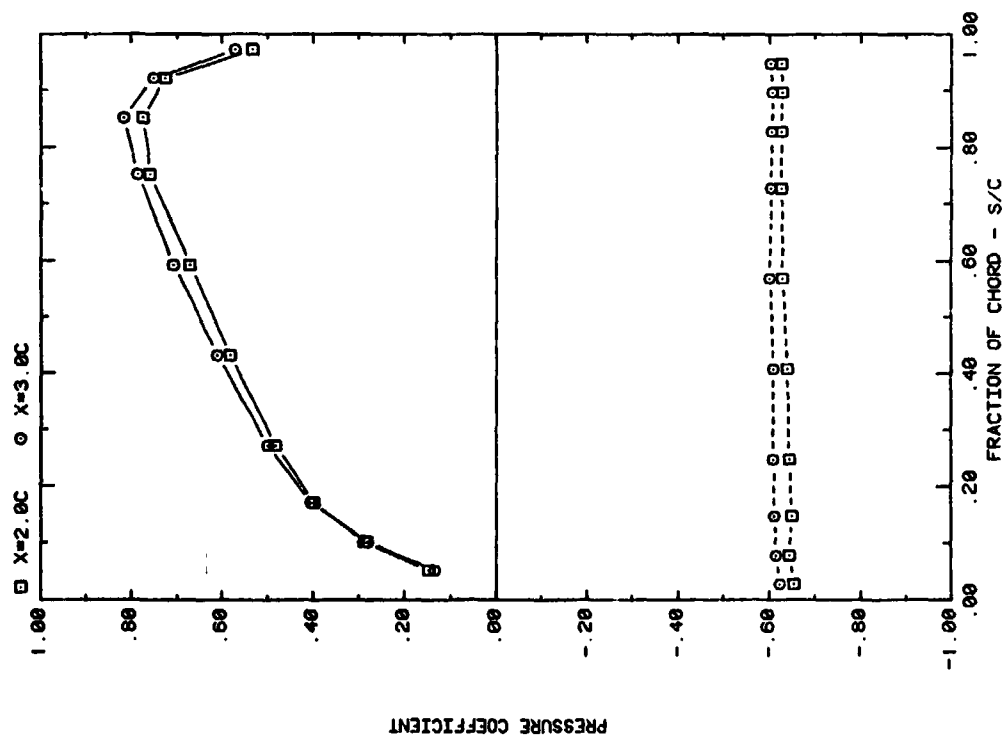


FRONT AND BACK PRESSURES ON ARRAY #1 IN UNIFORM FLOW  
EFFECT OF SEPARATION (X) ON ATTACK ANGLE 20, H/C = 0.25

Plot 2-1-2. Multiple Arrays without Fence, Uniform Flow Study  
Effect of Separation Distance

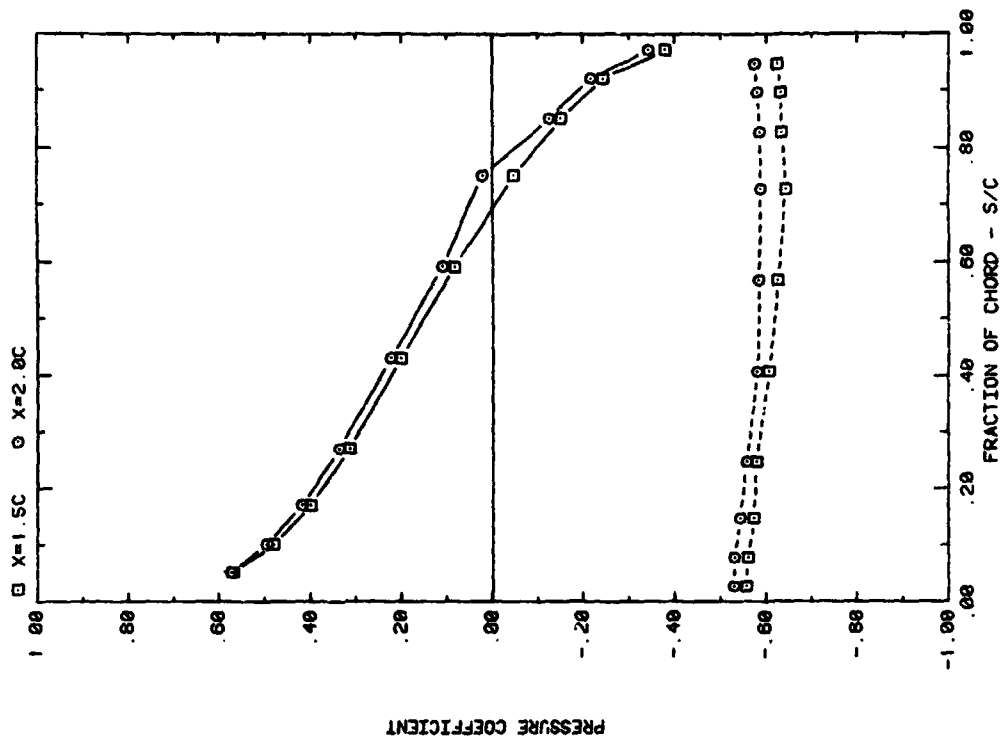


FRONT AND BACK PRESSURES ON ARRAY #1 IN UNIFORM FLOW  
EFFECT OF SEPARATION (X) ON ATTACK ANGLE 120, H/C = 0.25

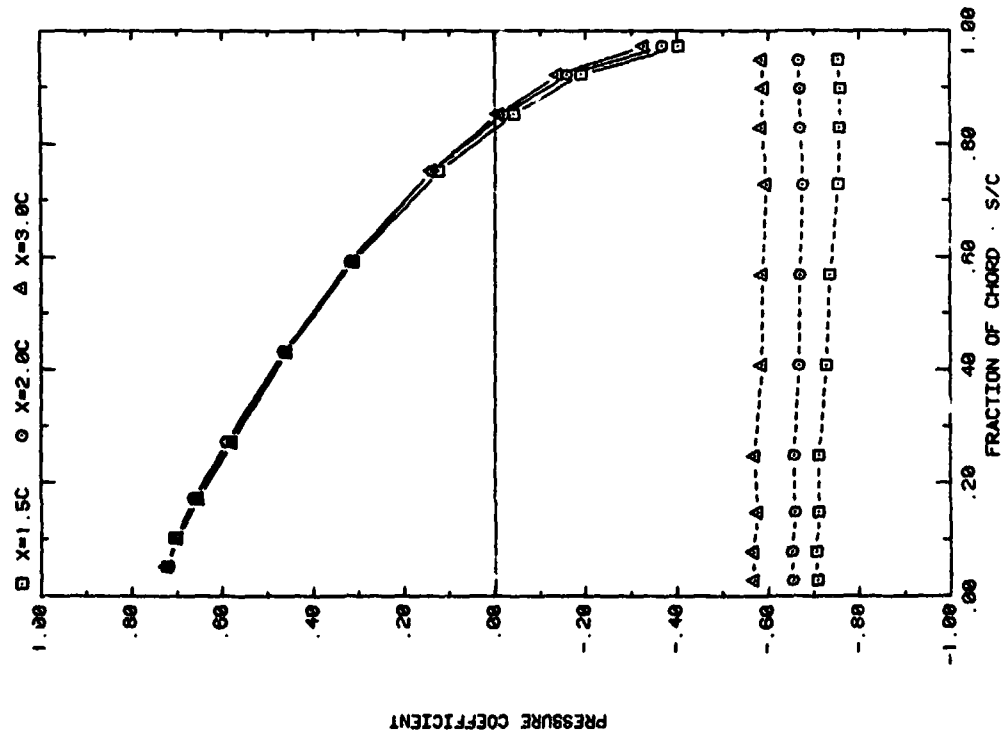


FRONT AND BACK PRESSURES ON ARRAY #1 IN UNIFORM FLOW  
EFFECT OF SEPARATION (X) ON ATTACK ANGLE 60, H/C = 0.25

Plot 2-1-2. (Continued)

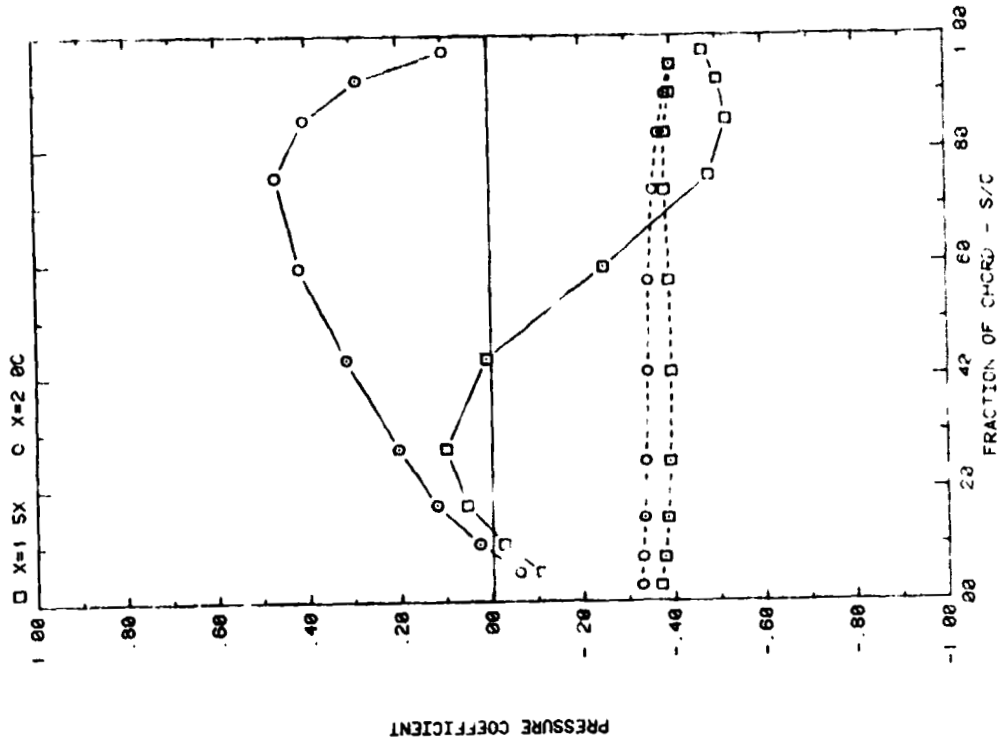


FRONT AND BACK PRESSURES ON ARRAY #1 IN UNIFORM FLOW EFFECT OF SEPARATION (X) ON ATTACK ANGLE 160, H/C = 0.25

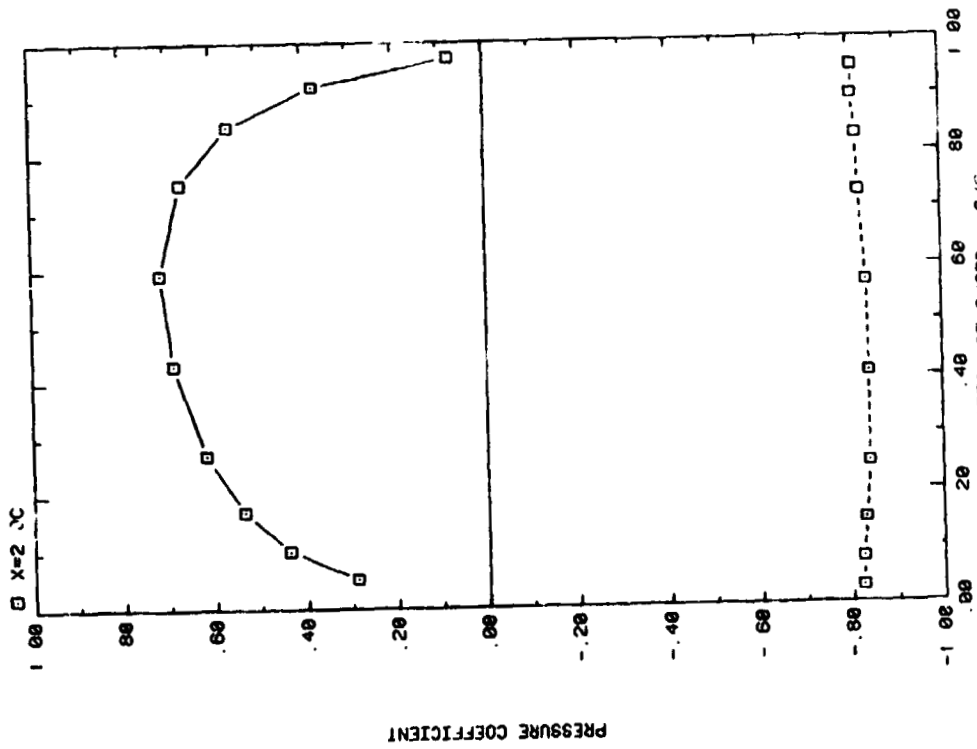


FRONT AND BACK PRESSURES ON ARRAY #1 IN UNIFORM FLOW EFFECT OF SEPARATION (X) ON ATTACK ANGLE 145, H/C = 0.25

Plot 2-1-2. (Continued)

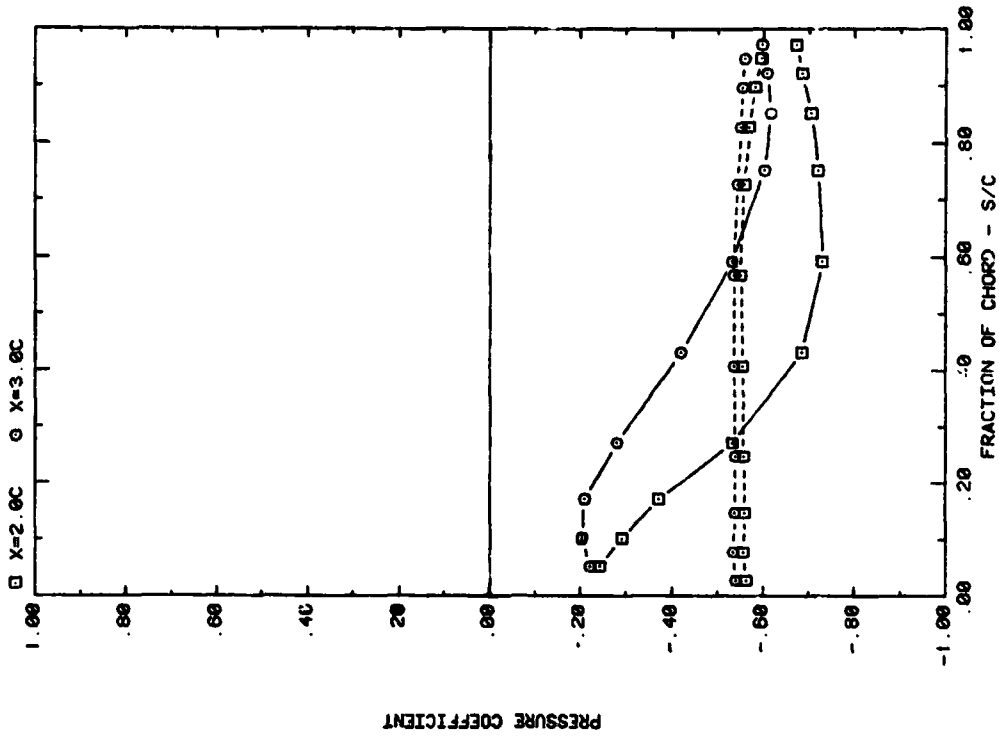


FRONT AND BACK PRESSURES ON ARRAY #2 IN UNIFORM FLOW  
EFFECT OF SEPARATION (X) ON ATTACK ANGLE 90, H/C = 0.25

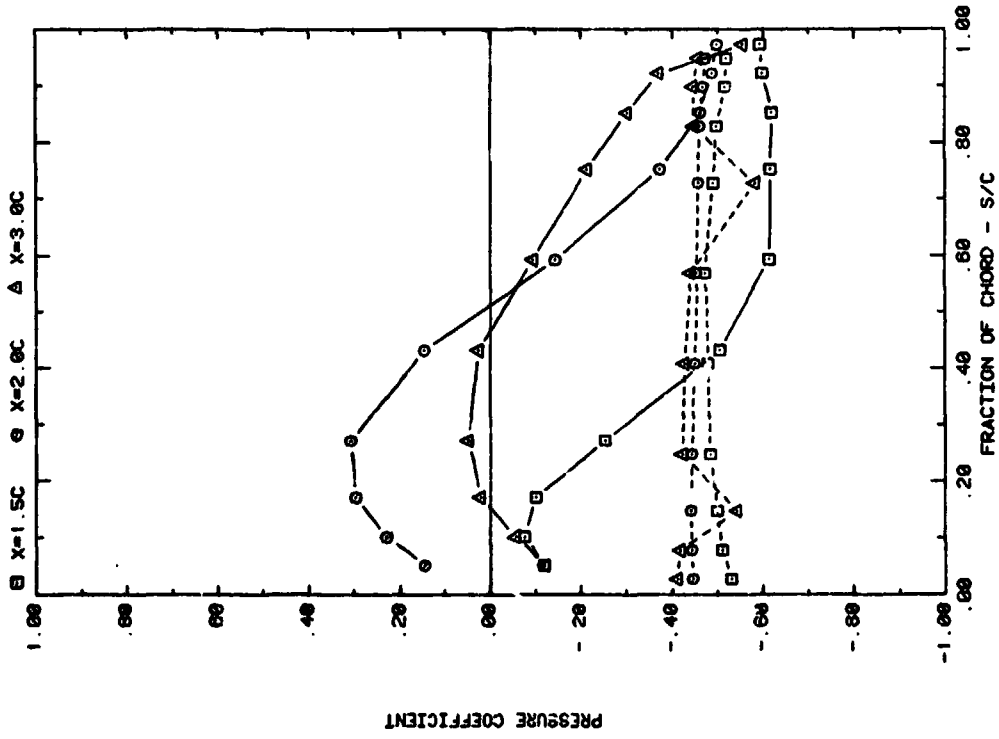


FRONT AND BACK PRESSURES ON ARRAY #1 IN UNIFORM FLOW  
EFFECT OF SEPARATION (X) ON ATTACK ANGLE 90, H/C = 0.25

Plot 2-1-2. (Continued)

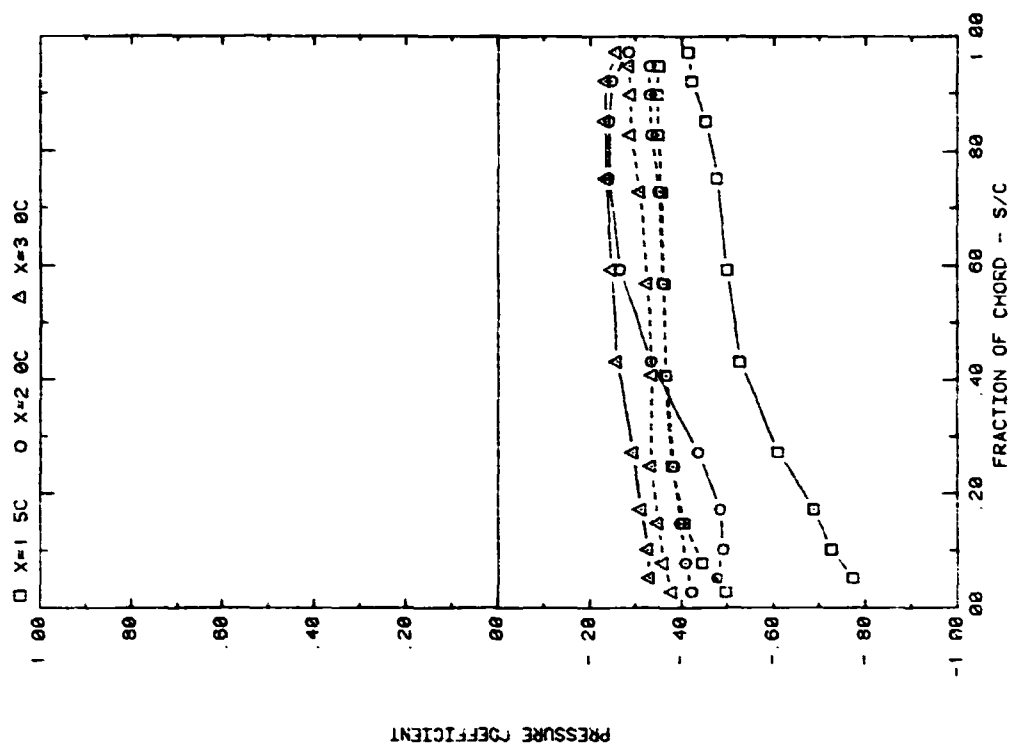


FRONT AND BACK PRESSURES ON ARRAY #2 IN UNIFORM FLOW  
EFFECT OF SEPARATION ANGLE ON ATTACK ANGLE 60, H/C = 0.25

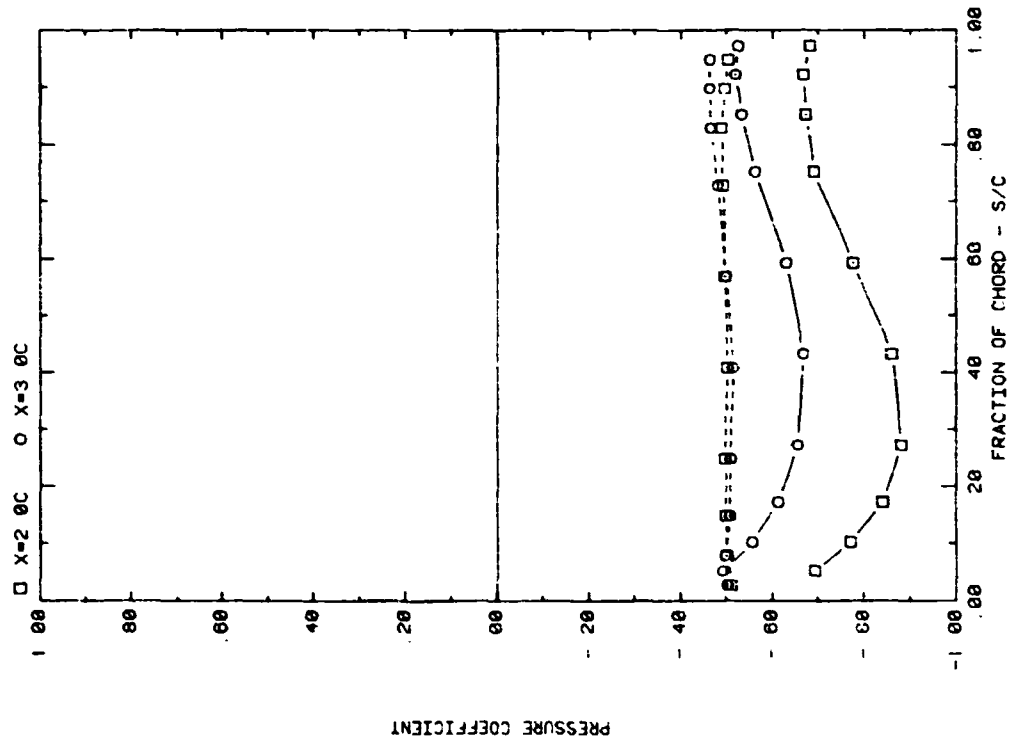


FRONT AND BACK PRESSURES ON ARRAY #2 IN UNIFORM FLOW  
EFFECT OF SEPARATION ANGLE ON ATTACK ANGLE 95, H/C = 0.25

Plot 2-1-2. (Continued)



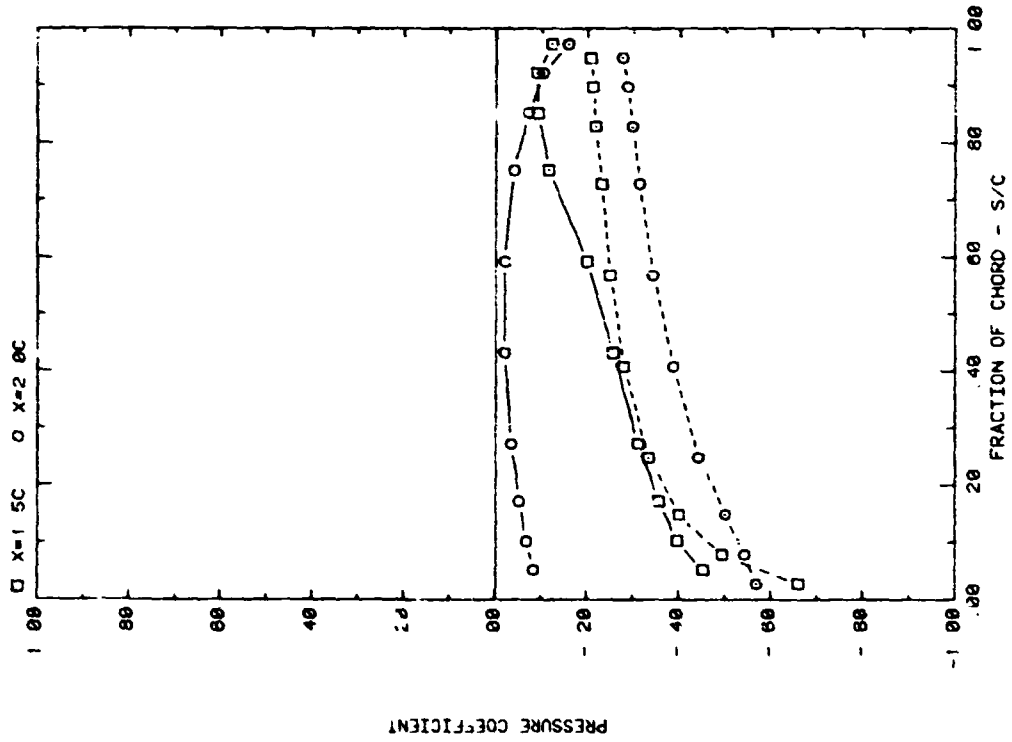
FRONT AND BACK PRESSURES ON ARRAY #2 IN UNIFORM FLOW  
EFFECT OF SEPARATION (X) ON ATTACK ANGLE 145, H/C = 0.25



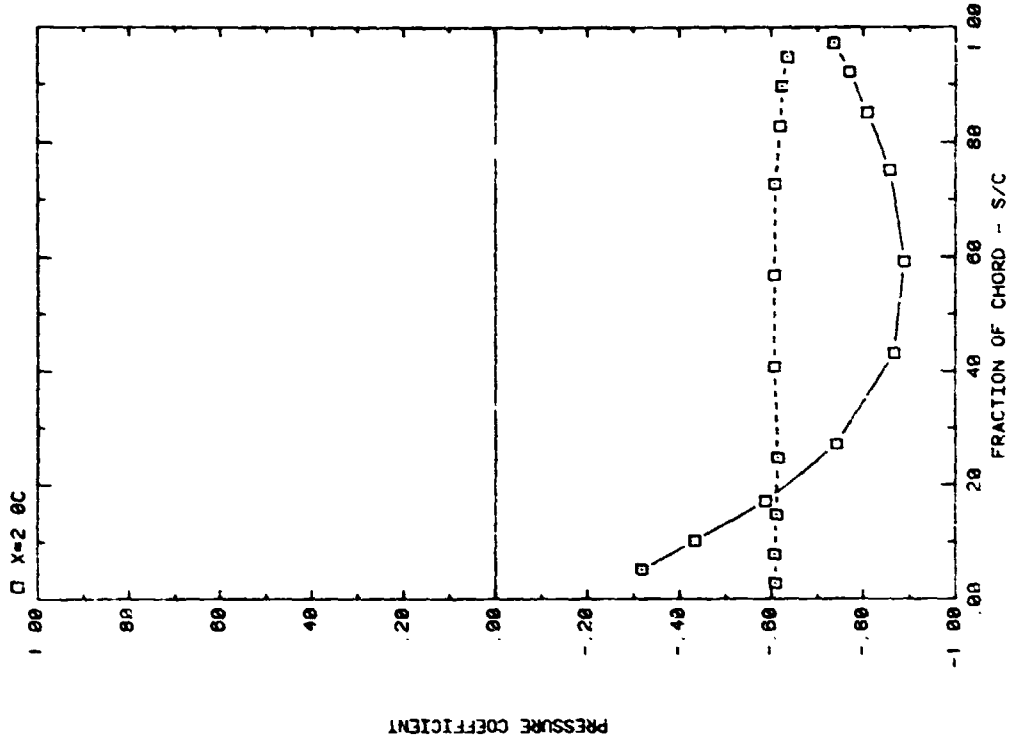
FRONT AND BACK PRESSURES ON ARRAY #2 IN UNIFORM FLOW  
EFFECT OF SEPARATION (X) ON ATTACK ANGLE 120, H/C = 0.25

Plot 2-1-2. (Continued)

4

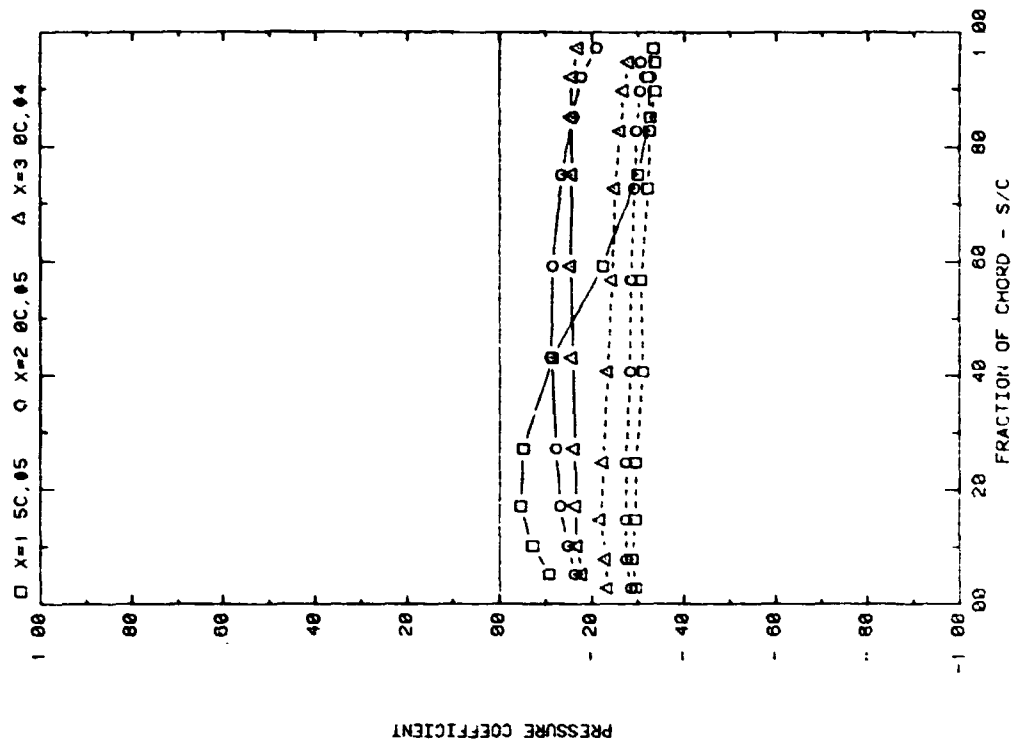


FRONT AND BACK PRESSURES ON ARRAY #2 IN UNIFORM FLOW  
EFFECT OF SEPARATION (X) ON ATTACK ANGLE 160, H/C = 0.25

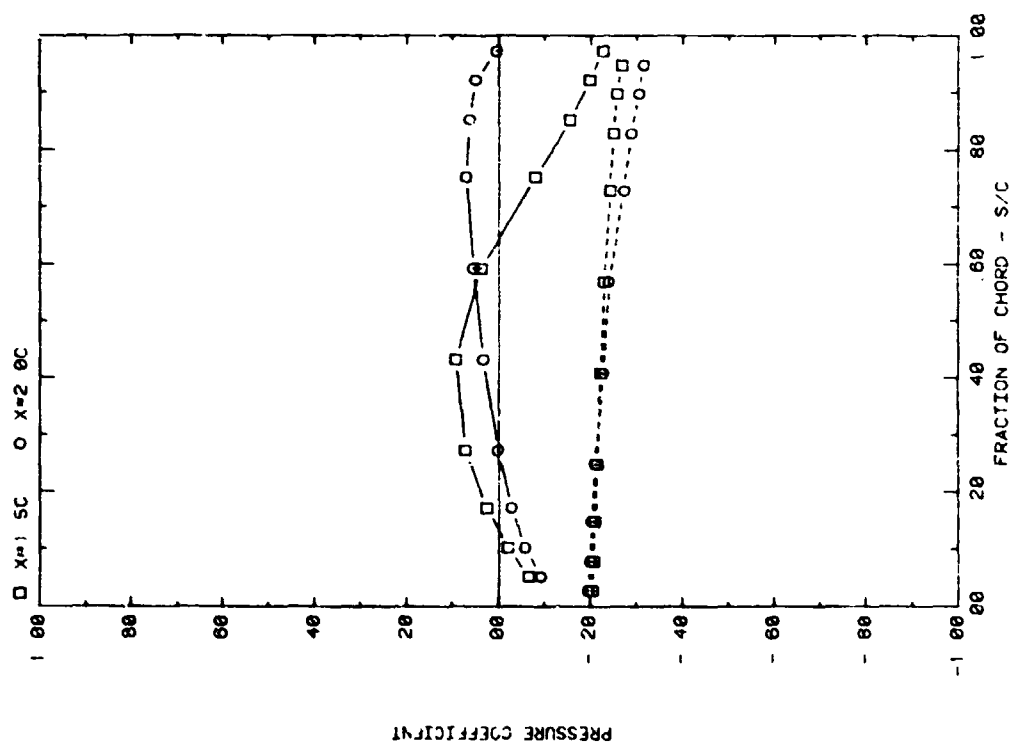


FRONT AND BACK PRESSURES ON ARRAY #2 IN UNIFORM FLOW  
EFFECT OF SEPARATION (X) ON ATTACK ANGLE 90, H/C = 0.25

Plot 2-1-2. (Continued)

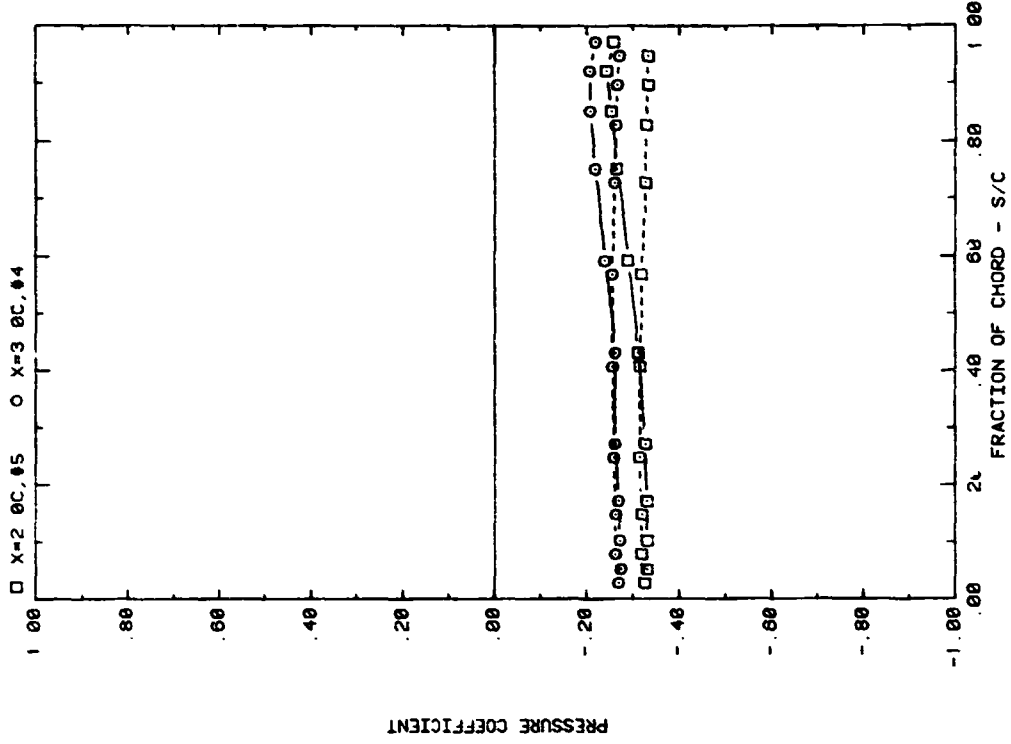


FRONT AND BACK PRESSURES ON ARRAY #4 OR #5 IN UNIFORM FLOW  
EFFECT OF SEPARATION (X) ON ATTACK ANGLE 35, H/C = 0.25

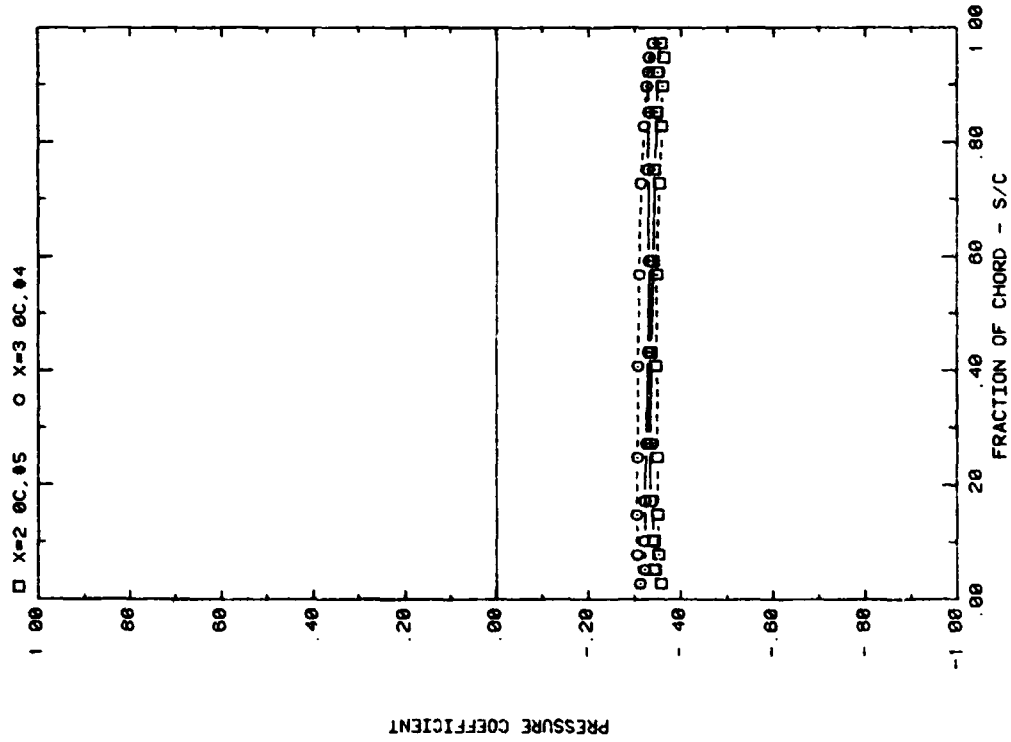


FRONT AND BACK PRESSURES ON ARRAY #5 IN UNIFORM FLOW  
EFFECT OF SEPARATION (X) ON ATTACK ANGLE 20, H/C = 0.25

Plot 2-1-2. (Continued)

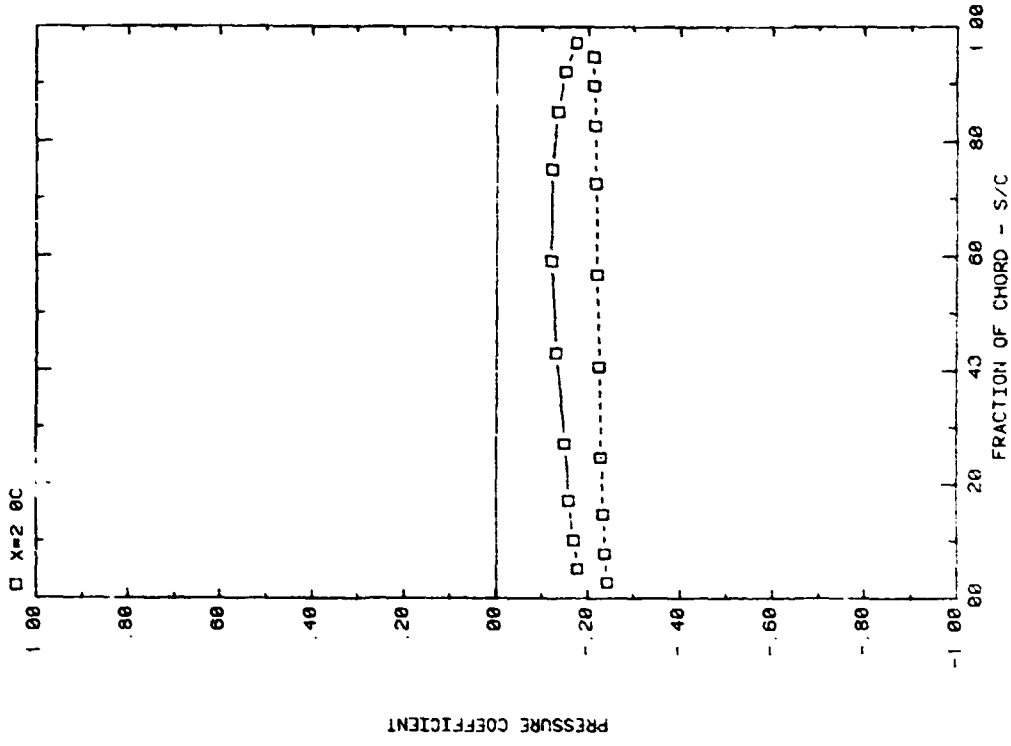


FRONT AND BACK PRESSURES ON ARRAY #4 OF #5 IN UNIFORM FLOW  
EFFECT OF SEPARATION (X) ON ATTACK ANGLE 120, H/C = 0.25

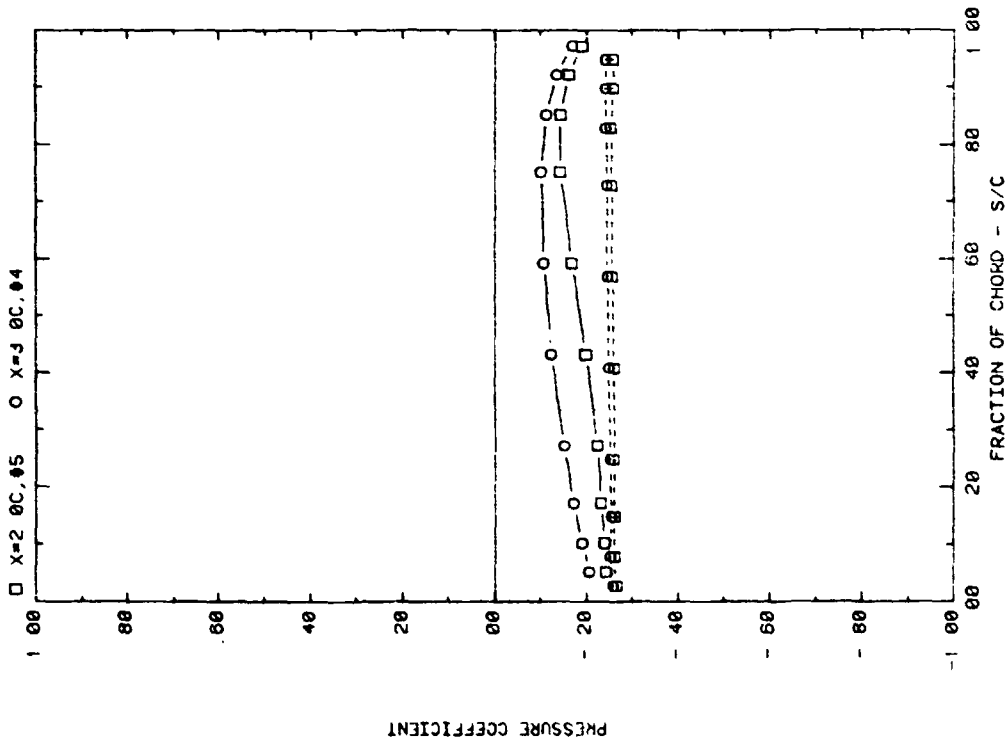


FRONT AND BACK PRESSURES ON ARRAY #4 OR #5 IN UNIFORM FLOW  
EFFECT OF SEPARATION (X) ON ATTACK ANGLE 60, H/C = 0.25

Plot 2-1-2. (Continued)

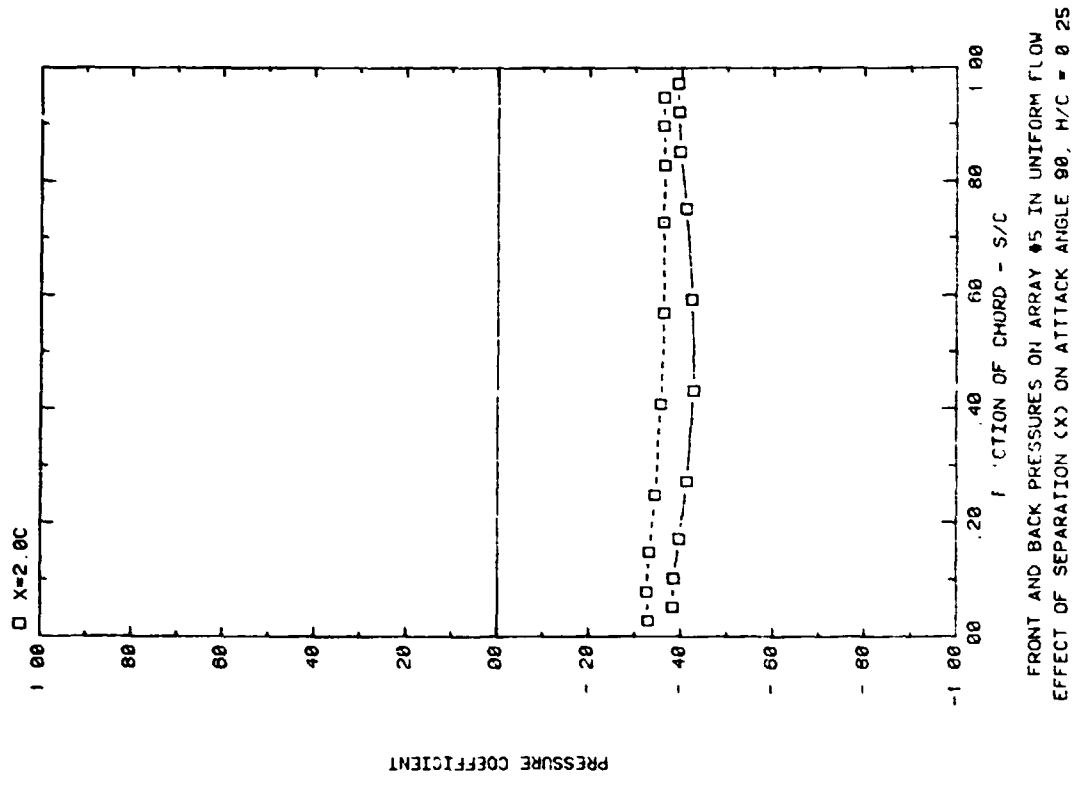


FRONT AND BACK PRESSURES ON ARRAY #5 IN UNIFORM FLOW  
EFFECT OF SEPARATION (Y) ON ATTACK ANGLE 160, H/C = 0.25

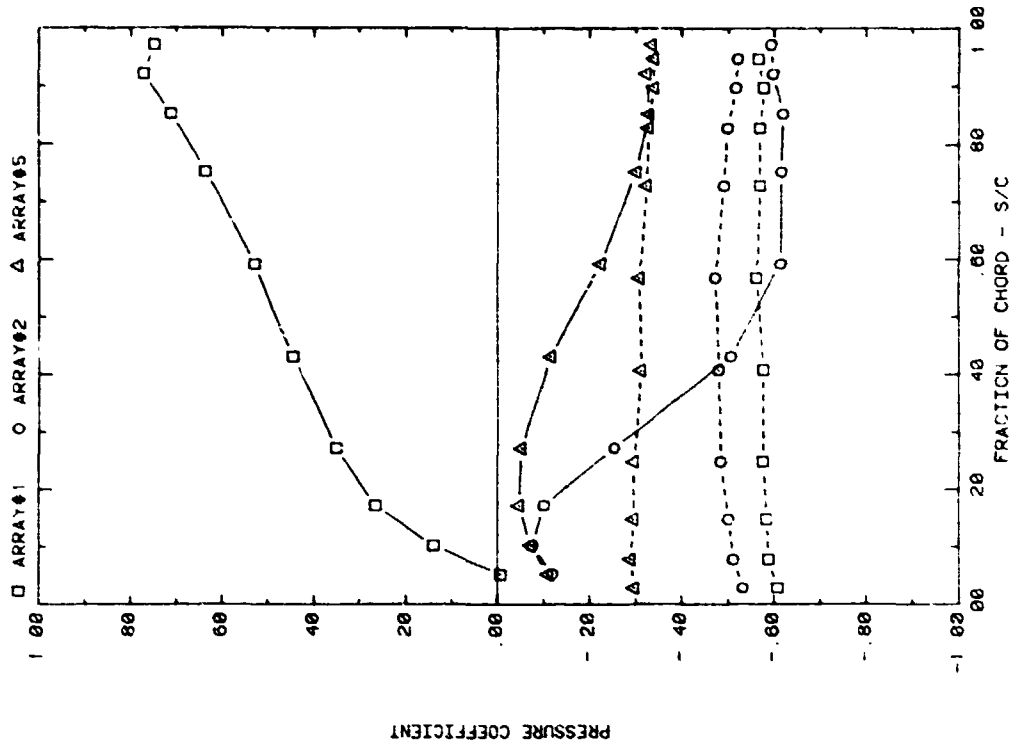


FRONT AND BACK PRESSURES ON ARRAY #4 OR #5 IN UNIFORM FLOW  
EFFECT OF SEPARATION (X) ON ATTACK ANGLE 145, H/C = 0.25

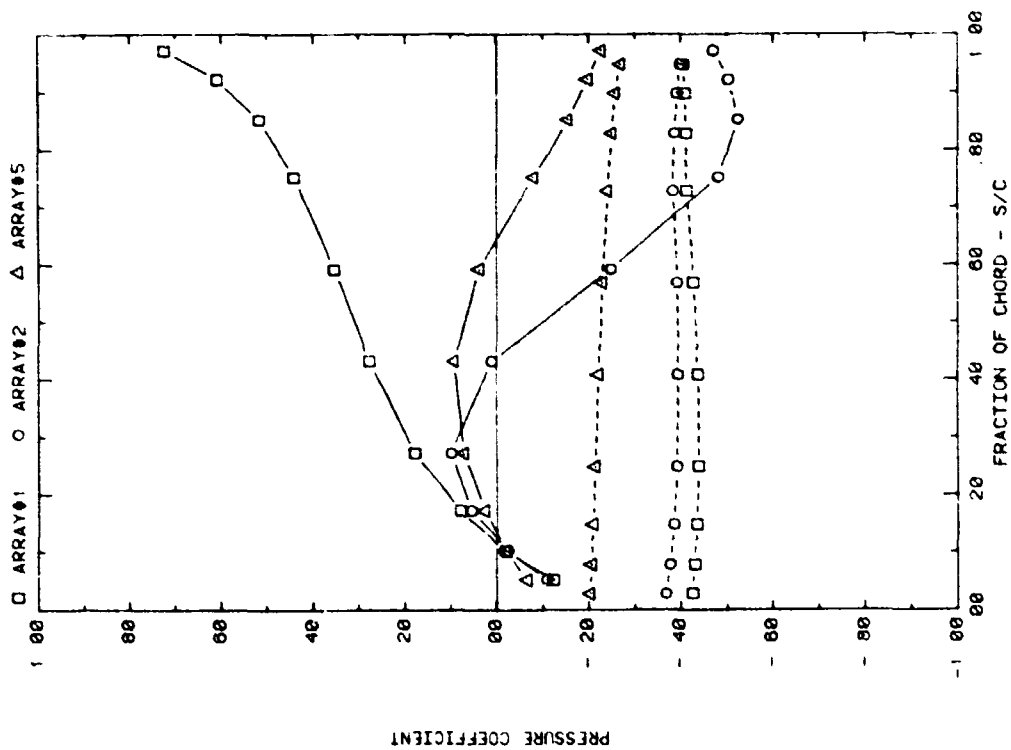
Plot 2-1-2. (Continued)



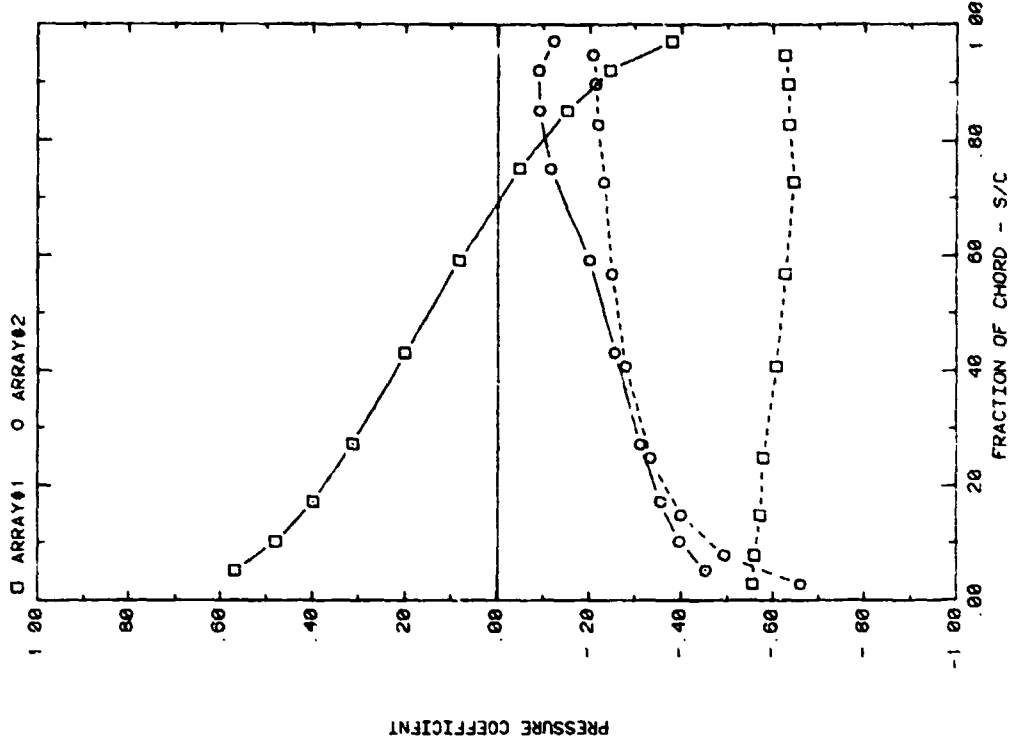
Plot 2-1-2. (Concluded)



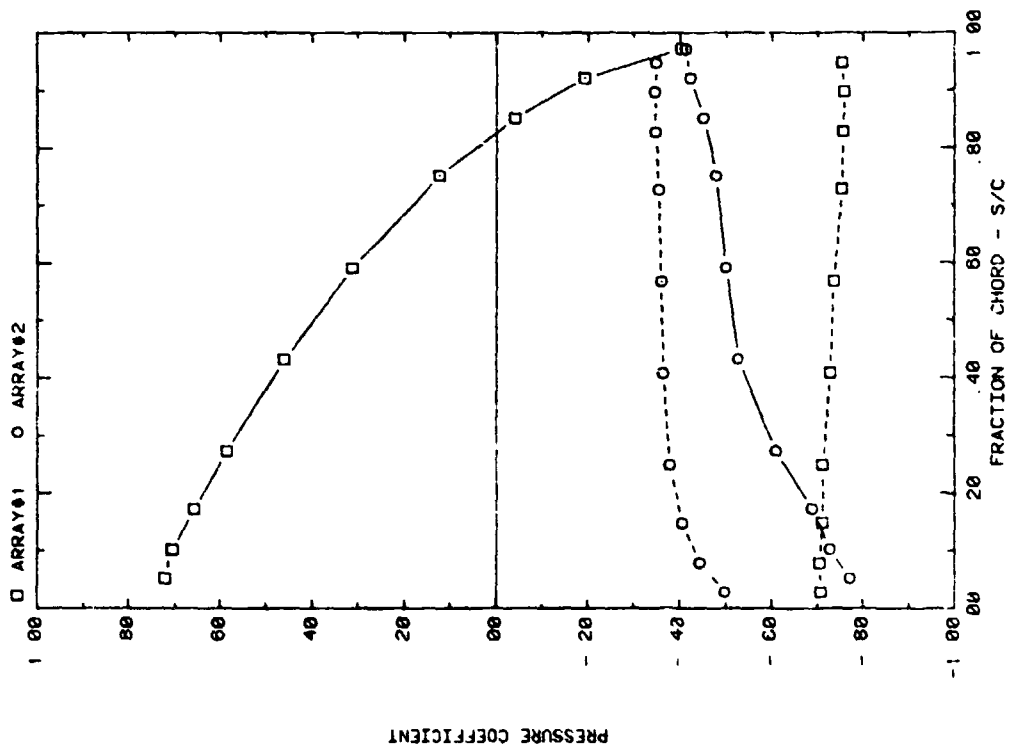
FRONT AND BACK PRESSURES ON VARIOUS ARRAYS FOR SEPARATION = 1.5C  
EFFECT OF ARRAY CONFIGURATION FOR ATTACK ANGLE, ALPHA = 35



FRONT AND BACK PRESSURES ON VARIOUS ARRAYS FOR SEPARATION = 1.5C  
EFFECT OF ARRAY CONFIGURATION FOR ATTACK ANGLE, ALPHA = 28  
Plot 2-1-3. Multiple Arrays without Fence, Uniform Flow Study  
Effect of Array Position

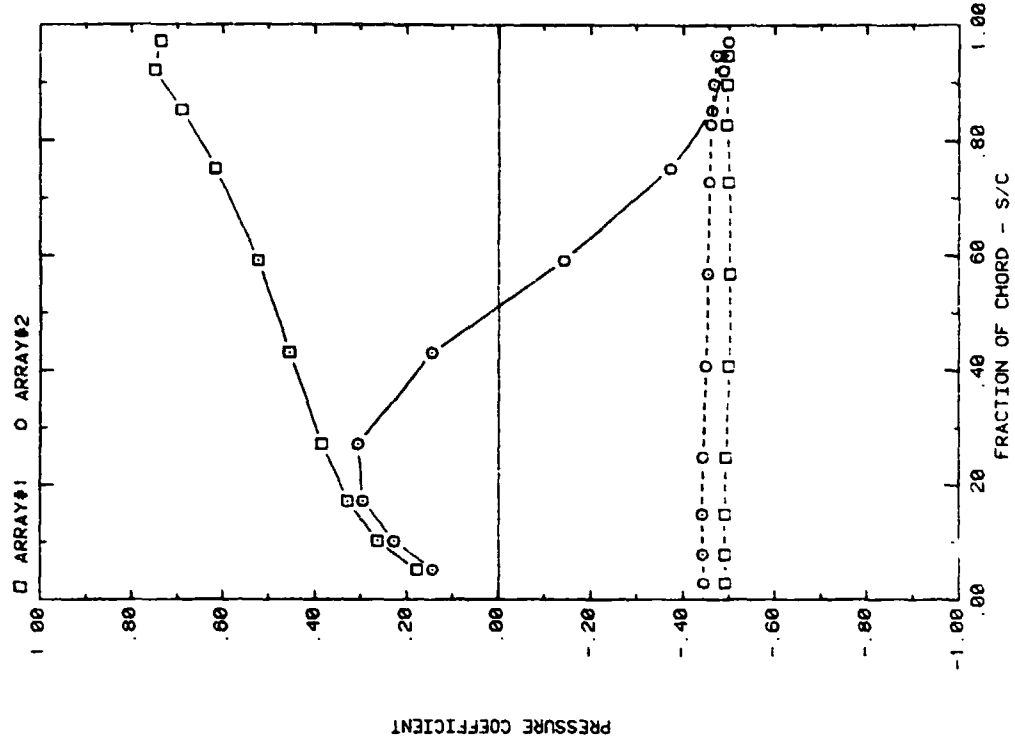


FRONT AND BACK PRESSURES ON VARIOUS ARRAYS FOR SEPARATION -1 SC  
EFFECT OF ARRAY CONFIGURATION FOR ATTACK ANGLE, ALPHA = 160

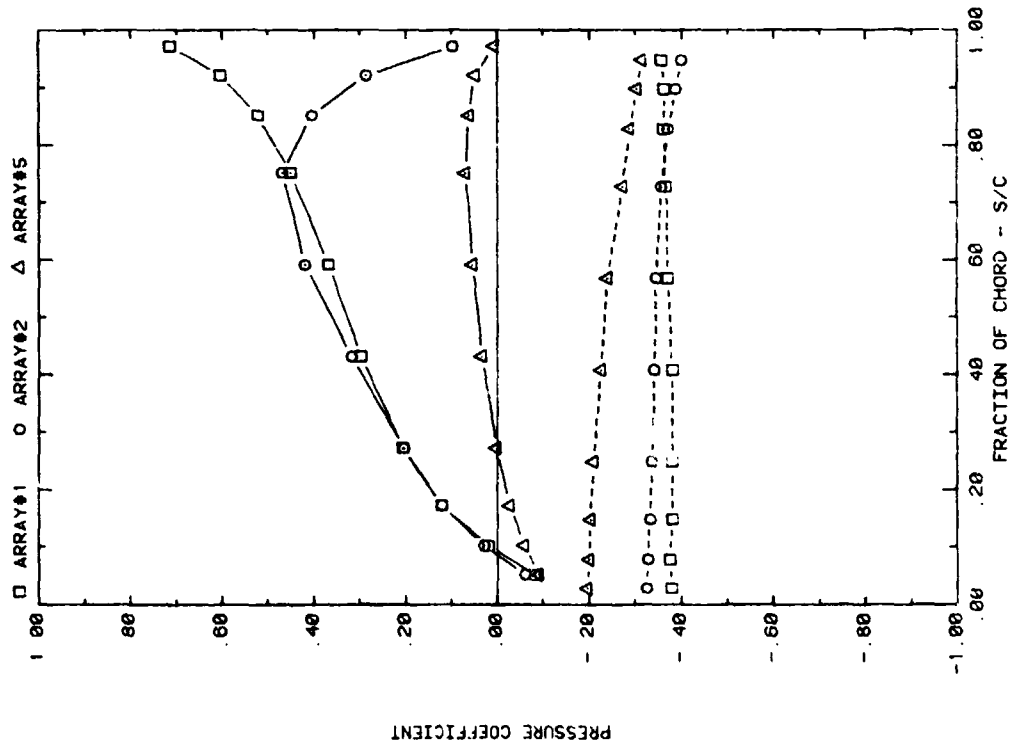


FRONT AND BACK PRESSURES ON VARIOUS ARRAYS FOR SEPARATION -1 SC  
EFFECT OF ARRAY CONFIGURATION FOR ATTACK ANGLE, ALPHA = 145

Plot 2-1-3. (Continued)

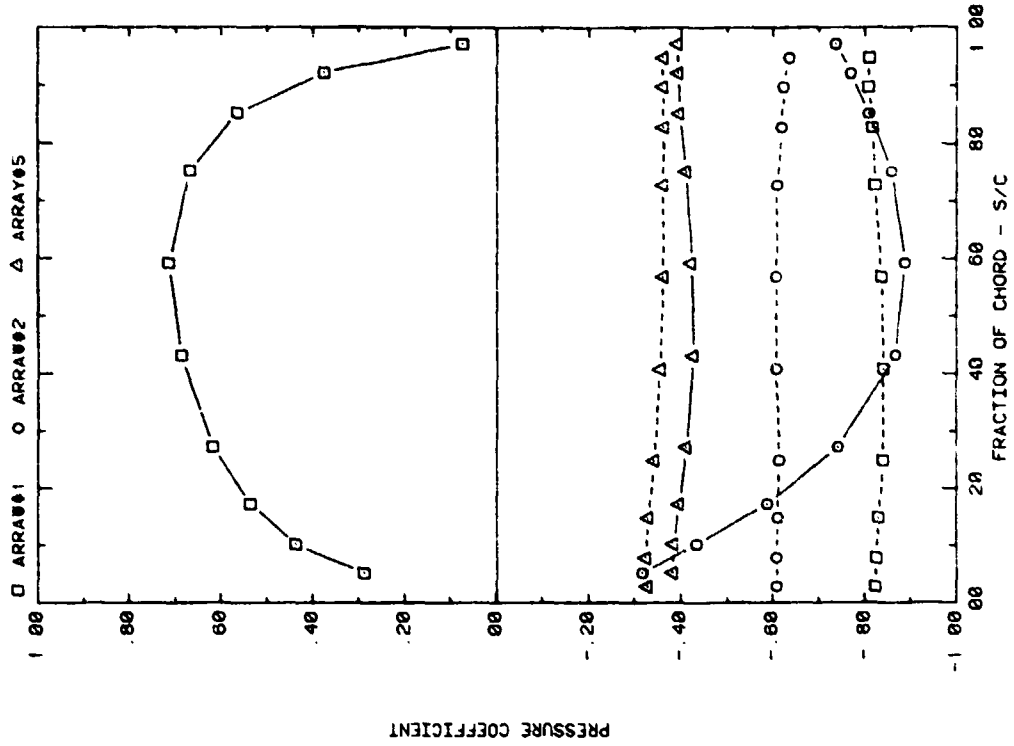


FRONT AND BACK PRESSURES ON VARIOUS ARRAYS FOR SEPARATION = 2C  
EFFECT OF ARRAY CONFIGURATION FOR ATTACK ANGLE, ALPHA = 35

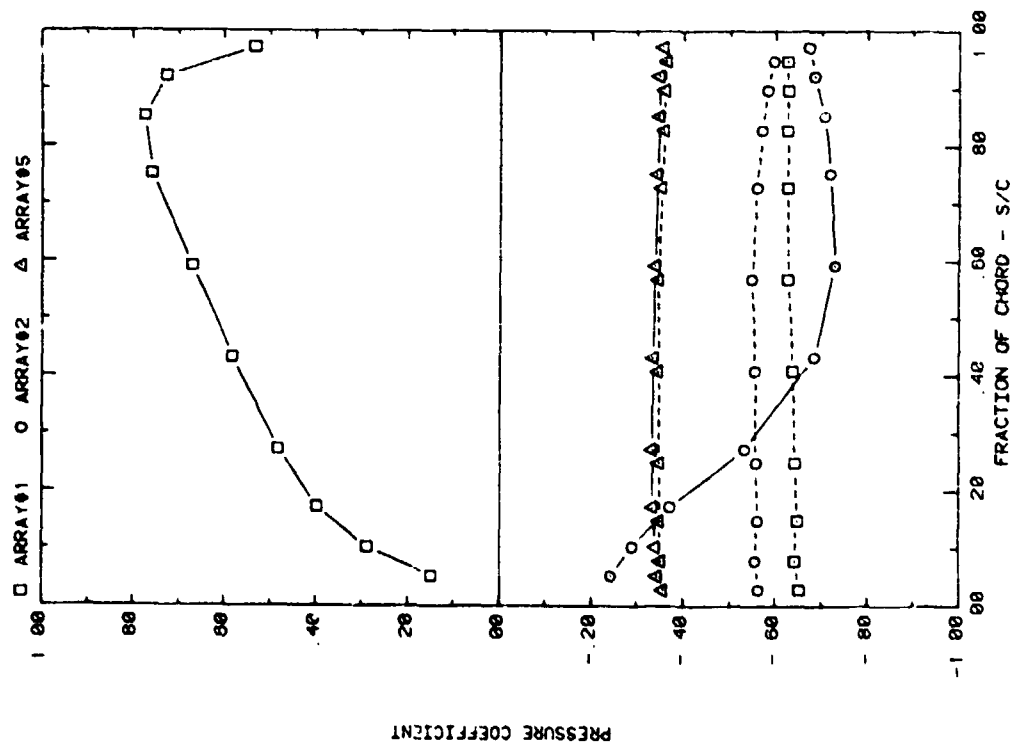


FRONT AND BACK PRESSURES ON VARIOUS ARRAYS FOR SEPARATION = 2C  
EFFECT OF ARRAY CONFIGURATION FOR ATTACK ANGLE, ALPHA = 20

Plot 2-1-3. (Continued)

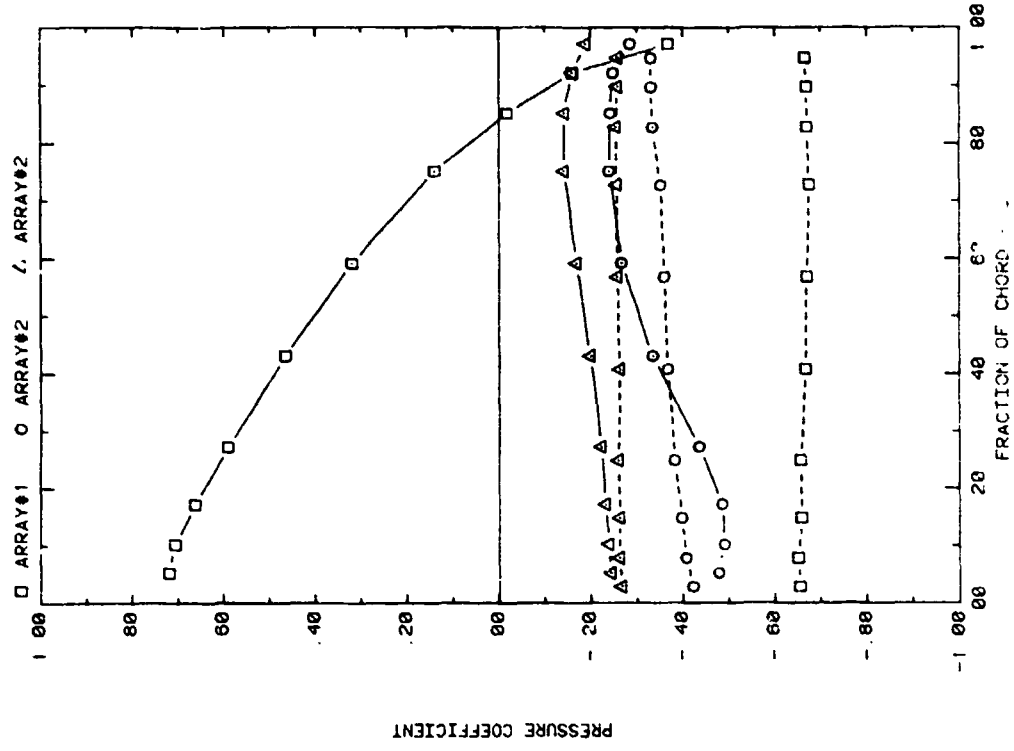


FRONT AND BACK PRESSURES ON VARIOUS ARRAYS FOR SEPARATION = 2C  
EFFECT OF ARRAY CONFIGURATION FOR ATTACK ANGLE, ALPHA = 90

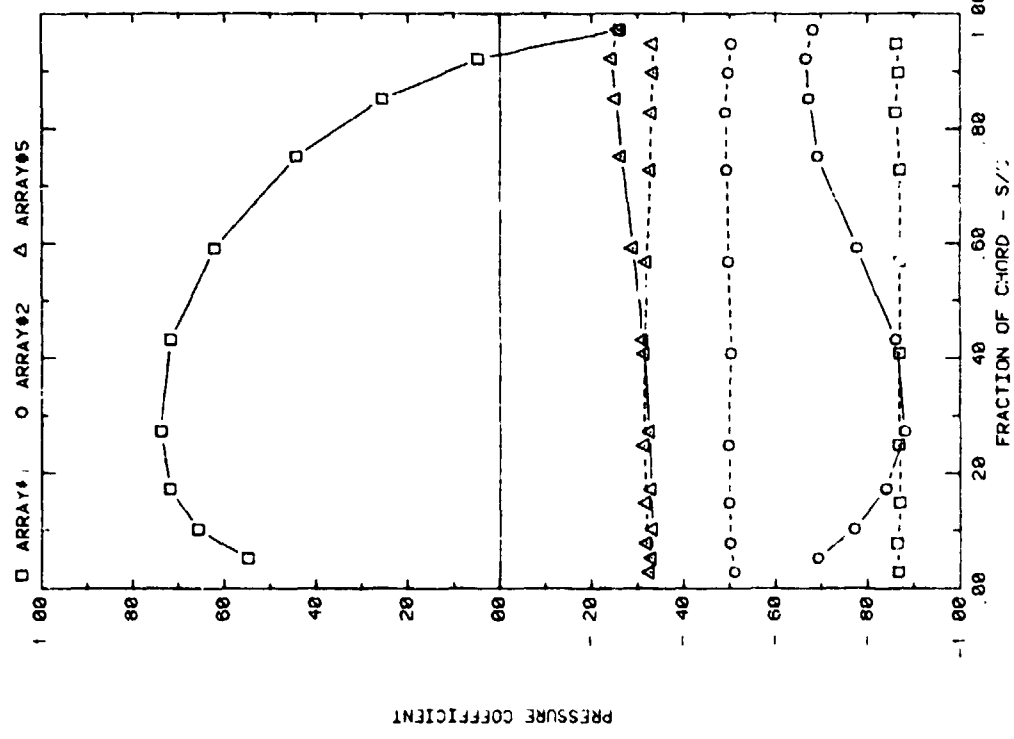


FRONT AND BACK PRESSURES ON VARIOUS ARRAYS FOR SEPARATION = 2C  
EFFECT OF ARRAY CONFIGURATION FOR ATTACK ANGLE, ALPHA = 60

Plot 2-1-3. (Continued)

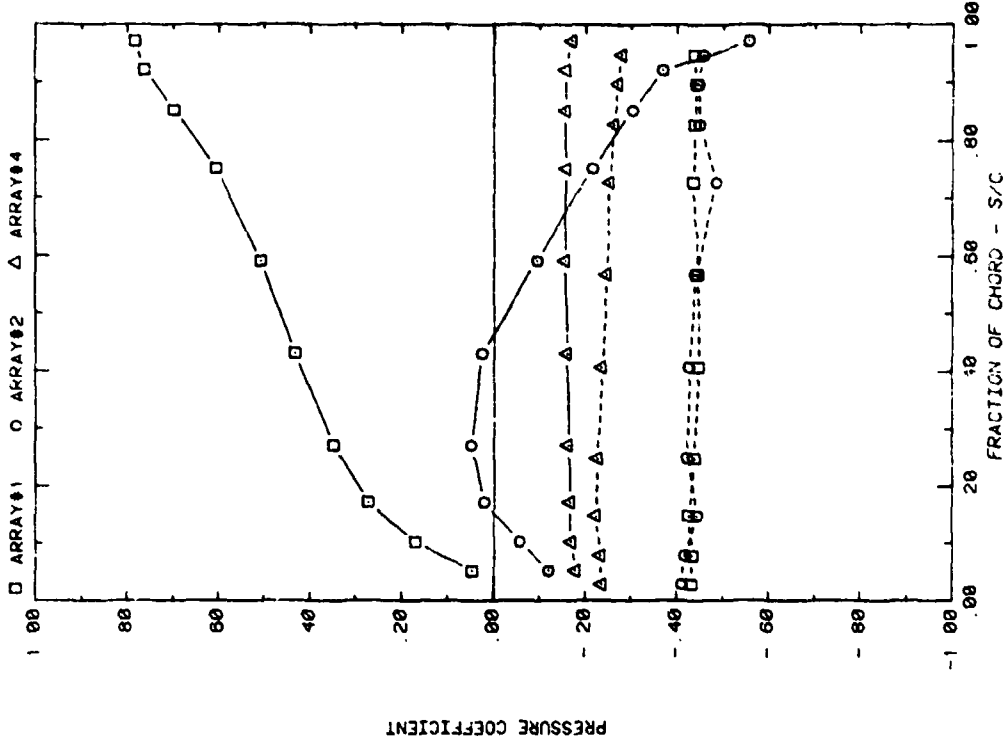


FRONT AND BACK PRESSURES ON VARIOUS ARRAYS . . . SEPARATION = 2C  
EFFECT OF ARRAY CONFIGURATION FOR ATTACK ANGLE  $\alpha$  = 145

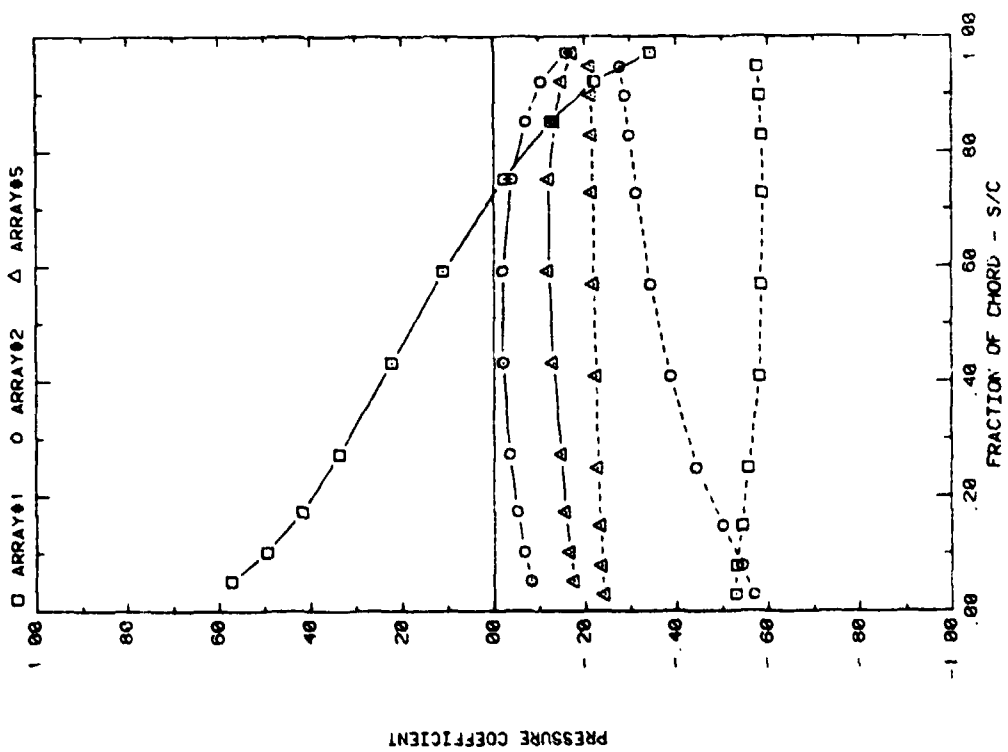


FRONT AND BACK PRESSURES ON VARIOUS ARRAYS FOR SEPARATION = 2C  
EFFECT OF ARRAY CONFIGURATION FOR ATTACK ANGLE, ALPHA = 120

Plot 2-1-3. (Continued)

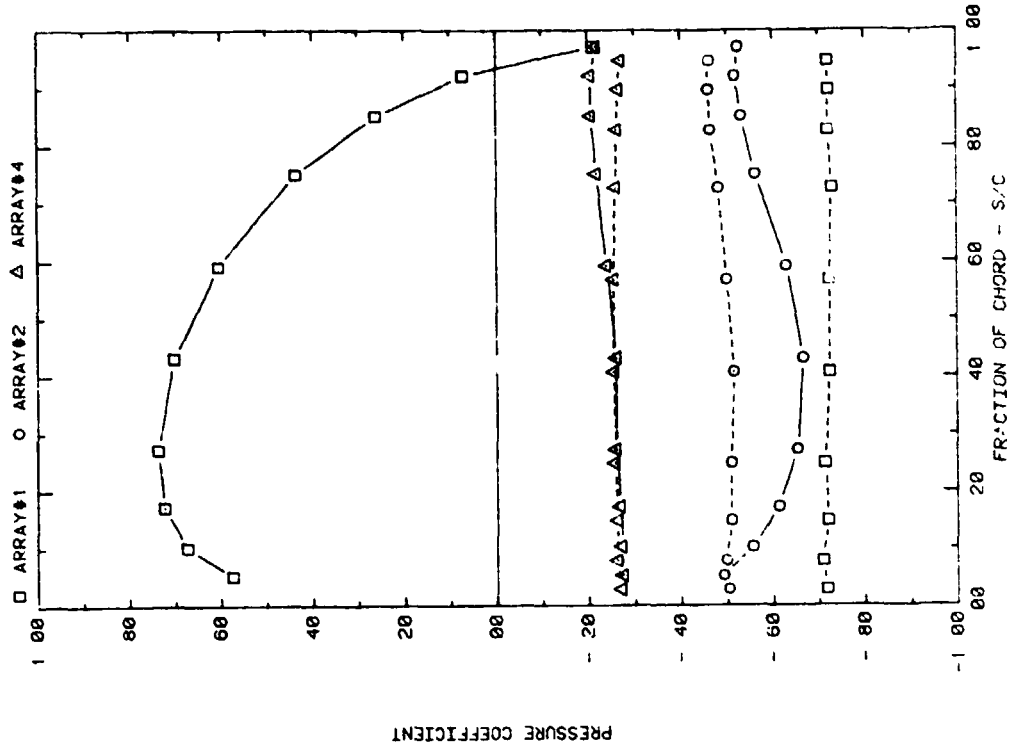


FRONT AND BACK PRESSURES ON VARIOUS ARRAYS FOR SEPARATION = 3C  
EFFECT OF ARRAY CONFIGURATION FOR ATTACK ANGLE, ALPHA = 35

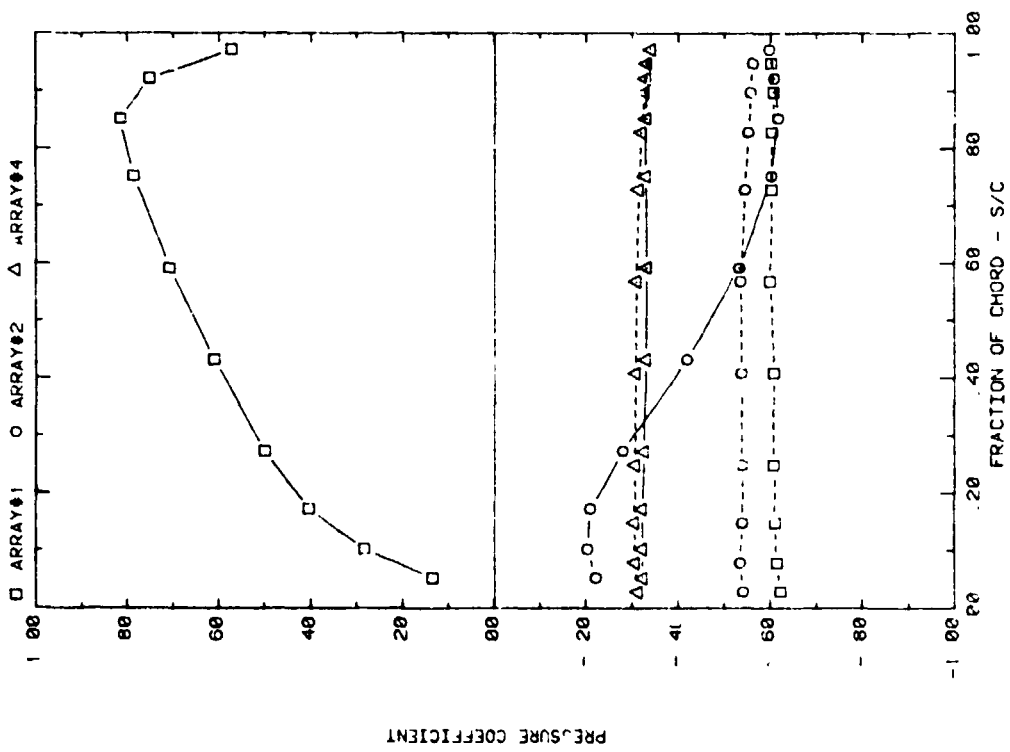


FRONT AND BACK PRESSURES ON VARIOUS ARRAYS FOR SEPARATION = 2C  
EFFECT OF ARRAY CONFIGURATION FOR ATTACK ANGLE, ALPHA = 16C

Plot 1-3. (Continued)

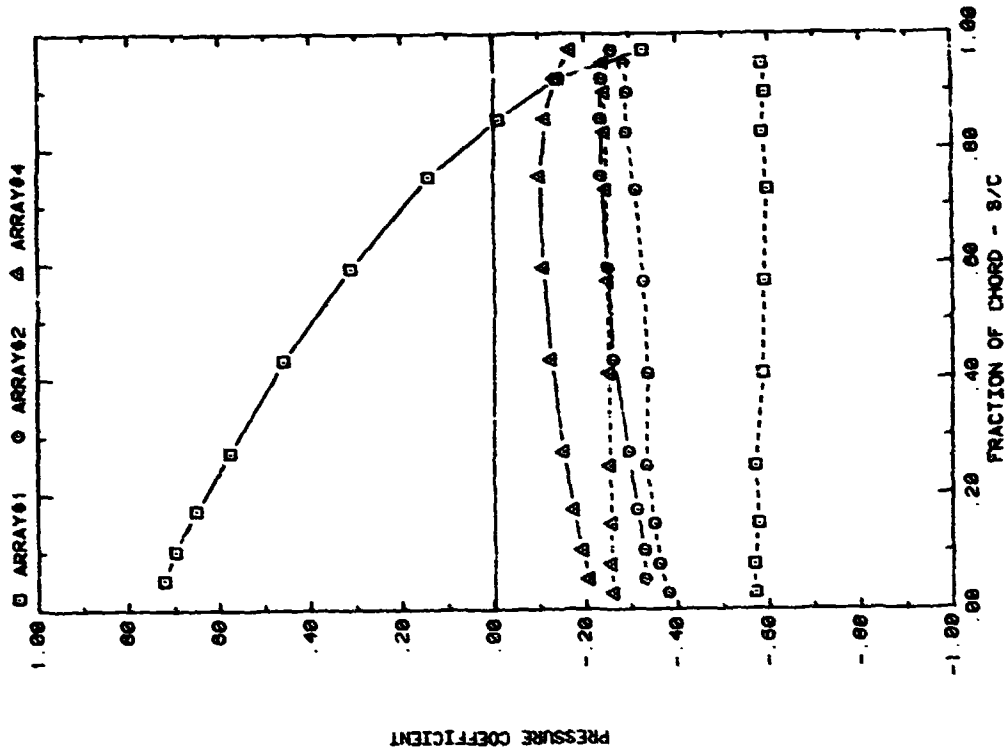


FRONT AND BACK PRESSURES ON VARIOUS ARRAYS FOR SEPARATION = 3C  
EFFECT OF ARRAY CONFIGURATION FOR ATTACK ANGLE, ALPHA = 120



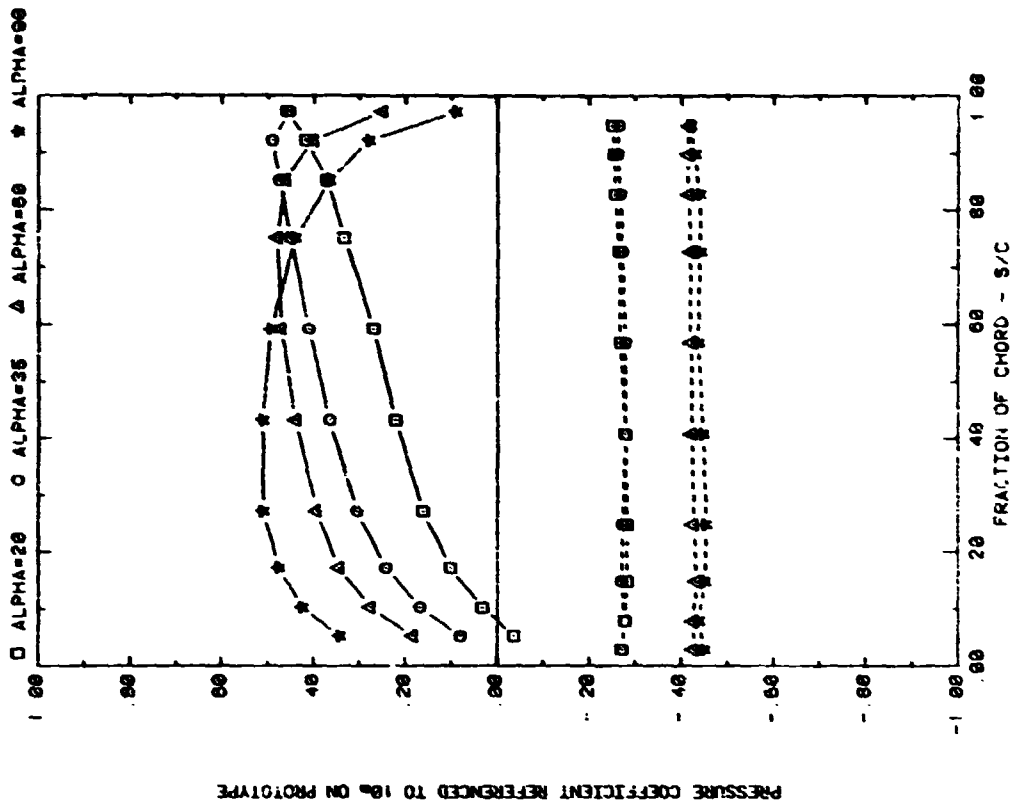
FRONT AND BACK PRESSURES ON VARIOUS ARRAYS FOR SEPARATION = 3C  
EFFECT OF ARRAY CONFIGURATION FOR ATTACK ANGLE, ALPHA = 60

Plot 2-1-3. (Continued)

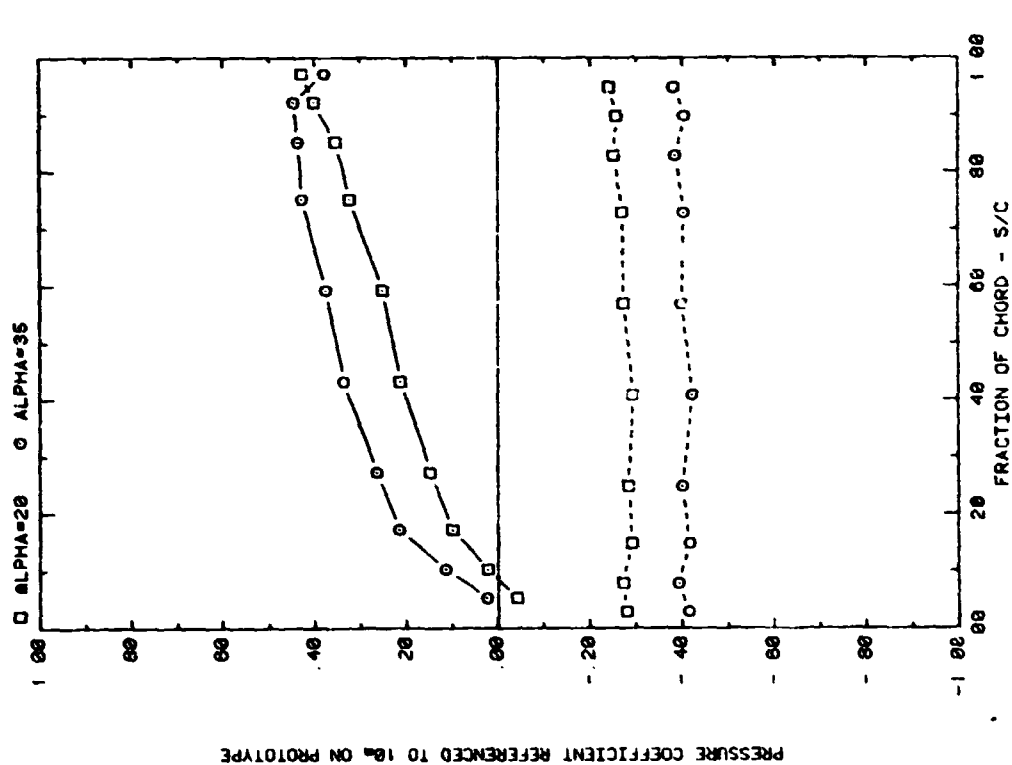


FRONT AND BACK PRESSURES ON VARIOUS ARRAYS FOR SEPARATION = 3C  
EFFECT OF ARRAY CONFIGURATION FOR ATTACK ANGLE, ALPHA = 145

Plot 2-1-3. (Concluded)

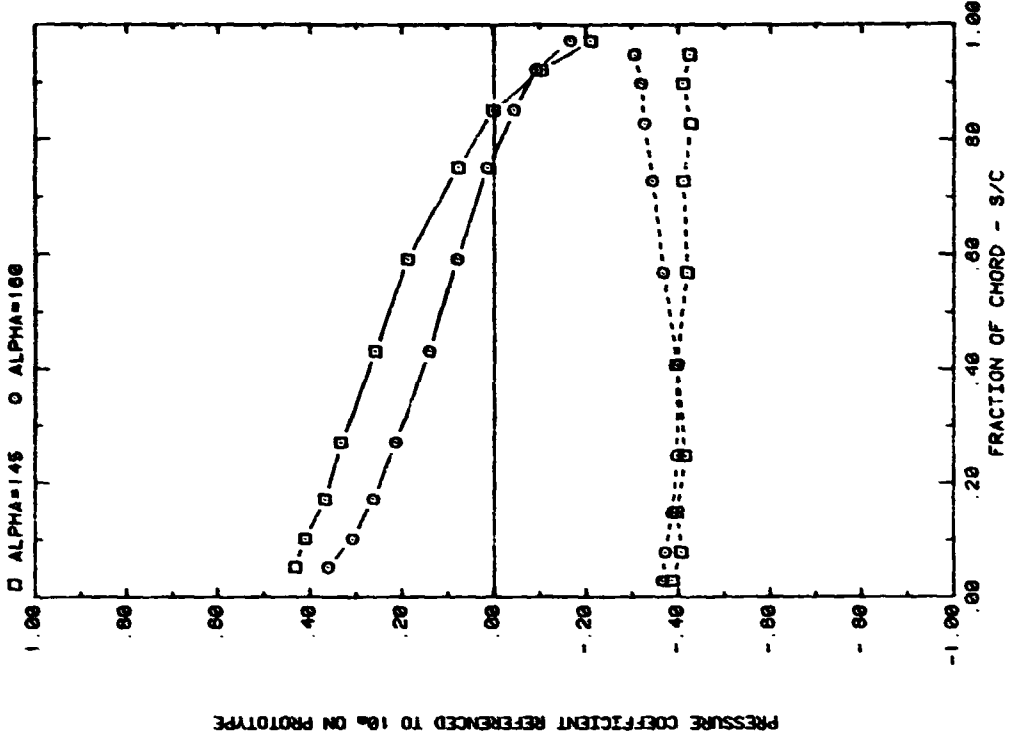


FRONT AND BACK PRESSURES ON ARRAY #1 IN BOUNDARY LAYER  
EFFECT OF ATTACK ANGLE FOR SPACING = 2C

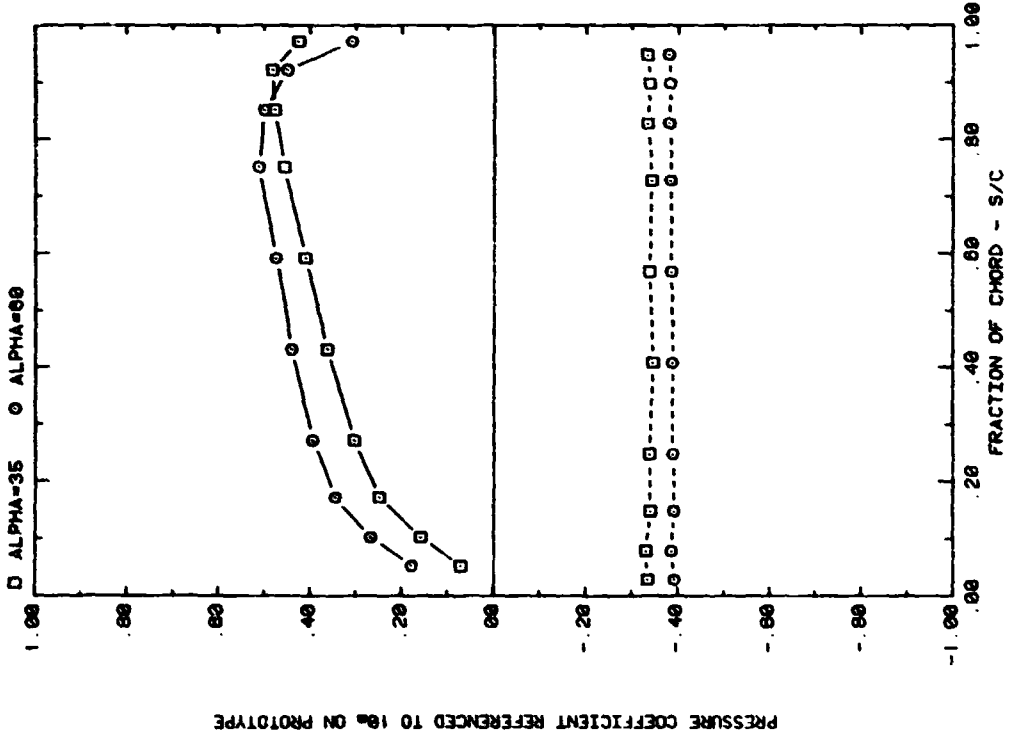


FRONT AND BACK PRESSURES ON ARRAY #1 IN BOUNDARY LAYER  
EFFECT OF ATTACK ANGLE FOR SPACING = 1.5C

Plot 2-2-1. Multiple Arrays without Fence, Nonuniform Flow  
Study Effect of Angle of Attack

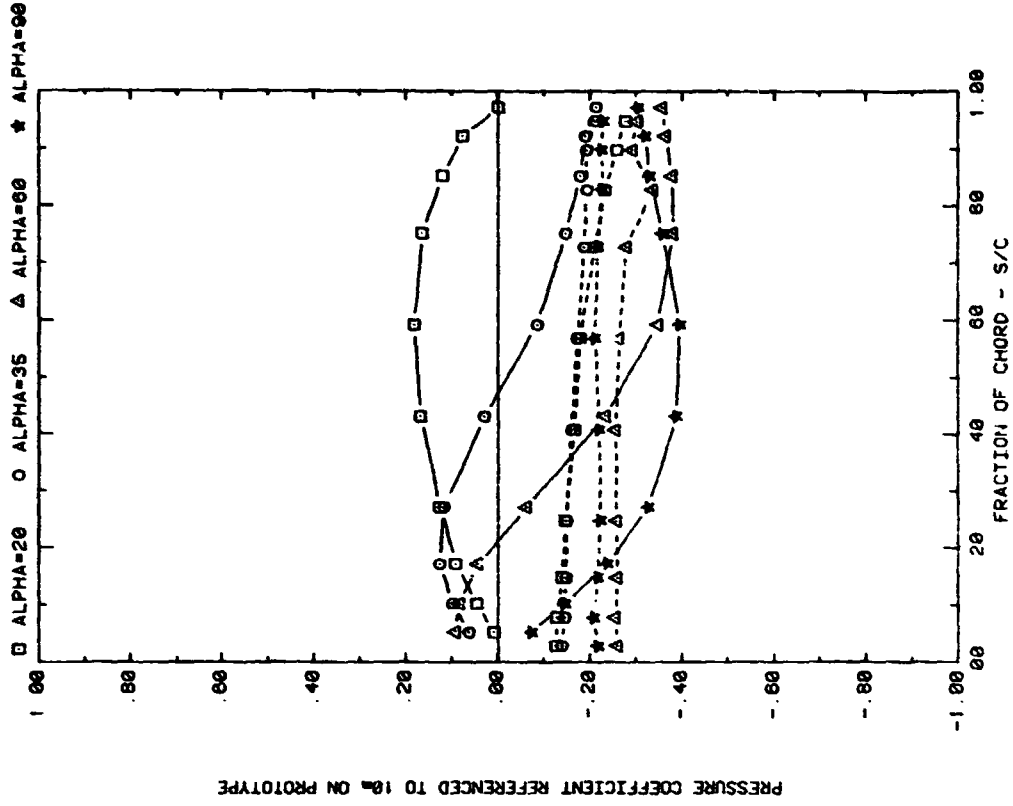


FRONT AND BACK PRESSURES ON ARRAY #1 IN BOUNDARY LAYER  
EFFECT OF ATTACK ANGLE FOR SPACING = 1.5C

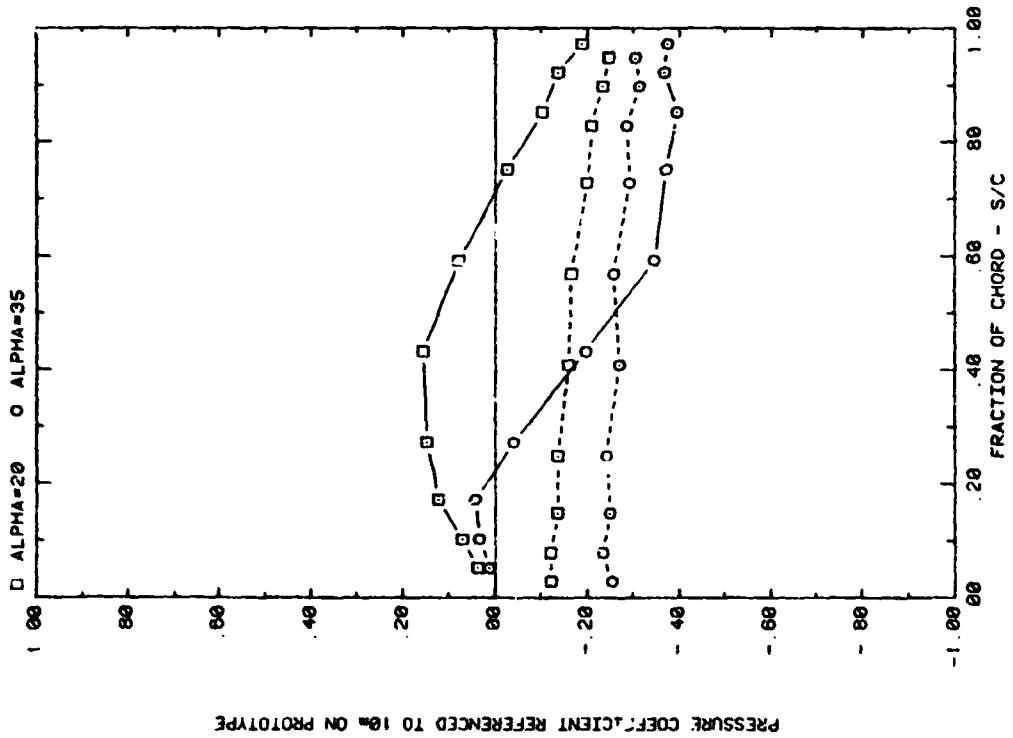


FRONT AND BACK PRESSURES ON ARRAY #1 IN BOUNDARY LAYER  
EFFECT OF ATTACK ANGLE FOR SPACING = 3C

Plot 2-2-1. (Continued)

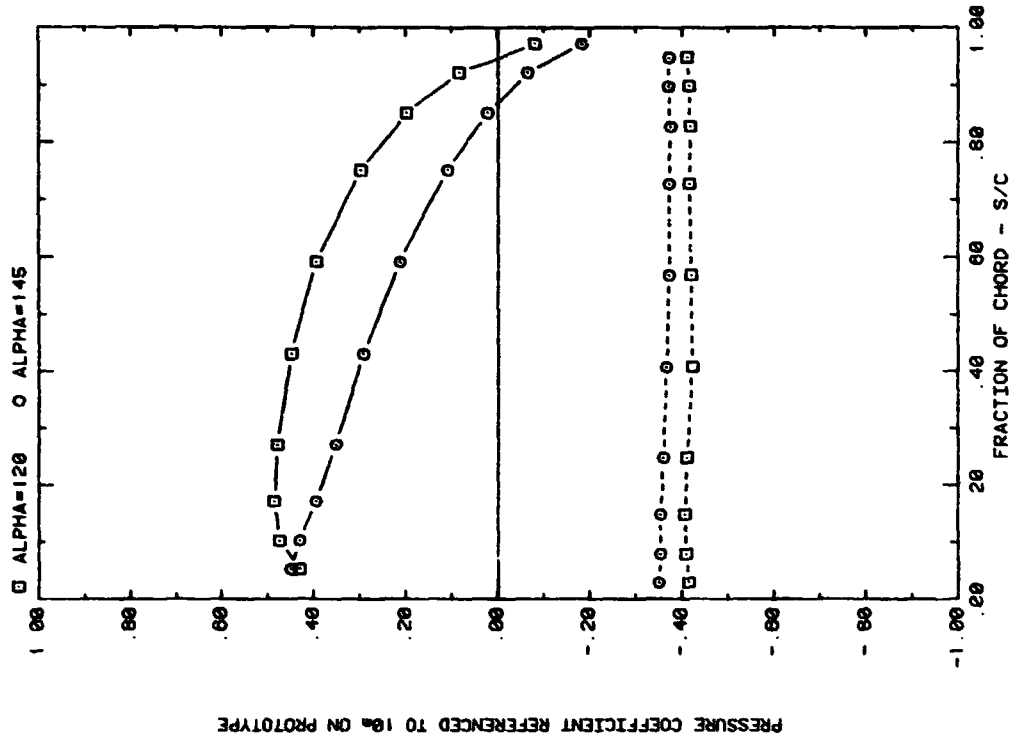


FRONT AND BACK PRESSURES ON ARRAY #2 IN BOUNDARY LAYER  
EFFECT OF ATTACK ANGLE FOR SPACING = 2C

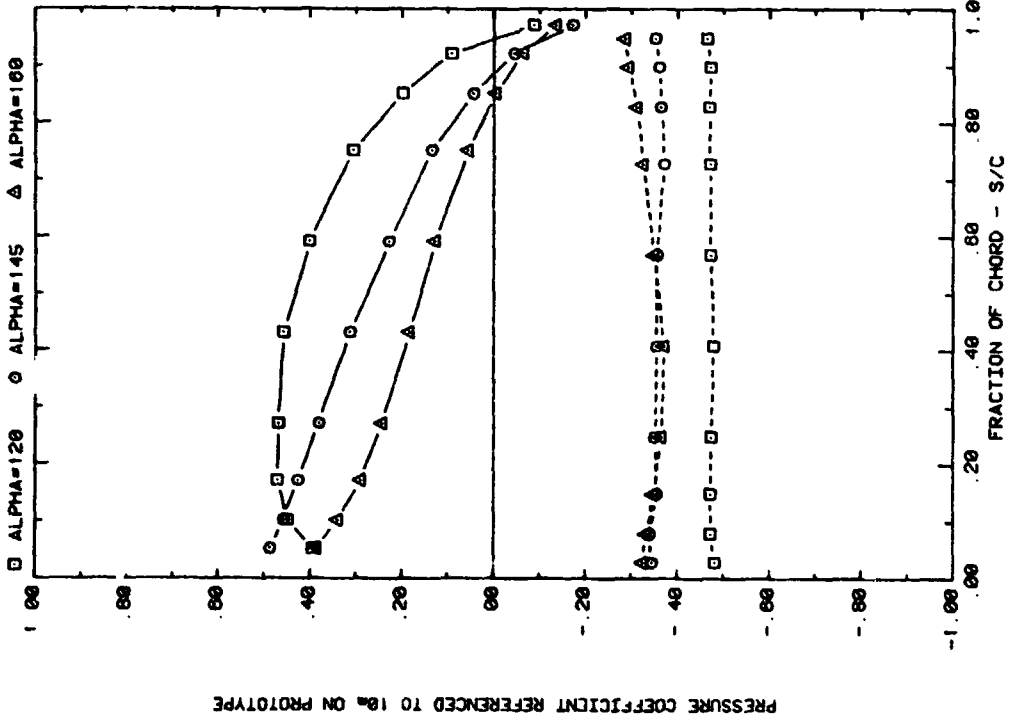


FRONT AND BACK PRESSURES ON ARRAY #2 IN BOUNDARY LAYER  
EFFECT OF ATTACK ANGLE FOR SPACING = 1.5C

Plot 2-2-1. (Continued)

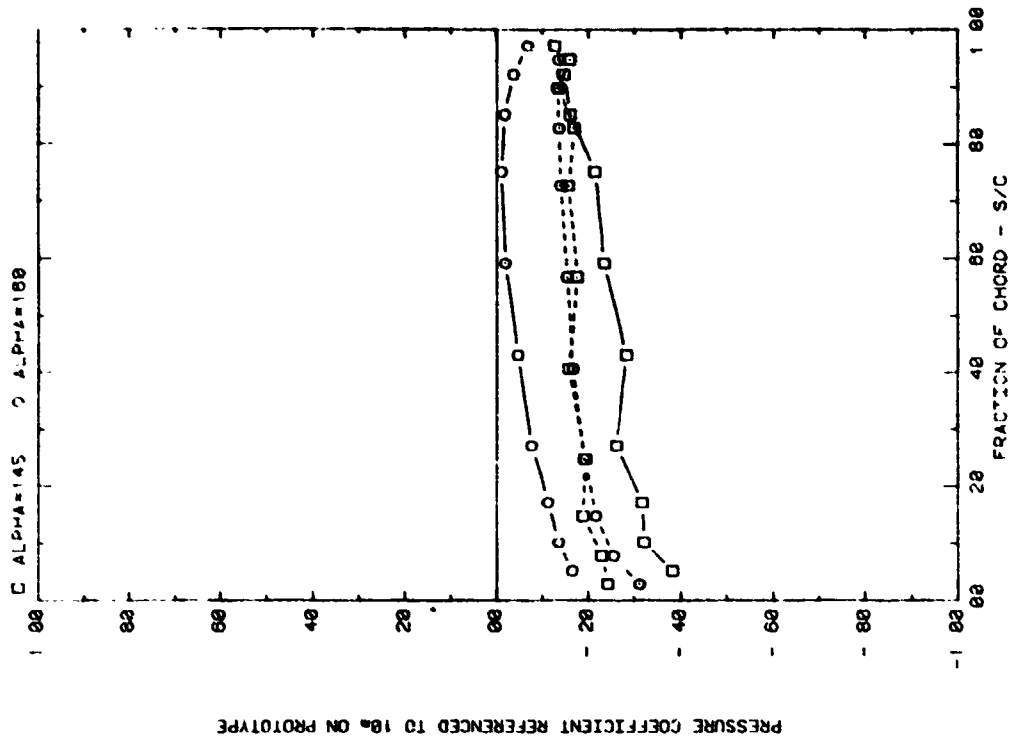
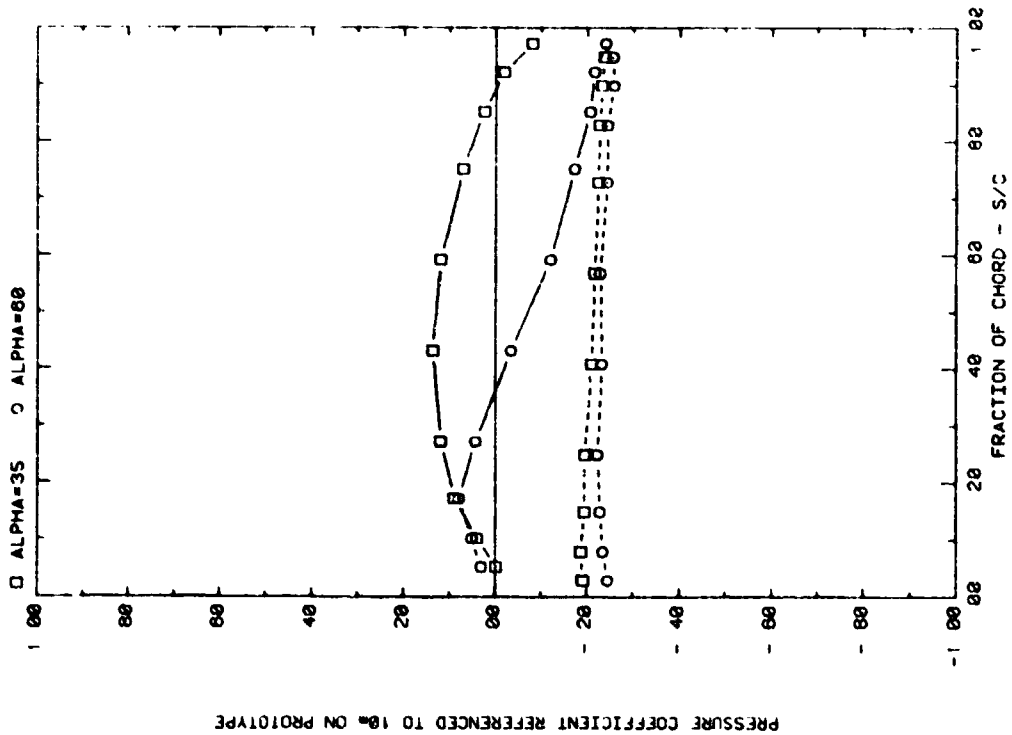


FRONT AND BACK PRESSURES ON ARRAY #1 IN BOUNDARY LAYER  
EFFECT OF ATTACK ANGLE FOR SPACING = 3C

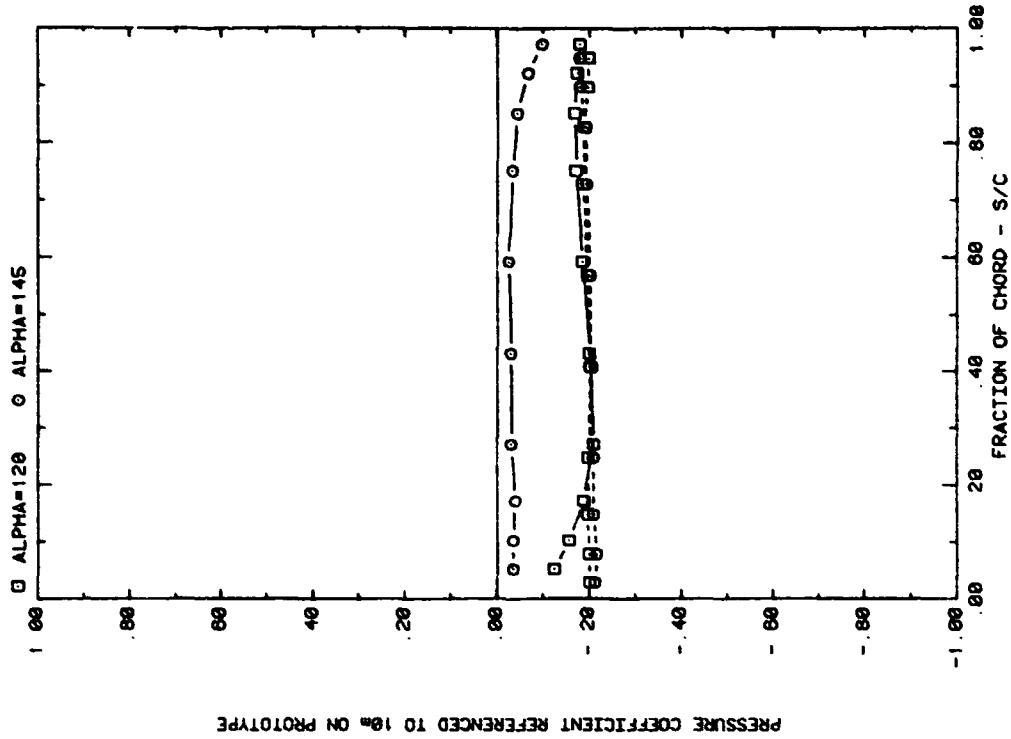


FRONT AND BACK PRESSURES ON ARRAY #1 IN BOUNDARY LAYER  
EFFECT OF ATTACK ANGLE FOR SPACING = 2C

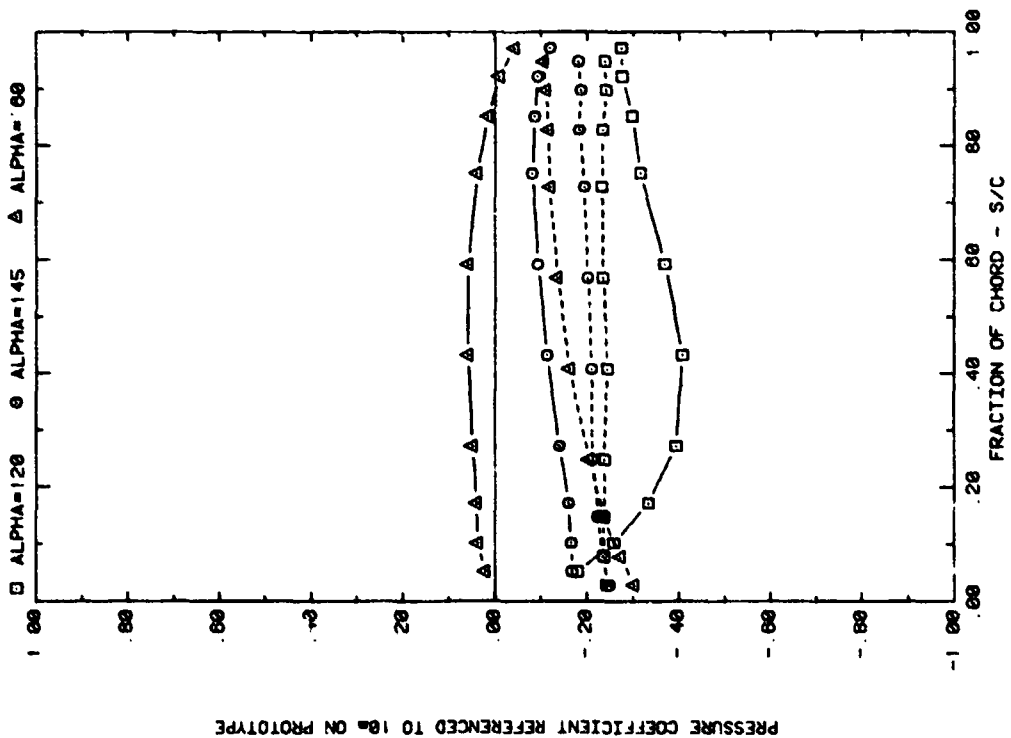
Plot 2-2-1. (Continued)



Plot 2-2-1. (Continued)

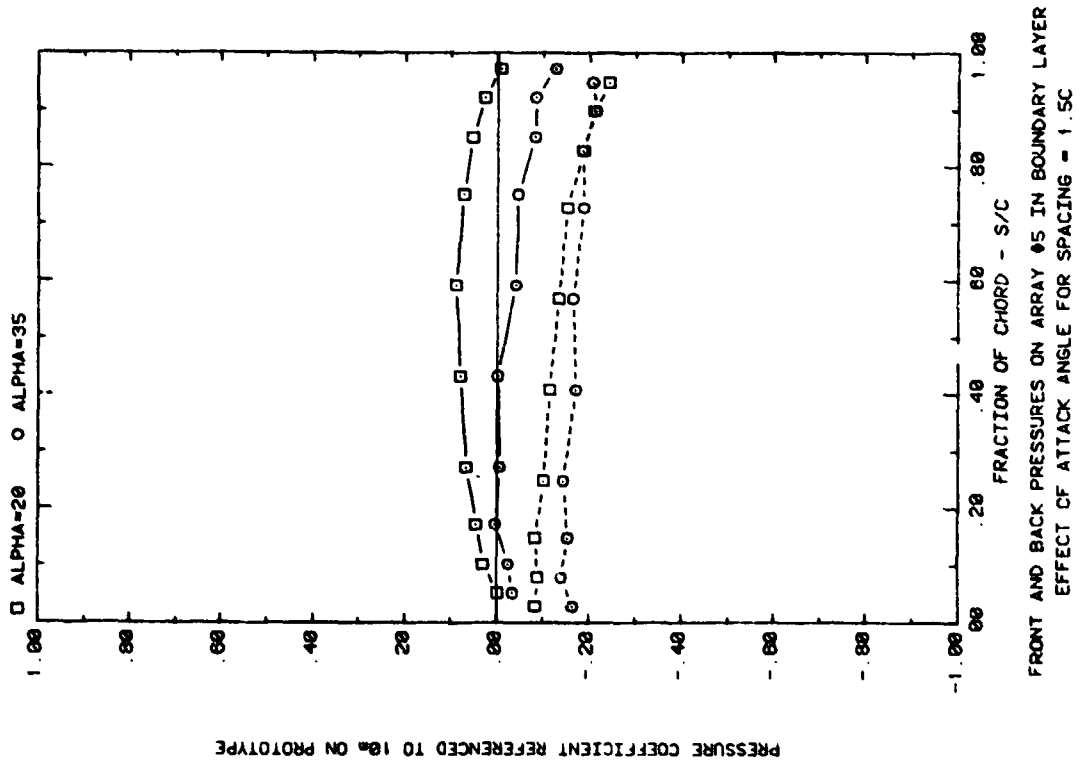
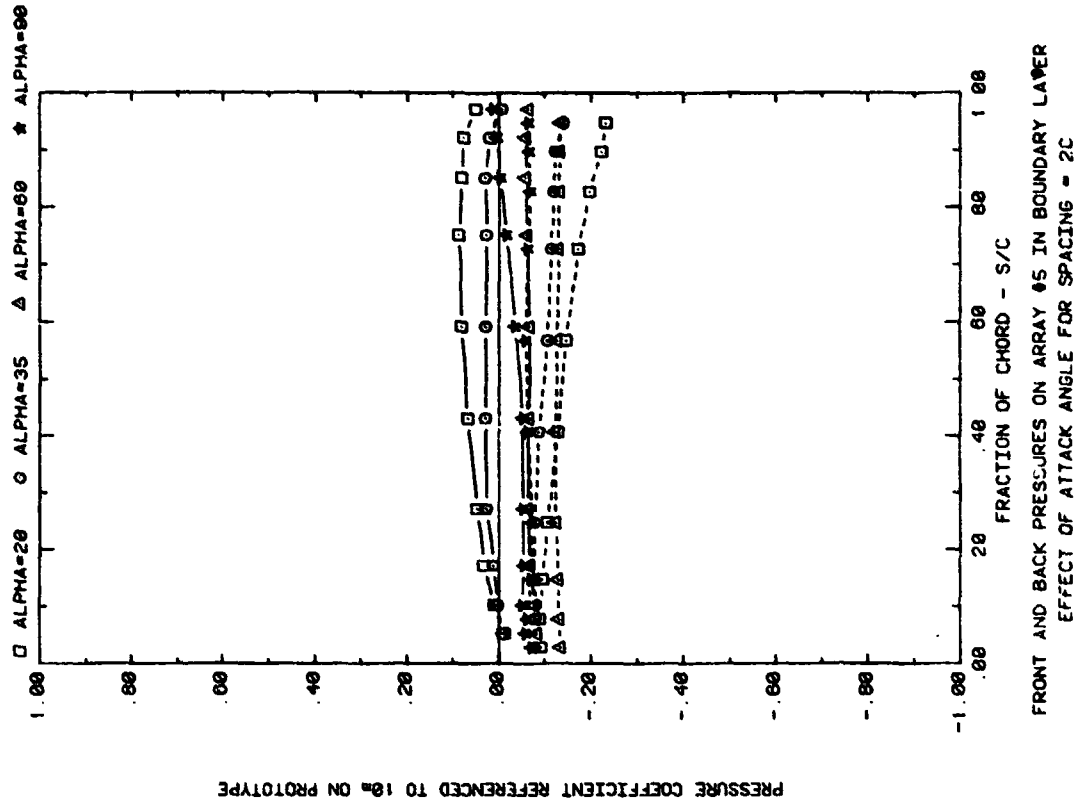


FRONT AND BACK PRESSURES ON ARRAY #2 IN BOUNDARY LAYER  
EFFECT OF ATTACK ANGLE FOR SPACING = 3C

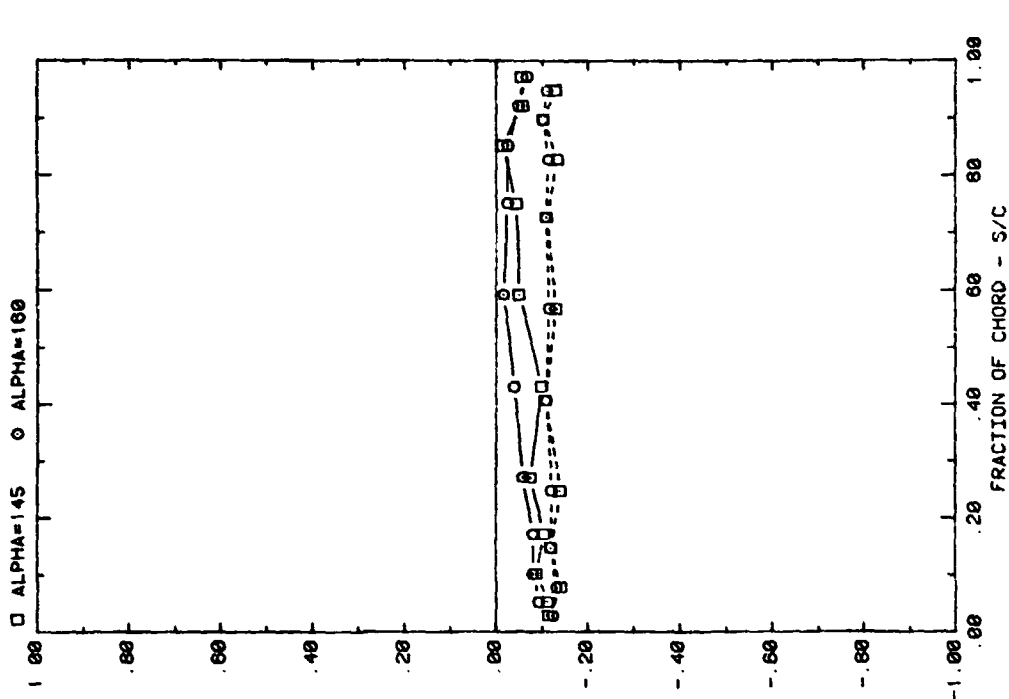


FRONT AND BACK PRESSURES ON ARRAY #2 IN BOUNDARY LAYER  
EFFECT OF ATTACK ANGLE FOR SPACING = 2C

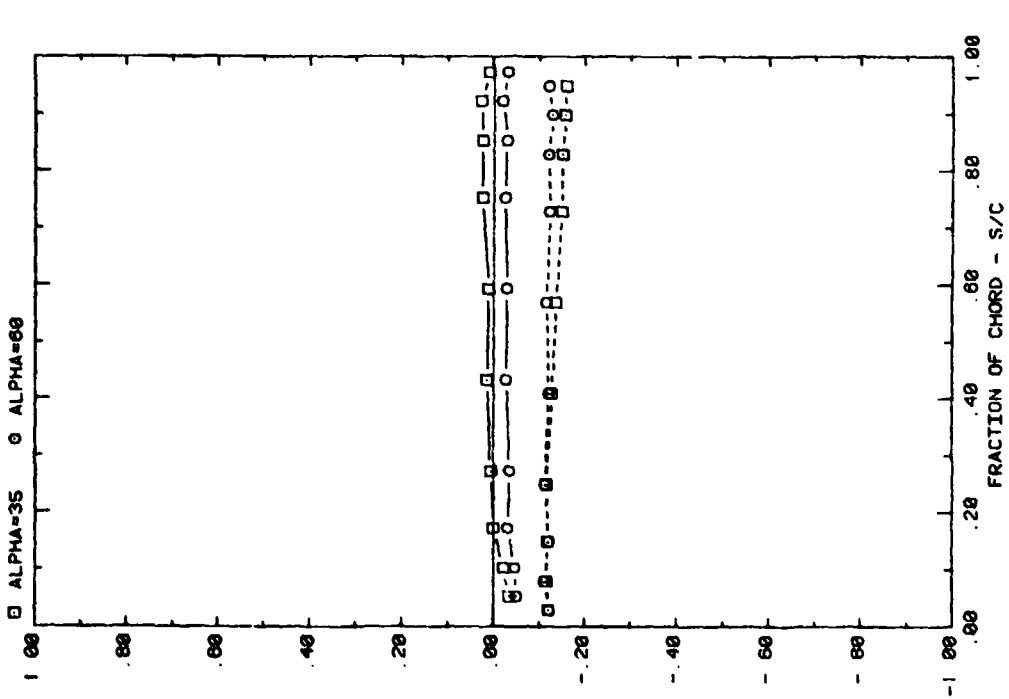
Plot 2-2-1. (Continued)



Plot 2-2-1. (Continued)

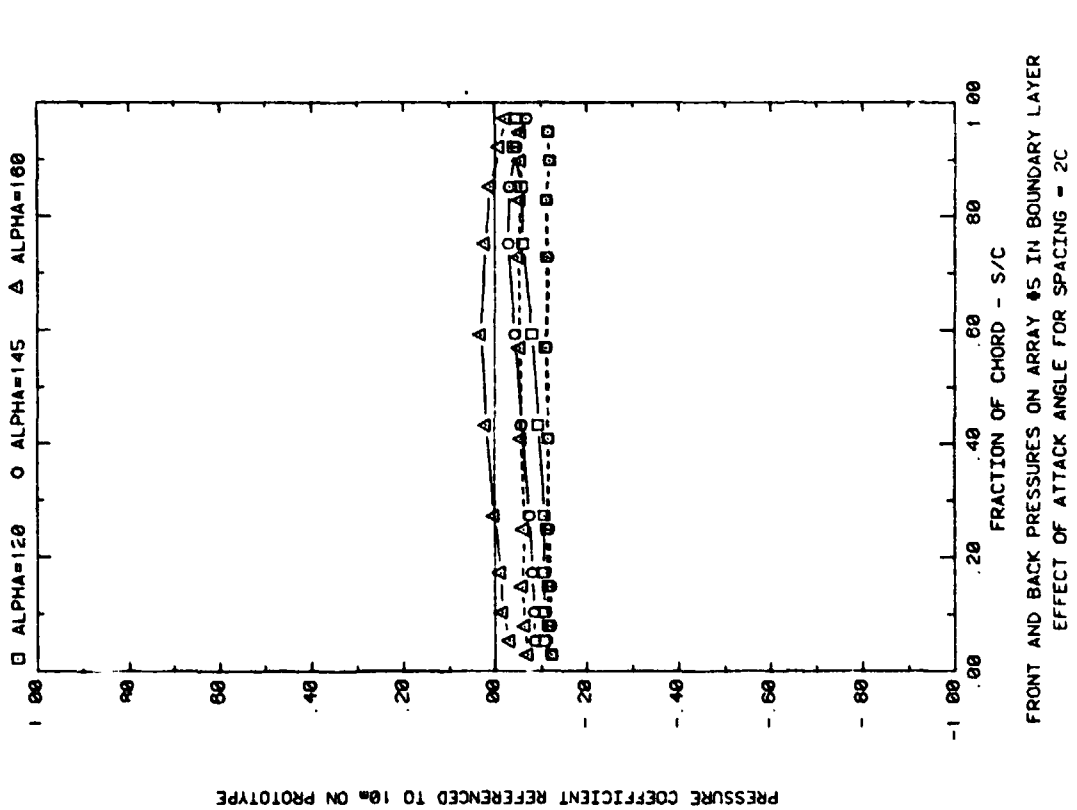
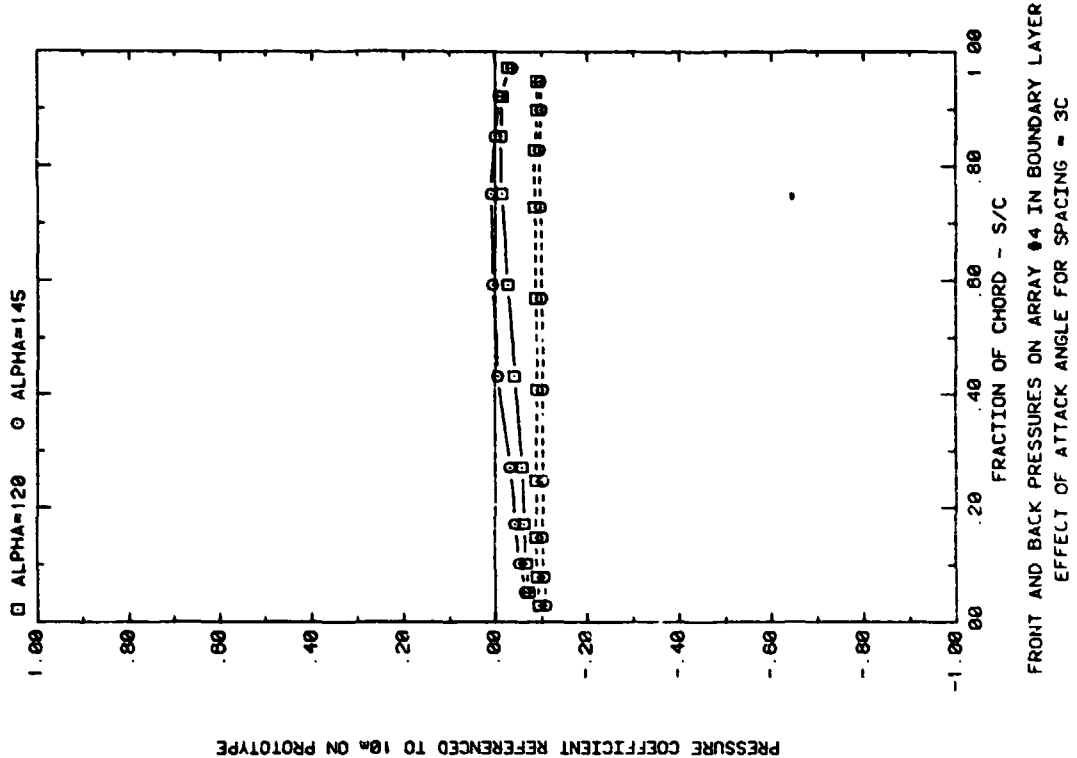


PRESSURE COEFFICIENT REFERENCED TO 10% ON PROTOTYPE

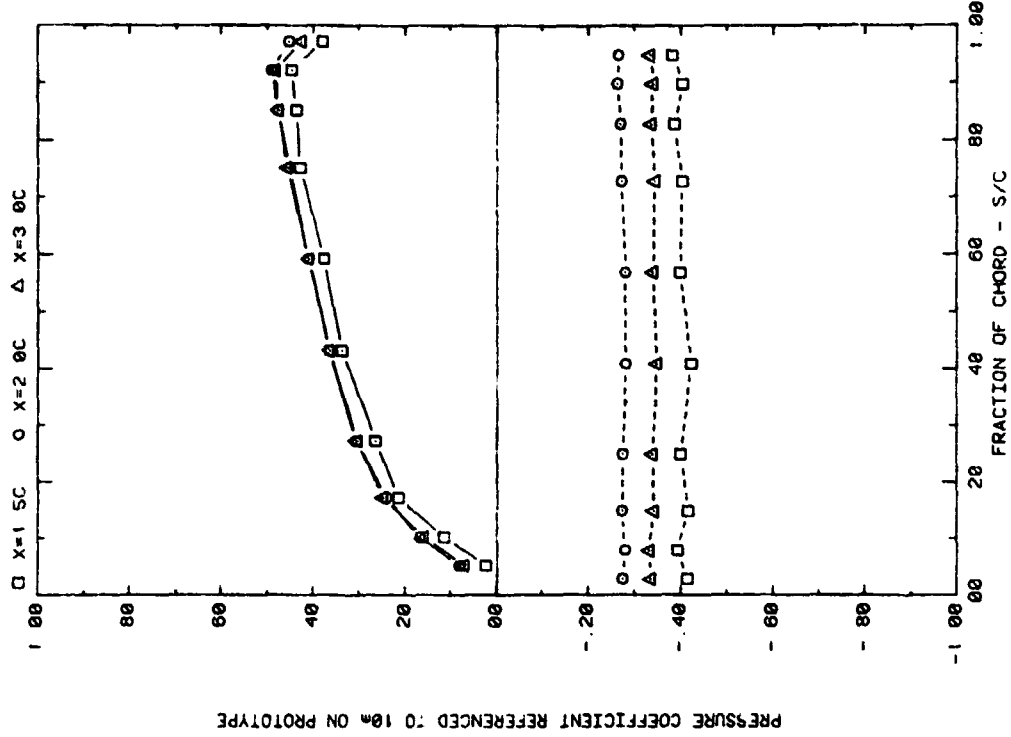


PRESSURE COEFFICIENT REFERENCED TO 10% ON PROTOTYPE

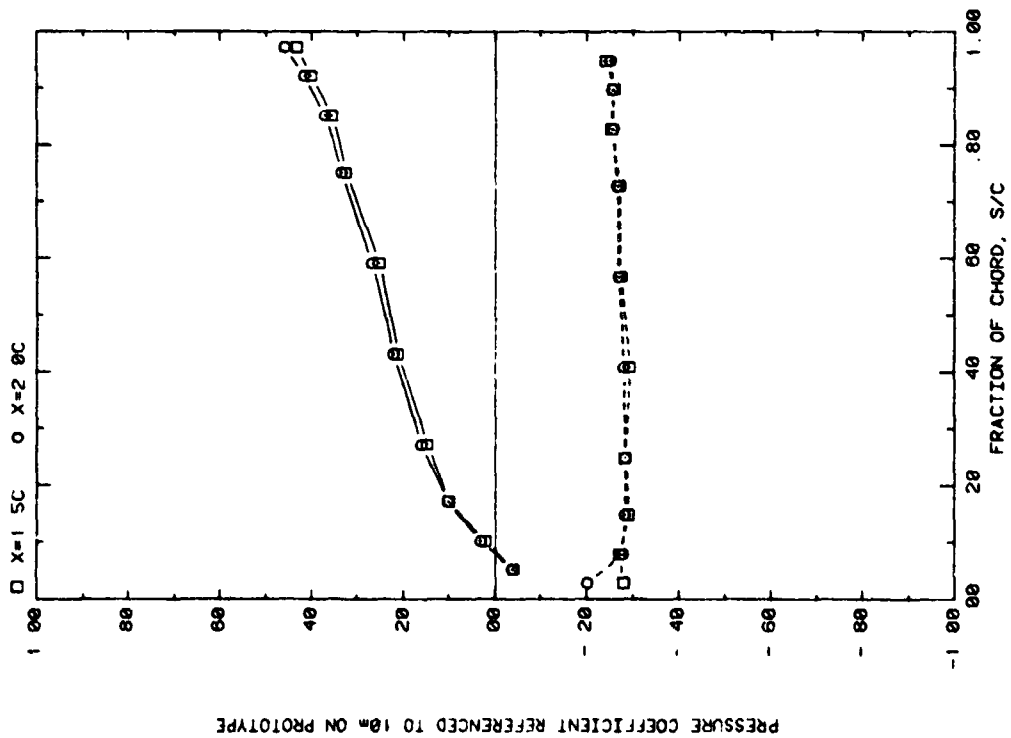
Plot 2-2-1. (Continued)



Plot 2-2-1. (Concluded)

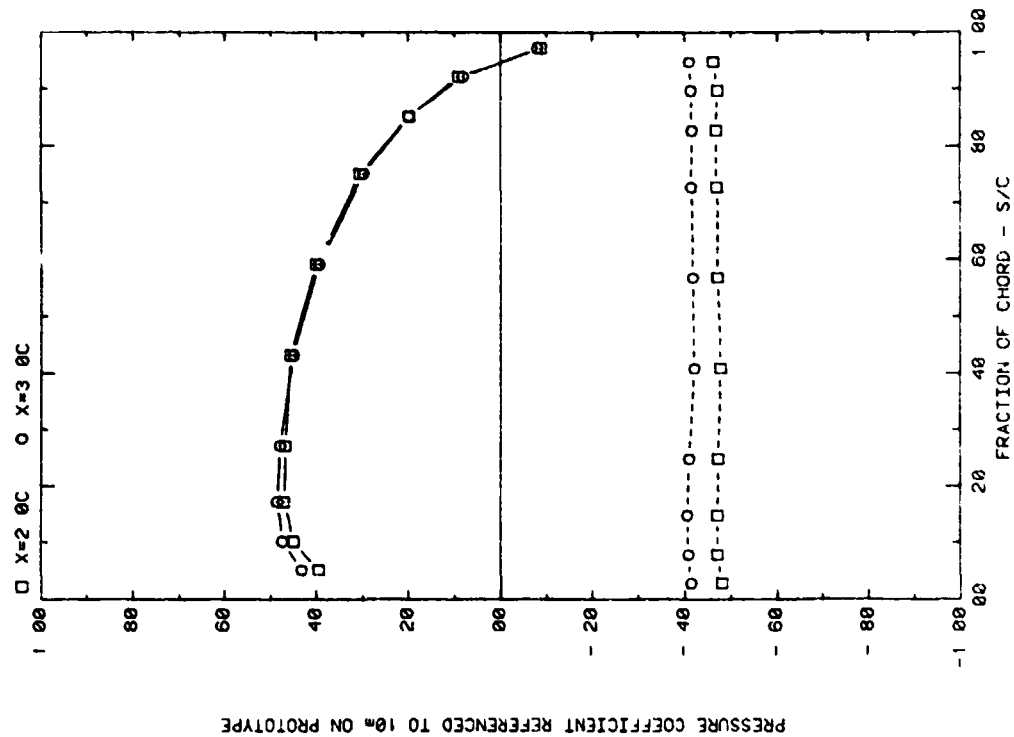


FRONT AND BACK PRESSURES ON ARRAY #1 IN BOUNDARY LAYER  
EFFECT OF SEPARATION (X) ON ATTACK ANGLE 35, H/C = 0.25

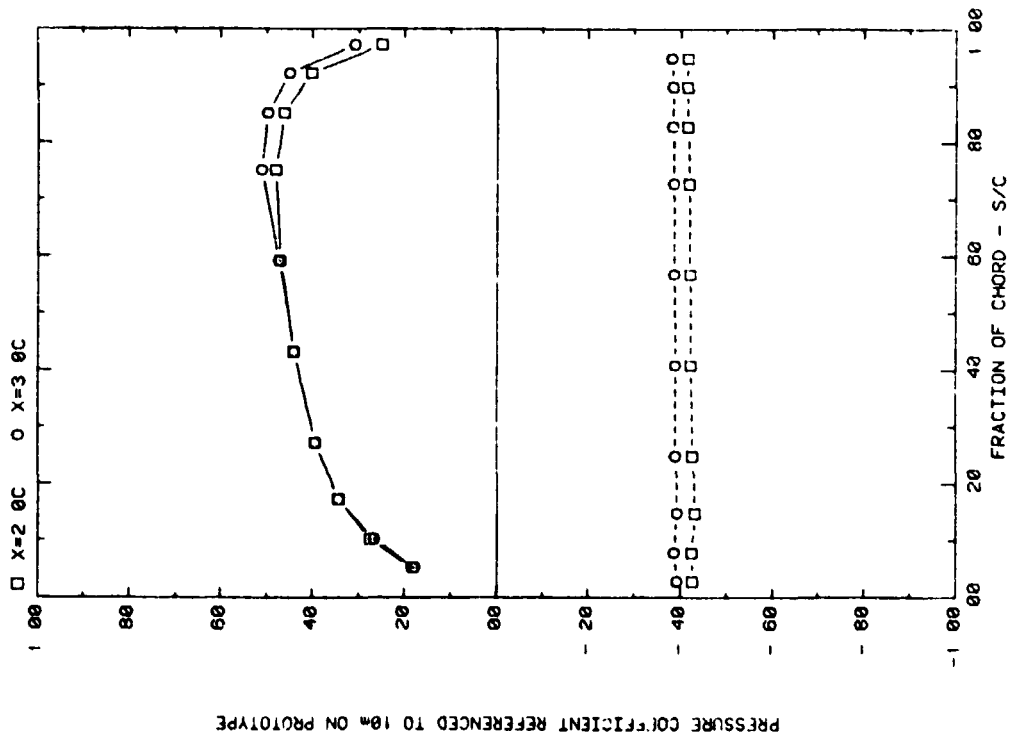


FRONT AND BACK PRESSURES ON ARRAY #1 IN BOUNDARY LAYER  
EFFECT OF SEPARATION (X) ON ATTACK ANGLE 20, H/C = 0.25

Plot 2-2-2. Multiple Arrays without Fence, Nonuniform Flow Study  
Effect of Separation Distance

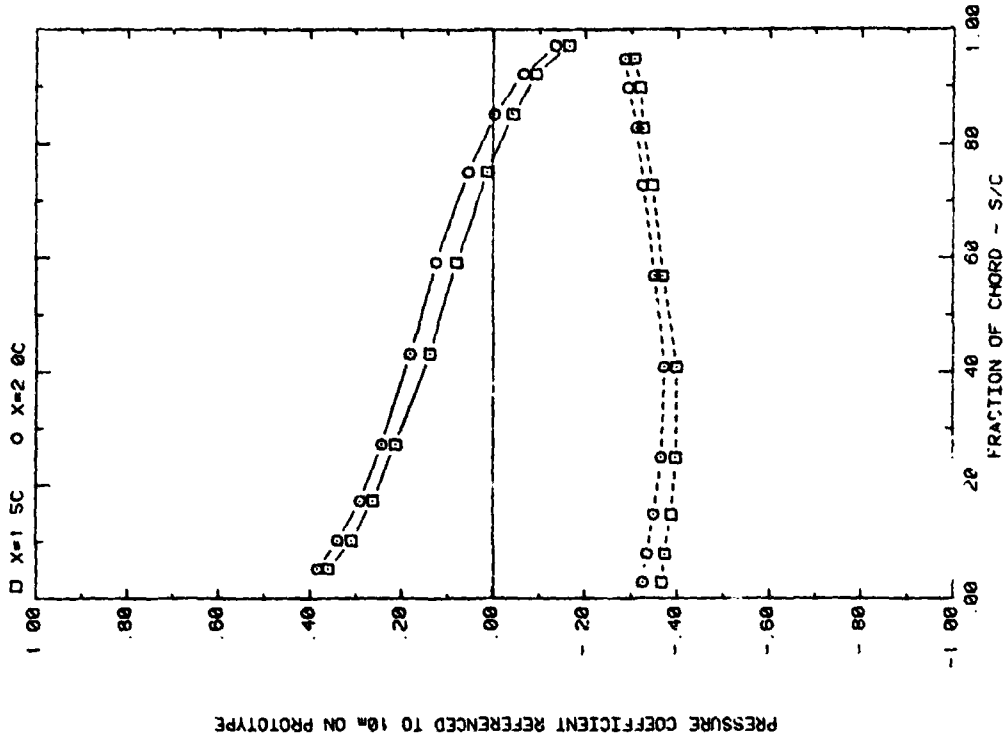


FRONT AND BACK PRESSURES ON ARRAY #1 IN BOUNDARY LAYER  
EFFECT OF SEPARATION (X) ON ATTACK ANGLE 120, H/C = 0.25

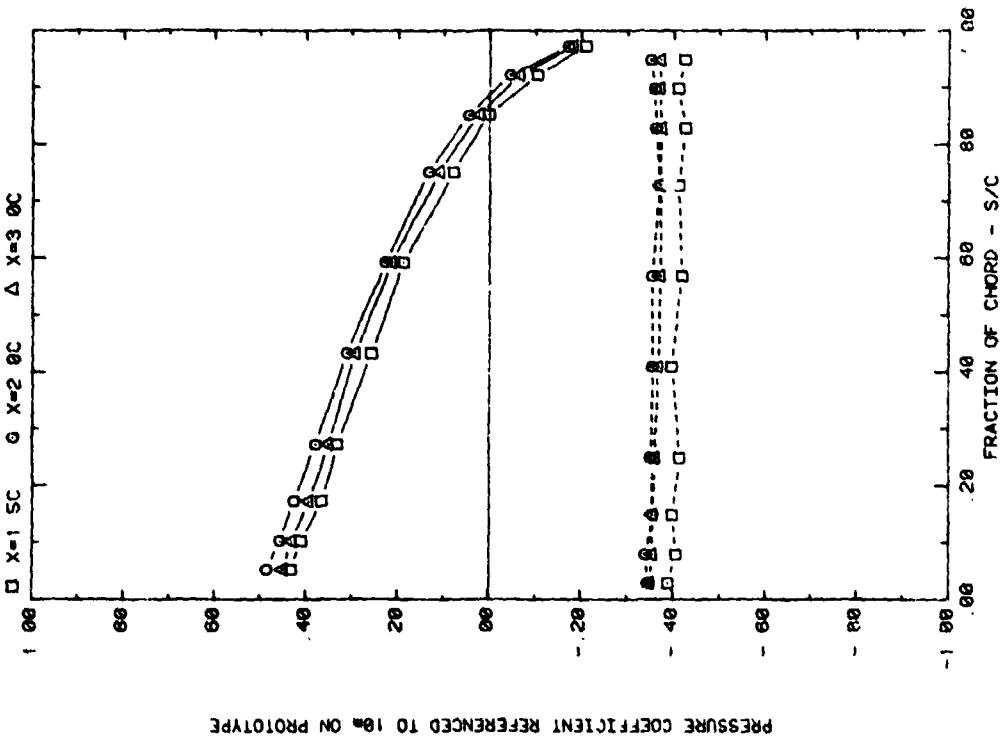


FRONT AND BACK PRESSURES ON ARRAY #1 IN BOUNDARY LAYER  
EFFECT OF SEPARATION (X) ON ATTACK ANGLE 60, H/C = 0.25

Plot 2-2-2. (Continued)

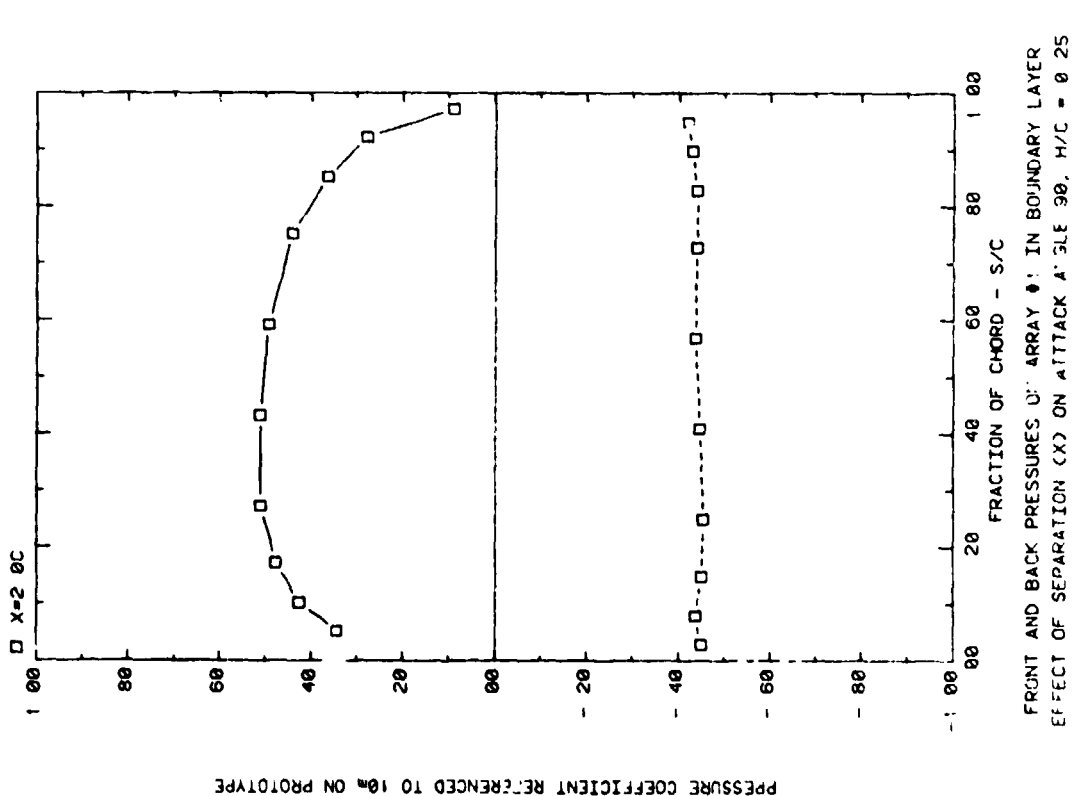
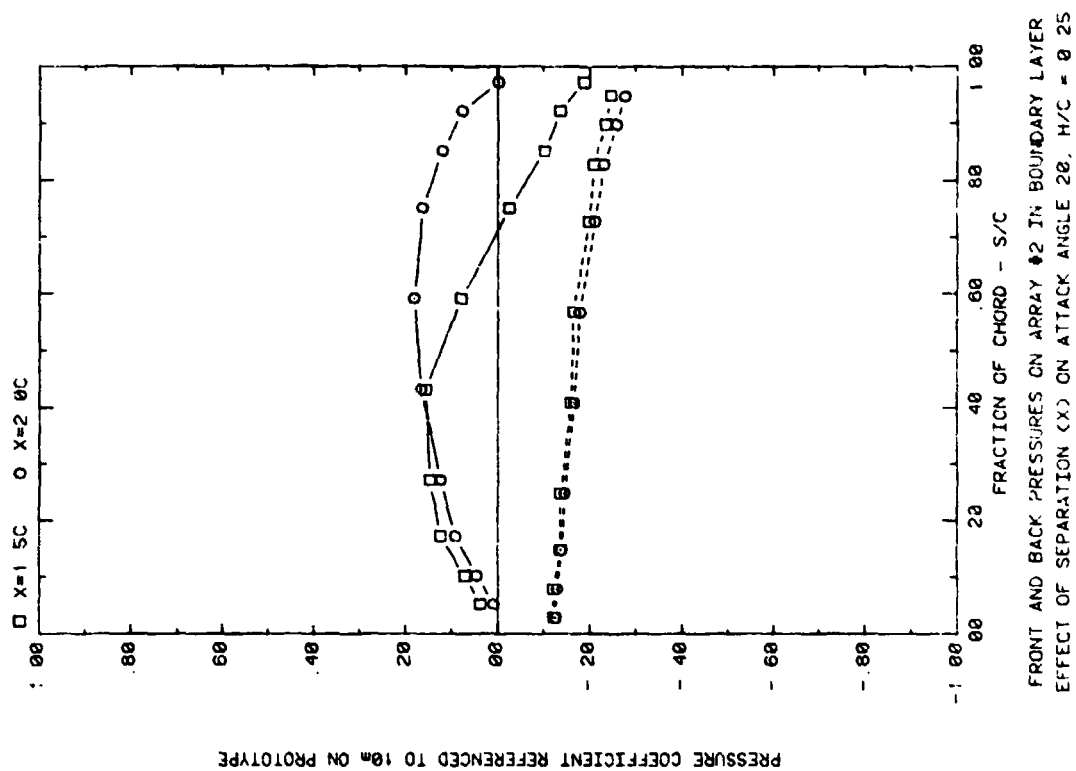


FRONT AND BACK PRESSURES ON ARRAY #1 IN BOUNDARY LAYER  
EFFECT OF SEPARATION (X) ON ATTACK ANGLE 160, H/C = 0.25

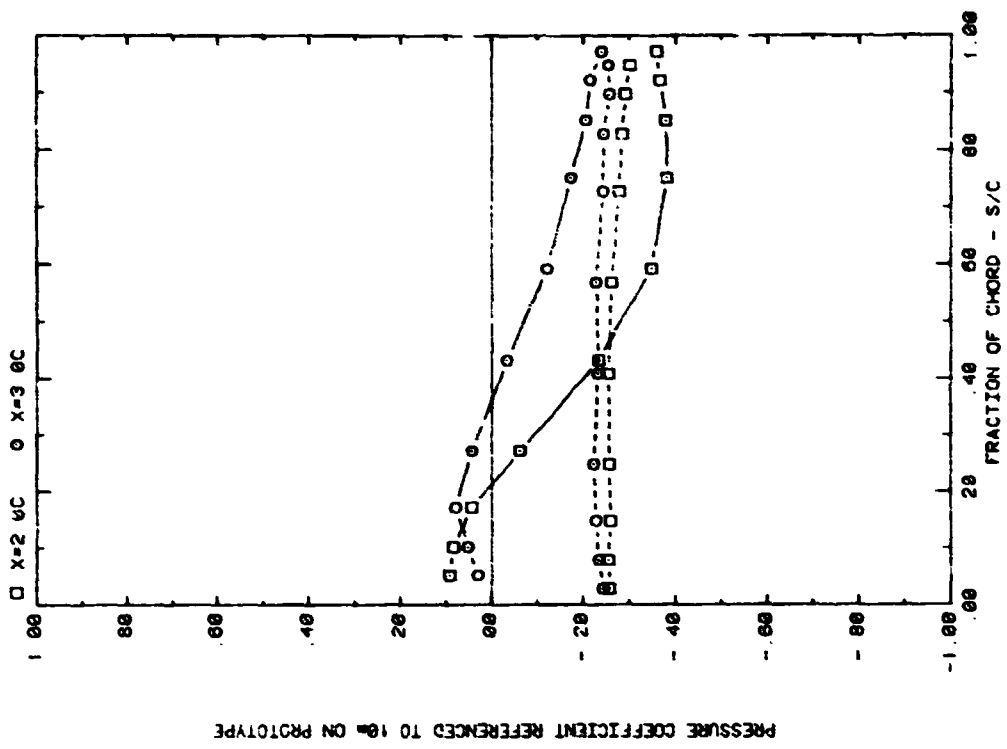


FRONT AND BACK PRESSURES ON ARRAY #1 IN BOUNDARY LAYER  
EFFECT OF SEPARATION (X) ON ATTACK ANGLE 145, H/C = 0.25

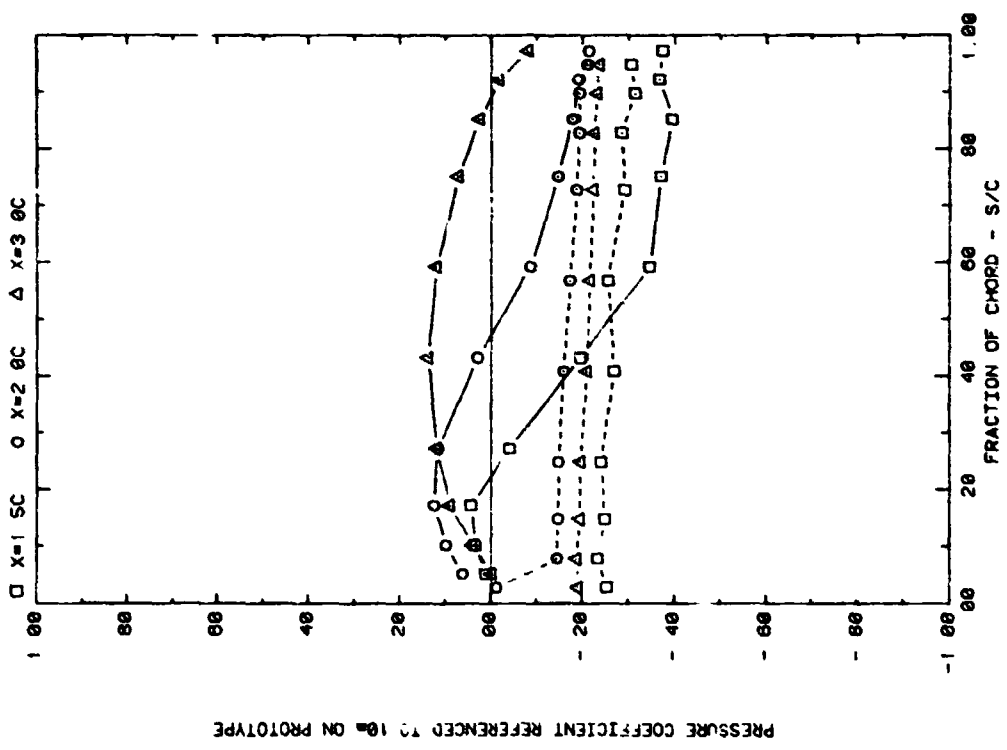
Plot 2-2-2. (Continued)



Plot 2-2-2. (Continued)

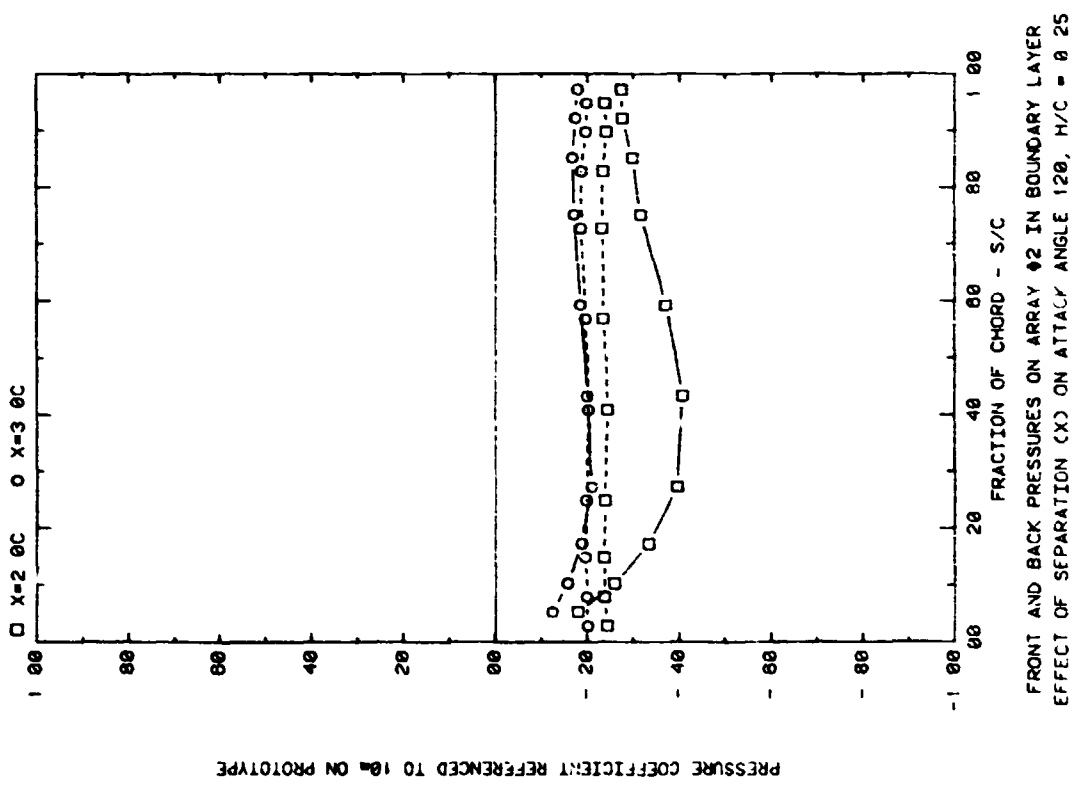
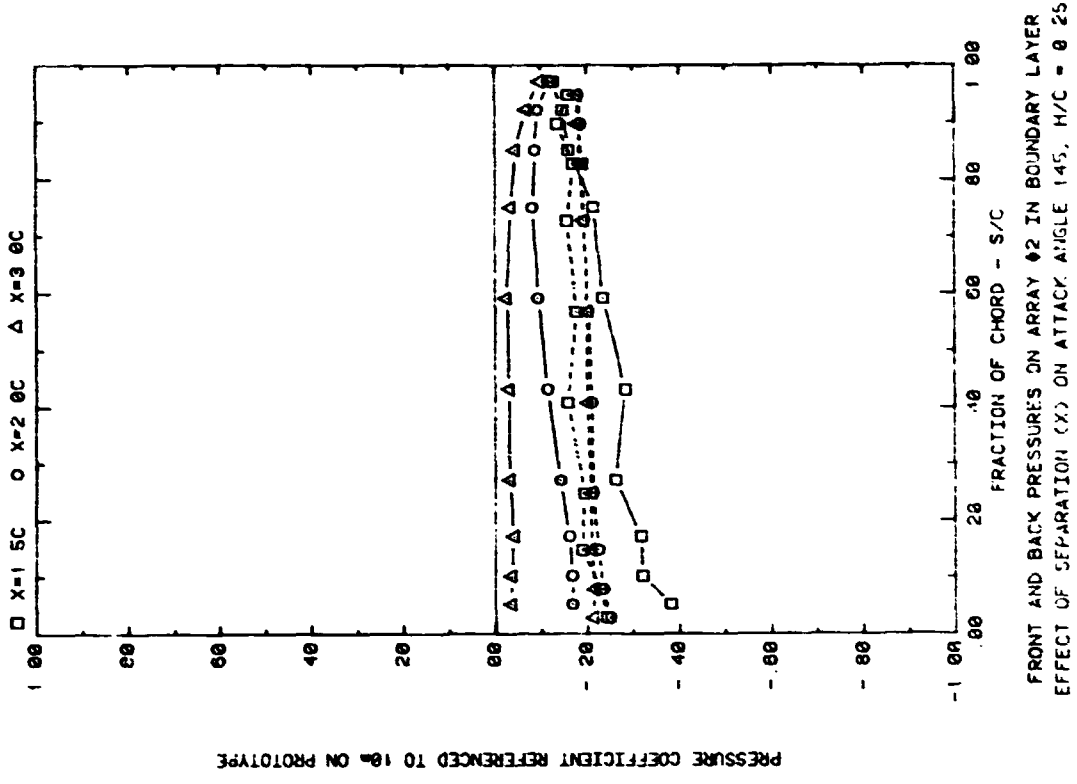


FRONT AND BACK PRESSURES ON ARRAY #2 IN BOUNDARY LAYER EFFECT OF SEPARATION (X) ON ATTACK ANGLE 60, H/C = 0.25

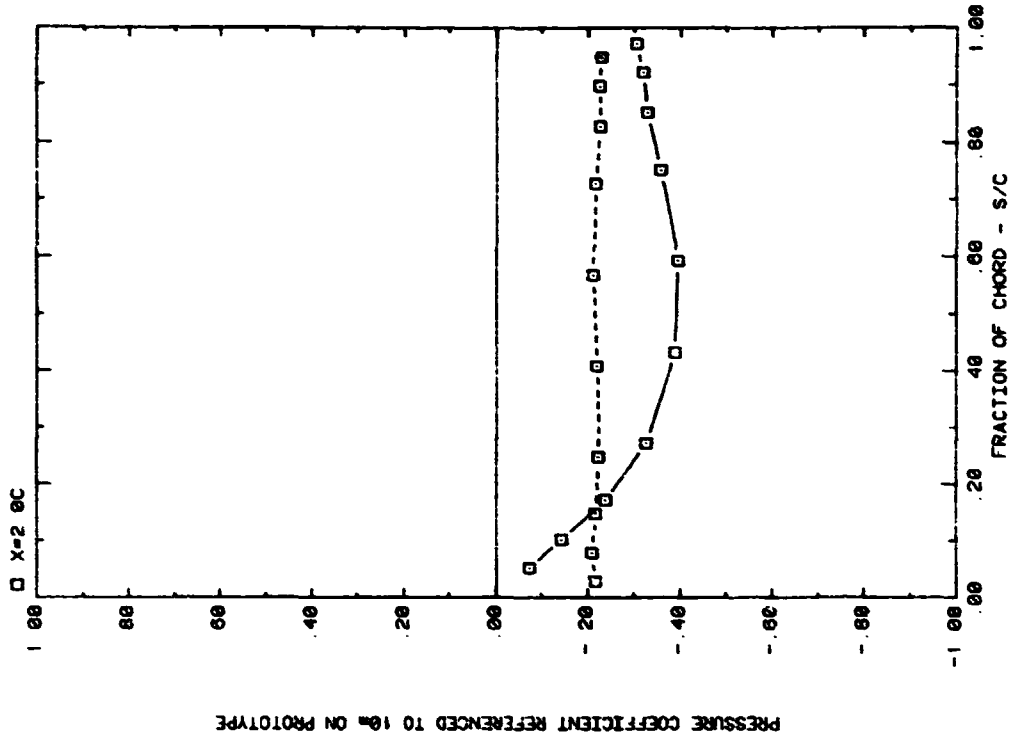


FRONT AND BACK PRESSURES ON ARRAY #2 IN BOUNDARY LAYER EFFECT OF SEPARATION (X) ON ATTACK ANGLE 35, H/C = 0.25

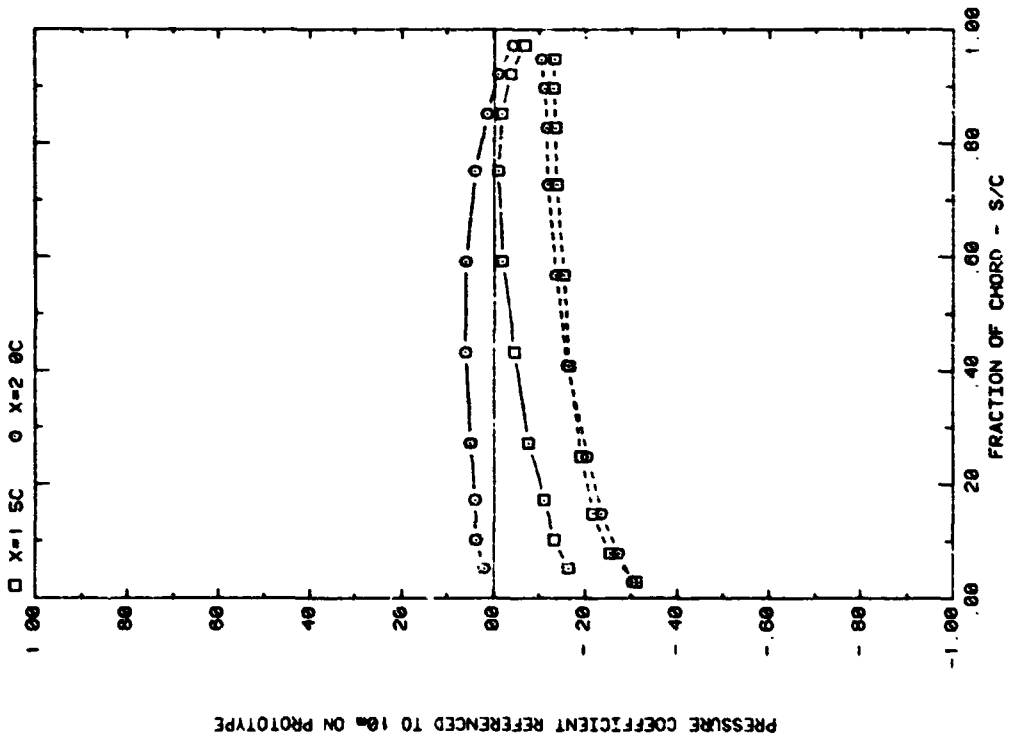
Plot 2-2-2. (Continued)



Plot 2-2-2. (Continued)

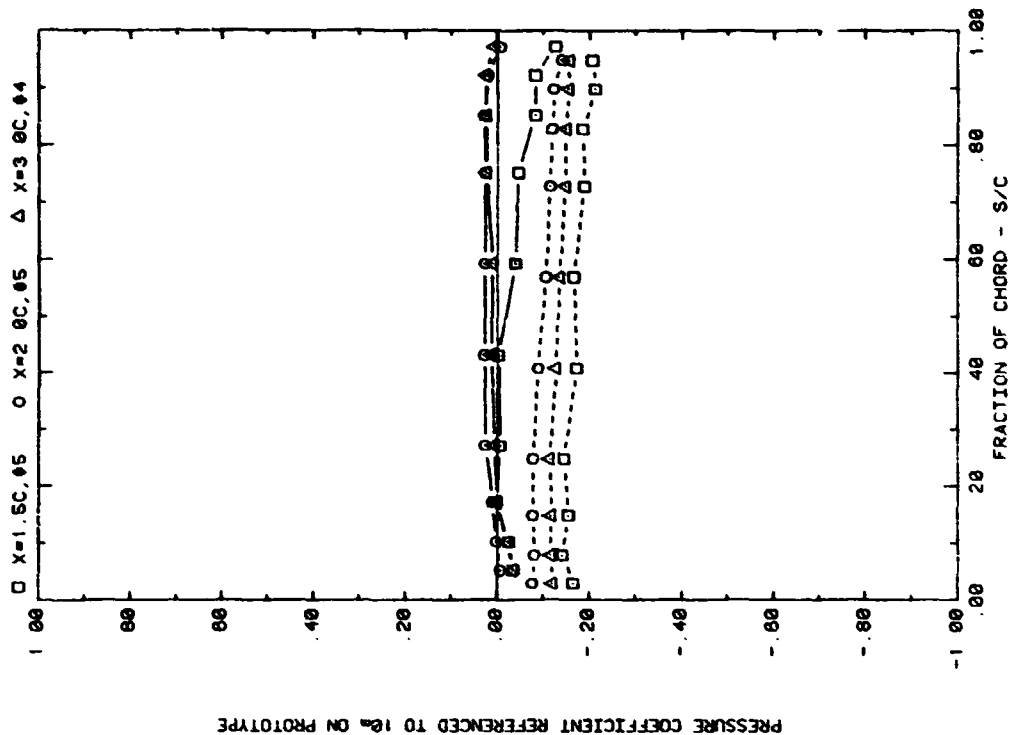


FRONT AND BACK PRESSURES ON ARRAY #2 IN BOUNDARY LAYER  
EFFECT OF SEPARATION (X) ON ATTACK ANGLE 90, H/C = 0.25

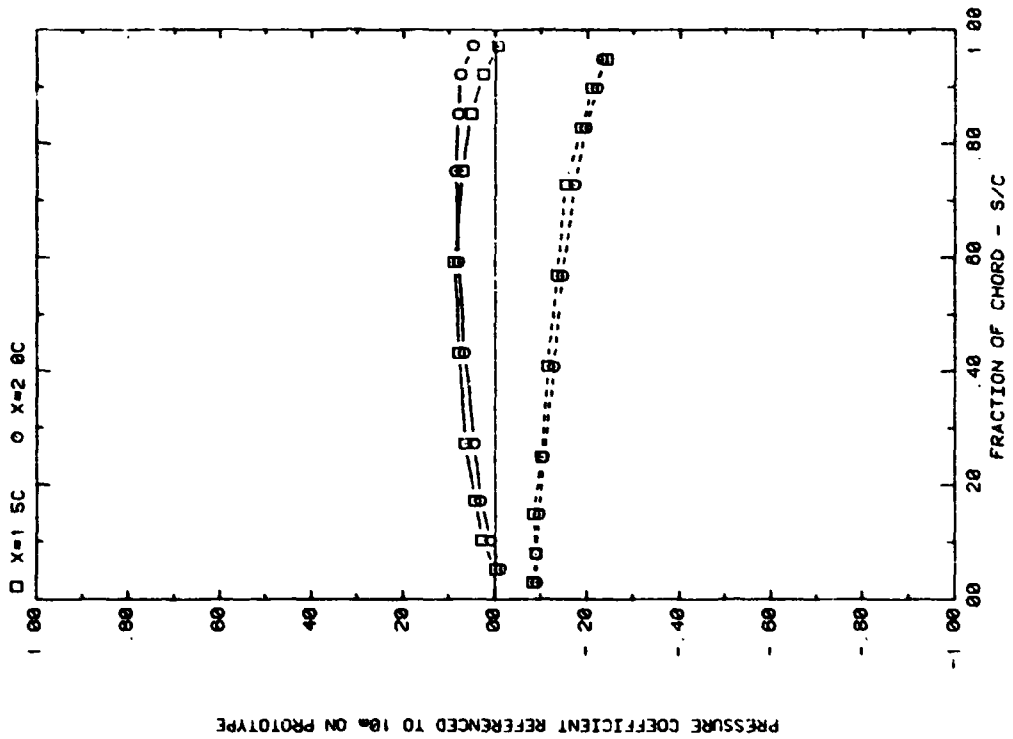


FRONT AND BACK PRESSURES ON ARRAY #2 IN BOUNDARY LAYER  
EFFECT OF SEPARATION (X) ON ATTACK ANGLE 180, H/C = 0.25

Plot 2-2-2. (Continued)

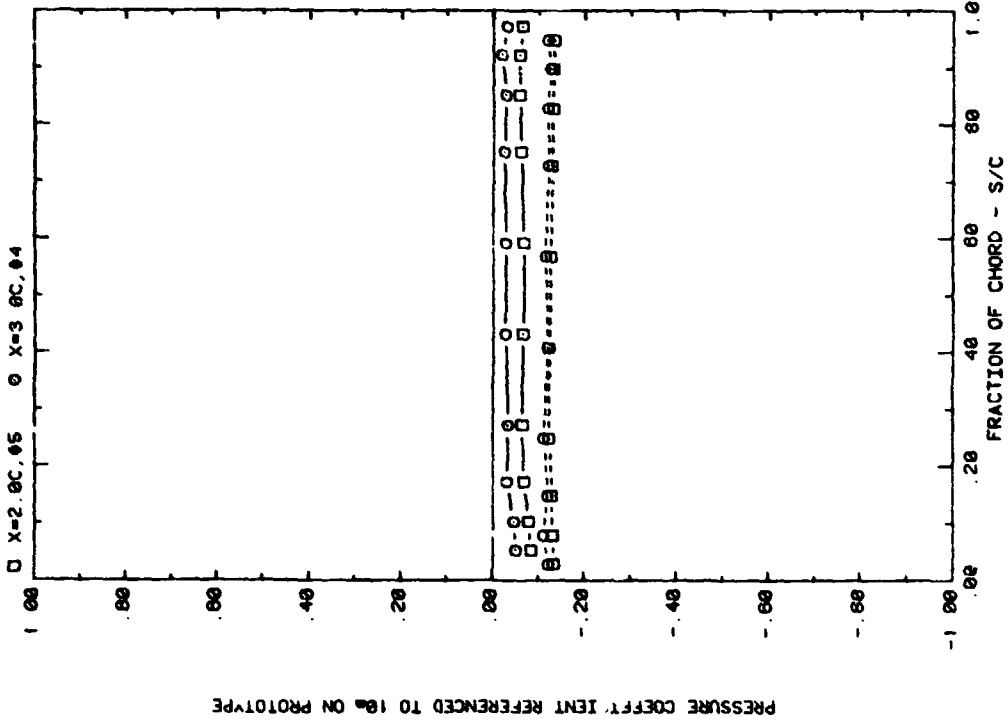


FRONT AND BACK PRESSURES ON ARRAY #5 IN BOUNDARY LAYER  
EFFECT OF SEPARATION (X) ON ATTACK ANGLE 20, H/C = 0.25

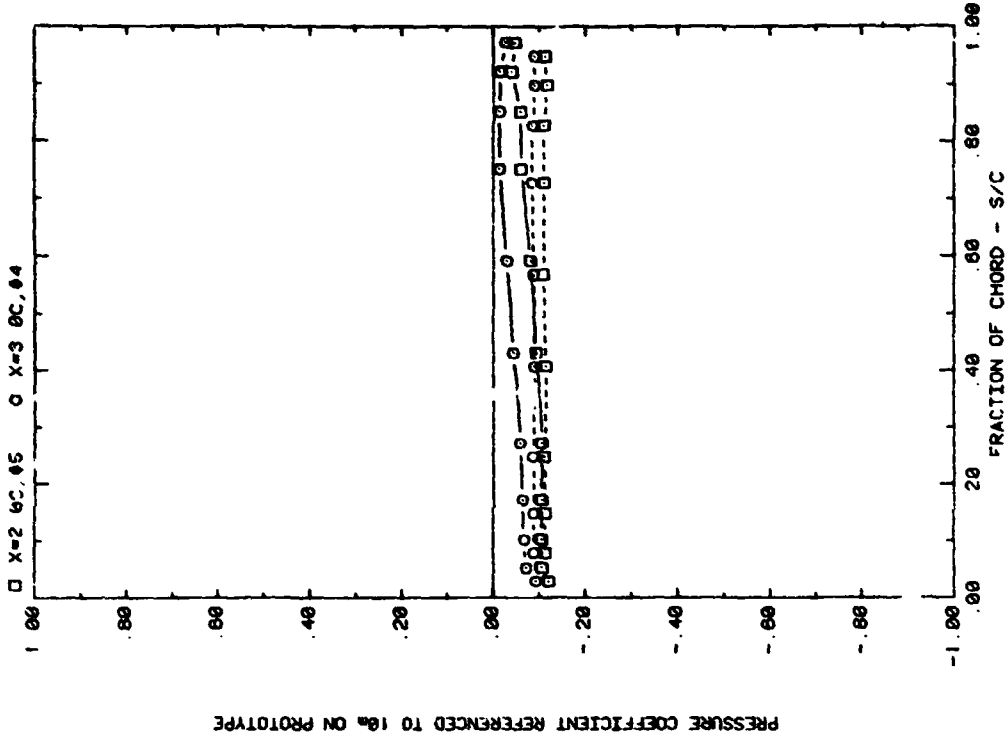


FRONT AND BACK PRESSURES ON ARRAY #5 IN BOUNDARY LAYER  
EFFECT OF SEPARATION (X) ON ATTACK ANGLE 35, H/C = 0.25

Plot 2-2-2. (Continued)

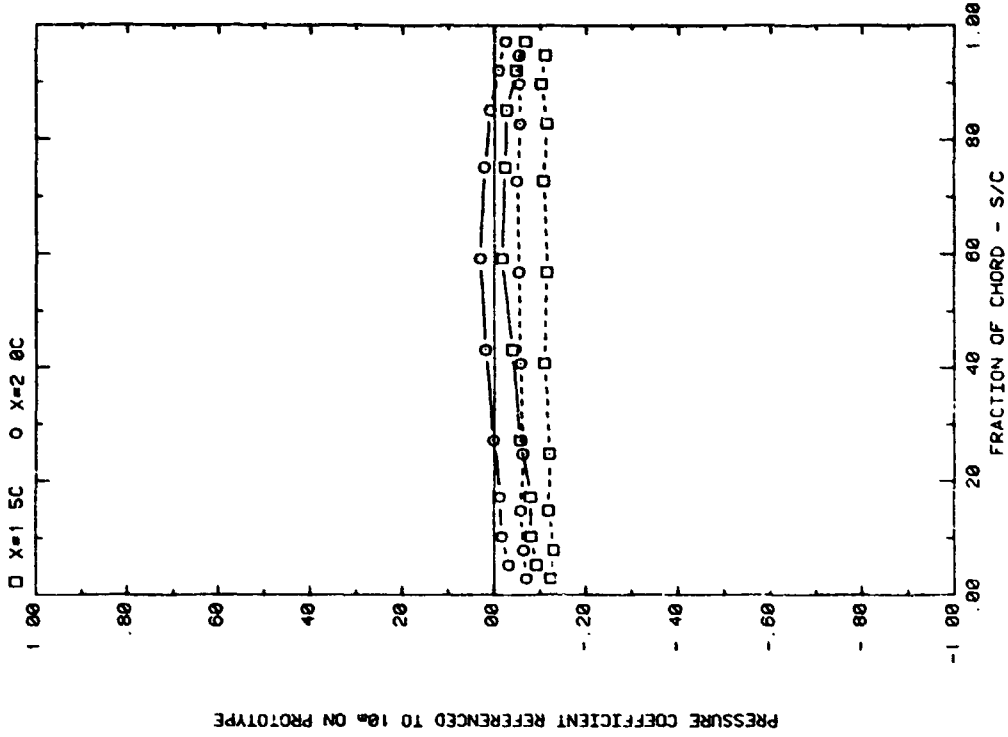


FRONT AND BACK PRESSURES ON ARRAY 60 OR 65 IN BOUNDARY LAYER  
EFFECT OF SEPARATION (X) ON ATTACK ANGLE 60, H/C = 0.25

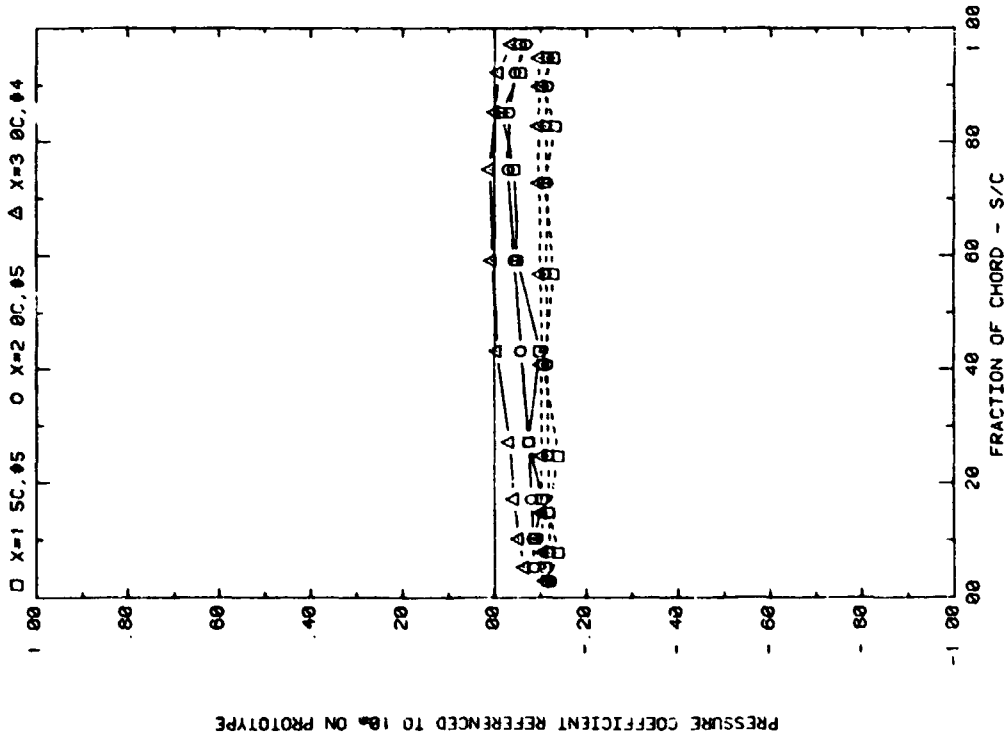


FRONT AND BACK PRESSURES ON ARRAY 64 OR 65 IN BOUNDARY LAYER  
EFFECT OF SEPARATION (X) ON ATTACK ANGLE 120, H/C = 0.25

Plot 2-2-2. (Continued)

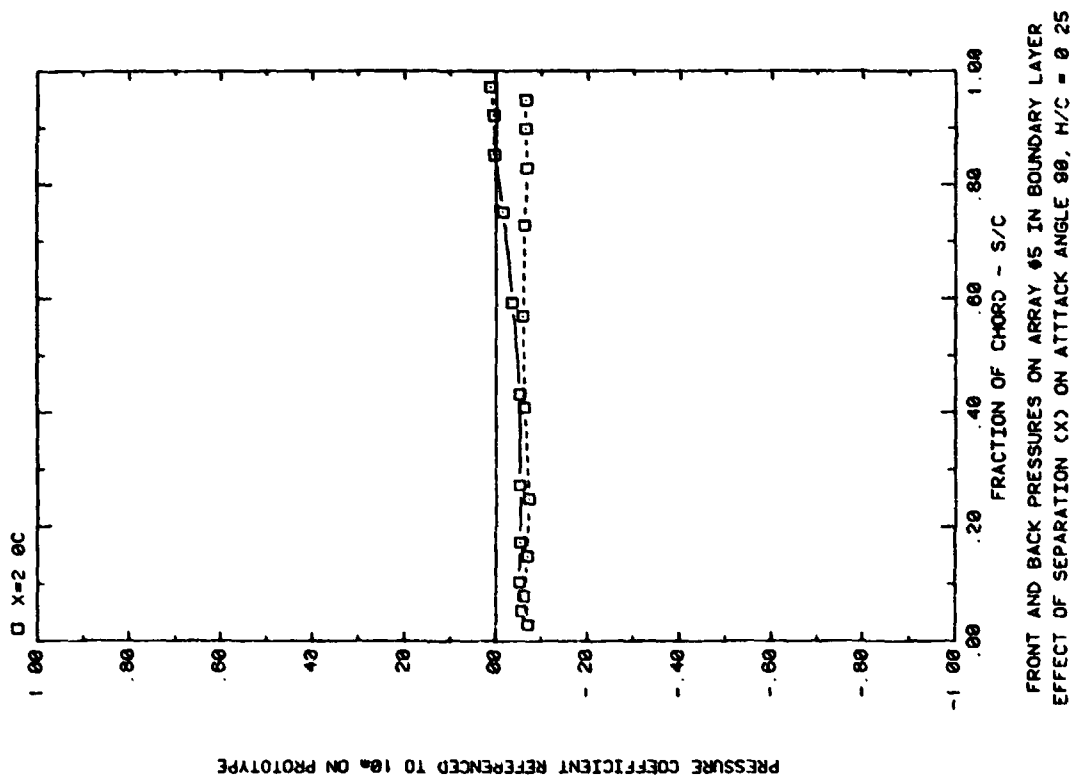


FRONT AND BACK PRESSURES ON ARRAY #5 IN BOUNDARY LAYER  
EFFECT OF SEPARATION (X) ON ATTACK ANGLE 160, H/C = 0.25

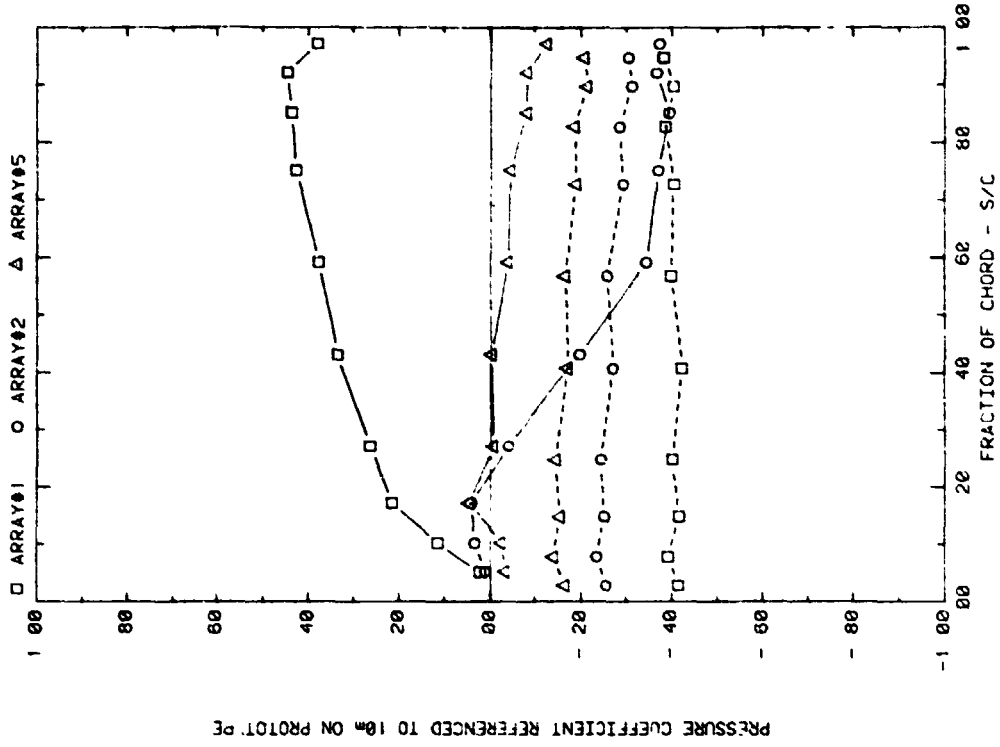


FRONT AND BACK PRESSURES ON ARRAY #4 OR #5 IN BOUNDARY LAYER  
EFFECT OF SEPARATION (X) ON ATTACK ANGLE 145, H/C = 0.25

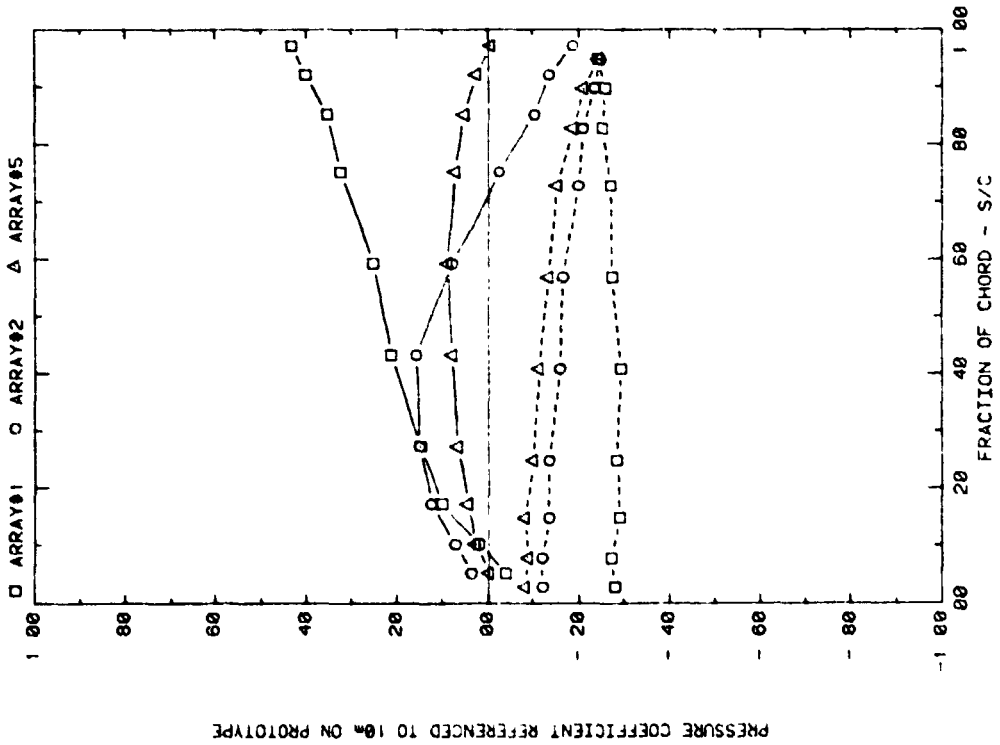
Plot 2-2-2. (Continued)



Plot 2-2-2. (Concluded)

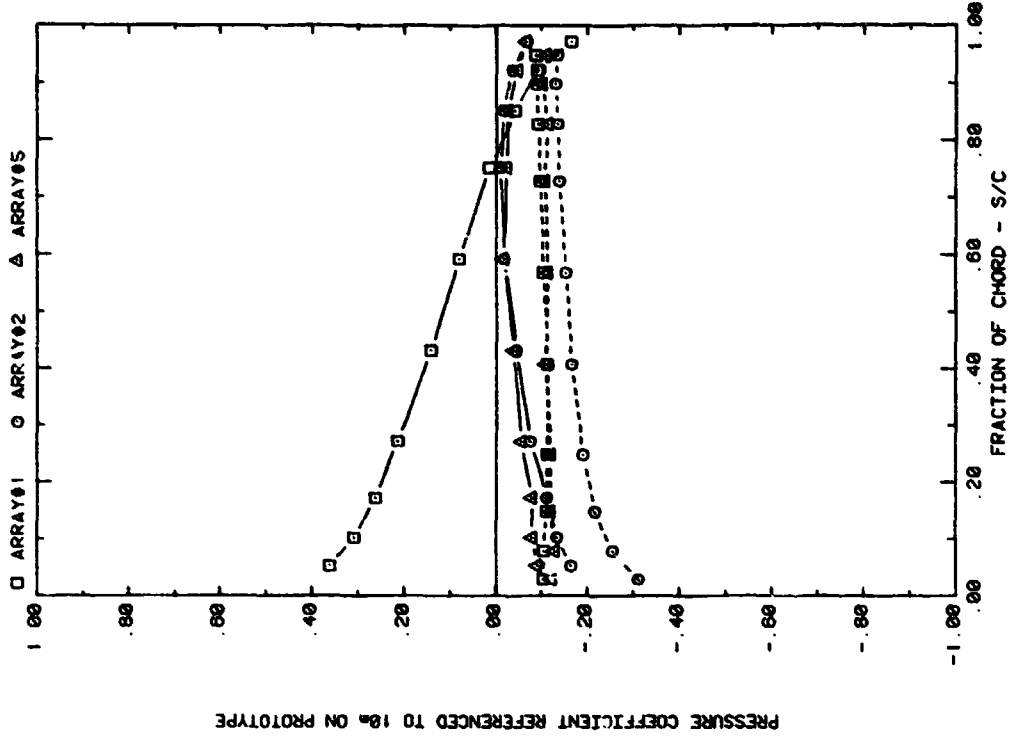


FRONT AND BACK PRESSURES ON ARRAYS IN BOUNDARY LAYER,  $X = 1.5C$   
EFFECT OF ARRAY CONFIGURATION ON ATTACK ANGLE 35,  $H/C = 0.25$

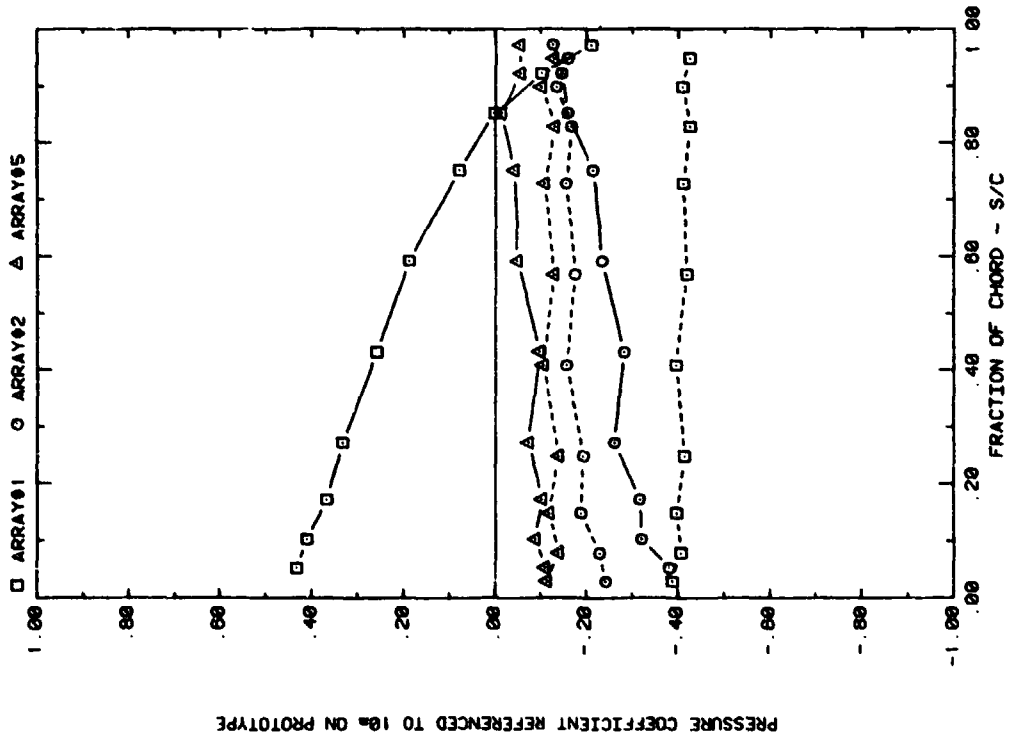


FRONT AND BACK PRESSURES ON ARRAYS IN BOUNDARY LAYER,  $X = 1.5C$   
EFFECT OF ARRAY CONFIGURATION ON ATTACK ANGLE 20,  $H/C = 0.25$

Plot 2-2-3. Multiple Arrays without Fence, Nonuniform Flow Study  
Effect of Array Position

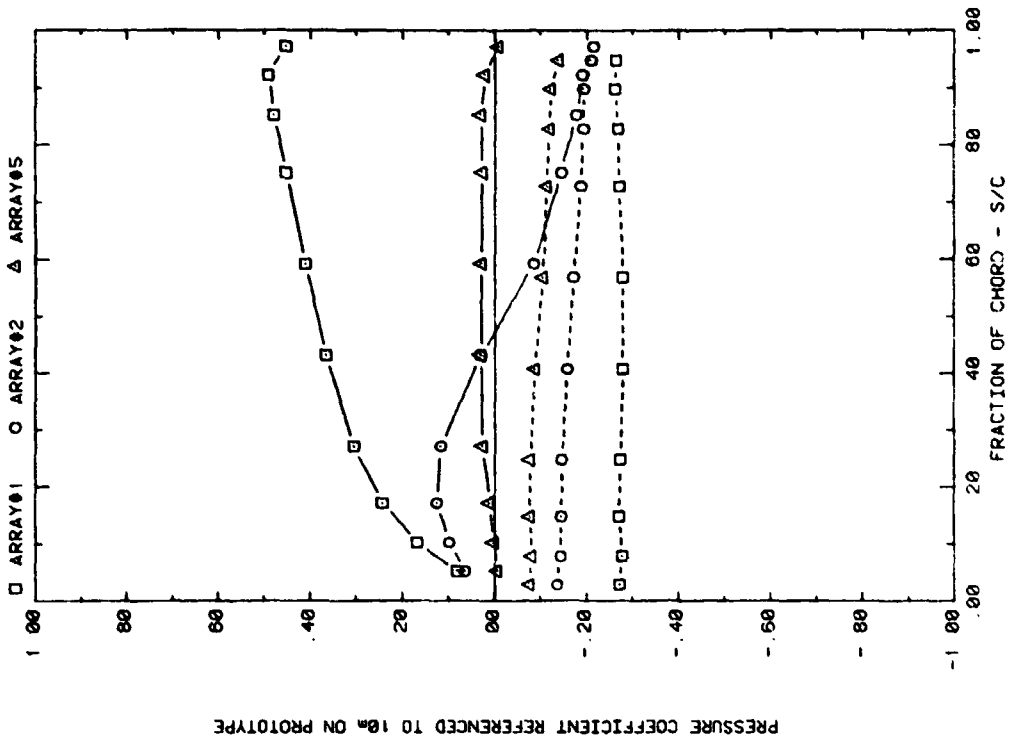


FRONT AND BACK PRESSURES ON ARRAYS IN BOUNDARY LAYER,  $x = 1.5c$   
EFFECT OF ARRAY CONFIGURATION ON ATTACK ANGLE 145,  $H/C = 0.25$

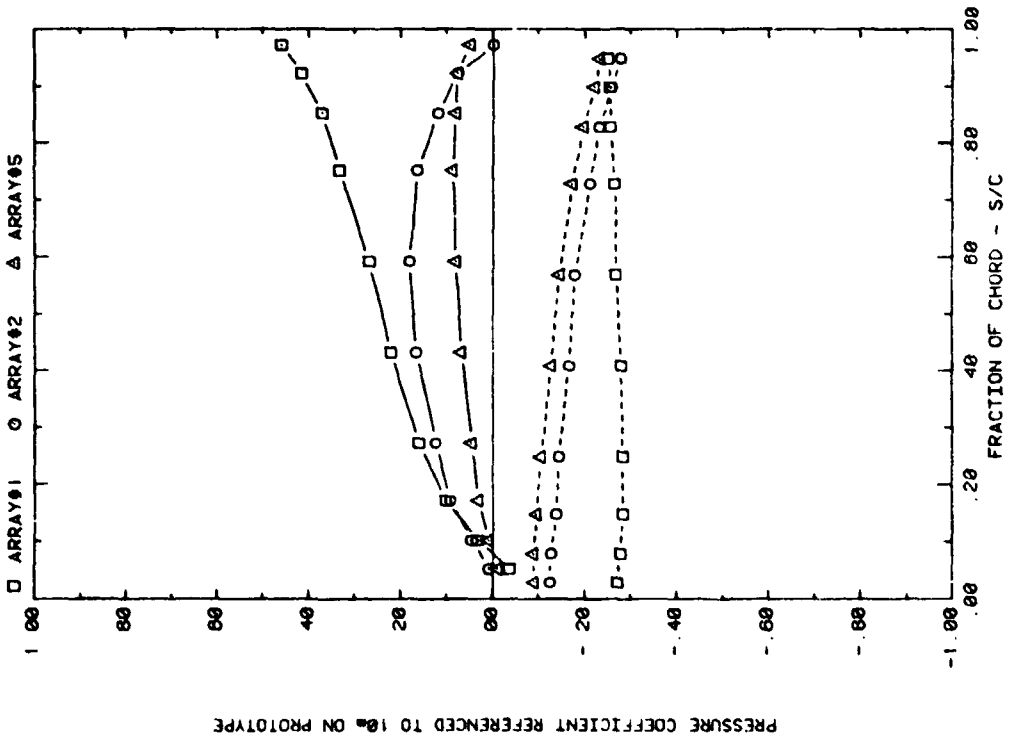


FRONT AND BACK PRESSURES ON ARRAYS IN BOUNDARY LAYER,  $x = 1.5c$   
EFFECT OF ARRAY CONFIGURATION ON ATTACK ANGLE 150,  $H/C = 0.25$

Plot 2-2-3. (Continued)

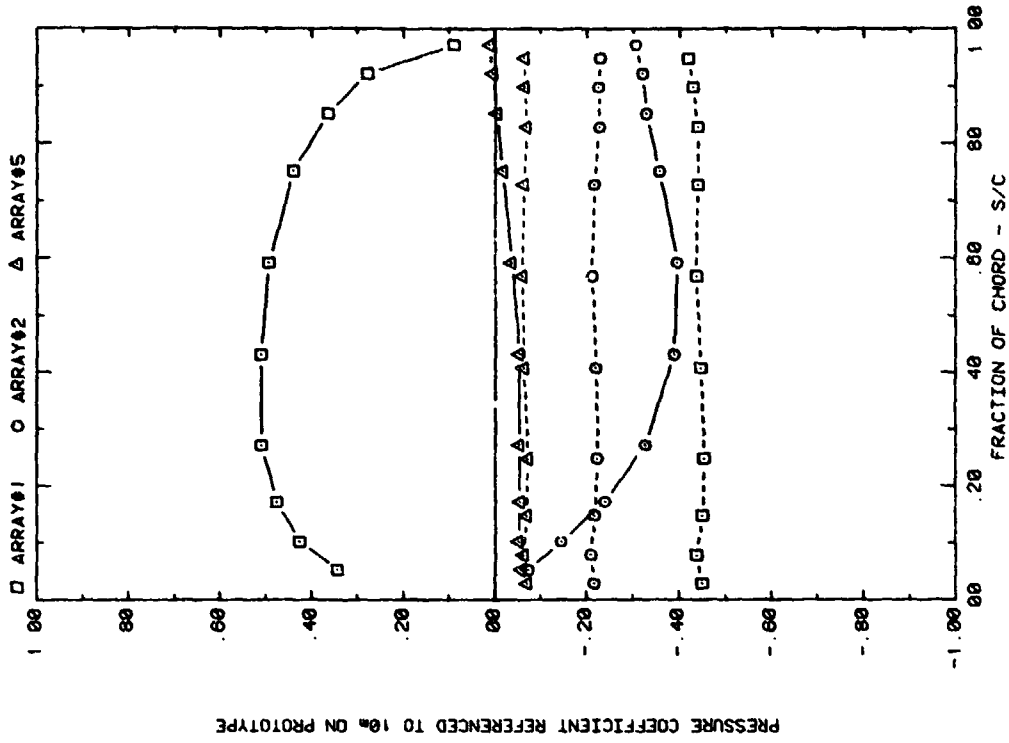


FRONT AND BACK PRESSURES ON ARRAYS IN BOUNDARY LAYER,  $X = 2.0C$   
EFFECT OF ARRAY CONFIGURATION ON ATTACK ANGLE 35,  $H/C = 0.25$

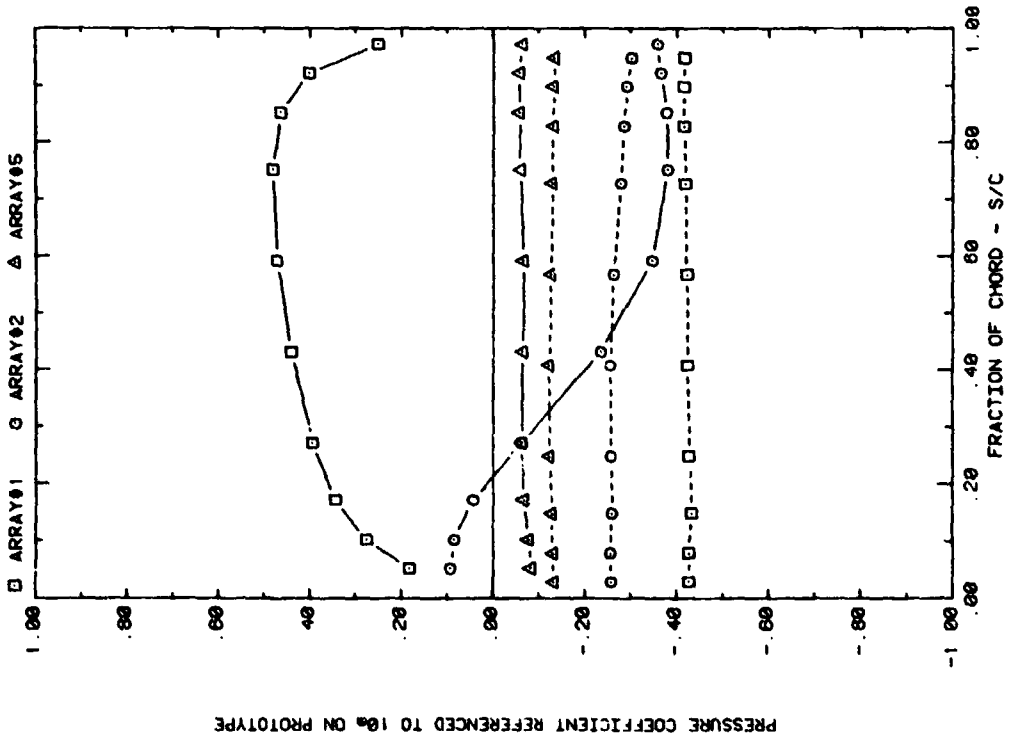


FRONT AND BACK PRESSURES ON ARRAYS IN BOUNDARY LAYER,  $X = 2.0C$   
EFFECT OF ARRAY CONFIGURATION ON ATTACK ANGLE 20,  $H/C = 0.25$

Plot 2-2-3. (Continued)

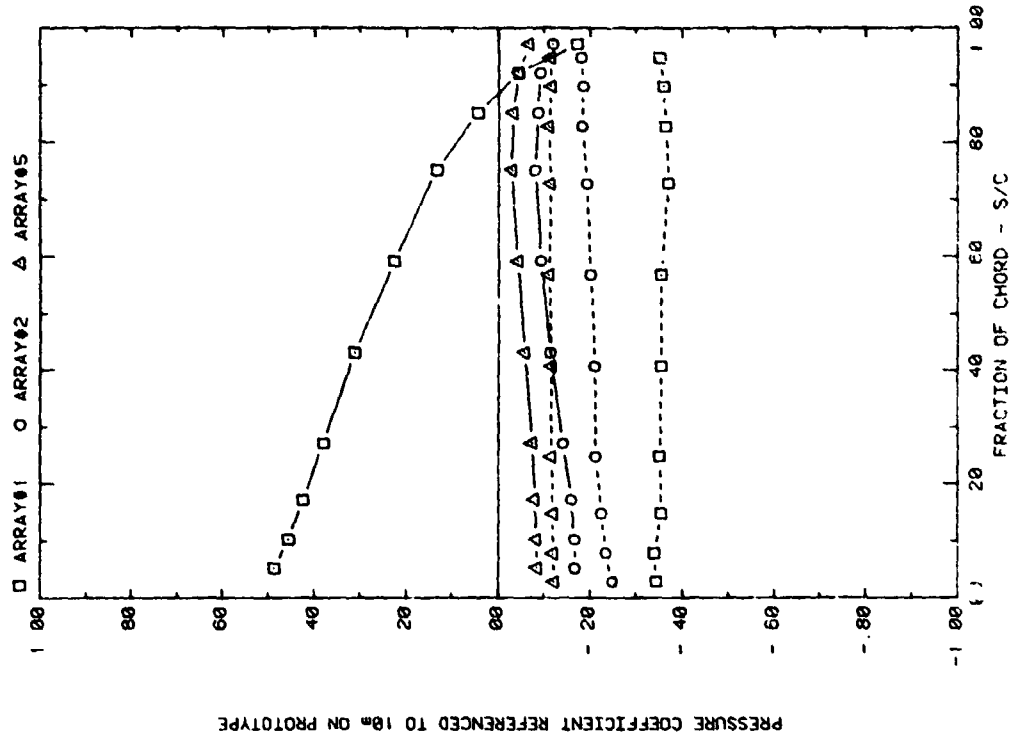


FRONT AND BACK PRESSURES ON ARRAYS IN BOUNDARY LAYER,  $X = 2.0C$   
EFFECT OF ARRAY CONFIGURATION ON ATTACK ANGLE 90,  $H/C = 0.25$

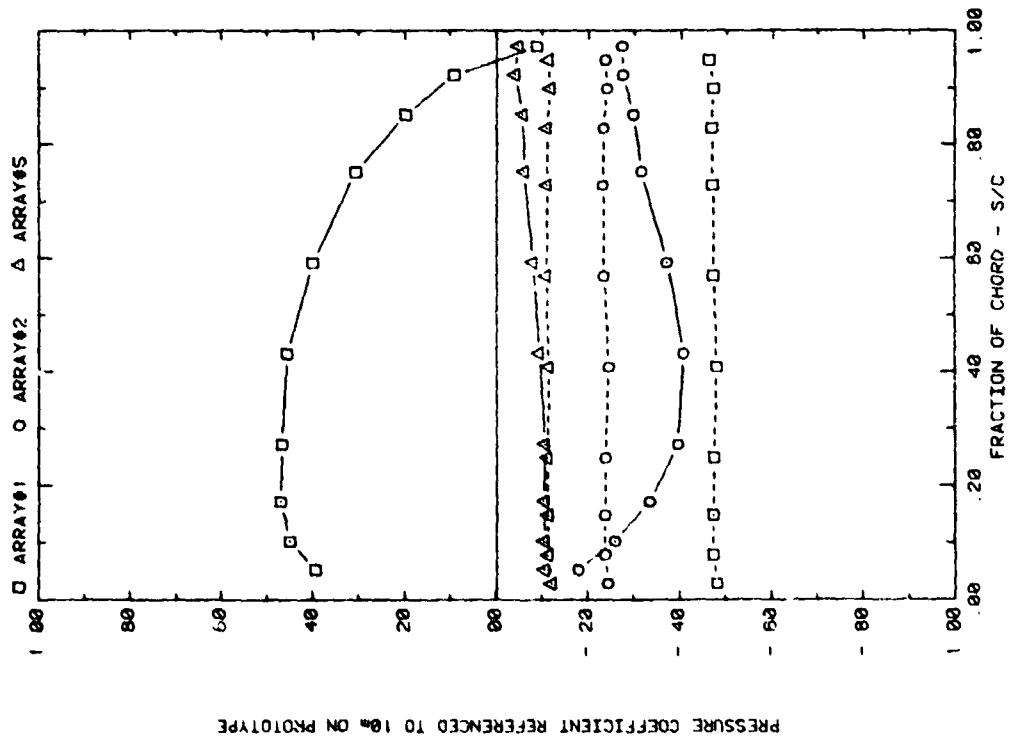


FRONT AND BACK PRESSURES ON ARRAYS IN BOUNDARY LAYER,  $X = 2.0C$   
EFFECT OF ARRAY CONFIGURATION ON ATTACK ANGLE 60,  $H/C = 0.25$

Plot 2-2-3. (Continued)

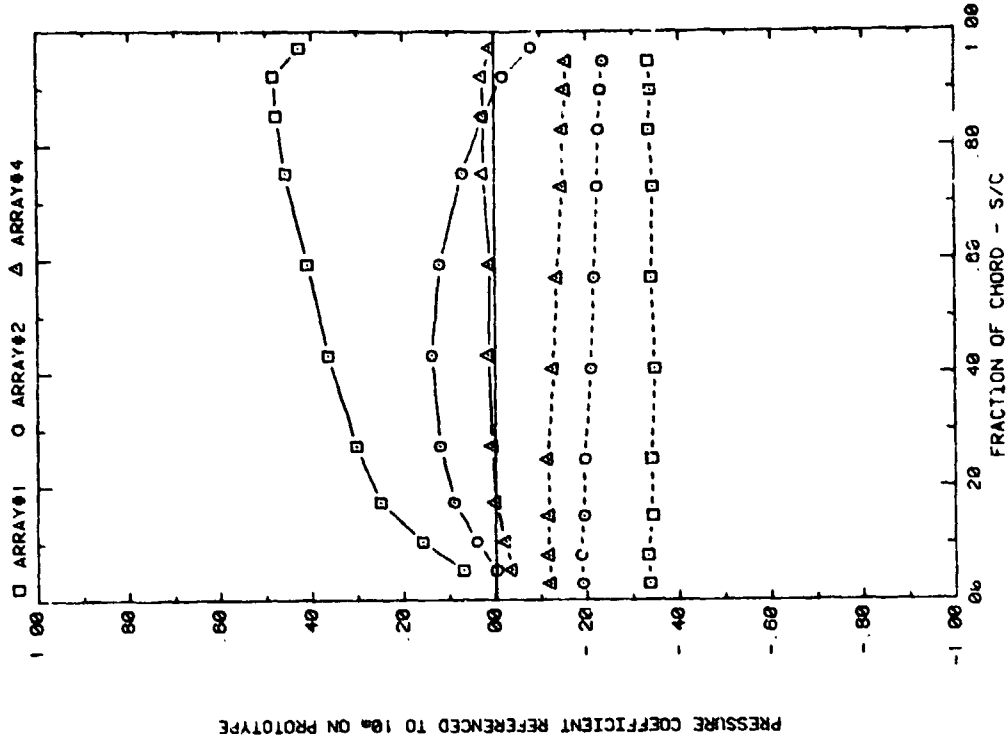


FRONT AND BACK PRESSURES ON ARRAYS IN BOUNDARY LAYER,  $\alpha = 145^\circ$   
EFFECT OF ARRAY CONFIGURATION ON ATTACK ANGLE 145,  $H/C = 0.25$

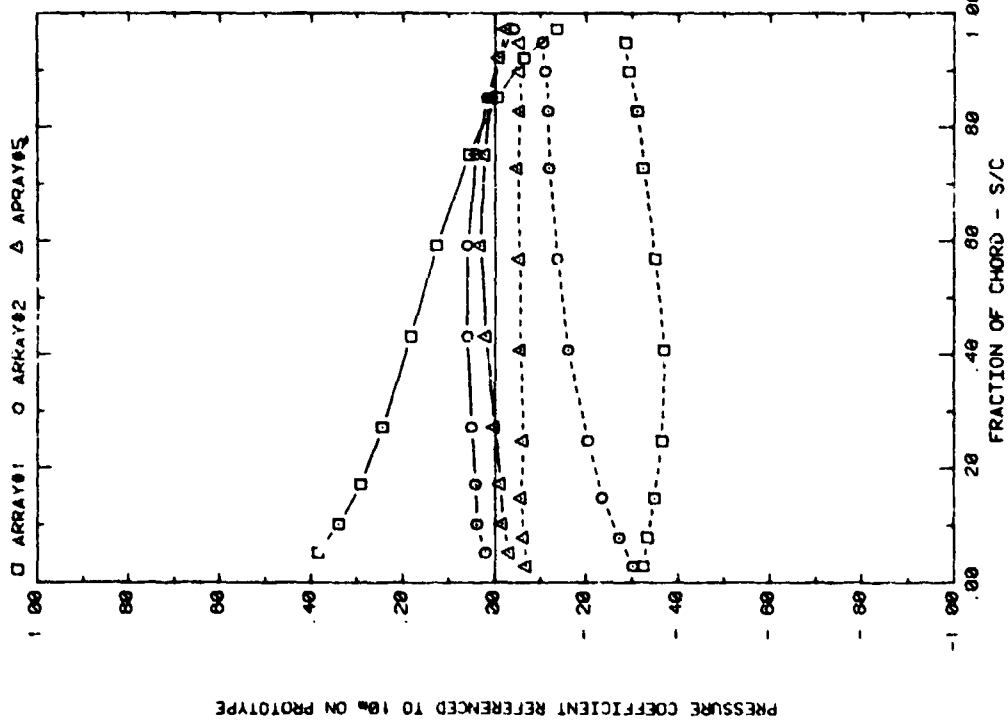


FRONT AND BACK PRESSURES ON ARRAYS IN BOUNDARY LAYER,  $\alpha = 120^\circ$   
EFFECT OF ARRAY CONFIGURATION ON ATTACK ANGLE 120,  $H/C = 0.25$

• Plot 2-2-3. (Continued)

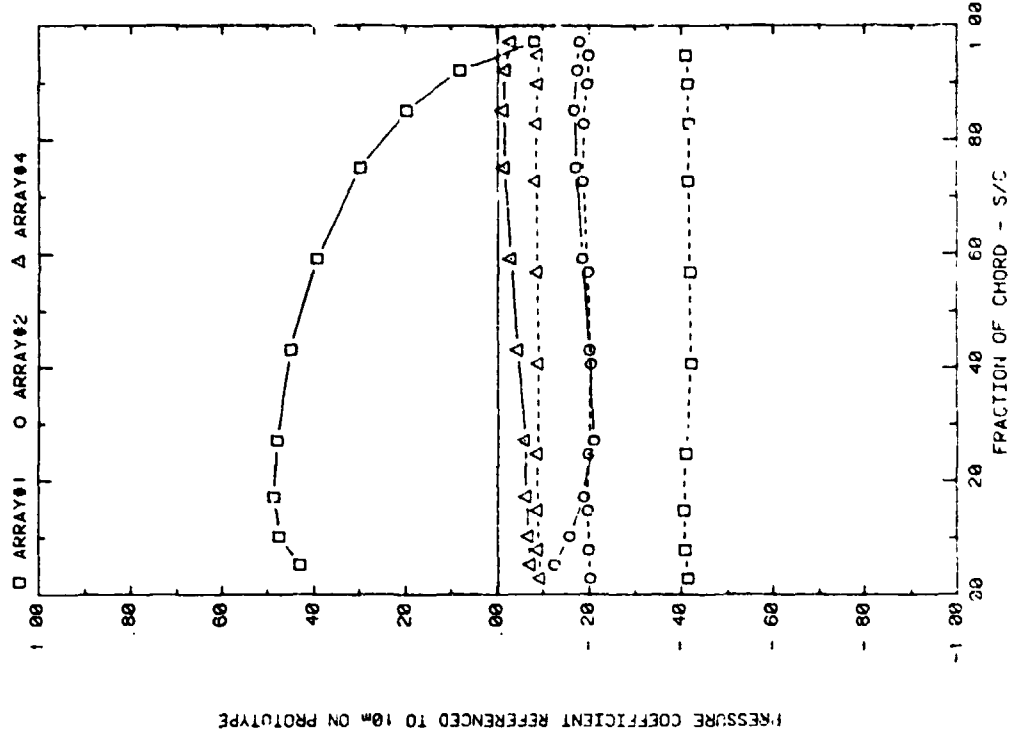


FRONT AND BACK PRESSURES ON ARRAYS IN BOUNDARY LAYER,  $x = 3.0c$   
EFFECT OF ARRAY CONFIGURATION ON ATTACK ANGLE 35,  $H/C = 0.25$



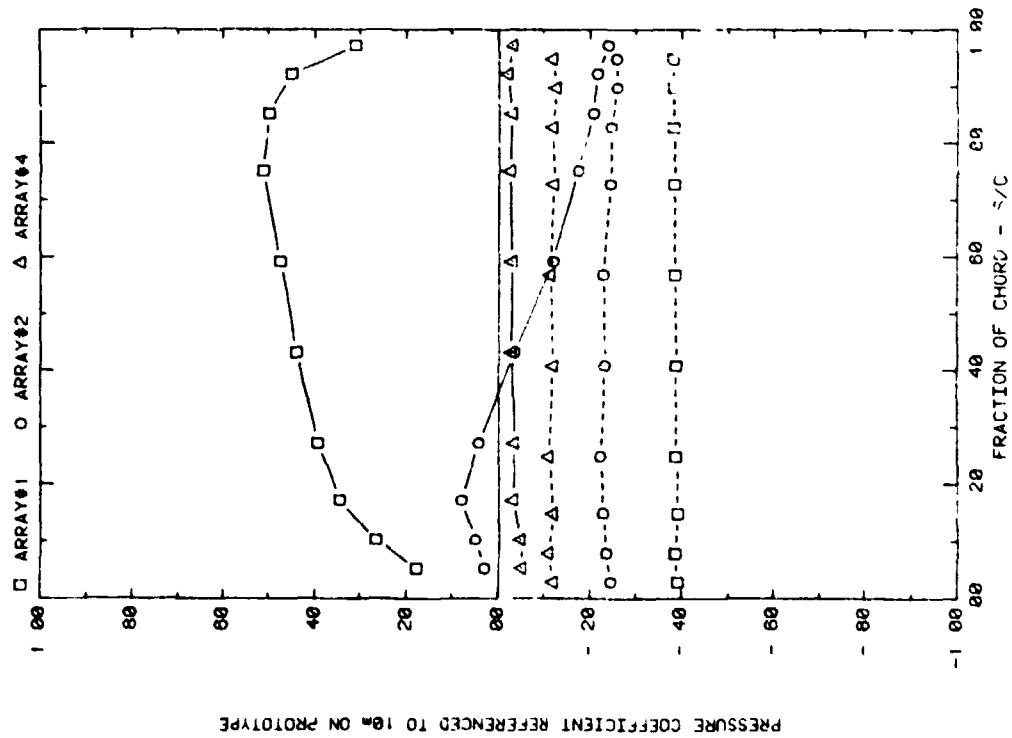
FRONT AND BACK PRESSURES ON ARRAYS IN BOUNDARY LAYER,  $x = 2.0c$   
EFFECT OF ARRAY CONFIGURATION ON ATTACK ANGLE 180,  $H/C = 0.25$

Plot 2-2-3. (Continued)



PRESSURE COEFFICIENT REFERENCED TO 10# ON PROTOTYPE

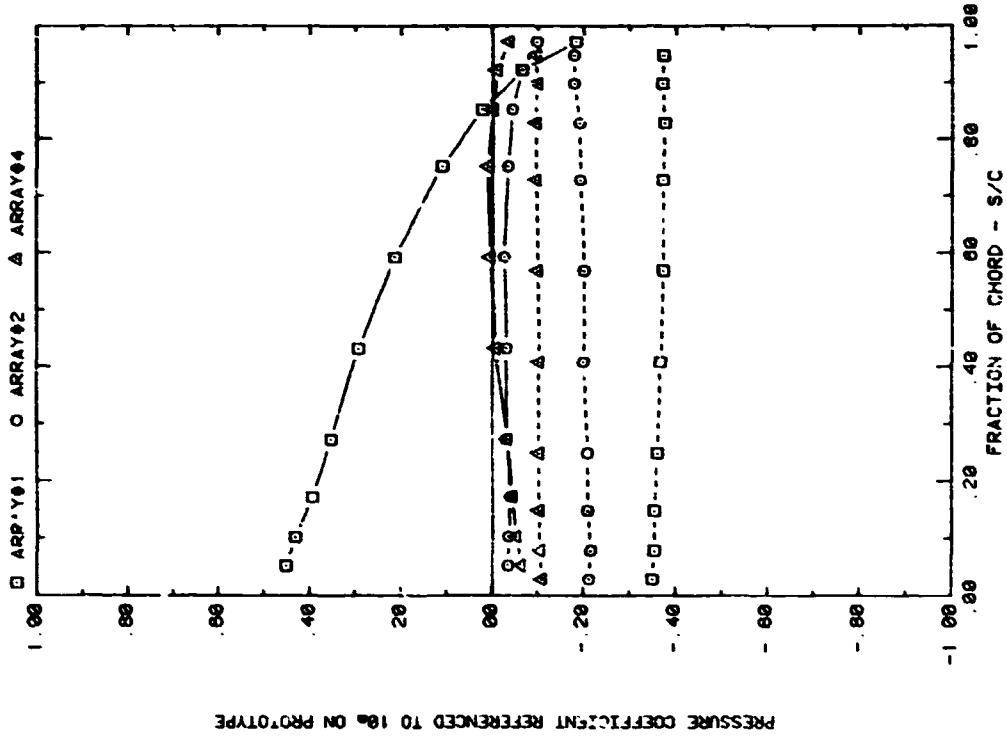
FRONT AND BACK PRESSURES OF ARRAYS IN BOUNDARY LAYER,  $\alpha = 30^\circ$   
EFFECT OF ARRAY CONFIGURATION ON ATTACK ANGLE 120,  $H/C = 0.25$



PRESSURE COEFFICIENT REFERENCED TO 10# ON PROTOTYPE

FRONT AND BACK PRESSURES ON ARRAYS IN BOUNDARY LAYER,  $\alpha = 30^\circ$   
EFFECT OF ARR Y CONFIGURATION ON ATTACK ANGLE 60,  $H/C = 0.25$

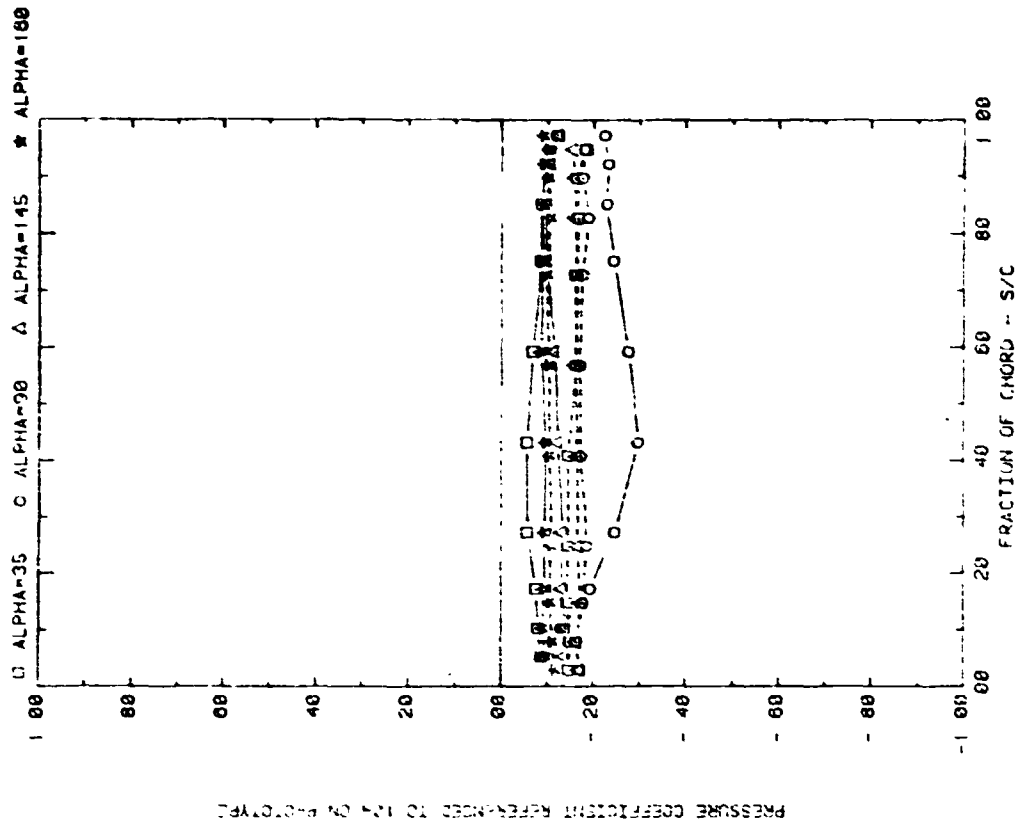
Plot 2-2-3. (Continued)



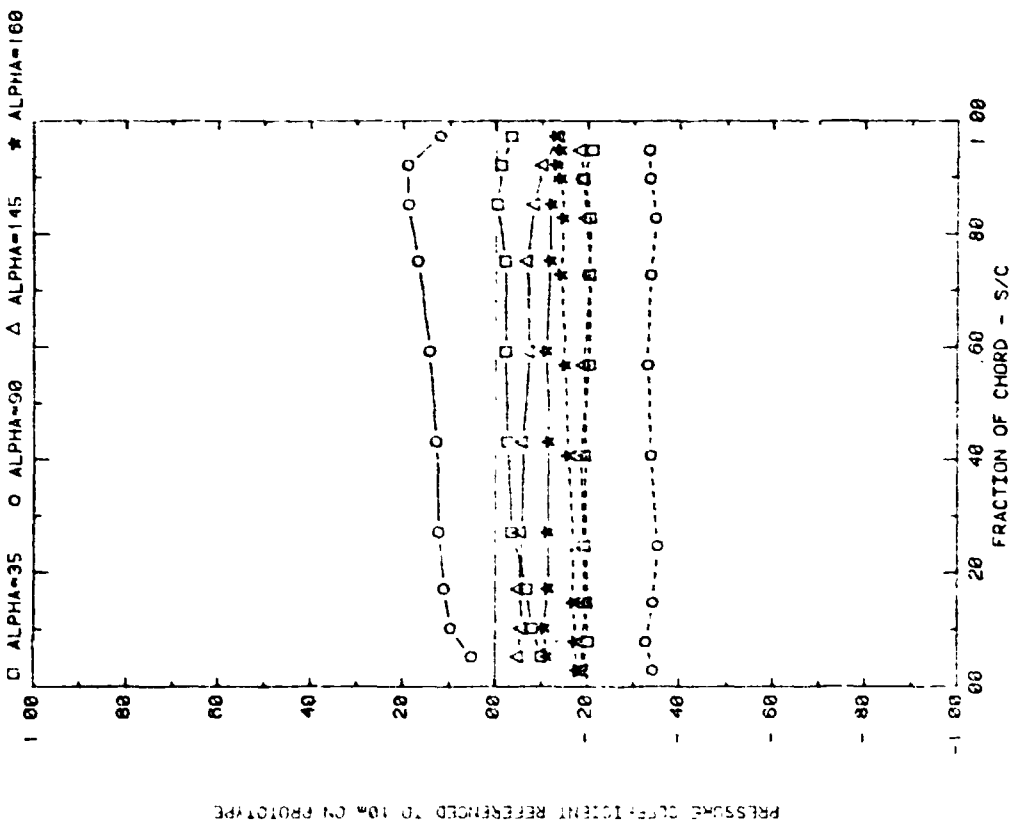
PRESSURE COEFFICIENT REFERENCED TO 10 ON PROTOTYPE

FRONT AND BACK PRESSURES ON ARRAYS IN BOUNDARY LAYER,  $X = 3.0C$   
EFFECT OF ARRAY CONFIGURATION ON ATTACK ANGLE 145,  $H/C = 0.25$

Plot 2-2-3. (Concluded)



FRONT AND BACK PRESSURES ON ARRAY #1 WITH SEPARATION = 2C  
EFFECT OF ATTACK ANGLE WITH  $M = 3^*$ ,  $P = 30\%$ , AND  $D = 5^*$

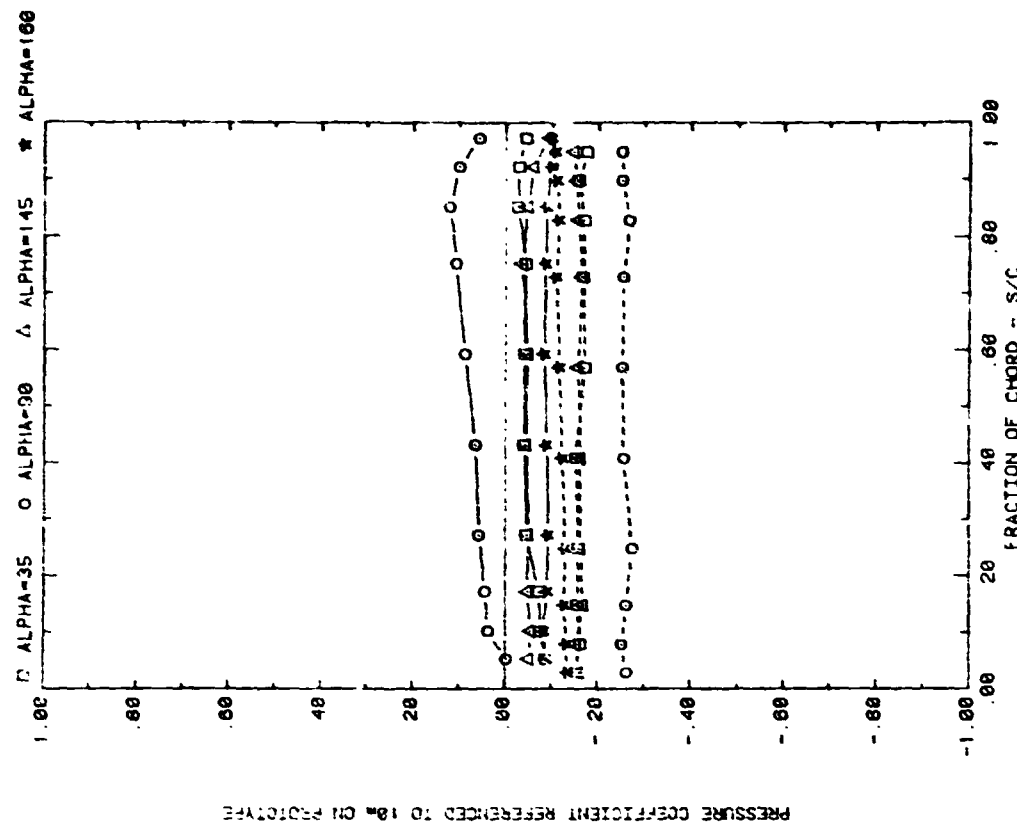


FRONT AND BACK PRESSURES ON ARRAY #1 WITH SEPARATION = 2C  
EFFECT OF ATTACK ANGLE WITH  $M = 3^*$ ,  $P = 30\%$ , AND  $D = 5^*$

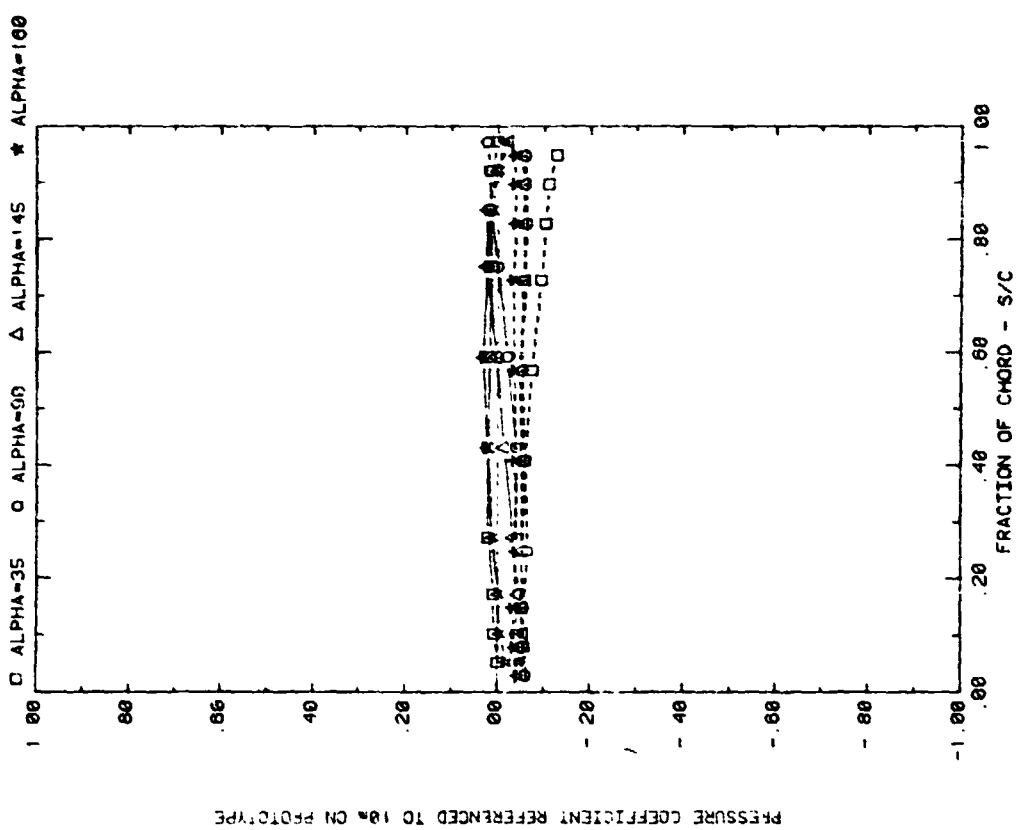
Plot 3-1. Multiple Arrays with Fence,  $WD = 0^\circ$   
Effect of Angle of Attack

PRESSURE COEFFICIENT REFERENCED TO 1% ON PROTOTYPE

PRESSURE COEFFICIENT REFERENCED TO 1% ON PROTOTYPE

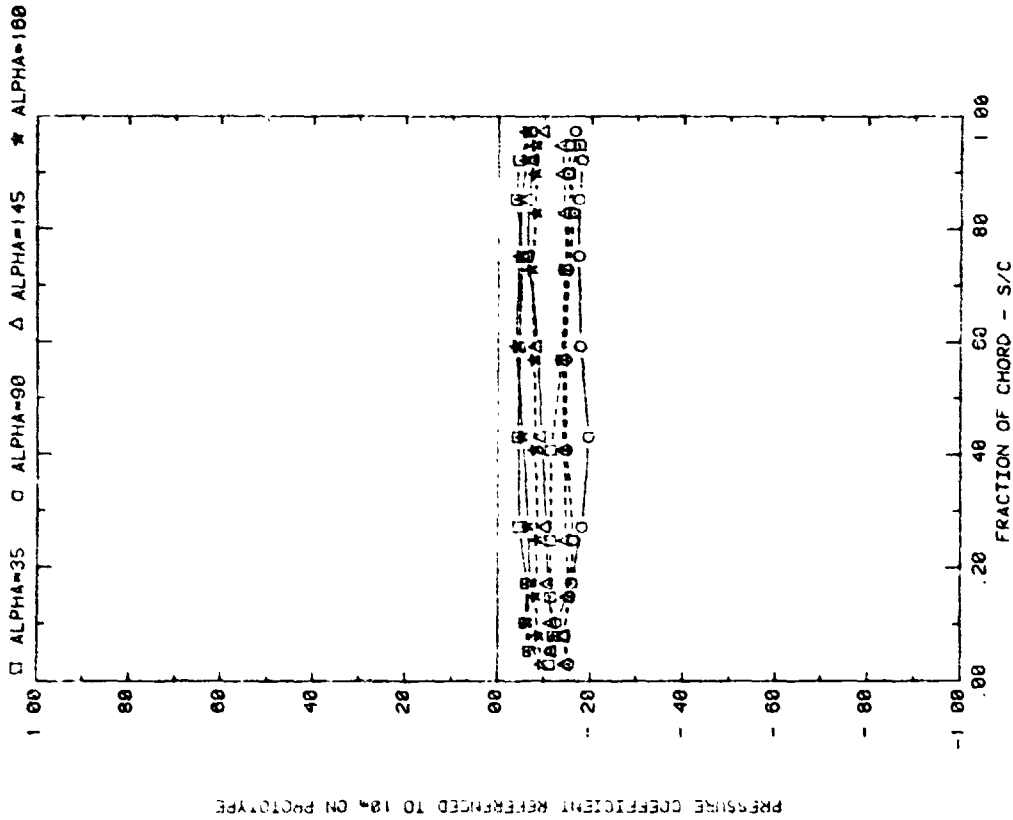
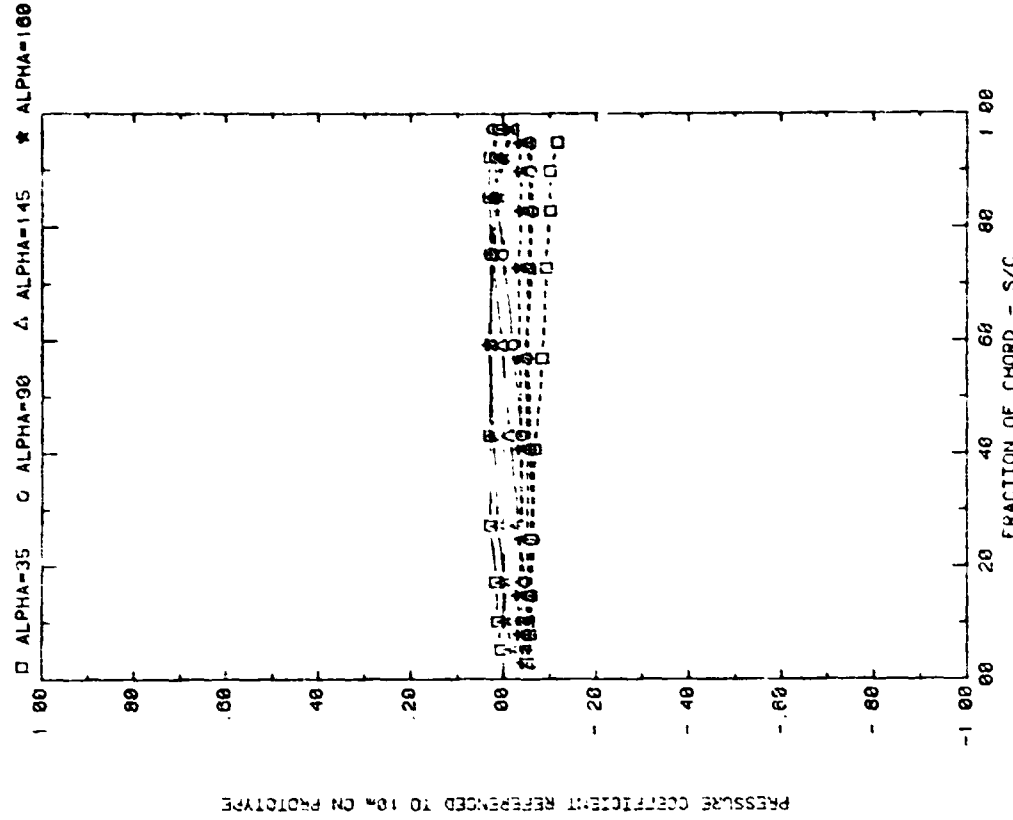


FRONT AND BACK PRESSURES ON ARRAY #1 WITH SEPARATION = 2C  
EFFECT OF ATTACK ANGLE WITH  $M=3$ ,  $P=30\%$ , AND  $D=10$ .

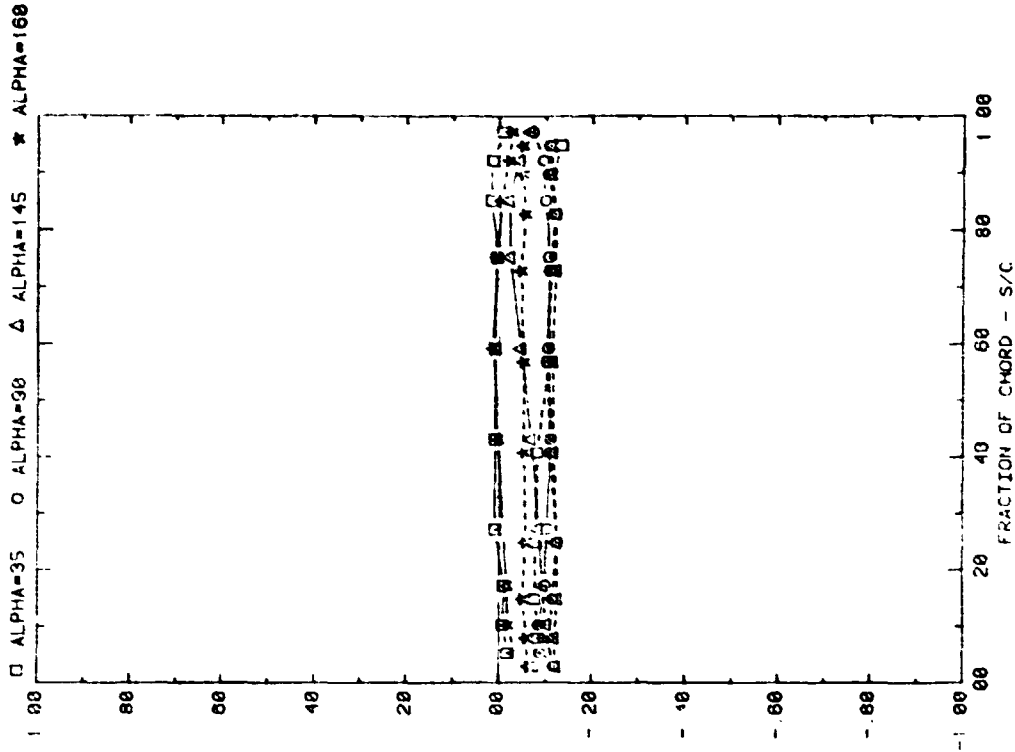


FRONT AND BACK PRESSURES ON ARRAY #5 WITH SEPARATION = 2C  
EFFECT OF ATTACK ANGLE WITH  $M=3$ ,  $P=30\%$ , AND  $D=5$ .

Plot 3-1. (Continued)

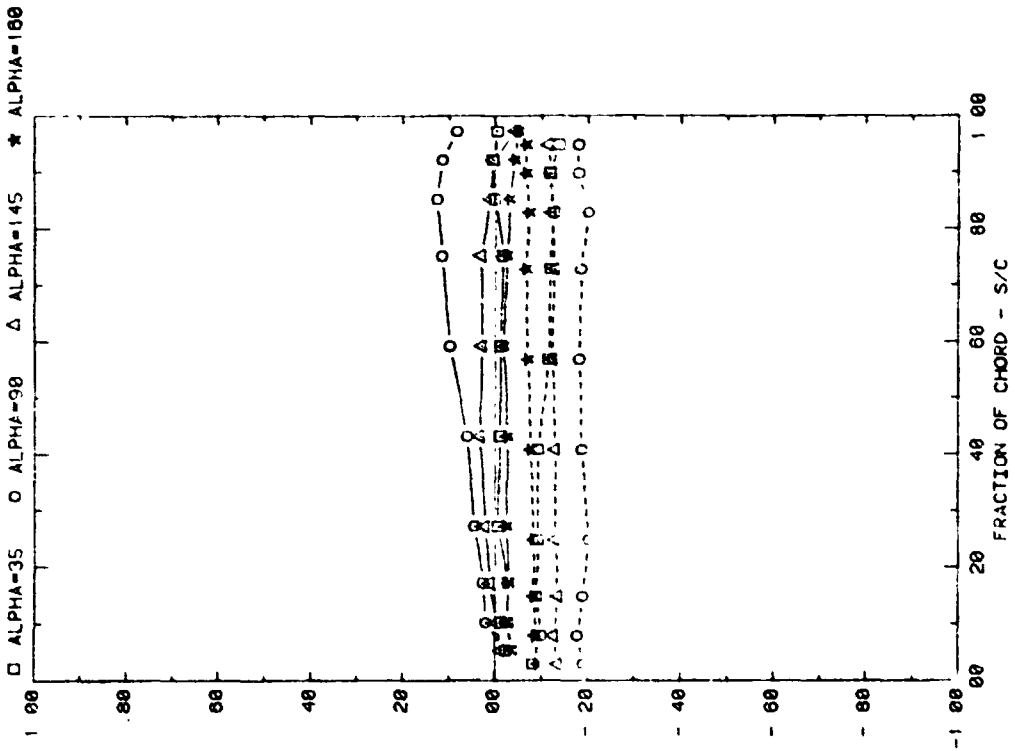


Plot 3-1. (Continued)



PRESSURE COEFFICIENT REFERENCED TO 10% ON PROTOTYPE

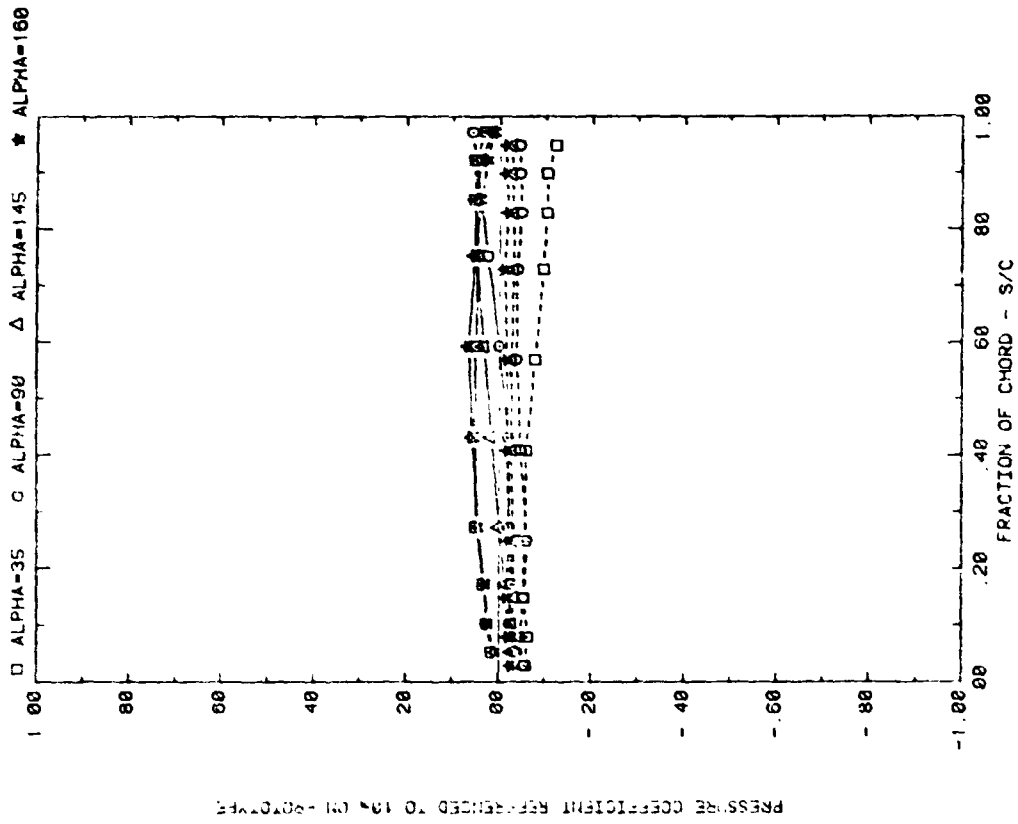
FRONT AND BACK PRESSURES ON ARRAY #2 WITH SEPARATION = 2C  
EFFECT OF ATTACK ANGLE WITH H=3", P=30%, AND D=20"



PRESSURE COEFFICIENT REFERENCED TO 10% ON PROTOTYPE

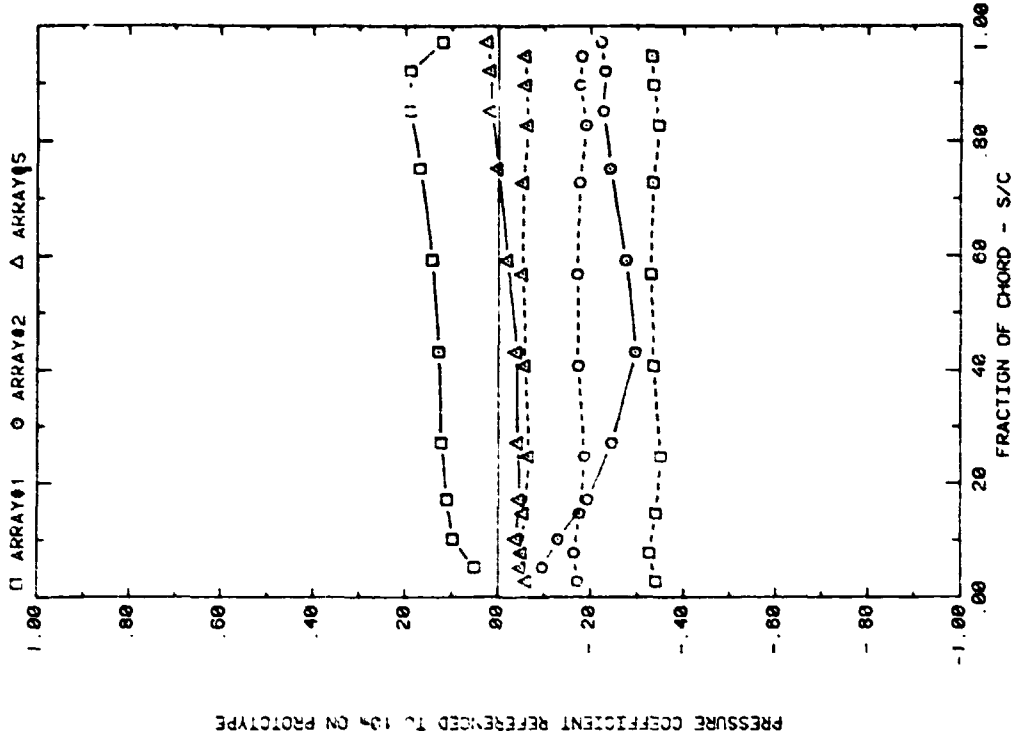
FRONT AND BACK PRESSURES ON ARRAY #1 WITH SEPARATION = 2C  
EFFECT OF ATTACK ANGLE WITH H=3", P=30%, AND D=20"

Plot 3-1. (Continued)



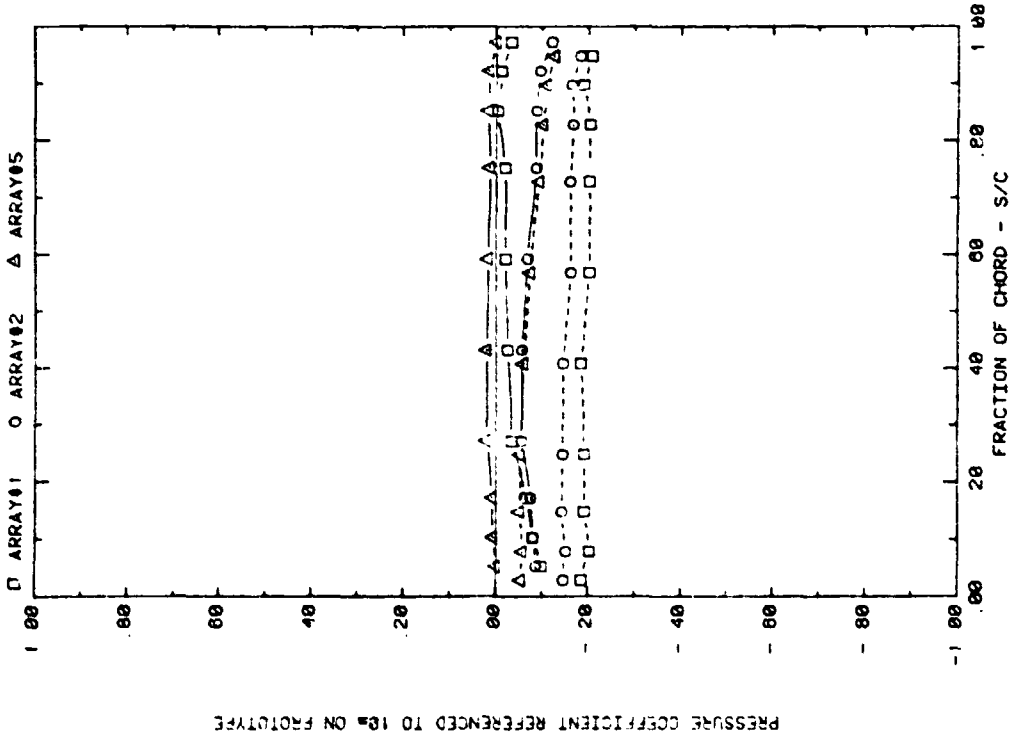
FRONT AND BACK PRESSURES ON ARRAYS WITH SEPARATION = 2C  
EFFECT OF ATTACK ANGLE WITH  $M=3$ ,  $P=30\%$ , AND  $D=20^\circ$

Plot 3-1. (Concluded)



PRESSURE COEFFICIENT REFERENCED TO 1.0 ON PROTOTYPE

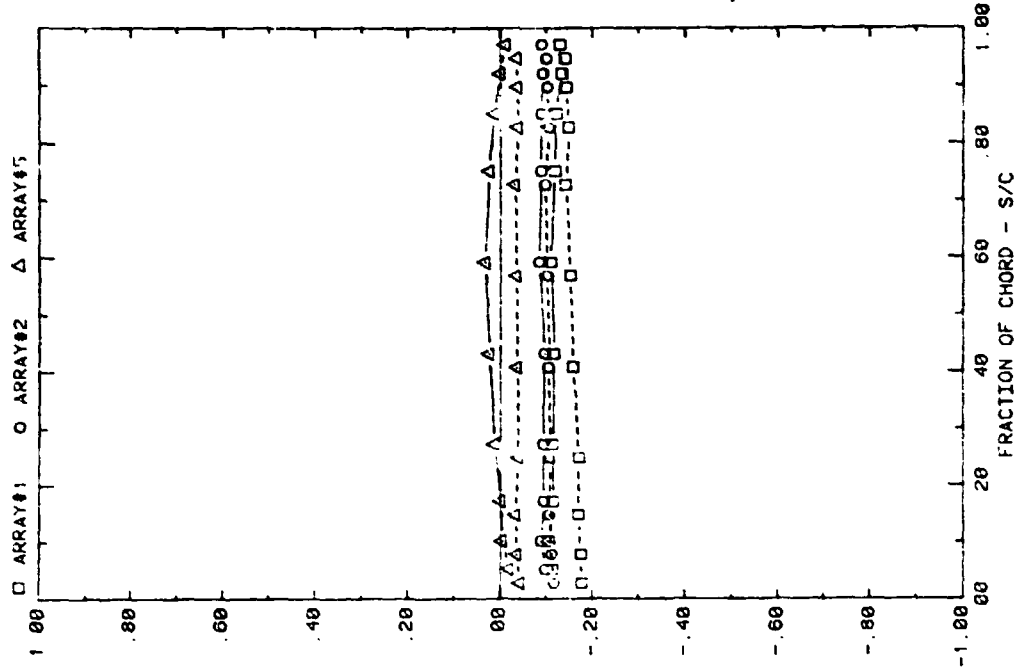
FRONT AND BACK PRESSURES ON VARIOUS ARRAYS WITH SEPARATION = 2C  
EFFECT OF ARRAYS WITH ATTACK ANGLE=00, H=3°, P=30%, AND D=5°



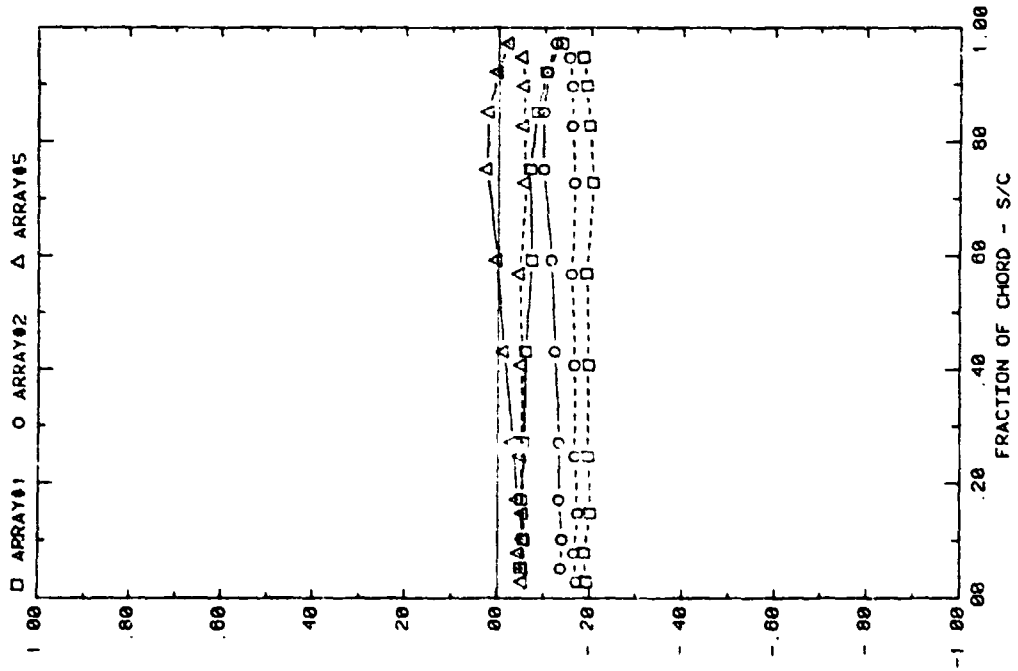
PRESSURE COEFFICIENT REFERENCED TO 1.0 ON PROTOTYPE

FRONT AND BACK PRESSURES ON VARIOUS ARRAYS WITH SEPARATION = 2C  
EFFECT OF ARRAYS WITH ATTACK ANGLE=35, H=3°, P=30%, AND D=5°

Plot 3-2. Multiple Arrays with Fence,  $WD = 0^\circ$   
Effect of Array Position



PRESSURE COEFFICIENT REFERENCED TO 10% ON PROTOTYPE

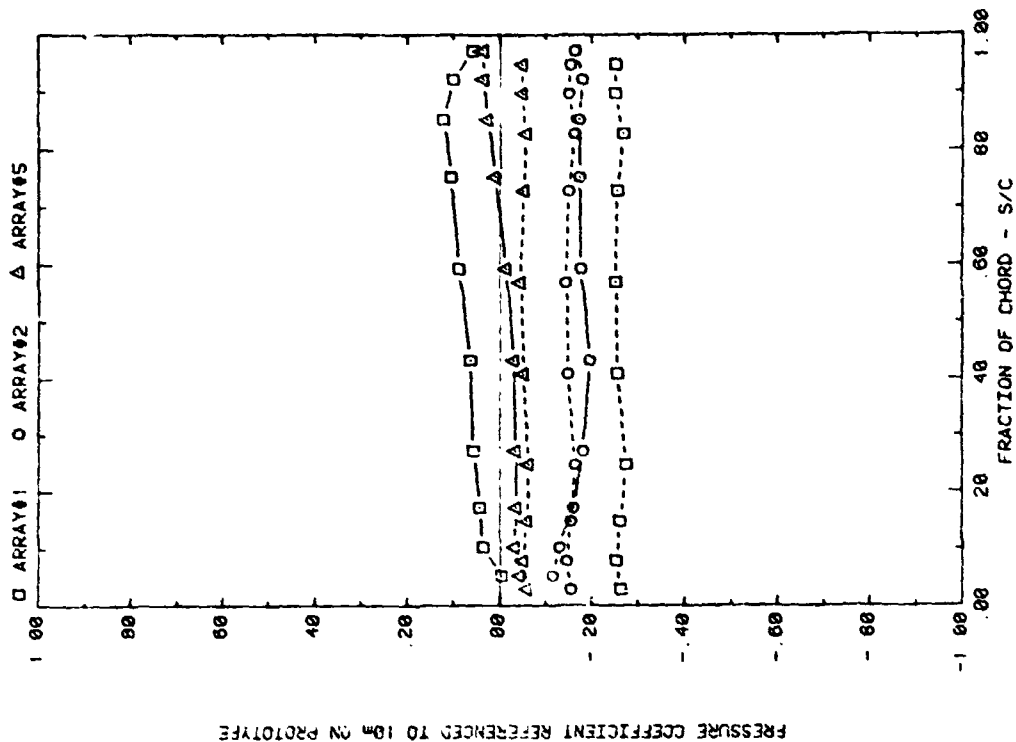


PRESSURE COEFFICIENT REFERENCED TO 10% ON PROTOTYPE

FRONT AND BACK PRESSURES ON VARIOUS ARRAYS WITH SEPARATION = 2C  
EFFECT OF ARRAYS WITH ATTACK ANGLE=10°, H=3", P=30%, AND D=5"

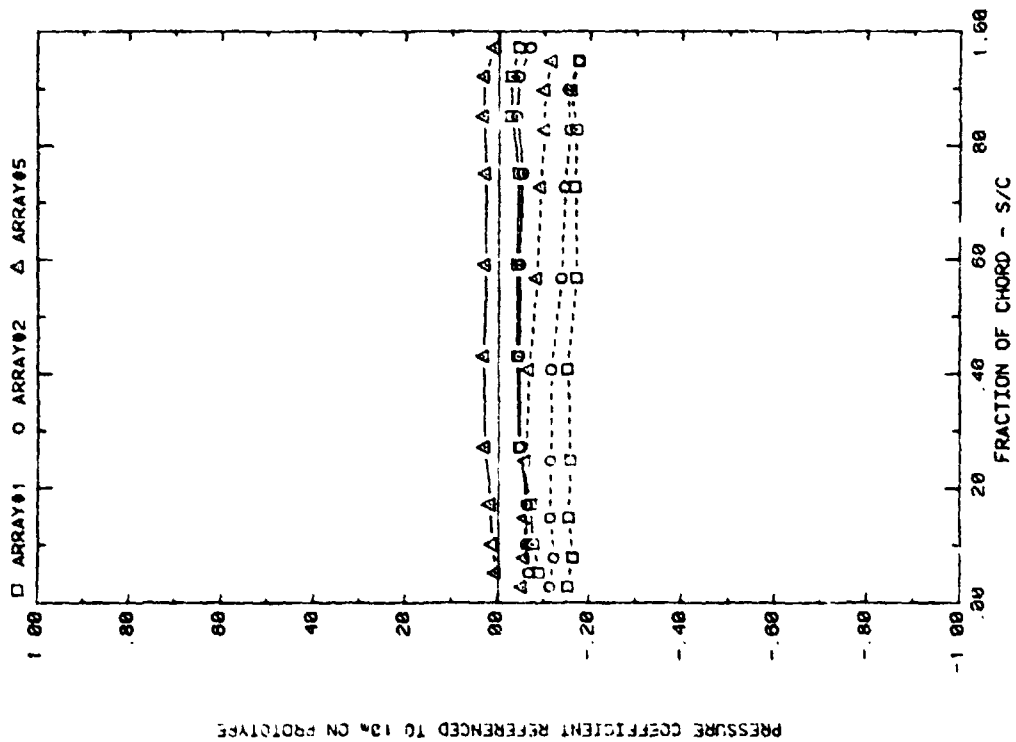
FRONT AND BACK PRESSURES ON VARIOUS ARRAYS WITH SEPARATION = 2C  
EFFECT OF ARRAYS WITH ATTACK ANGLE=145°, H=3", P=30%, AND D=5"

Plot 3-2. (Continued)



PRESSURE COEFFICIENT REFERENCED TO 10% ON PROTOTYPE

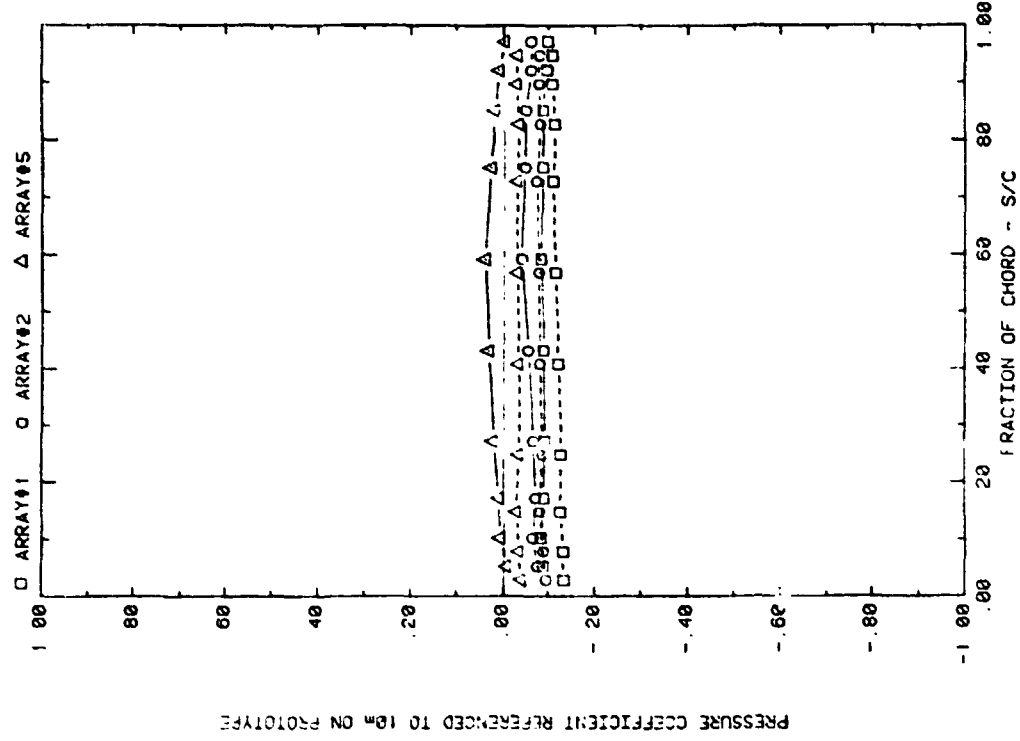
FRONT AND BACK PRESSURES ON VARIOUS ARRAYS WITH SEPARATION = 2C  
EFFECT OF ARRAYS WITH ATTACK ANGLE=90, M=3, P=30%, AND D=10.



PRESSURE COEFFICIENT REFERENCED TO 10% ON PROTOTYPE

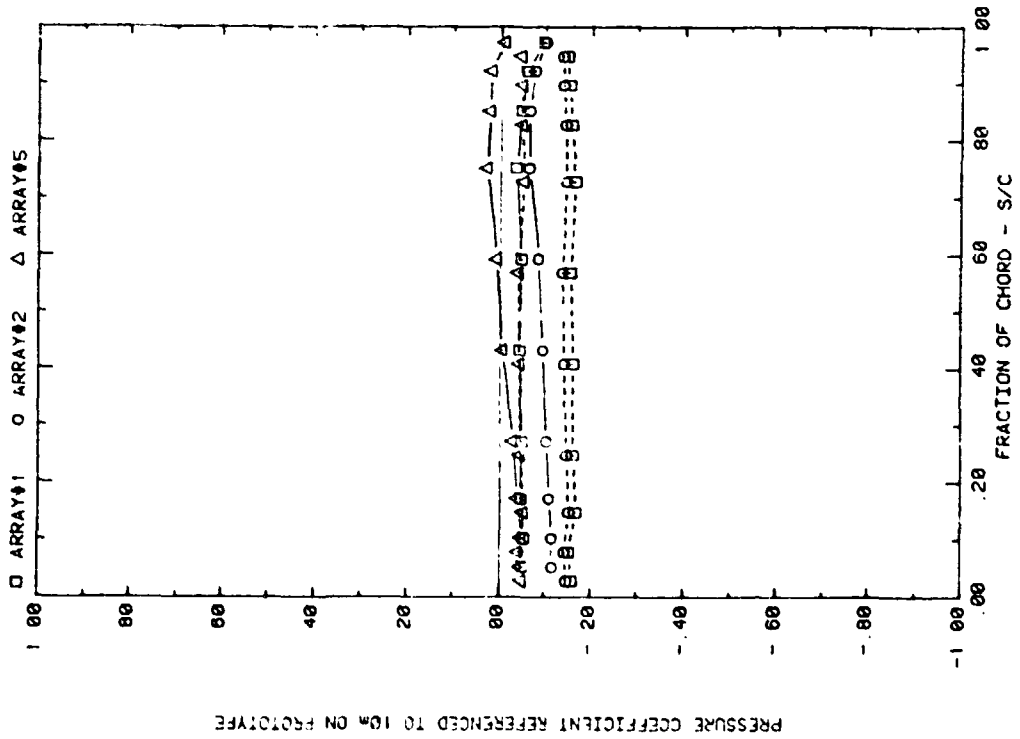
FRONT AND BACK PRESSURES ON VARIOUS ARRAYS WITH SEPARATION = 2C  
EFFECT OF ARRAYS WITH ATTACK ANGLE=35, M=3, P=30%, AND D=10.

Plot 3-2. (Continued)



PRESSURE COEFFICIENT REFERENCED TO 10% ON PROTOTYPE

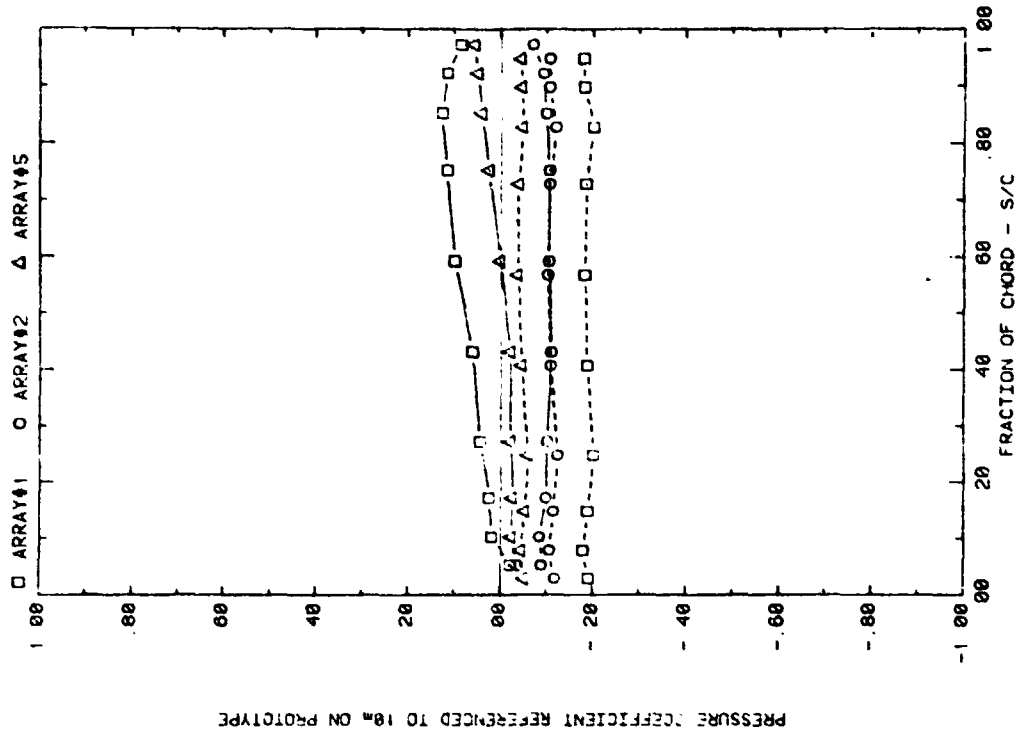
FRONT AND BACK PRESSURES ON VARIOUS ARRAYS WITH SEPARATION = 2C  
EFFECT OF ARRAYS WITH ATTACK ANGLE=10°, H=3°, P=30%, AND D=10°



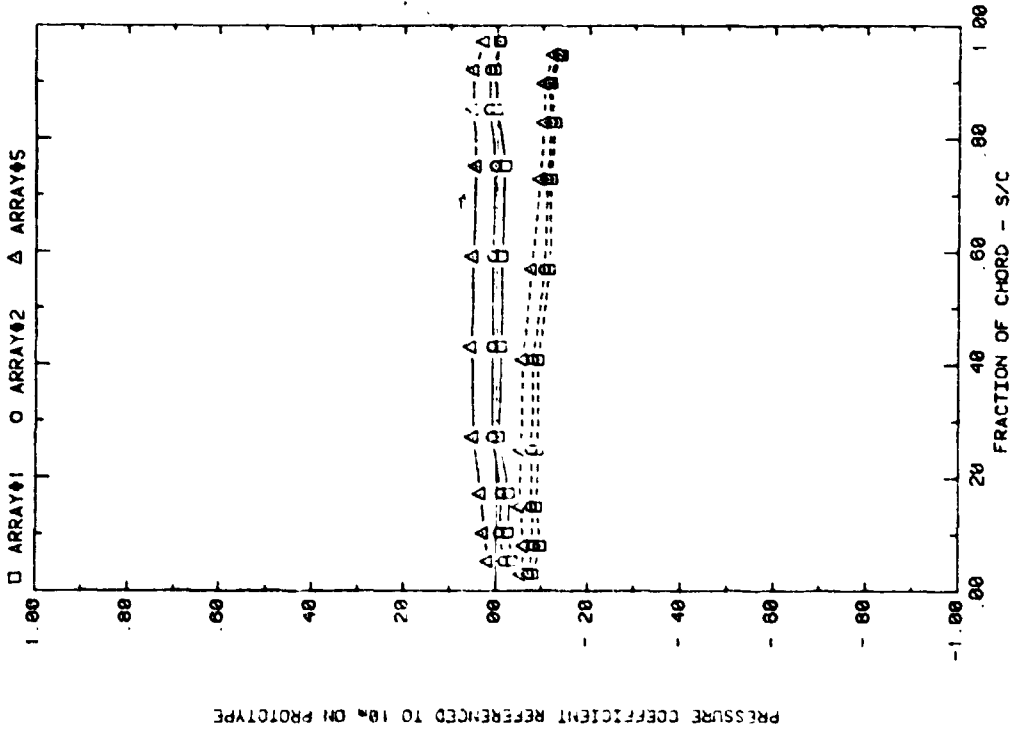
PRESSURE COEFFICIENT REFERENCED TO 10% ON PROTOTYPE

FRONT AND BACK PRESSURES ON VARIOUS ARRAYS WITH SEPARATION = 2C  
EFFECT OF ARRAYS WITH ATTACK ANGLE=145°, H=3°, P=30%, AND D=10°

Plot 3-2. (Continued)

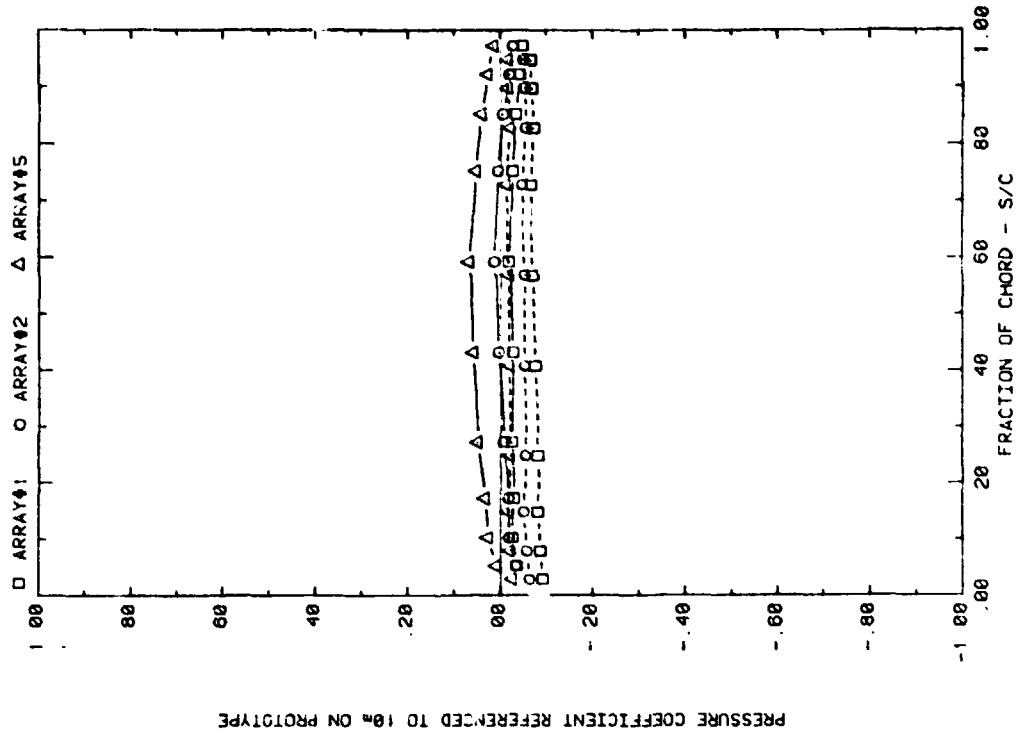


FRONT AND BACK PRESSURES ON VARIOUS ARRAYS WITH SEPARATION = 20  
EFFECT OF ARRAYS WITH ATTACK ANGLE=30, H=3', P=30%, AND D=20'



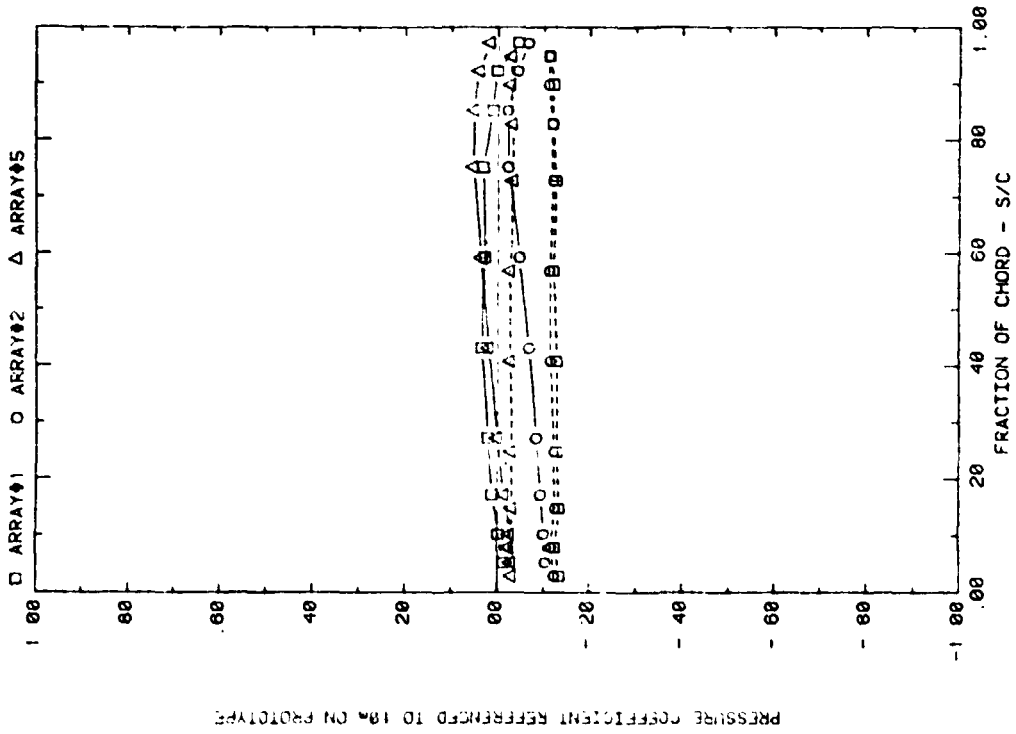
FRONT AND BACK PRESSURES ON VARIOUS ARRAYS WITH SEPARATION = 20  
EFFECT OF ARRAYS WITH ATTACK ANGLE=35, H=3', P=30%, AND D=20'

Plot 3-2. (Continued)



PRESSURE COEFFICIENT REFERENCED TO 10% ON PROTOTYPE

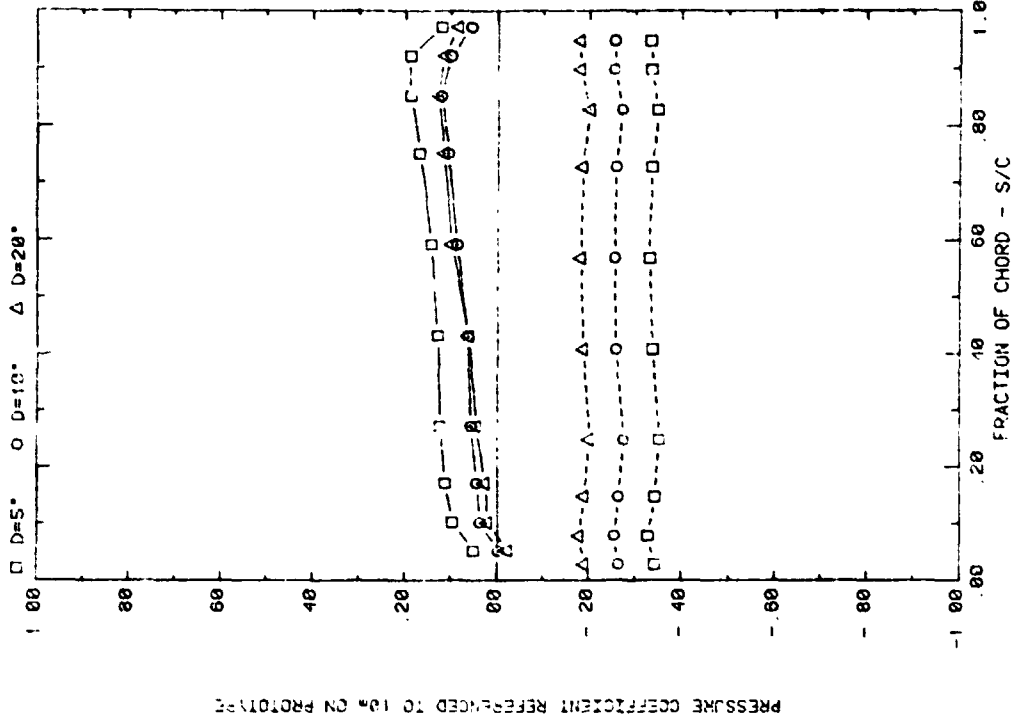
FRONT AND BACK PRESSURES ON VARIOUS ARRAYS WITH SEPARATION = 2C  
EFFECT OF ARRAYS WITH ATTACK ANGLE=160, H=3', P=30%, AND D=20.



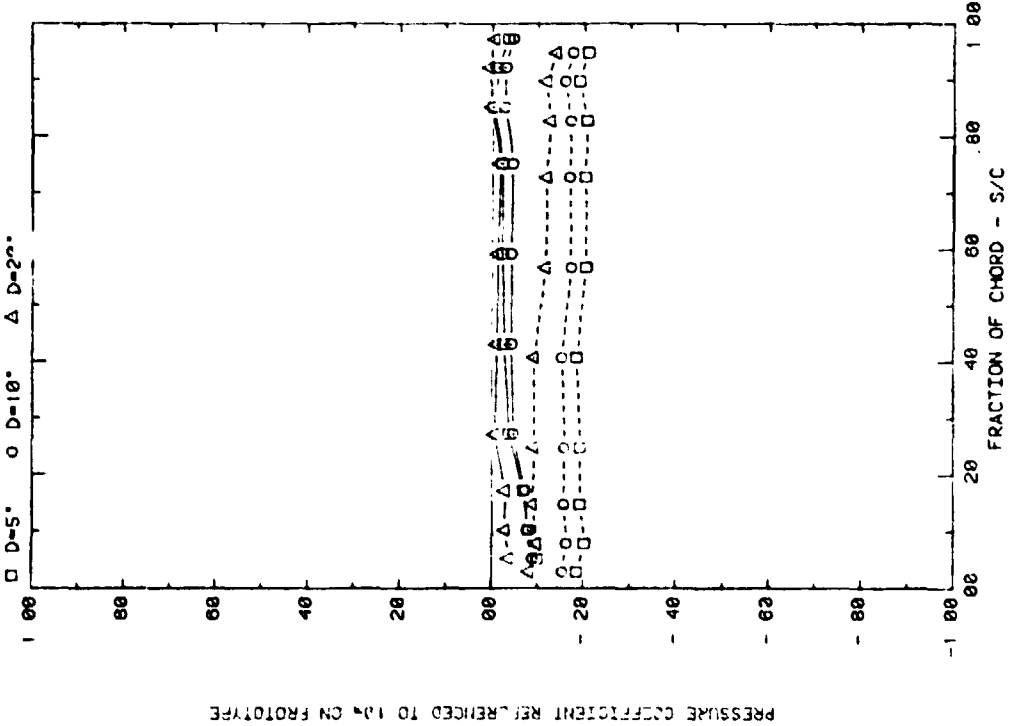
PRESSURE COEFFICIENT REFERENCED TO 10% ON PROTOTYPE

FRONT AND BACK PRESSURES ON VARIOUS ARRAYS WITH SEPARATION = 2C  
EFFECT OF ARRAYS WITH ATTACK ANGLE=145, H=3', P=30%, AND D=20.

Plot 3-2. (Concluded)

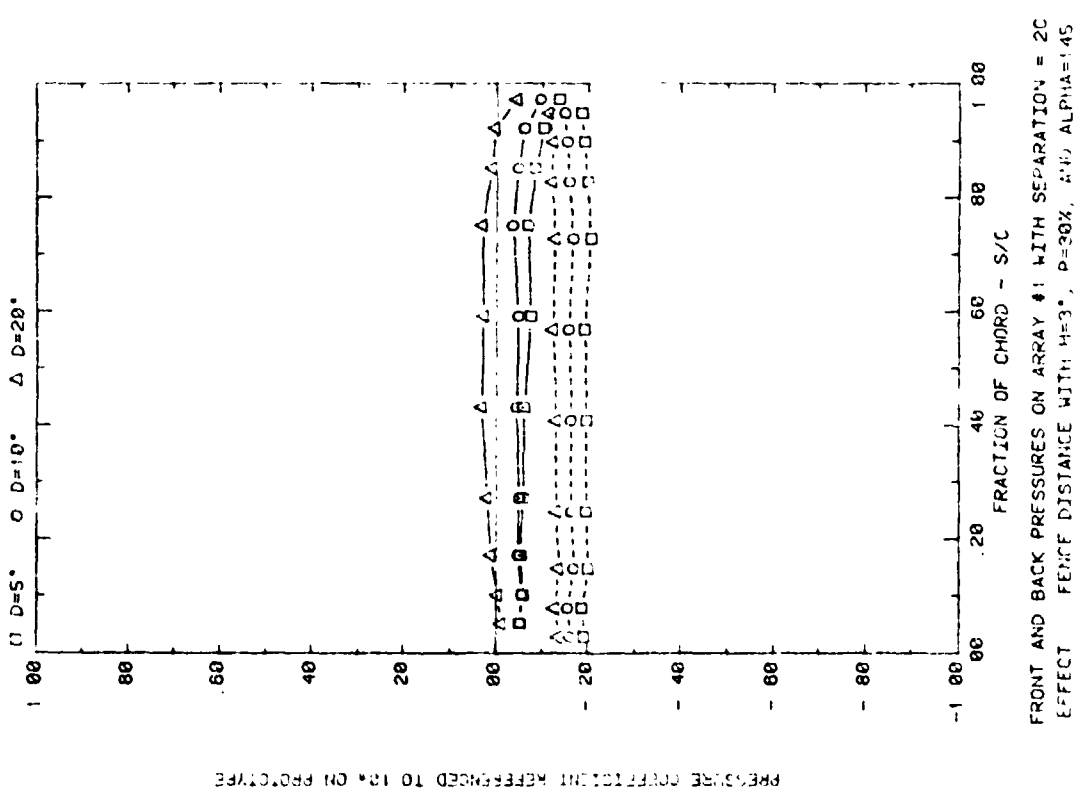
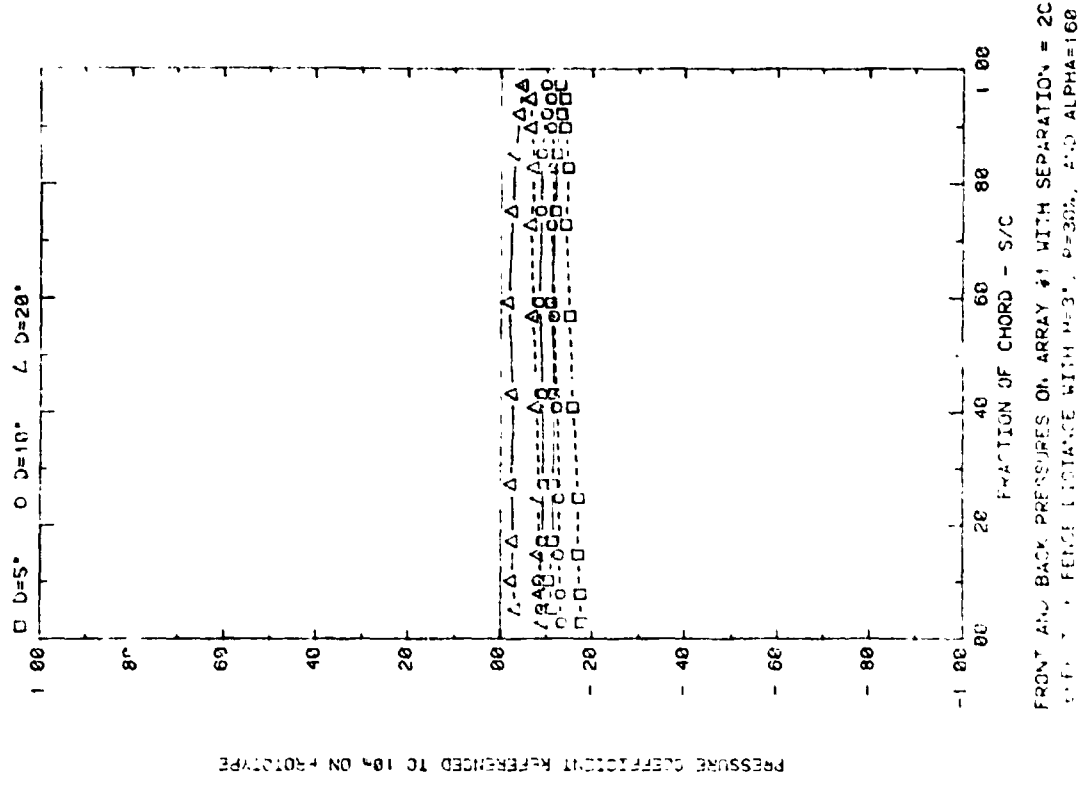


FRONT AND BACK PRESSURES ON ARRAY #1 WITH SEPARATION = 2C  
EFFECT OF FENCE DISTANCE WITH H=3°, P=30%, AND ALPHA=90

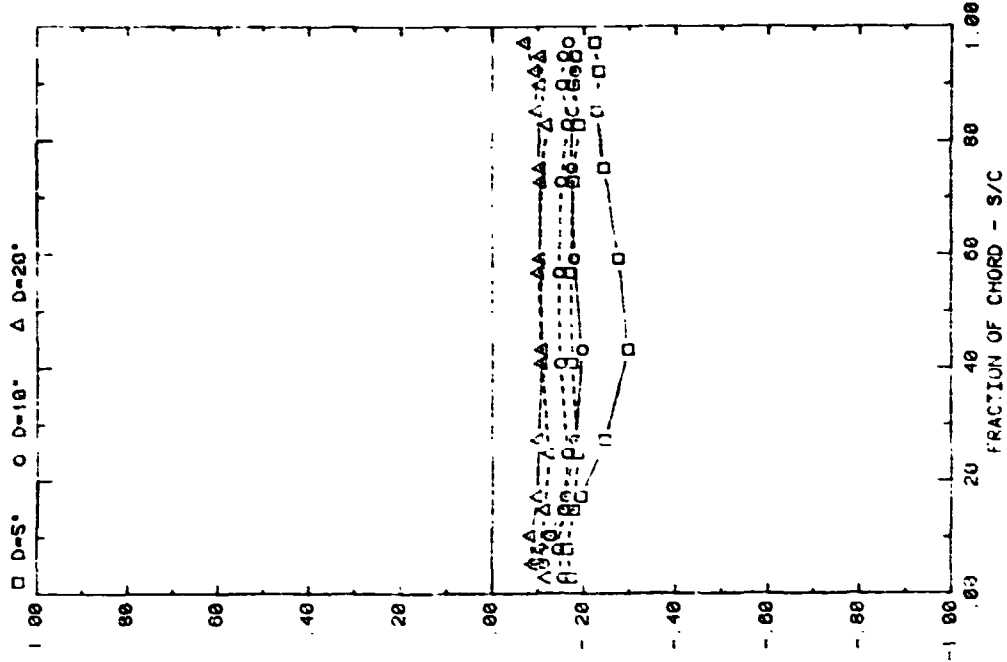


FRONT AND BACK PRESSURES ON ARRAY #1 WITH SEPARATION = 2C  
EFFECT OF FENCE DISTANCE WITH H=3°, P=30%, AND ALPHA=35

Plot 3-3. Multiple Arrays with Fence,  $WD = 0^\circ$   
Effect of Fence Distance

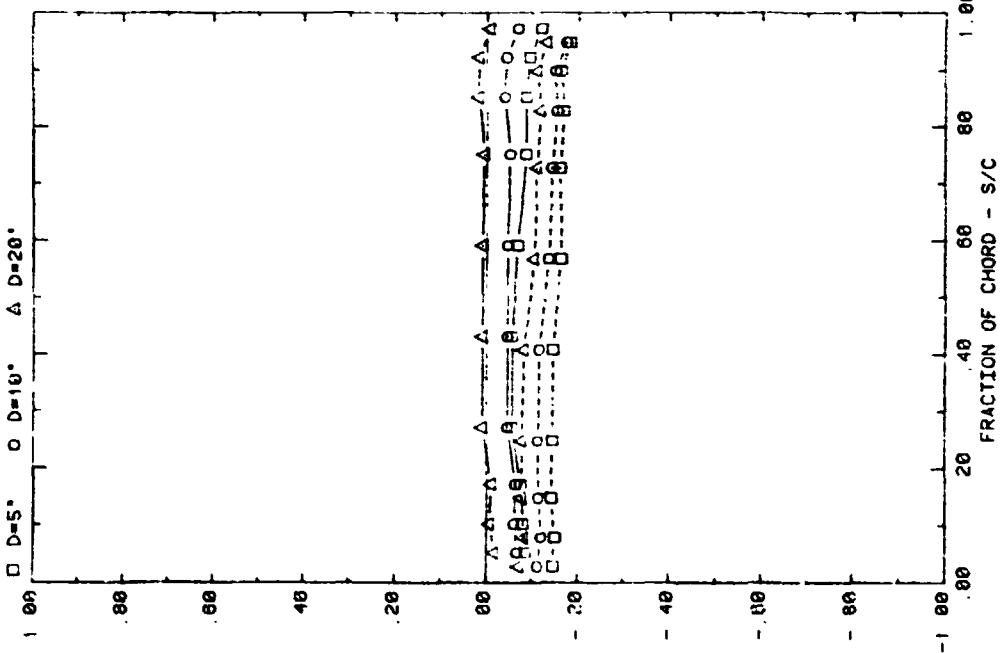


Plot 3-3. (Continued)



FRONT AND BACK PRESSURES ON ARRAY #2 WITH SEPARATION = 2C  
EFFECT OF FENCE DISTANCE WITH  $M=3$ ,  $P=30\%$ , AND  $\alpha=90$

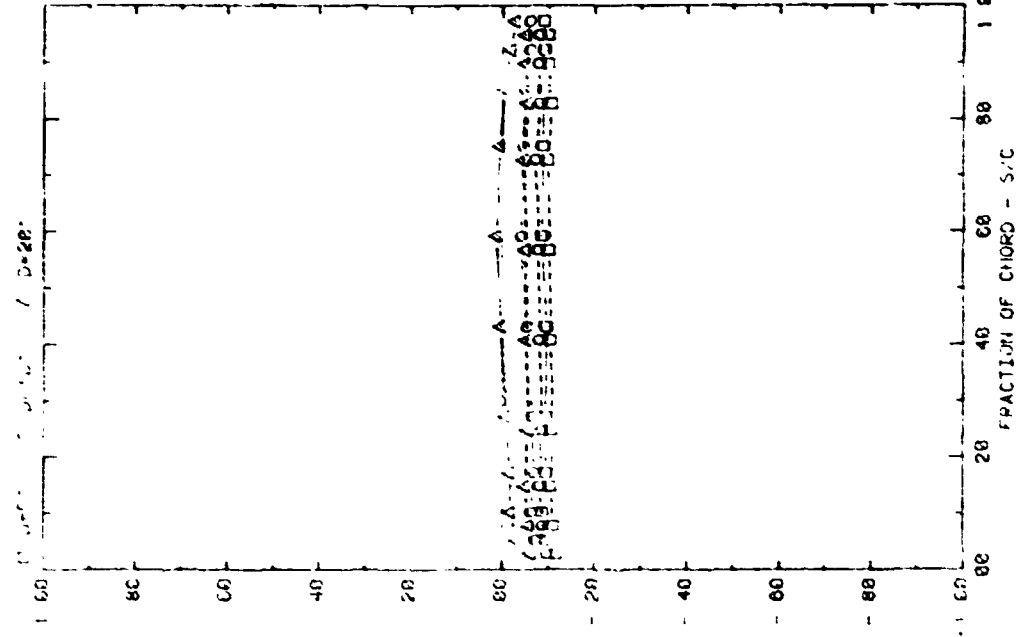
PRESSURE COEFFICIENT REFERENCED TO 10% ON PROTOTYPE



FRONT AND BACK PRESSURES ON ARRAY #7 WITH SEPARATION = 2C  
EFFECT OF FENCE DISTANCE WITH  $M=3$ ,  $P=30\%$ , AND  $\alpha=95$

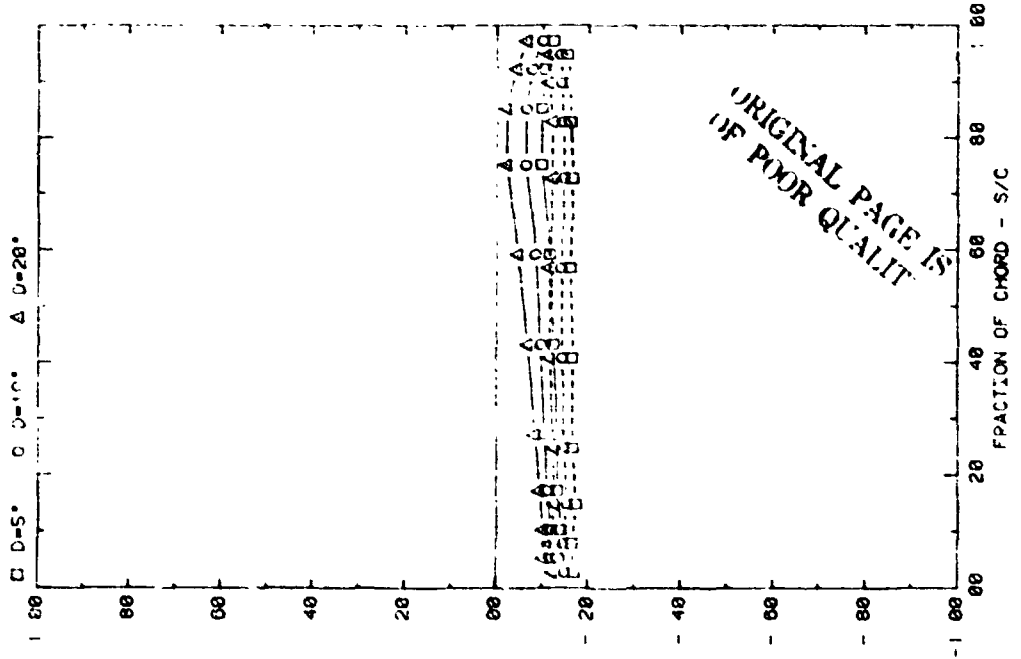
PRESSURE COEFFICIENT REFERENCED TO 10% ON PROTOTYPE

Plot 3-3. (Continued)



PRESSURE COEFFICIENT REFERENCED TO 1/4 IN ON PROTOTYPE

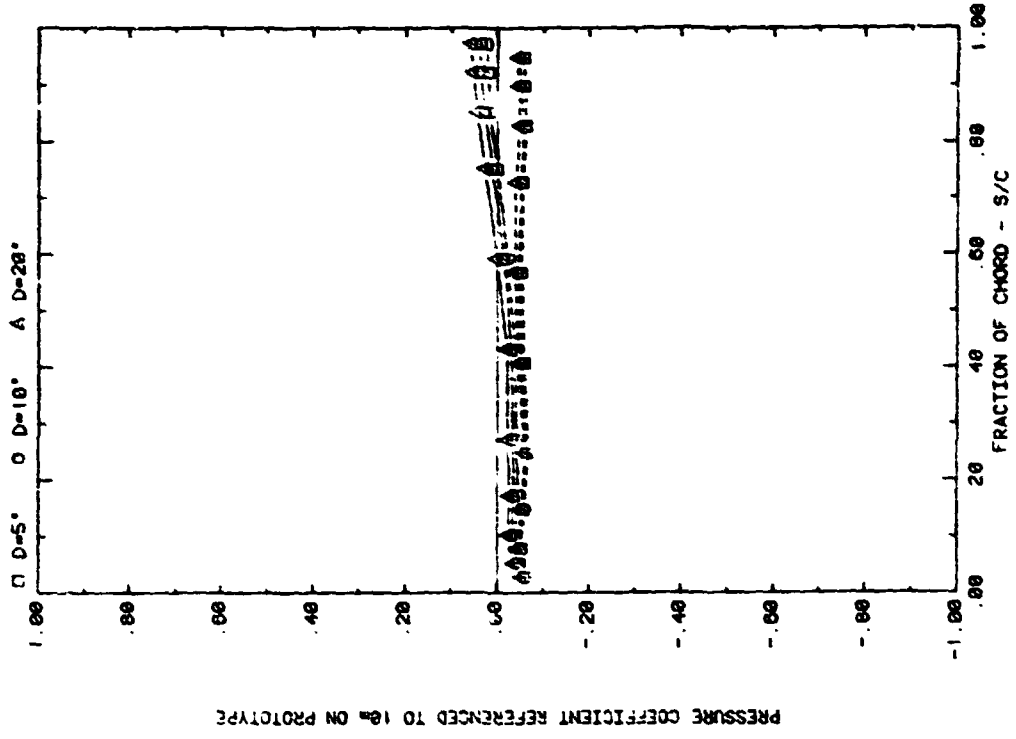
FRONT AND BACK PRESSURES ON ARRAY #2 WITH SEPARATION = 2C  
EFFECT OF FEINCE DISTANCE WITH H=3\*, P=30%, AND ALPHA=180



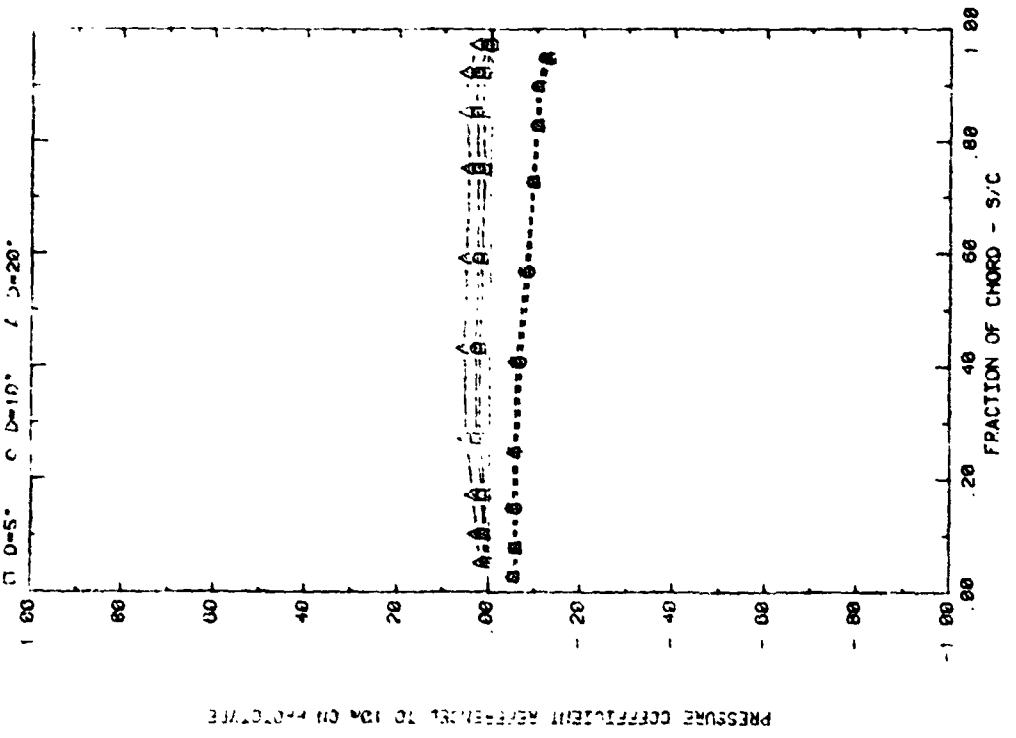
PRESSURE COEFFICIENT REFERENCED TO 1/4 IN ON PROTOTYPE

FRONT AND BACK PRESSURES ON ARRAY #2 WITH SEPARATION = 2C  
EFFECT OF FEINCE DISTANCE WITH H=3\*, P=30%, AND ALPHA=145

Plot 3-3. (Continued)



FRONT AND BACK PRESSURES ON ARRAY #5 WITH SEPARATION = 2C  
EFFECT OF FENCE DISTANCE WITH  $H=3^\circ$ ,  $P=38\%$ , AND  $\text{ALPHA}=30^\circ$

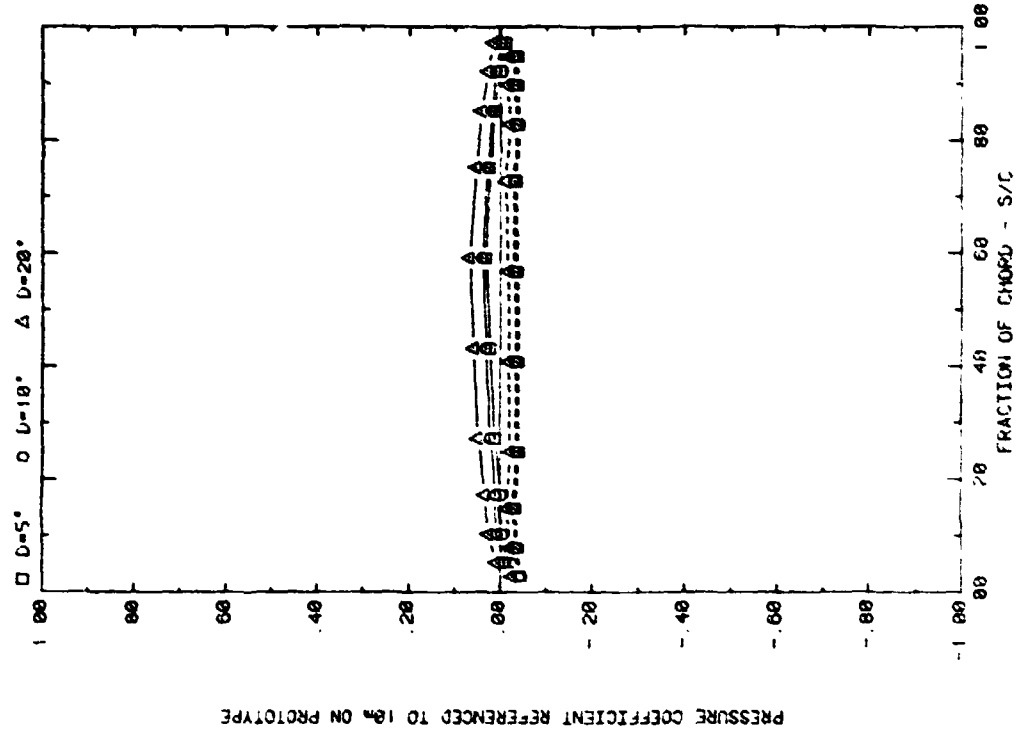


FRONT AND BACK PRESSURES ON ARRAY #5 WITH SEPARATION = 2C  
EFFECT OF FENCE DISTANCE WITH  $H=3^\circ$ ,  $P=30\%$ , AND  $\text{ALPHA}=35^\circ$

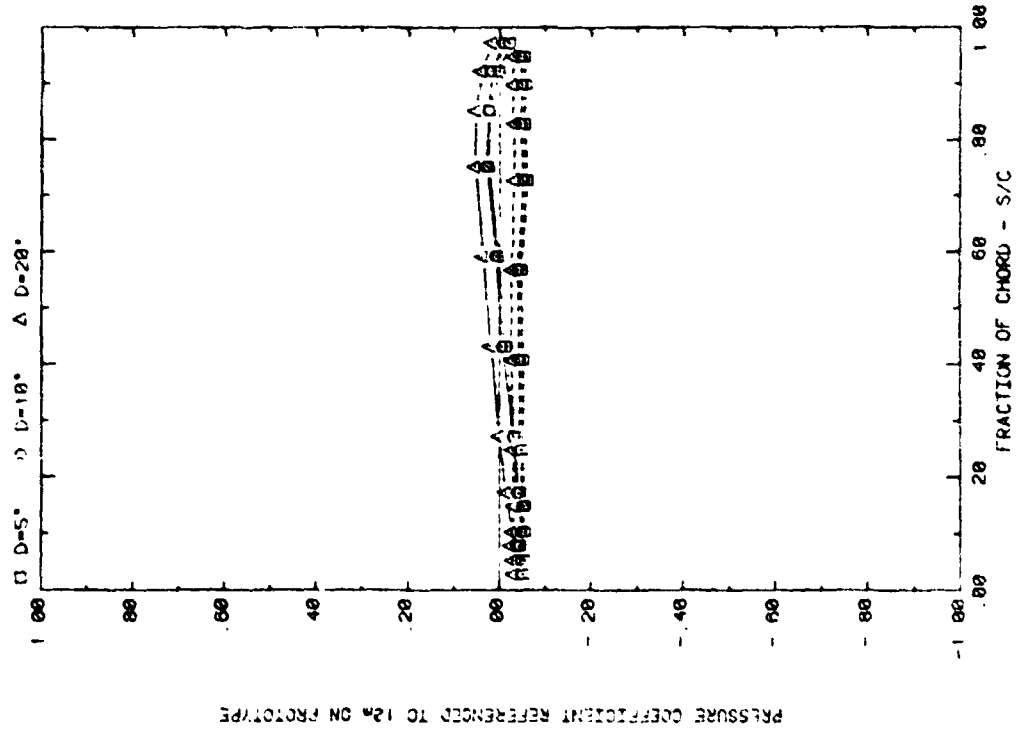
Plot 3-3. (Continued)

PRESSURE COEFFICIENT REFERENCED TO 10% ON PROTOTYPE

PRESSURE COEFFICIENT REFERENCED TO 10% ON PROTOTYPE

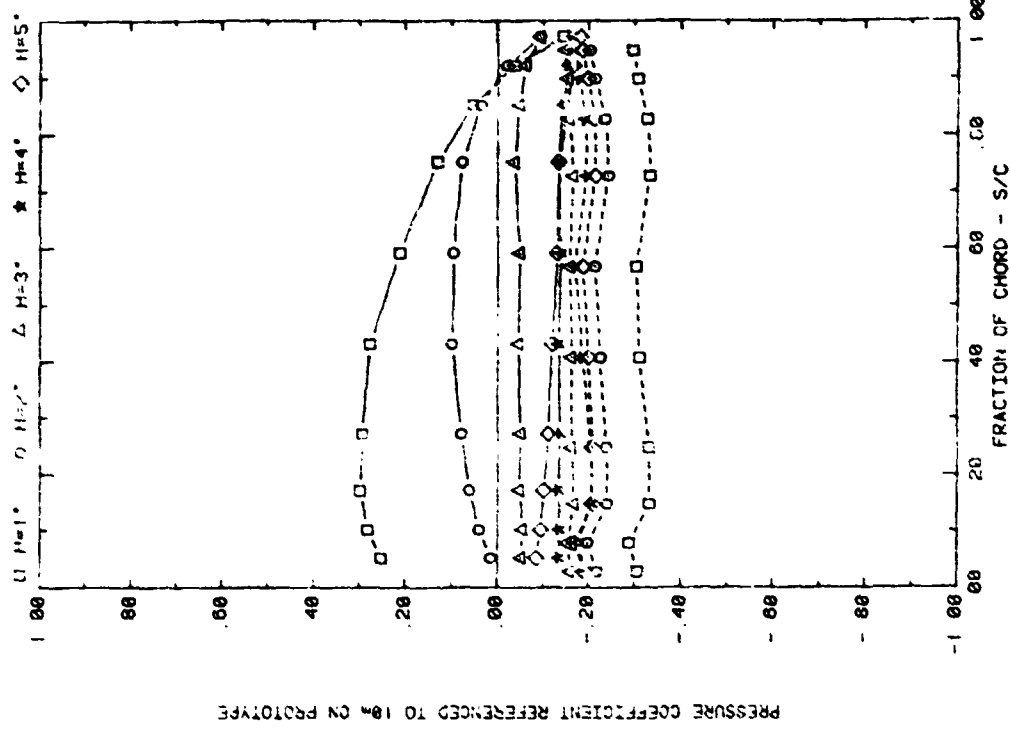


FRONT AND BACK PRESSURES ON ARRAY #5 WITH SEPARATION = 2C  
EFFECT OF FENCE DISTANCE WITH M=3°, P=30%, AND ALPHA=160

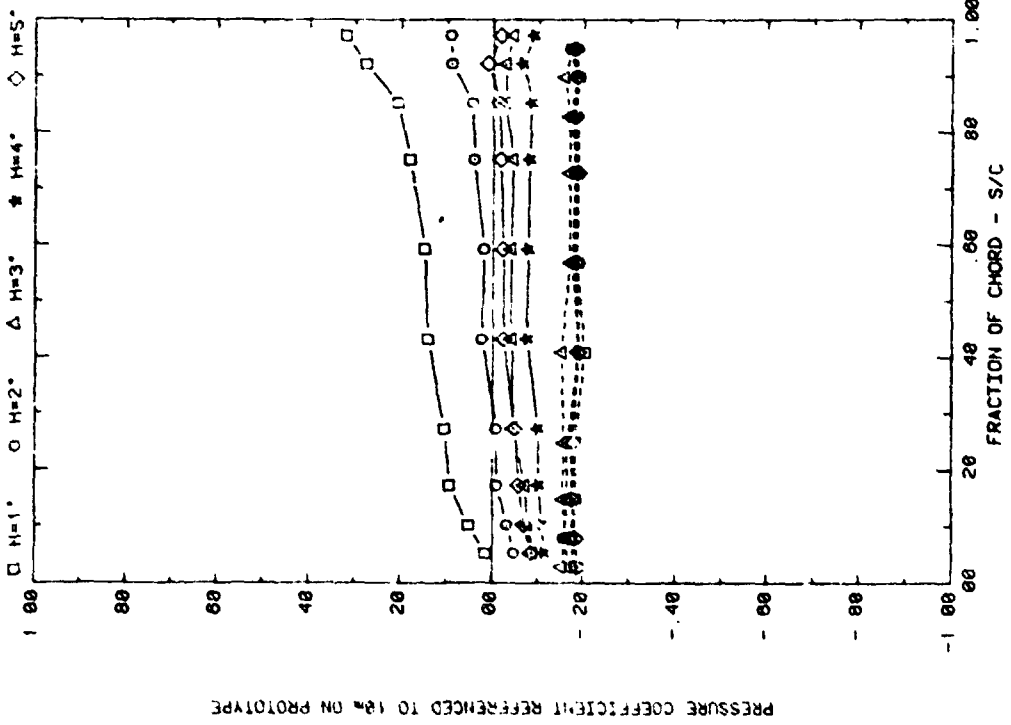


FRONT AND BACK PRESSURES ON ARRAY #5 WITH SEPARATION = 2C  
EFFECT OF FENCE DISTANCE WITH M=3°, P=30%, AND ALPHA=145

Plot 3-3. (Concluded)

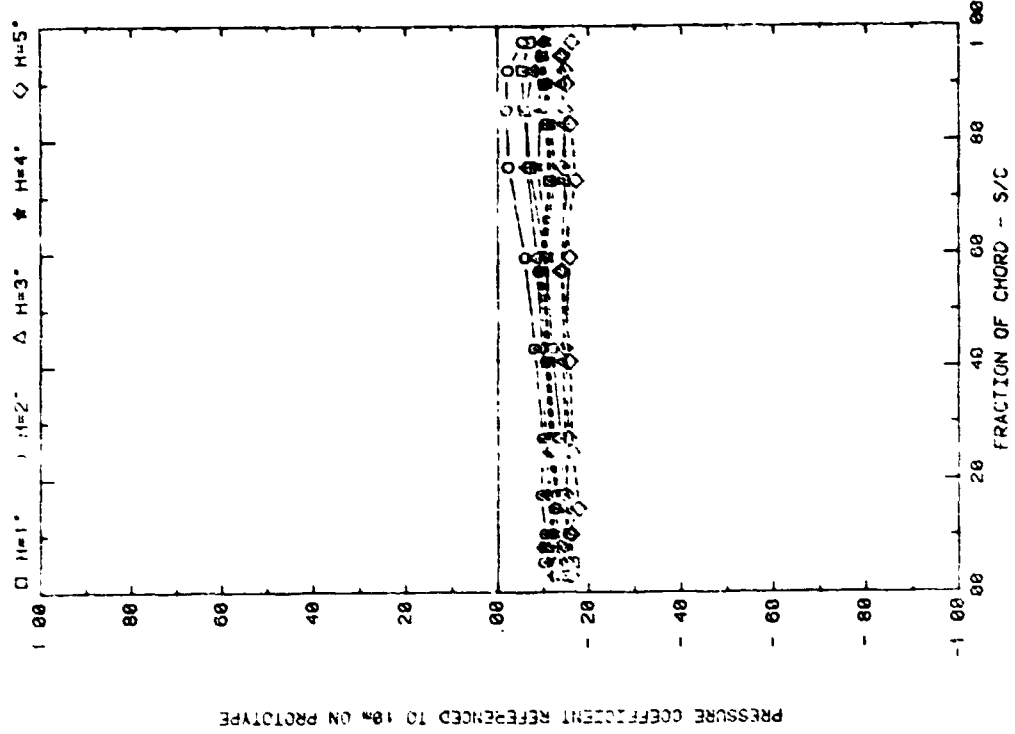


FRONT AND BACK PRESSURES ON ARRAY #1 WITH SEPARATION = 2C  
EFFECT OF FENCE HEIGHT WITH ALPHA=145, D=10", AND P=30%

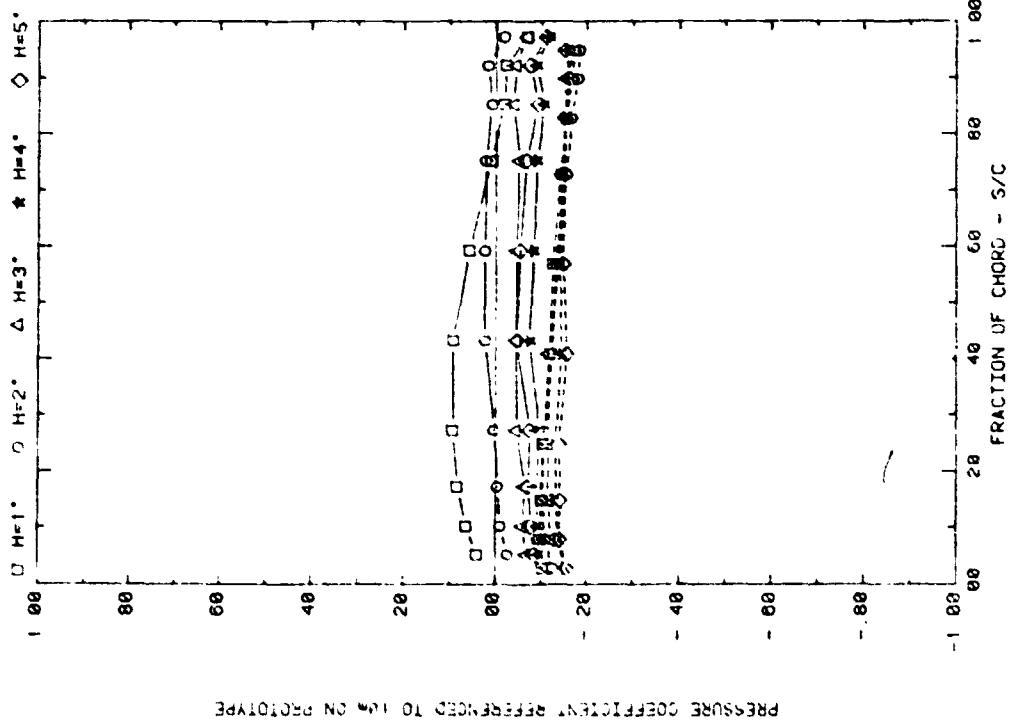


FRONT AND BACK PRESSURES ON ARRAY #1 WITH SEPARATION = 2C  
EFFECT OF FENCE HEIGHT WITH ALPHA=35, D=10", AND P=30%

Plot 3-4. Multiple Arrays with Fence,  $WD = 0^\circ$   
Effect of Fence Height

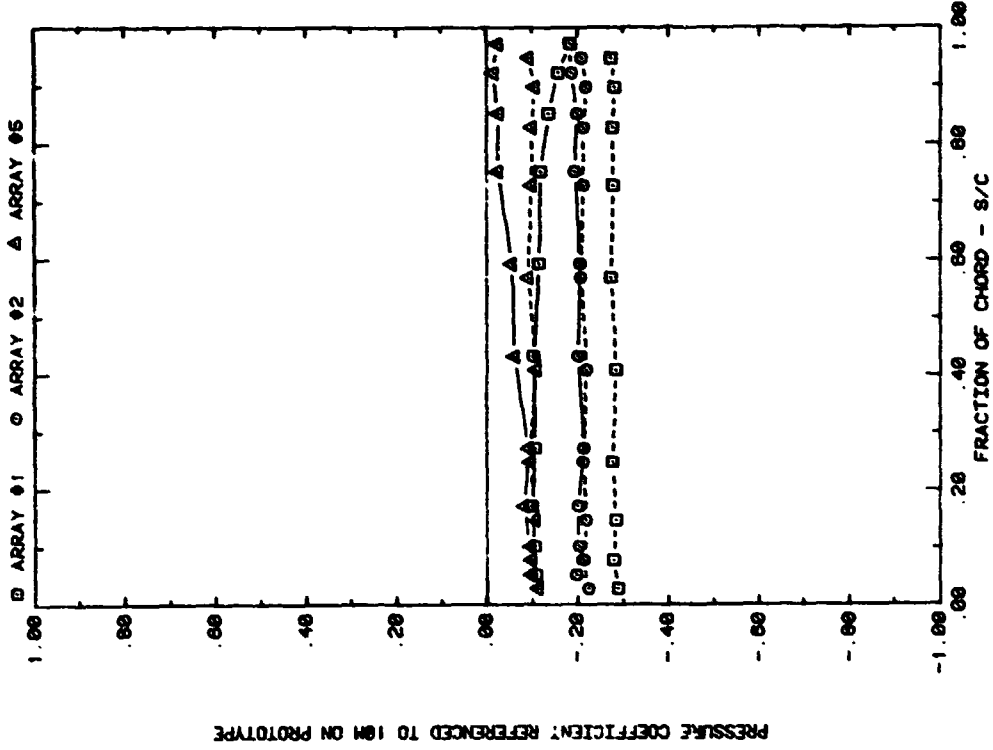


FRONT AND BACK PRESSURES ON ARRAY #2 WITH SEPARATION = 2C  
EFFECT OF FENCE HEIGHT WITH ALPHA=145, D=10°, AND P=30%



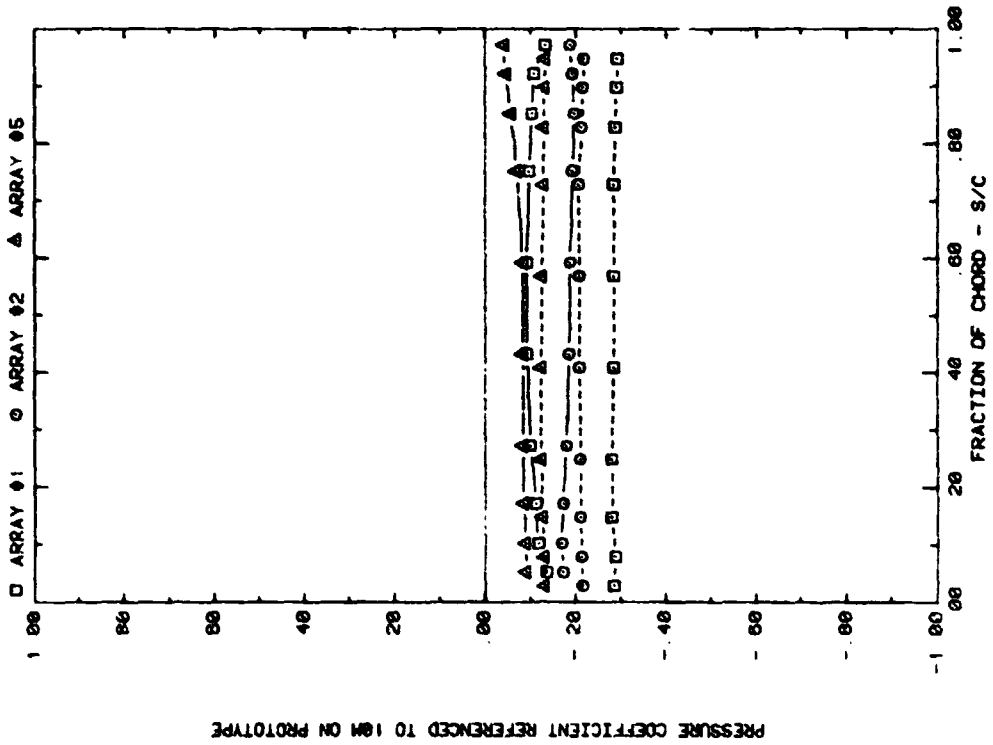
FRONT AND BACK PRESSURES ON ARRAY #2 WITH SEPARATION = 2C  
EFFECT OF FENCE HEIGHT WITH ALPHA=35, D=10°, AND P=30%

Plot 3-4. (Continued)



PRESSURE COEFFICIENT REFERENCED TO 14M ON PROTOTYPE

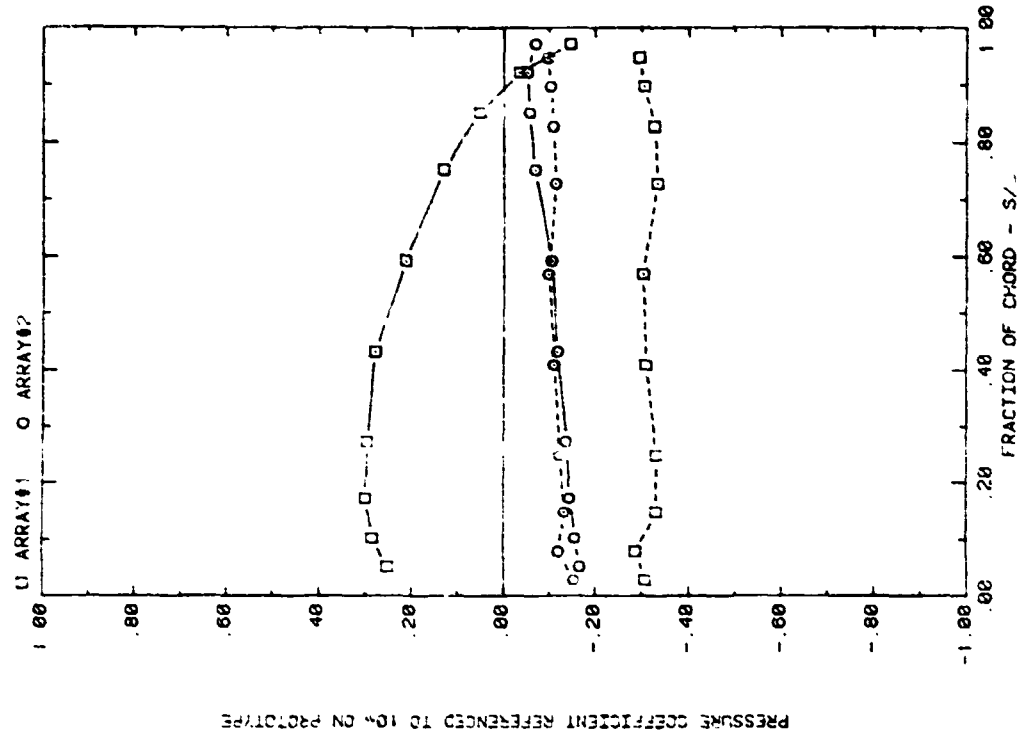
FRONT AND BACK PRESSURES ON ARRAYS #1, #2, #5 WITH SEPARATION = 2C  
EFFECT OF ARRAY WITH ALPHA = 0, WIND = 0, HF = 4°



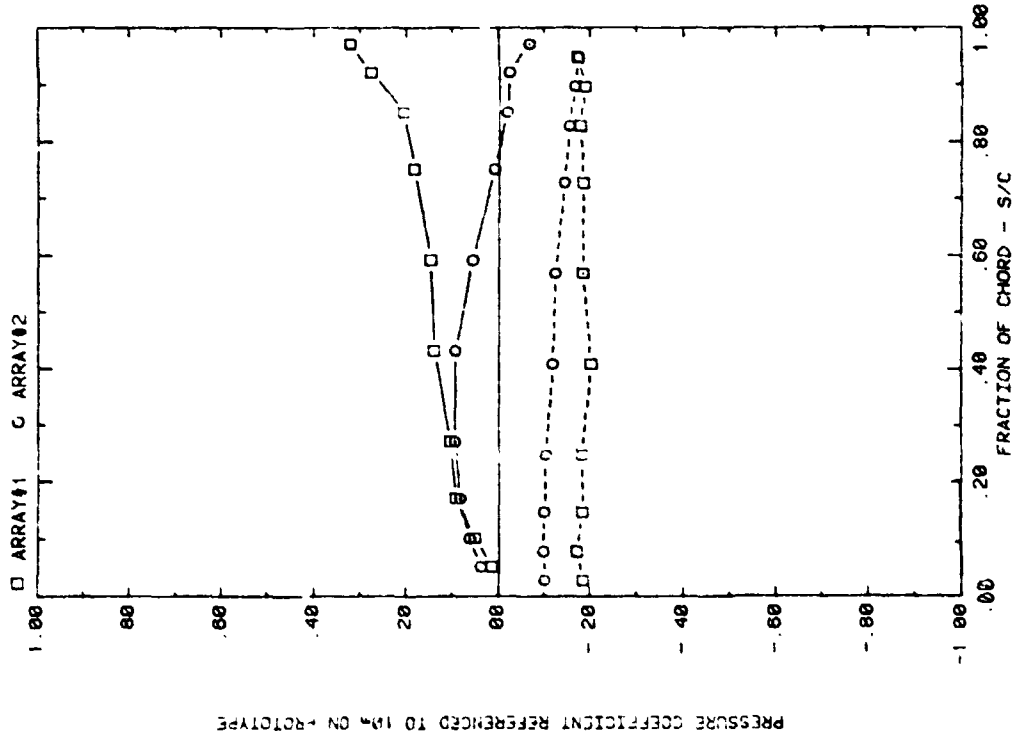
PRESSURE COEFFICIENT REFERENCED TO 14M ON PROTOTYPE

FRONT AND BACK PRESSURES ON ARRAYS #1, #2, #5 WITH SEPARATION = 2C  
EFFECT OF ARRAY WITH ALPHA = 4°, WIND = 0, HF = 4°

Plot 3-4. (Continued)

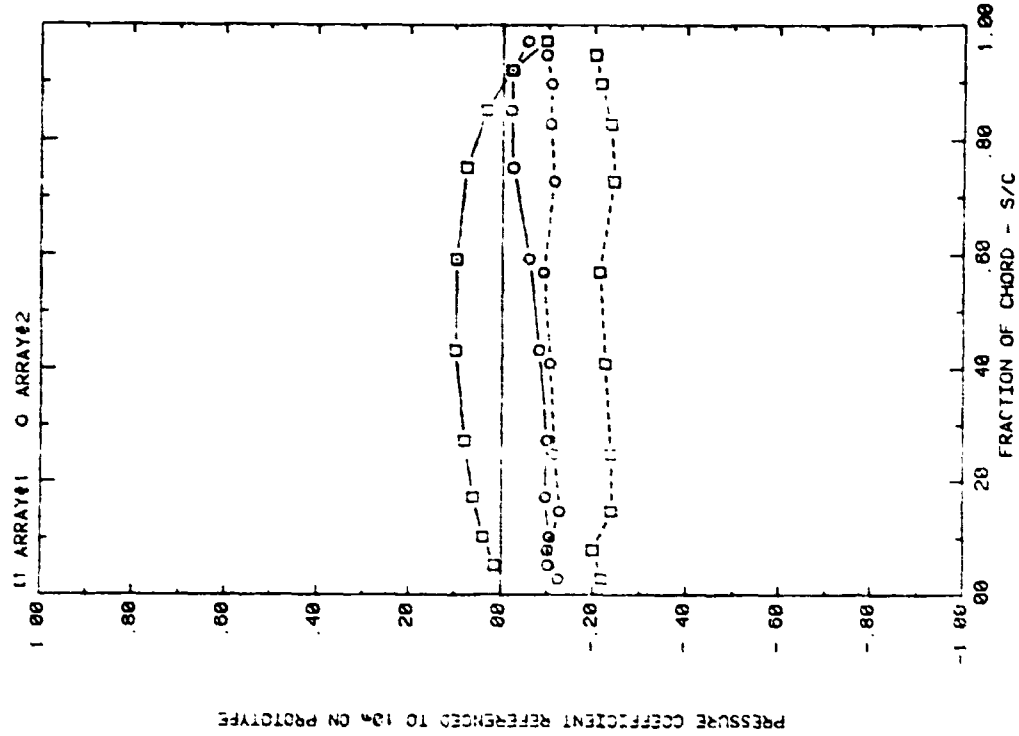


FRONT AND BACK PRESSURES ON ARRAYS #1&#2 WITH SEPARATION = 2C  
EFFECT OF ARRAY WITH ALPHA=145, H=1", D=10", AND P=30%

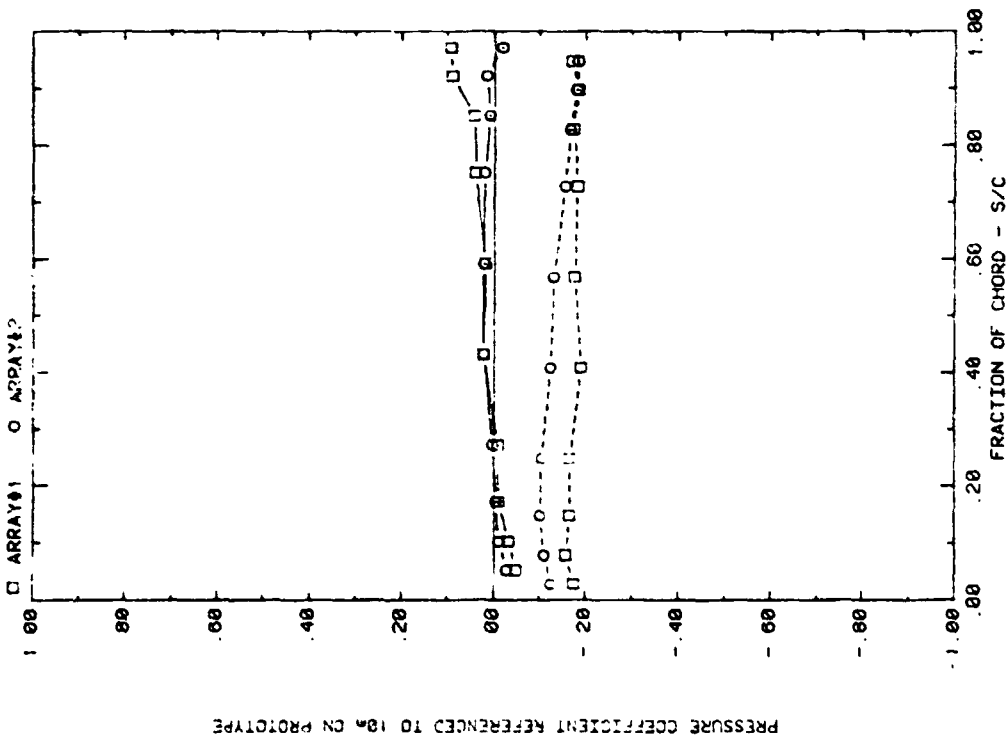


FRONT AND BACK PRESSURES ON ARRAYS #1&#2 WITH SEPARATION = 2C  
EFFECT OF ARRAY WITH ALPHA=35, H=1", D=10", AND P=30%

Plot 3-4. (Continued)

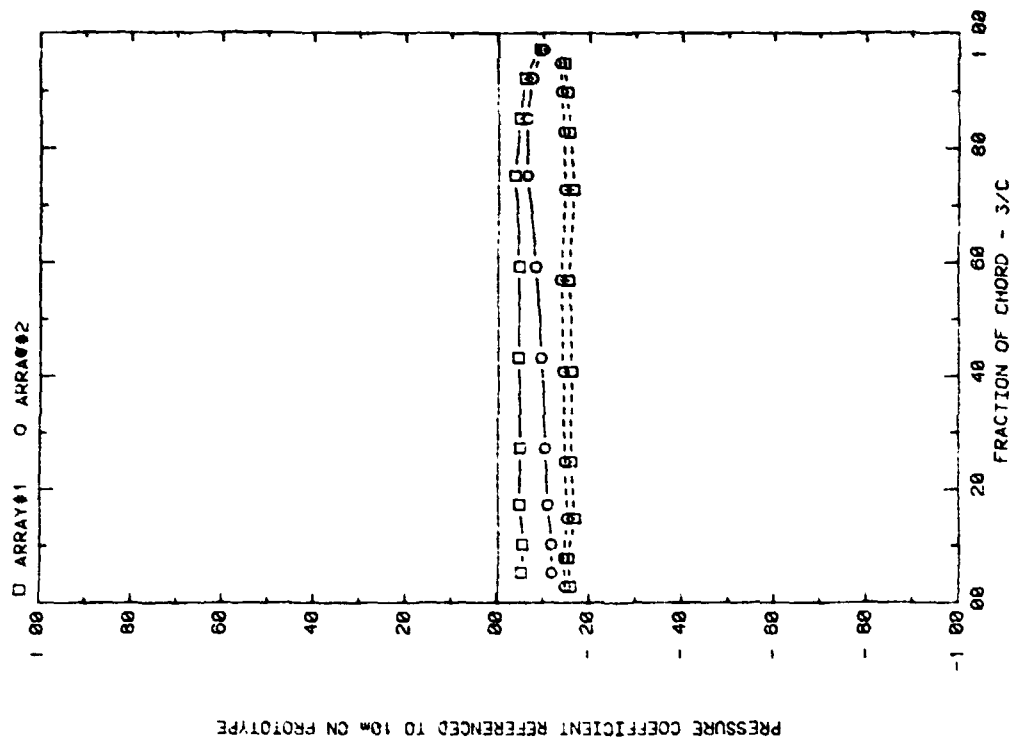


FRONT AND BACK PRESSURES ON ARRAYS #1&2 WITH SEPARATION = 2C  
EFFECT OF ARRAY WITH ALPHA=145, H=2', D=10', AND P=30%

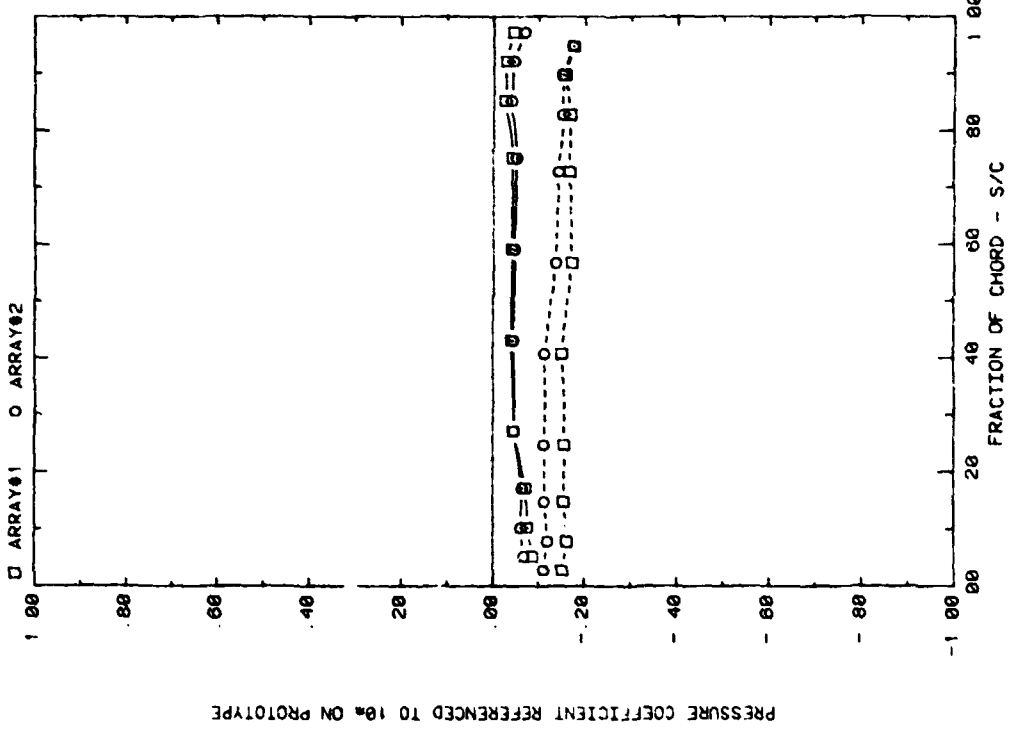


FRONT AND BACK PRESSURES ON ARRAYS #1&2 WITH SEPARATION = 2C  
EFFECT OF ARRAY WITH ALPHA=35, H=2', D=10', AND P=30%

Plot 3-4. (Continued)

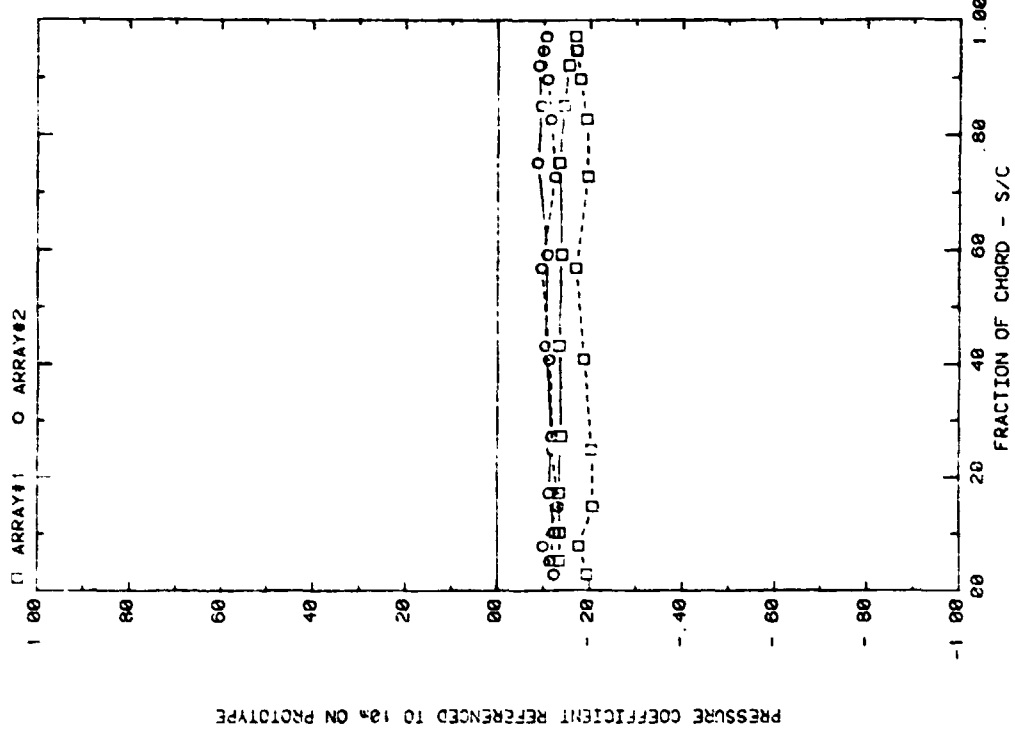


FRONT AND BACK PRESSURES ON ARRAYS #1&#2 WITH SEPARATION = 2C  
EFFECT OF ARRAY WITH ALPHA=15, H=3', D=10', AND P=30%



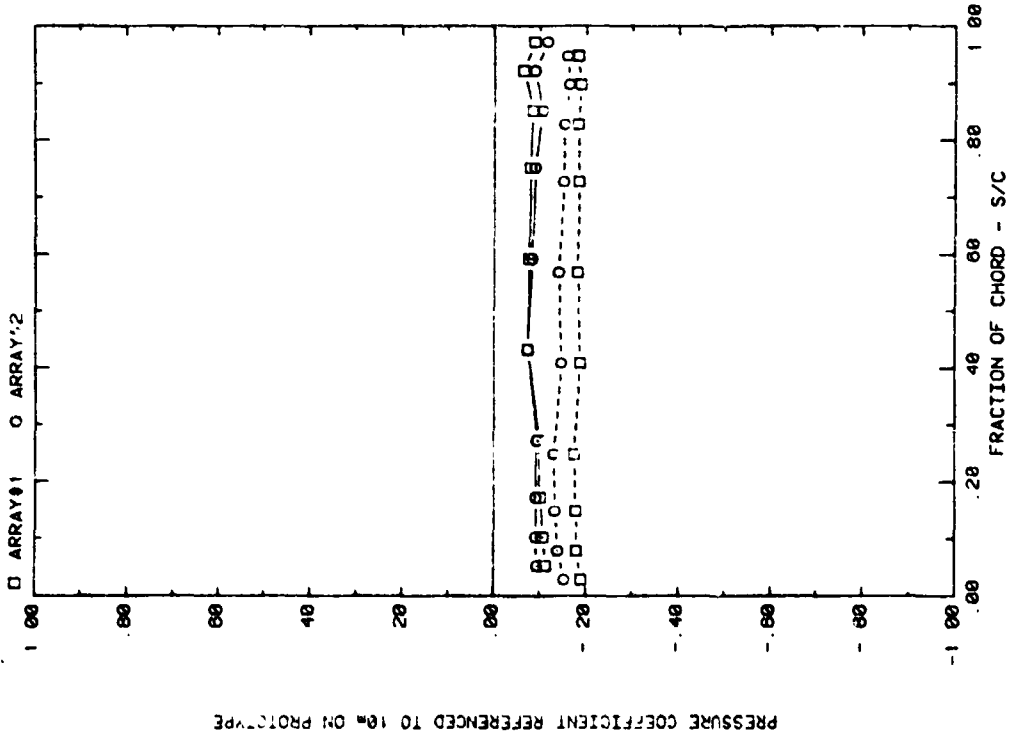
FRONT AND BACK PRESSURES ON ARRAYS #1&#2 WITH SEPARATION = 2C  
EFFECT OF ARRAY WITH ALPHA=35, H=3', D=10', AND P=30%

Plot 3-4. (Continued)



PRESSURE COEFFICIENT REFERENCED TO 12% ON PROTOTYPE

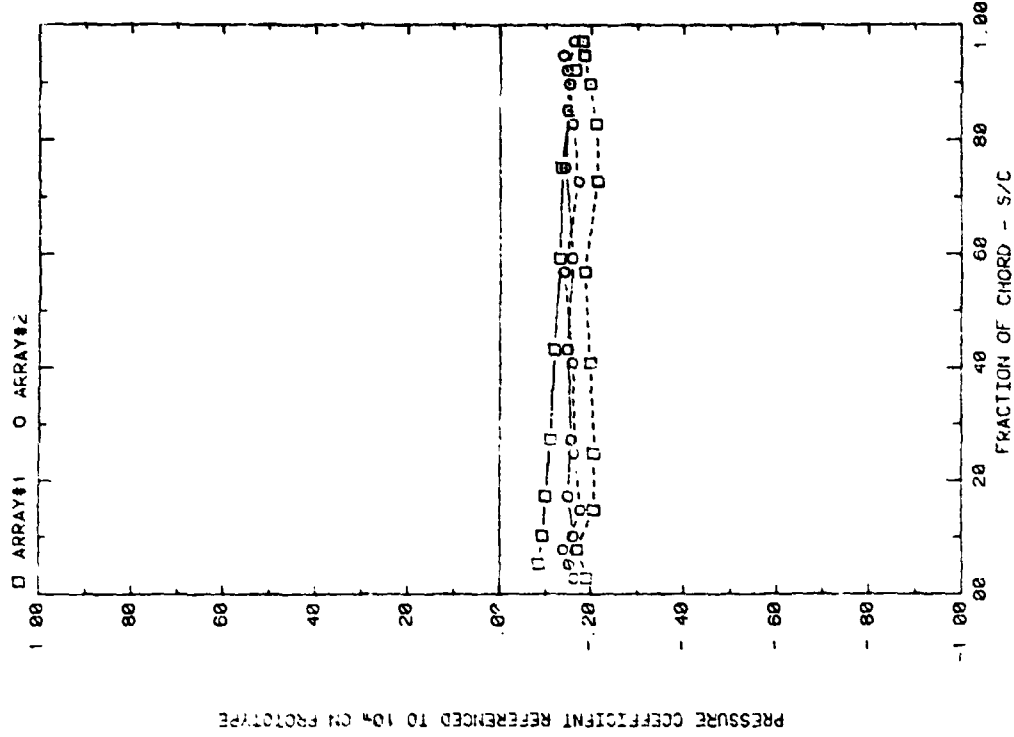
FRONT AND BACK PRESSURES ON ARRAYS #1&#2 WITH SEPARATION = 2C  
EFFECT OF ARRAY WITH ALPHA=145, H=4", D=10", AND P=30X



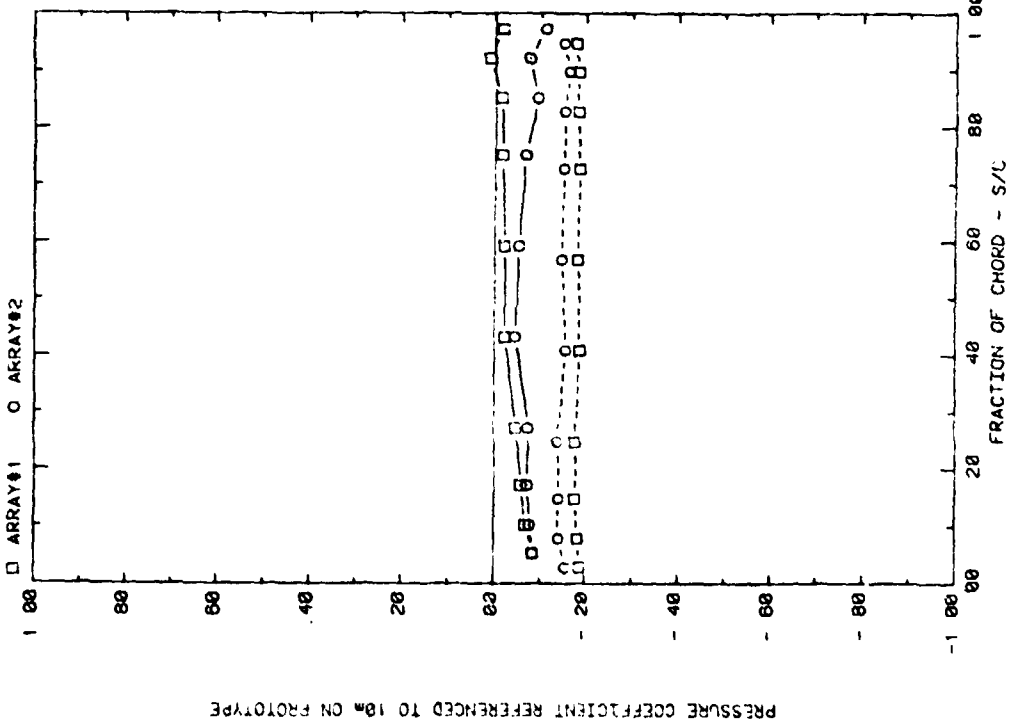
PRESSURE COEFFICIENT REFERENCED TO 10% ON PROTOTYPE

FRONT AND BACK PRESSURES ON ARRAYS #1&#2 WITH SEPARATION = 2C  
EFFECT OF ARRAY WITH ALPHA=35, H=4", D=10", AND P=30X

Plot 3-4. (Continued)

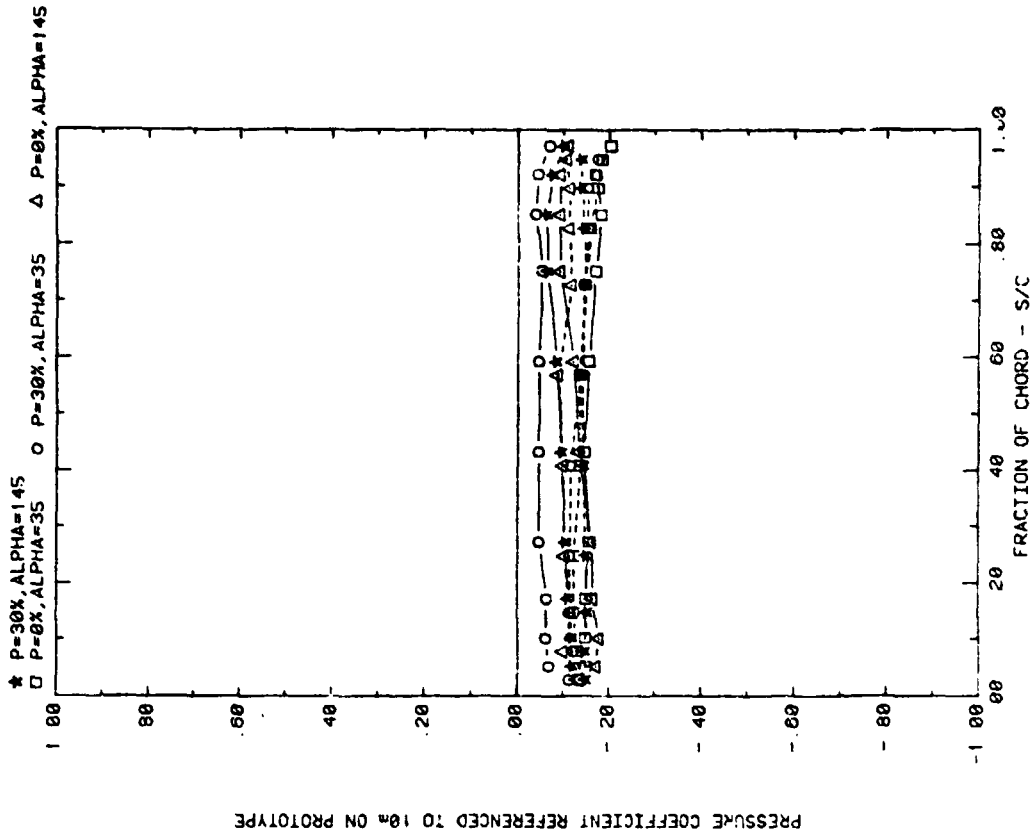


FRONT AND BACK PRESSURES ON ARRAYS #1&#2 WITH SEPARATION = 2C  
EFFECT OF ARRAY WITH ALPHA=14.5, H=5", D=10", AND P=30%

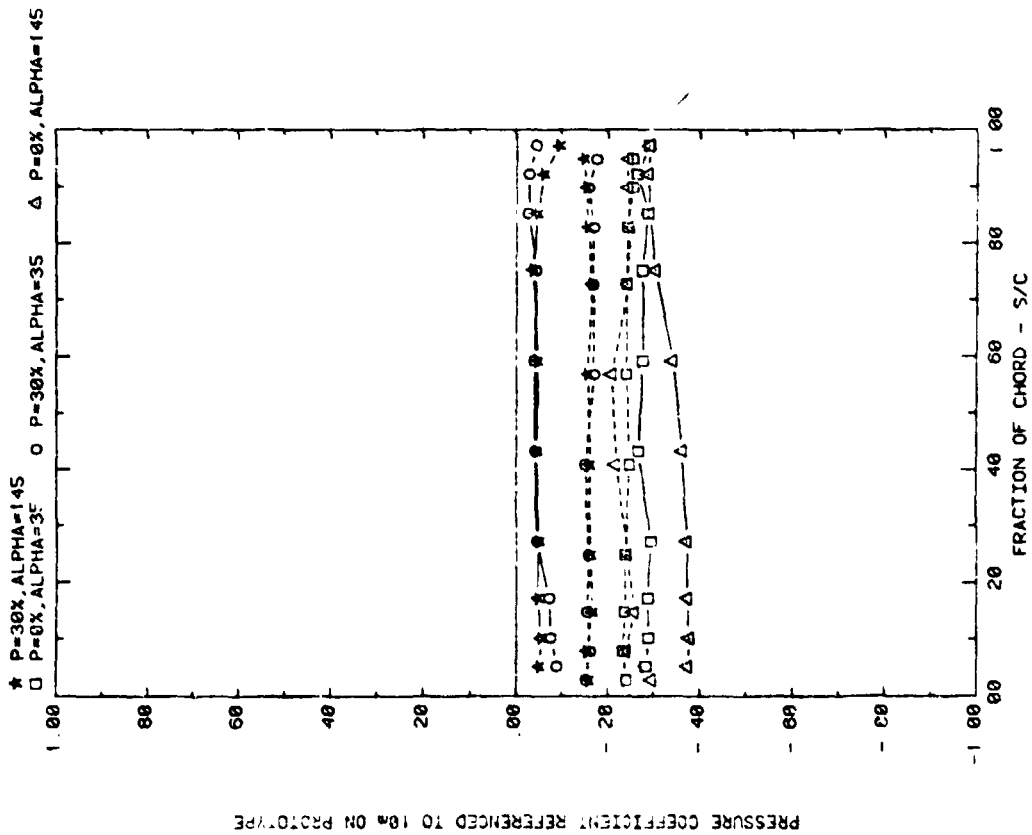


FRONT AND BACK PRESSURES ON ARRAYS #1&#2 WITH SEPARATION = 2C  
EFFECT OF ARRAY WITH ALPHA=35, H=5", D=10", AND P=30%

Plot 3-4. (Concluded)

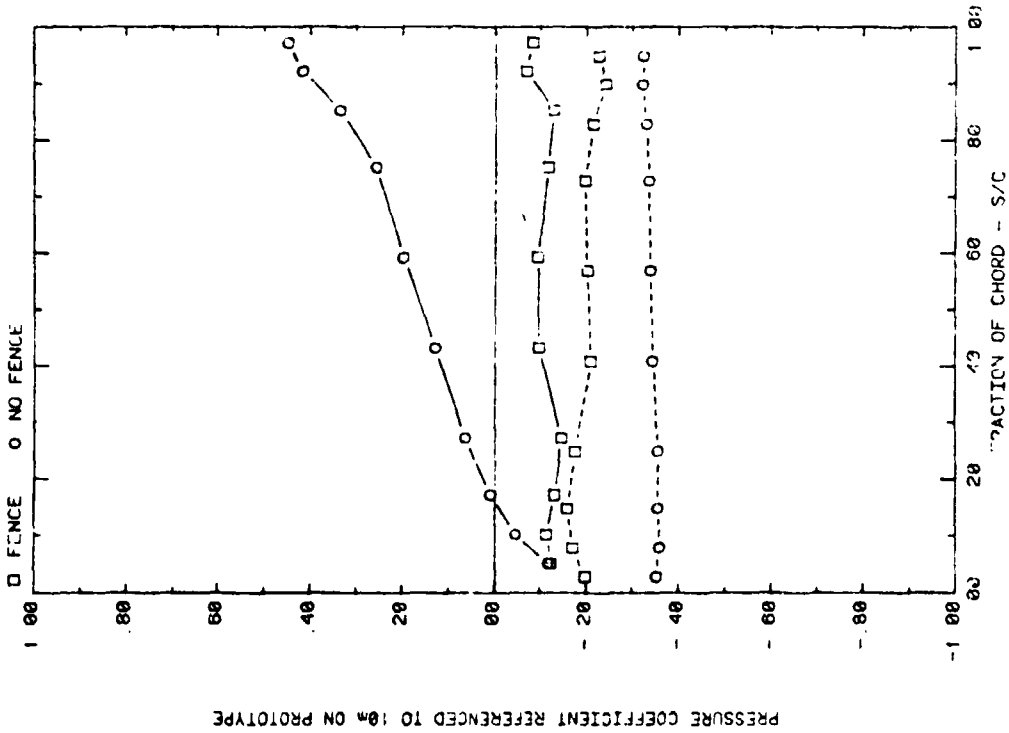
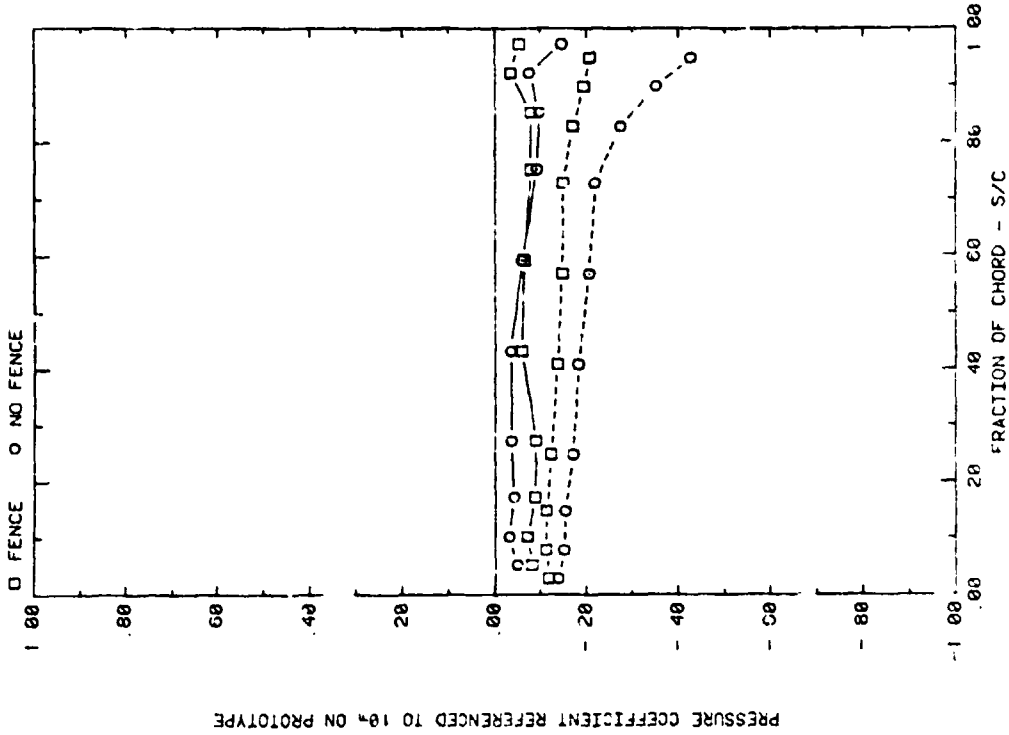


FRONT A J BACK PRESSURES ON ARRAY #2 WITH SEPARATION = 2C  
 EFFECT OF FENCE POROSITY WITH ALPHA=35 OR 145, D=10', AND H=3'

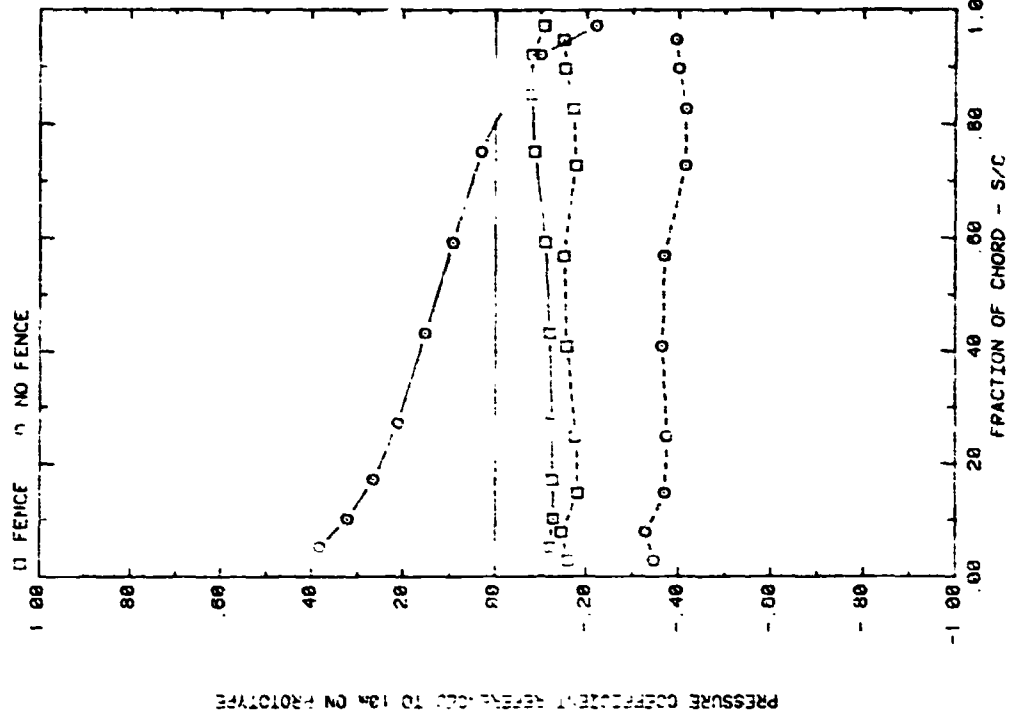


FRONT AND BACK PRESSURES ON ARRAY #1 WITH SEPARATION = 2C  
 EFFECT OF FENCE POROSITY WITH ALPHA=35 OR 145, D=10', AND H=3'

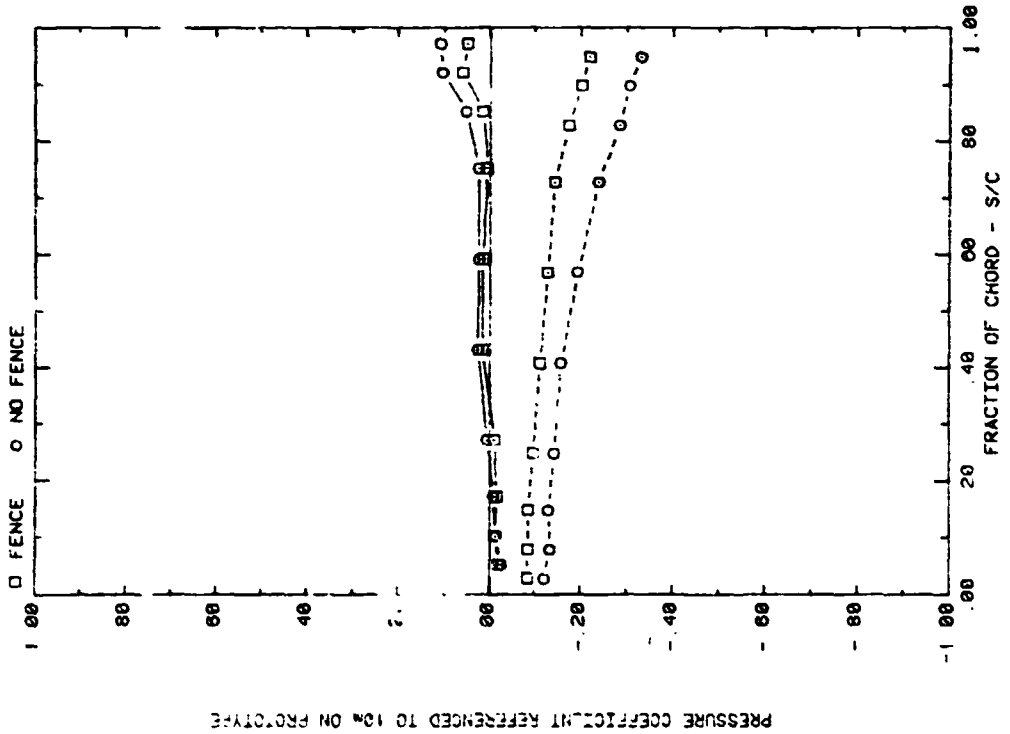
Plot 3-5. Multiple Arrays with Fence,  $WD = 0^\circ$   
 Effect of Fence Porosity



FRONT AND BACK PRESSURES ON ARRAY #1 WITH  $X=2C$ , AND WIND=0  
 EFFECT OF FENCE ON APPA EDGE, ALPHA=35, H=3", D=13", AND P=30%  
 FRONT AND BACK PRESSURES ON ARRAY #2 WITH  $X=2C$ , AND WIND=0  
 EFFECT OF FENCE ON ALRAY EDGE, ALPHA=35, H=3", D=13", AND P=30%  
 Plot 4-1. Edge Study,  $WD = 0^\circ$   
 Effect of Fence

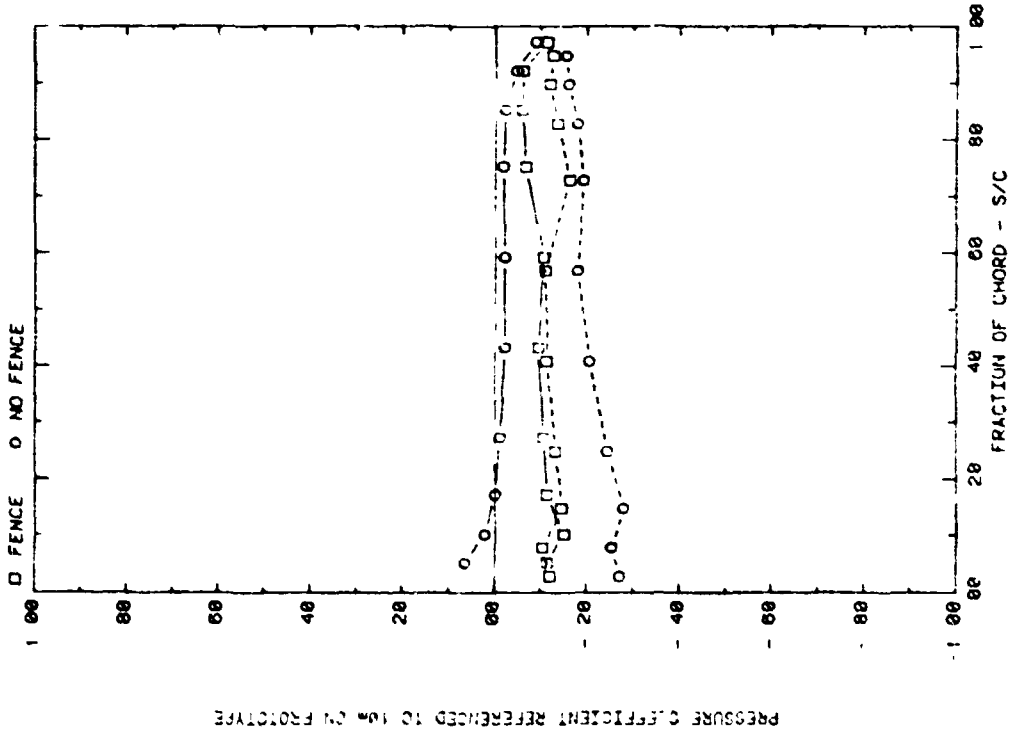
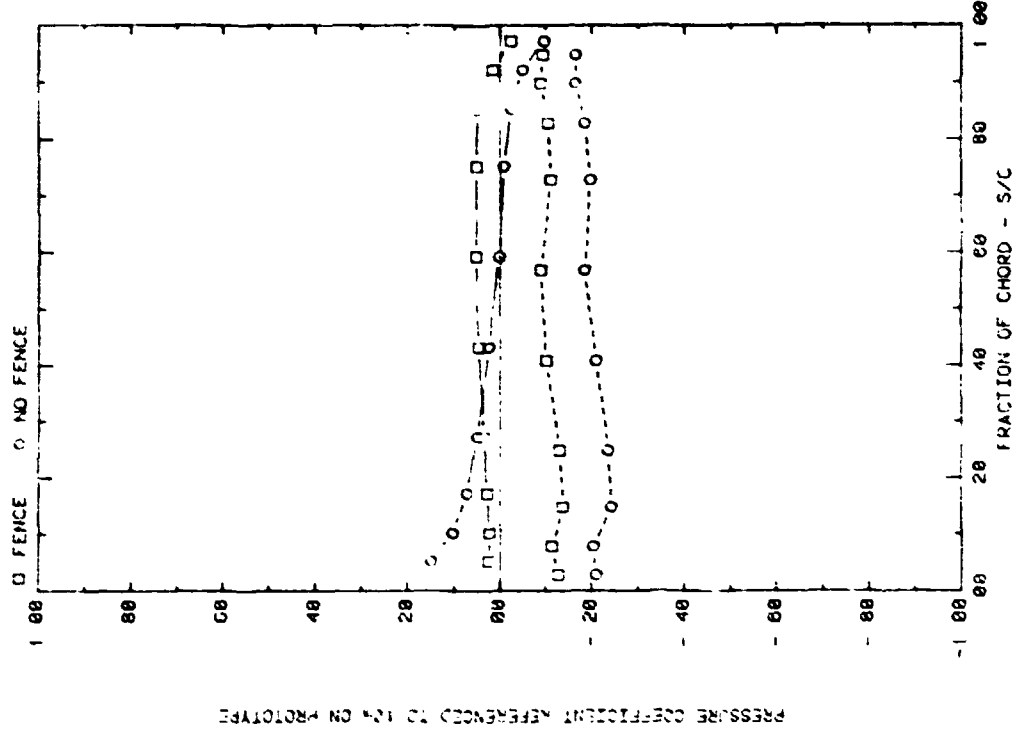


FRONT AND BACK PRESSURES ON ARRAY #1 WITH X=2C, AND WIND=0  
EFFECT OF FENCE ON ARRAY EDGE, ALPHA=145, H=3, D=10, AND P=30X



FRONT AND BACK PRESSURES ON ARRAY #5 WITH X=2C, AND WIND=0  
EFFECT OF FENCE ON ARRAY EDGE, ALPHA=35, H=3, D=10, AND P=30X

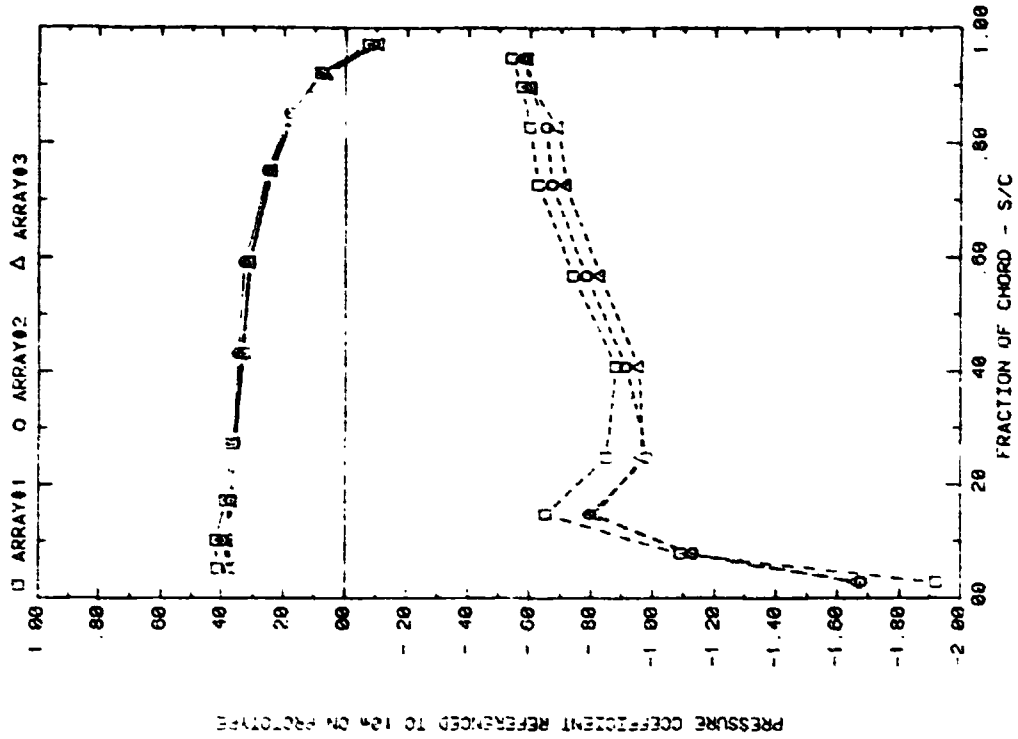
Plot 4-1. (Continued)



FRONT AND BACK PRESSURES ON ARRAY #2 WITH X=20, H=3, U=10, AND P=30X  
EFFECT OF FENCE ON ARRAY EDGE, ALPHA=145, H=3, U=10, AND P=30X

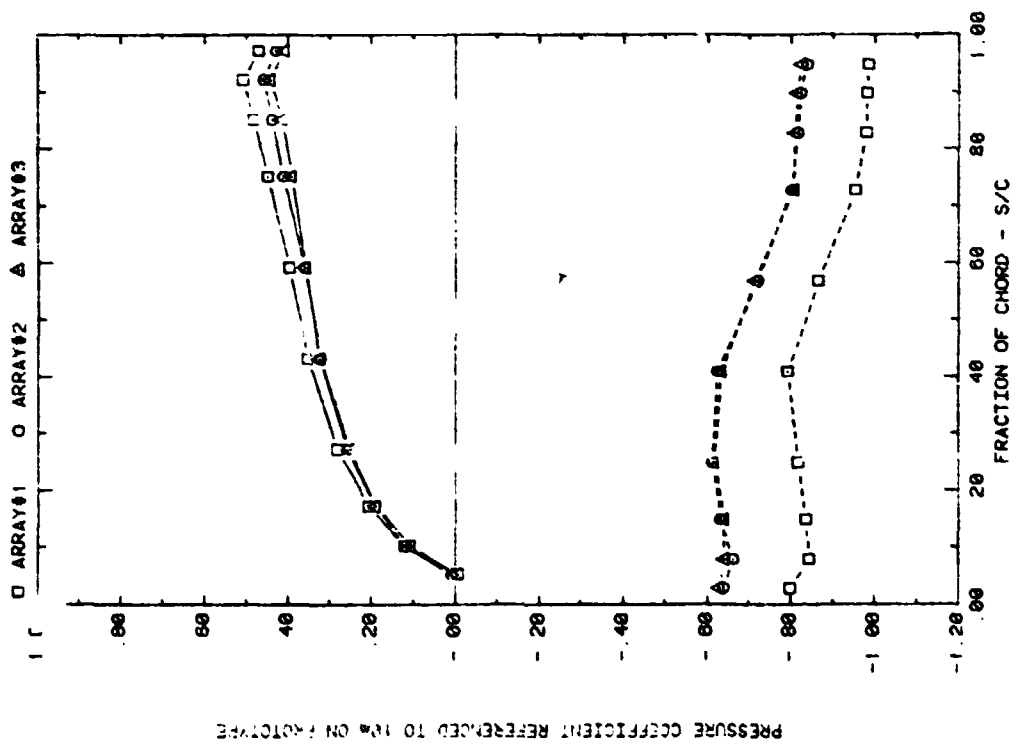
FRONT AND BACK PRESSURES ON ARRAY #2 WITH X=20, H=3, U=10, AND P=30X  
EFFECT OF FENCE ON ARRAY EDGE, ALPHA=145, H=3, U=10, AND P=30X

Plot 4-1. (Concluded)



PRESSURE COEFFICIENT REFERENCED TO 1/4 ON FACTIVE

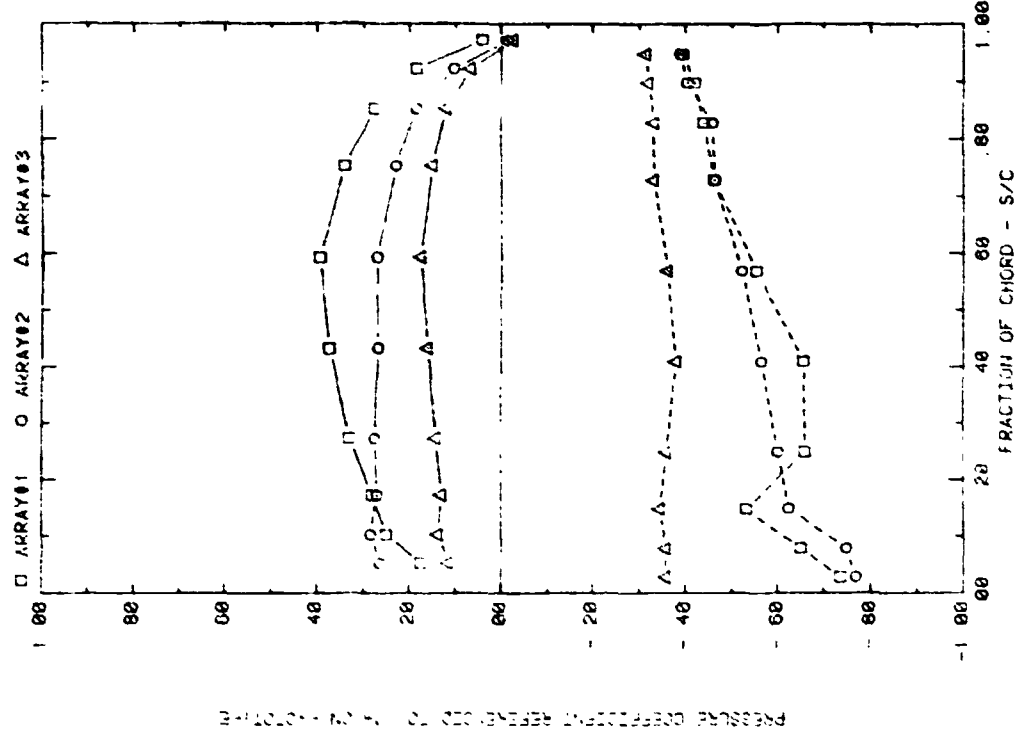
FRONT AND BACK PRESSURES 0.6° IN FROM ARRAY EDGE, X=2C, WIND=45  
EFFECT OF ARRAY WITH ALPHA=145, FC=0, H=3', D=10', AND P=30K



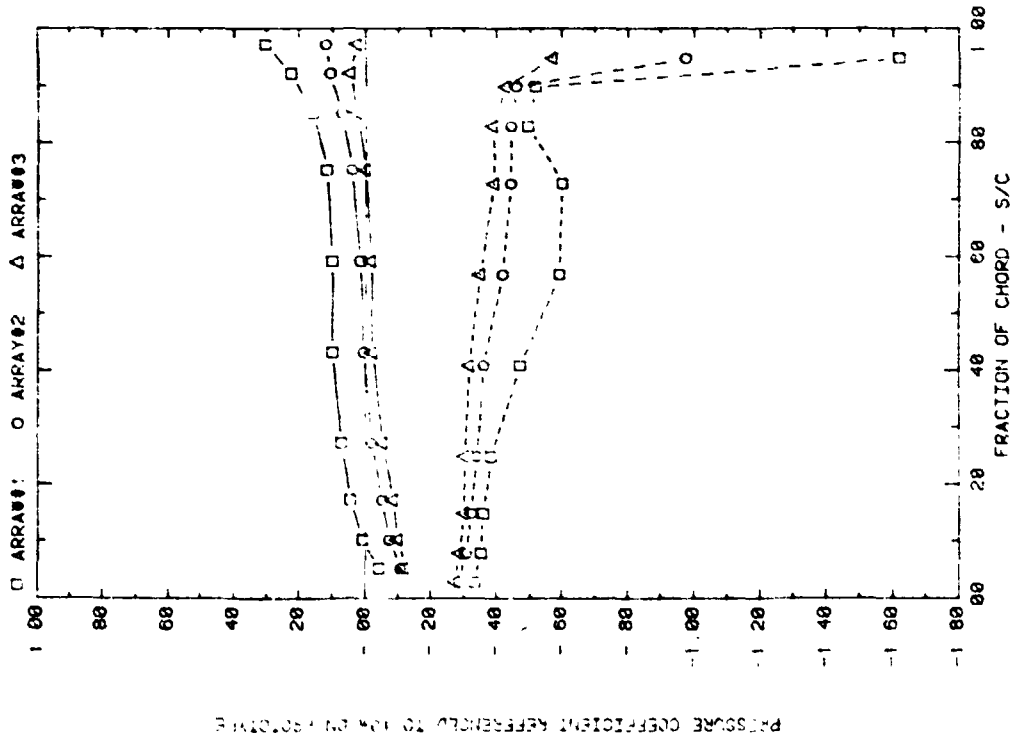
PRESSURE COEFFICIENT REFERENCED TO 1/4 ON FACTIVE

FRONT AND BACK PRESSURES 0.6° IN FROM ARRAY EDGE, X=2C, WIND=45  
EFFECT OF ARRAY WITH ALPHA=35, FC=0, H=3', D=10', AND P=30K

Plot 5-1-1. Corner Study, WD = 45°, Standard Model  
Effect of Array Position

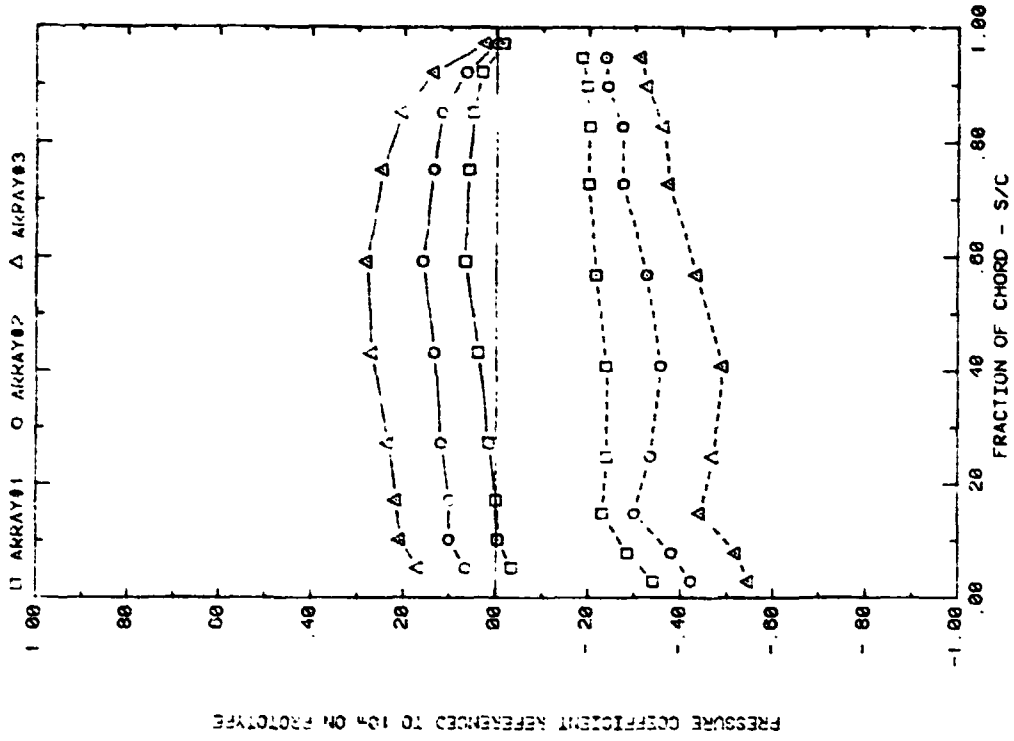


FRONT AND BACK PRESSURES 0.6" IN FROM ARRAY EDGE, X=2C, WIND=45  
EFFECT OF ARRAY WITH ALPHA=45, FC=1, H=3", D=12", AND P=30X

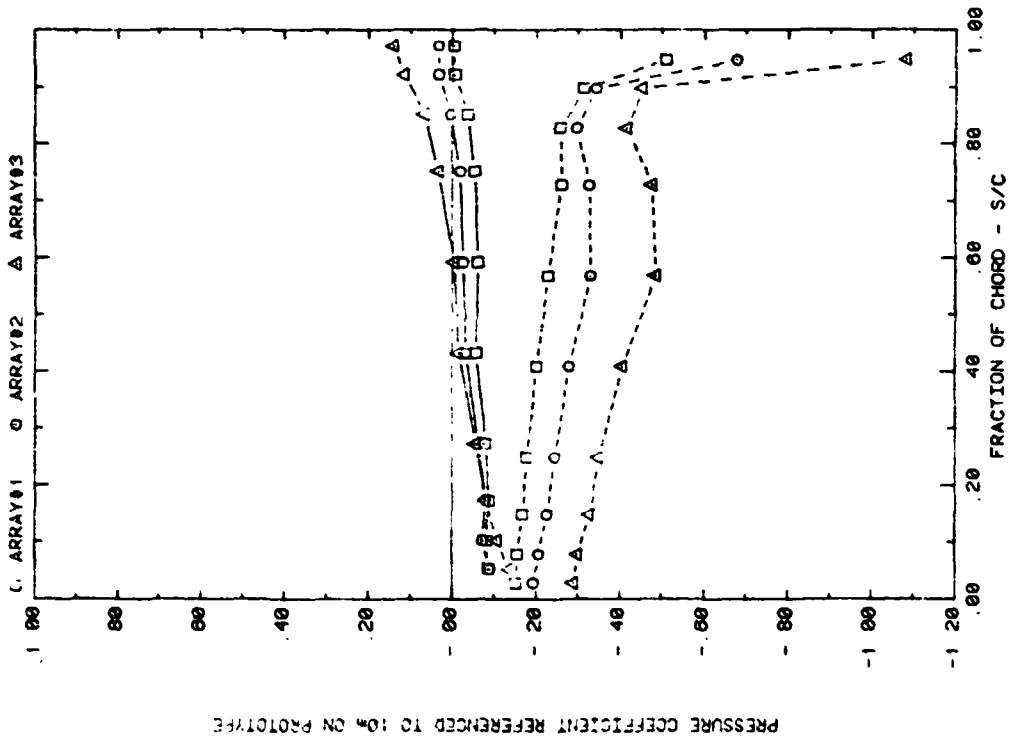


FRONT AND BACK PRESSURES 0.6" IN FROM ARRAY EDGE, X=2C, WIND=45  
EFFECT OF ARRAY WITH ALPHA=30, FC=1, H=3", D=12", AND P=30X

Plot 5-1-1. (Continued)

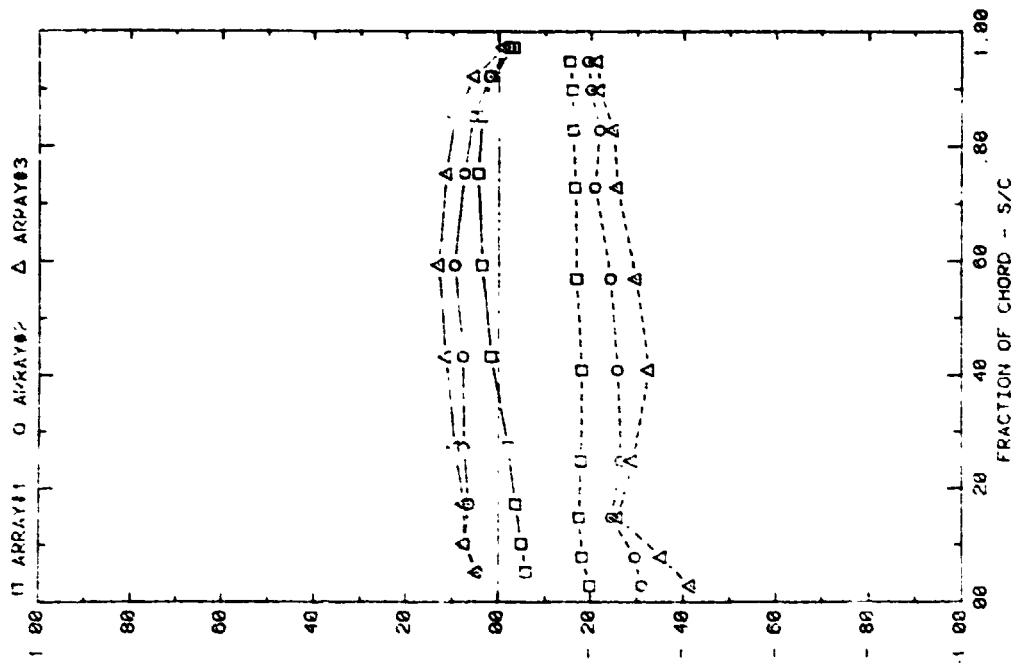


FRONT AND BACK PRESSURES  $\theta = 0^\circ$  IN FROM ARRAY EDGE,  $X=2C$ ,  $WIND=45$   
EFFECT OF ARRAY WITH ALPHA=145, FC=2, H=3, D=10, AND P=30%



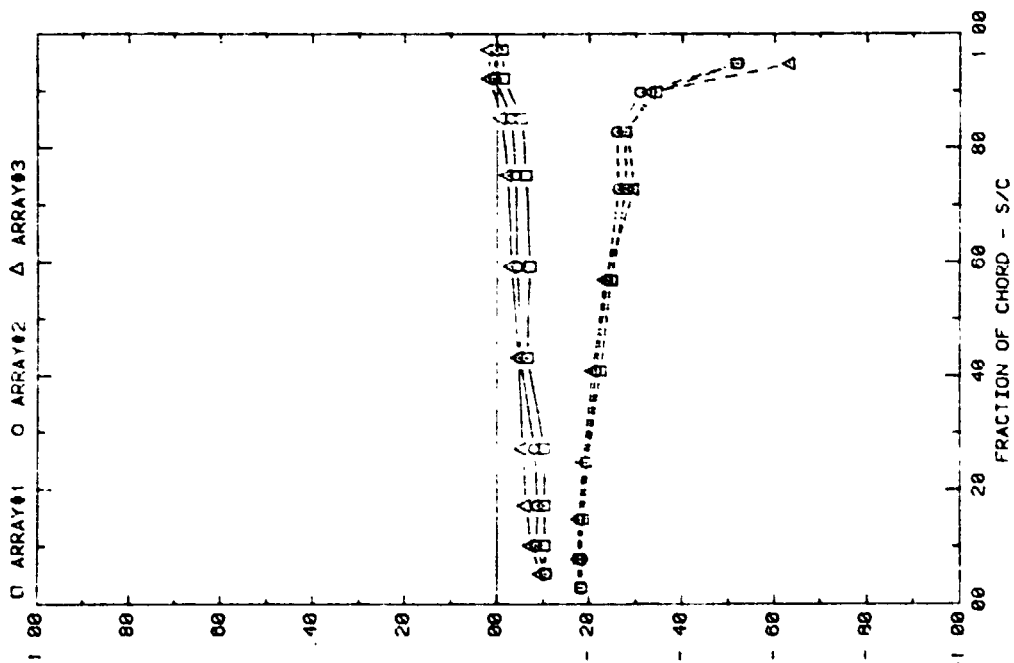
FRONT AND BACK PRESSURES  $\theta = 0^\circ$  IN FROM ARRAY EDGE,  $X=2C$ ,  $WIND=45$   
EFFECT OF ARRAY WITH ALPHA=35, FC=2, H=3, D=10, AND P=30%

Plot 5-1-1. (Continued)



PRESSURE COEFFICIENT REFERENCED TO 1/4 CHORD TYPE

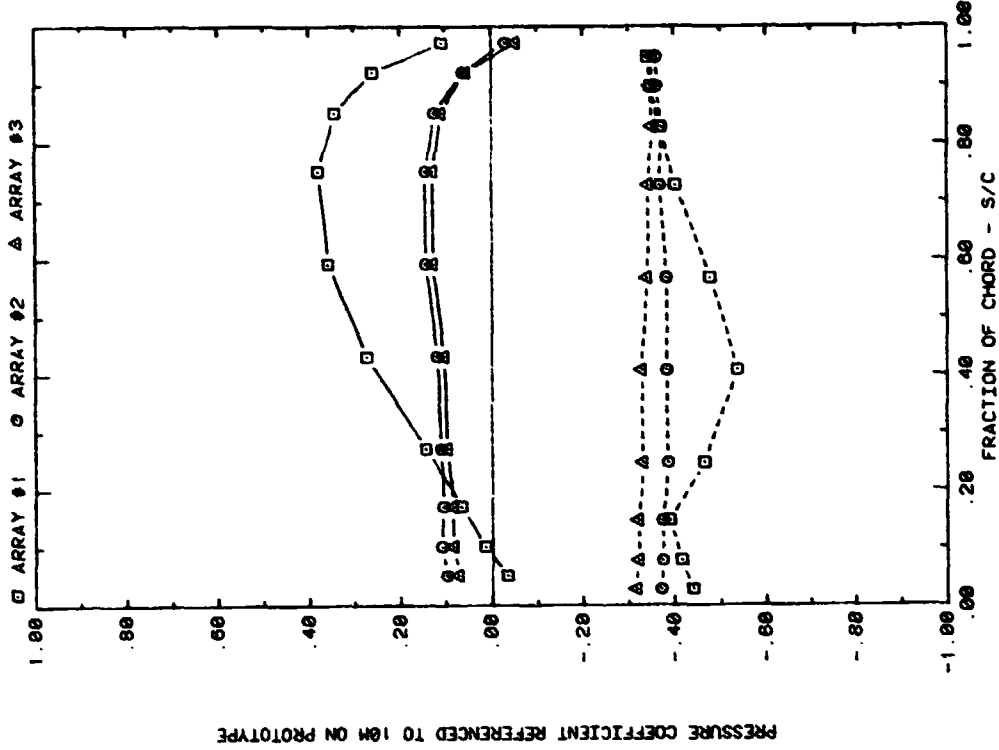
RIGHT AND BACK PRESSURES 0° IN FROM ARRAY EDGE, X=2C, WIND=45  
EFFECT OF ARRAY WITH ALPHA=145, FC=3, H=3°, D=10°, AND P=30%



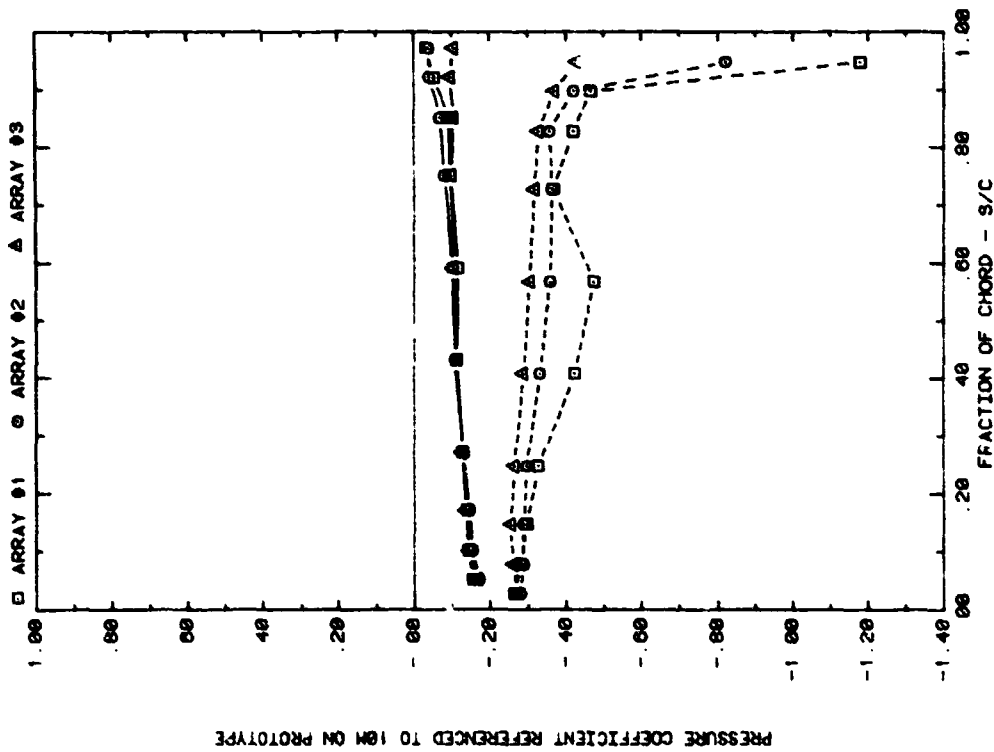
PRESSURE COEFFICIENT REFERENCED TO 1/4 CHORD TYPE

RIGHT AND BACK PRESSURES 0° IN FROM ARRAY EDGE, X=2C, WIND=45  
EFFECT OF ARRAY WITH ALPHA=35, FC=3, H=3°, D=10°, AND P=30%

Plot 5-1-1. (Continued)

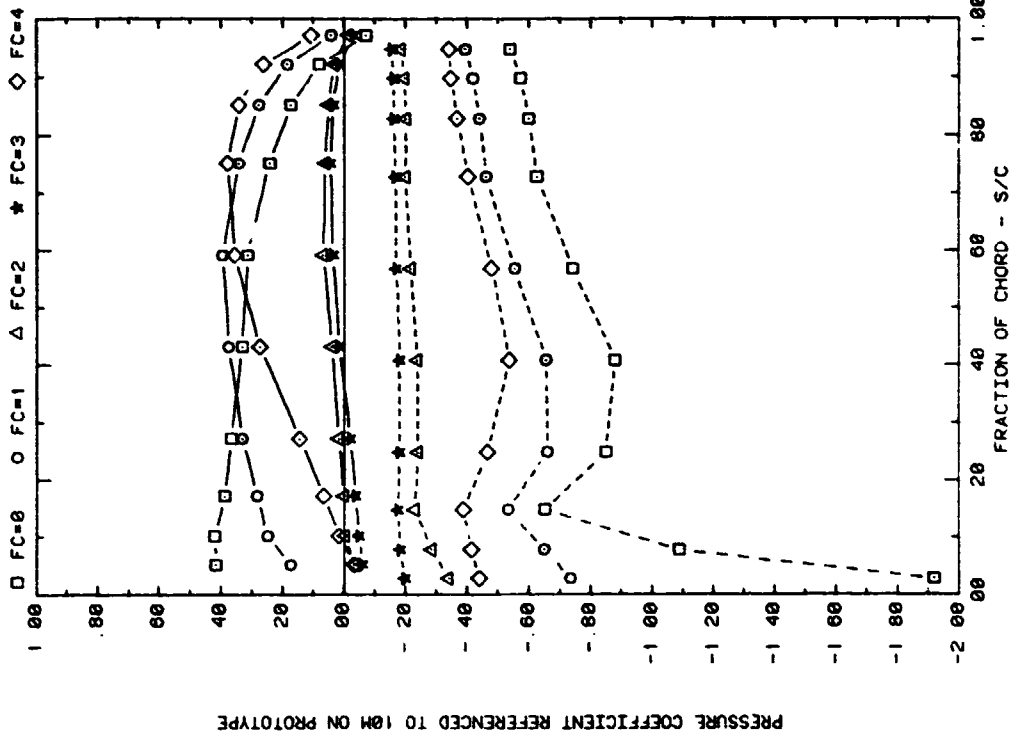


FRONT AND BACK PRESSURES ON ARRAYS #1, 2&3, WIND = 45  
EFFECT OF ARRAY WITH ALPHA = 145, X = 2C, FC = 4

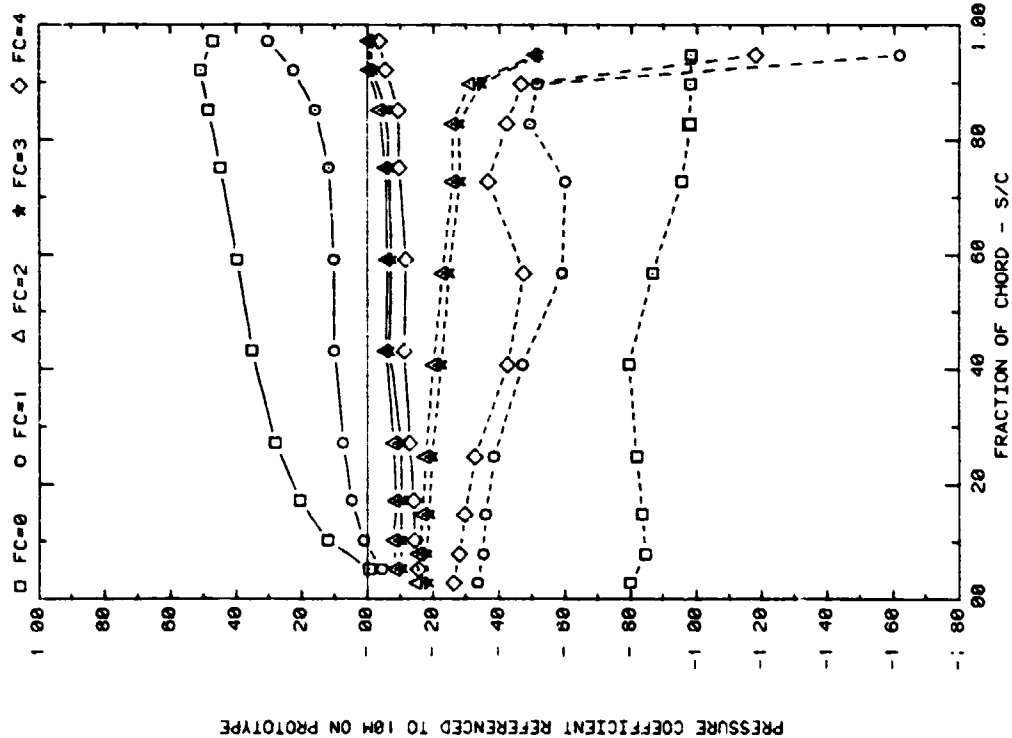


FRONT AND BACK PRESSURES ON ARRAYS #1, 2&3, WIND = 45  
EFFECT OF ARRAY WITH ALPHA = 35, X = 2C, FC = 4

Plot 5-1-1. (Concluded)

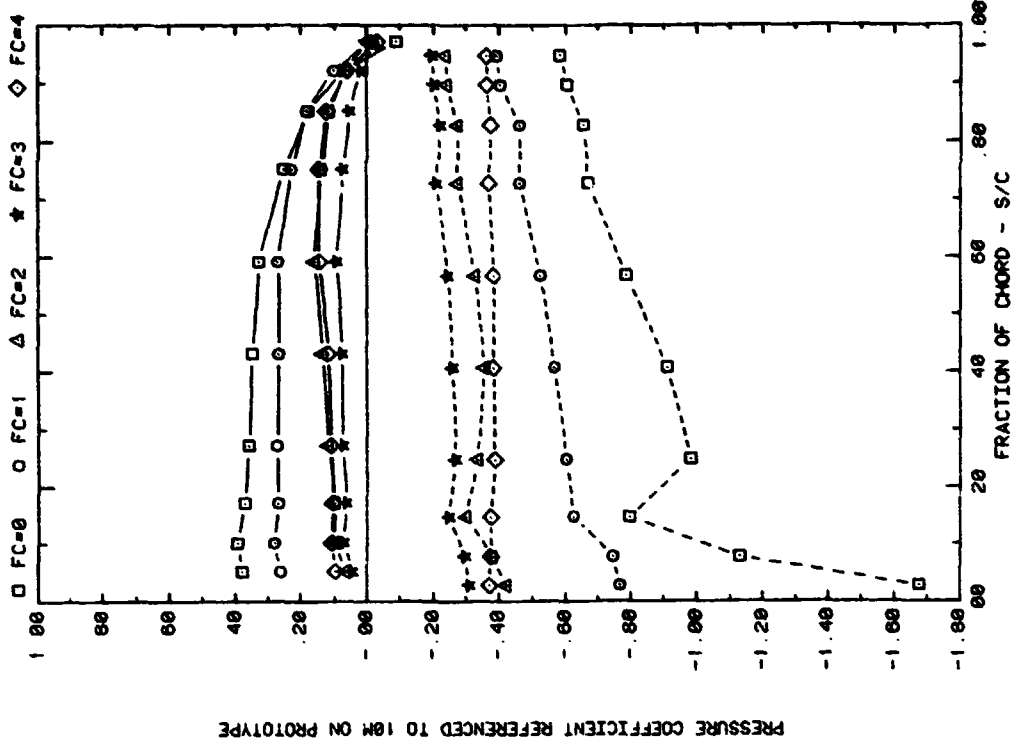


FRONT AND BACK PRESSURES 0.6" IN FROM EDGE OF ARRAY#1; WIND=45  
EFFECT OF FC WITH ALPHA=145, H=3", D=10°, P=30% AND X=2C



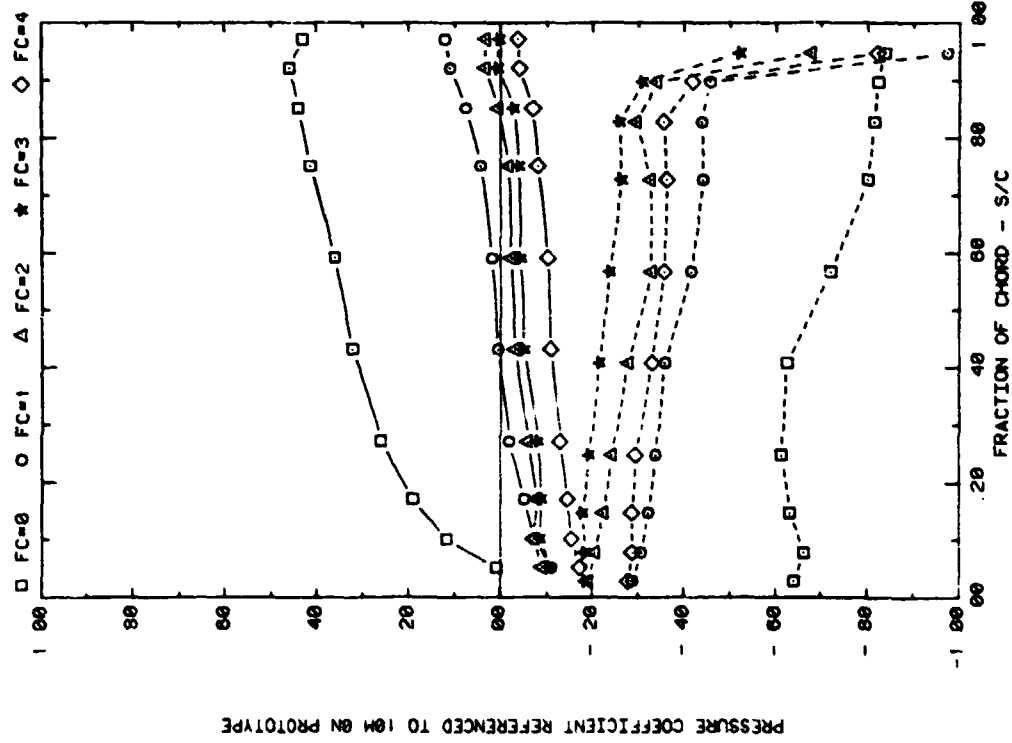
FRONT AND BACK PRESSURES 0.6" IN FROM EDGE OF ARRAY#1; WIND = 45  
EFFECT OF FC WITH ALPHA=35, H=3", D=10°, P=30%, AND X=2C

Plot 5-1-2. Corner Study, WD = 45°, Standard Model  
Effect of Fence Configuration



PRESSURE COEFFICIENT REFERENCED TO 10M ON PROTOTYPE

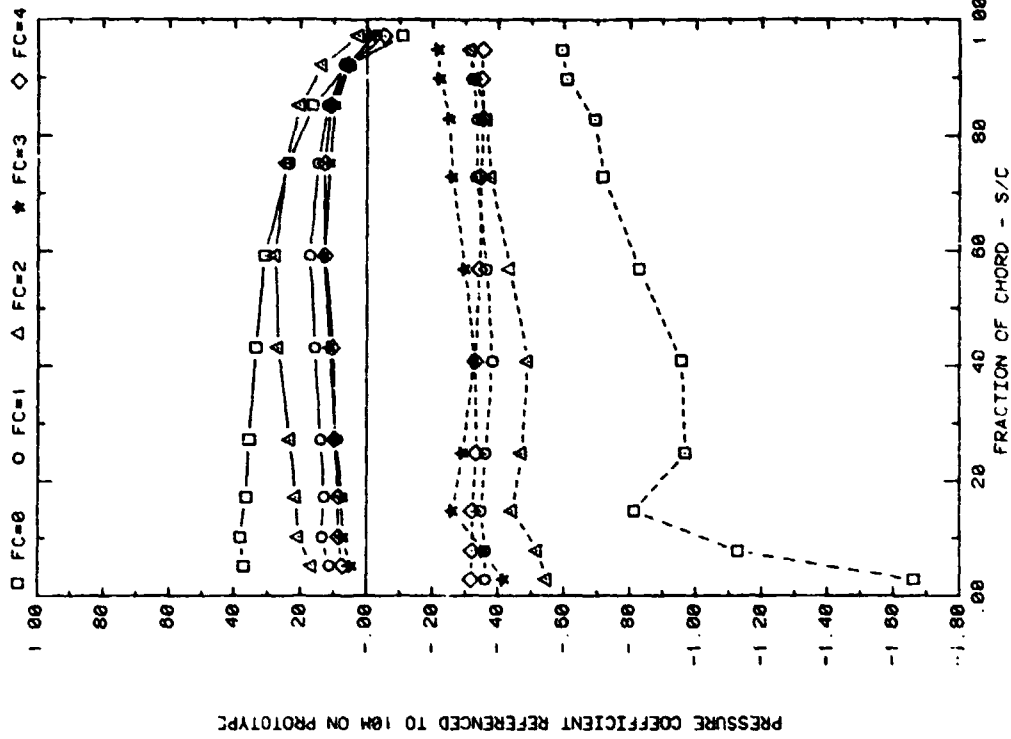
FRONT AND BACK PRESSURES  $\theta$  6° IN FROM EDGE OF ARRAY02; WIND=45  
EFFECT OF FC WITH ALPHA=145, H=3', D=10', P=38% AND X=2C



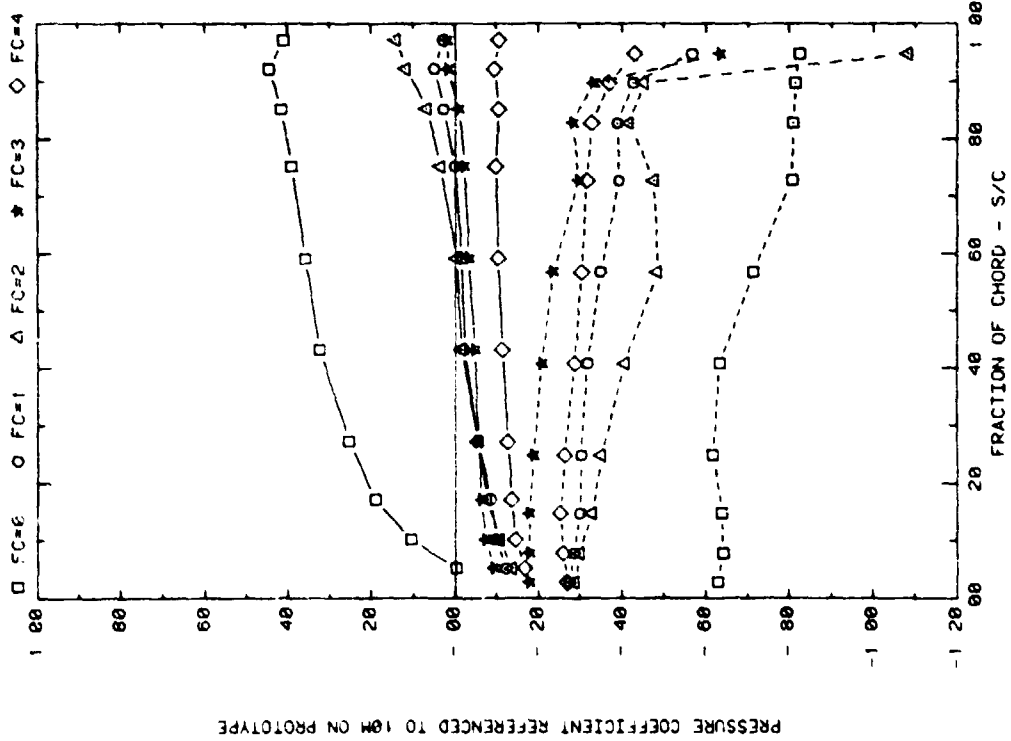
PRESSURE COEFFICIENT REFERENCED TO 10M ON PROTOTYPE

FRONT AND BACK PRESSURES  $\theta$  6° IN FROM EDGE OF ARRAY02; WIND=45  
EFFECT OF FC WITH ALPHA=95, H=3', D=10', P=38% AND X=2C

Plot S-1-2. (Continued)

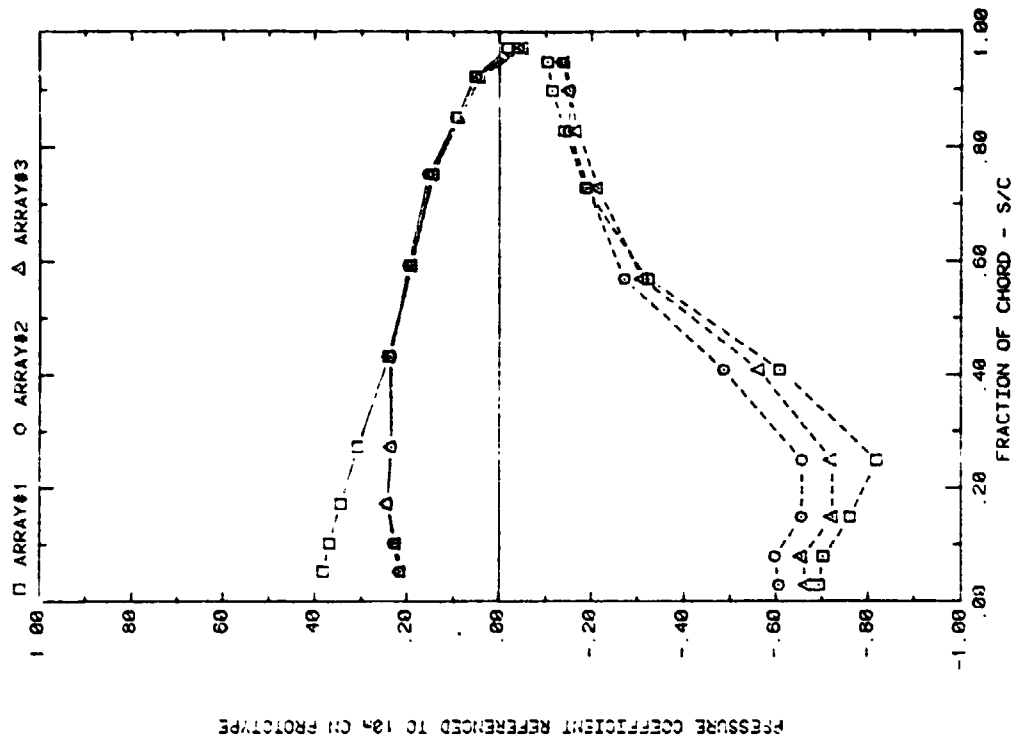


FRONT AND BACK PRESSURES  $\theta$  6° IN FROM EDGE OF ARRAY#3, WIND=45  
EFFECT OF FC WITH ALPHA=145, H=3°, D=10°, P=30%, AND X=2C



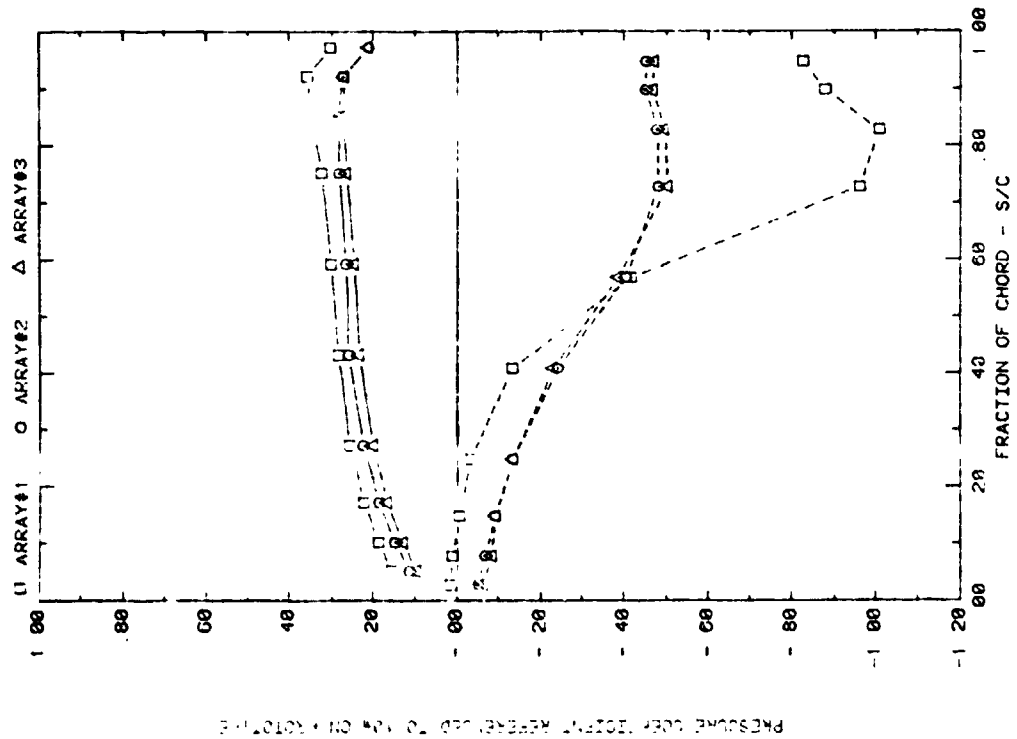
FRONT AND BACK PRESSURES  $\theta$  6° IN FROM EDGE OF ARRAY#3, WIND=45  
EFFECT OF FC WITH ALPHA=35, H=3°, D=10°, P=30%, AND X=2C

Plot 5-1-2. (Concluded)



PRESSURE COEFFICIENT REFERENCED TO 1/4 CH PROTOTYPE

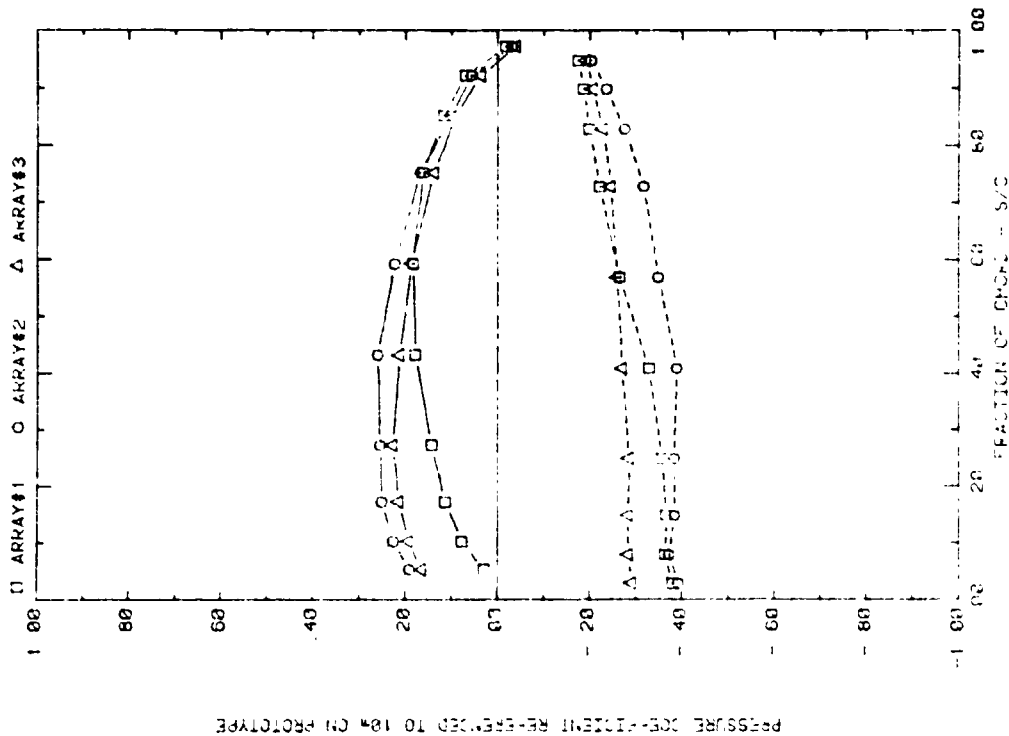
FRONT AND BACK PRESSURES 3.6° IN FROM ARRAY EDGE, X=2C, WIND=45  
EFFECT OF ARRAY WITH ALPHA=145, FC=0, H=3', D=10', AND P=30X



PRESSURE COEFFICIENT REFERENCED TO 1/4 CH PROTOTYPE

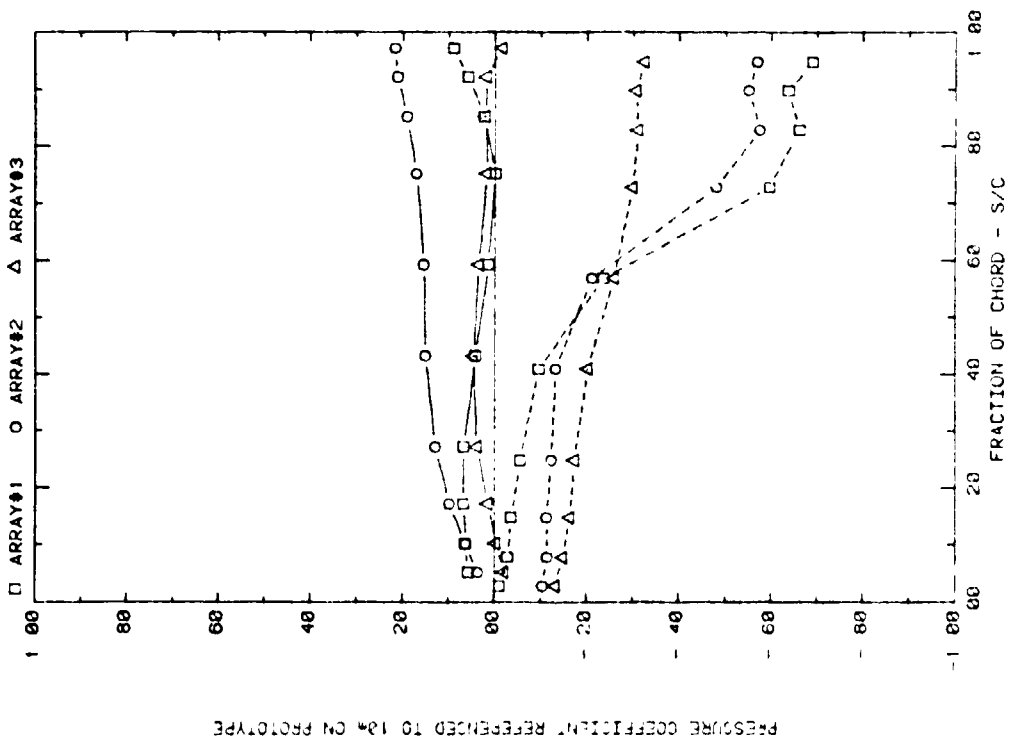
FRONT AND BACK PRESSURES 3.6° IN FROM ARRAY EDGE, X=2C, WIND=45  
EFFECT OF ARRAY WITH ALPHA=35, FC=0, H=3', D=10', AND P=30X

Plot 5-2-1. Corner Study, WD = 45°, Modified Model with Solid Extension  
Effect of Array Position



PRESSURE COEFFICIENT REFERENCED TO 10% CN PROTOTYPE

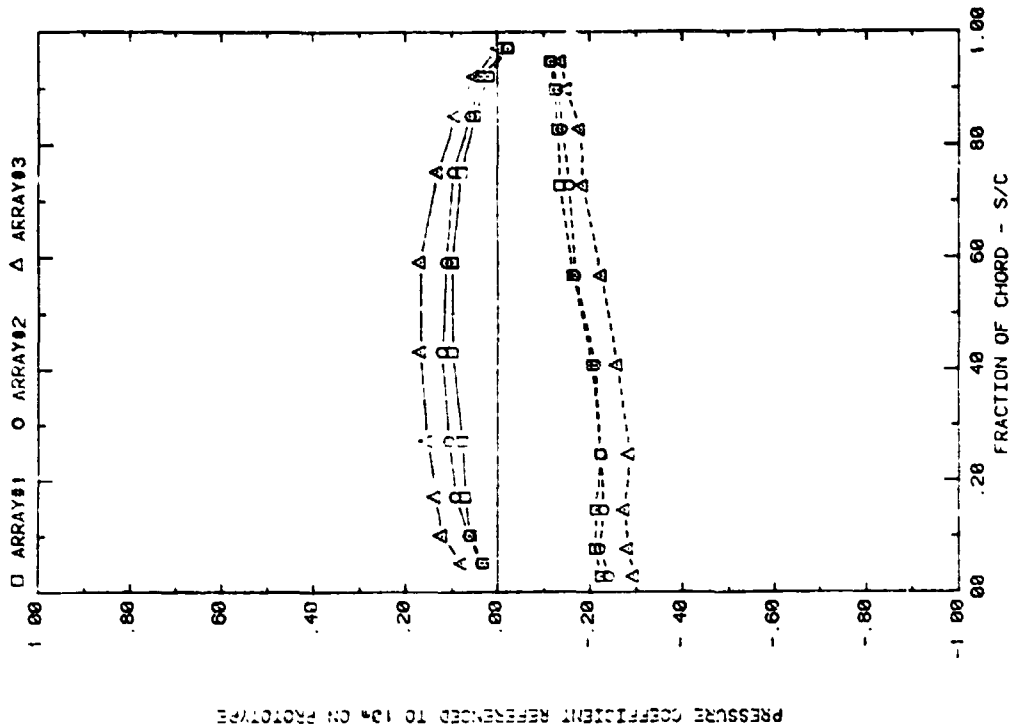
FRONT AND BACK PRESSURES 3.6" IN FROM ARRAY EDGE, X=20, WIND=45  
EFFECT OF ARRAY TIP ALPHA=45, FC=1, H=3°, D=18°, AND P=30%



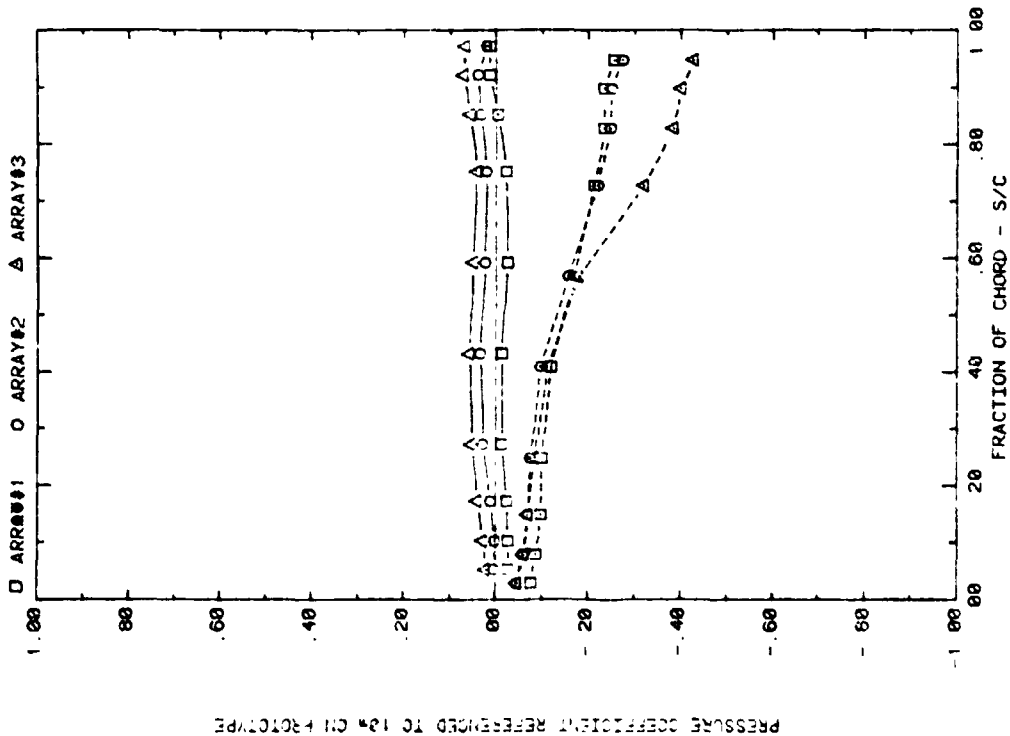
PRESSURE COEFFICIENT REFERENCED TO 10% CN PROTOTYPE

FRONT AND BACK PRESSURES 3.6" IN FROM ARRAY EDGE, X=20, WIND=45  
EFFECT OF ARRAY TIP ALPHA=35, FC=1, H=3°, D=18°, AND P=30%

Plot 5-2-1. (Continued)

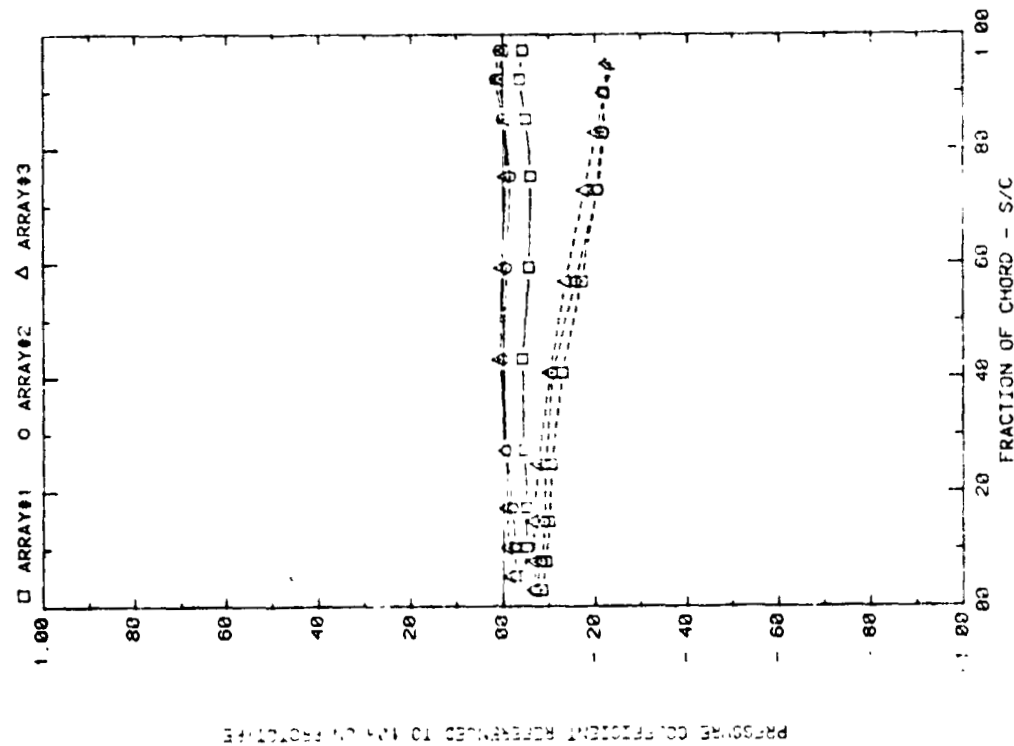
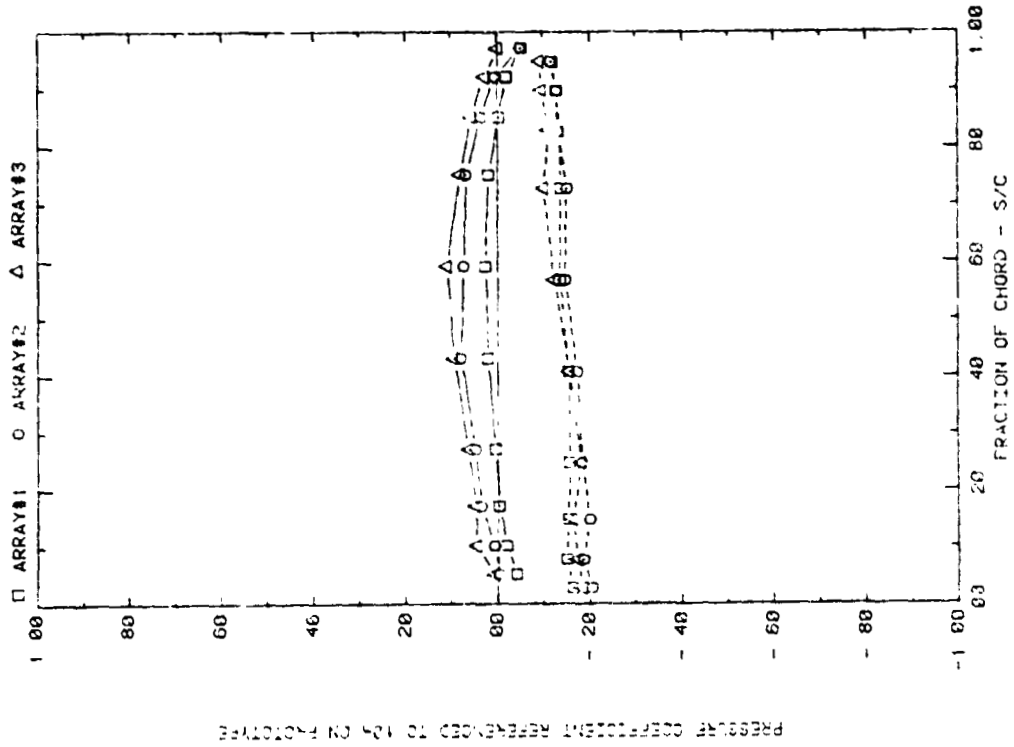


FRONT AND BACK PRESSURES 3.6° IN FROM ARRAY EDGE; X=2C, WIND=45  
EFFECT OF ARRAY WITH ALPHA=145, FC=2, H=3°, D=10°, AND P=30X



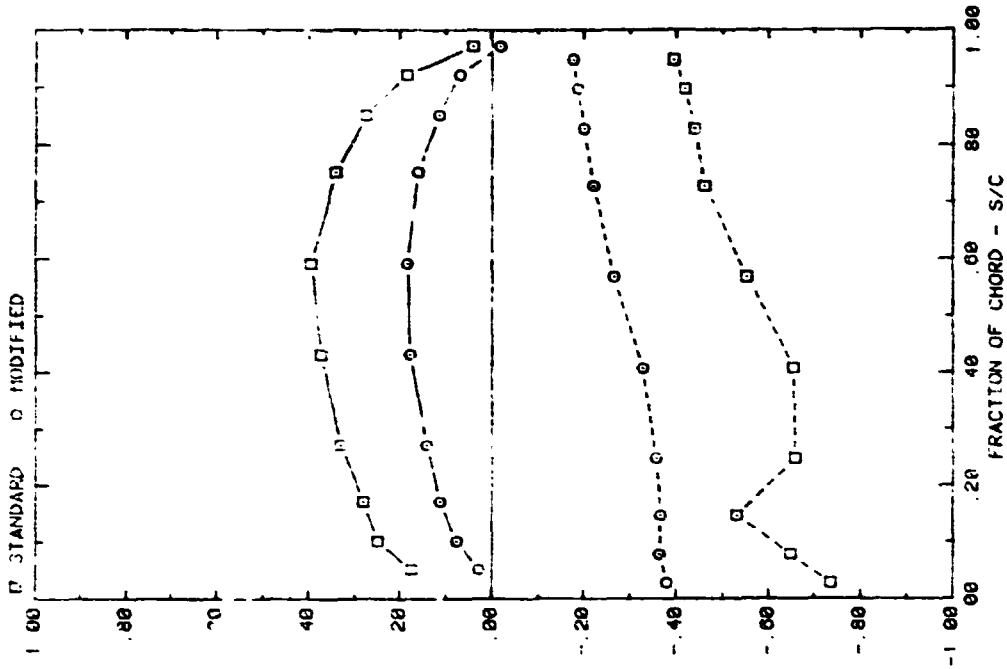
FRONT AND BACK PRESSURES 3.6° IN FROM ARRAY EDGE; X=2C, WIND=45  
EFFECT OF ARRAY WITH ALPHA=35, FC=2, H=3°, D=10°, AND P=30X

Plot 5-2-1. (Continued)

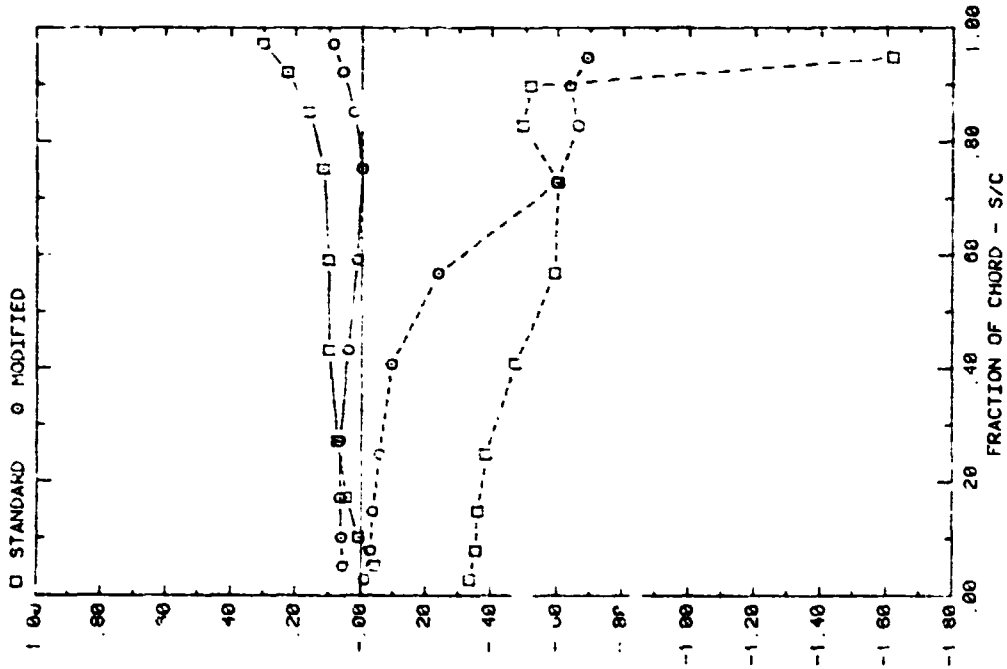


Plot 5-1-1. (Concluded)

ORIGINAL PAGE IS OF POOR QUALITY

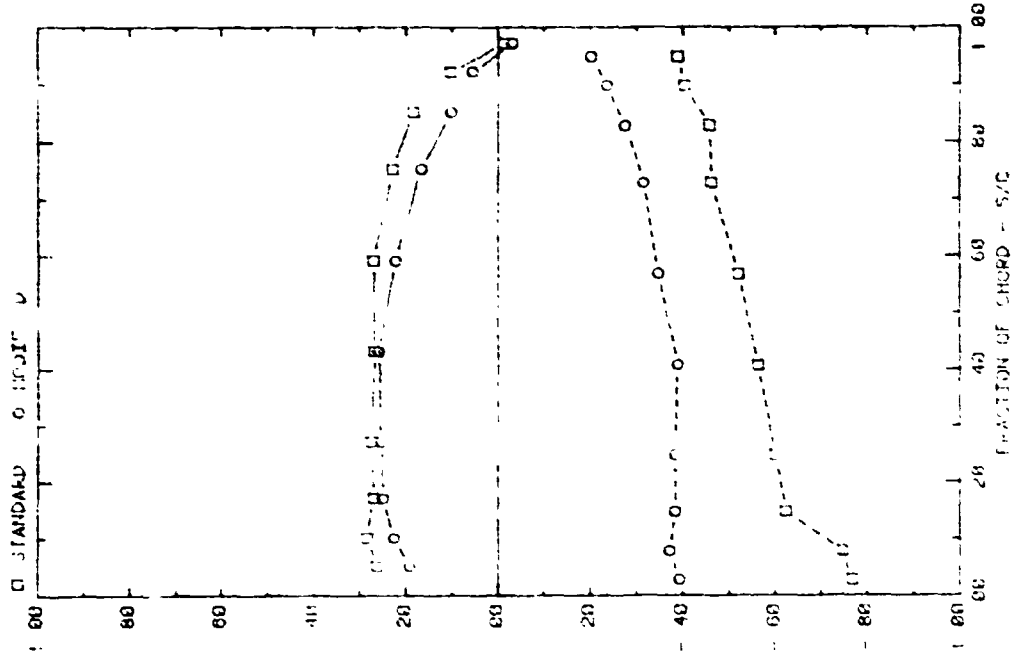


FRONT AND BACK PRESSURES ON ARRAY #1 WITH X=2C, AND WIND=45  
EFFECT OF TAP LOCATION, ALPHA=145, H=3", D=10", FC=1, AND P=30X

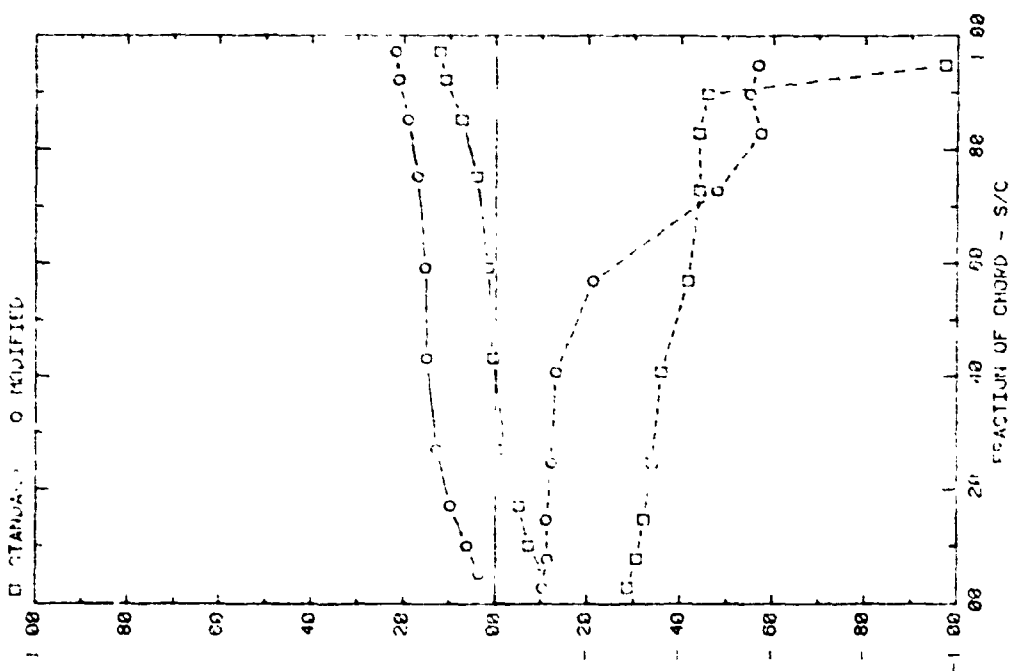


FRONT AND BACK PRESSURES ON ARRAY #1 WITH X=2C, AND WIND=15  
EFFECT OF TAP LOCATION, ALPHA=35, H=3", D=10", FC=1, AND P=30X

Plot 5-2-2. Corner Study, WD = 45°, Effect of Model Modification

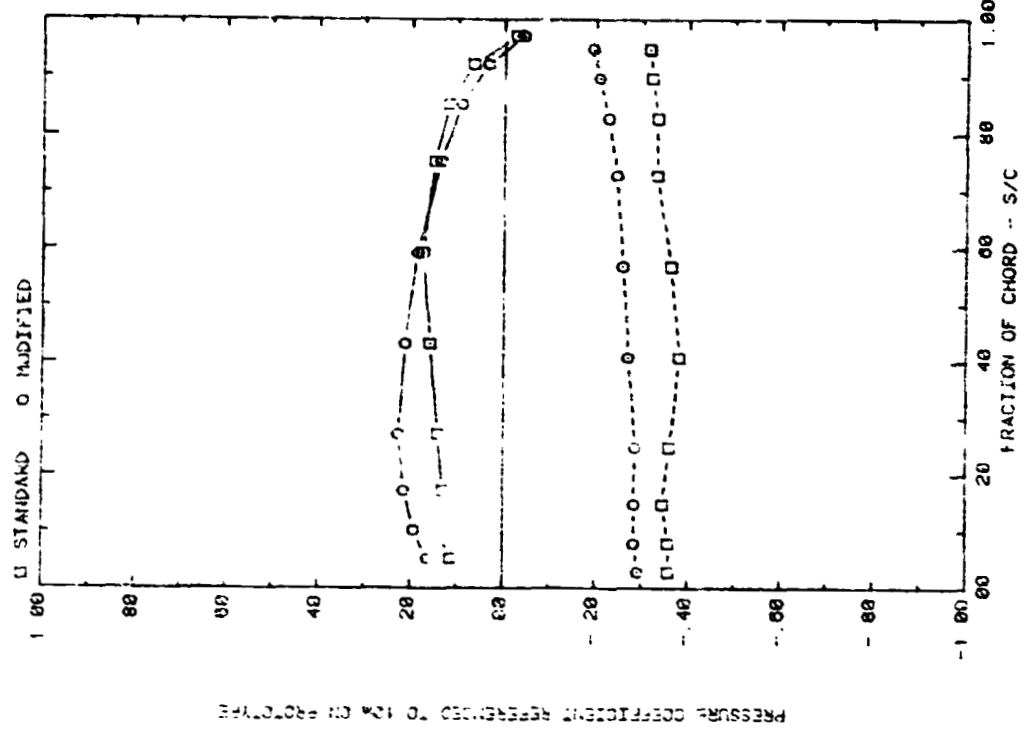


FRONT AND BACK PRESSURES ON ARRAY #2 WITH  $\alpha=20$ , AND WIND=45  
EFFECT OF TAP LOCATION, ALPHA=20, H=3', D=10", S/C=1, AND P=30%

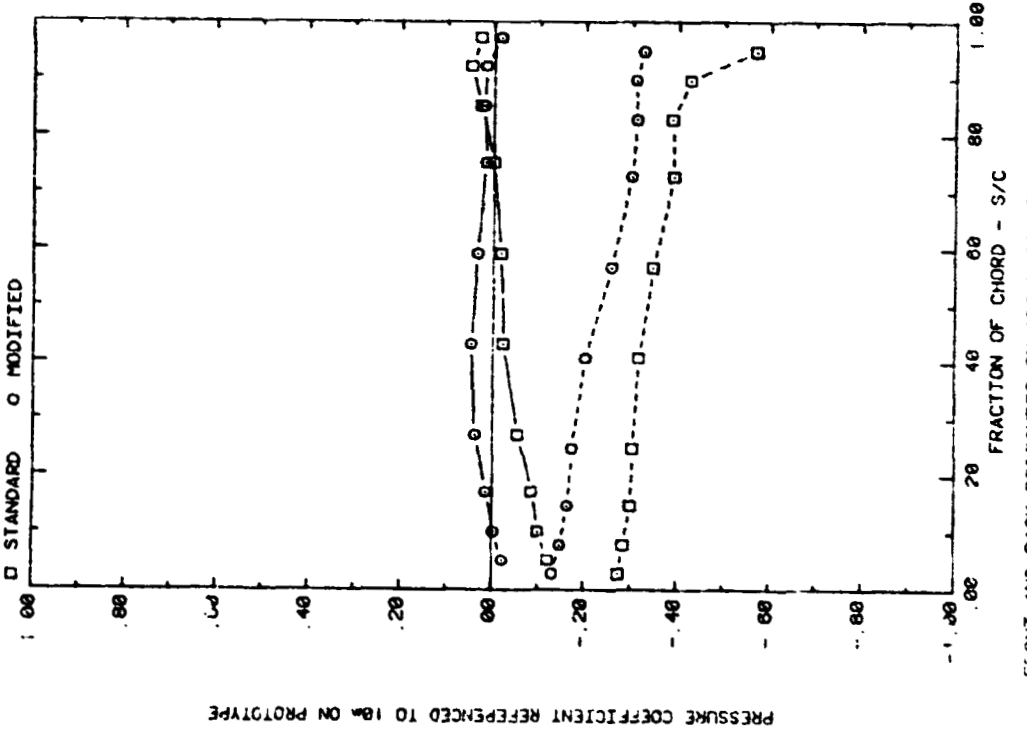


FRONT AND BACK PRESSURES ON ARRAY #2 WITH  $\alpha=10$ , AND WIND=45  
EFFECT OF TAP LOCATION, ALPHA=10, H=3', D=10", S/C=1, AND P=30%

Plot 5-2-2. (Continued)

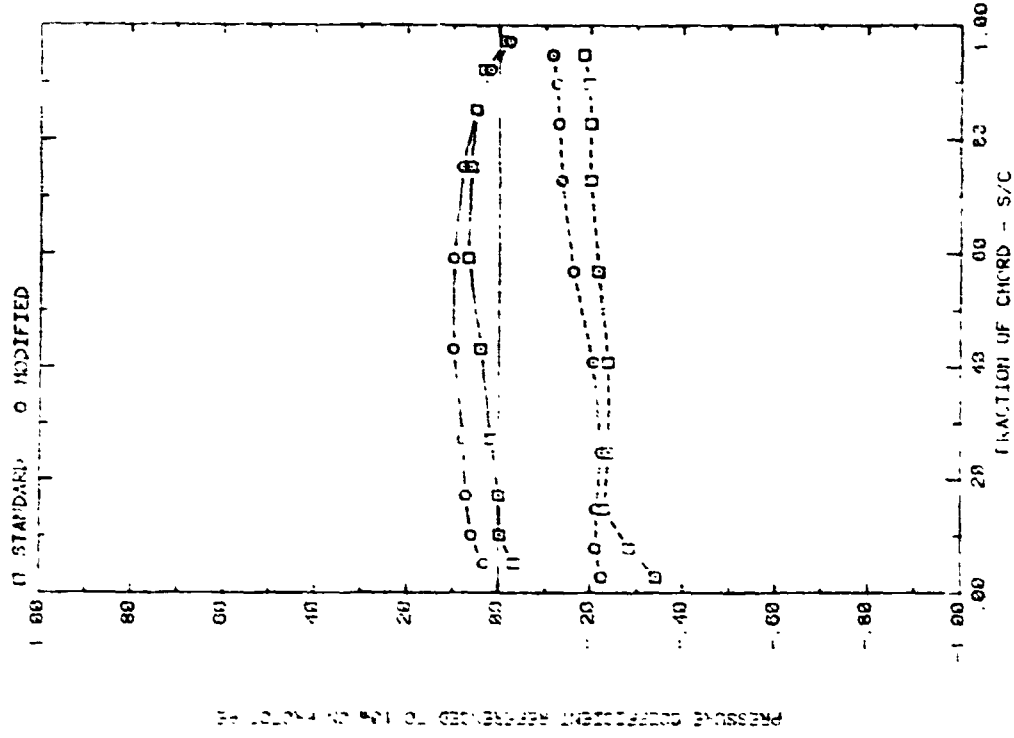


FRONT AND BACK PRESSURES ON ARRAY #3 WITH  $X=2C$ , AND WIND=45  
EFFECT OF TAP LOCATION, ALPHA=145, H=3', D=10', FC=1, AND P=30%

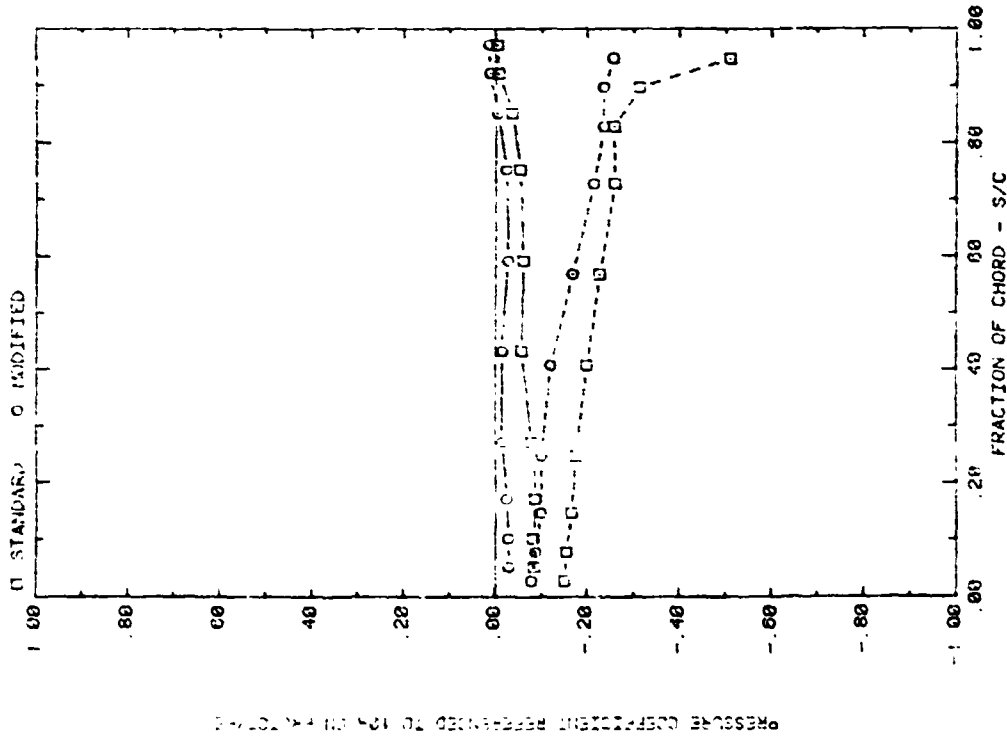


FRONT AND BACK PRESSURES ON ARRAY #3 WITH  $X=2C$ , AND WIND=45  
EFFECT OF TAP LOCATION, ALPHA=35, H=3', D=10', FC=1, AND P=30%

Plot 5-2-2. (Continued)

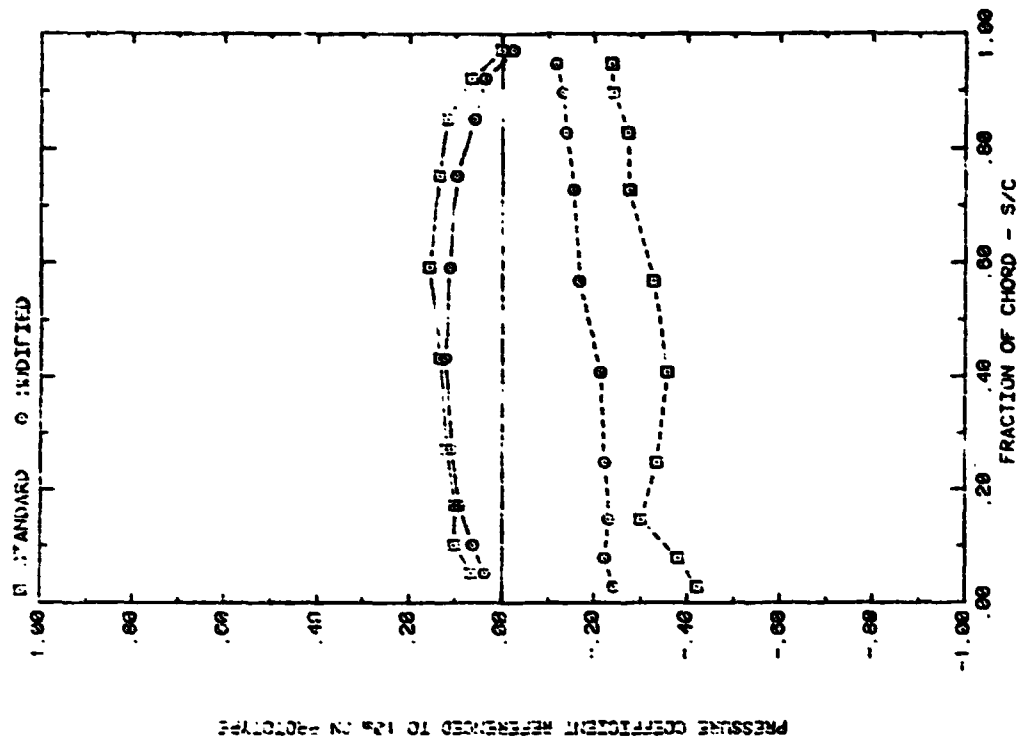


FRONT AND BACK PRESSURES ON ARRAY #1 WITH X=20, AND WIND=45  
EFFECT OF TAP LOCATION; ALPHA=145, H=3, D=10, FC=2, AND P=20X

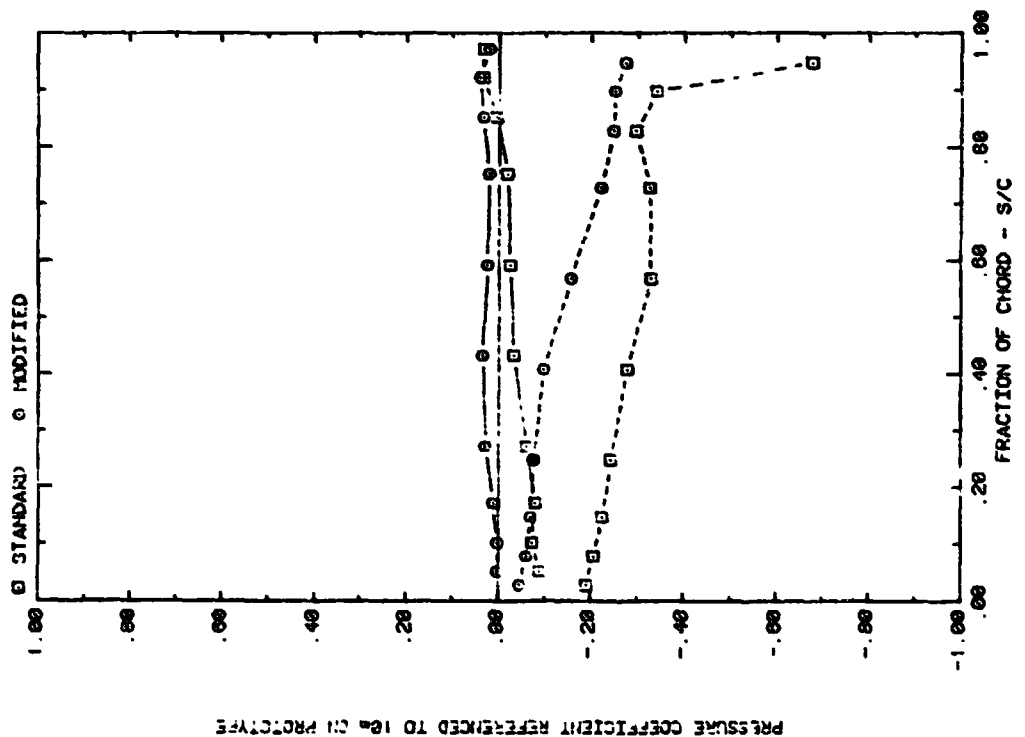


FRONT AND BACK PRESSURES ON ARRAY #1 WITH X=20, AND WIND=45  
EFFECT OF TAP LOCATION; ALPHA=35, H=3, D=10, FC=2, AND P=30X

Plot 5-2-2. (Continued)

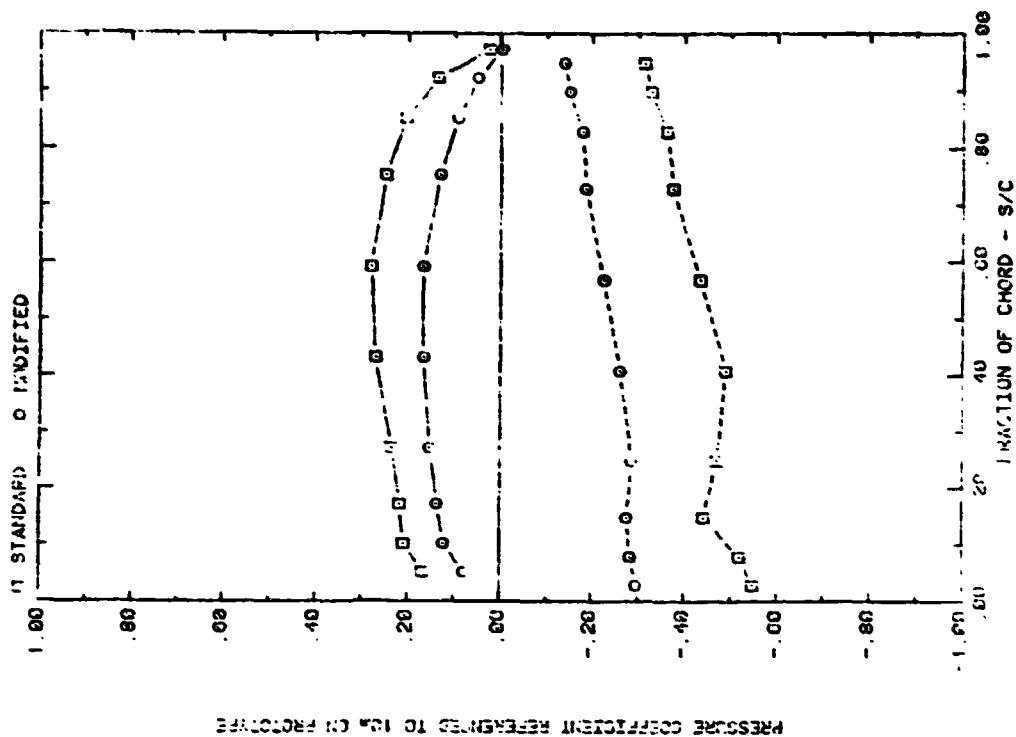


FRONT AND BACK PRESSURES ON ARRAY #2 WITH X=2C, AND WIND-45  
EFFECT OF TAP LOCATION; ALPHA=145, H=3, D=10°, FI=2°, FI=2°, AIJ P=30K

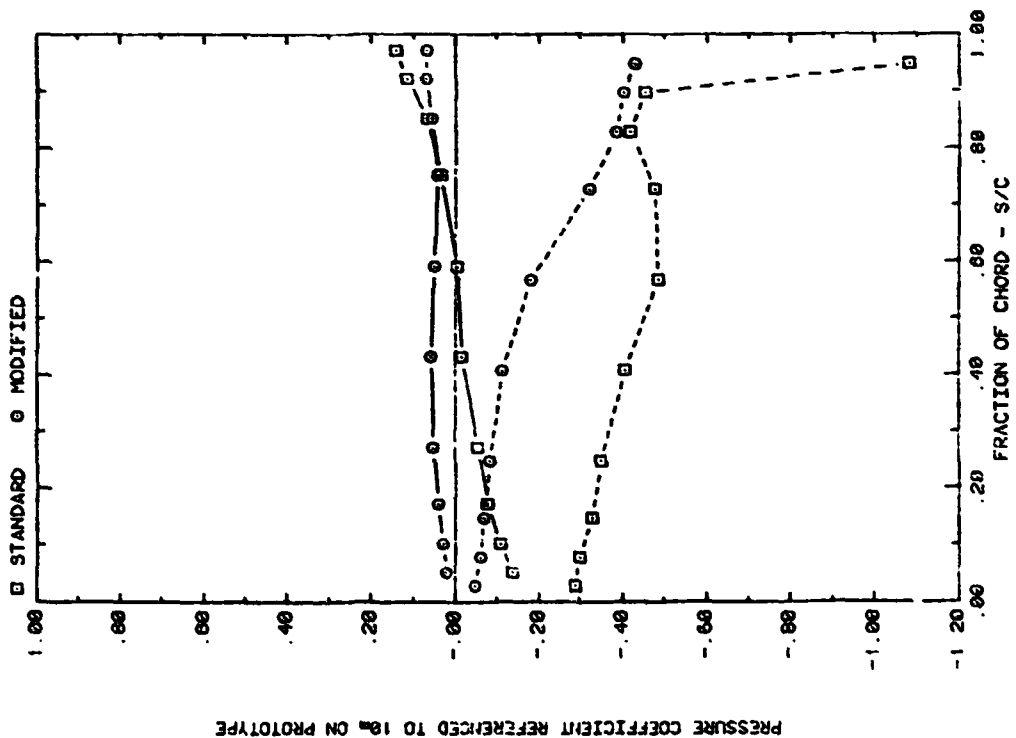


FRONT AND BACK PRESSURES ON ARRAY #2 WITH X=2C, AND WIND-45  
EFFECT OF TAP LOCATION; ALPHA=35, H=3, D=10°, FI=2°, FI=2°, AIJ P=30K

Plot 5-2-2. (Continued)

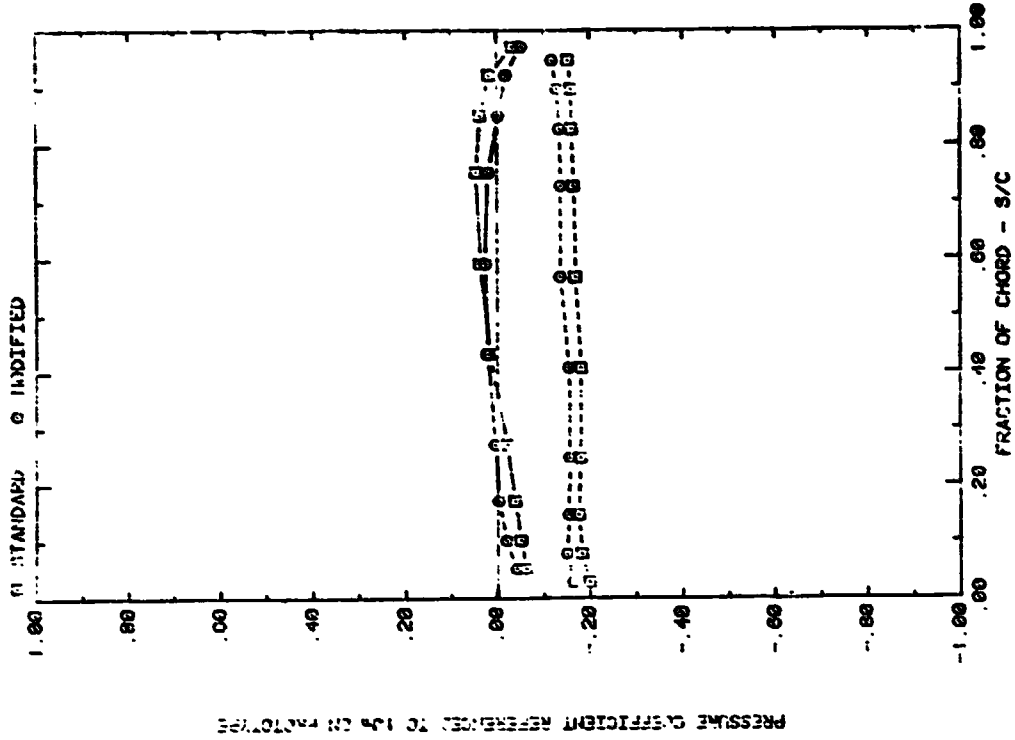


FRONT AND BACK PRESSURES ON ARRAY #3 WITH X=2C, AND WIND=45  
EFFECT OF TAP LOCATION, ALPHA=15, M=3, D=10, FC=2, AND P=30K

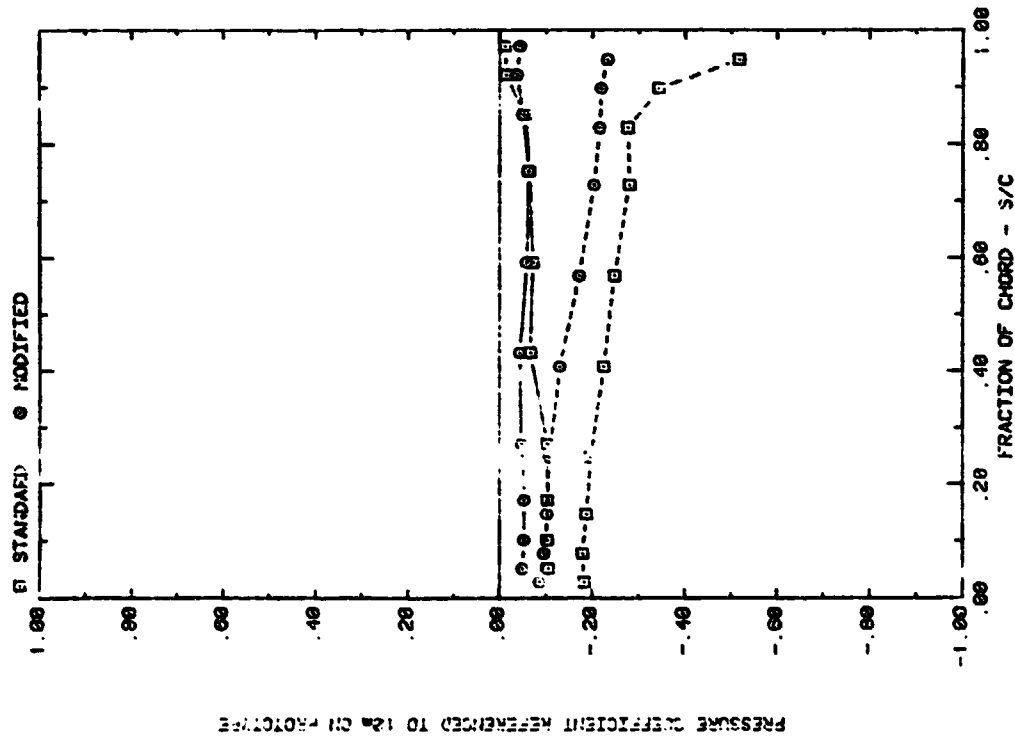


FRONT AND BACK PRESSURES ON ARRAY #3 WITH X=2C, AND WIND=45  
EFFECT OF TAP LOCATION, ALPHA=15, M=3, D=10, FC=2, AND P=30K

Plot 5-2-2. (Continued)

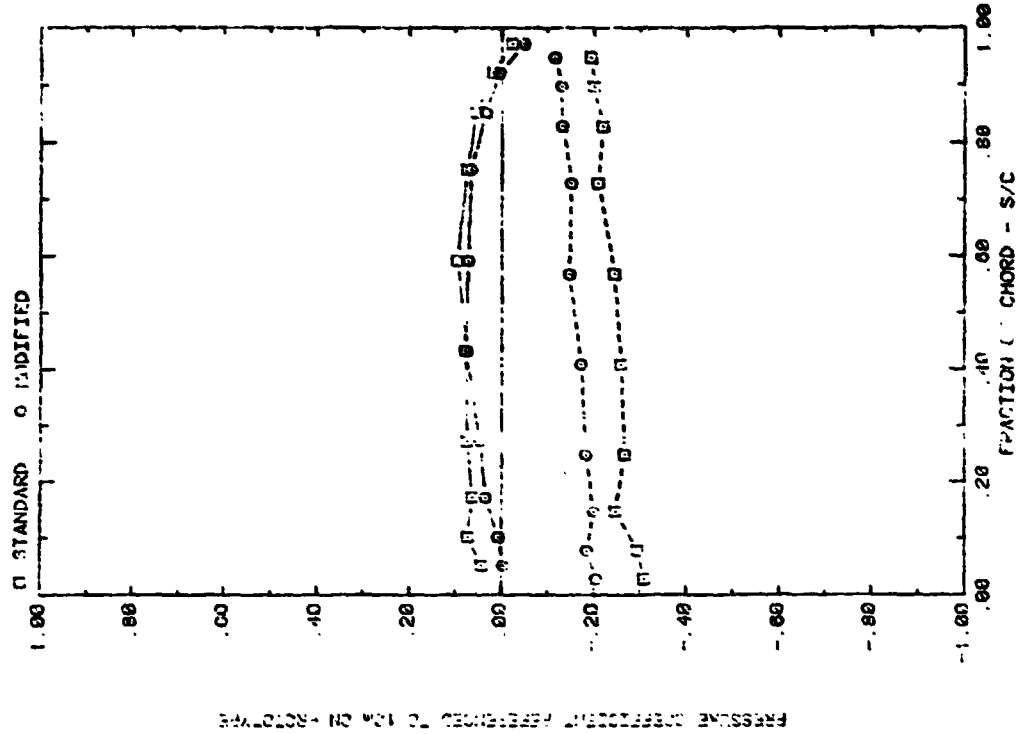


FRONT AND BACK PRESSURES ON ARRAY #1 WITH X=2C, AND WIND=45  
EFFECT OF TAP LOCATION; ALPHA=145, H=3', D=10°, FC=3, AND P=30%

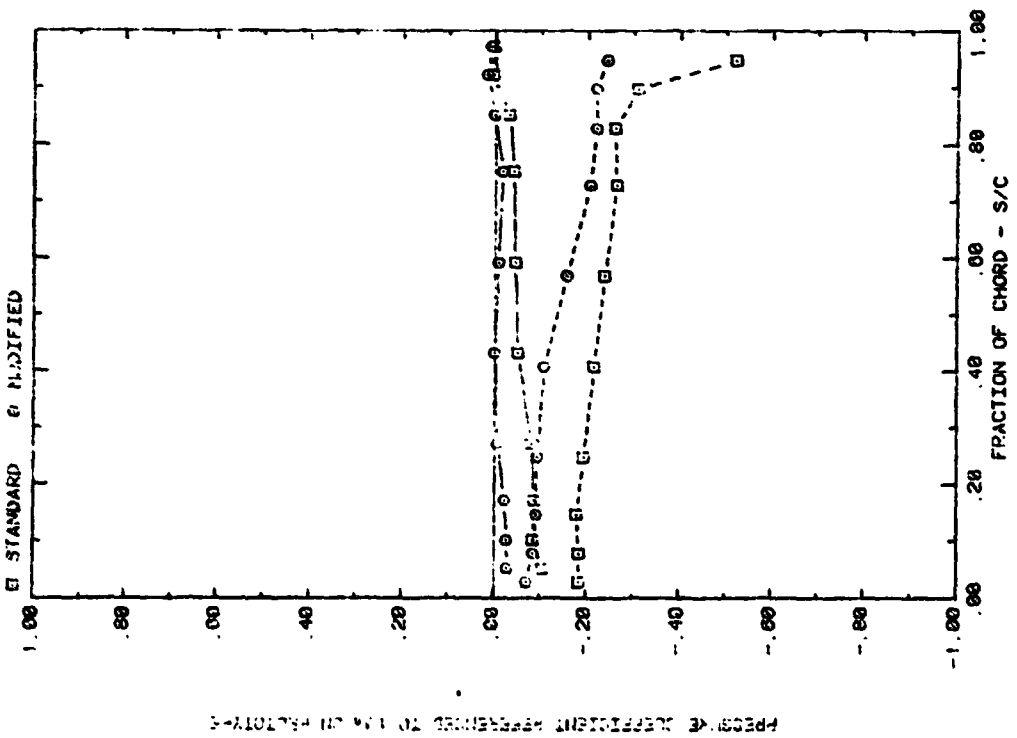


FRONT AND BACK PRESSURES ON ARRAY #1 WITH X=2C, AND WIND=45  
EFFECT OF TAP LOCATION; ALPHA=35, H=3', D=10°, FC=3, AND P=30%

Plot 5-2-2. (Continued)



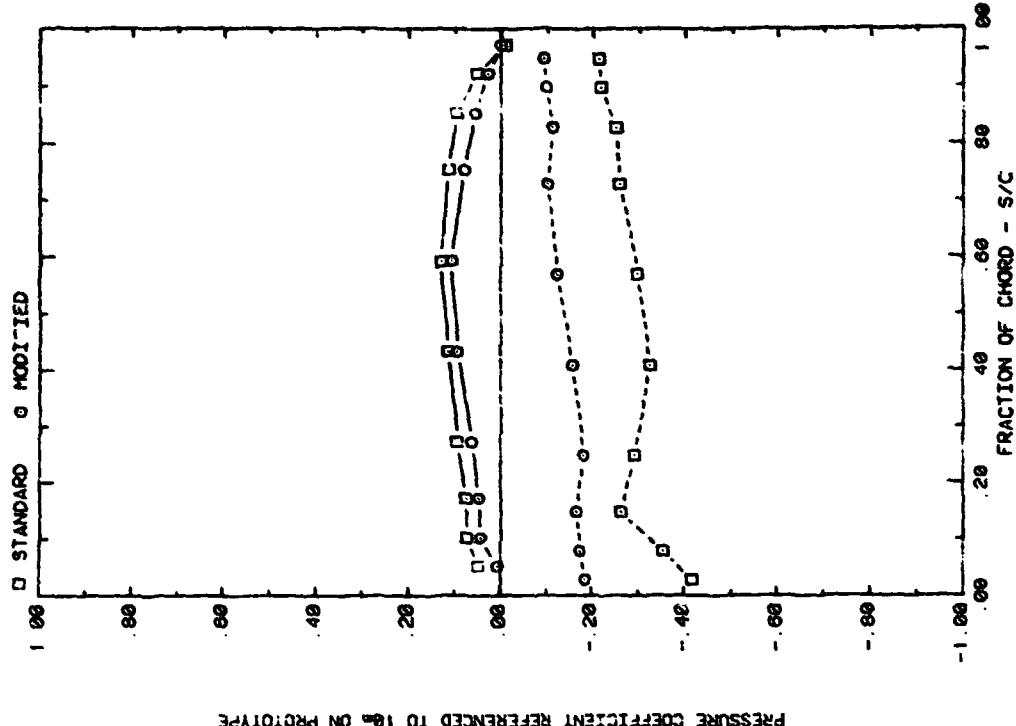
FRONT AND BACK PRESSURES ON ARRAY #2 WITH X=2C, AND WIND=45  
EFFECT OF TAP LOCATION; ALPHA=145, H=3, D=10, FC=3, AND P=30X



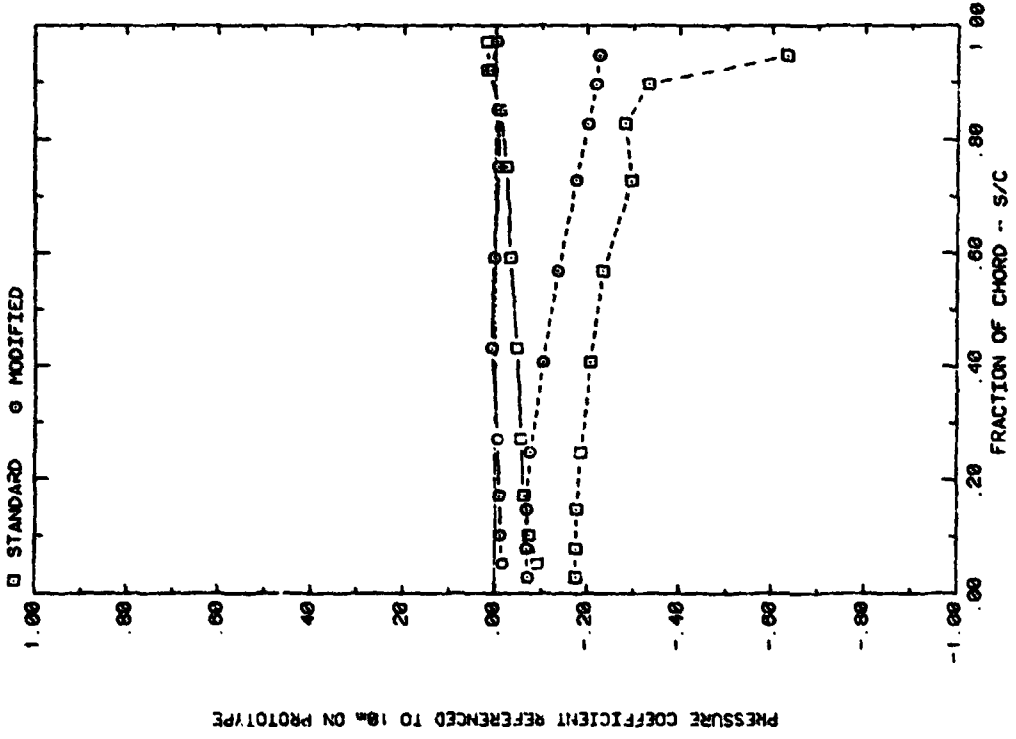
FRONT AND BACK PRESSURES ON ARRAY #2 WITH X=2C, AND WIND=45  
EFFECT OF TAP LOCATION; ALPHA=35, H=3, D=10, FC=3, AND P=30X

Plot 5-2-2. (Continued)

ORIGINAL PAGE IS  
OF POOR QUALITY

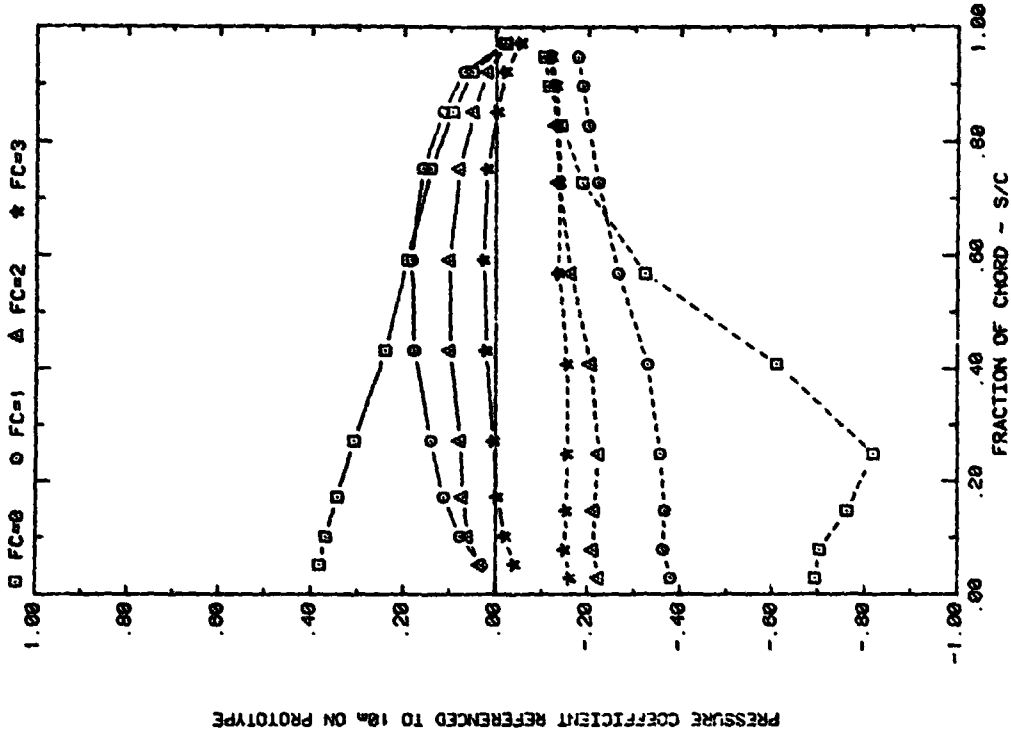


FRONT AND BACK PRESSURES ON ARRAY #3 WITH X=2C, AND WIND=45  
EFFECT OF TAP LOCATION, ALPHA=145, H=3, D=10, FC=3, AND P=30X

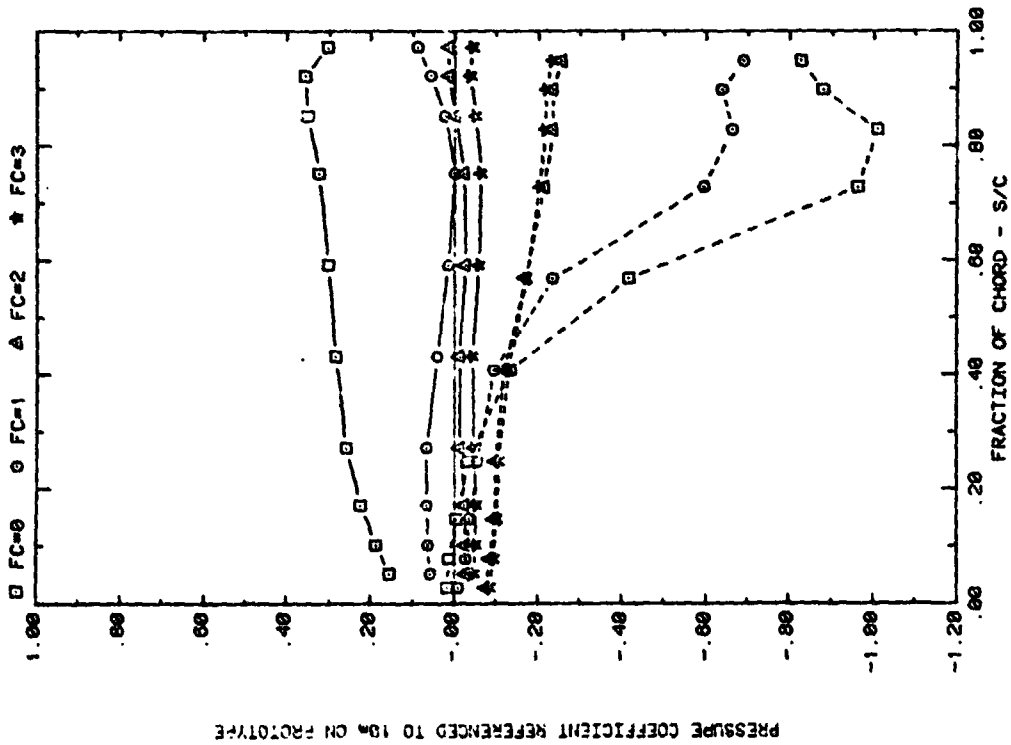


FRONT AND BACK PRESSURES ON ARRAY #3 WITH X=2C, AND WIND=45  
EFFECT OF TAP LOCATION, ALPHA=35, H=3, D=10, FC=3, AND P=30X

Plot 5-2-2. (Concluded)



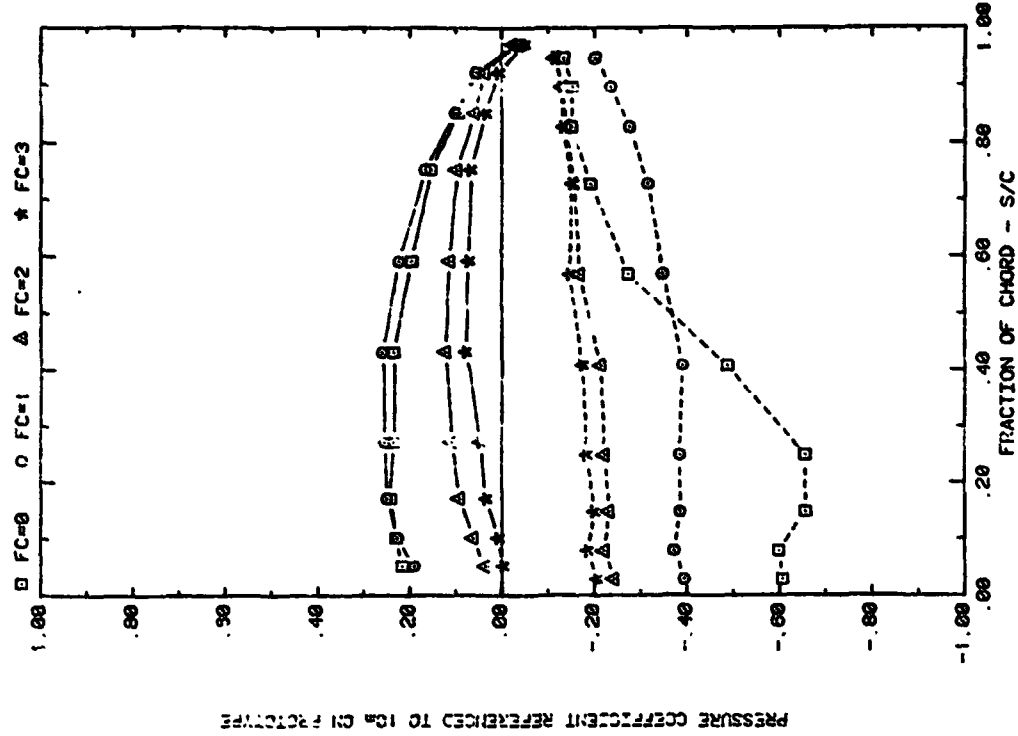
FRONT AND BACK PRESSURES 3.6° IN FROM EDGE OF ARRAY#1; WIND=45  
EFFECT OF FC WITH ALPHA=145, H=3', D=18', P=30%, AND X=2C



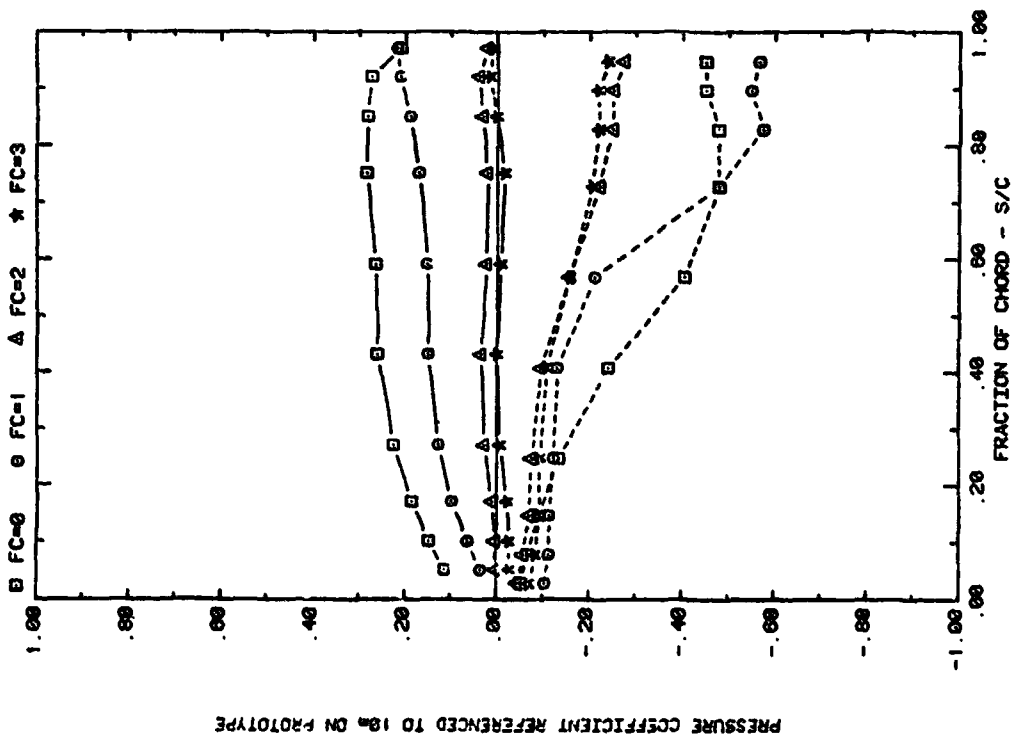
FRONT AND BACK PRESSURES 3.6° IN FROM EDGE OF ARRAY#1; WIND=45  
EFFECT OF FC WITH ALPHA=35, H=3', D=18', P=30%, AND X=2C  
Plot 5-2-3. Corner Study, WD = 45°, Modified Model with Solid Extension  
Effect of Fence Configuration

PRESSURE COEFFICIENT REFERENCED TO 10a ON PROTOTYPE

PRESSURE COEFFICIENT REFERENCED TO 10a ON PROTOTYPE

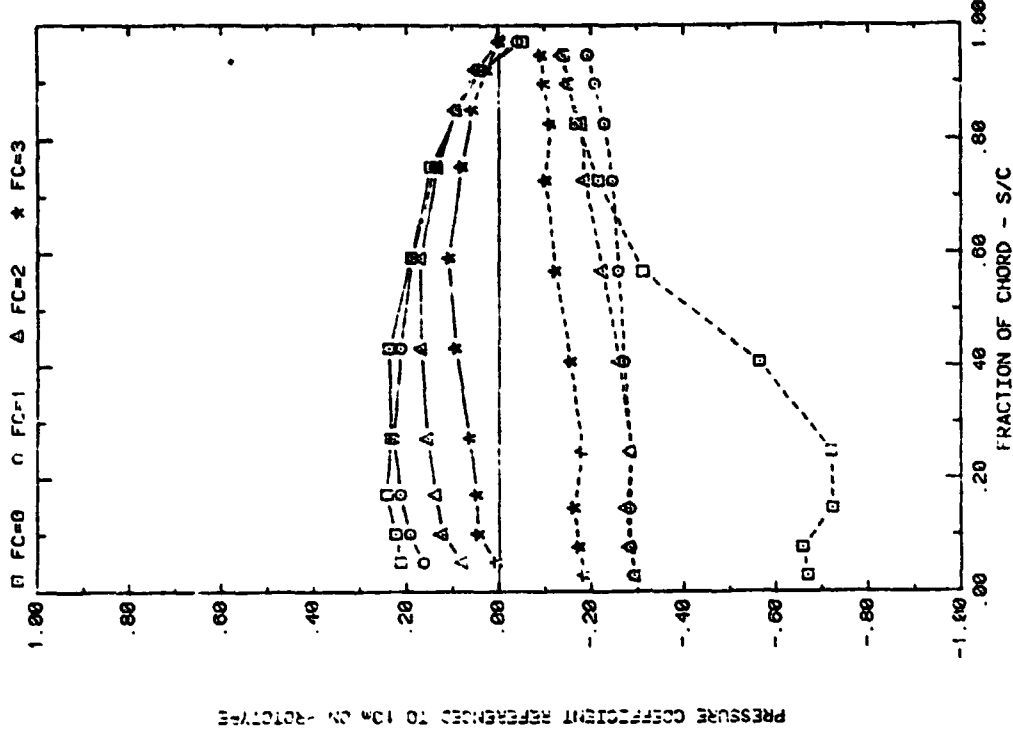


FRONT AND BACK PRESSURES 3.6" IN FROM EDGE OF ARRAY45, WIND=45  
EFFECT OF FC WITH ALPHA=145, H=3°, D=10°, P=30%, AND X=2C

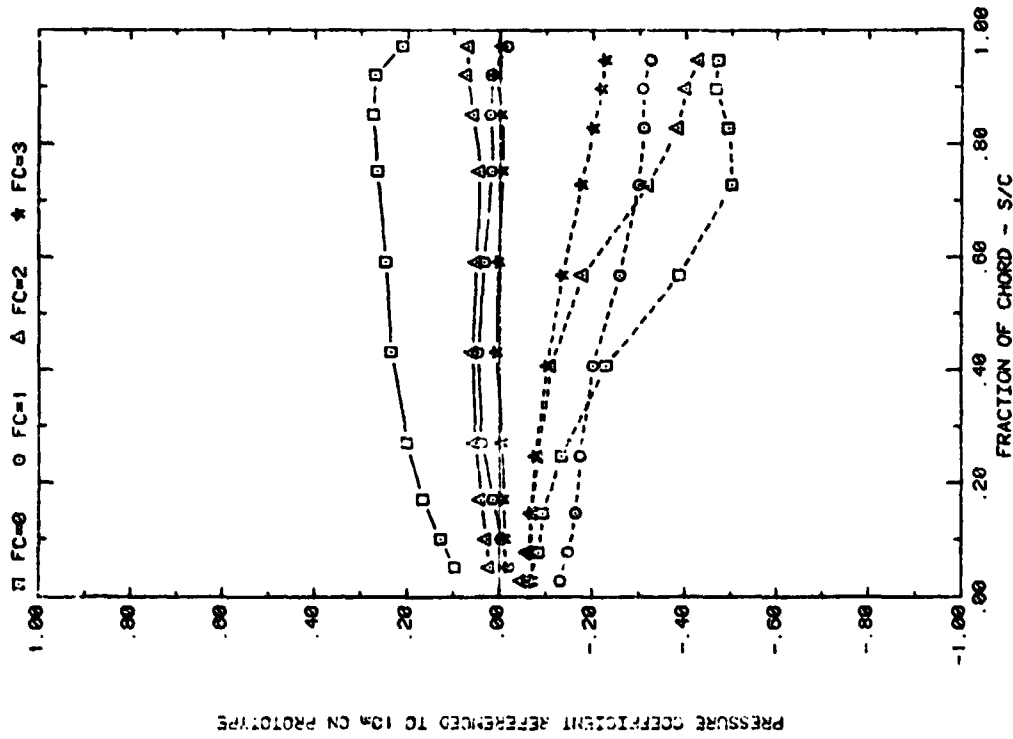


FRONT AND BACK PRESSURES 3.6" IN FROM EDGE OF ARRAY35, WIND=45  
EFFECT OF FC WITH ALPHA=35, H=3°, D=10°, P=30%, AND X=2C

Plot 5-2-3. (Continued)

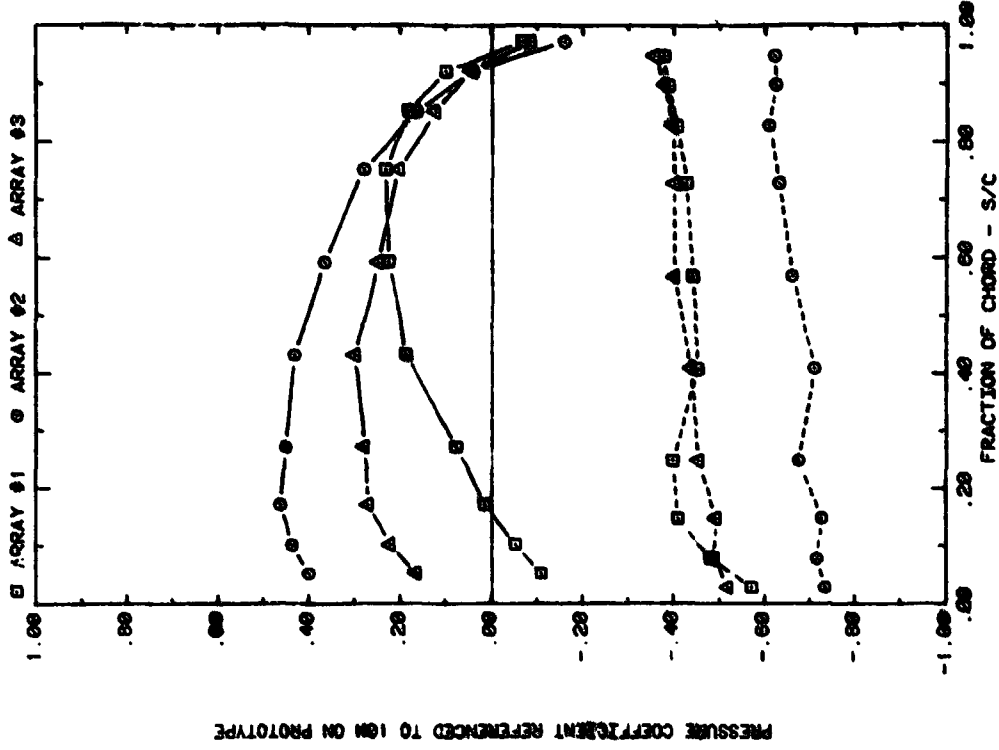


FRONT AND BACK PRESSURES 3.6° IN FROM EDGE OF ARRAY#3, WIND=45  
EFFECT OF FC WITH ALPHA=145, H=3°, D=10°, P=30%, AND X=2C

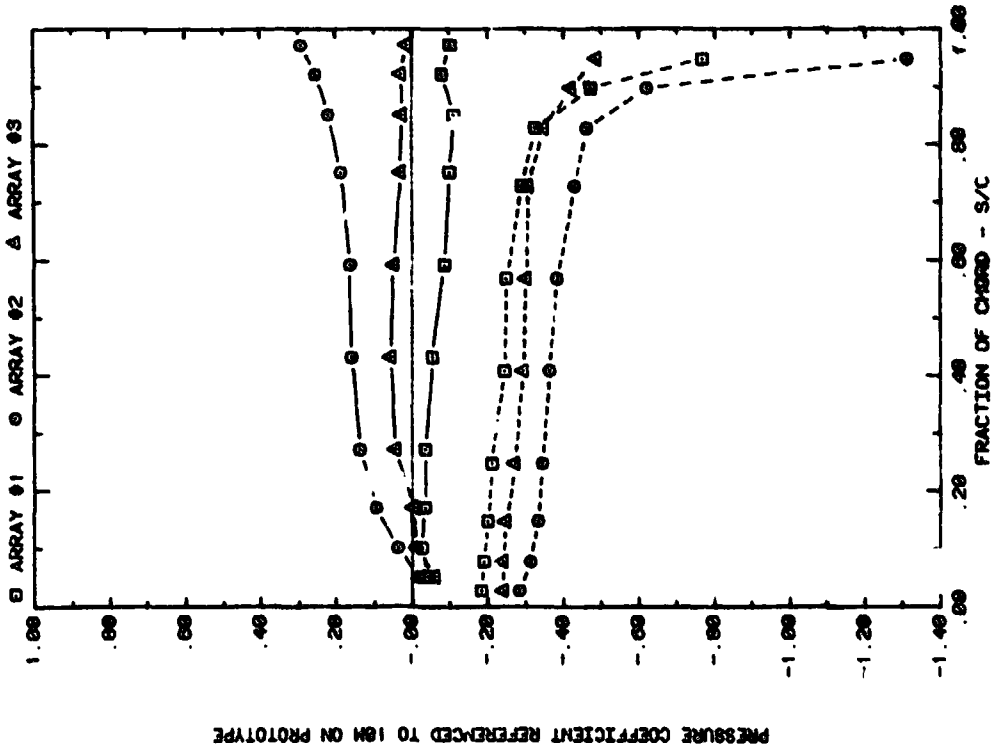


FRONT AND BACK PRESSURES 3.6° IN FROM EDGE OF ARRAY#3, WIND=45  
EFFECT OF FC WITH ALPHA=35, H=3°, D=10°, P=30%, AND X=2C

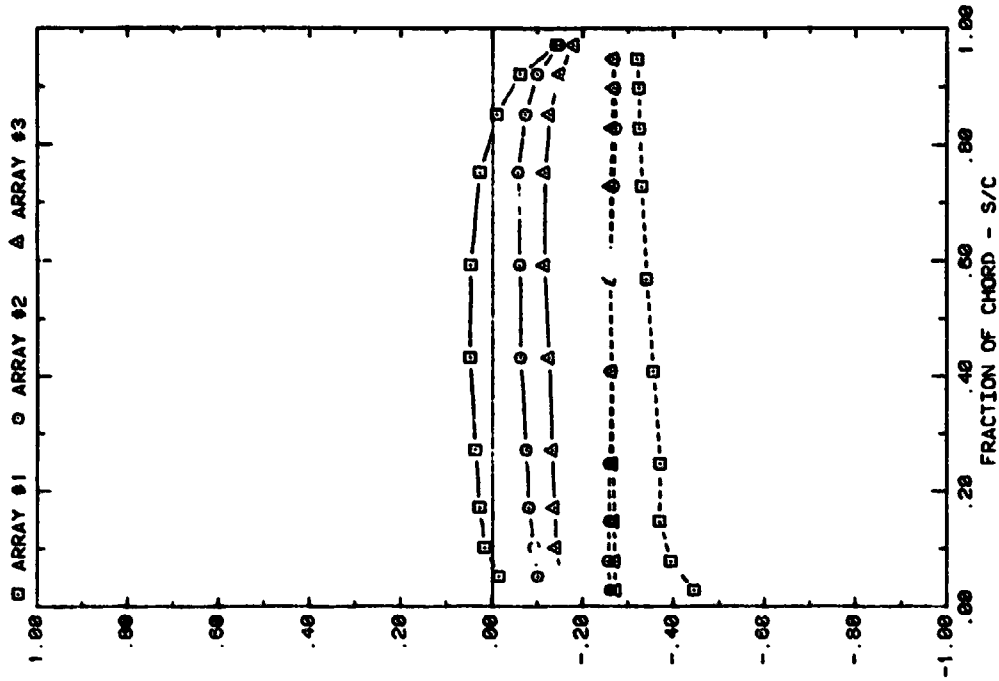
Plot 5-2-3. (Concluded)



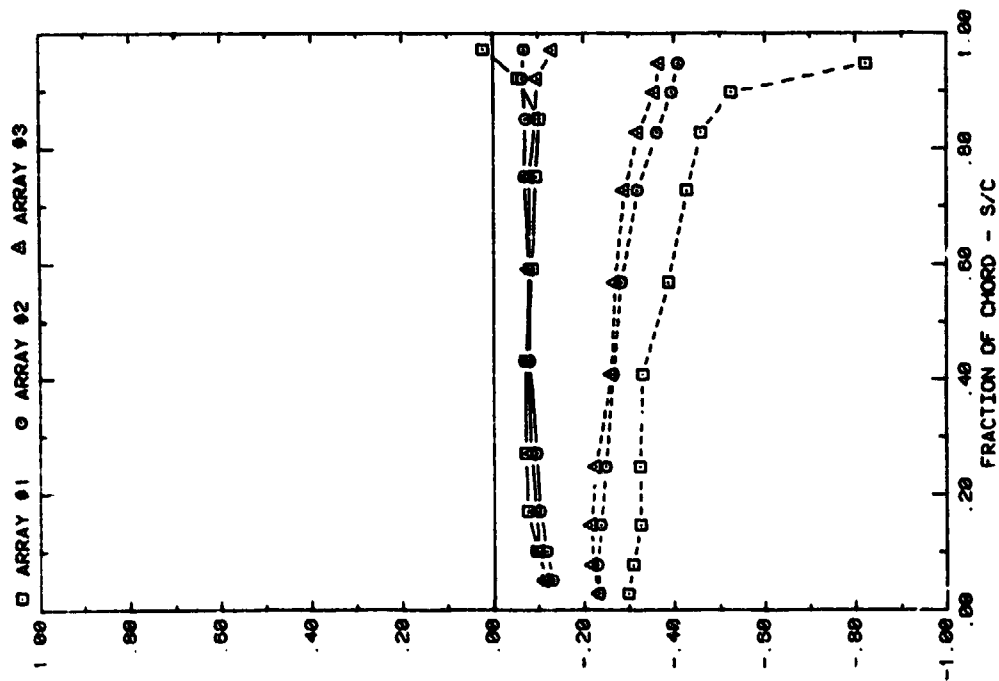
FRONT AND BACK PRESSURES ON ARRAYS #1, 2 & 3 ON POROSITY EXTENSION  
EFFECT OF ARRAY WITH ALPHA = 46, X = 2C, FC = 1



FRONT AND BACK PRESSURES ON ARRAYS #1, 2 & 3 ON POROSITY EXTENSION  
EFFECT OF ARRAY WITH ALPHA = 45, X = 2C, FC = 1  
Plot 5-3-1. Corner Study,  $\alpha = 45^\circ$ , Modified Model with Various Extension  
Effect of Array Position

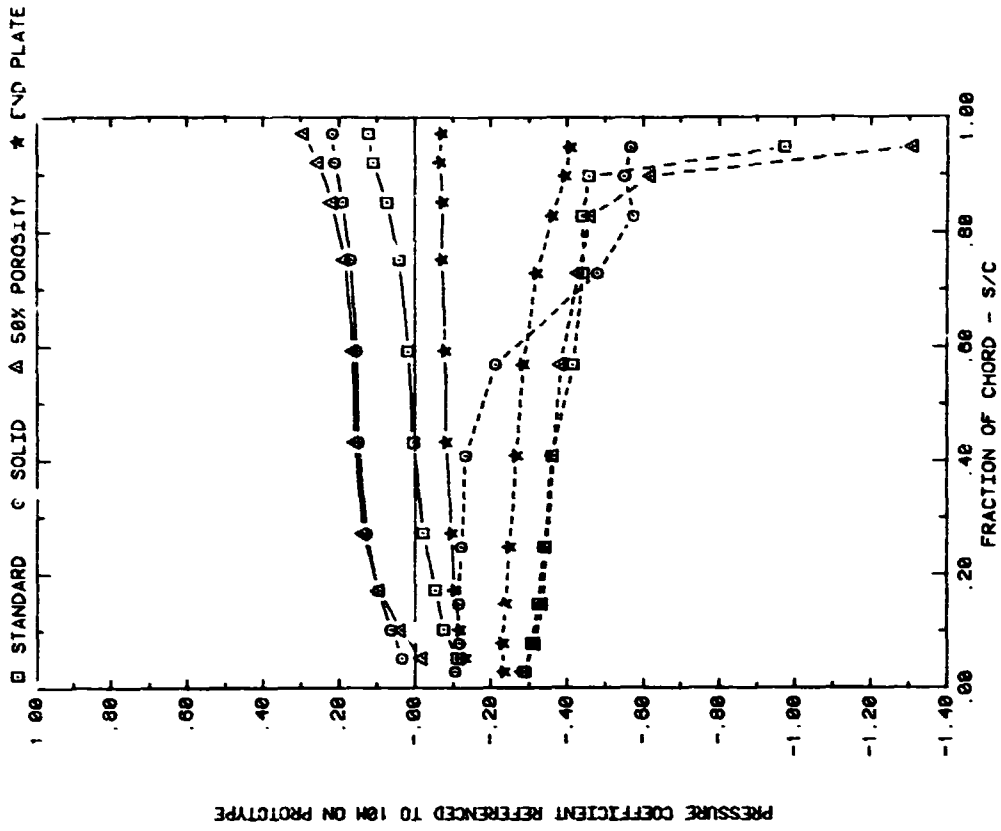


FRONT AND BACK PRESSURES ON ARRAYS #1, 2 & 3 END PLATE  
EFFECT OF ARRAY WITH ALPHA = 45, X = 2C, FC = 1

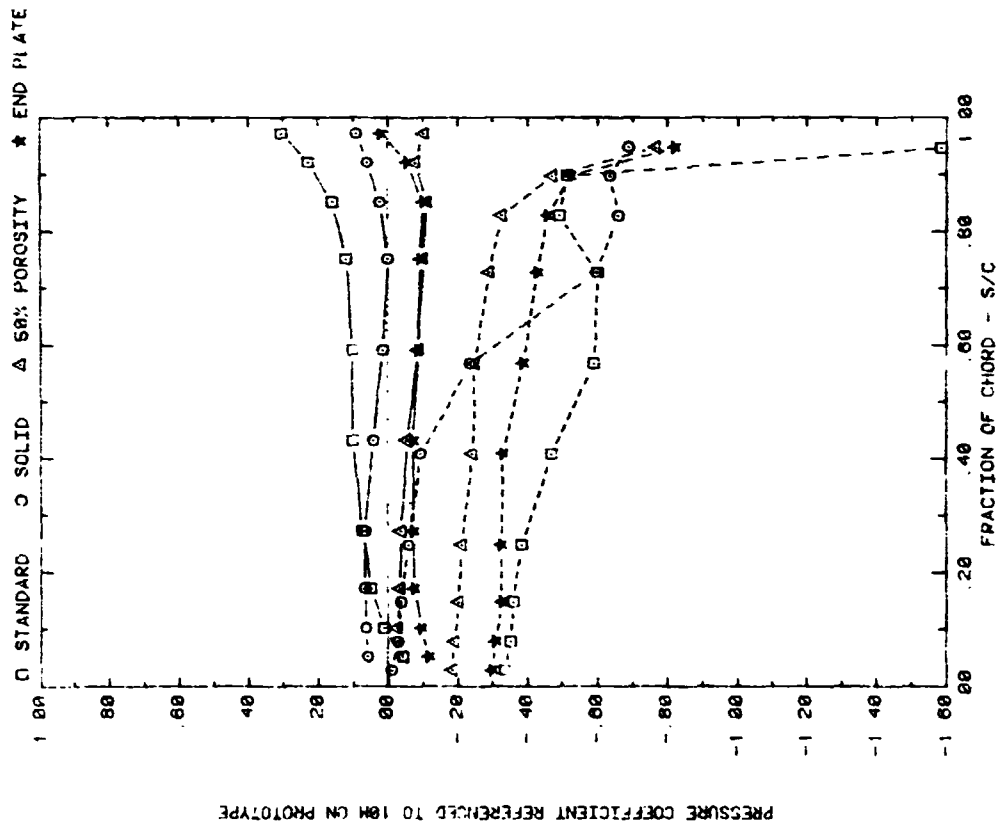


FRONT AND BACK PRESSURES ON ARRAYS #1, 2 & 3 END PLATE  
EFFECT OF ARRAY WITH ALPHA = 5, WIND = 45, X = 2C, FC = 1

Plot 5-3-1. (Continued)



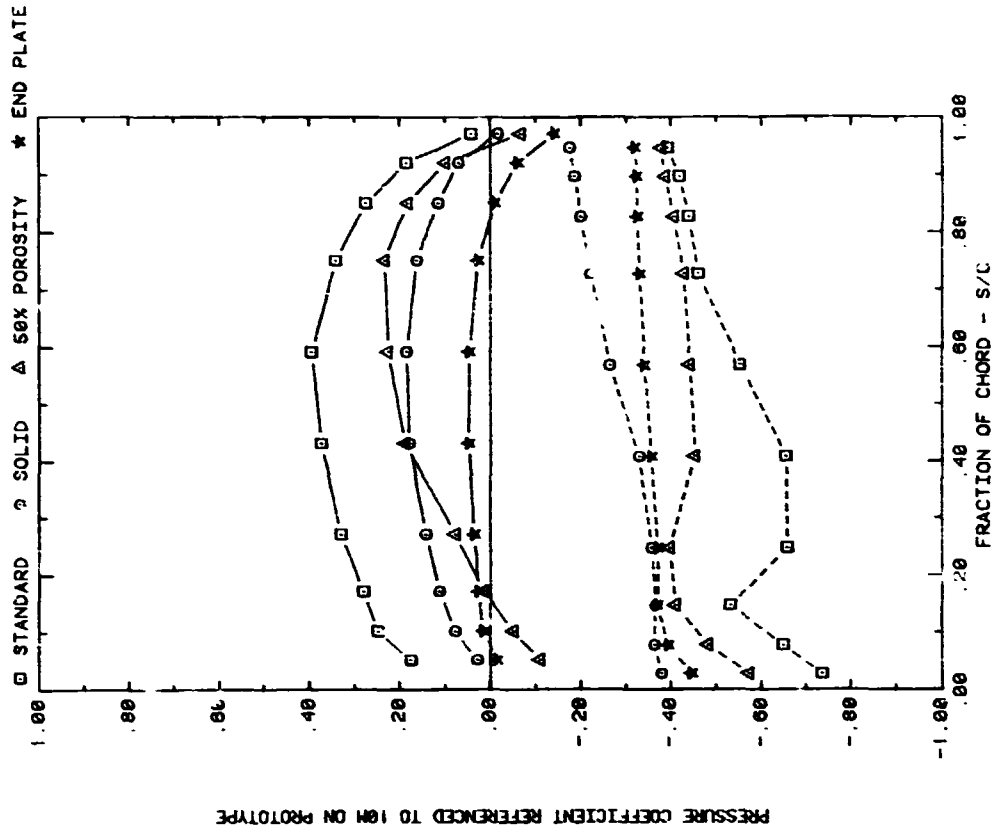
FRONT AND BACK PRESSURES ON ARRAYS; X = 2C, WIND = 45  
EFFECT OF EXTENSIONS; ARRAY = 2 ALPHA = 35, FC = 1



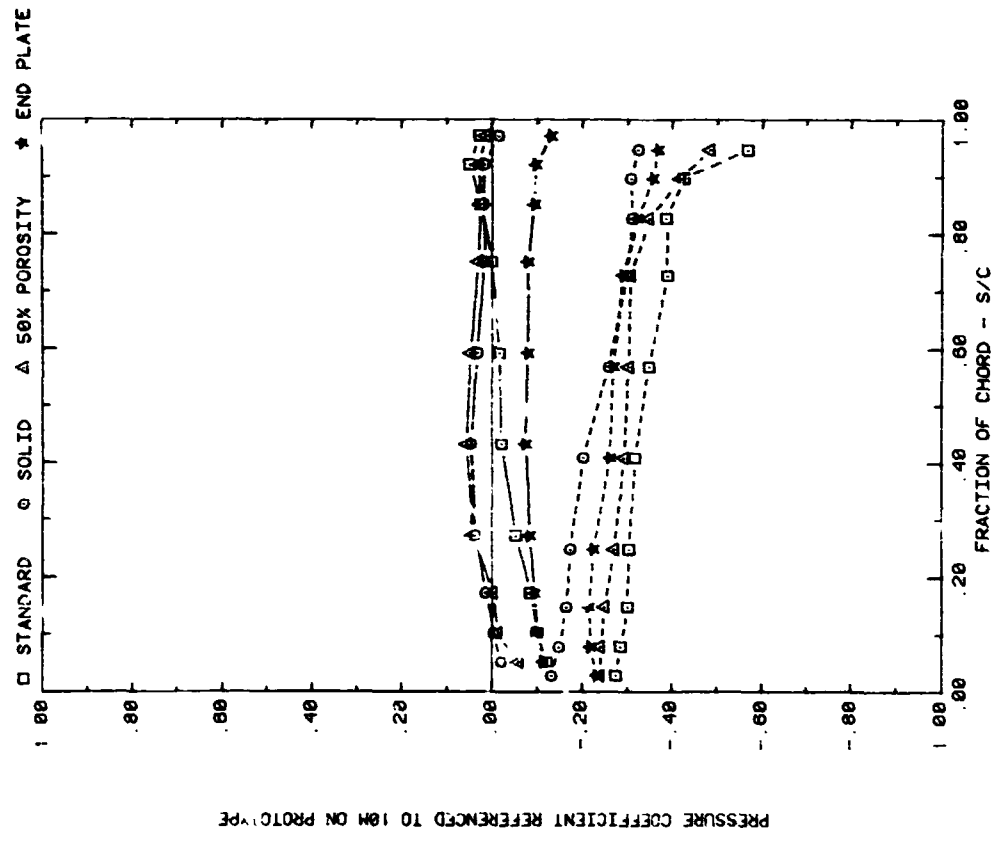
FRONT AND BACK PRESSURES ON ARRAYS; X = 2C, WIND = 45  
EFFECT OF EXTENSIONS; ARRAY = 1, ALPHA = 35, FC = 1

Plot 5-3-2. Corner Study, WD = 45°, Modified Model with Various Extension  
Effect of Model Configuration

C5

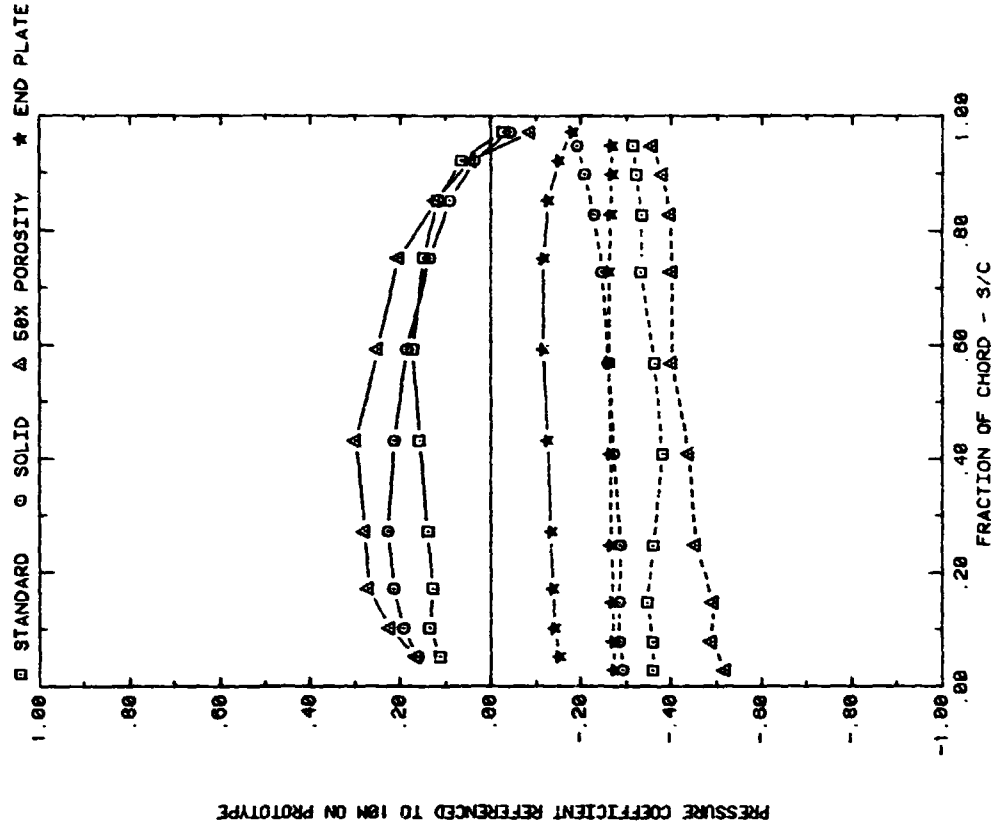


FRONT AND BACK PRESSURES ON ARRAYS; X = 2C, WIND = 45  
EFFECT OF EXTENSIONS, ARRAY = 1, ALPHA = 145, FC = 1

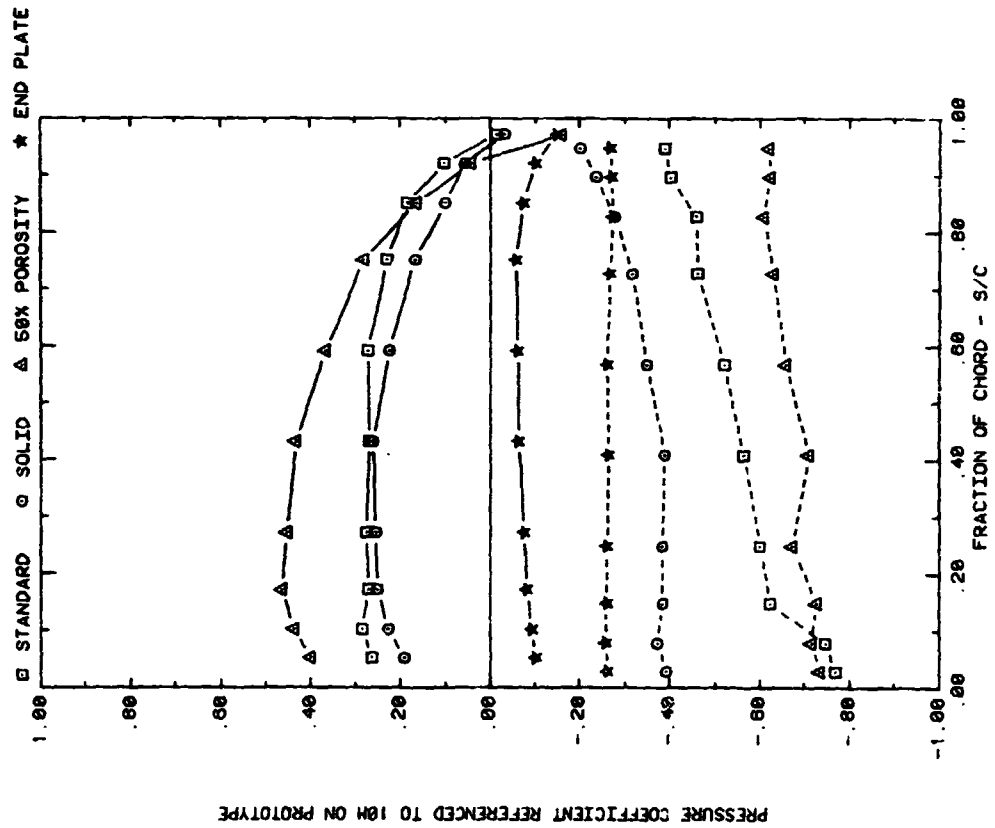


FRONT AND BACK PRESSURES ON ARRAYS; X = 2C, WIND = 45  
EFFECT OF EXTENSIONS, ARRAY = 3, ALPHA = 35, FC = 1

Plot 3-3-2. (Continued)



FRONT AND BACK PRESSURES ON ARRAYS, X = 2C, WIND = 45  
EFFECT OF EXTENSIONS, ARRAY = 3, ALPHA = 145, FC = 1



FRONT AND BACK PRESSURES ON ARRAYS, X = 2C, WIND = 45  
EFFECT OF EXTENSIONS, ARRAY = 2, ALPHA = 145, FC = 1

Plot 5-3-2. (Concluded)